



HAL
open science

Assessment of fresh and hardened properties of concrete made of crushed aggregates containing no natural sand

Faten Abi Farraj

► To cite this version:

Faten Abi Farraj. Assessment of fresh and hardened properties of concrete made of crushed aggregates containing no natural sand. Civil Engineering. Université Paul Sabatier - Toulouse III; Université Libanaise, 2021. English. NNT : 2021TOU30043 . tel-03343018

HAL Id: tel-03343018

<https://theses.hal.science/tel-03343018v1>

Submitted on 13 Sep 2021

HAL is a multi-disciplinary open access archive for the deposit and dissemination of scientific research documents, whether they are published or not. The documents may come from teaching and research institutions in France or abroad, or from public or private research centers.

L'archive ouverte pluridisciplinaire **HAL**, est destinée au dépôt et à la diffusion de documents scientifiques de niveau recherche, publiés ou non, émanant des établissements d'enseignement et de recherche français ou étrangers, des laboratoires publics ou privés.



THÈSE

En vue de l'obtention du DOCTORAT DE L'UNIVERSITÉ DE TOULOUSE

Délivré par l'Université Toulouse 3 - Paul Sabatier

Cotutelle internationale : Université libanaise

Présentée et soutenue par

FATEN ABI FARRAJ

Le 5 mai 2021

**Evaluation des propriétés du béton à l'état frais et l'état durci
composé des granulats concassés sans sable naturel**

Ecole doctorale : **MEGEP - Mécanique, Energétique, Génie civil, Procédés**

Spécialité : **Génie civil**

Unité de recherche :

LMDC - Laboratoire Matériaux et Durabilité des Constructions de Toulouse

Thèse dirigée par

Gilles ESCADEILLAS et Fadi HAGE CHEHADE

Jury

Mme Evelyne TOUSSAINT, Rapporteur

M. Ghassan CHEHAB, Rapporteur

M. André LECOMTE, Examineur

M. Fadi COMAIR, Examineur

M. Gilles ESCADEILLAS, Directeur de thèse

M. Fadi HAGE CHEHADE, Co-directeur de thèse

M. Thierry VIDAL, Co-directeur de thèse

M. Maher EL BARRAK, Co-directeur de thèse

Acknowledgments

"Don't let the sun go down without saying thank you to someone, and without admitting to yourself that absolutely no one gets this far alone," Stephen King.

First and foremost, I would like to express my sincere gratitude to Advanced Construction and Technology Services (ACTS) and its chairman Mr. Khaled Awad, for the funding opportunity to undertake this thesis. I would like to extend my deepest thanks to the country manager, Dr. Maher El Barrak, who never wavered in his determination to provide all the data and materials needed for the thesis, guide the experimental work, and assess the results.

I would like to place on record my extreme sense of gratitude to my supervisors for sharing immense knowledge, wide expertise, and valuable guidance which brought my work to a higher level. To Pr. Gilles Escadeillas for his steady patience and help through each stage of the process. To Pr. Fadi Hage Chehade for his advice and his belief in my capabilities. To Dr. Thierry Vidal for his devotion and excellent attention to detail. To Dr. Marie-Pierre Cubaynes for her consistent motivation and positive energy.

I would like to show my deepest appreciation for the members of the exam committee, Pr. Fadi Comair, Pr. Evelyne Toussaint, Pr. Ghassan Chehab, and Pr. André Lecomte, for generously devoting time to examine my work and offer valuable comments towards improving it.

I gratefully acknowledge the technical assistance and valuable contribution I have received from each and every member of the ACTS laboratory staff who has played an effective role in this project. I would like also to recognize the assistance I have received from the Laboratoire Matériaux et Durabilité de Constructions (LMDC), I was fortunate to benefit from the support of such professional staff.

Many thanks and appreciation for the quarries and concrete plants which have generously provided the materials and the information needed: SAD, BCL, and all those who preferred not to be mentioned.

I am grateful to my colleagues and friends for always being there for me to reduce the stress of this journey.

I owe the warmest thanks to my family for whom I am forever indebted. To my husband, for his significant patience and unconditional trust, and for sharing my goal to accomplish this thesis. To my dad for his tremendous encouragement and for teaching me how to believe in myself. To my mom for helping me go through this period in the most positive way with endless emotional support. To my elder sister for setting a great example and providing valuable advice. To my second sister for always being generous with her love and help. To my brother for knowing how to raise my spirit when I am down. To my parents-in-law for their heart-warming kindness. To the rest of my big family for their continuous love and encouragement. I am forever grateful they are all in my life!

Finally, I would like to thank all the amazing people who have been a part of this journey and have directly or indirectly contributed to this work.

Abstract

In Lebanon, good quality natural siliceous sand becomes rarely available, and for environmental reasons, its extraction is subjected to governmental restrictions. This problem affects the construction sector through the cost and the quality of concrete. Moreover, this sand is too fine to be used alone as fine aggregate in concrete mixes. Therefore, to meet the grading requirement of the ASTM C33, the standard applied in Lebanon, this sand is currently mixed with an appropriate proportion of a coarser crushed limestone sand which compensates the fineness of the natural sand.

Accordingly, finding an alternative to natural sand in concrete becomes essential to reduce its economic and environmental problems and to avoid the dependency of the construction field on its quality and availability in the Lebanese market. After a literature review of existing alternatives around the world, it seems that the replacement of natural sand by the local crushed limestone sand could be an appropriate solution in the Lebanese context due to the abundance and good quality of this sand. Hence, the current study is the first in this country that aims to give scientific evidence of this solution before being applied in the Lebanese market. Its objective is to assess the effect on the concrete performance of the total replacement of natural siliceous sand by crushed limestone sand.

In order to respond to the objective of the study, the behaviors of concrete mixes incorporating normalized crushed sands without natural sand are compared to those of reference concrete containing the conventional combination of natural sand and crushed sand, to verify that their performances could be maintained, for three normal strength concrete mixes and one high strength concrete. Since the crushed sand, provided currently from the limestone quarries, is too coarse to directly replace the natural sand, the first step consists of constructing two types of normalized crushed sand conforming to the standard grading requirements. For each type of fine aggregate, the fresh concrete properties, mechanical behavior, and durability are investigated. The effects of the mineralogy, morphology, and particle size distribution of fine aggregates on these various properties are then evaluated. A microstructural analysis is also conducted to depict the variations at the interface between the cement paste and the different types of sand grains and to try to explain the differences that could exist at the macro scale between the different types of concrete.

Furthermore, since the production of the normalized crushed limestone sand could impose many industrial and economic constraints to limit the high percentage of fines, the performance of normal and high strength concretes, incorporating crushed sand with a percentage of fines ($< 75 \mu\text{m}$ sieve) exceeding the limit imposed by ASTM C33 (7%), is evaluated following a performance-based approach.

For fixed water to cement ratio, cement content, and coarse aggregates proportions, and for different dosages of admixture to reach the same slump value, the results prove that the concrete performance could be maintained when using the normalized crushed limestone sand conforming to the standard grading requirements or the fine crushed limestone sand with a high percentage of fines. Additionally, the overview on the economic and environmental impacts on the Lebanese context verifies the feasibility of the use of crushed limestone sand as the only fine aggregate.

Keywords: Natural siliceous sand, crushed limestone sand, fines, fresh properties, admixture, mechanical resistances, shrinkage, durability, concrete microstructure, interfacial transition zone, feasibility study, economy, environment.

Résumé

La détérioration de la qualité du sable naturel siliceux au Liban et les restrictions imposées par l'Etat à son utilisation, suite aux effets néfastes de son exploitation, affectent le secteur de la construction libanais à travers le coût et la qualité du béton. Actuellement, ce sable trop fin pour être utilisé seul dans le béton selon la norme ASTM C33, en vigueur au Liban, est toujours mélangé avec un pourcentage approprié d'un sable calcaire concassé de carrière.

Une alternative à ce sable naturel doit être trouvée pour remédier aux problèmes environnementaux et économiques et limiter la dépendance actuelle du secteur de la construction libanais que son utilisation induit. Après avoir dressé un état de l'art des alternatives existantes à travers le Monde, il apparaît que le remplacement du sable naturel par le sable calcaire concassé local pourrait être une solution adaptée au contexte Libanais grâce à l'abondance et à la bonne qualité de ce sable. Ainsi, cette étude est la première menée au Liban visant à démontrer scientifiquement la pertinence de cette solution avant de la mettre en pratique. Elle a pour objectif d'évaluer les effets de la substitution totale du sable naturel siliceux par du sable calcaire concassé, sur les performances des bétons.

Pour répondre à l'objectif de l'étude, les bétons contenant des sables concassés normalisés sans sable naturel sont comparés à des bétons de référence constitués de la combinaison conventionnelle du sable naturel et du sable concassé, pour vérifier si leurs performances peuvent être maintenues, pour trois formulations de bétons ordinaires et une formulation de béton à hautes performances. Comme la granulométrie du sable concassé des carrières libanaises ne respecte actuellement pas la norme ASTM C33, un travail de construction de deux types de sable concassé calcaire dont la granulométrie est conforme à cette norme a été préalablement réalisé. Les propriétés à l'état frais, le comportement mécanique, et les propriétés de durabilité sont étudiés pour chaque type de sable. Les effets de la minéralogie, de la morphologie, et des distributions granulométriques des sables sont ainsi évalués. Cette étude est complétée par une analyse microstructurale visant à détecter les variations de l'état des interfaces entre la pâte de ciment et les grains de sable et à tenter d'expliquer les éventuelles différences qui peuvent survenir à l'échelle macrostructurale entre les différents types de béton.

En outre, étant donné que la limitation du pourcentage des fines lors de la production du sable concassé normalisé induit des contraintes industrielles et économiques, une étude complémentaire du comportement de deux formulations d'un béton ordinaire et d'un béton à hautes performances a été menée selon une approche performantielle afin d'évaluer l'influence de l'incorporation du sable concassé ayant un pourcentage de fines ($< 75 \mu\text{m}$) dépassant la limite imposée par la norme ASTM C33 (7%).

Les résultats obtenus permettent de conclure que, pour des mêmes rapports eau efficace sur ciment, dosages en ciment et proportions des gravillons, ainsi que pour un dosage de superplastifiant adapté de manière à atteindre le même affaissement au cône d'Abrams, les performances de ces bétons peuvent être maintenues lors d'une substitution totale du sable naturel par du sable concassé calcaire, que sa granulométrie ou que son pourcentage de fines soient conformes ou non à la norme. Du point de vue économique et environnemental, le sable concassé calcaire peut ainsi être considéré comme une solution alternative pertinente à l'utilisation du sable naturel siliceux.

Mots-clefs : Sable naturel siliceux, sable concassé calcaire, fines, propriétés à l'état frais, adjuvant, résistances mécaniques, retrait, durabilité, microstructure, zone d'interface, étude de faisabilité, économie, environnement.

List of Abbreviations and Definitions

Aggregates

NS	Natural sub-rounded siliceous sand, resulting from the fragmentation of friable sandstone, characterized by a particle size distribution that predominantly exceeds the maximum passing limit of the ASTM C33 standard
CS/CCS	Conventional crushed angular limestone sand, resulting from the crushing of limestone rocks, with a particle size distribution coarser than the lower limit of the ASTM C33 standard
FCS	Fine crushed sand, recently provided from the limestone quarries, with a particle size distribution that conforms to the standard requirements, except for the high percentage of fines that exceeds the allowable limit (7%) and varies between 13% and 18%
ECS	Equivalent crushed sand, constructed in the laboratory in order to get crushed sand with a particle size distribution strictly similar to the one used in the reference mix
MCS	Modified crushed sand, constructed in the laboratory with a well-distributed particle size distribution between the ASTM C33 limits with a fines percentage that does not exceed 7%
MA	Medium crushed limestone aggregate with a nominal diameter of 10-12 mm, resulting from the crushing of limestone rocks
CA	Coarse crushed limestone aggregate with a nominal diameter of 20 mm, resulting from the crushing of limestone rocks

Concrete mixes

CM	Control mix, incorporating adequate mass proportions of NS and CCS, to conform to the ASTM C33 grading requirements for fine aggregates and to serve as the reference concrete
EM	Equivalent mix, containing the ECS as the only fine aggregate without natural sand, to eliminate the effect of the gradation while studying the effect of the total substitution of the conventional combination of fine aggregates by the crushed sand
MM	Modified mix, consisting of the MCS as the only fine aggregate without natural sand, to study the effect of the well-graded crushed sand
FM	Fine mix, including the FCS as the only fine aggregate without natural sand, to assess the effect of the high percentage of fines in sand

TABLE OF CONTENTS

GENERAL INTRODUCTION.....	22
I. LITERATURE REVIEW.....	26
INTRODUCTION	27
1. OVERVIEW OF THE AGGREGATES PRODUCTION IN LEBANON	28
2. INTERNATIONAL PROBLEMS OF THE NATURAL SAND USED IN CONSTRUCTION	30
2.1 <i>River sand</i>	30
2.2 <i>Sea sand</i>	31
2.3 <i>Land pits sand</i>	32
2.4 <i>Dune sand</i>	32
3. REVIEW ON THE WORLDWIDE ALTERNATIVES TO NATURAL SAND	32
3.1 <i>Crushed rocks</i>	32
3.1.1 <i>Crushed limestone</i>	33
3.1.2 <i>Crushed marble</i>	33
3.1.3 <i>Crushed granite</i>	34
3.2 <i>Recycled wastes</i>	35
3.2.1 <i>Recycled concrete</i>	35
3.2.2 <i>Crushed bricks and tiles</i>	35
3.2.3 <i>Glass waste</i>	36
3.2.4 <i>Plastic waste</i>	38
3.3 <i>Industrial by-products</i>	39
3.3.1 <i>Bottom and fly ash</i>	39
3.3.1.1 <i>Bottom ash</i>	39
3.3.1.2 <i>Fly ash</i>	40
3.3.2 <i>Rubber ash</i>	41
3.3.3 <i>Foundry sand</i>	42
3.3.4 <i>Metals slag</i>	43
3.3.4.1 <i>Iron slag</i>	43
3.3.4.2 <i>Ferronickel slag</i>	44
3.3.4.3 <i>Ferrochrome slag</i>	44
3.3.4.4 <i>Copper slag</i>	45
3.4 <i>Summary of the literature review on the alternatives to natural sand</i>	45
3.5 <i>Available alternatives to natural sand in Lebanon</i>	47

4. EFFECTS OF FINE AGGREGATES CHARACTERISTICS ON CONCRETE PERFORMANCE	48
4.1 <i>Fine aggregates characteristics</i>	48
4.1.1 Mineralogy and chemical composition of fine aggregates.....	48
4.1.2 Morphology of fine aggregates	49
4.1.3 Physical characteristics of fine aggregates.....	52
4.1.4 Fines content and deleterious particles in fine aggregates	52
4.2 <i>Effects of fine aggregates characteristics' on concrete at the macroscale</i>	53
4.2.1 Effects of fine aggregates characteristics' on the fresh properties of concrete.....	53
4.2.1.1 <i>Effects of the mineralogy of fine aggregates</i>	53
4.2.1.2 <i>Effects of the morphology of fine aggregates</i>	54
4.2.1.3 <i>Effects of the physical properties of fine aggregates</i>	55
4.2.1.4 <i>Effects of the fines content of fine aggregates</i>	57
4.2.1.5 <i>Effects of the deleterious particles of fine aggregates</i>	58
4.2.1.6 <i>Effects of the proportion of fine aggregates</i>	58
4.2.1.7 <i>Summary of the fine aggregates characteristics' on the fresh properties of concrete</i>	59
4.2.2 Effects of fine aggregates characteristics' on the mechanical behavior of concrete: strengths and modulus of elasticity	59
4.2.2.1 <i>Effects of the mineralogy of fine aggregates</i>	59
4.2.2.2 <i>Effects of the morphology of fine aggregates</i>	61
4.2.2.3 <i>Effects of the physical properties of fine aggregates</i>	61
4.2.2.4 <i>Effects of the fines content of fine aggregates</i>	62
4.2.2.5 <i>Effects of the deleterious particles in fine aggregates</i>	65
4.2.2.6 <i>Summary of the effects of the fine aggregates' characteristics on the mechanical behavior of concrete</i>	65
4.2.3 Effects of fine aggregates' characteristics on the mechanical behavior of concrete: shrinkage deformations	66
4.2.3.1 <i>Types of shrinkage</i>	66
4.2.3.2 <i>Effects of the aggregates' inclusion on the shrinkage of the cement paste</i>	67
4.2.3.3 <i>Effects of the physical properties of fine aggregates</i>	68
4.2.3.4 <i>Effects of the deleterious particles in fine aggregates</i>	69
4.2.3.5 <i>Effects of the variations in the mix design parameters</i>	69
4.2.4 Effects of aggregates characteristics' on the durability properties of concrete	69
4.2.4.1 <i>Effects of the mineralogy of fine aggregates</i>	71
4.2.4.2 <i>Effects of the morphology of fine aggregates</i>	73
4.2.4.3 <i>Effects of the physical properties of fine aggregates</i>	73
4.2.4.4 <i>Effects of the fines content of fine aggregates</i>	73

Table of Contents

4.2.4.5	<i>Effects of the variations in the mix design parameters</i>	74
4.2.4.6	<i>Summary of the effects of the fine aggregates' characteristics on the durability properties of concrete</i>	75
4.3	<i>Effects of fine aggregates characteristics' on the concrete microstructure</i>	75
4.3.1	Effects of the mineralogy of fine aggregates	77
4.3.2	Effects of the morphology of fine aggregates	79
4.3.3	Effects of the fines content of sands	80
4.3.4	Summary of the effects of fine aggregates characteristics' on the concrete microstructure	80
	CONCLUSIONS.....	81
 II. AGGREGATES CHARACTERIZATION AND FINE AGGREGATES PREPARATION		
84		
	INTRODUCTION	85
1.	CHARACTERIZATION OF AGGREGATES.....	86
1.1	<i>Shape characteristics</i>	86
1.2	<i>Chemical composition</i>	88
1.3	<i>Mineralogical composition</i>	91
1.4	<i>Physical characterizations</i>	92
1.4.1	Gradation.....	93
1.4.2	Deleterious particles.....	96
1.4.2.1	<i>Clay lumps and friable particles</i>	96
1.4.2.2	<i>Sand equivalent</i>	97
1.4.2.3	<i>Methylene blue value</i>	98
1.4.2.4	<i>Lightweight particles</i>	98
1.4.2.5	<i>Organic impurities</i>	99
1.4.2.6	<i>Summary of deleterious particles</i>	99
1.4.3	Specific gravity and absorption.....	100
1.4.4	Resistance to soundness and degradation	101
2.	PREPARATION OF FINE AGGREGATES.....	102
2.1	<i>Provided crushed sand</i>	103
2.1.1	Conventional crushed sand	103
2.1.2	Fine crushed sand.....	104
2.2	<i>Constructed crushed sand</i>	106
2.2.1	Equivalent crushed sand.....	106
2.2.2	Modified crushed sand.....	107
	CONCLUSIONS.....	108

III. CONCRETE MIX DESIGN AND EXPERIMENTAL PROCEDURE	109
INTRODUCTION	110
1. CONCRETE MIX DESIGN	110
1.1 Materials	111
1.1.1 Aggregates	111
1.1.2 Cement	111
1.1.2.1 Chemical and mineralogical composition	112
1.1.2.2 Physical characterizations	113
1.1.3 Water	117
1.1.4 Admixture	117
1.2 Mix proportions	117
1.2.1 Mixes incorporating normalized crushed sand	117
1.2.1.1 Fine aggregates	118
1.2.1.2 Coarse aggregates	120
1.2.1.3 All-in aggregates	120
1.2.1.4 Concrete mixes	121
1.2.1.5 Additional concrete mix	122
1.2.2 Concrete mixes incorporating crushed sand with a high percentage of fines	123
1.2.3 Summary of materials and proportions	126
1.3 Mixing procedure	127
2. EXPERIMENTAL PROCEDURE	127
2.1 Fresh state properties of concrete	127
2.1.1 Fresh concrete temperature	128
2.1.2 Slump and slump retention	128
2.1.3 Setting time	129
2.1.4 Fresh density and air content	130
2.2 Mechanical behavior of concrete	130
2.2.1 Compressive strength	130
2.2.2 Modulus of elasticity	131
2.2.3 Flexural strength	133
2.3 Shrinkage of concrete	134
2.4 Durability properties of concrete	135
2.4.1 Porosity accessible to water	136
2.4.2 Water absorption by immersion	136
2.4.3 Depth of water penetration under pressure	136
2.4.4 Resistance to chloride ion penetration	137

Table of Contents

2.4.5	Resistivity	138
2.5	<i>Microstructural analysis of concrete</i>	139
2.6	<i>Summary of the concrete experimental program</i>	140
CONCLUSIONS.....		142
IV. EXPERIMENTAL STUDY ON CONCRETE MIXES INCORPORATING NORMALIZED CRUSHED SAND		143
INTRODUCTION		144
1.	COMPARISON OF CONCRETE PERFORMANCES.....	144
1.1	<i>Fresh properties</i>	145
1.1.1	Fresh concrete temperature	146
1.1.2	Workability	147
1.1.3	Loss of workability with time	149
1.1.4	Setting times.....	151
1.1.5	Density and air content	152
1.1.6	Summary of fresh properties.....	153
1.2	<i>Mechanical behavior</i>	153
1.2.1	Compressive strength.....	154
1.2.2	Modulus of elasticity.....	158
1.2.3	Flexural strength	159
1.2.4	Summary of the mechanical behavior.....	161
1.3	<i>Shrinkage</i>	161
1.3.1	Autogenous shrinkage.....	162
1.3.2	Total shrinkage.....	163
1.3.3	Drying shrinkage and mass loss.....	165
1.3.4	Summary of the shrinkage	166
1.4	<i>Durability Properties</i>	166
1.4.1	Porosity accessible to water	167
1.4.2	Water absorption by immersion.....	167
1.4.3	Water penetrability under pressure	170
1.4.4	Resistance to chloride ion penetration	172
1.4.5	Resistivity	174
1.4.6	Overall durability performance.....	176
1.4.7	Summary of the durability properties	178
1.5	<i>Microstructural analysis and correlation with the concrete performance</i>	179

Table of Contents

2. FEASIBILITY STUDY FOR USING THE NORMALIZED CRUSHED SAND AS THE ONLY FINE AGGREGATE	183
2.1 Technical overview	183
2.2 Environmental overview	184
2.3 Economic overview	185
CONCLUSIONS.....	186
V. PERFORMANCE-BASED APPROACH STUDY ON CONCRETE MIXES INCORPORATING CRUSHED SAND WITH HIGH PERCENTAGE OF FINES.....	188
INTRODUCTION	189
1. FRESH PROPERTIES.....	190
1.1 Fresh concrete temperature	191
1.2 Workability.....	191
1.3 Loss of workability with time	192
1.4 Setting times	194
1.5 Density and air content	194
1.6 Summary of fresh properties	195
2. MECHANICAL BEHAVIOR	195
2.1 Compressive strength.....	195
2.2 Flexural strength.....	198
2.3 Summary of the mechanical behavior.....	199
3. DURABILITY PROPERTIES.....	200
3.1 Porosity accessible to water	200
3.2 Water absorption by immersion.....	201
3.3 Water penetrability under pressure	202
3.4 Resistance to chloride ions penetration	203
3.5 Resistivity.....	205
3.6 Overall durability performance	205
3.7 Summary of durability properties	207
4. MICROSTRUCTURAL ANALYSIS AND CORRELATION WITH THE CONCRETE PERFORMANCE.....	207
5. FEASIBILITY STUDY FOR USING THE FINE CRUSHED SAND AS THE ONLY FINE AGGREGATE	209
5.1 Technical overview	210
5.2 Environmental overview	210
5.3 Economic overview	210
CONCLUSIONS.....	211

CONCLUSIONS AND FUTURE STUDIES	212
RESUME SUBSTANTIEL	218
ANNEXES	235
ANNEX A: PHYSICAL CHARACTERIZATION TESTS FOR AGGREGATES	236
ANNEX B: CRUSHED AGGREGATES PROPERTIES FROM DIFFERENT LEBANESE RESOURCES.....	256
ANNEX C: PHYSICAL CHARACTERIZATION TESTS FOR CEMENT	262
ANNEX D: CONCRETE TESTS	270
ANNEX E: COMPARISON BETWEEN CALCULATED AND EXPERIMENTAL FRESH CONCRETE DENSITIES.....	290
REFERENCES.....	295

List of Figures

Chapter I: Literature Review

<i>Figure I.1 Distribution of quarries, presented by the yellow points, all over Lebanon (Ministry of Environment, 2006).....</i>	<i>29</i>
<i>Figure I.2 Environmental impacts of sand mining on (a) Ramleh El Bayda beach, Beirut (L'Orient Le Jour, 2016) and (b) the pine forests in Jezzine district.....</i>	<i>29</i>
<i>Figure I.3 Direct and indirect impacts of the sand dredging on the marine environment (Tillin et al., 2011 cited by UNEP, 2014).....</i>	<i>31</i>
<i>Figure I.4 The difference of surface spalling, after exposure to a temperature of 1000 °C, between (a) concrete containing crushed bricks and roof tiles aggregates and (b) concrete containing crushed basaltic aggregates (Miličević et al., 2016).....</i>	<i>36</i>
<i>Figure I.5 Examples of glass waste used as fine aggregates in concrete (a) (Kim et al., 2018) and (b) (Ismail and AL-Hashmi, 2009).....</i>	<i>37</i>
<i>Figure I.6 (a) Image showing the appearance of the natural siliceous sand and the PVC sand and (b) SEM image of the ITZ between the PVC aggregate and the cement paste (x500) (Senhadji et al., 2015).....</i>	<i>38</i>
<i>Figure I.7 Polyethylene terephthalate (PET) bottle wastes: (a) Heat-treated spherical/cylindrical particles PP, and (b) Flaky fine particles PF (Saikia and De Brito, 2014).....</i>	<i>39</i>
<i>Figure I.8 Scanning electron microscope images of bottom ash as fine aggregate (a) (x300) (Rafieizonooz et al., 2017) and (b) (x230) (Singh and Siddique, 2014).....</i>	<i>40</i>
<i>Figure I.9 Different particle sizes of the geopolymers fly ash (Agrawal et al., 2017).....</i>	<i>41</i>
<i>Figure I.10 Scanning electron microscope image at the ITZ of a rubber ash particle for concrete containing 20% rubber ash as a replacement to natural sand (x13450) (Gupta et al., 2014).....</i>	<i>41</i>
<i>Figure I.11 Ferrochrome slag used as fine aggregate (Panda et al., 2013).....</i>	<i>44</i>
<i>Figure I.12 (a) Waste composition (GIZ, 2014) and (b) waste management in Lebanon (Abbas et al., 2017).....</i>	<i>48</i>
<i>Figure I.13 Determination of particles shape by (a) (Bengtsson and Evertsson, 2006) and (b) (He et al., 2016).....</i>	<i>50</i>
<i>Figure I.14 Schematic representation of the apparatus used to calculate the aggregate surface roughness (Tasong et al., 1998).....</i>	<i>51</i>
<i>Figure I.15 Rheological properties between mortars incorporating limestone crushed sand M1L0, siliceous crushed sand M1S0, and river natural sand M1R0 (Safiddine et al., 2017).....</i>	<i>54</i>
<i>Figure I.16 Mechanism of (a) dispersive action of water-reducing admixture and (b) steric hindrance of polycarboxylate water-reducing admixture (Thomas and Wilson, 2002).....</i>	<i>55</i>
<i>Figure I.17 Difference between continuous and discontinuous granular skeleton (Santos et al. 2015).....</i>	<i>56</i>
<i>Figure I.18 Rheological properties of mortar with optimized and original grading (Lagerblad et al. 2014).....</i>	<i>56</i>

List of Figures

<i>Figure I.19 Relationship between the methylene blue absorption of sand samples, the admixture content, and the compressive strength of concrete mixes in order to get the same slump for fixed water to cement ratio (Hasdemir et al., 2016)</i>	<i>58</i>
<i>Figure I.20 Effect of different types of fines on the compressive strength of concrete (Bonavetti & Irassar, 1994).....</i>	<i>60</i>
<i>Figure I.21 Effect of fines content on the mechanical behavior of concrete in terms of compressive and flexural strengths (a) (Çelik and Marar, 1996) and (b) (Li et al., 2011).....</i>	<i>63</i>
<i>Figure I.22 Evolution of the compressive strength with time for different water to cement ratio and different fines content (C: W/C = 0.56; D: W/C= 0.45; E: W/C= 0.40; 1: 5% fines; 2: 9% fines; 3: 13% fines); samples were water cured at 20 ± 2 °C (Ding et al., 2016).....</i>	<i>64</i>
<i>Figure I.23 Effect of fines content on the 28-day compressive strength of concrete (Gokce et al., 2016)</i>	<i>64</i>
<i>Figure I.24 Theoretical repartition of stress (Pons, 1998 as cited by Pons and Torrenti, 2008).....</i>	<i>67</i>
<i>Figure I.25 The effect of the volume of coarse aggregates on the drying shrinkage of concrete (Eguchi and Teranishi, 2005).....</i>	<i>68</i>
<i>Figure I.26 The effect of the incorporation of crushed limestone sand on the drying shrinkage of concrete containing mountain sand (Aquino et al., 2010).....</i>	<i>68</i>
<i>Figure I.27 Model of the three different forms of water in concrete (Metha and Monteiro, 2006 cited by Chen et al., 2012).....</i>	<i>70</i>
<i>Figure I.28 Schematic representation of materials of similar porosity but (a) high permeability: interconnected capillary pores by large passages, and (b) low permeability: partly connected and segmented capillary pores (Neville and Brooks, 1987)</i>	<i>70</i>
<i>Figure I.29 Effect of hydrochloric acid environment on concrete with different types of fine aggregates (a) C0: 100% Siliceous sand, (b) C2: 50% Siliceous sand + 50% Limestone sand, and (c) C4: 100% Limestone sand (Bederina et al., 2013)</i>	<i>72</i>
<i>Figure I.30 SEM images of the interfaces of aggregates and cement paste in mortars made of (a) siliceous sand and (b) calcareous sand after 168 days of immersion in 1% sulfuric acid (Chang et al., 2005).....</i>	<i>72</i>
<i>Figure I.31 Effect of fines content on the chloride ion diffusion coefficient on (a) loose microstructure (W/C: 0.55; cement: 327.5 kg/m^3) and (b) dense microstructure (W/C: 0.32; cement : 530 kg/m^3) (Li et al., 2009).....</i>	<i>74</i>
<i>Figure I.32 Effect of water to cement ratio on the absorption and porosity of mortar (Bonavetti and Irassar, 1994).....</i>	<i>75</i>
<i>Figure I.33 The effect of aggregates inclusion in the perturbation of the cement arrangement. The aggregates could not cut through cement grains (A), they form a wall for the distribution of cement grains (B) (Scrivener et al., 2004)</i>	<i>76</i>
<i>Figure I.34 SEM image showing (A) the Portlandite and (B) the footprint of the calcite attack in the cement paste (Grandet and Ollivier, 1980)</i>	<i>78</i>
<i>Figure I.35 Illustration of the different cracks propagation modes in mortars subjected to compression with (a) siliceous sand after 5 years of hydration and (b) calcareous sand after 1 year of hydration (Bachiorrini and Murat, 1987)</i>	<i>78</i>
<i>Figure I.36 The behavior of smooth plastic wastes after loading (Saikia and De Brito, 2014)</i>	<i>80</i>

Chapter II: Aggregates Characterization and Fine Aggregates Preparation

Figure II.1 Simple observation of (a) natural sand, (b) crushed sand, (c) medium aggregate, and (d) coarse aggregate..... 86

Figure II.2 Optical microscope images for the natural sand (a) x25 and (b) x100, and for the crushed sand (c): x25 and (d): x100..... 87

Figure II.3 Samples preparation of the two types of sand for SEM analysis..... 88

Figure II.4 Fine aggregates grains viewed on SEM (x30): (a) natural sand and (b) crushed sand..... 88

Figure II.5 TGA graphs for (a) natural sand and (b) crushed aggregates..... 90

Figure II.6 DTG graphs for (a) natural sand and (b) crushed aggregates 91

Figure II.7 XRD patterns for fine aggregates (NS and CS) and coarse aggregates (MA and CA)..... 91

Figure II.8 XRD patterns for the four size fractions of crushed sand (CS-1, CS-2, CS-3, and CS-4) compared to that of CS 92

Figure II.9 Sampling methods for (a) fine and (b) coarse aggregates 92

Figure II.10 The particle size distribution of fine aggregates compared to ASTM C33 grading limits94

Figure II.11 The particles size distribution of medium aggregates compared to size no.8 aggregates limits..... 95

Figure II.12 The particles size distribution of coarse aggregates compared to size no.6 aggregates limits 96

Figure II.13 Relation between sand equivalent value and fines percentage for natural and crushed sand (data collected from ACTS laboratory) 98

Figure II.14 Organic impurities detection for fine aggregates: (a) natural sand and (b) crushed sand 99

Figure II.15 Moisture conditions of aggregates (Kosmatka and Wilson, 2011)..... 100

Figure II.16 Crushing process for the production of the "Conventional crushed sand" 103

Figure II.17 The particle size distribution of the fine aggregates' combination in the reference concrete compared to the ASTM C33 grading limits 104

Figure II.18 The particle size distribution of the "Fine crushed sand" compared to ASTM C33 grading limit..... 105

Figure II.19 Crushing process for the production of the "Fine crushed sand" 106

Figure II.20 The particle size distribution of the "Equivalent crushed sand" compared to ASTM C33 grading limits..... 107

Figure II.21 The particle size distribution of the "Modified crushed sand" compared to ASTM C33 grading limits..... 107

Chapter III: Concrete Mix Design and Experimental Procedure

Figure III.1 XRD analysis of the cement sample 113

Figure III.2 TGA-DTG analysis of the cement sample 113

Figure III.3 The particle size distribution of cement represented by the histogram and the cumulative values 114

List of Figures

<i>Figure III.4 The apparatus used for the flow time test</i>	115
<i>Figure III.5 The Vicat apparatus used to determine the consistency of mortar</i>	115
<i>Figure III.6 The particle size distribution of the fine aggregates incorporated in the normal strength concretes compared to the gradation limits of ASTM C33</i>	118
<i>Figure III.7 The particle size distribution of the fine aggregates incorporated in the high-strength concrete compared to the gradation limits of ASTM C33</i>	119
<i>Figure III.8 The particle size distribution of medium and coarse aggregates compared to the gradation limits of no. 6.7 aggregate</i>	120
<i>Figure III.9 Example of the determination of aggregates proportions by Dreux method (assessment of the normalized crushed sand effect) for (a) normal strength concretes and (b) high-strength concrete</i>	121
<i>Figure III.10 The particle size distribution of the fine aggregates incorporated in the performance-based approach study compared to the gradation limits of ASTM C33</i>	123
<i>Figure III.11 Example of the determination of aggregates proportions by Dreux method (assessment of the fine crushed sand effect)</i>	125
<i>Figure III.12 Illustrations of the tests conducted on the concrete mixes at fresh state: (a) Temperature; (b) Slump and slump retention; (c-d) Setting time; (e) Density; and (f): Air content</i>	129
<i>Figure III.13 Neoprene pad and compressive strength machine</i>	131
<i>Figure III.14 The compressometer used to measure the longitudinal displacement of a specimen under uniaxial compressive load, allowing the determination of the modulus of elasticity</i>	132
<i>Figure III.15 Schematic of the apparatus of the flexural strength test by third-point loading (ASTM C78, 2016)</i>	133
<i>Figure III.16 The length change readings to determine the total and autogenous shrinkages</i>	134
<i>Figure III.17 The test of the depth of water penetration under pressure: (a) the samples under pressure (b) the sample at the end of the test</i>	137
<i>Figure III.18 The steps followed in the resistance to chloride ions penetration test: (a) epoxy coating; (b) vacuum; and (c) charge measurement</i>	138
<i>Figure III.19 The apparatus of the resistivity test for concrete specimens</i>	139

Chapter IV: Experimental Study on Concrete Mixes Incorporating Normalized Crushed Sand

<i>Figure IV.1 Evolution of slump over time for (a) "Mix 30", (b) "Mix 35-I " (c) "Mix 35-II ", and (d) "Mix 50"</i>	149
<i>Figure IV.2 Initial and final setting times function of admixture content in the normal strength concrete mixes</i>	152
<i>Figure IV.3 Fresh density and air content function of admixture content in all concrete mixes</i>	153
<i>Figure IV.4 Evolution of the compressive strength over time for all the studied concretes</i>	155
<i>Figure IV.5 Evolutions of the ratio of the compressive strength at different ages to the 28-day compressive strength for (a) "Mix 30", (b) "Mix 35-I", (c) "Mix 35-II", and (d) "Mix 50"</i>	156
<i>Figure IV.6 Average flexural strength values of all concrete mixes</i>	161

List of Figures

<i>Figure IV.7 Evolution with the concrete age of the autogenous shrinkage for the three types of concrete of "Mix 30a" in sealed conditions without moisture exchange</i>	162
<i>Figure IV.8 Evolution with the concrete age of the accidental mass loss measured on sealed samples of the three types of concrete of "Mix 30a"</i>	163
<i>Figure IV.9 Evolution with concrete age of the total shrinkage of the three types of concrete of "Mix 30a", stored in a climatic chamber (23 ± 2 °C and $50 \pm 4\%$ RH)</i>	164
<i>Figure IV.10 Total shrinkage of the three types of concrete of "Mix 30a" as a function of the mass loss of the total shrinkage samples</i>	165
<i>Figure IV.11 Relation between the average water absorption by immersion and the air content of fresh concrete</i>	169
<i>Figure IV.12 Relation between the average water absorption and the average compressive strength at 90 days for normal strength concretes and 135 days for "Mix 50", completed by confidential data from ACTS</i>	169
<i>Figure IV.13 An example of the specimens used for the test of water depth under pressure for (a) an uncracked specimen and (b) a cracked specimen</i>	170
<i>Figure IV.14 Relation between the average water depth and the average compressive strength at 90 days for normal strength concretes and 135 days for "Mix 50", completed by confidential data from ACTS and (Al-Amoudi et al., 2009)</i>	171
<i>Figure IV.15 Relation between the average passed charge and the average compressive strength at 90 days for normal strength concretes and 135 days for "Mix 50", completed by confidential data from ACTS and (Al-Amoudi et al., 2009; Kou and Poon, 2009)</i>	174
<i>Figure IV.16 Relation between the average resistivity and the average compressive strength at 90 days for normal strength concretes and 135 days for "Mix 50", completed by data from (Chen et al., 2014) and (AFGC, 2004) guide</i>	176
<i>Figure IV.17 Durability properties for (a) "Mix 30", (b) "Mix 35-I", (c) "Mix 35-II", and (d) "Mix 50"</i>	177
<i>Figure IV.18 SEI images (x800) for (a) CM, (b) EM, and (c) MM of "Mix 30a"</i>	180
<i>Figure IV.19 Graph of the elemental distribution (a) between two natural siliceous sand grains in CM and (b) two crushed limestone sand grains in MM</i>	181
<i>Figure IV.20 Interfacial transition zone between the sandstone and cement paste as observed by SEM (a) in our study and (b) by (Shen et al., 2017)</i>	182
 Chapter V: Performance-Based Approach Study on Concrete Mixes Incorporating Crushed Sand with High Percentage of Fines	
<i>Figure V.1 Slump evolution over time for (a) "Mix 30" and (b) "Mix 50"</i>	193
<i>Figure V.2 Evolution of (a) the compressive strength and (b) the compressive ratio versus time for all the studied concretes</i>	197
<i>Figure V.3 Relation between the average depth of water and the average compressive strength at 90 days for "Mix 30" and 135 days for "Mix 50", completed by data from (Gokce et al., 2016)</i>	203
<i>Figure V.4 Durability properties for the different types of concrete of (a) "Mix 30" and (b) "Mix 50"</i>	206

List of Figures

<i>Figure V.5 SEI images (x200) at ITZ of (a) natural sand grains CM-30a, (b) crushed sand grain FM-30b, and (c) crushed sand grain MM-30a</i>	<i>208</i>
<i>Figure V.6 The distribution map of calcium at the interface between the cement paste and the crushed sand grains of (a) FM-30b (x200) and (b) MM-30a (x500).....</i>	<i>209</i>

List of Tables

Chapter I: Literature Review

<i>Table I.1 Summary of the alternatives to natural siliceous sand and their effects on concrete.....</i>	<i>45</i>
<i>Table I.2 Shape classification of aggregates (BS 812-1, 1975).....</i>	<i>49</i>
<i>Table I.3 Effects of fine aggregates' characteristics on the fresh properties of concrete.....</i>	<i>59</i>
<i>Table I.4 Effects of fine aggregates characteristics on the mechanical behavior of concrete.....</i>	<i>65</i>
<i>Table I.5 Effects of fine aggregates characteristics on the durability properties of concrete.....</i>	<i>75</i>
<i>Table I.6 Effects of fine aggregates characteristics on the concrete microstructure</i>	<i>81</i>

Chapter II: Aggregates Characterization and Fine Aggregates Preparation

<i>Table II.1 Chemical characteristics of aggregates.....</i>	<i>89</i>
<i>Table II.2 Chemical characteristics of the different size fractions of crushed sand.....</i>	<i>90</i>
<i>Table II.3 The average values (and standard deviation values) of the percentage of materials finer than 75 μm sieve in aggregates.....</i>	<i>93</i>
<i>Table II.4 The average values (and standard deviation values) of the cumulative passing percentage of natural sand and crushed sand over a series of sieves</i>	<i>94</i>
<i>Table II.5 The average values (and standard deviation values) of the cumulative passing percentage of medium and coarse aggregates over a series of sieves.....</i>	<i>95</i>
<i>Table II.6 The average values (and standard deviation values) of deleterious particles content in aggregates.....</i>	<i>96</i>
<i>Table II.7 The average values (and standard deviation values) of the specific gravities and absorption of fine and coarse aggregates</i>	<i>101</i>
<i>Table II.8 The average values (and standard deviation values) of the mass loss percentage after immersion cycles in sodium sulfate solution and after Los Angeles machine test for aggregates of Series A.....</i>	<i>102</i>

Chapter III: Concrete Mix Design and Experimental Procedure

<i>Table III.1 Chemical composition of cement</i>	<i>112</i>
<i>Table III.2 Mineralogical composition of the clinker calculated by modified Bogue method.....</i>	<i>112</i>
<i>Table III.3 The characteristics of the particle size distribution of cement, in μm</i>	<i>114</i>
<i>Table III.4 Setting times of cement paste</i>	<i>116</i>
<i>Table III.5 The average values (and the standard deviation values) of the flexural and compressive strengths of the normalized mortars, in MPa</i>	<i>117</i>
<i>Table III.6 Characteristics of the water used in concrete mixes.....</i>	<i>117</i>
<i>Table III.7 Nomenclature of the different types of concrete according to the type of the fine aggregates (assessment of the normalized crushed sand effect on normal strength concretes).....</i>	<i>119</i>

List of Tables

<i>Table III.8 Nomenclature of the different types of concrete according to the type of the fine aggregates (assessment of the normalized crushed sand effect on the high-strength concrete)</i>	<i>120</i>
<i>Table III.9 Mix design proportions of concretes (assessment of the normalized crushed sand effect) (kg/m³).....</i>	<i>122</i>
<i>Table III.10 Mix design proportions of "Mix 30-a" (kg/m³)</i>	<i>123</i>
<i>Table III.11 Nomenclature of the different types of concrete according to the type of the fine aggregates (assessment of the fine crushed sand effect)</i>	<i>124</i>
<i>Table III.12 Mix design proportions of concrete mixes incorporating crushed sand with high fines percentage (kg/m³).....</i>	<i>124</i>
<i>Table III.13 Concrete mixes nomenclature according to the cement content, the water to cement ratio, and the aggregates series.....</i>	<i>126</i>
<i>Table III.14 The experimental program for measurements of fresh properties.....</i>	<i>127</i>
<i>Table III.15 The experimental program for mechanical characterization</i>	<i>130</i>
<i>Table III.16 The experimental program for durability properties.....</i>	<i>135</i>
<i>Table III.17 The experimental program for the microstructural analysis</i>	<i>140</i>
<i>Table III.18 Summary of the conducted tests on concrete</i>	<i>141</i>

Chapter IV: Experimental Study on Concrete Mixes Incorporating Normalized Crushed Sand

<i>Table IV.1 Fresh concrete temperature and admixture content of all concrete mixes</i>	<i>145</i>
<i>Table IV.2 Fresh state properties of all concrete mixes</i>	<i>146</i>
<i>Table IV.3 Average values (and standard deviations) of the compressive strength of all concrete mixes at different ages, in MPa.....</i>	<i>154</i>
<i>Table IV.4 Average experimental values (and standard deviations) of modulus of elasticity "Mix 30a" at 28 days and calculated values according to ACI 318 and Eurocode 2</i>	<i>159</i>
<i>Table IV.5 Average values (and standard deviations) of 28-day flexural strength of all the studied concretes</i>	<i>160</i>
<i>Table IV.6 Average values (and standard deviations) of the compressive strength of the three types of concrete of "Mix 30a"</i>	<i>164</i>
<i>Table IV.7 Average values (and standard deviations) of the durability properties at 90 days for normal strength concretes and at 135 days for "Mix 50".....</i>	<i>167</i>
<i>Table IV.8 Correlation between chloride ions penetrability and the passing charge (ASTM C1202, 2017).....</i>	<i>172</i>
<i>Table IV.9 Correlation between concrete resistivity and chloride ions penetration (Shane et al., 1999)</i>	<i>175</i>
<i>Table IV.10 Environmental and economic advantages and disadvantages of the normalized crushed sand as the only fine aggregate in concrete mixes.....</i>	<i>186</i>

Chapter V: Performance-Based Approach Study on Concrete Mixes Incorporating Crushed Sand with High Percentage of Fines

Table V.1 Fresh concrete temperature and admixture content of all concrete mixes 190

Table V.2 Fresh state properties of all concrete mixes..... 190

Table V.3 Average values (and standard deviations) of the compressive strength of all concrete mixes at different ages, in MPa..... 196

Table V.4 Average values (and standard deviations) of the 28-day flexural strength of all concrete mixes, in MPa..... 199

Table V.5 Average values (and standard deviations) of durability properties of all the studied concretes at 90 days for "Mix 30" and at 135 days for "Mix 50" 200

Table V.6 Correlation between chloride ions penetrability and the passing charge (ASTM C1202, 2017) 204

Table V.7 Correlation between concrete resistivity and chloride ions penetration (Shane et al., 1999 cited by the manual of the resistivity measuring machine Giatec-RCON) 205



General Introduction



General Introduction

Nowadays, the Lebanese construction field suffers from the scarcity of natural siliceous sand. The good quality is almost depleted and its mining is prohibited due to the negative environmental impacts, resulting from its extraction. Consequently, the natural sand is provided from the black market or imported from other countries and sold at high prices, affecting thereby the cost of concrete. In addition to these problems, the natural siliceous sand could not be used as the only fine aggregate in concrete since it is characterized by a particle size distribution finer than the limits imposed by ASTM C33, the standard applied in Lebanon. Therefore, currently, this sand is mixed with a convenient percentage of crushed limestone sand to conform to the standard limits.

Due to the worldwide expansion of concrete construction and since natural sand is the major fine aggregate used in concrete, the problems related to the overexploitation of this resource are not limited to Lebanon. Its quantity and quality have deteriorated internationally and its mining harmfully affects the environment. Therefore, the United Nations Environment Program UNEP encourages the governments to restrict the excavation of the natural sand and increase the taxes on its mining (*UNEP, 2014*). Consequently, it becomes challenging to supply good quality natural sand at a low cost.

To cope with these problems, many countries have found alternatives to natural sand in concrete. Thus, several studies assess the partial or total replacement of the natural sand by different types of manufactured sand, resulting from rock crushing, recycled concretes, domestic wastes, and industrial by-products.

The crushed limestone sand is one of the internationally recommended alternatives to natural sand in concrete. It could present several advantages on the concrete strengths and durability due to its mineralogy, morphology, and fines content. Currently, in the Lebanese context, the crushed limestone sand seems to be the most feasible, among the other alternatives, since there are no other solutions from the solid wastes in the short-term and since the crushed limestone quarries are spread all over the country. However, despite the abundance of the crushed limestone sand in Lebanon, and although its sole use in concrete could provide several environmental and economic benefits, this solution is not yet applied in the country, mainly due to the lack of a scientific reference in the Lebanese frame that could convince of its relevance all the concerned parties in the construction field.

For this reason, Advanced Construction and Technology Services (ACTS), a leading third-party engineering firm in the region, has funded this study, aiming to provide a scientific background for the use of crushed sand concretes without natural sand. Within the scope of a joint research program between Lebanon and France, this study is the first academic and industrial cooperation in Lebanon to answer the following questions:

- Could the use of natural siliceous sand in concrete be eliminated?
- Could the crushed limestone sand totally replace the natural siliceous sand, instead of being used as an additional fine aggregate in concrete?
- Could the concrete performance be maintained by this replacement?
- What could be the effect of this substitution on the fresh properties, mechanical behavior, and long-term performance of concrete?
- What could be the effect on the concrete microstructure at the interface between the cement paste and the sand grains?

General Introduction

The study leads to a better understanding of the positive effects resulting from the optimization of crushed sand production and the valorization of its high fines content. It encourages the use of good quality crushed limestone sand as the only fine aggregate in concrete, in order to remove the dependency of the construction field on the natural sand quality and availability in the Lebanese market.

By verifying the performance of crushed sand concretes that do not contain natural sand and by comparing it with the conventional concrete, the study presents the effect of the fine aggregates' morphology, mineralogy, particle size distribution, and fines content on the fresh properties and mechanical strengths of normal and high-strength concretes, commonly used in the Lebanese market. Additionally, the study evaluates the effects of the fine aggregates' characteristics on the shrinkage, durability, and microstructure of concrete, which have not been widely covered in previous studies.

During this study, two different approaches are followed. To comply with the specifications of the ASTM standard, in terms of the particle size distribution and fines content, the first approach consists of evaluating the performance of concrete incorporating normalized crushed sand with a particle size distribution within the limits and fines content lower than 7% (the maximum percentage of fines allowed in ASTM C33). Second, to valorize the high percentage of fines generated during the crushed sand production, a performance-based approach is applied to assess the behavior of concrete containing fine crushed limestone sand with high fines content (13-18%) exceeding the limit imposed by the standard (7%).

The main part of the experimental work conducted during this study is performed in the laboratories of ACTS, including the physical characterization of aggregates, the construction of normalized crushed sand, the concrete mixing, the preparation of concrete samples, and the majority of concrete tests. Some of the tests, such as the morphological, chemical, and mineralogical characterizations of aggregates, porosity accessible to water in concrete, and the microstructural analysis, are conducted in the Laboratoire Matériaux et Durabilité des Constructions LMDC in France since they require specific equipment available in this laboratory.

The thesis is divided into five chapters as follows:

The first chapter details the problems of the natural sand on the international and national levels and introduces some alternatives used worldwide for the natural sand. It also includes a literature review on the effects of the fine aggregates' characteristics on the concrete performance at macro and micro scales.

The morphological, chemical, mineralogical, and physical characteristics of the aggregates used in the study are presented in the second chapter. The developed experimental program on aggregates is conducted to serve two main objectives: first, to verify that the aggregates used conform to the ASTM C33 specifications, before being used in concrete mixes; second, to determine the differences between the natural sand and the crushed sand in order to be able to explain the variations between concretes and to deduce the effect of the fine aggregates' characteristics on concrete behavior.

These effects are assessed for four formulations of normal and high strength concretes, commonly used in Lebanon. For each formulation, the differences between the concrete mixes are limited to the fine aggregates' types and to the admixture content to obtain a workable concrete. The materials proportions of the seventeen different types of studied concrete are displayed in the third chapter. This chapter also presents the experimental program conducted on the different concrete mixes to evaluate their fresh properties, mechanical behavior, and durability. The tests performed in this study are the most commonly required in the Lebanese market, generally carried out following the ASTM standard. The macrostructural assessment is followed by a microstructural analysis to detect the differences in

General Introduction

concretes at the interface between the cement paste and the sand grains, to be able to explain the variations that could occur between the performances of the different types of concrete.

Since the crushed limestone sand, provided currently from the limestone quarries, presents a particle size distribution coarser than the one imposed by ASTM C33, the study consists of constructing, in the laboratory, a normalized crushed sand with a particle size distribution that conforms to the standard requirements. In the fourth chapter, the fresh, mechanical, and durability performances of two types of crushed sand concrete, containing this normalized crushed sand with two different gradations, are compared to those of the reference concrete incorporating the conventional combination of natural sand and crushed sand.

To reduce the coarseness of the crushed limestone sand, some quarries tried to improve the crushing process. They recently produce crushed limestone sand with a high percentage of fines (13-18%) exceeding the maximum limit imposed by the ASTM C33 (7%). Knowing that the reduction of fines could impose some industrial and economic limitations, a performance-based approach is followed to valorize the high percentage of fines and to evaluate the effect of this crushed limestone sand on the concrete performance, in the last chapter of the study. This chapter consists of comparing the properties of the concrete incorporating the fine crushed sand as the only fine aggregate with the reference concrete and the normalized crushed sand concrete, at fresh and hardened states.

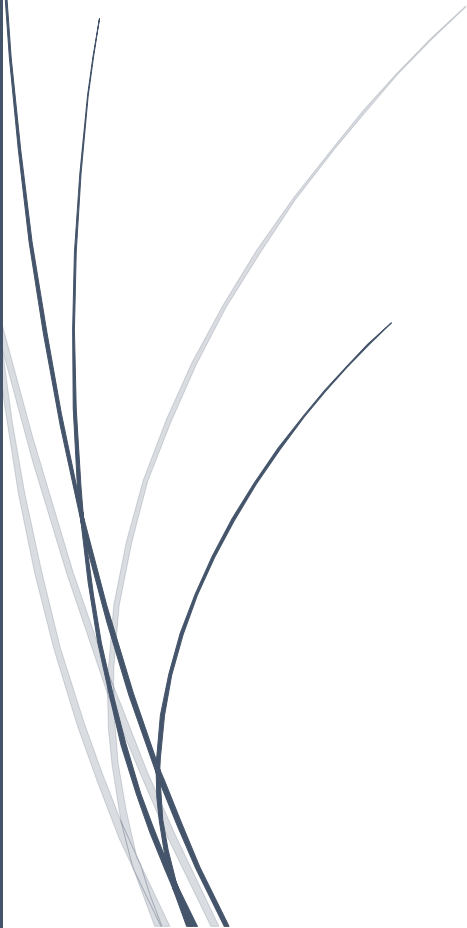
Furthermore, since this study aims to introduce a practical and effective solution that could be applied in the industry, it is essential to assess the feasibility of the total replacement of the natural sand by crushed sand on technical, environmental, and economic terms. This evaluation is conducted for the normalized crushed sand and the fine crushed sand and is presented in the fourth and fifth chapters respectively.

The obtained results are summarized in the conclusion and some recommendations are presented for the concerned parties in the Lebanese market.



Chapter I

Literature Review



I. Literature Review

Introduction

In Lebanon, the natural siliceous sand of good quality becomes more and more scarce and its extraction imposes serious environmental impacts. Thus, natural sand mining is now subjected to governmental restrictions and the sand production from quarries is ceased all over the country. These problems led to the importation of sand at high prices and the increase of the reliance on the black market, increasing thereby the cost of natural sand and consequently the cost of concrete. In addition to its scarcity and its environmental threats, the natural siliceous sand is characterized by a fine particle size distribution that does not conform to the grading limit of ASTM C33 (*ASTM C33, 2016*), the applied standard in Lebanon. Therefore, to be used in concrete, this sand should be combined with a coarser sand (*Kabbani, 1967*). Hence, the crushed limestone sand is always used in an adequate proportion, to compensate for the fineness of the natural sand.

In 2015, according to the research department of BLOMINVEST Bank (*BLOMINVEST Bank, 2016*), cement production in Lebanon was estimated at around 5.58 million tons. Since the cement production is an indication of concrete production, it is estimated that the concrete production in 2015 needed approximately 12.75 million tons of sand (natural and crushed sand). The amount of available natural siliceous sand could no longer respond to this need, even when it is combined with crushed limestone sand. Since the crushed limestone sand is abundantly available at an acceptable price, thus it could eliminate the dependency of the construction field on the quality and availability of the natural sand in the Lebanese market. The crushed limestone sand tends to be an effective alternative to natural siliceous sand in concrete, it could be used as the only fine aggregate instead of using it as an additional fine aggregate resource.

The problems of the natural sand are not limited to Lebanon, the scarcity and the negative impact of sand mining on the environment are an international concern, leading the United Nations Environment Program UNEP to address an alarming message to the governments declaring that the sand is rarer than one thinks (*UNEP, 2014*). Due to the worldwide expansion of the construction works, the natural sand resource is extracted at a rate that greatly exceeds its renewal. According to (*UNEP, 2014*), in 2012 the world consumed 25.9 to 29.6 billion tons of aggregates, representing enough concrete to build a 27x27 m wall around the equator. Hence, many countries have found solutions consisting of partially or totally replacing the natural sand with different types of manufactured sand such as crushed rocks, recycled concrete and domestic wastes, and industrial by-products.

The first part of this chapter consists of introducing an overview of the production of fine aggregates and the problems of the natural sand in Lebanon. Afterward, the main negative impacts of the different types of natural sand mining and some of the international alternatives are presented in the second and third parts of this literature review. The last part details the effects of the fine aggregates' characteristics on different stages of the concrete age and at different scales: the fresh state, mechanical behavior, durability properties, and microstructural characteristics.

1. Overview of the aggregates production in Lebanon

The aggregates are usually used in concrete as an economic skeleton for the cement paste (Kabbani, 1967). They occupy about 60 to 75% of concrete volume (Neville and Brooks, 1990; Kosmatka and Wilson, 2011). They strongly contribute to the concrete strengths and stiffness due to their generally high values of mechanical resistances and modulus of elasticity.

The aggregates are mainly divided into two major categories: coarse and fine aggregates. As defined by (ASTM C125, 2016), the coarse aggregates are formed of particles that are predominantly retained on the 4.75 mm sieve. The fine aggregates entirely pass the 9.5 mm sieve, almost entirely pass the 4.75 mm sieve, and are predominantly retained on the 0.075 mm sieve.

In Lebanon, the coarse aggregates are used in concrete production in two different sizes: the medium aggregate with a nominal diameter of 10-12 mm and the coarse aggregate with a nominal diameter of 20 mm. They are provided from limestone quarries distributed in most of the Lebanese districts (Ministry of Environment, 2006) since the majority of the Lebanese rocks are sedimentary and specifically of limestone nature (Walley, 1997).

As for the fine aggregates, the natural siliceous sand was the only type used historically for concrete production in Lebanon. This sand is a granular material resulting from the fragmentation of friable sandstone or natural disintegration and abrasion of rocks (ASTM C125, 2016). The Lebanese natural sand originates from rivers, alluvial fans, seashores, and disintegrated sandstones. The last two, mined from sea coasts and land pits, are the most predominant (Kabbani, 1967; Hamad et al., 1996). They are simply excavated and extracted by machines such as bulldozers and rippers (Khawlie and Hinai, 1980). The coastal natural sand in Lebanon originates from Egypt, where the water currents carried the quartz grains from the Nile and the Red Sea to the Lebanese shores millions of years ago (*L'Orient Le Jour*, 2016), and it is usually washed before being used in concrete. The sandstone is distributed in mountain areas, usually covered with vegetation and particularly pine trees forests, and it is used as it is found in nature. It is mainly formed of quartz grains coated with some traces of a variety of heavy minerals, i.e. calcite, iron oxide (hematite and limonite), or clay minerals (Hamad et al., 1996), giving the white sand grains different shades of yellow, brown, red, and violet.

For concrete construction, (Kabbani, 1967) proved that if the ASTM recommendations were to be strictly applied, the majority of these natural siliceous sand resources should not be used alone. They are generally characterized by poor gradation and excessive fineness. Therefore, the natural sand is nowadays mixed with crushed sand with adequate proportions, depending on the characteristics of each one of these two types of sand. The crushed sand is characterized by a coarser gradation which improves the overall fine aggregates gradation and fineness modulus (Kabbani, 1967). It results from breaking natural stones into smaller fragments by the use of mechanical devices (ASTM C125, 2016). It is first excavated by blasting vertical sheer-faced limestone quarries (Khawlie and Hinai, 1980), followed by a crushing and sieving process to collect particles that give an ideal gradation when mixed with the fine natural sand. The crushed sand is abundant in Lebanon, it is regularly produced in the rock quarries distributed all over the country (Figure I.1). Due to the crushing process, the crushed sand is usually formed of angular grains with rough surface. It is mainly composed of calcium carbonate (CaCO_3) in the form of calcite.



Figure I.1 Distribution of the quarries, presented by the yellow points, all over Lebanon (Ministry of Environment, 2006)

In addition to the gradation problems that could affect the concrete performance, the availability of good quality natural sand resources becomes scarce. Furthermore, the excessive exploitation of this sand increases the negative impacts on the environment. The coastal sand mining shrinks the beaches, threatens the shores, and disturbs the beach ecosystem (*The Daily Star, 2013; L'Orient Le Jour, 2016*), while the creation of land sand quarries destroys the pine trees forests, increases the deforestation risk, and affects the panorama (*Weltzien, 2006*). Accordingly, beach sand mining was long ago prohibited. As for land mining, the government decided, in 2003, to stop the operations of all sand quarries throughout the country (*Yager, 2004*). In order to respond to the market's need, many contractors import sand from other countries (*Yager, 2004*) or rely on the local black market. However, despite these restrictions, the beach sand is until today subjected sometimes to illegal mining in several areas along the coast, such as Tyre and Ramleh El Bayda (*The Daily Star, 2013; L'Orient Le Jour, 2016*), and some of the sand quarries are still operating illegally (*LBCI News, 2019*), as could be seen in Figure I.2.



Figure I.2 Environmental impacts of sand mining on (a) Ramleh El Bayda beach, Beirut (*L'Orient Le Jour, 2016*) and (b) the pine forests in Jezzine district

Consequently, due to the depletion of the good quality natural sand resources, the environmental impacts of its extraction, and the restrictions imposed on its mining, the price of the natural sand remarkably increases. Hence, the concrete prices are also affected.

All these problems, related to the natural sand production in Lebanon, prove the necessity of avoiding its use in construction. It becomes primordial to find an alternative that can totally replace the natural sand in concrete without affecting its performance. The crushed limestone sand could be this alternative, due to its wide availability in the Lebanese market at acceptable prices. Hence, the current study consists of assessing the effectiveness of this solution in the Lebanese context.

2. International problems of the natural sand used in construction

Because of the worldwide expansion of urban and infrastructure constructions, concrete production increases widely. Concrete becomes the most used building material with a production that exceeds the production of all the other materials combined (*Kosmatka and Wilson, 2011*). Consequently, the demand for aggregates rises remarkably, they are being extensively extracted at a rate that greatly exceeds their renewal (*UNEP, 2014*). Consequently, the demand for natural sand expands to meet this rapid growth of construction, since it is the major fine aggregate used in concrete.

Due to its extensive exploitation, there is a worldwide shortage of natural sand, and its good quality becomes more and more scarce. It risks disappearing and its consistent supply is not guaranteed anymore. Additionally, its extraction leaves harmful impacts on the environment. Consequently, the United Nations Environment Program UNEP urges the governments to set legislations to restrict the excavation and to intensify the taxes on natural sand mining (*UNEP, 2014*). Thus, the provision of this sand at an affordable cost becomes more and more challenging for the construction field despite the diversity of the natural sand types and origins.

The following sections detail the problems associated with each one of these natural sand types, including the river sand, sea sand, land pits sand, and dune sand.

2.1 River sand

River sand is the result of alluvial sedimentation of weathered rocks over the years and it is found on the river stream bank. Due to this natural process and the erosion caused by water, its particles are usually rounded, smooth, and well-graded (*Kabbani, 1967*). This sand is mainly formed of silica.

River sand mining imposes harmful consequences on the environment. The mining process reduces the groundwater level and increases the salinity intrusion into the river water (*Dolage et al., 2013; Patra and Mukharjee, 2017*). Besides, the river beds are eroded and the fauna and flora of the surrounding area are disturbed (*Patra and Mukharjee, 2017*). Due to the excessive exploitation of the river sand, several countries, such as Tunisia, Sri Lanka, and India, imposed restrictions on the extraction of this sand (*Akrouf et al., 2010; Dolage et al., 2013; Yajurved et al., 2015*). This fact had created problems in material supply, increasing thereby the conflicts in the market and the development of "Sand Mafias", criminal organizations that could kill to mine and sell illegal sand (*Environmental Justice Organization, 2014; New Yorker Magazine, 2017*). Therefore, the river sand price increases, creating instability in the construction sector.

In addition to its environmental problems, the river sand may contain a high amount of inorganic materials, impurities, deleterious particles (silt and clay), and chemical elements (chlorides and sulfates). Thus, it could be harmful to concrete and for the reinforced steel rebars, threatening thereby the durability of the structures.

Furthermore, (*Sadeghi and Harchegani, 2012*) confirmed that the sand mining activities do not only change the fluvial behavior of rivers but also produce considerable variations on the natural elements in the suspended sediments. They could alter the content of the deleterious particles in river sand.

2.2 Sea sand

The sea sand could be dredged from the sea and mined from the seashores. Usually, it is a fine poorly graded sand (*Kabbani, 1967*), mainly formed of quartz grains.

Marine sand mining causes a disturbance in the beach ecosystem by affecting the water currents and the sea bed biodiversity, as illustrated in Figure I.3. Also, the sand mining from beaches ruins the beach aesthetics and threatens the coastal infrastructures, due to the erosion of shorelines and the narrowing of the beach. It eliminates the shield protection from storms and tsunamis and it leads sometimes to a change in the international borders and the erosion and disappearance of islands. In Indonesia for example, at least 24 small islands have been eroded and entirely disappeared since 2005 (*Environmental Justice Organization, 2014*).

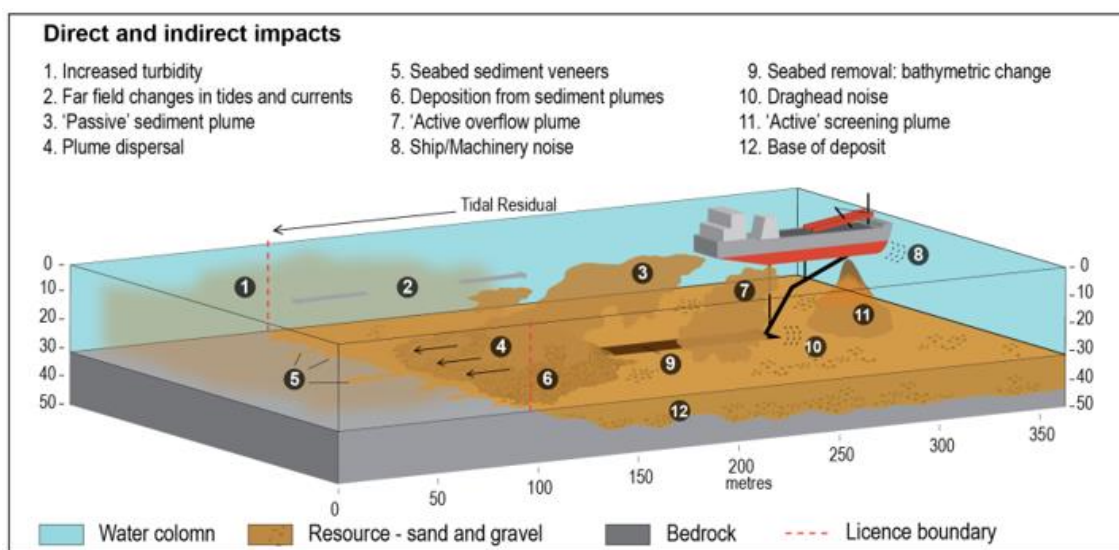


Figure I.3 Direct and indirect impacts of the sand dredging on the marine environment
(*Tillin et al., 2011 cited by UNEP, 2014*)

Furthermore, this sand has not widely gained confidence in concrete production. It may contain potentially harmful substances, such as seashells, chloride ions, organic matter, heavy metals, and other deleterious materials. These substances could affect the fresh, hardened, and durability properties of reinforced concrete structures and corrode the reinforced steel rebars. The world has known many structural failures due to the use of such sand as fine aggregate in concrete. Examples of these disasters are the collapse of structures that have occurred in Taiwan, South Korea, Turkey, and China (*Xiao et al., 2017; Liu et al., 2018*).

If it is intended to be used in concrete, the sea sand should be subjected to special treatments, such as washing, desalting, stabilization, and organic thermal elimination of heavy metals, or mixed with other

types of sand (Limeira et al., 2011; Xiao et al., 2017; Liu et al., 2018). On one hand, these techniques can decrease the concrete's permeability and avoid the steel rebars corrosion in the reinforced concrete structures. On the other hand, they increase construction costs.

2.3 Land pits sand

The land pits sand consists mainly of disintegrated sandstones mined from pits in the inland areas (Kabbani, 1967). They are mainly characterized by quartz mineralogy.

Internationally, the inland resources are almost depleted (Environmental Justice Organization, 2014; UNEP, 2014) and the creation of new quarries becomes more complicated (New Yorker Magazine, 2017). The inappropriate mining and quarrying of land sand deposits lead to significant environmental and socio-economic problems in the surrounding neighborhood. The excavation of sand from lands destroys the landscape and the natural coverage (Dos Anjos et al., 2017), and it threatens the stability of soils, infrastructures, and adjacent structures. The surrounding areas are also affected by the dust, the noise, and the reduction of the value and cost of the estates (El-Fadel et al., 2001; Ministry of Environment, 2006).

2.4 Dune sand

Dune sand is a fine aggregate resulting from the wind deposits and it is characterized by a low fineness modulus and high content of quartz particles (Kabbani, 1967).

Even though the use of this sand does not present remarkable impacts on the environment, its incorporation in concrete is restricted. The high fineness, surface area, and intergranular porosity of this sand could reduce the workability and strength of concrete (Zeghichi et al., 2012; Lee et al., 2016). For this reason, many countries were obliged to import sand for their huge construction projects, despite the large desert areas in their territory. Dubai, for example, imported sand from Australia for the concrete construction of its artificial islands and the tallest building in the world (Environmental Justice Organization, 2014; New Yorker Magazine, 2017).

3. Review on the worldwide alternatives to natural sand

To cope with the natural sand environmental problems and to reduce the construction cost imposed by its scarcity, it became primordial to many countries to find available and economical alternatives to natural sand in concrete.

To be adequately used in construction, these alternatives should not negatively affect concrete performance when they partially or totally replace the natural sand. Accordingly, many researchers assessed the behavior of concrete incorporating the most common alternatives, i.e., crushed rocks, recycled construction and domestic wastes, and industrial by-products.

3.1 Crushed rocks

During the crushing process of coarse aggregates, the particles passing the 4.75 mm sieve could not be sold as coarse aggregates. Thus, adequate processing in crushing, sieving, and grading optimization could generate a good quality of the materials passing the 4.75 mm sieve, which could be used as crushed sand in concrete. The use of this sand could eliminate the negative impacts of materials disposal and limit the exploitation of natural sand resources. Moreover, the cost of fine aggregates, in some cases, could be reduced since the crushed sand becomes more abundant in some countries.

Among the crushed sand studied in the literature, the effects of the crushed limestone, marble, and granite, are detailed in the following sections.

3.1.1 Crushed limestone

The limestone is a friable sedimentary rock mainly composed of calcium carbonate CaCO_3 in the form of calcite. It could also contain different amounts of other minerals such as silica, clay, silt, iron oxide, magnesium carbonate, and organic materials.

The main disadvantage related to the use of crushed limestone sand as fine aggregate in mortar and concrete is its negative effect on workability. The crushed limestone sand is usually characterized by high porosity and water absorption. Accordingly, many studies have shown that the crushed limestone sand increases the water demand of mixes and decreases the workability of mortar and concrete (*Donza et al. 2002, Akrouf et al., 2010; Bederina et al., 2013; Stefanidou, 2016*). Therefore, for a fixed slump and similar water to cement ratio, a higher percentage of superplasticizer is usually needed to obtain good workability without compromising the mechanical properties of concrete.

In terms of mechanical performance, overall, the studies conducted on the use of the crushed limestone sand in mortar and concrete have shown that crushed limestone as a fine aggregate presents several advantages over the natural siliceous sand. The angular shape and rough surface of its grains improve the bond with the cement paste (*Javelas et al., 1975; Grandet and Ollivier, 1980; Stefanidou, 2016*). Moreover, due to its calcite nature, the limestone crushed sand could react with the cement paste and the products of the hydration reaction to form the calcium hydro-carbo-aluminate (*Farran, 1956; Grandet and Ollivier, 1980; Ollivier et al., 1995*). The formation of this product reduces the porosity at the interfacial transition zone (ITZ) between the cement paste and the sand grains and densifies the concrete microstructure in this zone (*Javelas et al., 1975; Ollivier et al., 1995*). Thus, the crushed sand concrete could give higher compressive and flexural strengths than those of the conventional concretes composed of natural siliceous sand (*Bederina et al., 2013; Bentz et al., 2015*).

Due to the crushing process, the crushed limestone sand could have a high percentage of fines that exceeds the maximum allowable limits specified in the different standards. However, the microstructural analysis of these fines proves that they are generally not deleterious and they have the same composition as the original parent rock (*Makhloufi et al., 2014*). These fines could be advantageous for concrete. At an early age, they could act as a nucleation site and accelerate the hydration reaction of the cement paste (*Bonavetti and Irassar, 1994; Bentz et al., 2015; Benyamina et al., 2019*).

3.1.2 Crushed marble

The marble is a metamorphic rock formed when the limestone is exposed to pressure and high temperature. Thus, it has similar mineralogy as the limestone sedimentary rock and it is mainly composed of calcite, but with lower porosity.

To have comparable workability, the water to cement ratio tends to be increased with the replacement level of the natural river siliceous sand by crushed marble sand having a comparable particle size distribution (*Gameiro et al., 2014; Binici and Aksogan, 2018*).

On the other hand, the compressive strength is enhanced by 65%, 47%, and 34% at 7, 28, and 90 days respectively when the replacement level increases to 100% (*Binici and Aksogan, 2018*).

In terms of durability, the crushed marble concretes, without natural sand, exhibit 44% lower abrasion ratio, higher sulfate and freeze-thaw resistances (25% and 34% higher compressive strengths after the sulfate immersion and the freeze-thaw cycles respectively), and five times lower capillary permeability coefficient than the natural sand concrete at 90 days (*Binici and Aksogan, 2018*). In the study of (*Gameiro et al., 2014*), the durability properties (the water capillary permeability, the water absorption by immersion, the chloride migration, and the carbonation depth) remain in the same range when the crushed marble totally replaces the natural river sand. Nevertheless, the concrete durability seems not affected by 20% replacement, but above this level, the values of the durability properties begin to increase, indicating lower durability.

3.1.3 Crushed granite

The finely crushed granite is generated during the crushing of granite rocks in quarries. It is mainly formed of quartz, feldspar, and micas.

Many studies have assessed the effect of substitution of the river siliceous sand by the crushed granite sand, by comparing two types of concrete mainly differing by the proportions of the two types of sand. In the study of (*Cordeiro et al., 2016; Mundra et al., 2016; Shen et al., 2017*), the slump value is fixed and the admixture content varies to reach a similar slump, while the slump changes in the study of (*Kou and Poon, 2009*).

In these studies, the workability of concrete has been negatively affected by the incorporation of crushed granite due to the angular shape of the crushed sand grains. For the same water to cement ratio, the slump of concrete decreases progressively with the increase of the substitution rate of natural river sand by crushed granite sand (*Kou and Poon, 2009*): it varies from 65 to 30 mm when the replacement rate varies from 0 to 100%. Likewise, to reach a similar slump, the admixture demand increases by 40% with the replacement level of natural siliceous river sand by crushed granite sand up to 50% (*Cordeiro et al., 2016*). It increases by 14% when the crushed granite totally replaces the river sand in the study of (*Shen et al., 2017*), while the dosage of admixture remains comparable between both types of concrete in the experiments conducted by (*Mundra et al., 2016*).

For a replacement level up to 50%, the 28-day compressive strengths remain in the same range of strength with a slightly better behavior compared to the reference concrete (maximum increase of 9%) (*Kou and Poon, 2009; Cordeiro et al., 2016; Mundra et al., 2016*). Above this level, the compressive strength decreases gradually with the increase of the crushed granite sand (*Kou and Poon 2009; Mundra et al., 2016*). When the crushed granite sand fully replaces the river siliceous sand, the concrete compressive strength remarkably decreases by 20-25% in the study of (*Mundra et al., 2016*), whereas it remains in the same range of strength in the study of (*Kou and Poon, 2009; Shen et al., 2017*) with a maximum decrease of 7%. The negative effect of this substitution on the compressive strength is attributed to the high fines percentage of the crushed granite sand assessed by (*Mundra et al., 2016*), whereas the particle size distribution of the crushed granite in the other studies is comparable to the one of the river sand. Despite the decrease in the compressive strength in the study conducted by (*Mundra et al., 2016*), the total replacement of natural sand does not significantly affect the flexural strength of concrete: the crushed granite concrete presents 6% lower values than the reference concrete.

As for the durability, (*Kou and Poon, 2009*) do not detect a significant difference in the resistance to chloride ion penetration (< 10%) when the crushed granite sand partially (25-50%) or totally replaces the natural river sand, for the same water to cement ratio, cement content, and coarse aggregates proportions. In this study, the slightly higher passed charge in the crushed granite concrete is attributed

to its lower slump (65 and 30 mm for natural and crushed granite concretes respectively) that could generate a less compact microstructure, thus lower durability.

3.2 Recycled wastes

Rapid urban development produces a huge amount of construction and demolition wastes. Furthermore, the wide range of products consumed worldwide generates massive domestic wastes.

Using these wastes as fine aggregates in concrete could be a safe and effective solution to eliminate the environmental negative effects of their disposal and to minimize the extensive exploitation of natural sand resources.

The recycled concrete, crushed bricks and tiles, glass wastes, and plastic wastes are examples of the recycled materials studied as alternatives to natural sand in concrete production.

3.2.1 Recycled concrete

Usually, the concrete wastes could be used as aggregates in new concrete. These concrete wastes are generated from the demolition of construction, the return of fresh concrete after production, the waste of the fabrication of precast concrete, and the tested concrete cylinders from the laboratories and ready-mix plants. The aggregates from recycled concrete are usually characterized by the presence of adhered cement paste on their surface, resulting from the old concrete. Therefore, the fine recycled concrete is characterized by a significantly higher absorption than the natural sand. Since the proportion of the adhered cement paste in the fine aggregates is higher than that in the coarse aggregates due to the lower size of fine aggregates grains (*RECYBETON Recommendations, 2018*), the recycled concrete is used more as coarse aggregates than fine aggregates.

Accordingly, the concrete incorporating the recycled concrete sand as an alternative to natural sand could present a high water content, in order to attain acceptable workability. For a replacement level of 50% and 100% of the natural silica sand, (*Kurda et al., 2019*) have found that the water demand and the porosity of concrete increase, reducing thereby its durability performance in terms of its water absorption and resistivity.

Furthermore, due to the adhered cement paste on the surface of the recycled aggregates, these aggregates could liberate soluble alkalis and increase the alkali-silica expansion (*RECYBETON Recommendations, 2018*). The recycled aggregates could also liberate soluble silica originating from the impurities that these aggregates could englobe from the construction materials.

3.2.2 Crushed bricks and tiles

The waste crushed bricks and tiles mainly result from the demolished constructions and are usually manufactured from clay minerals or ceramic. To avoid their deposition in the environment, these wastes could be valorized and used as fine aggregates in concrete after a simple crushing process. As fine aggregates, they are usually characterized by higher absorption and lower density than natural sand.

Since the crushed tiles tend to absorb more water in concrete, they decrease the flow diameter and the workability of mortars for fixed water to cement ratio and the same superplasticizer content (*Topçu and Bilir, 2010*).

The incorporation of the crushed tiles decreases the concrete compressive strength since it increases its porosity. Yet, it gives an acceptable structural performance. For the same water to cement ratio, the decrease in 28-day compressive strength of 100% crushed brick concrete does not exceed 10% compared to the reference concrete containing siliceous sand as the only fine aggregate (*Alves et al., 2014*). In the study of (*Topçu and Bilir, 2010*), the replacement of the natural siliceous sand by crushed tiles up to 40% produces a concrete compressive strength higher than the target designed strength (30 MPa). Moreover, the flexural strength increases when the crushed tiles are added as fine aggregates, even for a total replacement of the natural sand by crushed tiles (increase by 20%). This result is attributed to the rough surface of the crushed tiles grains which enhances the bond with the cement paste. To compensate for the high water demand of the crushed bricks, (*Debieb and Kenai, 2008*) increase the water to cement ratio of concrete mixes from 0.61 to 0.93, for a total replacement of calcareous aggregate by fine crushed bricks, creating thus concrete with lower compressive strength (about 30%) and flexural strength (36%), and higher permeability (60%).

Furthermore, the low thermal conductivity of the crushed bricks and roof tiles could provide better resistance to high temperatures (*Miličević et al., 2016*). Since these wastes are thermally stable, they could thereby provide longer protection of the concrete structure when exposed to fire than the concrete with other types of aggregates, as illustrated in Figure I.4.



Figure I.4 The difference of surface spalling, after exposure to a temperature of 1000 °C, between (a) concrete containing crushed bricks and roof tiles aggregates and (b) concrete containing crushed basaltic aggregates (*Miličević et al., 2016*)

3.2.3 Glass waste

The use of waste glass in concrete production was assessed by many researchers. They indicate that the glass could be beneficial or detrimental to the concrete performance depending on the size of its particles. The coarse particles of the glass waste could present an alkali-silica reactivity and cause an expansion of concrete, while the fine particles are characterized by a pozzolanic activity and could improve the concrete performance. The threshold of the effect of waste glass is found to be 0.6 mm in the study of (*Rajabipour et al., 2010*) and 1 mm in the research conducted by (*Idir et al., 2010*). Examples of glass waste are illustrated in Figure I.5.



Figure 1.5 Examples of glass waste used as fine aggregates in concrete
 (a) (Kim et al., 2018) and (b) (Ismail and AL-Hashmi, 2009)

In the study of (Kim et al., 2018), a heavyweight glass, collected from the waste of cathode ray tube CRT funnels, is used as a substitute for river siliceous sand in concrete. The results showed that, for fixed water to cement ratio, the total replacement of the natural sand by the glass waste, with comparable particle size distribution, could increase the concrete slump and seems not significantly affecting the air content of fresh concrete. In contrast, (Ismail and AL-Hashmi, 2009) have found that the slump decreases from 7.5 to 5 cm with the replacement of the desert sand by 10, 15, and 20% of glass waste (collected from bottles, jars, and windows) characterized by a finer gradation than the natural sand. To compensate for the loss of workability, (De Castro and De Brito, 2013) increase the effective water to cement ratio from 0.55 to 0.58 when the glass waste replaces the river limestone sand from 10 to 20%.

For a replacement ratio of 10, 15, and 20%, (Ismail and AL-Hashmi, 2009) show that glass waste does not affect the concrete compressive strengths at 3, 7, 14, and 28 days, and increases its flexural strength for all the replacement levels and at different ages (11% increase at 28 days). They have also confirmed that the waste glass could have a pozzolanic activity that could reach 80% at 28 days. For a higher replacement ratio, 50 and 100%, the compressive and flexural strengths gradually decrease in the study conducted by (Kim et al., 2018). The concrete with the crushed glass as the only fine aggregate displays a reduction of 26% and 16% in the 28-day compressive and flexural strengths respectively, compared to the reference river sand concrete.

In terms of durability, the incorporation of glass waste, as 50 and 100% of the proportion of fine aggregates, produces concrete with lower water absorption, depth of water penetration under pressure, penetration to chloride ion, and diffusion coefficient (Kim et al., 2018). Thus, the natural sand substitution by glass waste could improve the durability of concrete structures in terms of the studied properties. However, in the study of (De Castro and De Brito, 2013), the higher water to cement ratio in the concretes containing 5, 10, and 20% of crushed glass increases the porosity of concrete and reduces its durability in terms of the water absorption by immersion and by capillary, the resistance to carbonation, and the resistance to chloride ion penetration. Nevertheless, this decrease in durability does not exceed 15% and is considered acceptable by these researchers.

Furthermore, (Ismail and AL-Hashmi, 2009) prove that the 10, 15, and 20% replacements of dune sand by glass waste do not increase the alkali-silica reactivity. The expansions of all mixes are far below the limit (0.1%) imposed by (ASTM C1260, 2001).

3.2.4 Plastic waste

There is international concern about finding a solution for the waste left by plastic consumption all over the world. One of these solutions could be the recycling of these plastic wastes, such as polyvinyl chloride PVC and polyethylene terephthalate PET, as fine aggregates in concrete. Generally, the low density and lower water absorption of these particles could promote their use in the lightweight concrete solving the problem of the high water absorption generally related to the lightweight aggregates (*Choi et al., 2009; Senhadji et al., 2015*).

The use of plastic wastes could be beneficial in increasing the flow of mortar and slump of concrete, even if their particle size distribution is coarser than the one of the natural siliceous sand concrete (*Choi et al., 2009; Senhadji et al., 2015*). In contrast, the use of this manufactured sand could induce negative effects on the compressive strength of concrete. In the study of (*Choi et al., 2009*), this strength decreases by 6%, 16%, and 30% with the increase of the replacement percentage of natural river sand to 25%, 50%, and 75% respectively. Similarly, a significant decrease (> 35%) in the compressive strength of self-compacting concrete is observed by (*Hama and Hilal, 2017*) when the replacement level of the fine aggregates combination (river sand and crushed limestone) reaches 12.5% for a comparable particle size distribution. Compared to the natural siliceous sand concrete, the 28-day compressive strength is 15, 27, and 49% lower when the replacement level is 30, 50, and 70% respectively (*Senhadji et al., 2015*). This effect of plastic waste on the compressive strength is attributed, in the study of (*Senhadji et al., 2015*), to the weak ITZ and the large air bubbles in the concrete, as seen in Figure I.6.

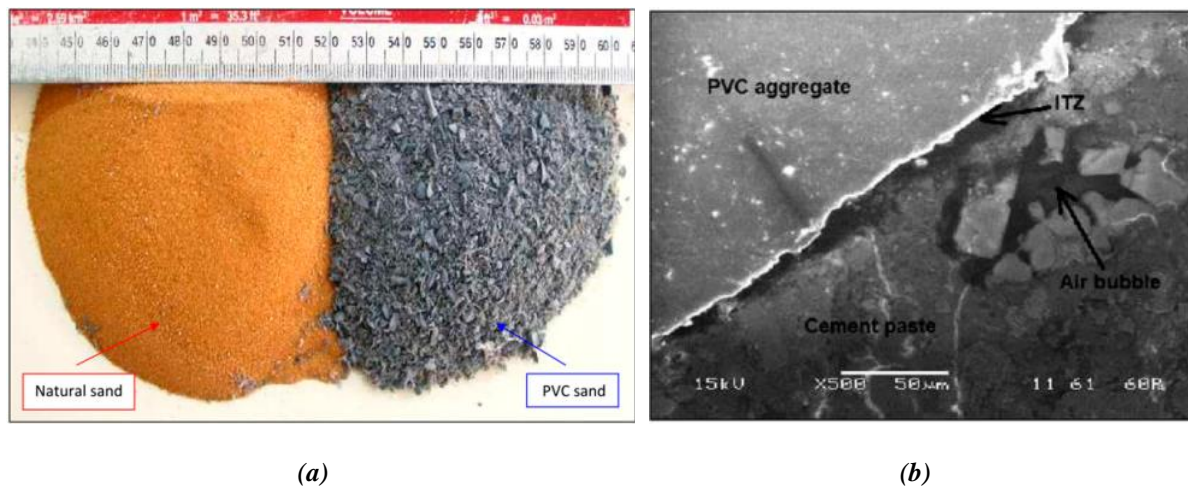


Figure I.6 (a) Image showing the appearance of the natural siliceous sand and the PVC sand and (b) SEM image of the ITZ between the PVC aggregate and the cement paste (x500) (*Senhadji et al., 2015*)

The effect of plastic waste as fine aggregate in concrete is also assessed by (*Saikia and De Brito 2014*). They study the effect of two shapes of polyethylene terephthalate (PET) bottle wastes as fine aggregates in concrete (Figure I.7): spherical/cylindrical particles that are heat-treated (PP), and flaky particles shredded in small sizes (PF). By conserving the same particle size distribution, the water to cement ratio is slightly decreased from 0.53 to 0.52 and the slump is increased from 122 to 132 mm, with the incorporation of PP due to the spherical and smooth surface texture of these particles. Despite the lower water demand, 5% and 10% PP replacement decreases the concrete compressive and splitting tensile strengths, and the modulus of elasticity (decrease > 15%). Hence, these particles could have created a weaker bond with the cement paste than the natural sand in the reference concrete. Besides, adding the flaky PF particles allows an increase in the water to cement ratio (0.57 to 0.64) and a decrease in the

slump (122 to 120 mm), leading to a significant reduction of the concrete compressive and splitting tensile strengths (decrease > 30%).

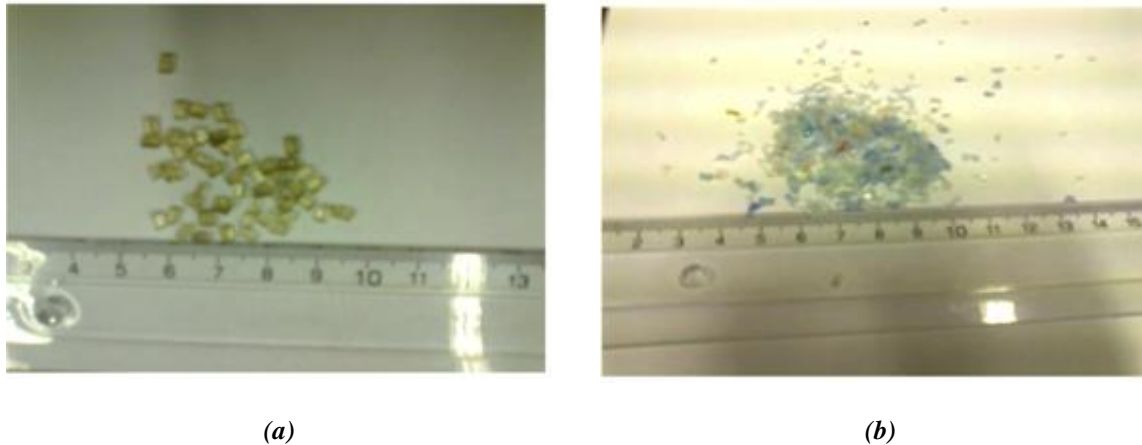


Figure I.7 Polyethylene terephthalate (PET) bottle wastes: (a) Heat-treated spherical/cylindrical particles PP, and (b) Flaky fine particles PF (Saikia and De Brito, 2014)

3.3 Industrial by-products

Due to the rapid industrial development worldwide, significant quantities of by-products are generated. This fact imposes environmental problems related to the pollution that could be produced by these substances, the lack of landfill areas, and the increased cost of waste disposal. Therefore, several studies have tried to find the optimum replacement percentage of natural sand by ash, slag, or foundry sand to produce good quality concrete. The application of this concept could contribute to the reduction of the landfills of the by-products while producing sustainable concrete.

3.3.1 Bottom and fly ash

The ash is an industrial by-product mainly formed during the coal burning process in thermal power plants. The ash particles agglomerate together at the bottom of the furnace to form the "Bottom ash". They are sieved and collected to have a particle size distribution close to one of the natural sand. The small particles which move upwards by the combustion gases are collected and named "Fly ash".

3.3.1.1 Bottom ash

The furnace bottom ash is mainly composed of silica, alumina, and iron, in addition to small amounts of other elements such as calcium, magnesium sulfate (Singh and Siddique, 2014), and some unburnt carbon. The stockpiling of the bottom ash in lagoons presents threats to the surrounding environment since it could be toxic. Hence, when used as fine aggregate in concrete (Figure I.8), the concentration of the elements leached from the bottom ash should not exceed the maximum allowable limit for toxic material (Rafieizonooz et al., 2017).

In terms of workability, at fixed water to cement ratio, the high specific surface and water absorption, the angular shape, and the rough surface texture of bottom ash could reduce the concrete workability with the increased level of natural sand substitution. In the study of (Singh and Siddique, 2014), the slump decreases from 70 to 10 mm when the bottom ash totally replaces the natural river sand.

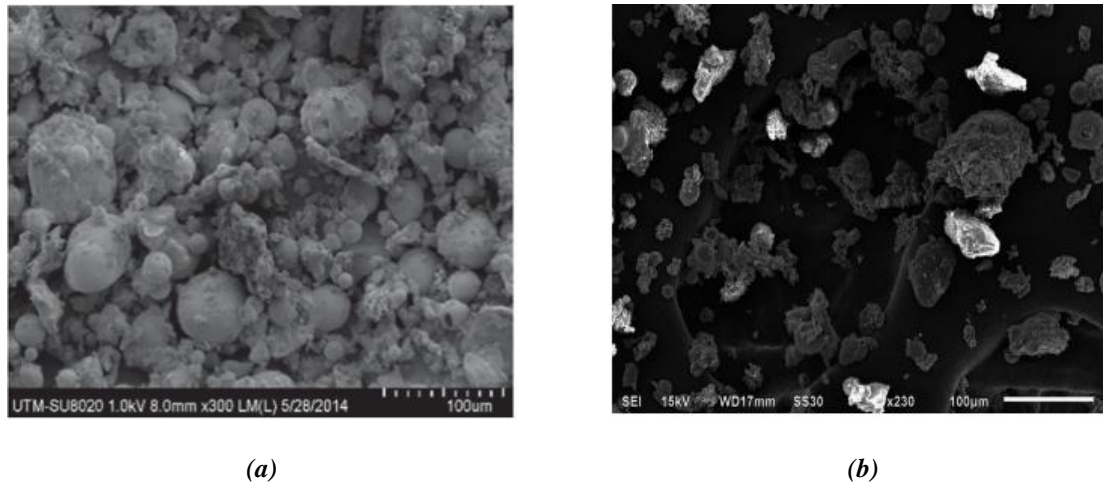


Figure I.8 Scanning electron microscope images of bottom ash as fine aggregate (a) (x300) (Rafieizonooz et al., 2017) and (b) (x230) (Singh and Siddique, 2014)

At a late age, the silica of the bottom ash could react with the calcium hydroxide produced from the cement hydration, to form calcium silicate hydrates. These products contribute to the increase in the compressive strength with time by filling the voids in concrete (Singh and Siddique, 2014; Rafieizonooz et al., 2017). At 7 days, the compressive strengths of mixes incorporating 25, 50, 75, and 100% bottom ash are 9, 18.6, 22.8, and 25.8% lower than the reference concrete without bottom ash in the study of (Rafieizonooz et al., 2017), while 50 and 100% replacements decrease the 7-day compressive strength by 9 and 15% respectively in the study of (Singh and Siddique, 2014). However, at 90 and 180 days, all mixes from each study present similar compressive strengths.

The bottom ash could also affect the permeability of concrete. At 180 days, the porosity accessible to water and the water absorption of concrete increase from 14.1% to 18.1% and 5.8% to 6.5% respectively when the natural river sand is totally replaced by bottom ash (Singh and Siddique, 2014).

3.3.1.2 Fly ash

Due to its fineness, the fly ash is studied as a partial replacement to coarser natural sand. (Saxena and Pofale, 2017) have found that the substitution level could reach 80% without compromising the concrete strengths (compressive strength, splitting tensile strength, and flexural strength) at 7 and 28 days. However, they have observed that it is preferable to limit its amount to 30% to avoid a high reduction in the workability of concrete.

Furthermore, to be used as the only fine aggregate in mortar, the fly ash could be transformed into a geopolymer fly ash (Figure I.9). (Agrawal et al., 2017) mix the fly ash with an alkaline solution of sodium hydroxide (NaOH) and sodium silicate (Na_2SiO_3), to form polymeric bonds of alumino-silicate. These researchers observe the same 28-day compressive strength for the fly ash and the natural sand mortars, while at early ages (3 and 7 days) the strength of the former is lower (difference around 20%). They conclude that, at a late age, the unreacted fly ash in the solution may have reacted with the hydration products, i.e, lime, and contributed to the enhancement of the 28-day compressive strength.



Figure I.9 Different particle sizes of the geopolymer fly ash (Agrawal et al., 2017)

3.3.2 Rubber ash

In addition to the bottom ash generated during the coal combustion, some studies assessed the effect of the ash that could result from the combustion of other materials. One of these materials is rubber tires, with a particle size distribution ranging between 0.15 and 1.9 mm.

At constant water to cement ratio, (Gupta et al. 2014) have found that the higher the addition of rubber ash, the more the admixture demand in the concrete mix to conserve the same workability. For a replacement ratio varying from 0 to 20%, the admixture dosage varies from 2.1 to 2.6%, 0.5 to 1.6%, and 0 to 0.9% for a W/C of 0.35, 0.45, and 0.55 respectively.

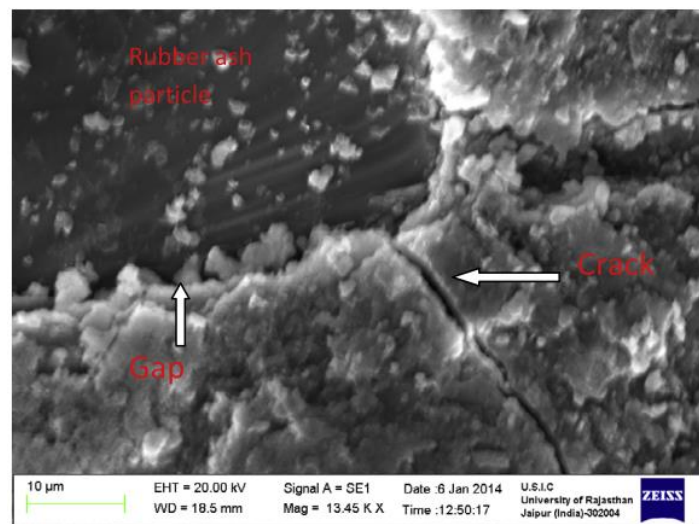


Figure I.10 Scanning electron microscope image at the ITZ of a rubber ash particle for concrete containing 20% rubber ash as a replacement to natural sand (x13450) (Gupta et al., 2014)

The addition of rubber ash at W/C of 0.35 and 0.45 lower the concrete compressive strength by 20 and 10% respectively for a replacement ratio of 20%, while this strength increases by around 10% at a W/C of 0.55. According to the researchers, due to the high workability of the mixes having a W/C of 0.55, the rubber ash particles induce efficient packing. Conversely, the reduction of the compressive strength

in the other mixes with lower water to cement ratio is related to the weaker stiffness of the rubber ash compared to the surrounding natural sand. On the other hand, the rubber ash presents a lower flexural strength for all the replacement levels and all the water to cement ratio, due to a poor interfacial bonding with cement paste (Figure I.10).

In terms of durability, in this study, the chloride diffusion tends to increase with the incorporation level of rubber ash.

3.3.3 Foundry sand

The foundry sand is high-quality silica sand used in the metal casting industry as a molding material, due to its high thermal conductivity (Aggarwal and Siddique, 2014). During the metal casting production, the molten metals are poured into preformed molds of foundry sand. This sand is used and recycled several times, and when it could no longer be used in the casting process, it is designated as a waste foundry sand and discarded in landfills (Aggarwal and Siddique, 2014; Coppio et al., 2019). The increasing amount of these wastes, due to the huge production of metal casted parts, drives some researchers to evaluate its effectiveness as a replacement to natural sand in concrete, although this sand could be polluted by the metal residues.

(Coppio et al., 2019) study the effect of the total replacement of natural sand A by two types of foundry sand: long-ago discarded foundry sand F and recently discarded foundry sand G. The three fine aggregates present close fineness modulus (2.45, 2.06, 2.45 for A, F, and G respectively) and they differ by their fines content (1.90, 6.35, and 3.22% for A, F, and G respectively). The cement content slightly varies between the three concrete mixes (361, 352, and 358 kg/m³ for A, F, and G respectively) while the water to cement ratio (0.5) is fixed. The replacement of natural sand with foundry sand decreases the slump of concrete (50, 20, and 45 mm for A, F, and G respectively). As for the mechanical behavior, the compressive strength is reduced by 43% (long-ago discarded foundry sand F) and 22% (recently discarded foundry sand G) compared to the conventional concrete. The compressive strength tends to be lower when the foundry sand contains greater fines materials (1.90, 6.35, and 3.22% for A, F, and G respectively). Moreover, the metal residues contained in the foundry sand could have affected their adherence with the cement paste, reducing thereby the concrete strength. The researchers then deduce that the long-ago discarded foundry sand should not be used as a total replacement to natural sand in concrete, while the recently discarded foundry sand could be used for non-structural purposes only. In terms of durability, (Coppio et al., 2019) do not observe a clear tendency of the effect of foundry sand on the electrical resistivity of concrete. It could be lower, equal, or higher than the one of the natural sand concrete depending on the composition and the content of the metal residues and fine materials in the foundry sand.

(Aggarwal and Siddique, 2014) do not study the foundry sand as the only substitute for natural sand in concrete. They have mixed it with an equal proportion of bottom ash and have assessed the effect of this mix as a partial replacement to natural sand, in proportions varying between 0% and 60%. To reach a fixed slump, the water to cement ratio has to be increased with the natural sand substitution rate, due to the lower fineness moduli of the foundry sand and bottom ash which increase the water demand. Hence, the results show a significant decrease (reached 47%) in the 7, 28, 90, and 365-day compressive, flexural, and splitting tensile strengths of concrete at 60% substitution. At 30%, the lower values of the compressive strength remain in the same range with the reference concrete, while the flexural and splitting tensile strengths slightly exceed those of the natural sand concrete. In terms of durability, the combination of these by-products sands provides a very low permeability to chloride ions with slightly lower resistance than the natural sand concrete.

3.3.4 Metals slag

The metal slags are defined as by-products of metal productions. They could be divided into two types according to the cooling process applied. The air-cooled slag is the crystalline dense material produced after slowly cooling the slag in the air. The foam slag is a lightweight material formed when the slag is directly discharged and rapidly cooled with water jets.

The following sections feature the effects of the incorporation of different kinds of metal slags on the concrete performance: iron slag, blast furnace slag, ferrochrome slag, ferronickel slag, and copper slag.

3.3.4.1 Iron slag

The iron slag is produced as a by-product generated from the iron industry and it is collected during the separation of the molten steel from the impurities by high-pressure oxygen (*Qasrawi et al., 2009; Noufal and Manju, 2016*). In the studies of (*Qasrawi et al., 2009; Singh and Siddique, 2016*), the chemical analysis of the steel slag revealed a high content of iron oxide Fe_2O_3 .

The incorporation of steel slag in concrete tends to decrease the workability. For the same water to cement ratio, the higher the incorporation level of the iron slag in concrete, the lower its slump. (*Qasrawi et al., 2009*) use steel slag with a particle size distribution within the ASTM limits except for the high percentage of fines (20.5%). They have found that the slump varies from 12 to 2 cm when the natural sand replacement varies from 0 to 100%. Similarly, the slump flow decreases from 774 to 687 mm with an iron slag proportion of 0 and 40% respectively characterized by a fineness modulus (2.83) within the acceptable range (2.3-3.1) (*Singh and Siddique, 2016*). In contrast, (*Noufal and Manju, 2016*) observe that the slump increases from 95 to 112 mm when the iron slag, with a particle size distribution that falls within the recommended range for concrete, totally replaces the natural river sand.

As for the strengths, (*Qasrawi et al., 2009*) show that a replacement percentage up to 15% seems beneficial for the compressive strength of the normal strength concrete, whereas, for a replacement of 50%, the flexural strength exceeds the one of the natural river sand concrete. (*Noufal and Manju, 2016*) have found that the replacement percentage could be increased to 50% (with an optimum percentage of 30%) without compromising the compressive and splitting tensile strengths of concrete. (*Singh and Siddique, 2016*) prove that the use of steel slag as a 40% substitute for natural sand improves the strengths of concrete at 7, 28, and 91 days. At 28 days, the compressive, flexural, and splitting tensile strengths of the self-compacting concrete increase by 20%, 14%, and 21% respectively compared to the concrete without iron slag. It should be noted that, in addition to the difference in the particle size distribution between the various slags used, the distinction in the optimum replacement level between the three mentioned studies could be due to the variation in the quality of the steel slag used. The steel slag properties could depend on many factors associated with the steel production (such as the target grade of the steel being produced) and the slag characteristics (such as the metal content) (*Noufal and Manju, 2016*).

In terms of durability, the resistance of concrete to chloride ion penetration increases with the replacement ratio of natural sand by iron slag. In the study of (*Noufal and Manju, 2016*), the permeability of concrete passes from moderate without replacement (2240 C) to very low with 100% replacement (800 C). Thus, the steel slag could improve the durability of concrete. This result could be attributed to the enhancement of the concrete microstructure created by the steel slag aggregate. (*Singh and Siddique, 2016*) have observed an additional formation of calcium silicate and aluminates hydrates,

as products of the reaction between the reactive silica in iron slag and the calcium hydroxide produced by the hydration of cement.

3.3.4.2 Ferronickel slag

The ferronickel slag is a by-product of nickel production. If the radioactivity of this slag is too high, it could be harmful and cannot be used in concrete.

In the study of (*Liu et al., 2020*), the radiation indices of the ferronickel slag used were close to zero. Since the particle size distribution of the ferronickel slag lies outside the limits imposed by the Chinese standard, the incorporation of this sand does not exceed 50% to meet the grading limits. The microstructural analysis demonstrates that this slag could actively contribute to the hydration production of concrete and produce more hydration products than the natural river sand concrete. Consequently, the internal structure of concrete could become denser and the concrete durability could be improved. Therefore, when the replacement level reaches 27%, the resistance to chloride-ion penetration is increased by 21% compared to the reference concrete. However, the addition of iron slag in a proportion of 50% decreases the resistance of concrete to the chloride ion penetration. The researchers explain these results by the effect of the high content of iron in this mix which is more pronounced in reducing the concrete resistance than the positive blocking effect of the hydration products.

3.3.4.3 Ferrochrome slag

The ferrochrome slag is a by-product of the process of manufacturing ferrochrome alloy in electric arc furnaces. Ferrochrome is the most used alloy in stainless-steel production. This slag usually contains 6-12% of deleterious particles such as chromium, one of the most toxic heavy metals found in the environment (*Panda et al., 2013*). It could only be used in concrete if the leaching of chromium to the environment does not exceed the regulatory norms.

By performing leaching experiments, (*Panda et al., 2013*) prove that, even though this slag contains a high amount of chromium, this substance remains immobilized in concrete, with a negligible leaching level. In their study, the molten ferrochrome slag is cooled by the means of a high-pressure water jet to have a granulated slag with a particle size distribution comparable to the one of the fine aggregate suitable for the concrete production (Figure I.11).



Figure I.11 Ferrochrome slag used as fine aggregate (Panda et al., 2013)

They have found that the granulated ferrochrome slag as partial and total substitutions to natural sand produced concrete with approximately the same slump, same hardened density, and same compressive strength as the natural sand concrete. Thus, they deduce that the ferrochrome slag could be safely used as fine aggregate in concrete.

3.3.4.4 Copper slag

Copper slag is a by-product generated during the production of copper. Most of the generated slag is rejected as waste, despite its use in the sandblasting industry and the production of abrasive tools (Al-Jabri *et al.*, 2011; Dos Anjos *et al.*, 2017).

When used in concrete, the particle size distribution of the copper slag is adopted to be comparable to the one of the conventional fine aggregates used in concrete. The glassy surface of this slag, its sphericity, and its low water absorption could reduce the water demand of concrete and promote higher workability compared to the natural ravine sand concrete (Dos Anjos *et al.*, 2017) and the crushed sand concrete (Al-Jabri *et al.*, 2011).

The 50% replacement of crushed sand by copper slag seems to affect the concrete strengths (Al-Jabri *et al.*, 2011). For 80 and 100% replacements, the compressive, splitting tensile, and flexural strengths of concrete decrease by 22, 13, and 23% compared to the crushed sand concrete. The results of the strengths are related to the porosity of concrete and the surface of the slag which lowers the cohesion with the cement paste. In their study, (Al-Jabri *et al.*, 2011) found that the incorporation of copper slag up to 50% of the fine aggregate mass decreases the porosity accessible to water by approximately 15%. Above this substitution rate, the porosity begins to increase but it remains lower than the porosity of the reference concrete, even when the copper slag totally replaces the crushed sand.

(Dos Anjos *et al.*, 2017) observe a decrease in the compressive and splitting tensile strengths of concrete with the replacement level of copper slag. The reduction becomes remarkable when the substitution rate exceeds 40% to reach 11.5% and 33.5% for compressive and splitting tensile strengths respectively, compared to reference concrete with ravine sand. Despite this decrease, the compressive strength remains higher than the designed strength. According to the researchers, this reduction in the concrete strengths is due to the residual impurities on the copper slag particles, such as paint particles and anti-oxides, reducing thereby the bond with the cement paste.

3.4 Summary of the literature review on the alternatives to natural sand

Table I.1 summarizes the effect on the concrete performance of the different types of alternatives in the studies reviewed.

Table I.1 Summary of the alternatives to natural siliceous sand and their effects on concrete

Study	Alternative	Maximum Replacement level	Effects on concrete
(Akrouf <i>et al.</i> , 2010)	Crushed limestone	100%	Decrease in workability Decrease in compressive strength
(Bederina <i>et al.</i> , 2013)		100%	Decrease in workability Increase in the compressive and flexural strengths
(Stefanidou, 2016)		100%	Decrease in workability Increase in flexural strength
(Donza <i>et al.</i> , 2002)		100%	Decrease in workability Increase in compressive strength

Study	Alternative	Maximum Replacement level	Effects on concrete
(Gameiro et al., 2014)	Crushed marble	100%	Decrease in workability Same range of durability
(Binici and Aksogan, 2018)		100%	Decrease in workability Increase in compressive strength Increase in durability
(Kou and Poon, 2009)	Crushed granite	100%	Decrease in workability Same range of compressive strength Same range of durability
(Cordeiro et al., 2016)		50%	Decrease in workability Same range of compressive strength
(Shen et al., 2017)		100%	Decrease in workability Same range of compressive strength
(Mundra et al., 2016)		100%	Same range of workability Decrease in compressive strength Same range of flexural strength
(Kurda et al., 2019)	Recycled concrete	100%	Decrease in workability Decrease in durability
(Topçu and Bilir, 2010)	Crushed tiles	100%	Decrease in workability Decrease in compressive strength Increase in flexural strength
(Alves et al., 2014)		100%	Same range of compressive strength
(Kim et al., 2018)	Glass waste	100%	Increase in workability Decrease in compressive and flexural strengths Increase in durability
(Ismail and AL-Hashmi, 2009)		20%	Decrease in workability Same range of compressive strength Increase in flexural strength
(Choi et al., 2009)	Plastic waste	75%	Increase in workability Decrease in compressive strength
(Senhadji et al., 2015)		70%	Increase in workability Decrease in compressive strength
(Hama and Hilal, 2017)		12.5%	Decrease in compressive strength
(Saikia and De Brito 2014)		10%	Decrease in workability Decrease in compressive and splitting tensile strengths
(Singh and Siddique, 2014)	Bottom ash	100%	Decrease in workability Decrease in 7-day compressive strength Same range of 90 and 180-day compressive strengths Decrease in durability
(Rafieizonooz et al., 2017)		100%	Decrease in 7-day compressive strength Same range of 90 and 180-day compressive strengths
(Saxena and Pofale, 2017)	Fly ash	80%	Decrease in workability Same range of compressive, splitting tensile, and flexural strengths
(Agrawal et al., 2017)		100%	Decrease in 3 and 7-day compressive strength Same range of 28-day compressive strength
(Gupta et al. 2014)	Rubber ash	20%	Decrease in workability Decrease in compressive and flexural strengths Decrease in durability
(Coppio et al., 2019)	Foundry sand	100%	Decrease in workability Decrease in compressive strength

Study	Alternative	Maximum Replacement level	Effects on concrete
(Aggarwal and Siddique, 2014)	Foundry sand and bottom ash	60%	Decrease in workability Decrease in compressive, splitting tensile, and flexural strengths Same range of durability
(Qasrawi et al., 2009)		100%	Decrease in workability Decrease in compressive strength Increase in flexural strength
(Singh and Siddique, 2016)	Iron slag	40%	Decrease in workability Increase in compressive strength, splitting tensile, and flexural strengths
(Noufal and Manju, 2016)		50%	Increase in workability Increase in compressive strength and splitting tensile strengths Increase in durability
(Liu et al., 2020)	Ferronickel slag	50%	Decrease in durability
(Panda et al., 2013)	Ferrochrome slag	100%	Same range of workability Same range of compressive strength
(Dos Anjos et al., 2017)	Copper slag	100%	Increase in workability Decrease in compressive and splitting tensile strengths

3.5 Available alternatives to natural sand in Lebanon

In Lebanon, there is no proper sorting process for wastes, and recycling practices are not widespread in the country (*Ministry of Environment, 2018*). As illustrated in Figure I.12a, 37% of the total generated wastes could be recycled or reused (glass, plastic wastes, metal, and paper/cardboard), while actually only 8% are recycled (Figure I.12b). Recyclable materials, including plastic, glass, and rubber, are generally mixed and treated with other types of wastes (*GIZ, 2014; Abbas et al., 2017*). Similarly, the construction and demolition wastes are not collected separately and they are treated as the other solid waste materials (*GIZ, 2014*), despite their significant quantity that can be recycled (*Srouf et al., 2012*). In rare cases, these construction and demolition wastes are used as backfilling materials in landfills or in some construction site activities, for example behind retaining walls. Thus, it is very difficult to collect a sufficient quantity of these recyclable and construction wastes from the unsegregated waste stream (*Abbas et al., 2017*), and to use it as fine aggregates in concrete.

Lebanon is also characterized by a relatively small industrial sector, where 84% of the industries employ less than 10 workers (*El-Fadel et al., 2001*). Most of these industries are light manufacturing industries (*El-Fadel et al., 2001; GIZ, 2014; Ministry of Environment, 2018*) and they generate around 188,000 tons of industrial wastes per year (8.38% of the total wastes) (*GIZ, 2014*). The composition of these wastes is poorly documented and there are no adequate factories for industrial wastes treatment (*Abbas et al., 2017*). Thus, most of these wastes are mixed with municipal wastes and placed in sanitary landfills due to a lack of clear legislation and strict controls (*El-Fadel et al., 2001; GIZ, 2014; Abbas et al., 2017*). It should also be noted that, among these Lebanese industries, the basic metal industry occupies only 4% (*Ministry of Environment, 2018*), thus they do not generate a sufficient quantity of metal slag to be used as fine aggregate in concrete.

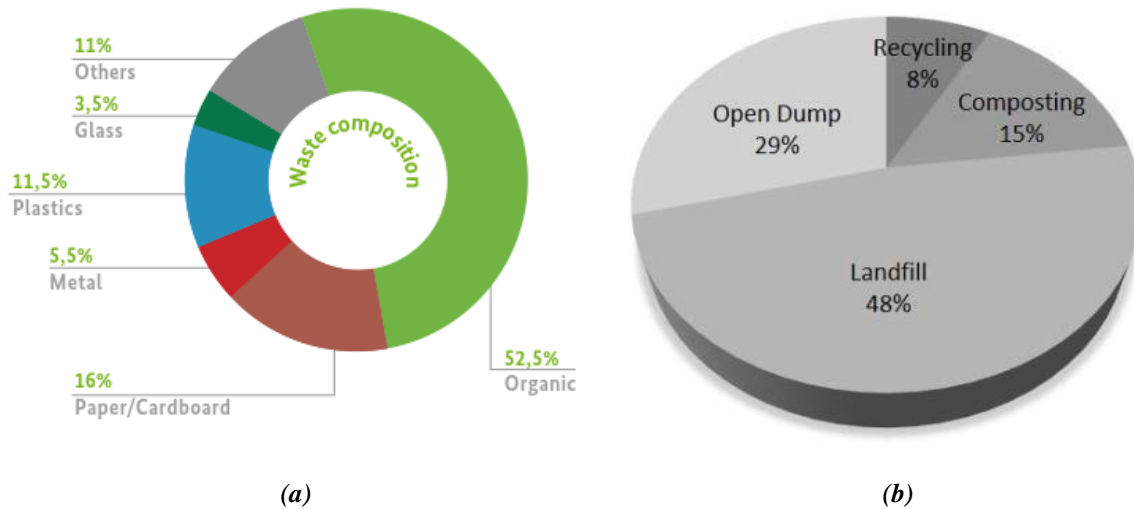


Figure I.12 (a) Waste composition (GIZ, 2014) and (b) waste management in Lebanon (Abbas et al., 2017)

Since there are no upcoming initiatives for solid waste management that could be expected in the near future (GIZ, 2014) and since the crushed limestone sand quarries are already widely available almost all over the country (as discussed in Section 2), currently, the crushed limestone sand tends to be the most adequate alternative to natural sand in the Lebanese context.

4. Effects of fine aggregates characteristics on concrete performance

The physical and chemical characteristics of aggregates are of great importance in determining concrete performance (Neville and Brooks, 1987). The fine aggregate, in particular, is an essential material in the concrete mix which ensures a granular continuity between the cement and coarse aggregates, and its properties could influence the concrete performance.

In consideration of the important role that the fine aggregates could play on concrete, a literature review on their effects is presented in this section. This review features the effects on the fresh state, mechanical behavior (resistances and deformation), and durability properties of concrete. Also, the effects of the different characteristics of fine aggregates on the concrete microstructure are presented in the last part of this section to be able to explain the differences between the concrete behaviors at the macroscale.

4.1 Fine aggregates characteristics

Before focusing on the effect of fine aggregates characteristics on the concrete performance, the following section presents an overview of the mineralogy, morphology, physical characteristics, and fines content of fine aggregates.

4.1.1 Mineralogy and chemical composition of fine aggregates

The mineralogy of sand depends on its origin. The natural sand is usually siliceous formed of quartz particles. The crushed sand mineralogy depends on the nature of its parent rock. For example, limestone and marble are mainly formed of calcite, while granite is typically composed of feldspar, quartz, and micas. Likewise, as already detailed previously, each type of the manufactured sands presented in Section 3 is characterized by specific mineralogy depending on the origin of the material used in its manufacture.

To determine the mineralogy of sand, the X-Ray Diffraction technique XRD is usually used. This method helps to identify the spacing of the planes of the crystalline solid present in a sample by detecting the diffraction pattern for X-ray wavelengths directed toward the sample. The sample is introduced into the diffractometer in powder form and maintained at an angle θ from the incident beam. The diffracted rays are continuously collected by the X-ray detector, rotating at an angle of 2θ . The constructive interference of X-rays and a crystalline sample occurs when Bragg's Law is satisfied:

$$n \lambda = 2d \sin \theta \quad (\text{Eq. I.1})$$

Where n : diffraction order; λ : wavelength of the target material in the X-ray tube, commonly the copper (1.5406 Å) and the cobalt (1.7902 Å); d : plans spacing; θ : half of the deviation angle between the incident and the diffracted rays.

The Scanning Electron Microscope SEM coupled with the Energy Dispersive Spectrometer EDX are used to determine the chemical composition of aggregates. In the SEM/EDX, the sample surface is coated with electrically conducting material and introduced into the machine chamber. An electron gun generates an electron beam which is accelerated. When the primary electrons hit the specimen, they excite the electrons of the atoms in the sample to create secondary electrons, backscattered electrons (from deeper locations), and X-ray waves. The detectors collect the signals emitted by the sample and display them as images on a computer screen. Due to the relation between the energy revealed by backscattered electrons and the atomic number of the chemical element, the information related to the distribution of different elements in the sample and their concentrations are determined by the analysis of the backscattered electrons images and their energetic intensity.

4.1.2 Morphology of fine aggregates

The morphology characteristics mainly depend on the formation history of the sand particles. Also, the surface texture of the aggregates varies with the crystalline texture of each rock, its hardness, and the intergranular bond between the mineral grains (*Tasong et al., 1998*).

According to (*Neville and Brooks, 1987*), a US classification is usually used to categorize the aggregates shape into five types:

- Well rounded: with no original faces left
- Rounded: faces almost disappeared
- Sub-rounded: considerable wear, faces reduced in area
- Sub angular: some wear, but faces untouched
- Angular: little evidence of wear

Table I.2 presents the classification of aggregates based on their shape as per (*ASTM D4791, 2019*) standard.

Table I.2 Shape classification of aggregates (ASTM D4791, 2019)

Shape classification	Description
Elongated	Particles of aggregate having a ratio of length to width greater than a specified value
Flat	Particles of aggregate having a ratio of width to thickness greater than a specified value
Flat and elongated	Particles of aggregate having a ratio of length to thickness greater than a specified value

The determination of the exact shape of fine aggregates is a complex process and there is no specified normalized method to determine it. However, previous studies presented some rules to assess certain properties that could estimate the shape of the fine aggregates' grains.

• Aspect ratio and elongation

The aspect ratio is the ratio of the minimum diameter of the particle over its maximum diameter (*Bengtsson and Evertsson, 2006*) (Figure I.13a), detected by SEM after dividing the sample into narrow fractions by sieving and casting it in epoxy molds.

$$\text{Aspect Ratio} = \frac{\text{Minimum Diameter}}{\text{Maximum Diameter}} \quad (\text{Eq. I.2})$$

The elongation also depends on the length and width of the particle (Figure I.13b). In the study of (*He et al., 2016*), this characteristic was studied by a combination of high-quality optical components and two systems of image analysis equipment: 500 Nano working in dry samples and Flowcell operating in a liquid environment.

$$\text{Elongation} = 1 - \frac{\text{Width}}{\text{Length}} \quad (\text{Eq. I.3})$$

The particle is spherical if the aspect ratio is equal to one, while for irregular-shaped particles, the aspect ratio is lower than one. On the other hand, the higher the elongation value, the more elongated the particle is (*He et al., 2016*).

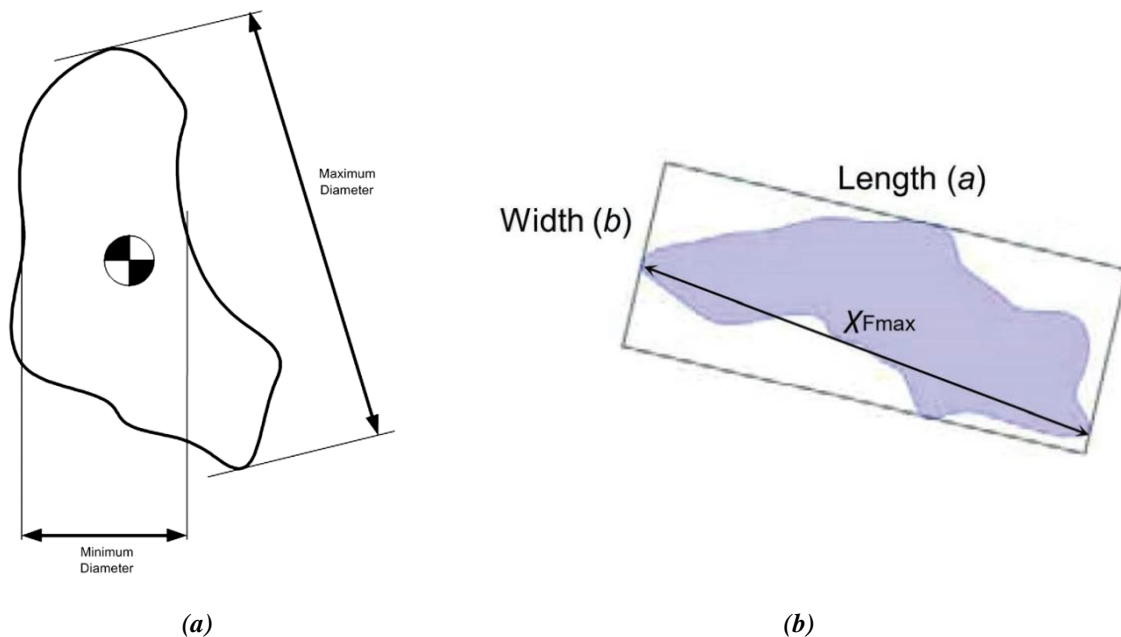


Figure I.13 Determination of particles shape by (a) (*Bengtsson and Evertsson, 2006*) and (b) (*He et al., 2016*)

• Roundness

The roundness parameter is calculated to assess how close the particle is to a circle (*Cordeiro et al., 2016; He et al., 2016*). The diameter and the projected area of the particle are determined using digital image software. A value equal to one indicates a spherical particle.

$$\text{Roundness} = \frac{4 \cdot \text{Particle projected area}}{\pi \cdot \text{Diameter}^2} \quad (\text{Eq. I.4})$$

• Angularity

The angularity defines the sharpness of corners of a 2D image of aggregate particles. A small value characterizes a perfect circle. It could be calculated based on the gradient method. By using a binary particle image (silhouette), the variation of the gradient is measured all over the boundary of the particle, and the following formula is applied (*Rajan and Singh, 2017*):

$$\text{Angularity} = \frac{1}{\frac{n}{3}-1} \sum_{i=1}^{n-3} |\theta_i - \theta_{i+3}| \quad (\text{Eq. I.5})$$

Where θ_i : the orientation angle of the edge point i ; n : the total number of points; i : the i^{th} point on the edge of the particle.

• Roughness

The surface roughness could be detected by a laser microscope system. This technique could measure very small topographic height change (up to 0.001 mm) (*Tasong et al., 1998*) as illustrated in Figure I.14. The roughness is calculated as follows (*Shen et al., 2016*):

$$\text{Roughness} = \frac{1}{L} \int_0^L |y(x)| dx \quad (\text{Eq. I.6})$$

Where L : the length in μm ; x : the length variable; $y(x)$: the height variation versus x in μm between the detecting point and the base face.

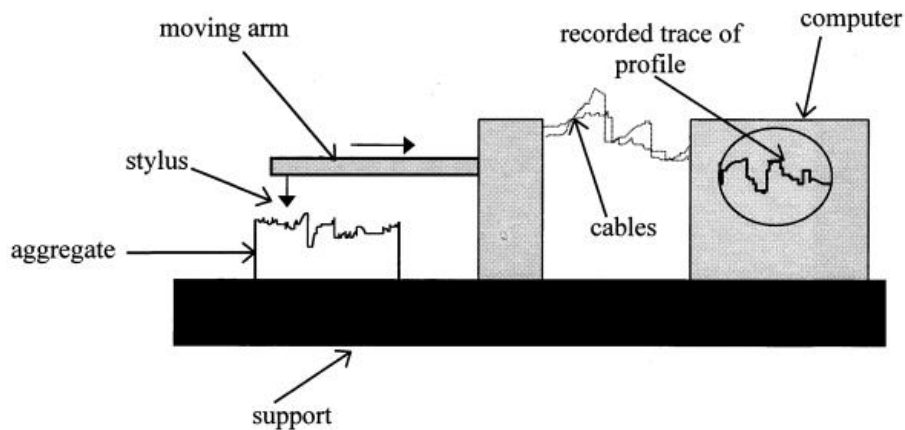


Figure I.14 Schematic representation of the apparatus used to calculate the aggregate surface roughness (*Tasong et al., 1998*)

• Bluntness

The bluntness perimeter describes the degree of abrasion of a particle (*He et al., 2016*). A higher value indicates an important abrasion of the sand grains.

$$\text{Bluntness} = \frac{1}{\sqrt{\bar{V}} - 1} \quad (\text{Eq. I.7})$$

$$\text{in which } \bar{V} = \frac{1}{N} \sum_{i=1}^N \left(1 + \frac{r_{\max}}{r_i}\right)^2 \quad (\text{Eq. I.8})$$

Where r_i : radius of the maximum inscribed circle on point i ; r_{\max} : the maximum value of r_i ; N : number of points.

Usually, the natural sand is formed of smooth grains close to a sphere as a result of the multiple collisions, frictions, and abrasions forces exerted on these grains before their extraction (Neville and Brooks, 1987; Cortes et al., 2008; He et al., 2016; Yamei and Lihua, 2017). On the other hand, the manufactured sand which results from a crushing process tends to have rough flat angular particles, with a degree of angularity and elongation depending on the parent rock, the crusher type, and the reduction ratio, which is the ratio of the feed size to the production size in a crusher (Neville and Brooks, 1987; He et al., 2016; Yamei and Lihua, 2017; Shen et al., 2018).

4.1.3 Physical characteristics of fine aggregates

The studied physical properties of aggregates include the particle size distribution, the specific gravity, the absorption, and the porosity.

The particle size distribution and fineness modulus of fine aggregate are usually determined by sieve analysis. The diameters of the sieves depend on the standard applied. In the American standard (ASTM C136, 2014), 4.75, 2.36, 1.18, 0.60, 0.30, 0.15 mm sieves are used, while the particle size distribution is determined in the European standard (BS EN 933-1, 2012) using 4, 2, 1, 0.500, 0.250, and 0.125 mm sieves. The sieves are placed in decreasing order according to their diameter, and the retained mass on each sieve is determined as a percentage of the original mass of the sample. The fineness modulus consists of dividing over 100 the sum of the cumulative percentage retained on 0.15, 0.30, 0.60, 1.18, 2.36, and 4.75 mm sieves following (ASTM C136, 2014) and 0.125, 0.250, 0.500, 1, 2, and 4 mm as per (BS EN 933-1, 2012).

The specific gravity (relative density) is determined as the ratio of the density of the aggregate particles to the density of water, and it does not take into consideration the voids between these particles. The 24-hour absorption of aggregate represents its ability to absorb water and it is calculated as the difference between the mass of the aggregate in a saturated-surface dried condition and an oven-dried condition to the mass of the sample in the oven-dried condition (ASTM C128, 2015; BS EN 1097-6, 2013). The total porosity of aggregate particle corresponds to the ratio of the total voids space to the total volume, while the porosity accessible to water is determined by the ratio of the open pores to water to the total volume.

4.1.4 Fines content and deleterious particles in fine aggregates

The fines are the fraction of particles passing the 0.075 mm sieve (ASTM C117, 2013) or the 0.063 mm sieve (BS EN 12620, 2002). These fines could contain a high content of deleterious materials, such as silt and clay minerals, which could be detrimental to concrete performance. Therefore, the standards impose a maximum percentage of fines in aggregates used for concrete.

The production of crushed rocks usually generates fine crushed sand with a high percentage of fines, which could reach 20% by mass of the fine aggregate. By increasing the limits of the fines allowable to be present in sands, the high percentage of fines could then be valorized, reducing thereby the environmental and economic effects of their stockpiling as wastes. Therefore, for fine aggregates, the standards differentiate between the natural and the manufactured sands. They raise the limits for the fines content in crushed sand since these fines are mainly generated from the parent rocks during the crushing process and are usually free of deleterious particles. (ASTM C33, 2016) increases the maximum allowable fines percentage from 5% for natural sand to 7% for crushed sand. The British standard (BS 882, 1992) allows a maximum fines percentage of 4% for uncrushed, partially crushed, or

crushed gravel sand and 16% for crushed rock sand. However, later on, the European standard (*BS EN 12620, 2002*) does not set a specified limit for the fines content in both types of sand.

The mineral and physical properties of the crushed sand and its fines depend on the steps of the crushing process. If they are collected from a primary crusher, they could have a higher content of deleterious particles. However, they are usually of good quality if they result from a secondary or tertiary crusher.

The effects of the low and high percentage of fines in sands on some concrete properties were evaluated in some previous studies and are presented in the following sections.

4.2 Effects of fine aggregates characteristics' on concrete at the macroscale

Different sand characteristics could influence the concrete properties: the sand mineralogy, morphology, physical properties, fines content, and deleterious particles. Thus, it is sometimes difficult to decouple the effects of each characteristic and determine the most influential factor. In addition to the characteristics of fine aggregates, the variation of the parameters of the concrete mix design could impact the concrete performance. In some studies, by changing the type of fine aggregates, the water to cement ratio is fixed leading to a different slump value or a variation in the superplasticizer dosage if a fixed slump is targeted. In other studies, the variation in the water demand is compensated by a variation in the water to cement ratio of the mix.

The following sections detail the effect of the fine aggregates' characteristics on the fresh state, mechanical behavior, and durability properties of concrete.

4.2.1 Effects of fine aggregates characteristics' on the fresh properties of concrete

Fresh concrete is defined in (*ASTM C125, 2016*) as concrete that possesses enough of its original workability to be placed and consolidated by the intended consolidation methods.

4.2.1.1 Effects of the mineralogy of fine aggregates

The mineralogy of fine aggregates is not considered an influential factor on the fresh properties of mortar and concrete. Thus, the differences that could be detected in the behavior of fresh concrete incorporating fine aggregates with different mineralogy are mainly not related to the difference in the mineralogy, but to the other sand characteristics, such as the shape and the high percentage of fines (*Akrout et al., 2010*).

In the study conducted by (*Safiddine et al., 2017*), despite the difference in their mineralogy, the siliceous (M1S0) and the limestone (M1L0) crushed sands, with the same grains shape and particle size distribution, present close rheological properties (Figure I.15). However, a remarkable difference is detected between the crushed sand mortars and the natural sand mortar (M1R0), due to the difference in the shape and the particle size distribution of these two types of sand.

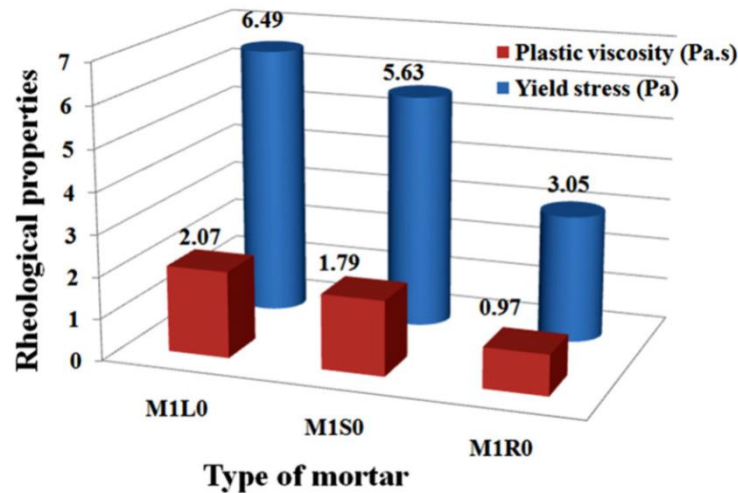


Figure 1.15 Rheological properties between mortars incorporating limestone crushed sand MIL0, siliceous crushed sand MISO, and river natural sand MIR0 (Safiddine et al., 2017)

4.2.1.2 Effects of the morphology of fine aggregates

The fine aggregates morphology could play an important role in the workability of concrete. For the same mineralogy, (Saikia and De Brito, 2014) observe that the slump of concrete changes when the plastic wastes are used in different shapes, as an alternative to natural sand. When incorporated as pellet-shaped (cylindrical/spherical) particles, the slump of concrete is slightly increased (from 122 to 132 mm) with a lower water to cement ratio (from 0.53 to 0.52). Contrarily, the use of flaky particles negatively affects the workability and requires a higher amount of water (the water to cement ratio is increased from 0.57 to 0.64) to reach a comparable slump (120 mm) as the quartzite natural sand concrete (122 mm).

Sand composed of spherical particles with a smooth surface could induce a positive effect on the fresh behavior of concrete by reducing the friction between the particles in the fresh mix. The more spherical the particle is, the more beneficial it could be. In the study conducted by (Choi et al., 2009), compared to natural river sand mortar, the mortar flow increases linearly with the incorporation of the plastic wastes grains with a glassy surface. The 25% replacement produces a combination of fine aggregates with a particle size distribution similar to the one of the natural sand. The researchers observe that the flow slightly increases by 4% and it could reach 16% with the total replacement, even though the plastic wastes are characterized by a poor gradation. In this study, the concrete behavior is also assessed and the results show that the slump increases from 100 to 223 mm, 105 to 214 mm, and 135 to 205 mm for fixed water to cement ratio of 0.53, 0.49, and 0.45 respectively. Similarly, in the study of (Dos Anjos et al., 2017), the improvement of the workability with the addition of copper slag as fine aggregate in concrete is attributed to the smooth and spherical particles of the blasted copper slag.

On the contrary, the angularity and rough surface of crushed sand tend to increase the friction between grains and reduce the workability of fresh concrete. The slump decreases from 65 to 35 mm for the total replacement by crushed granite (Kou and Poon, 2009) and 70 to 10 mm when the bottom ash totally replaces the natural river sand (Singh and Siddique, 2014). Likewise, the admixture demand has to be increased by 40% for 50% replacement of the natural siliceous river sand by crushed granite sand in the study of (Cordeiro et al., 2016) and 14% for total replacement in the study of (Shen et al., 2017). Similarly, for an addition of 20% of angular rubber ash, the admixture dosage varies from 2.1 to 2.6%, 0.5 to 1.6%, and 0 to 0.9% for a W/C of 0.35, 0.45, and 0.55 respectively (Gupta et al., 2014).

Thus, the angular sand requires a higher paste demand to provide adequate flowability to concrete (Cortes *et al.*, 2008). Besides, to get the same workability for the same cement content, the angular sand particles with a rough surface require more water than the rounded sand particles with a smooth surface (Kabbani, 1967).

The common practice adopted in several studies to compensate for the water demand consists of increasing the water content of the concrete mixes incorporating angular and rough sand particles. However, instead of adding water and increasing the water to cement ratio of mixes, the loss in the workability of concrete with angular and rough sand particles could be overcome by the addition of an adequate quantity of superplasticizer. This chemical admixture reduces the agglomeration of the cement grains and reduces the amount of water needed to maintain workability (Bederina *et al.*, 2013). In virtue of this deflocculation effect, the superplasticizer reduces the porosity between the cement particles and increases the fresh density, limiting thus the voids ratio (the ratio of the difference between the total volume and the solid volume to the solid volume) of fresh concrete. In the study of (Li and Kwan, 2014), the addition of the superplasticizer attenuates the voids ratio of the concrete mix by 39%, it varies from 0.28 to 0.17%. However, it should be noted that, despite its positive effect on the initial workability of concrete, certain types of superplasticizers could present a negative effect on slump retention since the electrostatic repulsion effect of the admixture (Figure I.16a) depends on the dissolved ions and could diminish as far as the cement is hydrated (Thomas and Wilson, 2002). Hence, the slump loss could increase more rapidly in mixes containing water-reducing admixture, compared to the mixes where the required workability is achieved by increasing the water content (Makhloufi *et al.*, 2014). This effect is reduced in the admixtures operating with the steric hindrance mechanism (Figure I.16b): a long side-chain still operates and keeps the cement grains physically dispersed even when the effect of the electrostatic repulsion is reduced (Thomas and Wilson, 2002).

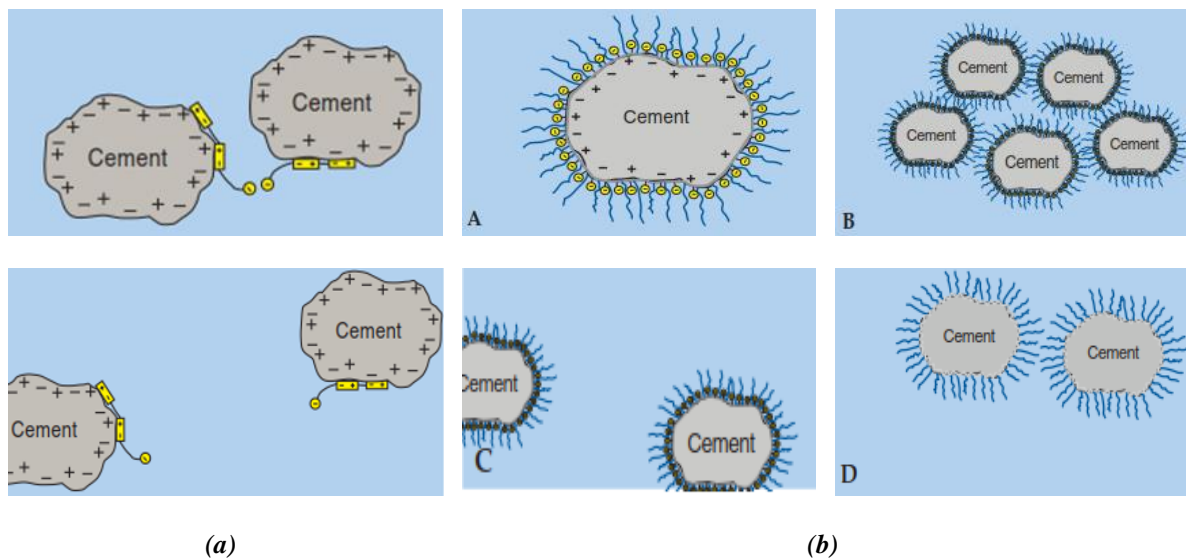


Figure I.16 Mechanism of (a) dispersive action of water-reducing admixture and (b) steric hindrance of polycarboxylate water-reducing admixture (Thomas and Wilson, 2002)

4.2.1.3 Effects of the physical properties of fine aggregates

In addition to the morphology of sand, the particle size distribution could also have a significant effect on the properties of fresh concrete. It was even proved that the particle size distribution of fine aggregates could be a predominant factor in the fresh properties of concrete over the morphology of its

grains. Indeed, for the same gradation and fines content of sand, (Shen *et al.*, 2018) observe the same slump values for two types of concrete with two different sand shapes: spherical and angular.

In a continuous granular skeleton, the quantity of cement paste needed to fill the intergranular voids between aggregates particles decreases, providing an additional quantity available to cover the surface of aggregates and to lubricate them. Therefore, for the same cement content, the discontinuous granular skeleton reduces the flowability of concrete (Santos *et al.*, 2015; Jiao *et al.*, 2017). Additionally, the risk of segregation and bleeding could be limited with the well-graded fine aggregates. The intermediate and small size particles fill the intergranular voids and prevent the coarser particles to settle and segregate (Figure I.17).

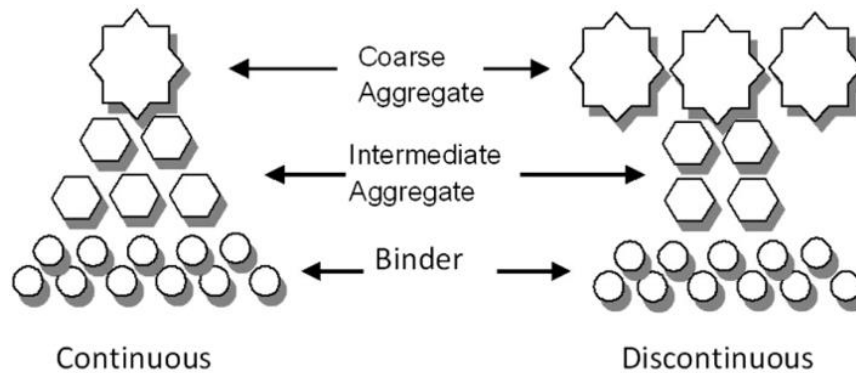


Figure I.17 Difference between continuous and discontinuous granular skeleton (Santos *et al.* 2015)

(Lagerblad *et al.*, 2014) show that, when the grading of sand is optimized, the yield stress and the plastic viscosity of mortar decrease (Figure I.18) since the well-graded fine aggregates reduce the voids between particles and thus provide to mortar a better ability to flow.

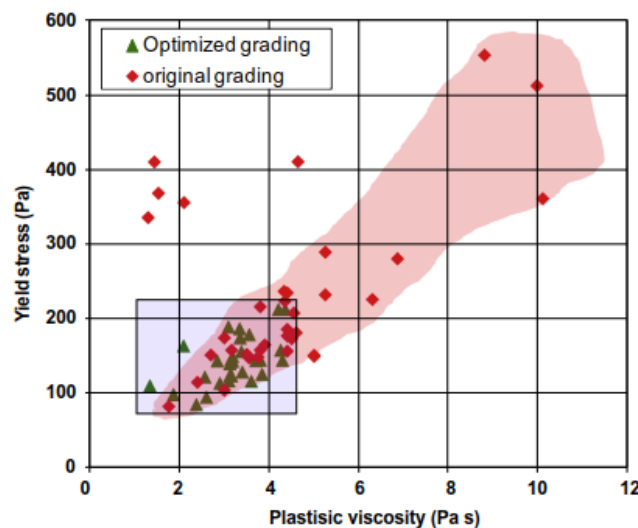


Figure I.18 Rheological properties of mortar with optimized and original grading (Lagerblad *et al.* 2014)

In addition to the particle size distribution, the absorption and the porosity of fine aggregate could also influence the fresh behavior of concrete. The higher absorption and porosity of the sand leads to higher water demand in concrete mixes. Accordingly, the water that could be absorbed by the fine aggregate is usually determined and added to the water that would be used for the cement hydration, to avoid any effect on the workability of concrete. However, in some studies, such as those conducted by (Kou and

Poon, 2009; Akrouf et al., 2010; Saikia and De Brito, 2014), the absorption of the different types of fine aggregate is not taken into consideration in the mixing and the water demand of concrete is affected.

The specific gravity of fine aggregates could also be an influential factor on the fresh properties of concrete, particularly its fresh density. This effect is observed in previous studies when the natural sand is replaced by different types of fine aggregates. When the specific gravity of the alternative sand is lower than the specific gravity of the original natural sand, the fresh density of concrete is obviously reduced, while it is increased when the alternative sand is characterized by higher specific gravity. Accordingly, the fresh density of concrete decreases with the coal bottom ash (*Singh and Siddique 2014*) and the crushed tiles (*Topçu and Bilir, 2010*), whereas it increases with the slag (*Qasrawi et al., 2009*).

4.2.1.4 Effects of the fines content of fine aggregates

In addition to the morphology and physical properties, the fines content in the sand could also affect the fresh behavior of concrete. At fixed cement content and water to cement ratio, the incorporation of fine aggregate with an adequate percentage of fines fills the gaps between the aggregates and increases the fluidity of mortar. This effect remains beneficial as far as the percentage of fines is equal to or below the optimum level required to fill the interparticle voids. Above this level, the surface area of fine aggregates increases, leading to higher water demand. Since the water absorbed by the fines is usually not taken into consideration in the determination of the effective water in the concrete mix design, the workability could decrease.

The two opposite effects of the fines content in the sand on the fresh behavior of concrete are observed in several studies. For fixed water to cement ratio (0.4) and the same admixture content (0.7%) (*Ding et al., 2016*), the increment of the percentage of the limestone fines from 5 to 9% of the crushed limestone sand mass, have played a positive role in increasing the slump of concrete, from 110 to 160 mm. On the other hand, when the percentage of fines reaches 13%, the slump decreases to 45 mm. (*Westerholm et al., 2008*) also observes that the yield stress of mortar begins to increase linearly when the fines content exceeds 16%.

For the same reasons, similar fines content could differently affect loose and dense concrete microstructures. The beneficial effect of fines is more pronounced in the loose microstructure with high water to cement ratio and low cement content. However, in a dense microstructure, the fines could negatively affect the concrete workability since a high content of fines is not required to fill the intergranular voids of such microstructure. At fixed water to cement ratio and cement content of 0.5 and 420 kg/m³ respectively, (*Çelik and Marar, 1996*) have found that, when the crushed rock fines replace the limestone crushed sand from 0 to 30% by mass, the slump decreases from 92 to 60 mm. It is remarkable that, despite the high addition of the fines content in the fine aggregates, the difference is not so significant since the precision of the slump test is 10 mm. Similarly, the slump flow of self-compacting concrete decreases from 845 to 665 mm with the incorporation of the fines content up to 20%, in a concrete mix with a water to cement ratio of 0.4 and a cement content of 490 kg/m³ (*Benyamina et al., 2019*).

In addition to the workability, the density of fresh concrete could be increased by the high percentage of fines generated by the sand. Thus, they act as a filler and reduce the air content in concrete mixes. In the study of (*Çelik and Marar, 1996*), when the percentage of fines varies from 0 to 30%, the air content decreases from 2.77 to 1.28%.

4.2.1.5 Effects of the deleterious particles of fine aggregates

The nature of the fines particles ($< 75 \mu\text{m}$ sieve) contained in the fine aggregates could also play a significant role in the workability of concrete. The presence of high content of deleterious particles, such as clay, could form a coating at the surface of sand grains, increasing thereby the water demand of concrete (Hasdemir *et al.*, 2016). By comparing several manufactured sand with different stone powder, gradation, and impurities percentage, (Shen *et al.*, 2016; Shen *et al.*, 2018) have found that the effects of the gradation and the contents of stone powder and clay lumps in fine aggregates predominate those of the particle shape and the micro-roughness of the sand grains. The concrete incorporating angular manufactured sand, with lower stone powder and clay lump content than the rounded natural sand, demands a lower dosage of superplasticizer than the natural sand concrete, even though the shape of the manufactured sand is more detrimental for the concrete workability.

(Hasdemir *et al.*, 2016) conduct the methylene blue absorption test (EN 933-9, 2010) to have an indication of the clay content in the sand and to evaluate its effect on the concrete workability. They have reported that, in order to reach a similar slump for fixed water to cement ratio, the dosage of admixture in concrete mixes evolves in the same way as that of the methylene blue absorption value of the sand samples (Figure I.19). The higher the methylene blue value, the higher the clay minerals which demand a high amount of water and absorb a part of the admixture quantity. (Lagerblad *et al.*, 2014) also observe that a high quantity of mica and clays in the fine fraction of aggregates could increase the water demand and decrease the concrete workability.

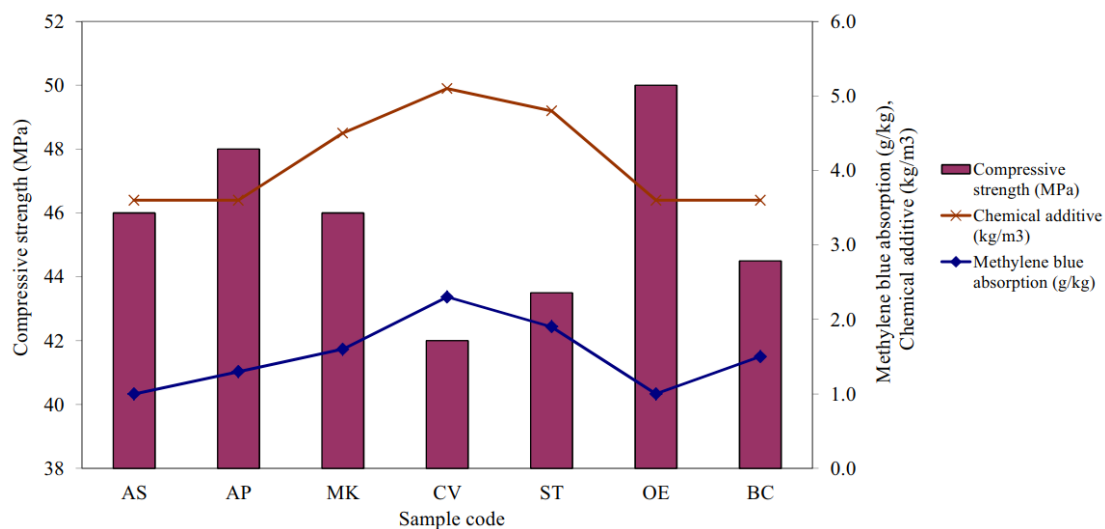


Figure I.19 Relationship between the methylene blue absorption of sand samples, the admixture content, and the compressive strength of concrete mixes in order to get the same slump for fixed water to cement ratio (Hasdemir *et al.*, 2016)

4.2.1.6 Effects of the proportion of fine aggregates

It is worth noting that some studies show that the effect of fine aggregates on workability and rheological properties of mortar and concrete could be less or more pronounced depending on the contribution of the fine aggregates' proportions and the solid phase in concrete mixes. In concrete with low water to cement ratio, the effects of the solid phase, and thus those linked to the fine aggregates' characteristics, could be predominant, whereas they could be non-influent for high water to cement ratio. (Kim *et al.*, 2018) notice that the increase in the slump, due to the total replacement of natural sand by the glass waste, varies from 186% to 46% when the water to cement ratio changes from 0.35

to 0.55, due to the higher water content and lower proportion of the solid phase (cement added to the fine aggregates) in the latter mix. (Gonçalves *et al.*, 2007) observe that for water to cement ratio equal to 0.4, the consistency of mortar depends on fine aggregates' characteristics, specifically the particle shape and grading. In contrast, for the water to cement ratio of 0.5, the workability of mortar is quasi-independent on fine aggregates' properties due to the lower proportion of the solid phase in the mix.

4.2.1.7 Summary of the fine aggregates characteristics' on the fresh properties of concrete

Table I.3 summarizes the main effects of the fine aggregates characteristics' on the fresh properties of concrete.

Table I.3 Effects of fine aggregates' characteristics on the fresh properties of concrete

Fine aggregates characteristics	Effects and mechanisms
Mineralogy	No reported effect
Morphology	Spherical-Smooth surface Positive effect: Reduce the interparticle friction
	Angular-Rough surface Negative effect: Increase the interparticle friction
Gradation	Well-graded Positive effect: Increase the mix compactness
	Non-conform grading Negative effect: Increase the cement demand to fill the interparticle voids
Fines content	Lower than the optimum Positive effect: Help to lubricate the coarser aggregates particles
	Higher than the optimum Negative effect: Increase the water demand
Deleterious particles and impurities	Negative effect: Increase the water demand

4.2.2 Effects of fine aggregates characteristics' on the mechanical behavior of concrete: strengths and modulus of elasticity

The compressive strength, the tensile strength determined by splitting or by flexural tests, and the modulus of elasticity are important criteria to characterize the mechanical behavior of concrete. Hence, the effects of the characteristics of fine aggregates on these properties are assessed in several studies.

4.2.2.1 Effects of the mineralogy of fine aggregates

The compatibility between the mineralogy of fine aggregates and the hydration products could create a chemical reaction that enhances the bond between the paste and the sand, leading to the improvement of concrete mechanical behavior. For example, the carbonate ions in the limestone sand could react with the primary hydration product to form a secondary hydration product, the calcium hydro-carbo-aluminate (Farran, 1956; Grandet and Ollivier, 1980; Ollivier *et al.*, 1995). Conversely, some types of fine aggregates, such as plastic wastes, could not allow a chemical reaction with the hydration products of concrete. The weak resulting bonding with cement paste reduces the compressive strength of concrete by approximately 40% for a replacement level of 12.5-15% (Saikia and De Brito, 2014; Hama and Hilal, 2017).

Additionally, the fines particles of the sand could behave differently in the concrete according to their mineralogy and affect the mechanical behavior of concrete. (Bonavetti and Irassar, 1994) evaluate this difference by adding three types of fines to natural siliceous sand in concrete (Figure I.20).

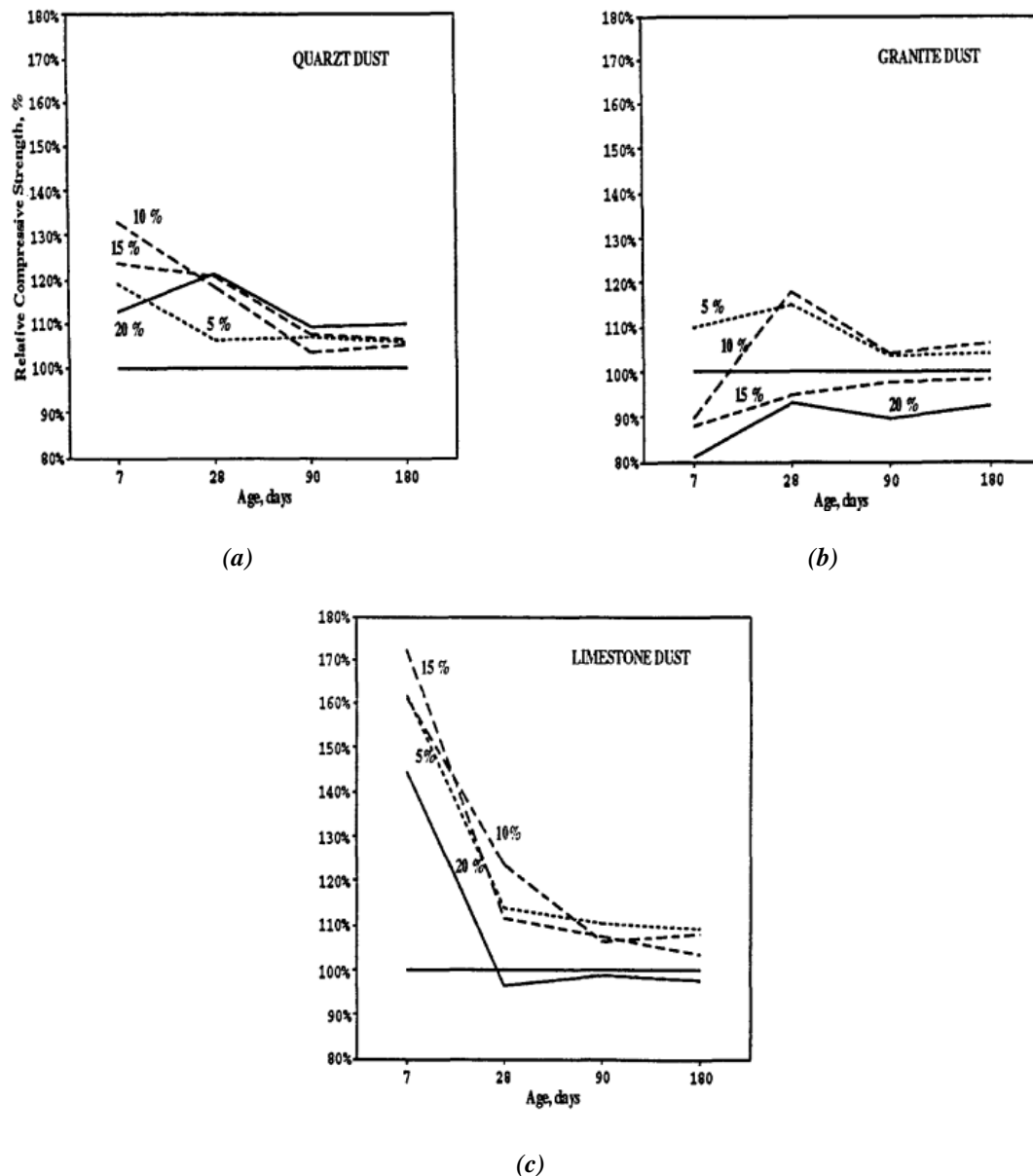


Figure I.20 Effect of different types of fines on the compressive strength of concrete (Bonavetti & Irassar, 1994)

5-20% of quartz dust improves the strength with a maximum increase of 32%. 15-20% of granite dust tends to decrease the compressive strength at all ages, while a percentage of 10% seems detrimental only at 7 days. The addition of limestone fines leads to a strong enhancement of compressive strength (44-72%) at 7 days, with no detrimental effect at a later age. The limestone fines could act as nucleation sites for the hydration products which accelerate the cement hydration at early age (Bonavetti and Irassar, 1994). This effect is also observed by (Benyamina et al., 2019) where the incorporation of the limestone fines increases the compressive strength of concrete at 3 and 7 days, despite the slight decrease of the 28-day compressive strength.

Due to their pozzolanic properties, the fines of some types of sand could also react with the free lime in concrete to form C-S-H gels which improve the mechanical behavior at a late age. This activity is detected in several studies, where the incorporation of some alternative sand provides a significant increase in the compressive strength, at an age above 28 days, compared to the natural sand concrete. In the bottom ash concrete and the natural sand concrete, the 90-day compressive strength increases from the 28-day compressive strength by 19.1 and 6.8% (*Singh and Siddique, 2014*), and 42 and 10% (*Rafieizonooz et al., 2017*) respectively. Similarly, in the study of (*Aggarwal and Siddique, 2014*), the gain in compressive strength from 28 days to 365 days, in the concrete containing ash and foundry sand is higher (34-40%) than that in the control mix (22%).

4.2.2.2 Effects of the morphology of fine aggregates

The morphology of fine aggregates is reported to be an influential factor in the mechanical behavior of concrete. The angular sand with a rough surface improves the bond between the sand grains and the cement paste, thus providing higher strength than the concrete incorporating rounded or spherical sand particles with a smooth surface.

At fixed water to cement ratio for different slumps or different admixture content, the crushed sand concrete is characterized by a higher compressive strength (10%) compared to concrete incorporating natural siliceous sand with similar fineness modulus as the crushed granite sand (*Donza et al., 2002*). However, this positive effect of the angular rough sand is undetectable in some studies, where the loss of workability in concrete is compensated by the addition of the water content. Thus, the total replacement of natural sand by angular crushed sand reduces the compressive strength of concrete by 7% and by 12-19% in the study of (*Kou and Poon, 2009; Akrouf et al., 2010*) respectively. Since each mix is characterized by optimum water to cement ratio for which the maximum solid concentration and minimum void ratio are attained (*Li and Kwan, 2014*), the excess water content above this optimum decreases the solid concentration and increases the voids ratio, modifying thereby the concrete behavior at the hardened state.

It should be noted that, despite the variation of the water to cement ratio, the effect of shape could sometimes be predominant. In the study of (*Saikia and De Brito, 2014*), when comparing two mixes incorporating 5% of plastic wastes with two different shapes, the concrete with the angular particles presents close strengths to the concrete with the spherical particles, despite the lower water to cement ratio in the latter (0.57 and 0.53 respectively), emphasizing the beneficial effect of the angularity of fine aggregate on concrete strengths. However, at higher incorporation levels of plastic wastes (10 and 15%), this effect is replaced by that of the higher water to cement ratio (0.60 and 0.64 respectively) in the mixes containing angular sand grains. Similarly, an 8-11% higher compressive strength is observed for the concrete incorporating manufactured sand with angular shape grains even if its water content is 10% higher than the one of the natural sand concrete (*Yamei and Lihua, 2017*).

4.2.2.3 Effects of the physical properties of fine aggregates

As already discussed in the previous section, if the granular distribution is too coarse, the concrete mix risks segregating and bleeding. On the contrary, if it is too fine, the concrete mix will require higher water demand. (*Sabih et al., 2016*) study the effect of the optimization of the gradation and fineness modulus of different types of sand on the concrete compressive strength. They have found that, for the same water to cement ratio and cement content, the optimization of sand gradation to conform to the ASTM specifications, significantly increases the concrete compressive strength (8-39%). In the study of (*Shen et al., 2018*), the 28-day compressive strength is not affected by the

optimization of the gradation of a metasandstone manufactured sand, while it increases by approximately 12% when the natural river sand gradation is optimized. Thus, the researchers conclude that the original gradation of the manufactured sand does not play a significant negative role in the concrete compressive strength and does not negatively affect the concrete even if this sand is not well-graded.

The crushing value of fine aggregate, which indicates the ability of an aggregate to resist crushing by measuring the percentage by weight of the crushed materials, could also be an influential factor in the mechanical behavior of concrete. (*Li et al., 2011*) observe that the concretes incorporating sand with the lowest crushing value are characterized by the highest flexural strengths. However, they do not detect a clear relationship between the crushing value of sand and the compressive strength of concrete. In their study, the limestone manufactured sand characterized by lower crushing values than the river siliceous sand helps to improve the flexural strength of concrete.

In addition to the gradation and the crushing value, the modulus of elasticity of the fine aggregate could also influence that of the concrete. Usually, the dependence of the modulus of elasticity of concrete on the modulus of elasticity of coarse aggregates is more pronounced than the one of fine aggregates since the coarse aggregates occupy a relatively higher volume in concrete. However, some studies show that the modulus of elasticity of concrete could also depend on the modulus of elasticity of fine aggregates, according to their proportions in the mix. In the study of (*Gupta et al. 2014*), for a high water to cement ratio of 0.55, the modulus of elasticity seems not affected by the 20% replacement of natural sand by rubber ash in concrete. In contrast, when the water to cement ratio is reduced to 0.35, the modulus of elasticity of concrete decreases by 17%. In the study of (*Singh and Siddique, 2014*), for water to cement ratio of 0.45, the use of coal bottom ash which is characterized by a finer particle size distribution induces a 21% lower modulus of elasticity, which remains in the typical range of the modulus of elasticity for the designed compressive strength.

In other studies, the reduction of the modulus of elasticity of concrete with different alternative sands is mainly the result of a higher porosity of concrete due to the higher water to cement ratio in these mixes, compared to the reference concrete. In the study of (*Saikia and De Brito, 2014*), the modulus of elasticity is 60% lower when the water to cement ratio is increased from 0.53 to 0.74 to compensate for the high water demand of 15% content of plastic wastes in concrete. On the other hand, in the same study, when the water to cement ratio remains the same, the modulus of elasticity decreases by 12.5%, due to the lower stiffness of the plastic wastes compared to that of the quartzite sand.

By working in the mortar, (*Topçu and Bilir, 2010*) observe that the lower modulus of elasticity and the porous structure of the crushed tiles decrease the modulus of elasticity, compared to a mortar incorporating normalized sand. The modulus of elasticity decreases by 52-83% for a replacement ratio varying between 0 and 100%.

4.2.2.4 Effects of the fines content of fine aggregates

Concerning the effect of the content of fine particles in the sand, studies show that a high percentage of fines could be beneficial for the mechanical behavior of concrete. Generally, the enhancement of the mechanical behavior is attributed to the improvement of the bond between the cement paste and aggregates due to a better homogeneity of the system (*Achour et al., 2008*) and the increase of the mix packing density (*Gonçalves et al., 2007*).

(*Gonçalves et al., 2007*) compare two types of concrete with crushed sand characterized by two different content of fines. The classified sand is subjected to an air classification technique to limit the fines

generated during the crushing process, and the unclassified sand is used without the reduction of its fines content. The reduction of fines from 14.5% to 1.6% and 17.7% to 4.8% lower the packing density of the mixes and reduce the 28-day compressive strength of about 23-25% and 10-19% for a vertical shaft crusher and cone crusher respectively. However, this positive effect of the high percentage of fines could be lowered or eliminated if the fines content exceeds the optimum percentage of each mix. Fines content above the optimum percentage could even negatively affect the concrete mechanical behavior. This optimum content differs from one mix to another. It depends on the concrete microstructure, which is determined by the water to cement ratio, the cement content, and the granular skeleton of aggregates.

The effect of the variation of the fines percentage on mechanical behavior is illustrated in (Figure I.21). The 7 and 28-day compressive and flexural strengths increase linearly with the percentage of dust until 10% (Çelik and Marar, 1996). Above this value, both types of strengths begin to decrease. Despite this reduction, the strengths remain higher than the ones of the control mix (0% dust) even with a dust percentage of 30%, except for the 28-day flexural strength which is slightly (< 10%) lower than the flexural strength of the control mix (Figure I.21a). The same trend and optimum percentage are observed for the 28-day compressive strength in the study of (Li et al., 2011). As for the flexural strength, when the fines content exceeds 10%, the values slightly change but remain in the same range (Figure I.21b).

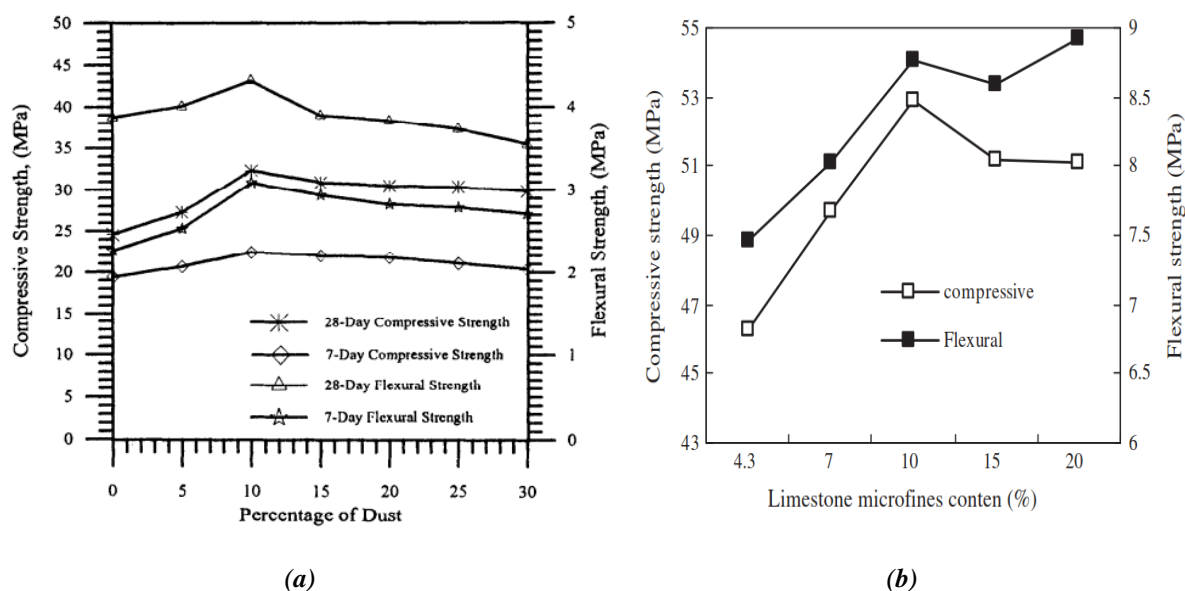


Figure I.21 Effect of fines content on the mechanical behavior of concrete in terms of compressive and flexural strengths (a) (Çelik and Marar, 1996) and (b) (Li et al., 2011)

In a lean microstructure, the high percentage of fines contributes to filling the intergranular voids (Kronlof et al., 1994). However, in a dense microstructure, the cement content could be high enough to fill the intergranular voids. Thus, the excess quantity of fines that is not beneficial to fill the voids, requires a higher amount of cement to cover the grains, decreasing thereby the compressive strength of concrete. Accordingly, (Ding et al., 2016) prove that, for minimum water to cement ratio of 0.45, the use of manufactured sand with limestone powder content up to 13% gives a high long-term compressive strength (Figure I.22). However, for lower water to cement ratio, this fines content should be reduced to 9% to avoid any decrease in the concrete compressive strength.

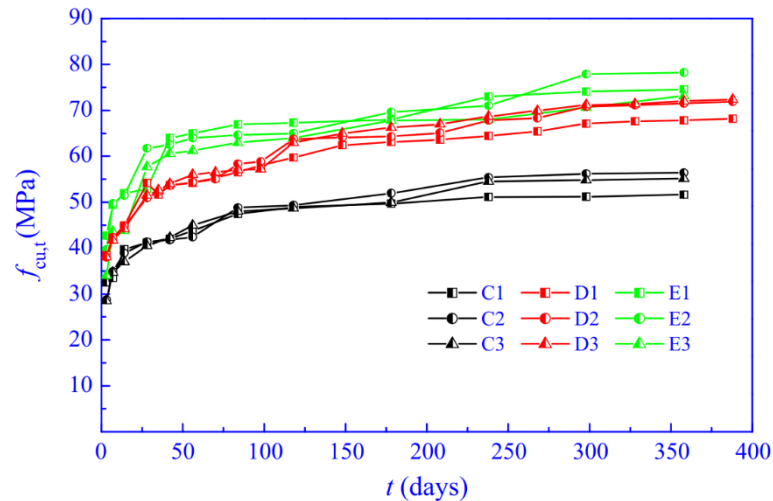


Figure I.22 Evolution of the compressive strength with time for different water to cement ratio and different fines content (C: W/C = 0.56; D: W/C= 0.45; E: W/C= 0.40; 1: 5% fines; 2: 9% fines; 3: 13% fines); samples were water cured at 20 ± 2 °C (Ding et al., 2016)

This effect of fines in a dense microstructure is also observed in the study conducted by (Qasrawi et al., 2009). The adequate replacement percentage of natural sand by steel slag depends on the cement content (50% for 330 kg/m^3 and 427 kg/m^3 , and 30% for 536 kg/m^3). The steel slag sand is characterized by angular grains and high fines percentage (20.5%). Thus, at low cement content, its fines enhance the bond between aggregates and cement paste, densify the concrete structure, and increase the compressive strength of concrete. In the study of (Akrouf et al., 2010), when the fine crushed limestone sand (14.2% of fines) replaces the siliceous sand (1.7% of fines), the decrease in the compressive and flexural strengths of concrete is more remarkable (about 13%) at a high cement content of 400 kg/m^3 . Additionally, the increment of fines content could be detrimental to the mechanical behavior of high water to cement ratio concrete (0.6) if additive cementitious materials (10-15% of pozzolan or slag) are incorporated (Khouadjia et al., 2015). It should be noted that, in all the aforementioned studies, the samples used for the assessment of the concrete strengths are water cured at room temperature (20 ± 2 °C).

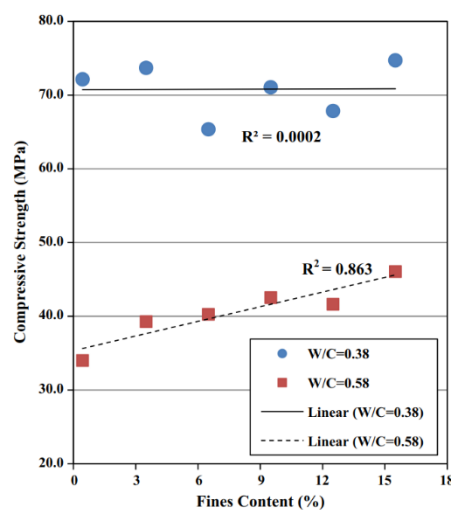


Figure I.23 Effect of fines content on the 28-day compressive strength of concrete (Gokce et al., 2016)

In some studies, such as the one of (Gokce et al., 2016), at low water to cement ratio of 0.38 and cement content of 380 kg/m³, the variation of the content of the limestone fines from 0 to 15% does not influence the 28-day compressive strength of concrete samples, cured in lime-saturated water at 20 ± 2 °C (Figure I.23).

4.2.2.5 Effects of the deleterious particles in fine aggregates

The presence of impurities in fine aggregates could also change the mechanical performance of concrete. They could form a coating at the surface of sand grains and thus reduce the adherence of the latter with the cement paste. Thus, the higher the content of these impurities, the lower could be the compressive strength of mortar and concrete.

In the study of (Hasdemir et al., 2016), the compressive strength of concrete is determined for different concrete mixes incorporating fine aggregates with different content of deleterious particles. The presence of high clay amount in the fine aggregate (translated by high methylene blue value 2.3 g/kg and low sand equivalent 78%) reduces the concrete compressive strength from 50 to 42 MPa compared to the concrete incorporating fine aggregate with comparable mineralogy but with lower clay content (methylene blue value 1 g/kg and sand equivalent 93%). (Coppio et al., 2019) have assessed the effect of foundry sand, previously used as a molding material in the metal industry, as an alternative to natural sand in concrete. They have concluded that the presence of metal residues in the foundry sand could explain the decrease of the compressive strength of the foundry sand concrete (a decrease of 22 to 43%). Additionally, (Dos Anjos et al., 2017) attribute the cause of the decrease of compressive (11.5%) and splitting tensile strengths (33.5%) of concrete containing 40% of copper slag as a replacement to natural ravine sand, to the organic impurities present on the surface of the blasting copper slag (i.e. paint particles, anti-oxides, and rust).

4.2.2.6 Summary of the effects of the fine aggregates' characteristics on the mechanical behavior of concrete

The effects of fine aggregates characteristics' on the mechanical behavior of concrete are recapitulated in Table I.4.

Table I.4 Effects of fine aggregates' characteristics on the mechanical behavior of concrete

Fine aggregates characteristics		Effects and mechanisms
Mineralogy		<p>Positive effect:</p> <ul style="list-style-type: none"> - Create a nucleation site that accelerates the cement hydration at early age - Produce secondary C-S-H as a consequence of the pozzolanic activity - The calcite could react with the hydration products to form hydro-carbo-aluminate
		<p>Negative effect:</p> <p>Decrease the bond with the cement paste</p>
Morphology	Spherical-Smooth surface	<p>Positive effect:</p> <p>Increase the bond with the cement paste</p>
	Angular-Rough surface	<p>Negative effect:</p> <p>Decrease the bond with the cement paste</p>
Gradation	Well-graded	<p>Positive effect:</p> <p>Increase the compactness of the mix</p>
	Non-conform grading	<p>Negative effect:</p> <p>Increase the interparticle voids</p>

Fine aggregates characteristics		Effects and mechanisms
Fines content	Lower than the optimum	Positive effect: Fill the interparticle voids
	Higher than the optimum	Negative effect: Increase the uncoated sand particles by the cement paste
Deleterious particles and impurities		Negative effect: Lower the adherence of sand grains with the cement paste

4.2.3 Effects of fine aggregates' characteristics on the mechanical behavior of concrete: shrinkage deformations

The presence of water in the concrete is essential for the hydration reaction of the cement paste, but when this water is used for hydration or leaves the concrete by evaporation, it creates a shrinkage in concrete volume (*Neville and Brooks, 1987*).

4.2.3.1 Types of shrinkage

The origin of the shrinkage in concrete could be classified into different categories:

- **Plastic shrinkage**

Plastic shrinkage is the contraction that occurs when the cement paste is in its plastic state before hardening, thus it is usually of short duration. It is the result of the surface water evaporation due to hydric exchange with a dryer environment or the suction of water from concrete by adjacent dry concrete or soil (*Neville and Brooks, 1987*), coupled with the effects of settling and bleeding of the material. Due to the difference in the hydric conditions between the surface and the inner concrete, this shrinkage induces tensile stress during concrete hardening. Thus, the cracks could occur when the evaporation process at the surface is faster than the bleeding process to the surface (*Lerch, 1957 as cited by Cohen et al., 1990; Kosmatka and Wilson, 2011*).

- **Chemical shrinkage**

The chemical shrinkage is the reduction in the volume of the cementitious paste due to the hydration reaction since the hydration products occupy less volume in the mix than the volume originally occupied by the water and the unreacted materials (*Le Chatelier, 1900*). The chemical shrinkage could be presented as the ratio of the volume reduction during hydration to the initial volume of the cement paste (unhydrated cement and water) before hydration (*Tazawa et al., 1995*).

- **Autogenous shrinkage**

Even when there is no moisture exchange to or from the concrete, a shrinkage still occurs (*Neville and Brooks, 1987*). This shrinkage is known as autogenous shrinkage. It develops within sealed conditions, without subjection to change in external hydrothermal conditions (*Neville and Brooks, 1987; ASTM C125, 2016*). Thus, during the autogenous shrinkage, the cementitious materials shrink without any weight change.

The contraction of the material is caused by the capillary forces which occur in the pores when their water content decreases due to hydration. The capillary pores are assumed to have a spherical form and the pressure is determined by the Laplace formula:

$$P_w = \frac{2 \sigma_w}{r_w} \quad (\text{Eq. I.9})$$

Where σ_w is the surface tension of water (0,073 N/m) and r_w the radius of the capillary pore (m).

A higher cement quantity needs higher free water for hydration. Thus, the higher the available free water, the lower the autogenous shrinkage since the needed water for hydration is easily used without inducing capillary tensions. Moreover, a concrete structure with finer pores presents higher capillary tensions. Hence, this shrinkage increases when the microstructure becomes denser, and when the water to cement ratio decreases (*Tazawa and Miyazawa, 1995; Pons and Torrenti, 2008; Kosmatka and Wilson, 2011*). Consequently, the autogenous shrinkage is higher in the high-performance concrete compared to that of the normal strength concrete.

- **Desiccation shrinkage**

The desiccation or drying shrinkage is determined as the strain which occurs in the hardening concrete due to the loss by drying of the absorbed and free water when the concrete is placed in an unsaturated air of lower relative humidity compared to that of concrete (*Neville and Brooks, 1987; Topçu and Bilir, 2010*). During the drying process, the loss of water begins with the evaporation of the free water in the capillaries (*Neville and Brooks, 1987*).

The drying shrinkage could be reduced by appropriate curing (*Cortas et al., 2014*) since it is maximum at the surface and decreases at the inner parts of the concrete member (*Topçu and Bilir, 2010*). This variation in shrinkage induces tension at the surface of the concrete and compression at the inner parts of the concrete member, as illustrated in Figure I.24 (*Pons, 1998 as cited by Pons and Torrenti, 2008*). If tensile stress becomes higher than the material tensile strength, microcracks occur.

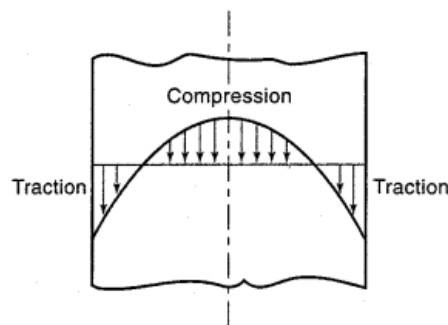


Figure I.24 Theoretical repartition of stress (Pons, 1998 as cited by Pons and Torrenti, 2008)

4.2.3.2 Effects of the aggregates' inclusion on the shrinkage of the cement paste

The inclusion of aggregates in concrete is beneficial in reducing the paste shrinkage (*Tazawa and Miyazawa, 1995*). First, by adding aggregates, the volume of the cement paste is reduced. Second, conventional aggregates are characterized by higher stiffness than cement paste, attenuating its shrinkage. This restraining action of the aggregates depends on the quality of the bond between the cement paste and the aggregates at the interface. Hence, the shrinkage behavior of concrete does not only depend on the paste characteristics but is also affected by the properties of the aggregates (*Belaribi et al., 1997*). Consequently, changing the type of aggregates in the concrete mixes could exhibit different shrinkage behavior (*Aquino et al., 2010; Lee et al., 2016*). The restraining of the shrinkage by the aggregates is more important when their modulus of elasticity is high. However, this confinement causes tensile stress in concrete at the ITZ, thus if the latter is of poor quality, the inclusion of aggregates could cause microcracks and make the concrete more vulnerable to the penetration of deleterious particles (*Topçu and Bilir, 2010; Cortas et al., 2014; Rezvani and Proske, 2017*). Furthermore, (*Pons*

and Torrenti, 2008) state that the aggregates of poor quality characterized by a low modulus of elasticity and a high porosity could produce concrete shrinkage deformations higher than expected.

The following sections consist of presenting the effect of fine aggregates characteristics on the shrinkage of concrete. It should be noted that the effect of coarse aggregates could be more pronounced than the effect of fine aggregates, since the higher the size and volume of aggregates, the higher the restraining action, thus the lower the drying shrinkage of concrete (Eguchi and Teranishi, 2005; Kou and Poon 2009; Lee et al., 2016), as shown in Figure I.25.

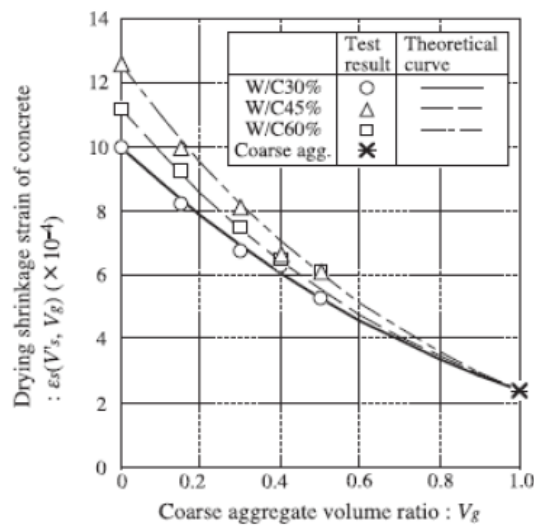


Figure I.25 The effect of the volume of coarse aggregates on the drying shrinkage of concrete (Eguchi and Teranishi, 2005).

4.2.3.3 Effects of the physical properties of fine aggregates

(Aquino et al., 2010) have found that despite the similarity in the size and volume of pores between the crushed limestone sand and the mountain sand (with no specification about the mineralogy), these two types of sand present different drying shrinkage behavior in concrete. For the same water to cement ratio, the concrete mixes incorporating crushed limestone sand develop less shrinkage than those with natural sand as the only fine aggregate. This reduction becomes significant (15%) for a replacement ratio that exceeds 40% (Figure I.26).

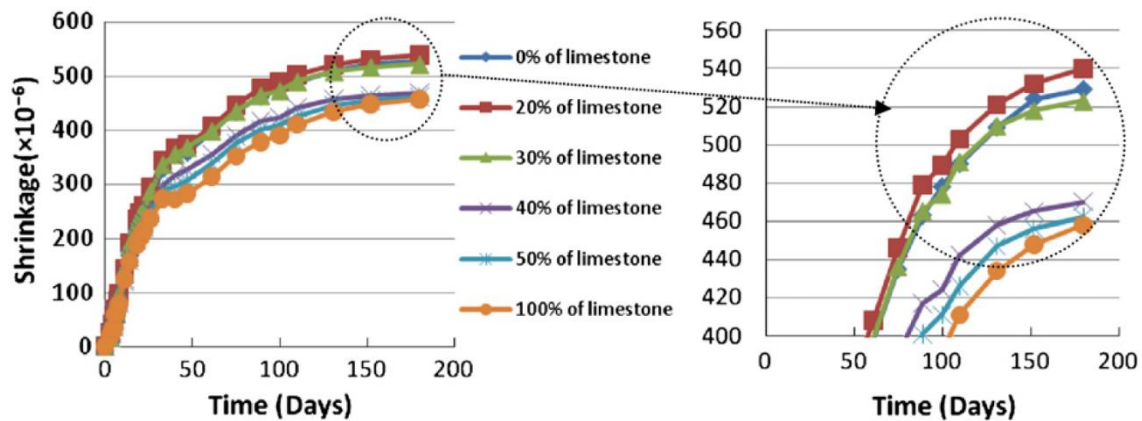


Figure I.26 The effect of the incorporation of crushed limestone sand on the drying shrinkage of concrete containing mountain sand (Aquino et al., 2010)

The researchers explain this result by the higher elastic modulus of the crushed limestone sand and the higher porosity of the mountain sand (0.021 and 0.025 mL/g for crushed limestone sand and mountain sand respectively). They consider that the more pores at the sand surface, the higher the adhered paste and its shrinkage. Besides, they consider that the additional water content in these pores could be detrimental and increase the shrinkage when the water escapes from aggregates.

Conversely, due to their high porosity, some alternatives to natural sand could act as a water reservoir in concrete. They could retain the moisture and then release it during the drying process, reducing thereby the shrinkage of concrete (*Aquino et al., 2010*). Due to this property, the shrinkage of concrete is decreased with the incorporation of furnace bottom ash, for the same water to cement ratio and volume of fine and coarse aggregates (*Bai et al., 2005; Kou and Poon, 2009*).

4.2.3.4 Effects of the deleterious particles in fine aggregates

The impurities in aggregates could also affect the shrinkage of concrete. The higher the clay and silt content, the higher the shrinkage deformation (*Kosmatka and Wilson, 2011*). This effect is demonstrated when the limestone is used as a filler in the study done by (*Rezvani and Proske, 2017*). They conclude that a higher content of shrinking clay in limestone produces a higher disjoining pressure, and increases the drying shrinkage of concrete.

4.2.3.5 Effects of the variations in the mix design parameters

In some studies, when the water to cement ratio is increased to compensate for the high water demand of fine aggregates (due to their shape or their high fines percentage), the drying shrinkage becomes higher as a result of the increase of the porosity in the mix. For example, in the study of (*Bonavetti and Irassar, 1994*), the incorporation of the limestone fines increases the water content in the mix and consequently the drying shrinkage of concrete.

4.2.4 Effects of aggregates characteristics' on the durability properties of concrete

Concrete durability is its ability to resist aggressive environmental, physical, and chemical conditions while maintaining its desired structural properties throughout its service life. The concrete durability mainly depends on the capacity of fluids to ingress and move through the concrete microstructure.

The transport of fluid and ions in the concrete microstructure is mostly governed by three mechanisms. The first is permeability, defined as the penetration of the fluid into the porous solid under a pressure gradient (*Khatib and Mangat, 1995*). The second mechanism is governed by diffusion due to the concentration gradient (*Atkinson and Nickerson, 1984*). The third is the absorption by capillary suction due to the surface stress created by the water in the interconnected voids (*Khatib and Mangat, 1995*).

These transport mechanisms mainly depend on the pore structure of concrete, created by a part of the mixing water and the entrapped and entrained air in the hardened cement paste (*Chen et al., 2012*). The evolution of hydration leads to a reduction of pores' size and their connection.

The water is present in concrete in three different forms (Figure I.27): chemically bonded if used in hydration, physically bonded to the solid particles by Van der Waals forces, and free water in capillary voids. Accordingly, the pores in the concrete could be classified into two categories (*Powers and Brownyard, 1946; Mindess et al., 1981 cited by Zhao et al., 2014; Chen et al., 2012*). The gel pores or

micropores (dimension < 100 nm) are the interlayer pores present in the cluster C-S-H sheets and are considered as part of the hydration products, while the capillary pores consist of the spaces originally occupied by mixing water.

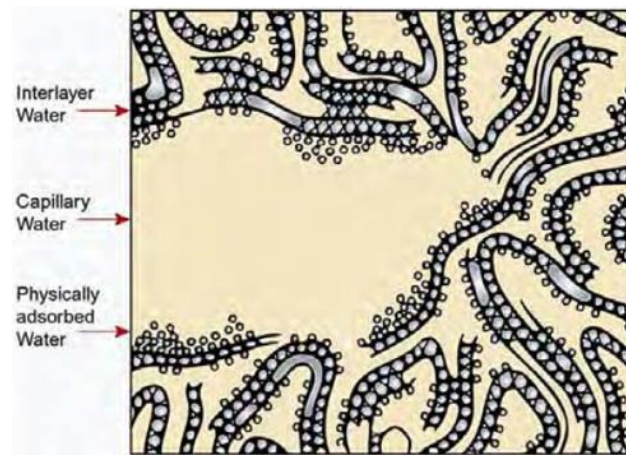


Figure I.27 Model of the three different forms of water in concrete
(Metha and Monteiro, 2006 cited by Chen et al., 2012).

The size and connectivity of capillary pores are the main factors that govern the transport mechanisms in concrete. The connectivity mainly dominates the effect of the porosity in determining permeability and diffusion (Neville and Brooks, 1987; Bellanger et al., 1993; Chia and Zhang, 2002; Yang et al., 2006; Neithalath and Jain, 2010). Thus, a material with high porosity but with a closed pore system could be tighter than a material with low porosity and open pores, since the higher the interconnectivity of pores, the higher the permeability (Figure I.28).

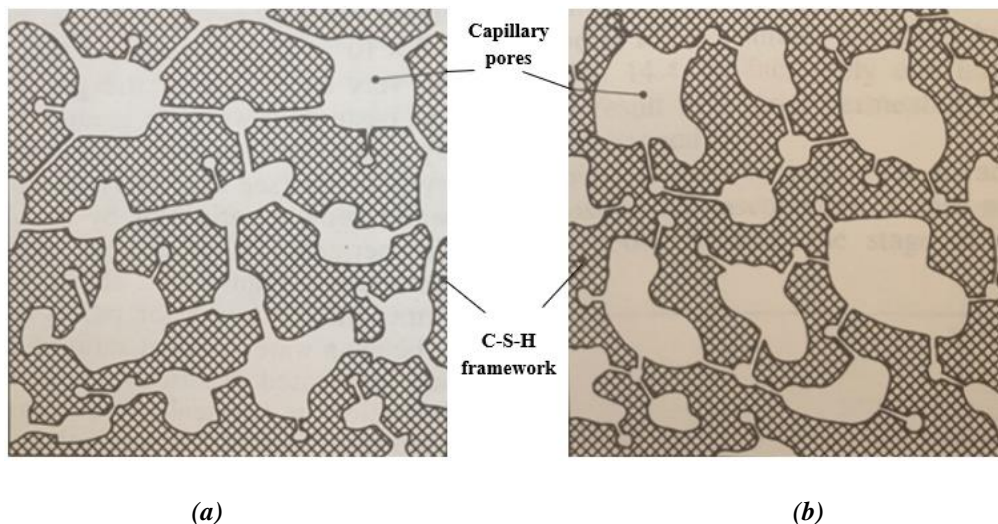


Figure I.28 Schematic representation of materials of similar porosity but (a) high permeability: interconnected capillary pores by large passages, and (b) low permeability: partly connected and segmented capillary pores (Neville and Brooks, 1987)

Thus, the pore structure of concrete cement paste is the main factor influencing its durability. However, this structure depends on the aggregates types. (Huiguang et al., 2011) demonstrated that the type of fine aggregate tends to be the second most influential factor in determining the permeability of concrete, after the curing conditions, for the same water to cement ratio and the same cement content. They conduct an analysis of the variance on the chloride ion penetration values for different factors (curing

time, type of sand, water consumption, and water to cement ratio). Hence, the effect of the fine aggregate characteristics, especially its mineralogy and fines content, should not be neglected while studying concrete durability.

4.2.4.1 Effects of the mineralogy of fine aggregates

The mineralogy of fine aggregates could also affect the durability of concrete. As already discussed in the previous section, some types of sand, such as limestone, could react with the hydration products and densify the microstructure of concrete. Thus, the porosity of concrete could be reduced and the durability enhanced. In the study of (*Binici and Aksogan, 2018*), the improvement of the durability of concrete by the incorporation of basalt is attributed to the chemical reactivity of this material which could create a more compacted matrix. According to (*Coppio et al., 2019*), the foundry sand with high calcite and alkali metal contents could result in the improvement of the hydration reaction and could lead to higher concrete resistivity. Likewise, (*Liu et al., 2020*) observe by SEM technique that the incorporation of the ferronickel slag as an alternative to natural sand increases the amount of the hydration products and densifies the microstructure, enhancing thus the resistance to chloride ion penetration by 21% compared to the natural river sand concrete.

However, the mineralogy of some types of fine aggregates could be detrimental to concrete. As already discussed in Section 3, a fraction of the siliceous fine aggregates and the glass wastes could be active in the alkali-silica reaction and lead to an expansion of concrete (*Idir et al., 2010; Rajabipour et al., 2010*) and its cracking, affecting thereby its durability. On the other hand, the addition of the calcite could induce the formation of thaumasite (*Labidi et al., 2019*), (a calcium sulfate carbonate silicate hydrate), which could also generate an expansion and cracking of concrete (*Wimpenny et al., 2015*). This mineral is a product of the reaction between the sulfate, the silicate, and the carbonate when concrete is exposed to a low temperature and a sulfate attack during the cement hydration (*Wimpenny et al., 2015*).

Furthermore, the mineralogy of fine aggregate could degrade the behavior of concrete when subjected to aggressive environments, such as acid solutions. The acid ions in hydroxylic and sulfuric acids react with the alkalis of the cement paste by dissolving the Portlandite and C-S-H gel, increasing thereby the porosity and permeability of mortar (*Bederina et al., 2013*). Some studies detect different behaviors of siliceous and limestone mortars and concrete when subjected to acid attacks. Figure I.29 presents the effects of the hydrochloric acid attack on different types of mortar with different types of sand. It illustrates the darker and thicker layer of the calcium chloride formed at the surface of the siliceous sand mortar compared to that of the limestone sand. Due to its high content in calcium carbonate, the limestone aggregate could play a sacrificial role in the concrete and reacts with the surrounding acid. Thus, it contributes to the reduction of the acid concentration near concrete surfaces, protects the paste-aggregate interfacial zone, and reduces the negative effects of the acid ions on the durability of concrete (*Chang et al., 2005; Bederina et al., 2013*). However, in concrete containing siliceous aggregates, the acid ions do not attack the aggregates. Then, they directly neutralize the alkaline cement paste and dissolve the hydration products (*Chang et al., 2005; Bederina et al., 2013*). Hence, the limestone sand seems to be beneficial for the concrete during this acid attack: it lowers the detrimental effect of the acid solutions and produces a more resistant and durable concrete than the siliceous sand.

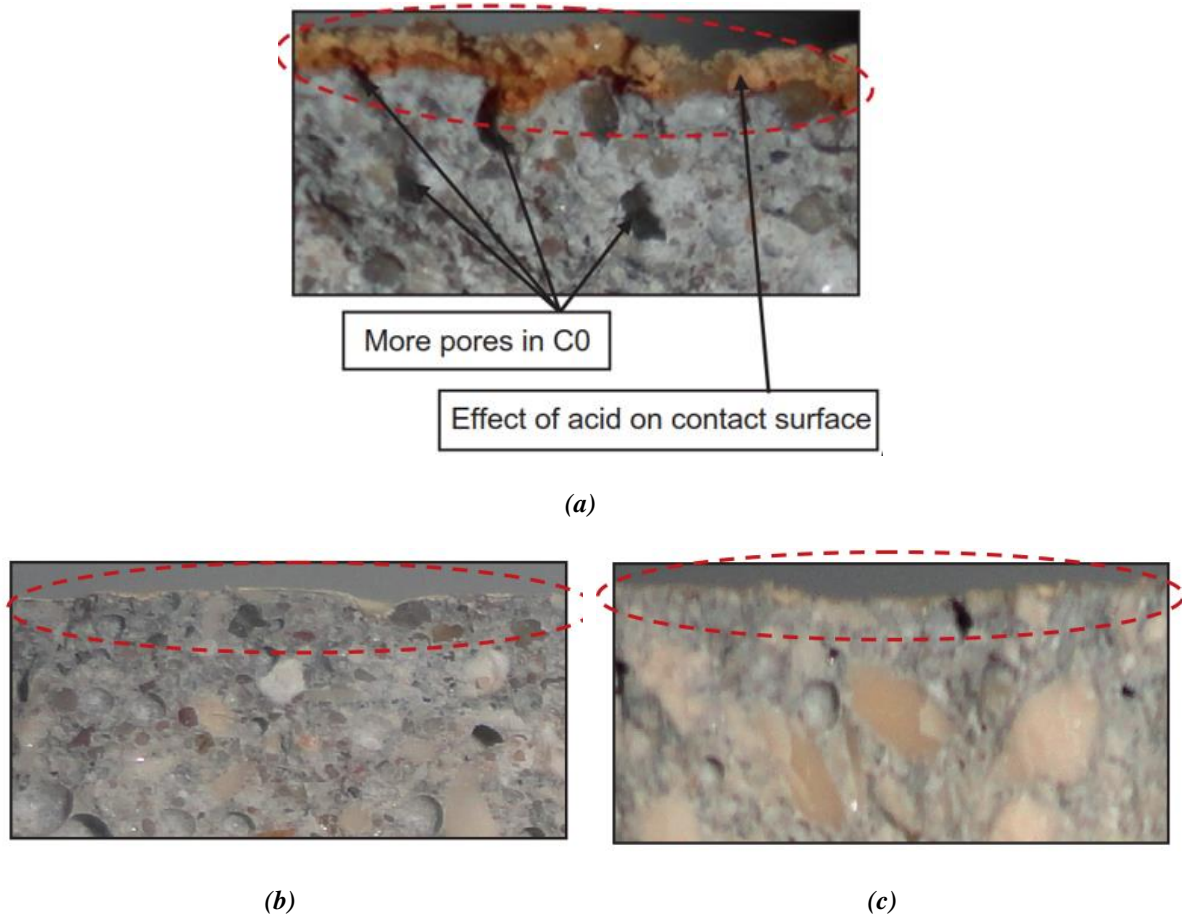


Figure I.29 Effect of hydrochloric acid environment on concrete with different types of fine aggregates (a) C0: 100% Siliceous sand, (b) C2: 50% Siliceous sand + 50% Limestone sand, and (c) C4: 100% Limestone sand (Bederina et al., 2013)

These effects could also be observed in the SEM images of Figure I.30. After 168 days of immersion in 1% sulfuric acid, the siliceous aggregates in Figure I.30a seem intact, while the interfacial transition zone and the surrounding mortar are cracked. In contrast, in Figure I.30b, there are no visible cracks in the paste surrounding the calcareous aggregate which is attacked by the acid solution.

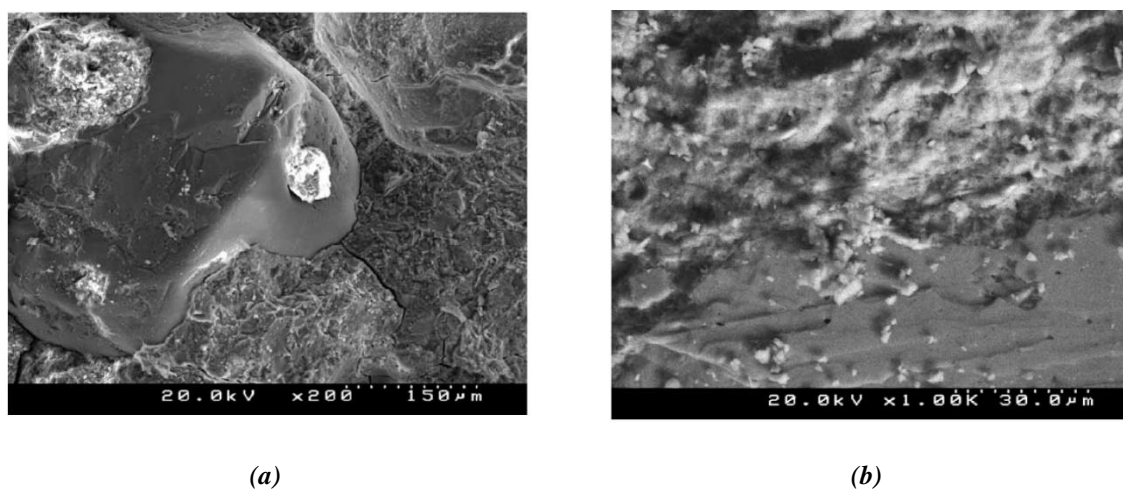


Figure I.30 SEM images of the interfaces of aggregates and cement paste in mortars made of (a) siliceous sand and (b) calcareous sand after 168 days of immersion in 1% sulfuric acid (Chang et al., 2005)

4.2.4.2 Effects of the morphology of fine aggregates

The morphology of the fine aggregates seems not to be an important influential factor in the durability properties of concrete, contrarily to the cases of fresh properties and mechanical behavior.

4.2.4.3 Effects of the physical properties of fine aggregates

The particle size distribution of fine aggregate seems to have a negligible influence on the permeability of concrete. (*Shen et al., 2018*) have found that the chloride ion penetration is not significantly modified when the gradation of the fine aggregate is optimized.

The durability seems to be more dominated by the packing density of the mixture than by the shape and grading of fine aggregates (*Gonçalves et al., 2007; Shen et al., 2018*). This packing density depends on the intrinsic packing capacity of the grains in the mixture and the method used for packing.

4.2.4.4 Effects of the fines content of fine aggregates

(*Shen et al., 2018*) have observed that for different shapes of sand grains, a similar gradation and content of fines lead approximately to the same permeability. However, for different fines content, the researchers observe a difference in the chloride ion permeability between river sand concrete and manufactured sand concrete, attributed to the difference in fines content instead of the difference in their shapes. Likewise, in the study of (*Gonçalves et al., 2007*), the mortar made of angular crushed sand with 14.5% of fines is characterized by a significant lower absorptivity (24-28%) than the mortar made with subrounded natural sand (0.5% of fines), whereas, when the fines content of the crushed sand is reduced to 1.6%, this difference is limited to 8-19%. Thus, the highest difference seems to be provided by the fines content and not by the shape of the fine aggregate. Furthermore, for the same shape and type of crushed sand, the authors observe a remarkable increase in the absorptivity (42-65%) of the mortar containing crushed sand with low fines percentage (1.6 and 4.8%), reduced by air classified technique, compared to those incorporating crushed sand with high fines percentage (14.5 and 17.7%).

The effect of sand fines on the durability of concrete could be more prominent in a loose microstructure (Figure I.31). When the concrete mixes are characterized by a low cement content and high water to cement ratio, their microstructure develops a high volume of pores with large sizes. Thus, the incorporation of fines could contribute to filling the pores, blocking the capillary passages, reducing the porosity, and thus decreasing the permeability of concrete (*Bonavetti and Irassar, 1994; Li et al., 2009; Menadi et al., 2009; Gokce et al., 2016*). Hence, the fines could provide an effective and beneficial effect by increasing the durability of concrete, favoring a thinner capillary vessel within the mortar (*Silva et al., 2009*).

However, in a dense microstructure, the effect of fines content could be limited. The low water to cement ratio and relatively high cement content create a concrete structure with few interconnected pores. Thus, the increment of fines could have little influence on this dense structure, as illustrated in Figure I.31. In the study of (*Li et al., 2009*), the chloride ion diffusion decreases linearly with the incorporation of fines when the water to cement ratio is 0.55 and the cement content 327.5 kg/m^3 , while no remarkable effect is detected with the incorporation of fines for water to cement ratio of 0.32 and cement content of 530 kg/m^3 . Similarly, the same trend is observed in the study of (*Gokce et al., 2016*) for the chloride migration coefficient and the depth of water penetration for two concrete types characterized by a water to cement ratio of 0.58 and 0.38 and cement content of 280 and 380 kg/m^3 respectively.

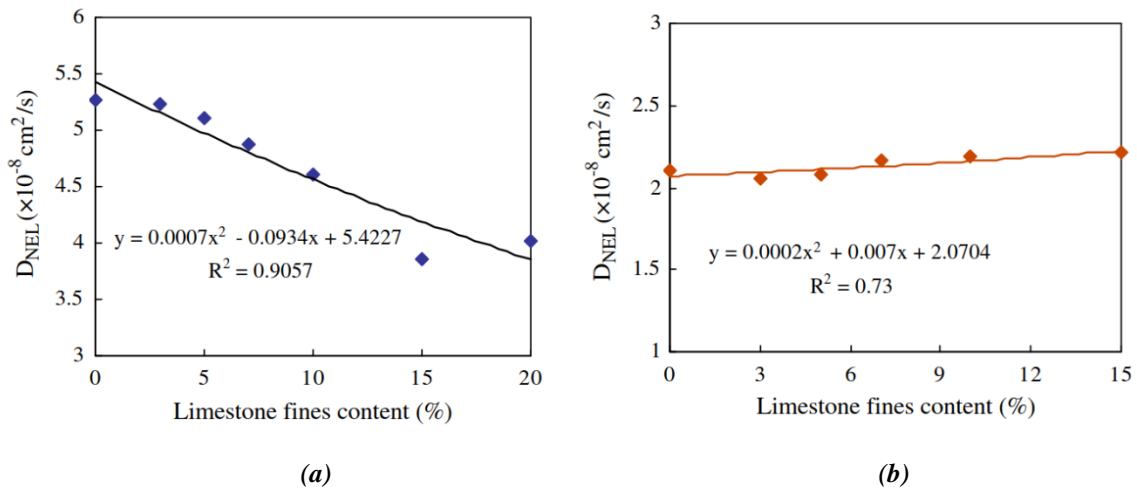


Figure I.31 Effect of fines content on the chloride ion diffusion coefficient on (a) loose microstructure (W/C: 0.55; cement: 327.5 kg/m³) and (b) dense microstructure (W/C: 0.32; cement : 530 kg/m³) (Li et al., 2009)

Besides, if the fines content exceeds the optimum level, the cement paste could be insufficient to cover the excess of fines particles, reducing thus the compaction of concrete and negatively affecting its durability (Vijayalakshmi et al., 2013). Accordingly, in the study of (Çelik and Marar, 1996), for water to cement ratio of 0.5 and cement content of 420 kg/m³, the addition of 15% of fines fills the voids and slightly decreases the water absorption of concrete (2%) compared to the reference concrete without fines, while beyond this threshold, the absorption begins to increase to reach a difference of 12% at 30% incorporation. In contrast, in the study of (Benyamina et al., 2019), for water to cement ratio of 0.4 and cement content of 490 kg/m³, even a high percentage of limestone fines (20%) is beneficial for concrete durability: it decreases the capillary water absorption, the chloride migration, and the porosity of concrete by 20%, 49.5%, and 12% respectively.

4.2.4.5 Effects of the variations in the mix design parameters

It is worth mentioning that if the loss in the workability of the fresh concrete, due to the difference in the characteristics of the fine aggregates, is compensated by the addition of the water content in concrete mixes, the durability of concrete could be affected. The water to cement ratio is an effective factor in determining durability (Huiguang et al., 2011), the highest the water to cement ratio the highest the group of large pores (Zhao et al., 2014). Thus, the porosity and the concrete permeability increase with the water content in the mix due to a looser microstructure as observed in the studies of (Bonavetti and Irassar, 1994; Kou and Poon, 2009; De Castro and De Brito, 2013; Aggarwal and Siddique, 2014) and demonstrated in Figure I.32.

Furthermore, the durability properties of concrete could be affected by the initial slump of the fresh mix. When the type of fine aggregate reduces the concrete workability, the compaction of the mix becomes more difficult and its porosity increases (Vijayalakshmi et al., 2013). Thus, the stiffest fresh concrete produces the highest water absorption by capillary (De Castro and De Brito, 2013). Accordingly, since the bottom ash concretes in the study of (Singh and Siddique, 2014) present a lower slump, they are characterized by higher porosity (14.25%-20.02%) and higher water absorption (5.9%-7.2%) than the natural sand concrete.

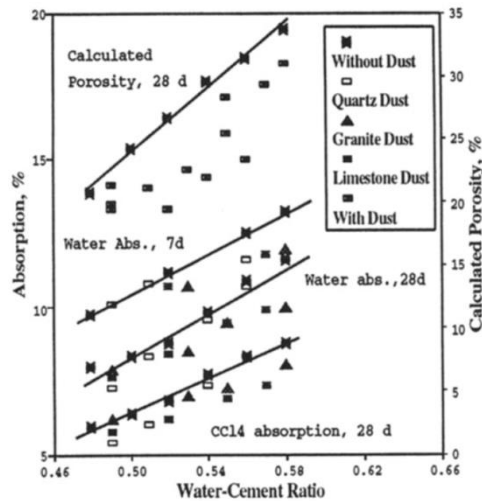


Figure I.32 Effect of water to cement ratio on the absorption and porosity of mortar (Bonavetti and Irassar, 1994)

4.2.4.6 Summary of the effects of the fine aggregates' characteristics on the durability properties of concrete

Table I.5 presents the general effects of the characteristics of fine aggregates on the durability properties of concrete.

Table I.5 Effects of fine aggregates' characteristics on the durability properties of concrete

Fine aggregates characteristics	Effects and mechanisms
Mineralogy	<p>Positive effect:</p> <ul style="list-style-type: none"> - Densification of the structure due to the production of additional hydrations products at long term - Sacrificial role under acid attack <p>Negative effect:</p> <ul style="list-style-type: none"> - The alkali-silica reactivity and thaumasite formation lead to concrete expansion and cracking
Morphology	No direct reported effect
Gradation	No direct reported effect
Fines content	<p>Lower than the optimum</p> <p>Positive effect:</p> <p>Fill the interparticle voids</p>
	<p>Higher than the optimum</p> <p>Negative effect</p> <p>Reduce the bond with cement paste and the compactness</p>
Deleterious particles and impurities	No reported effect

4.3 Effects of fine aggregates characteristics' on the concrete microstructure

The cement matrix and the aggregates are not the only two microstructural phases in concrete. A thin porous layer separates these two phases to form a third phase called Interfacial Transition Zone (ITZ).

The ITZ is defined as a zone around the aggregates particles where the mineralogical characteristics of the cement paste differ from those of the bulk (Farran, 1956; Ollivier et al., 1995). This layer is due to the inclusion of aggregates in concrete. By wall effect (Figure I.33), they disturb the geometrical distribution and packing of cement grains in water (Ollivier et al., 1995; Scrivener et al., 2004). Thus, this effect creates a gradient in the water to cement ratio and in the anhydrous and hydrated phases in concrete at the vicinity of aggregates (Monteiro et al., 1985; Ollivier et al., 1995). Accordingly, this zone is characterized by higher water to cement ratio and a loose arrangement of the small anhydrous cement grains (Breton et al., 1993; Scrivener et al., 2004).

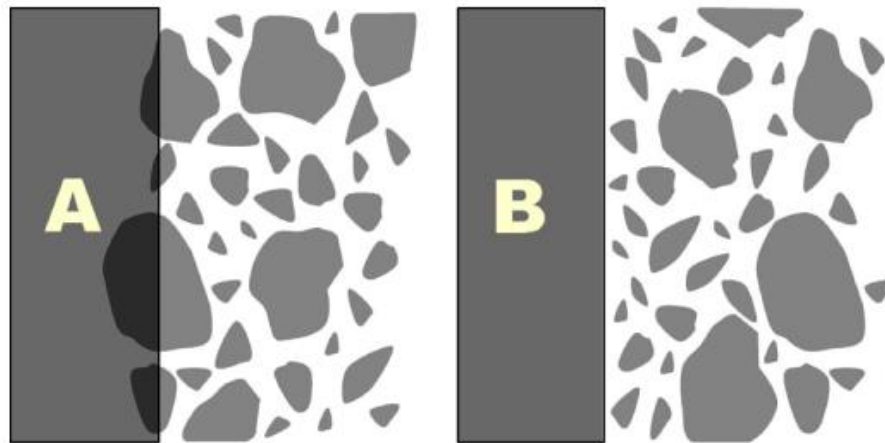


Figure I.33 The effect of aggregates inclusion in the perturbation of the cement arrangement. The aggregates could not cut through cement grains (A), they form a wall for the distribution of cement grains (B) (Scrivener et al., 2004)

Compared to the bulk cement paste, the ITZ is characterized by a higher porosity at all stages of hydration, since the pores to be filled in this zone are higher (Ollivier et al., 1995). However, with increasing time, the porosity at the ITZ reduces in the same range as the porosity in the bulk paste. Since the anhydrous cement amount is lower at the ITZ, the reduction of porosity in this zone is thus attributed to the formation of hydration products from the migrated ions into the interface (Scrivener et al., 2004). This migration is facilitated by the higher porosity of the ITZ and then a higher amount of ions is mobilized towards it (Monteiro et al., 1985; Breton et al., 1993; Ollivier et al., 1995). During hydration, mainly two hydrates phases are produced: the calcium silicate hydrate C-S-H and the calcium hydroxide Ca(OH)_2 , the Portlandite. The concentration of silicate in the solution is low and does not increase due to the low mobility of silicate ions. Thus, the C-S-H are rapidly formed around the cement particles (Scrivener et al., 2004). The concentration of calcium is higher in solution due to the mobility of these ions from the bulk paste towards the ITZ, leading to the preferential formation of calcium hydroxide which is mainly deposited in open pores. Most of the mobilized calcium ions are precipitated on the first day and slightly increase up to 28 days (Scrivener et al., 2004). As for the ettringite, since the ions forming this crystal are mobilized into the ITZ, the ettringite is also crystallized in pores and voids of the ITZ (Monteiro et al., 1985; Scrivener et al., 2004). It is also observed that the hydrates formed in the ITZ are well-formed large crystals, not randomly oriented in the contact of aggregates, due to the presence of few nucleation sites in this zone (Monteiro et al., 1985; Ollivier et al., 1995).

The ITZ width and boundary with the bulk cement paste are unobvious and unfixed. It could be detected by a rapid change of mineralogical compositions within 10-20 microns at the vicinity of the aggregates (Monteiro et al., 1985; Scrivener et al., 2004; An et al., 2017). (Monteiro et al., 1985) determine the thickness of this zone by removing, several times, the interface near the cement paste and analyzing the mass, density, and mineralogy of the newly exposed surface, until two consecutive removals present

the same characteristics, while (*Scrivener et al., 2004*) relate the thickness of this zone to the lack of anhydrous cement grains.

Given all the mentioned characteristics, the ITZ is considered the weakest zone in concrete, since it is less resistant than the bulk cement paste. Thus, it influences the behavior of concrete at the macroscale. When the concrete is subjected to mechanical or hygrothermal actions, the first microcracks initiate in this zone. They begin to grow in length, width, and number and propagate through the matrix (*Ollivier et al., 1995; Akçaoğlu et al., 2005; Bederina et al., 2013*). Thus, the mechanical and durability properties of concrete are dependent on the quality of its microstructure. This zone is also known to play a major role in controlling the performance of concrete exposed to fire (*Mazzucco et al., 2013*).

To improve the strength of this zone and reduce its voids, superplasticizers and cementitious materials could be added to limit the cement grains agglomeration and increase the nucleation sites (*Ollivier et al., 1995*). However, the quality of the ITZ is mainly determined by the interlocking between the aggregates and the cement grains, thus it depends on the morphology, mineralogy, and fines content of the aggregates used in concrete. Consequently, a review of the effect of fine aggregates on the concrete microstructure at the interfacial transition zone is detailed in the following sections.

4.3.1 Effects of the mineralogy of fine aggregates

The characteristics of the interfacial transition zone depend on the chemical reactions that could take place between the aggregates and the cement paste within this zone. Thus, the ITZ microstructure could be affected by the mineralogy of aggregates and its characteristics depend on the types of fine and coarse aggregates (*Ollivier et al., 1995; Tasong et al., 1998; Tasong et al., 1999*). The chemical reactivity of aggregates with the cement paste is proved in the study of (*Tasong et al., 1998*) by comparing the ions concentration in a cement solution with different types of aggregates (basalt, limestone, silica sand, and quartzite), crushed into a fine powder, to those in a control solution of cement without the aggregates. They demonstrate that there is a variety of chemical interactions that could occur between the aggregates and the cement paste.

In concrete, the silicate ions could leach from the siliceous, quartz, and basaltic aggregates to enter into the composition of C-S-H (*Javelas et al., 1975; Struble et al., 1980; Tasong et al., 1999*). However, these hydration products are present in the cement matrix as in the ITZ. Thus, no specific products are present in the ITZ of these aggregates. Additionally, the microscopical observation does not reveal any chemical bonding between the cement paste and the siliceous aggregates (*Struble et al., 1980*).

The calcium carbonate of the carbonate aggregates is dissolved by the concrete liquid phase and its ions are concentrated in the ITZ (*Grandet and Ollivier, 1980; Ollivier et al., 1995*). These ions could react in two different ways in concrete (*Struble et al., 1980*). First, due to the attack of the aggregates by the alkali solution, the calcite ions could be transformed into calcium hydroxide (*Farran, 1956; Grandet and Ollivier, 1980*). Secondly, the carbonate ions resulting from the dissolution of the calcium carbonate could react with the Portland cement and its hydration product (hydrated calcium aluminate) to form the calcium hydro-carbo-aluminate $C_3A.CaCO_3.11H_2O$ (*Farran, 1956; Grandet and Ollivier, 1980; Ollivier et al., 1995*). This reaction is limited to the ITZ and it is delayed because it should follow the slow dissolution of calcite from the aggregates (*Grandet and Ollivier, 1980; Ollivier et al., 1995*).

Consequently, the chemical and mineralogical compatibility between the limestone aggregates and the cement paste improves the cement-aggregate bond and the continuity in the mix, to produce a denser microstructure with higher mechanical strength (*Javelas et al., 1975; Ollivier et al., 1995; Bederina et al., 2013*). Furthermore, the attack of the calcite by the liquid phase etches the surface of the limestone

aggregate and increases its roughness (Figure I.34), increasing thus the cohesiveness and the bond with the surrounding cement paste, and enhancing the concrete mechanical properties (*Javelas et al., 1975; Grandet and Ollivier, 1980*).

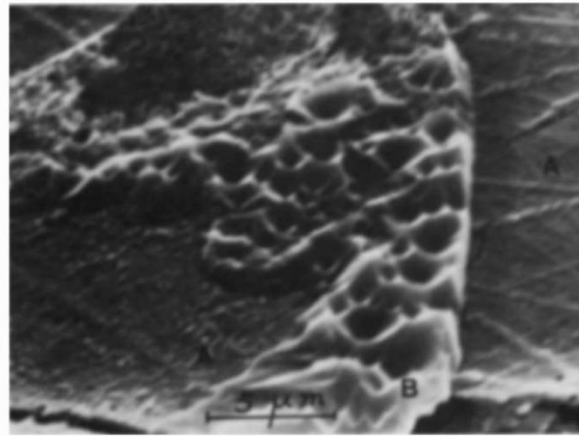
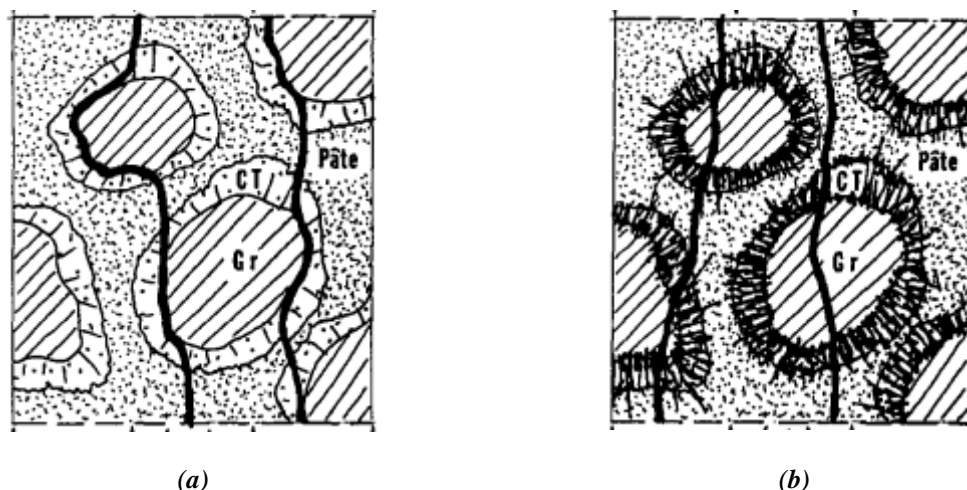


Figure I.34 SEM image showing (A) the Portlandite and (B) the footprint of the calcite attack in the cement paste (*Grandet and Ollivier, 1980*)

Accordingly, by comparing the behavior of mortar with calcareous and siliceous fine aggregates, (*Bachiorrini and Murat, 1987*) have found that the chemical active calcareous aggregates increase by 78% the long-term flexural strength of mortar by creating a denser and less porous ITZ than that around the siliceous aggregates characterized by larger and more developed pores. Furthermore, the adherence of the calcareous aggregate to the cement paste due to the formation of carbo-aluminate plays an important role in controlling crack propagation. The carbo-aluminate crystals are strongly anchored on the surface of the aggregates and, in the long-term, the cracks propagate throughout the aggregates, neither in the interface nor the surrounding bulk paste (Figure I.35). However, in the mortar with siliceous aggregates, the propagation follows the intergranular process regardless of the mortar age due to the lack of reactivity of the siliceous aggregate.



**Gr: aggregate, CT: interface, Pâte: cement paste*

Figure I.35 Illustration of the different cracks propagation modes in mortars subjected to compression with (a) siliceous sand after 5 years of hydration and (b) calcareous sand after 1 year of hydration (*Bachiorrini and Murat, 1987*)

Additionally, as already detailed in Section 4.2.4, the aggregates with different mineralogy could behave differently when subjected to acid attack. (Chang *et al.*, 2005) have found that the cracks are more developed in the interfacial transition zone of siliceous aggregates due to the direct attack of the hydration products by acid ions, while the calcareous aggregates protect the interfacial transition zone by the sacrificial role that they play during the acid attack.

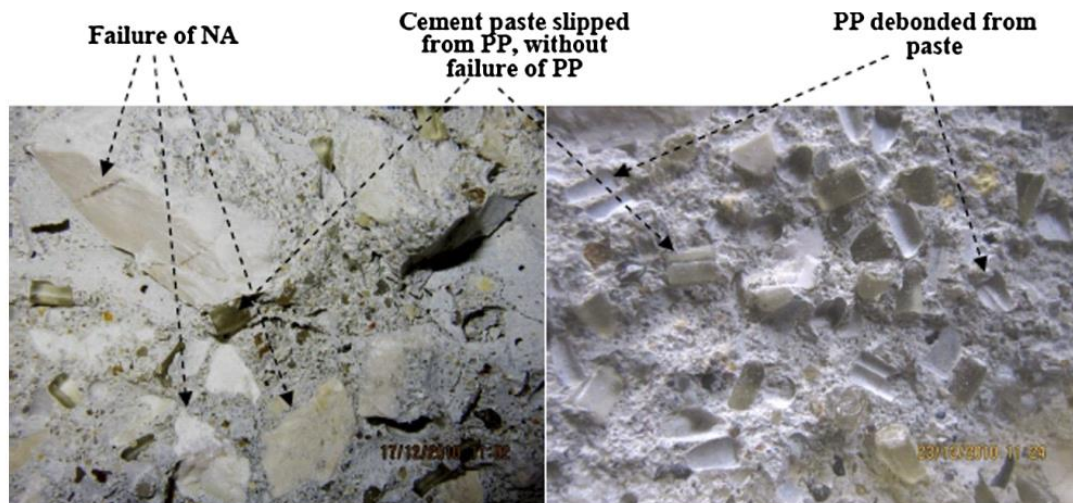
In addition to crushed limestone sand, some alternatives to natural sand could also have a positive effect on the microstructure of concrete and consequently on its mechanical and durability behavior. The incorporation of 10% of bottom ash as a replacement to natural sand reduces the porosity of the microstructure due to its pozzolanic activity (Yüksel *et al.*, 2007). The ferronickel slag could also densify the microstructure by increasing the hydration products (needle-shaped ettringite crystals, C-S-H gels, and a quantity of $\text{Ca}(\text{OH})_2$), compared to the reference concrete where the amount of voids is higher with no remarkable presence of C-S-H gels (Liu *et al.*, 2020). Additionally, 30% replacement of natural sand by ash and foundry sand increases the formation of C-S-H gels which act as a thick impermeable membrane for the penetration of deleterious ions into the concrete (Aggarwal and Siddique, 2014). Likewise, the incorporation of iron slag in concrete densifies the concrete microstructure with a better distribution of C-S-H gels and a higher amount of ettringite formed in the voids (Singh and Siddique, 2016).

Contrarily, some alternative sands could produce a more porous microstructure with a weak bonding with the cement paste. Microcracks could develop at the interface since their mineralogy does not allow a chemical reaction, as is the case of the rubber ash (Gupta *et al.*, 2014) and plastic wastes (Saikia and De Brito, 2014).

4.3.2 Effects of the morphology of fine aggregates

Since the lower the size of the fine aggregate, the lower the accumulated bleeding water and water to cement ratio around the aggregate particles, the reduction of size grains could reduce the porosity of the ITZ (Elsharief *et al.*, 2003).

In addition to the size of particles, the shape of the sand grains could also affect the thickness (Monteiro *et al.*, 1985) and the resistance of the ITZ. The rough texture and angular shape of some manufactured sand could enhance the bond at the ITZ (Bederina *et al.*, 2013; An *et al.*, 2017; Liu *et al.*, 2020), thus the propagation of cracks could be attenuated (Bederina *et al.*, 2013). In contrast, the ITZ of the smooth natural sand is weaker and the sand grains could be detached from the cement paste after reaching the ultimate load when the plastic wastes with a smooth surface are used as an alternative to natural sand (Saikia and De Brito, 2014), as demonstrated in Figure I.36. Similarly, when studying the coarse aggregates, (Ribeiro *et al.*, 2011) show that the aggregates could be dislodged from the matrix in case of a weak bond or be fractured without dislodgment in case of a better bond. They have found that the surface roughness of the crushed aggregate provides a good anchorage that exhibits the second behavior and favors a strong interface between the cement paste and the aggregate. However, the smooth surface of the natural aggregate does not create such an effective bond and they present the first behavior.



*NA: natural aggregate, PP: smooth rounded plastic wastes used as fine aggregate

Figure I.36 The behavior of smooth plastic wastes after loading (Saikia and De Brito, 2014)

However, the aggregates' surface roughness cannot be considered as the single parameter controlling their bond with the cement paste. This bond is also affected by the strength and the internal structure of aggregates (Tasong *et al.*, 1998; De Larrard and Belloc, 1997), and the chemical reaction that could occur between the aggregates and the cement paste, as explained previously.

4.3.3 Effects of the fines content of sands

The content of fines in the sands could also play a significant role in determining the quality of the interfacial transition zone. The high fines content could reduce the enriched water at the surface of the sand to produce a more homogeneous ITZ with lower voids (Shen *et al.* 2017; Shen *et al.*, 2018). They could fill the voids, densify the interfacial transition zone, and reduce the microstructure difference between the ITZ and the bulk paste. Hence, they lead to less permeable concrete (Li *et al.*, 2009; Bederina *et al.*, 2013). (Shen *et al.* 2017; Shen *et al.*, 2018) observe that, for the same mineralogy, the higher the fines content in sand, the denser the concrete microstructure and the narrower the ITZ. They also detect the presence of more cracks at the interface of the river sand grains with a weaker bond and more voids, giving more space for Portlandite and ettringite crystals to grow. However, for the manufactured sand concrete, they do not observe cracks at the interface, and the hydration products are finer and homogeneously distributed with a higher formation amount of C-S-H gels. However, when the content of fines in the transition zone exceeds the optimum required of each mix design, the excessive fines could form a coating surface on the aggregates which affect the bond between the aggregates and cement paste (Çelik and Marar, 1996; Li *et al.*, 2009), reducing in this way the durability of concrete.

4.3.4 Summary of the effects of fine aggregates characteristics' on the concrete microstructure

The properties of the concrete microstructure are strongly related to the characteristics of the fine aggregates used in concrete, as presented in Table I.6.

Table I.6 Effects of fine aggregates' characteristics on the concrete microstructure

Fine aggregates characteristics	Effects and mechanisms
Mineralogy	<p>Positive effect (in case of limestone):</p> <ul style="list-style-type: none"> - Densification of the structure due to the production of additional hydrations products at long term - Sacrificial role in acid attack
Gradation	No reported effect
Morphology	<p>Negative effect:</p> <p>Lower the bond between the cement paste and sand grains and increase the cracks initiation</p>
	<p>Positive effect:</p> <p>Increase the bond between the cement paste and sand grains and reduce the cracks initiation</p>
Fines content	<p>Positive effect:</p> <p>Reduce the porosity and densify the microstructure</p>
	<p>Negative effect</p> <p>Reduce the bond due to the coating of aggregates</p>
Deleterious particles and impurities	No reported effect

Conclusions

The good quality natural siliceous sand becomes less available in Lebanon, and the government imposed restrictions in the mining of the remaining quantity. In addition to its scarcity, this sand could not be used as the only fine aggregate in concrete due to its fineness. Thus, it is nowadays combined with an adequate proportion of crushed limestone sand to conform to the grading requirement of the ASTM C33 standard applied in Lebanon.

Several countries suffer from the scarcity of the different types of natural sand, their detrimental effects on concrete performance, and the negative environmental impacts of their excessive exploitation. Due to the river mining, the water level is reduced, the fauna and flora of the surrounding area are disturbed, and the river bed is eroded. Moreover, this sand may contain a high content of impurities and deleterious particles that could affect concrete performance. Sea mining causes a disturbance in the beach ecosystem and threatens the coastal infrastructures. The sea sand may contain high amounts of ions that cause rebars corrosion and should be washed before used in concrete. The sand mined from land pits presents negative impacts on the environment and the surrounding areas and its good quality is decreasing at an alarming rate. As for the dune sand, it is not widely used in concrete despite its high availability. It presents poor grading and high fineness and surface area, leading thereby to poor workability and low strength in concrete.

For these reasons, many studies have evaluated the effect of different alternatives as a partial or total substitute to natural sand in concrete. In this way, the exploitation of natural sand resources will be minimized and the environmental impacts of the disposal of these alternatives will be attenuated. The use of crushed limestone, marble, and granite sand in concrete contributes to valorizing the fine aggregates generated from the crushing process. The huge amount of construction and demolition wastes and domestic wastes, such as concrete, bricks, tiles, glass, and plastic, could be recycled as fine aggregate in concrete. The industrial by-products, such as the ash and the slag, and the foundry sand could also be incorporated as a replacement to natural sand in concrete.

Among these alternatives, the crushed limestone sand tends to be the most effective solution in the Lebanese context to totally replace the natural sand. It differs by its rough angular calcite grains in

comparison to the natural sand which is formed of sub-rounded siliceous grains. It could contain a high content of fines due to the crushing process.

Since the properties of sand could define the performance of concrete, a literature review was conducted to assess the effects of the fine aggregates on several concrete properties. The main observations could be summarized as follows:

The mineralogy of fine aggregates does not seem to be an influential factor in the fresh properties of concrete. In contrast, the shape of the sand grains could regulate the workability. Using rough angular sand grains favors the interparticle friction that lowers the concrete workability. A well-graded particle size distribution produces a compact mix, while a non-conform grading increases the cement needed to fill the interparticle voids in the concrete mix. Adequate fines content helps to lubricate the coarser aggregates particles by filling the intergranular voids and keeping excess cement content. However, in some cases, the fines content could increase the water demand affecting the workability, when it exceeds the optimum percentage of the mix or when it contains a high amount of impurities and deleterious particles.

The chemical compatibility of the sand grains with the hydration products leads to a strong bond with the cement paste. The morphology of sand has also a strong influence on concrete mechanical performance. In comparison with a spherical smooth surface, the angular rough sand grains could enhance the bond with the cement paste and thus the concrete strengths. Additionally, the well-graded sand with an adequate content of fines could improve the strengths of concrete by producing a compact mix. On the other hand, a non-conform grading could increase the interparticle voids, and the high content of fines could increase the quantity of the uncoated sand particles, affecting thereby the mechanical behavior of concrete. Besides, when the content of the deleterious particles and impurities in the fine aggregate exceeds the allowable limits, they could affect the adherence of the sand grains with the cement paste and thus decrease the concrete strengths.

The effect of the characteristics of fine aggregates seems less significant on the shrinkage of concrete than the coarse aggregate. The few studies which assessed this effect mainly related the difference in the concrete deformations to the porosity of fine aggregates.

The effect of the characteristics of the fine aggregate on the durability of concrete is not extensively developed in the literature. The content of fines is the most studied parameter. Similar to their effect on the fresh state and the mechanical behavior, the fines content could be increased, beyond the limits imposed by several standards, as far as it is beneficial or without effect on concrete. The high content of fines could fill the voids in concrete and increase its durability, while it could provide the opposite effect by coating the coarser particles and downgrading the bond. The mineralogy of the fine aggregate could also influence the concrete durability. The incorporation of certain types of sand reduces the porosity due to the formation of additional hydration products, while others lead to a detrimental expansion and then microcracking in concrete.

A literature review was also conducted on the microstructure of concrete to explain the origin of the differences in the behavior of concretes with different fine aggregates. Remarkably, the effect of coarse aggregates is more developed in the literature, and few studies concern the effect of fine aggregates on the concrete and ITZ microstructures. It was found that the chemical reactivity of certain types of aggregates, such as the limestone, could densify the concrete microstructure and reduce its porosity by producing secondary hydration products. Moreover, the bond between the cement paste and the sand grains depends on the morphology of the sand grains. Furthermore, as already explained, an optimum

percentage of fines seems beneficial in the densification of the concrete microstructure, in particular at the ITZ.

According to the literature review, several points could be taken into consideration while assessing the total replacement of natural siliceous sand by crushed limestone sand in the current study:

- It is crucial to study the characteristics of the fine aggregates used in our study, before conducting the experimental program on concrete, to be able to evaluate their potential effects on various concrete properties, especially those that were not widely covered in the literature, such as the shrinkage and the durability.
- In some studies, the effect of the different characteristics of fine aggregates could not be obviously concluded since many mix parameters differ between the compared concretes and it was difficult to decouple the effects of the different influential factors. Thus, to allow a comparison based on the only effect of the fine aggregates, it is essential to fix the cement content, the effective water to cement ratio, and the slump. If needed, to compensate for the loss of workability, a superplasticizer could be used instead of increasing the water content in the concrete formulations.
- Furthermore, since the concrete properties were not significantly affected when the fines content in the sand exceeded the maximum allowable percentage imposed by the different standards, thus it worth evaluating the effect of the crushed limestone sand with a high percentage of fines in the Lebanese context, instead of normalizing its particle size distribution.

Consequently, the results of the experimental program aim to determine if the replacement of the natural siliceous sand by crushed limestone sand could resolve the industrial problems and could emphasize the effects of the fine aggregates on concrete performance. For this purpose, the next chapter presents the first step of this program which consists of determining the characteristics of the fine aggregates to be able to assess their effects on concrete properties.



Chapter II

**Aggregates
Characterization
and Fine Aggregates
Preparation**



II. Aggregates Characterization and Fine Aggregates Preparation

Introduction

In Lebanon, two types of coarse aggregates, predominantly retained on a 4.75 mm sieve, are used in concrete mixes: the coarse aggregate having a nominal diameter of 20 mm and the medium aggregate with a nominal diameter of 10-12 mm. They are usually provided from the limestone quarries in the Lebanese mountains and are generally of good quality for concrete production. As for fine aggregates, they almost entirely pass the 4.75 mm sieve and are divided into two types: the crushed sand originated mainly from limestone rocks and the natural siliceous sand provided by simple excavation from sea, river, or mainly from the land quarries. Other fine aggregates exist in Lebanon but with smaller quantities, such as the basalt, with different performance and higher cost.

For this study, the natural sand NS is provided from a sandstone quarry (SAD Abou-Mizane) located in Mayrouba, Mount-Lebanon. Due to the lack of storage, the needed quantity of sand is divided into two stocks from two different pits (NS-Series A and NS-Series B). The crushed sand CS, medium aggregate MA, and coarse aggregate CA are provided from a quarry located in Bikfaya, Mount-Lebanon. The same stock of crushed sand is used throughout the study. However, the medium and coarse aggregates are not provided on the same day, they are thus collected from 5 different pits of the same quarry, nominated Series A to Series E.

An extensive experimental program is conducted on representative samples of these aggregates to be sure that the different characteristics of coarse and fine aggregates conform to the ASTM specifications, the standards applied in Lebanon. The current chapter presents the characteristics of each type of aggregates from the different pits, while the distribution of the aggregates series in concrete mixes is detailed in Chapter 3.

Recalling that the main objective of the study is to totally replace natural siliceous sand with crushed limestone sand in concrete mixes, and knowing that the fine aggregates could have a great influence on concrete properties, the second objective of this chapter is to detect the differences between natural sand and crushed sand in order to interpret the differences that could be present in the concrete performance.

For this purpose, the morphological study of grains is conducted using optical and scanning electron microscopes. The Induced Coupled Plasma ICP, ion chromatography, loss on ignition, and thermogravimetric analysis methods are used to evaluate the chemical composition of all aggregates, while the X-ray diffraction technique is applied to provide the mineralogical characterization. Physical characterization tests are also carried out on these aggregates. They include tests on gradation, deleterious particles' content, relative density, water absorption, resistance to abrasion and impact, and soundness.

The second part of this chapter covers the crushed sand production in the Lebanese quarries. It also describes the laboratory construction process of the different types of crushed sand that are used in this study, to have an effective general comparison between concrete mixes.

The procedures for sampling, testing, and properties calculations of each test applied to the aggregates are detailed in Annex A. All the aggregates characteristics are determined using the ASTM standards, except for the Methylene Blue value which is evaluated according to the European Standard.

Furthermore, the properties of the crushed aggregates are compared to those of crushed aggregates from different Lebanese quarries, distributed over seven different regions. This parallel study (Annex B) is conducted to ensure that the properties of the aggregates in Lebanon are comparable and that the final results of this thesis could be applicable even though the origin of the aggregates changes.

1. Characterization of aggregates

The characteristics of aggregates are determined by an exhaustive experimental program conducted on their different types. These characteristics include the shape, chemical and mineralogical compositions, and physical characterization (i.e., the gradation, content of fines and deleterious particles, specific gravity, absorption, resistance to soundness by sodium sulfate solution, and resistance to abrasion and impact by Los Angeles machine).

1.1 Shape characteristics

As detailed in Section 4 of Chapter I, the shape of aggregates plays an important role in concrete behavior at fresh and hardened states. It governs the friction between grains which affects concrete workability. It also influences the mix compactness, thus the concrete porosity, and the bond between the cement paste and the aggregates. Therefore, it could indirectly have a significant effect on mechanical and durability properties.

Hence, it is primordial to conduct a morphological study on aggregates, and especially on the two types of sand, to establish a detailed comparison between the fine aggregates samples and to depict the differences in their shape. This knowledge is useful to analyze the concrete performance, in particular when the natural sand is totally replaced by the crushed sand. For this purpose, an optical microscope and a scanning electron microscope SEM are used.

Before conducting the morphological tests, a simple observation of the different types of aggregates (Figure II.1) shows that the natural sand (Figure II.1a) is characterized by smooth sub-rounded grains, while the crushed sand (Figure II.1b) is formed of rough and angular particles, due to the crushing process. This figure also reveals the angular shape of medium (Figure II.1c) and coarse (Figure II.1d) aggregates, that are also provided from quarries by crushing.

In addition to the shape, the color is a remarkable difference between both types of sand. The natural sand is formed of yellow-orange grains while the crushed sand is greyish. This color difference could induce a difference in concrete color when the crushed sand totally replaces the natural sand.



(a)



(b)



Figure II.1 Simple observation of (a) natural sand, (b) crushed sand, (c) medium aggregate, and (d) coarse aggregate

By the transmission of light through the sample, the optical microscope gives 2D enlarged images of the natural and crushed sand specimens. Figure II.2 presents some representative images from the observations done by the mean of the optical microscope. The morphological difference between the two types of fine aggregates is confirmed: the natural sand (Figure II.2a and Figure II.2b) is sub-rounded in shape, while the crushed sand (Figure II.2c and Figure II.2d) is formed of angular grains, even in its smaller grains fraction. The crushed sand grains are bigger in size than those of the natural sand.

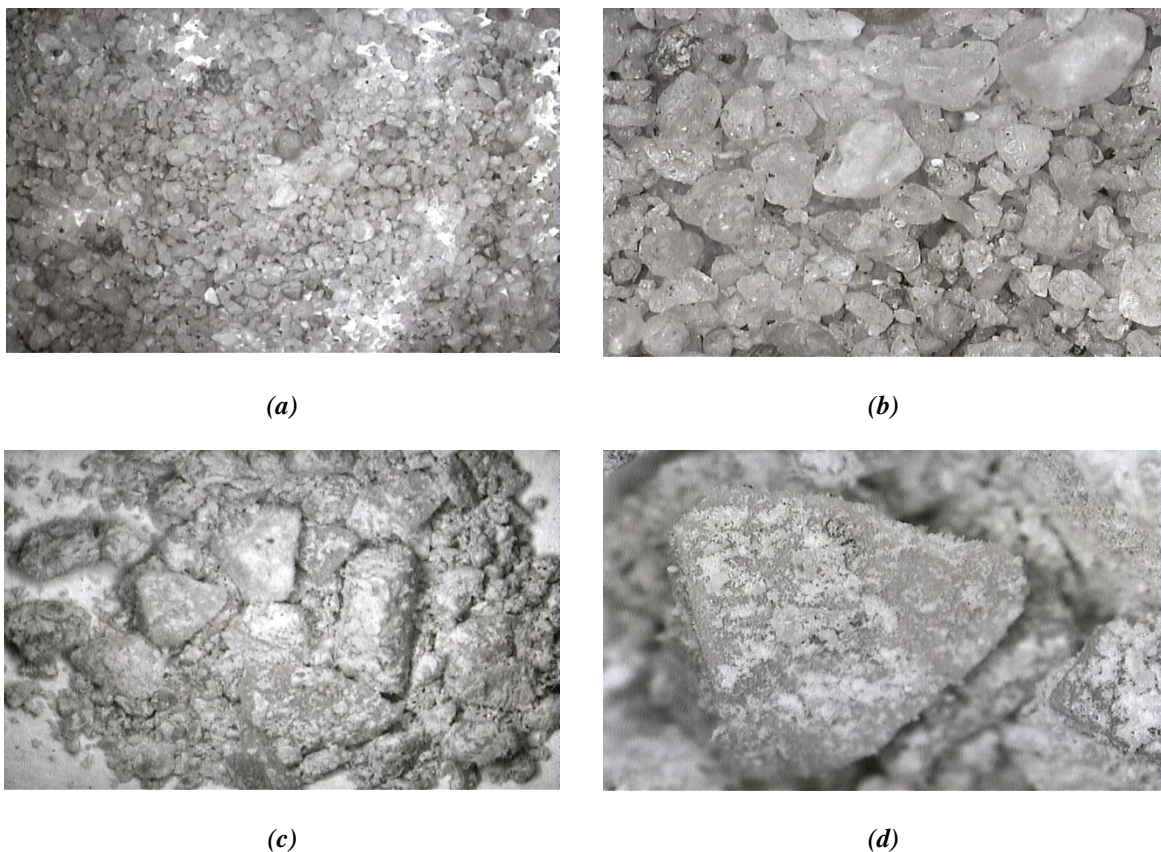


Figure II.2 Optical microscope images for the natural sand (a) x25 and (b) x100, and for the crushed sand (c): x25 and (d): x100

The SEM technique provides images of higher resolution and better quality compared to those of the optical microscope. Before being introduced into the vacuumed sample chamber of the SEM, the sand

specimens were embedded in a resin, polished to a mirror finish, and then coated with carbon to improve the electrical conductivity of the sample (Figure II.3).



Figure II.3 Samples preparation of the two types of sand for SEM analysis

Comparing the shape of the grains of the natural sand and the crushed sand of Figure II.4, we can confirm the sub-rounded shape of the natural sand (Figure II.4a) and the angularity of the crushed sand grains (Figure II.4b). These images also reveal cracks on the surface of the crushed sand. These cracks could be due to the crushing process during the crushed sand production.

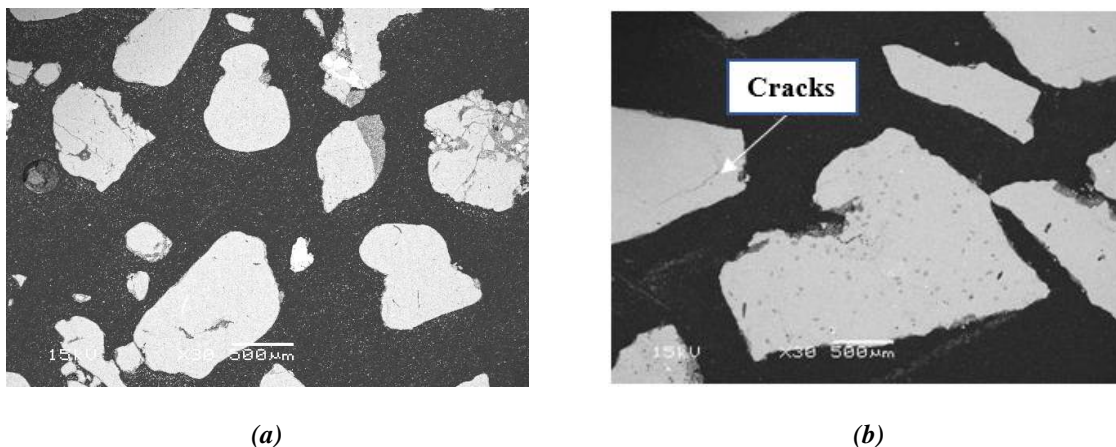


Figure II.4 Fine aggregates grains viewed on SEM (x30): (a) natural sand and (b) crushed sand

These differences in shape between the natural and crushed sands are also emphasized by previous studies (Yamei and Lihua, 2017; He et al., 2016) which observe that the natural sand grains are close to a sphere in shape, while the crushed sand grains are more flat, angular, and rough.

1.2 Chemical composition

The two types of sand used in Lebanon, provided from two distinct origins, could have different chemical compositions. To underline these differences and to be able to study their effects on concrete performance, chemical characterization tests are conducted on natural and crushed sands. The chemical compositions of the medium and coarse aggregates are also investigated to determine their nature. For this purpose, the induced coupled plasma, ion chromatography, loss on ignition, and thermogravimetric analysis methods are applied.

The induced coupled plasma method aims to identify the constituent elements of each type of aggregate by atomic emission spectrum (ICP-AEC) according to the (NF EN 196-2, 2013) standard, after grinding the solid sample into powder and converting it into liquid solution by fusion method.

During the fusion process, some sulfates could have been lost by volatilization. Therefore, the ICP is followed by the ion chromatography method that identifies some sulfates and quantifies their concentration in the samples.

These two experiments are completed by the determination of the loss on ignition of each sample. The method consists of measuring the percentage ratio of the mass loss of the sample after heating in a furnace at 975 °C, to its initial mass.

The results of the ICP, ion chromatography, and the loss of ignition methods, for each type of aggregates, are presented in Table II.1. The main chemical compound present in the natural sand is silica SiO_2 (87.25%). The crushed sand is mostly formed of calcium oxide (54.03%) and it is characterized by a high loss on ignition (43.20%). Thus, this sand is principally composed of calcite CaCO_3 (the sum of the percentages of CaO and the loss on ignition are equal to 97.23%), confirming its limestone nature.

The chemical compositions of medium and coarse aggregates are comparable to the composition of the crushed sand since the three types of aggregates originate from the same parent rock.

Table II.1 Chemical characteristics of aggregates

Mass Percentage (%)	NS	CS	MA	CA
SiO₂	87.25	1.22	0.90	0.57
CaO	4.95	54.03	53.18	55.22
Al₂O₃	0.63	0.33	0.26	0.16
Fe₂O₃	1.93	0.26	0.14	0.10
K₂O	0.06	0.10	0.08	0.06
Na₂O	0.11	0.04	0.03	0.04
MgO	0.18	0.64	0.64	0.60
Mn₂O₃	0.018	0.004	0.003	0.003
TiO₂	0.15	0.03	0.02	0.01
SO₃	0.03	0.14	0.12	0.08
P₂O₅	0.04	0.01	0.01	0.01
Cr₂O₃	0.005	0.001	0.001	0.001
Loss on ignition	4.64	43.20	44.60	43.15

During the production of crushed sand, the crushing process could generate high content of fines. These fines could have different mineralogy from the coarser particles and could be deleterious to the concrete performance. To ascertain that the crushed sand is homogeneous for all its grain size fractions, in addition to the general characterization of this sand, the sample is divided into four narrow size range fractions, and each fraction is chemically analyzed. The following nominations are applied for each section of crushed sand, and the results are detailed in Table II.2:

- CS-01: Passing 0.16 mm sieve;
- CS-02: Passing 0.63 mm sieve and retained on 0.16 mm sieve;
- CS-03: Passing 2.50 mm sieve and retained on 0.63 mm sieve;
- CS-04: Retained on 2.50 mm sieve.

This table shows that the mass proportions are very close in CS-02, CS-03, and CS-04. The finer fraction of this sand CS-01 also exhibits comparable values to the coarser ones but with small differences. It presents slightly higher proportions of SiO_2 , Al_2O_3 , Fe_2O_3 , K_2O , and TiO_2 .

Generally, these results prove that the crushed sand used in the study is chemically homogenous in all its grain size fractions.

Table II.2 Chemical characteristics of the different size fractions of crushed sand

Mass Percentage (%)	CS-01	CS-02	CS-03	CS-04
SiO ₂	1.40	0.53	0.69	0.50
CaO	53.67	54.86	54.85	54.51
Al ₂ O ₃	0.45	0.09	0.08	0.09
Fe ₂ O ₃	0.40	0.10	0.08	0.09
K ₂ O	0.14	0.05	0.05	0.05
Na ₂ O	0.05	0.05	0.05	0.05
MgO	0.66	0.67	0.65	0.66
Mn ₂ O ₃	0.005	0.004	0.004	0.004
TiO ₂	0.05	0.01	0.01	0.01
SO ₃	0.10	0.10	0.10	0.10
P ₂ O ₅	0.01	0.01	0.01	0.01
Cr ₂ O ₃	0.001	0.001	0.001	0.001
Loss on ignition	43.07	43.52	43.44	43.92

To complement the chemical analysis of the ICP and the ion chromatography, a thermogravimetric analysis TGA is applied. The TGA (Figure II.5) aims to record the mass variation of a sample subjected to a gradual elevation of temperature, to detect, in the case of the aggregates' samples, the decarbonization of calcite accompanied by the emission of CO₂. During this test, the temperature varies from 30 °C to 1050 °C at a rate of 10 °C/min, under an inert environment of Argon gas. To simplify the reading of the mass loss, the derivative thermogravimetry DTG, which corresponds to the rate of the mass loss during heating, is coupled with the TGA (Figure II.6).

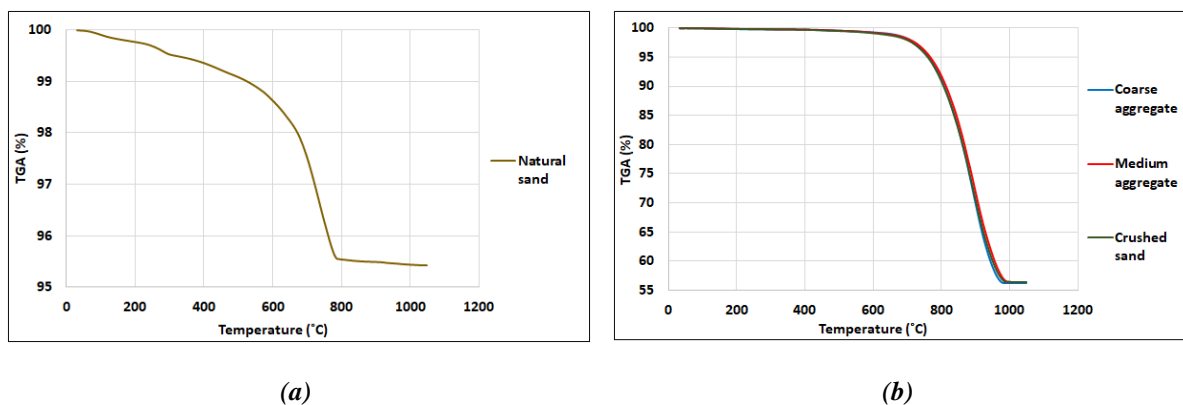


Figure II.5 TGA graphs for (a) natural sand and (b) crushed aggregates

The results of the TGA-DTG test for the four types of aggregates are compatible with the loss on ignition of the chemical characterization test. For the natural sand, the small percentage of mass loss (4.58%), becoming more significant at a temperature close to 600 °C, is an indication of a probable presence of some clay minerals or small quantities of calcite in this sand (Table II.1). The crushed sand, medium aggregate, and coarse aggregate lose respectively 43.58%, 43.61%, and 43.76% in mass at the end of the test. This loss significantly begins at a temperature of around 600-700 °C, indicating a calcite

presence since, around this temperature, the calcite is converted into lime CaO while releasing CO_2 . This observation is in accordance with the results of previous studies conducted on the limestone aggregates (González-Gómez *et al.*, 2015; Zhang *et al.*, 2017).

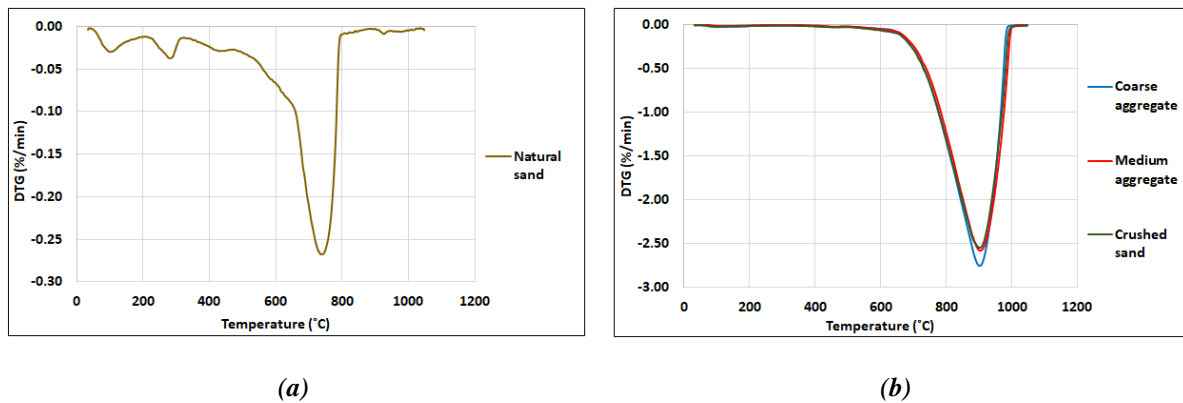


Figure II.6 DTG graphs for (a) natural sand and (b) crushed aggregates

1.3 Mineralogical composition

The mineralogical characterization is a complementary method for chemical analysis. It helps to determine the crystals' composition and the presence or not of clay phases in aggregates. By determining the mineralogical composition of the two types of sand, the effect of mineralogy on the concrete performance could be assessed.

Since each crystalline solid is characterized by a unique diffraction pattern for X-ray wavelengths, depending on the spacing of planes in its crystal lattice, X-Ray Diffraction (XRD) method is used to identify the type of crystalline solids present in each sample. Before being introduced into the diffractometer, the four types of aggregates are ground into a powder finer than $80\ \mu\text{m}$.

The XRD spectrum for all the aggregates is presented in Figure II.7.

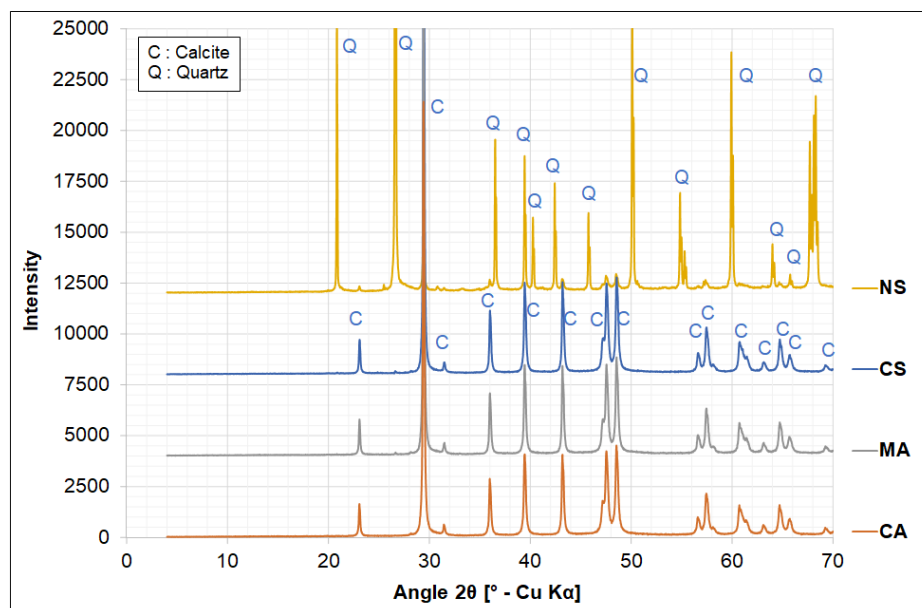


Figure II.7 XRD patterns for fine aggregates (NS and CS) and coarse aggregates (MA and CA)

The natural sand NS consists primarily of quartz with minor quantities of calcite, while the crushed sand CS shows a crystalline composition of calcite. The diagrams of both types of sand do not present clay phases. The XRD patterns for medium MA and coarse aggregates CA are complying with their chemical analysis and reveal that these aggregates are mainly composed of calcite.

The four size fractions of crushed sand studied for chemical constituents are also investigated for mineralogical composition for the same purpose. The comparison of the results of the four size fractions of the crushed sand sample (Figure II.8), shows that the four graphs are superimposed. This result proves that the crushed sand is mineralogically homogeneous in all its size fractions.

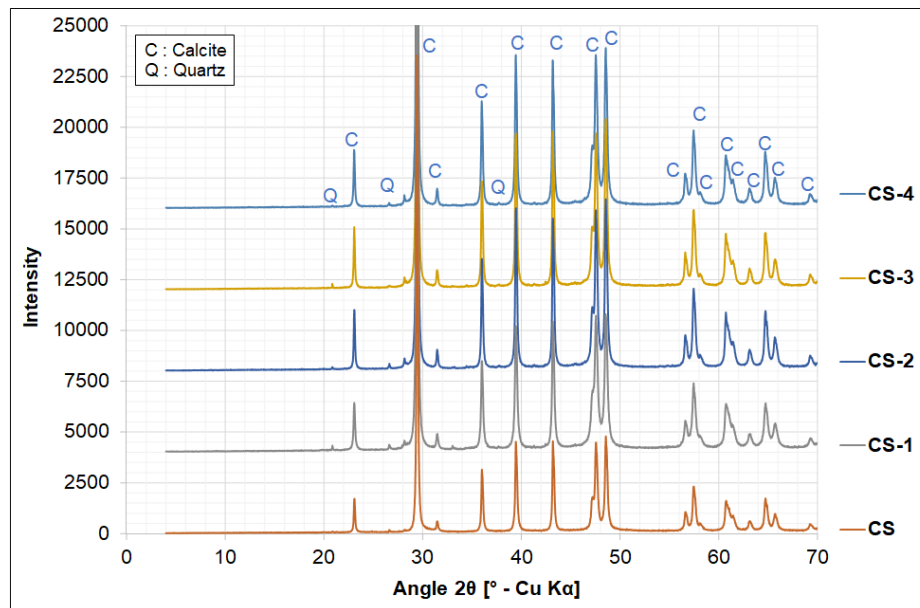


Figure II.8 XRD patterns for the four size fractions of crushed sand (CS-1, CS-2, CS-3, and CS-4) compared to that of CS

1.4 Physical characterizations

Before assessing the physical properties of the aggregates used in this study, they are sampled following the (*ASTM C702, 2011*) standard to obtain a sample portion representative of the entire provided quantity from the quarries. As shown in Figure II.9, the fine aggregates are sampled by the quartering method (Figure II.9a), while the splitting machine is used for sampling the coarse and medium aggregates (Figure II.9b).



(a)



(b)

Figure II.9 Sampling methods for (a) fine and (b) coarse aggregates

1.4.1 Gradation

Knowing the particle size distribution of each aggregate, the aggregates' proportions could be estimated to obtain a well-compacted concrete mix. The gradation of fine and coarse aggregates is determined by the dry sieve analysis test detailed in (*ASTM C136, 2014*) standard. It consists of separating a specified mass of the sample through a series of wire-mesh sieves placed in decreasing order from top to bottom according to the diameters of their openings, and by determining the mass retained on each sieve as a percentage of the total original dry mass.

Since the dry sieve analysis test does not give an accurate percentage of materials finer than 75 μm sieve, the (*ASTM C117, 2013*) standard is used for this purpose. Before applying the dry sieve, this test consists of washing the sample over a 75 μm sieve and calculating the percentage of particles removed after being dispersed by water.

The results of the percentage of fines for all aggregates are detailed in Table II.3. (*ASTM C33, 2016*) imposes a maximum fines percentage of 1% for coarse aggregates and 3% for natural sand. For crushed sand, knowing that the fines could consist of the fracture dust resulting from the crushing process, this limit is increased to 7%. The table shows that the percentage of fines of coarse and medium aggregates for all the provided series is within the acceptable limit (0.3-0.7 for CA and 0.6-0.8 for MA of series A, B, and E) except for medium aggregates of series C and D (1.5% and 1.9% respectively). The fines percentage of the natural sand of Series A (2.3%) does not exceed the percentage limit while the natural sand of Series B surpasses it (6.3%). The fines percentage of crushed sand presents a value close to the threshold of the standard limit (7.2%).

Table II.3 *The average values (and standard deviation values) of the percentage of materials finer than 75 μm sieve in aggregates*

Series	NS	CS	MA	CA
Series A	2.3 (0.34)	7.2 (0.15)	0.8 (0.07)	0.3 (0.02)
Series B	6.3 (0.47)	-	0.6 (0.04)	0.4 (0.06)
Series C	-	-	1.5 (0.05)	0.5 (0.07)
Series D	-	-	1.9 (0.04)	0.7 (0.10)
Series E	-	-	0.8 (0.16)	0.4 (0.16)

(-): aggregates not provided

The results of the dry sieve test for the fine aggregates used in this study are presented in Table II.4. For each type of sand, the fineness modulus FM is also calculated as the sum of the cumulative percentage retained on 0.15, 0.30, 0.60, 1.18, 2.36, and 4.75 mm sieves, divided by 100. The two types of natural sand present low fineness modulus values FM: 1.8 and 1.6 for NS-Series A and NS-Series B respectively. The FM of the crushed sand reaches a higher value of 3.4. To be used in concrete, the FM of sand should be between 2.3 and 3.1 (*ASTM C33, 2016*). The use of very fine sands (FM < 2.3) is uneconomical since it increases the surface area of sand and accordingly the cement demand of concrete, while the sand, with a fineness modulus higher than 3.1, negatively affects the workability of concrete (*Kosmatka and Wilson, 2011*). Therefore, each type of Lebanese sand cannot be used alone in concrete mixes, they are mixed in adequate proportions to have an acceptable fineness modulus.

Table II.4 The average values (and standard deviation values) of the cumulative passing percentage of natural sand and crushed sand over a series of sieves

Sieve diameter (mm)	NS-Series A	NS-Series B	CS
9.5	100.0 (0.00)	100.0 (0.00)	100.0 (0.00)
4.75	96.8 (0.81)	96.7 (0.67)	97.6 (0.29)
2.36	93.1 (1.12)	94.6 (0.79)	67.9 (1.09)
1.18	90.8 (1.31)	92.5 (0.97)	42.8 (1.01)
0.60	87.7 (1.33)	85.1 (1.26)	26.3 (0.63)
0.30	41.6 (1.52)	56.1 (1.01)	16.3 (0.51)
0.15	5.6 (0.50)	19.1 (0.34)	10.3 (0.44)
0.075	2.3 (0.20)	6.3 (0.47)	7.2 (0.15)
Fineness Modulus (FM)	1.8 (0.06)	1.6 (0.06)	3.4 (0.03)

(ASTM C33, 2016) imposes minimum and maximum allowable values for the cumulative passing percentages of fine aggregates. For each type of sand, Figure II.10 compares the cumulative passing percentage from each sieve with the grading envelope imposed by the standard.

The analysis of the particle size distribution of NS-Series A, NS-Series B, and CS of this figure shows that the Lebanese natural sand is characterized by a gradation that predominantly exceeds the maximum passing limit, while the crushed sand gradation is coarser than the lower limit. Therefore, to conform to the standard grading requirements, the natural sand and the crushed sand are always combined in appropriate proportions in all the concrete mixes in Lebanon.

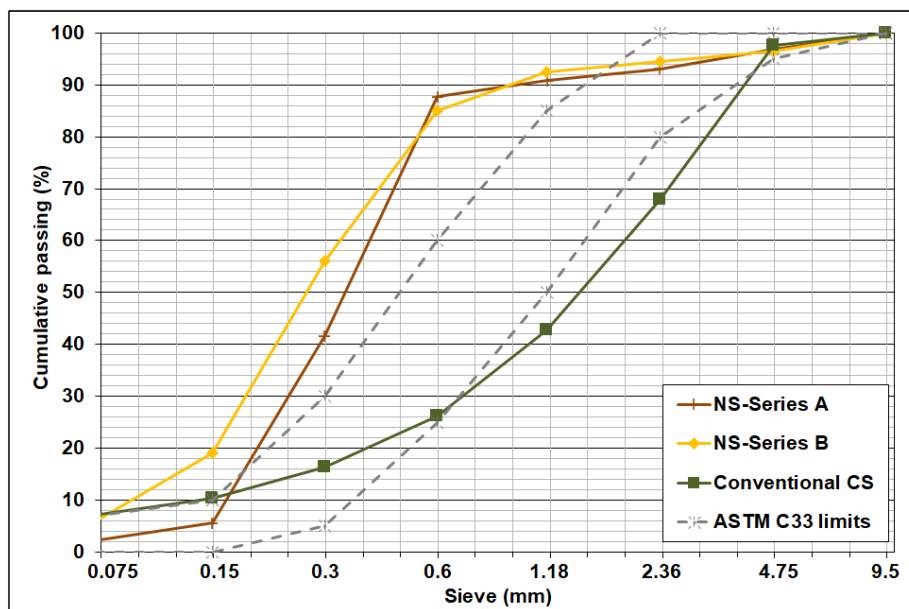


Figure II.10 The particle size distribution of fine aggregates compared to ASTM C33 grading limits (logarithmic scale)

The medium and coarse aggregates are provided from the Lebanese limestone quarries with two different nominal maximum sizes 9.5 and 19 mm respectively, as shown in Table II.5.

Table II.5 The average values (and standard deviation values) of the cumulative passing percentage of medium and coarse aggregates over a series of sieves

Sieve diameter (mm)	25	19	12.5	9.5	4.75	2.36	1.18	0.3	
MA	Series A	100.0 (0.00)	100.0 (0.00)	100.0 (0.00)	90.0 (1.75)	6.3 (2.42)	0.9 (0.23)	0.7 (0.17)	0.6 (0.14)
	Series B	100.0 (0.00)	100.0 (0.00)	100.0 (0.00)	81.3 (3.43)	3.6 (1.45)	0.9 (0.12)	0.8 (0.10)	0.7 (0.07)
	Series C	100.0 (0.00)	100.0 (0.00)	99.6 (0.21)	81.1 (0.22)	7.6 (0.11)	3.0 (0.27)	2.5 (0.22)	1.9 (0.07)
	Series D	100.0 (0.00)	100.0 (0.00)	99.6 (0.39)	88.4 (0.63)	22.4 (0.26)	8.5 (0.70)	6.2 (2.21)	2.8 (0.22)
	Series E	100.0 (0.00)	100.0 (0.00)	100.0 (0.00)	89.1 (1.23)	6.7 (3.32)	1.3 (0.41)	1.1 (0.23)	1.0 (0.18)
CA	Series A	100.0 (0.00)	94.4 (1.43)	23.9 (6.84)	1.5 (0.63)	0.4 (0.03)	0.4 (0.03)	-	-
	Series B	100.0 (0.00)	96.0 (0.86)	34.8 (1.50)	3.5 (0.38)	0.7 (0.05)	0.6 (0.06)	-	-
	Series C	100.0 (0.00)	95.6 (0.00)	36.7 (1.47)	4.0 (0.19)	1.3 (0.07)	1.1 (0.05)	-	-
	Series D	100.0 (0.00)	98.3 (0.80)	46.7 (0.28)	8.1 (1.05)	1.5 (0.13)	1.1 (0.19)	-	-
	Series E	100.0 (0.00)	98.9 (0.26)	36.4 (4.82)	2.5 (1.24)	0.8 (0.32)	0.6 (0.17)	-	-

(-): not measured

For all series, the diameter of the medium aggregate's particles mainly extends from 9.5 mm to 1.18 mm, it has a gradation close to the gradation of size no. 8 aggregate defined in the (ASTM C33, 2016) standard (Figure II.11).

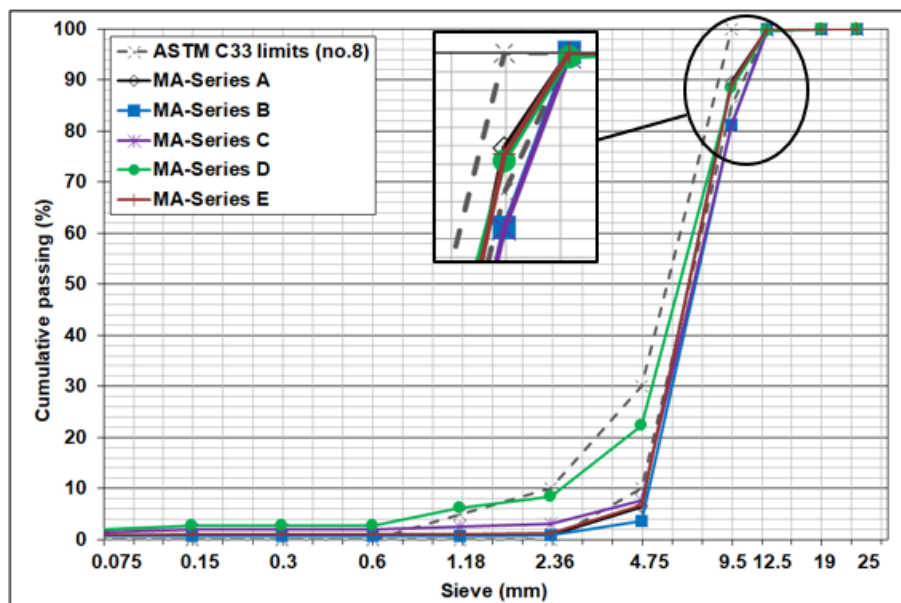


Figure II.11 The particles size distribution of medium aggregates compared to size no.8 aggregates limits (logarithmic scale)

The coarse aggregates are similar to no. 6 aggregate (*ASTM C33, 2016*) and they have predominantly grain sizes between 19 mm and 9.5 mm sieves (Figure II.12).

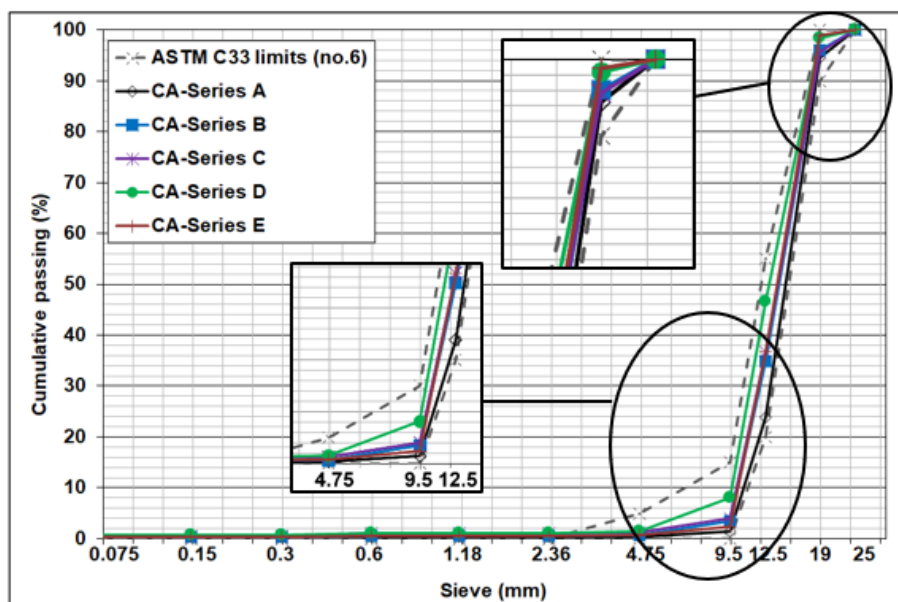


Figure II.12 The particles size distribution of coarse aggregates compared to size no.6 aggregates limits (logarithmic scale)

1.4.2 Deleterious particles

The nature and the content of deleterious particles are also effective indices of the quality of the fine aggregates and, in consequence, of the performance of concrete, as detailed in Section 4 of Chapter I. The percentage of deleterious particles in aggregates must be limited. They could increase the water requirements in the concrete mixes. Additionally, they could coat the surface of the aggregates, reducing thereby their adherence to the cement paste and degrading the concrete mechanical strengths.

To have a detailed perception of the nature of the deleterious materials, several tests are applied on the aggregates, including the percentage of clay lumps and friable particles, the sand equivalent, the methylene blue value, and the lightweight particles. The results are summarized in Table II.6 and the tests are detailed in the following.

Table II.6 The average values (and standard deviation values) of deleterious particles content in aggregates

Properties	NS		CS	MA	CA
	Series A	Series B	Series A	Series A	Series A
Clay lumps & friable particles (%)	5.3 (1.09)	5.0 (-)	0.7 (0.05)	0.2 (0.03)	0.2 (0.01)
Sand equivalent (%)	60 (1.9)	58 (1.4)	73 (1.1)	-	-
Methylene blue value (g)	1.9 (0.16)	1.3 (-)	0.9 (0.07)	-	-
Lightweight particles (%)	0.2 (0.04)	-	0.0 (0.00)	0.0 (0.00)	0.0 (0.00)

(-): not measured

1.4.2.1 Clay lumps and friable particles

The clay lumps and friable particles present on the aggregates could affect the water demand of the concrete mixes. To be sure that the materials finer than 75 μm sieve are free of clay lumps and friable particles, the percentage of these particles is determined for the four types of aggregates following (*ASTM C142, 2017*) standard.

After applying the test of materials finer than 0.075 mm sieve, this test is applied to the fraction coarser than 1.18 mm in fine aggregates and coarser than 4.75 mm sieve in coarse aggregates. The material sample is first weighed and then immersed in distilled water for 24 hours. After this period, the particles are rolled and squeezed between the fingers to break the friable particles into smaller portions. After wet sieving, the sample is oven-dried to constant mass and weighed. The percentage of clay lumps and friable particles is then calculated as the ratio of the difference in mass to the initial mass of the sample.

Table II.6 shows that the percentage of clay lumps and friable particles is low for the two types of coarse aggregates (0.2%) and the crushed sand (0.7%), while the natural sand presents a high value (around 5%) that exceeds the maximum allowable limit imposed by (*ASTM C33, 2016*) standard (3%).

When these two types of sand are combined with CS in equal mass proportions for NS-Series A and a proportion of 35% for NS-Series B, they are characterized by a percentage of clay lumps and friable particles of 3%, at the threshold of the limit.

Similar to the crushed sand of this study, the crushed aggregates from the different Lebanese resources reveal low percentages of clay lumps and friable particles (Annex B).

1.4.2.2 Sand equivalent

The sand equivalent value of fine aggregates aims to determine the proportions of clay-size particles in the sample's portion smaller than 4.75 mm sieve according to (*ASTM D2419, 2014*).

A flocculating solution is used to suspend the clay or clay size particles above the sand, and after sedimentation, the ratio of the height of the sand to the total height of the sand and the flocculating material is determined. Hence, the higher this value, the better the quality of sand.

Even though the crushed sand presents a higher percentage of fines compared to the natural sand, Table II.6 indicates that its sand equivalent value (73%) is higher than the value of the natural sand (60% and 58% for NS-Series A and NS-Series B respectively). This comparison demonstrates that the fines in the crushed sand are of better quality compared to those of the natural sand.

These results are confirmed by a wide range of data collected from the ACTS laboratory for both types of sand used in Lebanon. Figure II.13 proves that the crushed sand could present a higher sand equivalent value even if it is characterized by a higher content of fines.

It should be noted that the (*ASTM C33, 2016*) does not give a specific limit for the sand equivalent percentage in fine aggregates. Commonly, a fine aggregate with a sand equivalent value higher than 70% is usually accepted in concrete mixes.

The different resources of the Lebanese crushed sand present a wide range of sand equivalent values. For the resources studied in the parallel study of (Annex B), this characteristic varies between 61 and 78%.

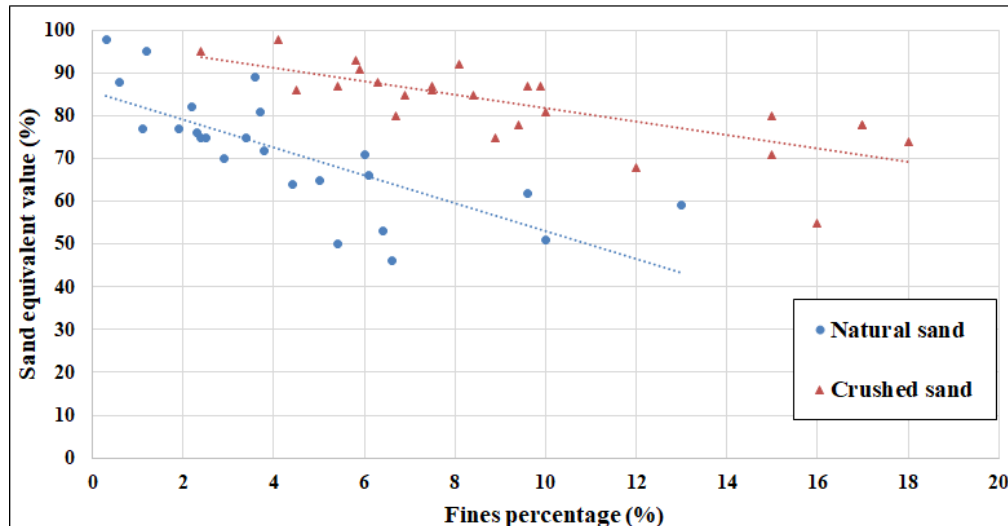


Figure II.13 Relation between sand equivalent value and fines percentage for natural and crushed sand (data collected from ACTS laboratory)

1.4.2.3 Methylene blue value

To assess the amount of clay material in the 0/2 mm fraction of sand, the methylene blue value test is applied on both types of fine aggregates following the (*BS EN 933-9, 1999*).

After successive additions of methylene blue solution to a suspension of the tested material in water, the reach of a free dye solution is confirmed by the presence of a colorless halo around the dark blue spot of the solution on a filter paper. The methylene blue value is then calculated as the total mass of dye absorbed until the sight of the halo per one kg of the sample. Thus, the high value is an indication of a high amount of clay in the sand.

Compared to the value of the crushed sand (0.9 g), the natural sand is characterized by a higher value (1.8 g and 1.3 g for NS-Series A and NS-Series B respectively), and thus a higher clay content (Table II.6). However, the values for both types of sand remain lower than 5 g, the maximum allowable limit for aggregates to be safely used in concrete (*ASTM C33, 2016*).

Generally, the study conducted on different resources of crushed sand in Lebanon reveals low values of methylene blue, thus low clay content in the crushed sand fraction smaller than 2 mm sieve (Annex B).

1.4.2.4 Lightweight particles

During placing and compacting concrete, the lightweight particles, having a density less than the aggregates, rise to the surface. During the finishing process, they could be covered by a thin mortar surface that could later reveal holes in the concrete surface, affecting thereby its durability. Hence, it is important to use aggregates with low content of lightweight particles. To assess the amount of these particles in aggregates, a zinc chloride solution, having a specific gravity of 2, is used to separate the lightweight particles from the aggregates, particularly coal and lignite, following the (*ASTM C123, 2014*) method.

This test is conducted on a saturated-surface dry fraction coarser than 0.30 mm sieve in fine aggregates and coarser than 4.75 mm sieve in coarse aggregates. The particles floating at the surface of the heavy

liquid are collected, washed, dried, and then weighed. The percentage of the lightweight particles is calculated as the percentage of the mass of the floating particles to the initial mass of the tested fraction.

The zero values in Table II.6 for coarse aggregates, medium aggregates, and crushed sand confirm the absence of lightweight particles in these aggregates. The natural sand presents an acceptable percentage of lightweight particles, with a value of 0.2%, lower than 0.5%, the maximum limit imposed by (*ASTM C33, 2016*).

1.4.2.5 Organic impurities

The presence of organic impurities in fine aggregates could have a detrimental effect by causing deterioration of concrete and by delaying its setting and hardening. Their presence is detected qualitatively following the (*ASTM C40, 2016*) standard.

The sample of sand is mixed with a hydroxide solution, and after 24 hours its color is compared to a standard color solution made of potassium dichromate in concentrated sulfuric acid.

For both types of sand, Figure II.14 shows that the color of the sample solution is lighter than the color of the standard solution (in the right of each picture). This means that the natural and crushed sands are both free from organic impurities.



Figure II.14 Organic impurities detection for fine aggregates: (a) natural sand and (b) crushed sand

1.4.2.6 Summary of deleterious particles

Generally, the limestone crushed coarse aggregates are characterized by low content of deleterious particles (clay lumps and friable particles, and lightweight particles) and they could be considered of good quality.

The natural sand presents higher content of deleterious particles than the crushed sand, even though the crushed sand contains higher amounts of fines ($< 75 \mu\text{m}$ sieve). The natural sand is characterized by a percentage of clay lumps and friable particles that exceeds the limits imposed by the standard and a sand equivalent value lower than the one usually accepted for concrete. In contrast, the content of deleterious particles for the crushed sand is within the limits. The fines of the crushed sand are mainly generated during the crushing process and originated from the parent rock rather than from impurities.

As expected, for both types of sand, there is a correlation between the results of the percentage of clay lumps and friable particle, the sand equivalent, and the methylene blue value: the higher the percentage of clay lumps, the higher the methylene blue value, and the lower the sand equivalent.

Similarly, (Wang *et al.* 2009) have found a linear relationship between the methylene blue value and the clay content in the crushed sand. The methylene blue value remarkably increases with the clay content. On the other hand, they have also observed that the clay content and the methylene blue value are not related to the content of limestone fines in the crushed sand. The sample with the highest fines content is not that the one which contains the highest clay content and methylene blue value.

1.4.3 Specific gravity and absorption

The aggregates' density and absorption are important characteristics to assess. The density is necessary to calculate the volume occupied by aggregates in concrete mixes. Its value depends on the mineralogical nature of the aggregate and its intrinsic porosity. The absorption of aggregates is used to determine the required mixing water in concrete mixes. Knowing that the densities and absorption of aggregates could differ from one pit to another, and to avoid any inaccuracy in the mix design proportions, these physical characteristics are calculated for each type of aggregate for all the series as per (ASTM C127, 2015) for coarse aggregates and (ASTM C128, 2015) for fine aggregates.

By definition, the specific gravity (relative density) is the ratio of the density of the aggregate particles to the density of water. It represents the mass of an aggregate to the mass of a volume of water equal to the volume of the absolute aggregate particles. It differs from bulk density (unit weight) which includes the volume of voids between the aggregates' particles.

For each type of aggregate, three types of relative densities are calculated depending on the moisture conditions of aggregates (Figure II.15):

- Oven Dry (OD) specific gravity: it is related to the aggregates that have been oven-dried to reach a constant mass. It is calculated as the ratio of the oven-dried mass to the difference between the saturated-surface dried mass and the mass in water;
- Saturated Surface Dry (SSD) specific gravity: it is used when the permeable pores of aggregates are filled with water but without free water on their surface. It is calculated as the ratio of the saturated-surface dried mass to the difference between the saturated-surface dried mass and the mass in water;
- Apparent specific gravity: it refers to the solid material making up the constituent particles excluding the pores that are accessible to water. It is calculated as the ratio of the oven-dried mass to the difference between the oven-dried mass and the mass in water.

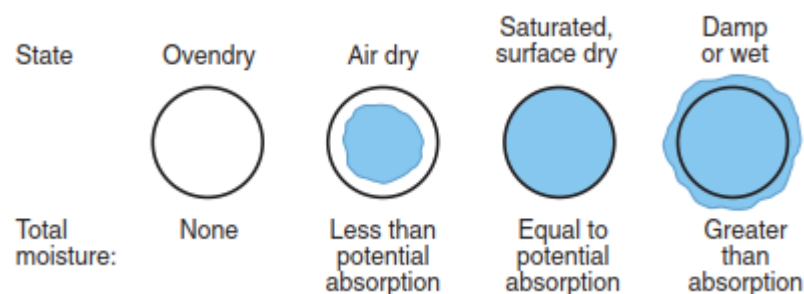


Figure II.15 Moisture conditions of aggregates (Kosmatka and Wilson, 2011)

The absorption is defined as the percentage increase in the mass of aggregate due to the penetration of water in its permeable voids after 24 hours of immersion in water. It is calculated as the percentage ratio of the difference between the saturated-surface dried mass of the specimen and the oven-dried mass (110 ± 5 °C) to the oven-dried mass.

The results of the different relative densities and the absorption of the four types of aggregates are presented in Table II.7. This table shows that the crushed sand is characterized by a higher absorption with a lower oven-dry density than the natural sand.

The densities and absorption of medium and coarse aggregates slightly vary from one pit to another. This slight variation is reasonable since the medium and coarse aggregates are extracted from different zones and depths of the same quarry (Ioannou *et al.*, 2014). Their oven-dry densities vary between 2.64 and 2.67 for medium aggregates and 2.65 and 2.69 for coarse aggregates, and their absorptions do not exceed 1%. These values are common for these types of aggregates since the densities range between 2.4 and 2.9 (Kosmatka and Wilson, 2011).

Table II.7 The average values (and standard deviation values) of the specific gravities and absorption of fine and coarse aggregates

Series	Properties	NS	CS	MA	CA
Series A	OD specific gravity	2.62 (0.010)	2.55 (0.026)	2.66 (0.001)	2.67 (0.003)
	SSD specific gravity	2.64 (0.005)	2.62 (0.024)	2.67 (0.002)	2.68 (0.003)
	Apparent specific gravity	2.68 (0.005)	2.74 (0.026)	2.70 (0.003)	2.70 (0.003)
	Absorption (%)	1.1 (0.19)	2.6 (0.28)	0.6 (0.04)	0.5 (0.02)
Series B	OD specific gravity	2.59 (0.001)	-	2.65 (0.003)	2.66 (0.002)
	SSD specific gravity	2.61 (0.002)	-	2.68 (0.002)	2.68 (0.002)
	Apparent specific gravity	2.66 (0.006)	-	2.71 (0.000)	2.71 (0.001)
	Absorption (%)	1.1 (0.10)	-	0.8 (0.04)	0.7 (0.01)
Series C	OD specific gravity	-	-	2.66 (0.000)	2.65 (0.009)
	SSD specific gravity	-	-	2.68 (0.000)	2.66 (0.010)
	Apparent specific gravity	-	-	2.71 (0.000)	2.70 (0.011)
	Absorption (%)	-	-	0.7 (0.01)	0.7 (0.03)
Series D	OD specific gravity	-	-	2.64 (0.026)	2.66 (0.013)
	SSD specific gravity	-	-	2.66 (0.022)	2.68 (0.012)
	Apparent specific gravity	-	-	2.70 (0.015)	2.71 (0.010)
	Absorption (%)	-	-	0.8 (0.16)	0.6 (0.04)
Series E	OD specific gravity	-	-	2.67 (0.001)	2.69 (0.000)
	SSD specific gravity	-	-	2.68 (0.002)	2.70 (0.001)
	Apparent specific gravity	-	-	2.71 (0.003)	2.72 (0.003)
	Absorption (%)	-	-	0.6 (0.02)	0.5 (0.03)

(-): aggregates not provided

The comparison between the results of crushed aggregates provided from different resources (Annex B) shows non-negligible differences in the values of relative densities and absorption, hence the necessity to determine these characteristics values before designing the concrete mixes.

1.4.4 Resistance to soundness and degradation

During its service life, the concrete could be subjected to severe weathering conditions including the freezing and thawing cycles and other factors leading to its abrasion. Thus, the aggregate should be resistant enough to contribute to the concrete resistance to these conditions. Additionally, the aggregate characterized by a low abrasion and impact resistances could generate more fines in the mix and thus increase its water requirement.

(ASTM C88, 2013) is used to simulate the freezing and thawing cycles, by subjecting the aggregates to five cycles of 16 to 18 hours of immersion in a sodium sulfate solution, followed by oven drying until stabilization of weight. The resistance of aggregates to the internal expansion force derived from successive precipitation and dissolution of salts in the pores is then estimated by the percentage of mass loss at the end of the final cycle to the original mass of the sample.

For medium and coarse aggregates, a supplementary test is used to assess the resistance to abrasion and impact. The method consists of determining the difference between the original mass sample and the proportion of materials retained on a 1.7 mm sieve after 500 revolutions in the Los Angeles machine (ASTM C131, 2014). The abrasion is expressed as a percentage corresponding to the mass loss divided by the original mass.

For the aggregates of Series A, four samples of each type are tested and the results of the average values and standard deviations are presented in Table II.8.

For soundness, (ASTM C33, 2016) imposes a maximum limit of 12% for coarse aggregates and 10% for fine aggregates. The coarse and medium aggregates used in this research present an acceptable soundness percentage of 8% and 9% respectively. By comparing the values of fine aggregates, the natural sand reaches a high value that overpasses the acceptable limit (11% > 10%) while the soundness of crushed sand is within the standard limit (5%). However, the combination of these two types of sand in equal mass proportions in concrete is characterized by a soundness value (8%) within the limit. Generally, the range of soundness percentage of the crushed aggregates evaluated from different Lebanese resources (Annex B) conforms to the standard requirement (CS: 1-4%; MA: 0.4-9%; CA: 0.5-3%).

The results of Table II.8 show an acceptable percentage of abrasion and impact loss by the Los Angeles machine for medium and coarse aggregates. For both types of aggregates, the loss (24%) is lower than the (ASTM C33, 2016) limit (50%). This value is also within the range of the values found for different aggregates resources in Lebanon, detailed in Annex B (MA: 22-24%; CA: 19-26%).

Table II.8 The average values (and standard deviation values) of the mass loss percentage after immersion cycles in sodium sulfate solution and after Los Angeles machine test for aggregates of Series A

Properties (%)	NS	CS	MA	CA
Soundness loss by sodium sulfate solution	11 (1.2)	5 (0.1)	9 (1.3)	8 (0.1)
Abrasion and impact loss by Los Angeles machine	-	-	24 (0.1)	24 (0.4)

(-): not measured

2. Preparation of fine aggregates

As already mentioned, for the concrete production in Lebanon, the natural sand is simply excavated from the land quarries, whereas the crushed sand is provided by crushing limestone rocks from the Lebanese mountains.

This section details the crushing process followed to produce the crushed sand in quarries. Furthermore, it develops the preparation methods adopted to construct two different gradations of normalized crushed sand, in order to respond to the objective of the study and to assess the effect of the total replacement of natural sand by normalized crushed sand in concrete.

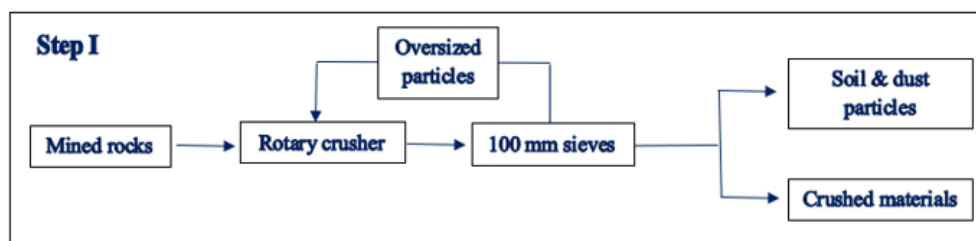
2.1 Provided crushed sand

The "Conventional crushed sand" is considered as coarse sand and its gradation should be optimized to be used as the only fine aggregate in concrete. Therefore, some Lebanese quarries began recently to optimize the gradation of the crushed sand, by producing "Fine crushed sand" with a finer particle size distribution, but with a high percentage of fines.

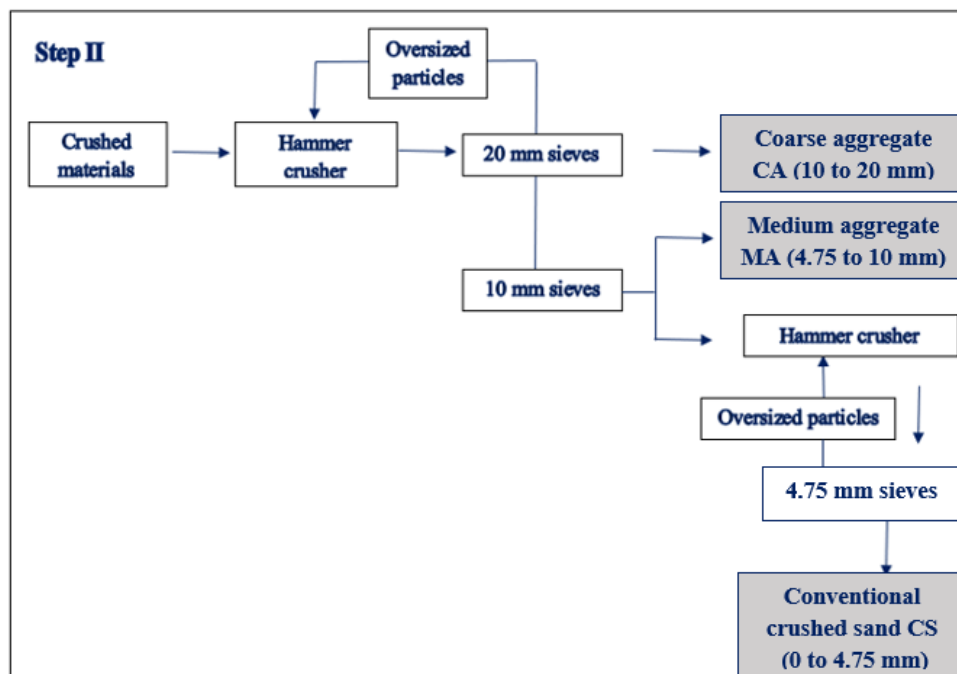
During this study, these two types of crushed sand are provided from the same quarry and their crushing process is explained in this part.

2.1.1 Conventional crushed sand

The "Conventional crushed sand" is used as an additional fine aggregate in all concrete mixes of the Lebanese market, to compensate for the fineness of the natural sand in concrete. Throughout this study, all the quantities of the conventional crushed sand used in the mixes are provided from the same quarry stock and are crushed according to the procedure described below (Figure II.16).



(a)



(b)

Figure II.16 Crushing process for the production of the "Conventional crushed sand"

The rotary crusher is used as a primary crusher to clean and reduce the size of the heavy rocks. During the first crushing step (Figure II.16a), the soil and the dust particles are removed from the crushed rocks

and carried by a conveyor belt to a separate pile. These particles are then used as fill materials in road construction or deposited in landfills. The rotary crushing process consists of crushing the materials previously mined from the Lebanese limestone mountains, by the means of blades fixed on a rotating rotor. The crushed materials are then screened over 100 mm sieves and carried by a conveyor belt to the second crusher (hammer crusher). The oversized particles are re-fed into the crusher.

The crushing materials resulting from the rotary crusher are crushed in the hammer crusher. In this step (Figure II.16b), heavy hammers crush the materials by an impact force. Four lines of hammers with seven hammers each are fixed on a spinning rotor. The motor of the crusher puts the rotor in quick rotation, imposing a high rotation speed on the hammers. The hammers hit the materials and crush them, then the finished product escapes from the cage of the crusher through openings of the desired size.

At the outlet of the hammer crusher, a conveyor belt transports the materials to two different sieves, 20 and 10 mm, to collect respectively the coarse aggregate and the medium aggregate. To produce the conventional crushed sand, a part of the produced medium aggregate is crushed again in a hammer crusher, then sieved over a 4.75 mm sieve. For the three sieves, the oversized particles are carried again to the crusher to be reduced to the desired sizes.

To obtain a control mix that simulates the one usually used in Lebanon, this sand is combined with the natural sand in an appropriate mass proportion. An example of the gradation of this fine aggregates' combination (50% Conventional CS – 50% NS-Series A) compared to the ASTM C33 grading limits are shown in Figure II.17, while the mix design proportions are detailed in the next chapter.

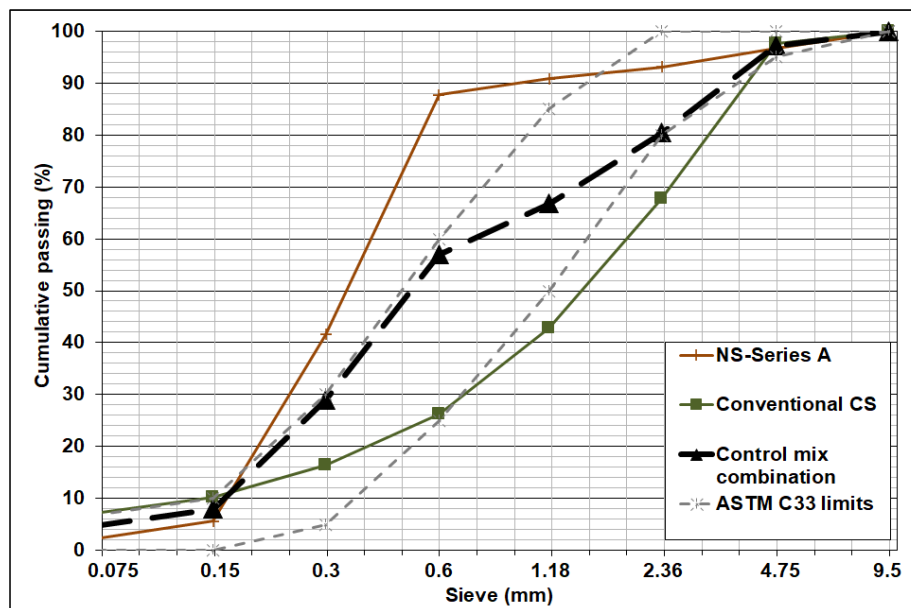


Figure II.17 The particle size distribution of the fine aggregates' combination in the reference concrete compared to the ASTM C33 grading limits (logarithmic scale)

2.1.2 Fine crushed sand

To be used as the only fine aggregate in concrete while respecting the (*ASTM C33, 2016*) grading limits, the crushed sand production should be optimized and its coarseness should be reduced. For this purpose, the same quarry that provided the conventional crushed sand has tried to improve its production by newly producing the "Fine crushed sand" with a particle size distribution that respects

the standard requirements, except for the high percentage of fines that exceeds the allowable limit (7%) and varies between 13% and 18%.

The "Fine crushed sand" of this study is provided from two different stocks of the same quarry, thus each stock is characterized by different fines percentages, 13% and 18%, and different fineness moduli, 2.7 and 2.1.

An example of this crushed sand gradation, compared to the ASTM C33 limits, is presented in Figure II.18. As will be seen in Chapter 3, this sand is used in some concrete mixes of the study to investigate, following a performance-based approach, if the performance of concrete could be maintained when using crushed sand that does not conform to the limits imposed by the standard, in terms of the percentage of the fines.

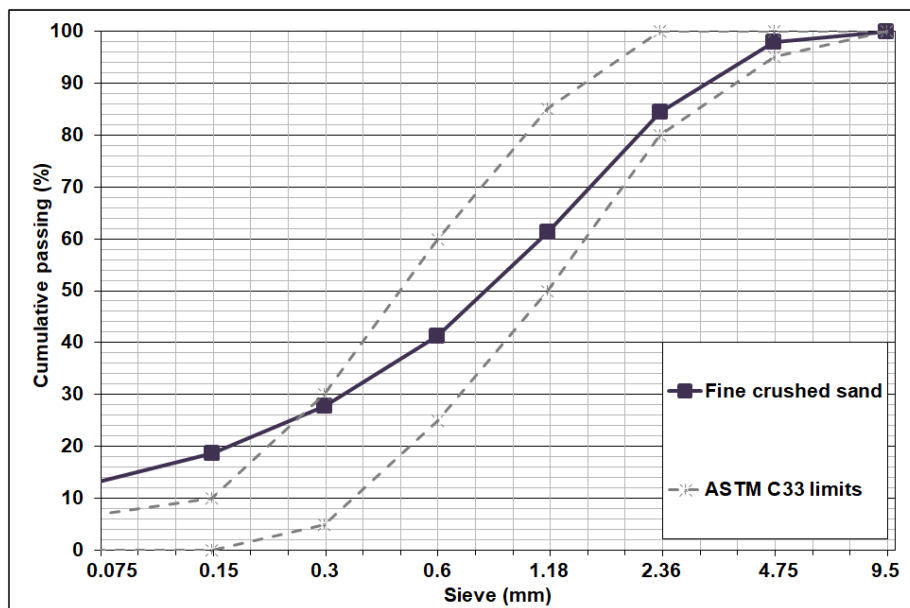


Figure II.18 The particle size distribution of the "Fine crushed sand" compared to ASTM C33 grading limits (logarithmic scale)

The first step in the production of this sand is similar to the one of the "Conventional crushed sand". However, to produce finer sand, an additional sieving step is applied (Figure II.19). A part of the material passing the 4.75 mm sieve is conveyed over sieves of 2.36 mm. The materials passing the 3 mm sieves form the "Fine crushed sand", while the retained particles (2.36 to 4.75 mm) are added to the "Conventional crushed sand" pile.

It should be noted that, sometimes, depending on the crushed rock characteristics, the crushing of the medium aggregates does not generate a sufficient volume of materials finer than 2.36 mm sieves. Therefore, before conveying the crushed sand to these sieves, an additional crushing could be applied to increase the production of the "Fine crushed sand".

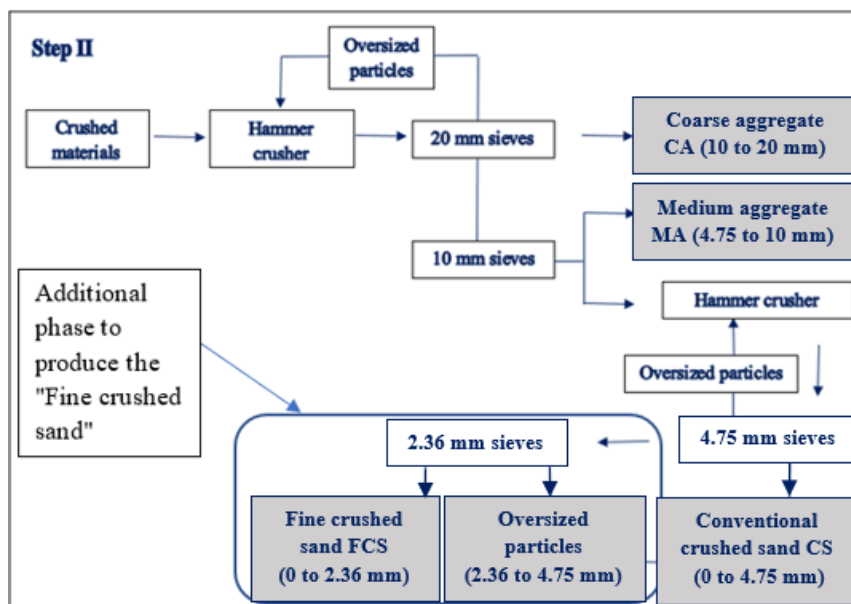


Figure II.19 Crushing process for the production of the "Fine crushed sand"

2.2 Constructed crushed sand

Aiming to evaluate the effect of the fine aggregate type and gradation on the concrete performance, two types of crushed sand are constructed during this study. To assess the only influence of the sand type on concrete behavior while avoiding the influence of the gradation, the "Equivalent crushed sand" is constructed with a gradation similar to that of the combination of the fine aggregates of the reference concrete. On the other hand, to investigate the effect of gradation, the well-graded "Modified crushed sand" is constructed.

2.2.1 Equivalent crushed sand

The "Equivalent crushed sand" is constructed in the laboratory in order to get crushed sand with a particle size distribution similar to the one used in the reference mix with natural sand NS-Series A. A large quantity of this crushed sand is constructed using the provided "Conventional crushed sand" and the "Fine crushed sand".

The "Conventional crushed sand" is dried, sieved, and divided into several size fractions, retained on the 4.75, 2.36, 1.18, 0.60, 0.30, 0.15, and 0.075 mm sieves. This first step aims to collect a large mass of the particles retained on each sieve, separately.

The second step of the construction consists of working on the provided "Fine crushed sand". The sieve and fines percentage analyses are conducted on each bag of this sand, and then compared to the gradation of the control mix combination, to know, for each sieve, the exact retained mass that needed to be added or removed from this bag. Afterward, the following steps are applied:

- The excess of fines is removed by washing;
- The excess mass retained on some sieves is removed by sieving;
- The extra mass that needed to be added on some sieves is brought from the quantities collected in step one from the "Conventional crushed sand".

The result of this construction is crushed sand with a particle size distribution that conforms to the (*ASTM C33, 2016*) grading requirements, identical to the gradation of the fine aggregates combination of conventional crushed sand and natural sand used in the control mix (Figure II.20).

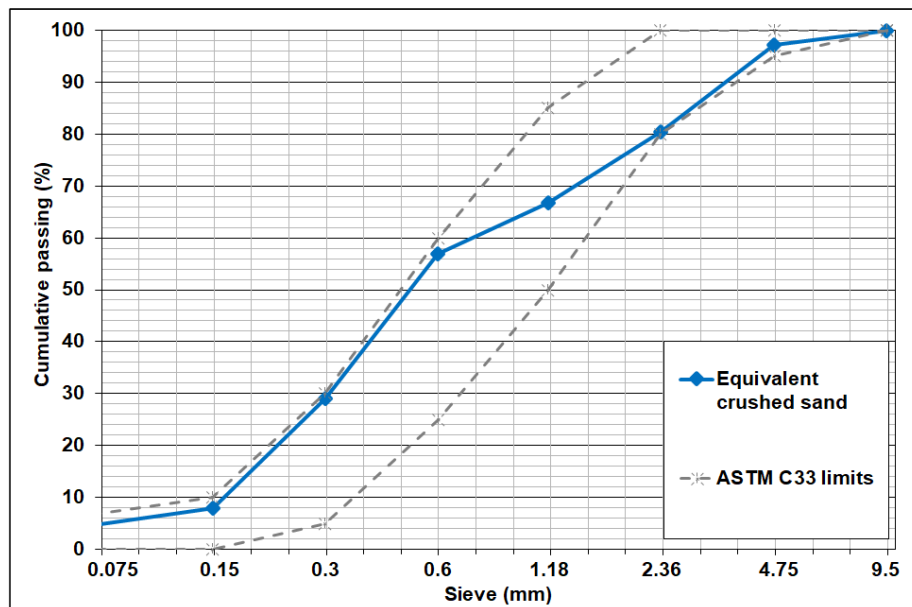


Figure II.20 The particle size distribution of the "Equivalent crushed sand" compared to ASTM C33 grading limits (logarithmic scale)

2.2.2 Modified crushed sand

The "Modified crushed sand" corresponds to a crushed sand that is well-distributed between the standard limits with a fines percentage that does not exceed 7% (Figure II.21).

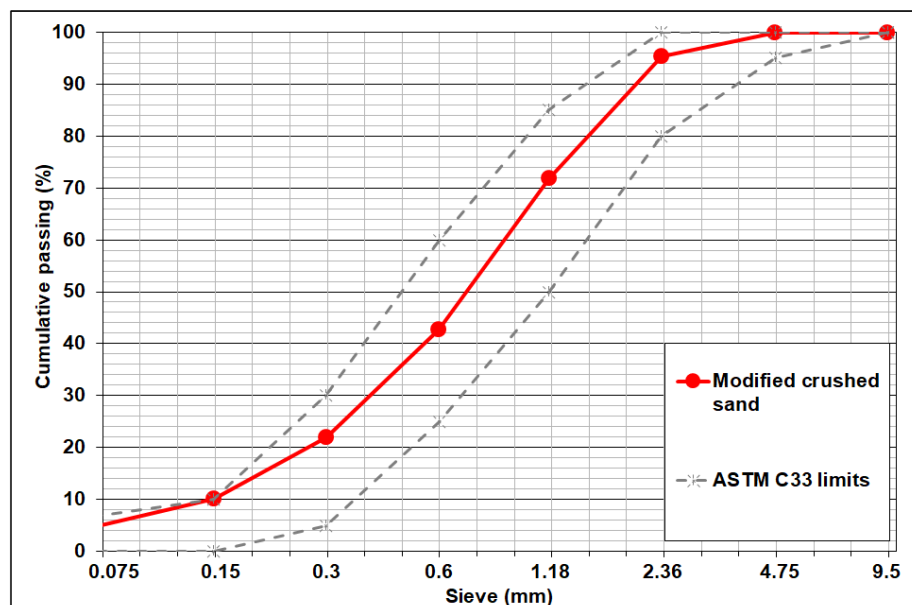


Figure II.21 The particle size distribution of the "Modified crushed sand" compared to ASTM C33 grading limits (logarithmic scale)

To construct this sand, an appropriate proportion of the "Fine crushed sand" is washed to reduce the high percentage of fines. Two stocks of the "Modified crushed sand" are constructed while reducing the percentage of fines to 3% in the first and 5% in the second with a fineness modulus of 2.6.

Conclusions

The experimental work conducted on aggregates aims to characterize each type of fine and coarse aggregates before using them in concrete and to highlight the difference in shape, chemical composition, mineralogy, and physical properties between natural and crushed sand.

The results reveal that the natural sand is siliceous rounded sand mainly formed of quartz grains, while the angular grains of crushed sand originate from calcite minerals. Compared to the standard grading requirements, the natural sand is characterized by a finer gradation, while the crushed sand presents a coarser one. Additionally, the physical characterization shows some differences between the two types of sand: the natural sand has higher fineness, specific gravity, deleterious particles, and soundness percentage, while the crushed sand presents higher absorption and a higher percentage of fines. This comparison shows that, even though the crushed sand contains a higher percentage of fines, its fines have better quality because they mainly result from the fragmentation of rocks during a secondary crushing process of this sand. The content of clay lumps and the soundness of the natural siliceous sand exceed the limit imposed by the standards applied in Lebanon. Since there is no scientifically proven alternative to natural sand so far, this sand is used nowadays in concrete mixes, despite its detrimental quality, providing that it is mixed with the crushed limestone sand, in order to have a combination of fine aggregates conforming to the specifications of ASTM C33.

The medium and coarse aggregates used are crushed limestone aggregates of good quality: they are characterized by good resistance to soundness and abrasion with low absorption and low percentages of deleterious particles.

The properties of the crushed aggregates used in this study are comparable to those of aggregates from different quarries located in different Lebanese regions, except for the densities and the absorption percentage. Thus, the results that will be found in this thesis could remain valid by changing the crushed aggregates in concrete mixes, providing that the densities and absorption are determined for each source of aggregate before mixing.

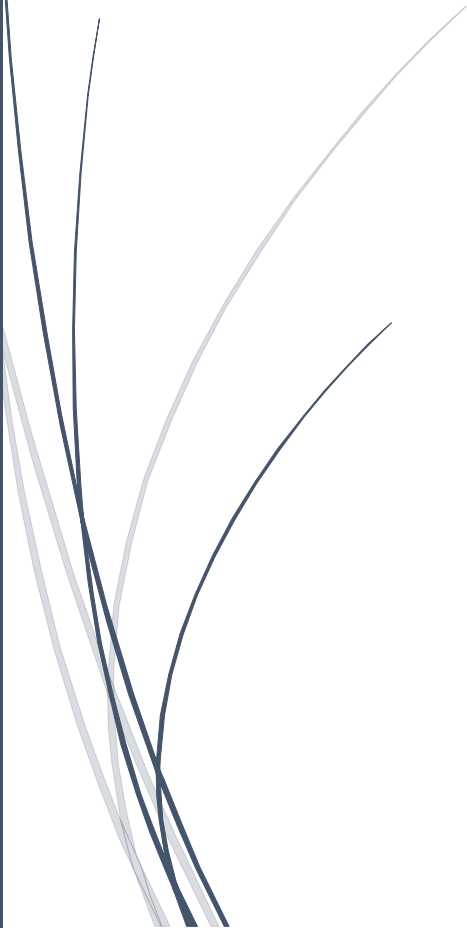
Since the study consists of assessing if the concrete performance could be maintained by the total substitution of natural sand by crushed sand, and since fine aggregates with different characteristics could behave differently in concrete, two types of crushed sand are specifically constructed for the experimental program. The effects related to the shape and physicochemical characteristics of fine aggregates are evaluated by using the "Equivalent crushed sand". This sand is constructed in the laboratory with a particle size distribution similar to that of the conventional combination of fine aggregates ("Natural sand" and "Conventional crushed sand") used in the Lebanese construction market. Then, the effect of the gradation of fine aggregates is investigated by using the constructed well-graded "Modified crushed sand" with a fine content conforming to the ASTM limits.

After determining all the aggregates' characteristics, in particular the gradation, the specific gravity, and the absorption, and after preparing the different types of crushed sand, the concrete mixes are designed and are presented in the next chapter.



Chapter III

Concrete Mix Design and Experimental Procedure



III. Concrete Mix Design and Experimental Procedure

Introduction

Chapter II has depicted many differences between the natural and crushed sand, including the shape of their grains, their chemical composition, mineralogical characterization, particle size distribution, fineness modulus, absorption, and the quantity and quality of their fines. Knowing that the differences between these two fine aggregates could directly affect the concrete performance on fresh and hardened states, the concrete mixes presented in this chapter are designed to compare, for several concrete strengths, different concrete formulations differing only by the fine aggregates type and/or gradation.

The study consists of evaluating the effect of substituting the typical combination of natural sand and the conventional crushed sand with crushed sand which gradation conforms to the grading requirements. Thus, a total of 9 mixes are compared for 3 different normal strength concretes, and two additional mixes for one high-strength concrete. Secondly, following a performance-based approach, the effect of crushed sand which gradation does not conform to the standard requirements in terms of fines content is evaluated, by comparing three types of concrete for two different strengths each. The mixing procedure and the materials proportions of each type of concrete are detailed in the first part of this chapter.

The last part describes the experimental program conducted to set a comparison between the different types of concrete in terms of the fresh properties, mechanical behavior, and long-term performance. Within the framework of this joint-program study between Lebanon and France, the concrete mixing, the preparation of the cylinders, and the concrete tests have been conducted in the laboratories of ACTS in Lebanon except for the porosity test and the microstructural analysis that have been carried out in LMDC in France. The concrete tests that are applied in this study are the most commonly required in Lebanon, usually conducted following the ASTM standards, except for some of them that are mostly carried out as per the British or European standards. Annex D presents more details on the procedure of each concrete test and compares the ASTM and the European standards.

1. Concrete mix design

Recalling that the objective of studying the concrete performance is to assess the effect of the different types of fine aggregate, the choice of the concrete formulations consists of limiting the differences between the various concrete types to the fine aggregates only.

For each concrete mix, the cement, effective water, and coarse aggregates contents are fixed and the only variable is the fine aggregates type and/or gradation. The slump value is fixed and a high-range water-reducing admixture is used with an adapted amount to attain the target workable concrete.

The materials used, their proportions in the different concretes, and the mixing procedure are detailed in the following sections.

1.1 Materials

The aggregates whose properties were detailed in the previous chapter are used in the concrete formulations. The characteristics of the cement and the water added to the concrete mixes are presented in this section.

1.1.1 Aggregates

Usually, in concrete plants, the aggregates are neither saturated nor dried before being incorporated in concrete, they are used in their natural moisture condition. Therefore, to simulate in our study the most realistic mixing process that is generally applied in concrete plants, the choice was to use the aggregates in their real moisture condition, as received from the suppliers.

All the coarse aggregates were received in their air-dry condition, their surface was dry and their pores were partially filled with water.

As for the fine aggregates, the preparation of the constructed crushed sand required a drying process, as detailed in Chapter II. Therefore, to let the fine aggregates be partially filled with water before being used in concrete, the prepared crushed sands were mixed with a small quantity of water that did not exceed the needed quantity to saturate them. Moreover, to obtain a valid comparison between the different mixes and to avoid the effect of the moisture condition on the concrete properties, the natural sand, the conventional crushed sand, and the fine crushed sand were also mixed with water before being used in concrete mixes to reach a moist condition close to the one of the constructed crushed sand.

All aggregates were then covered and stored at room temperature in the range of 20-30 °C.

On the eve of the mixing day, a representative sample of each type of aggregates was taken to determine its moisture content following the (*ASTM C566, 2013*) standard. The mass of the sample is measured before and after being oven-dried (105 ± 5 °C) to constant mass, and its moisture content is computed as the ratio of the difference in mass to the dried mass. Knowing the absorption (Chapter II) and the moisture content of each type of aggregates, the estimated quantity of water that will be absorbed by each aggregate is determined and added to the water of each mix.

1.1.2 Cement

In this study, all concrete mixes are prepared with a commercial limestone cement known as PA-L 42.5, provided by Holcim in bags of 50 kg each, and stored in a dry place until the mixing day. This cement is widely used in Lebanon and it is produced by grinding limestone (6%-15%) and calcium sulfate in addition to the clinker. The limestone enhances the workability of mortar and concrete and reduces the carbon footprint of cement production, while calcium sulfate is added to regulate the setting time of concrete.

The characteristics of this cement conform to the requirements of the American standard (*ASTM C595, 2017*) as Portland-Limestone cement Type I-L, and those of the European standard (*BS EN 197-1, 2011*) as CEM-II/A-L 42.5 N. To have a detailed view of the cement's characteristics, several chemical and physical characterization tests are conducted.

In the Lebanese construction field, cement production should conform to the Lebanese standard (*NL 53, 1999*) based on the *EN-197-1* standard, and the European standards are usually used to characterize

the cement. In some projects, American standards are also required. Accordingly, for some of the cement characteristics, both standards are represented in this study.

1.1.2.1 Chemical and mineralogical composition

The X-ray fluorescence spectrometry by fusion method, ion chromatography, and the loss on ignition are the methods applied to assess the nature and the quantity of the chemical elements present in the cement. The free lime is found by Ethylene glycol and HCl titration method, while the percentage of insoluble is detected by (*ASTM C114, 2004*).

Table III.1 details the chemical composition of the cement used in the study. The addition of limestone and calcium sulfate to the clinker is revealed by the high loss on ignition (7.23%) in the cement.

Table III.1 Chemical composition of cement

Compound	Mass percentage (%)
SiO ₂	17.21
CaO	62.60
Al ₂ O ₃	4.16
Fe ₂ O ₃	2.86
K ₂ O	0.30
Na ₂ O	0.27
MgO	1.16
Mn ₂ O ₃	0.03
TiO ₂	0.40
SO ₃	3.42
P ₂ O ₅	0.36
Cr ₂ O ₃	0.02
Insoluble	0.50
Free CaO	0.08
Loss on ignition	7.23

To determine the mineralogical composition of the cement, the modified Bogue method is used. The estimation of the mineralogical compounds in terms of mass percentage is presented in Table III.2.

Table III.2 Mineralogical composition of the clinker calculated by modified Bogue method

Compound	C ₃ S	C ₂ S	C ₃ A	C ₄ AF
Mass percentage (%)	64.7	15.4	8.3	11.7

Additionally, the XRD analysis is illustrated in Figure III.1. This graph shows that, in addition to the classical presence of calcite and the anhydrous compounds, a presence of Portlandite and ettringite is also detected.

The TGA-DTG analysis of the cement is presented in Figure III.2. Figure III.2a reveals a calcite content of 11.1% and 0.5% of gypsum. Figure III.2b confirms the presence of Portlandite and C-S-H in the cement. Hence, the studied cement could be slightly hydrated.

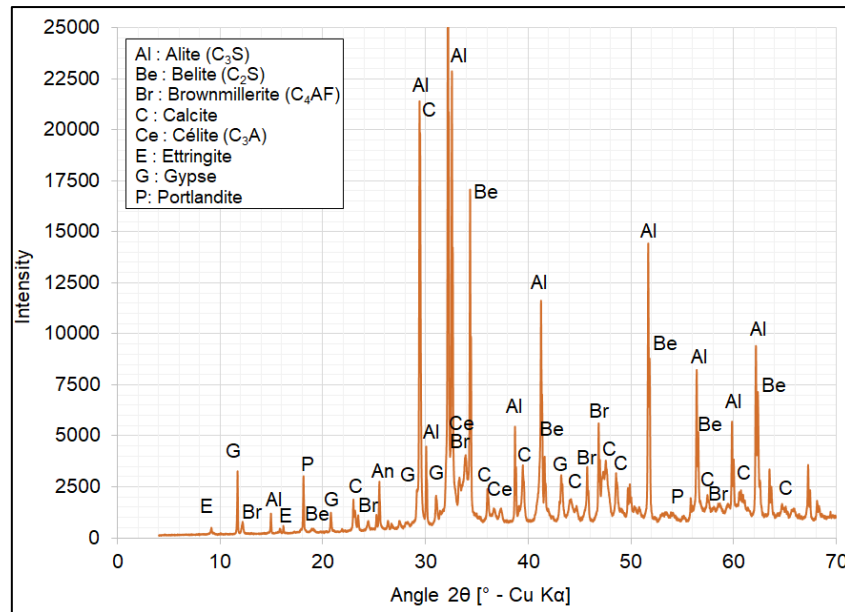
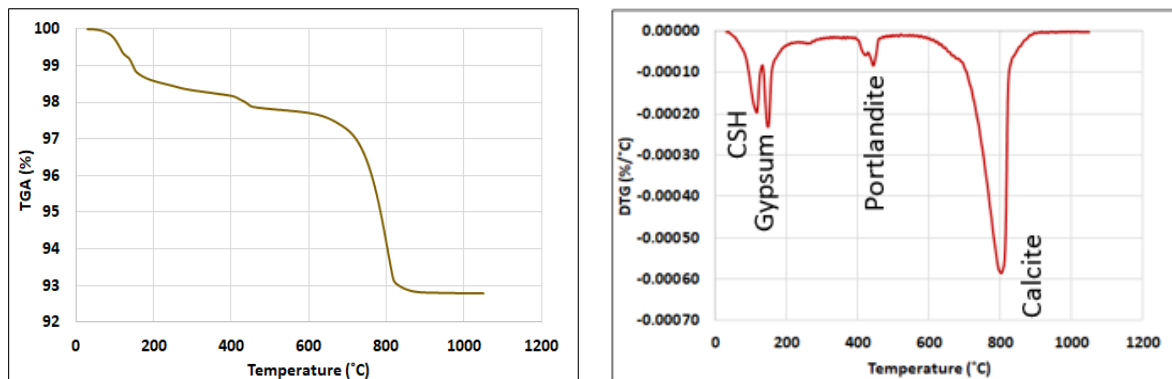


Figure III.1 XRD analysis of the cement sample



(a)

(b)

Figure III.2 TGA-DTG analysis of the cement sample

1.1.2.2 Physical characterizations

To determine the physical characteristics of the cement, several tests are applied: gradation, density, fineness and specific surface, flow time, setting time, and mechanical strengths.

- **Gradation**

The cement gradation is determined by the laser diffraction technique using the Fraunhofer model. After the emission of incident rays, the diffracted ray is detected and the diameters of the particles are calculated based on the spherical assumptions of cement grains; the calculated value is the equivalent diameter of a sphere having the same volume as the studied particle.

The sample is in the range of milligrams and is representative of the entire specimen. To avoid cement hydration by water, ethanol is used as the fluid that carries the cement powder. The ultrasounds technique allows the elimination of the particles' agglomeration.

The particle size distribution of the cement used in this study is represented by the red curve of Figure III.3.

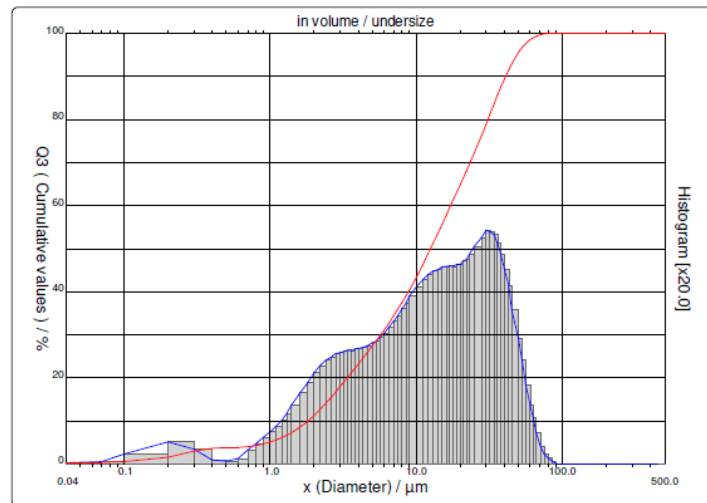


Figure III.3 The particle size distribution of cement represented by the histogram and the cumulative values

This cement is characterized by a maximum diameter of 80 μm and a mean diameter of 17.44 μm (Table III.3). 90% of the particles have a diameter below 40.87 μm , while 10% of particles have diameters below 1.81 μm . The cement is characterized by a D_{50} of 12.51 μm . These values are comparable to the results observed in the study of (Bentz *et al.*, 2015) for cement with a 3.82% addition of limestone by mass (the cement in their study is characterized by a D_{90} , D_{50} , and D_{10} of 30.8, 10.6, and 1.32 μm respectively).

Table III.3 The characteristics of the particle size distribution of cement, in μm

D_{max}	D_{mean}	D_{10}	D_{50}	D_{90}
80	17.44	1.81	12.51	40.87

- **Density**

In the (ASTM C188, 2017) standard, the Le Chatelier flask is used to determine the cement density. The measured density is equal to $3.09 \pm 0.003 \text{ g/cm}^3$ and it is lower than the density of the ordinary Portland cement (3.15 g/cm^3), due to the presence of limestone in this cement.

- **Fineness and specific surface**

The specific surface is defined as the surface of a solid in a unit mass and it is related to the fineness of the cement; the greater the specific surface the greater the fineness. The fineness of the cement affects its hydration rate and it is determined by applying the permeability principle conforming to (ASTM C204, 2017; NF EN 196-6, 2018). To obtain a representative result, the test is repeated on three samples of 5 g each.

The calculated values of the specific surface are $4170 \text{ cm}^2/\text{g}$ and $4272 \pm 236.4 \text{ cm}^2/\text{g}$ while applying the American and the European standard respectively. These values give an indication of the high fineness of the cement used and are higher than $3000 \text{ cm}^2/\text{g}$, conforming to the minimum limit imposed by (NL 53, 1999) for this type of cement.

- **Flow time**

To assess the influence of the cement on the workability of mortar or concrete and the water demand of cement, the flow time is evaluated as per (NF P 18-452, 2017) on a normalized mortar mix. The method consists of measuring the time that the normalized mortar takes, under vibration, to pass from a vertical position to an almost horizontal one in the apparatus machine illustrated in Figure III.4.



Figure III.4 The apparatus used for the flow time test

The cement used in the concrete mixes of this study is characterized by a mortar flow time of 2 seconds. This short flow time characterizes a cement that provides good workability to mortar or concrete without a need for a high amount of water. This could be attributed to the addition of the limestone to the clinker of the cement since this addition increases the packing of the cement grains.

- **Normal consistency and setting time of cement paste**

The paste used in the setting time test should have a normal consistency; it should not be too dry or too wet. Thus, to prepare the cement paste for the setting time test, the water to cement ratio which gives a normal consistency should be determined.

For this purpose, (ASTM C187, 2011; BS EN 196-3, 2016) are applied and the Vicat apparatus presented in Figure III.5 is used.



Figure III.5 The Vicat apparatus used to determine the consistency of mortar

The amount of water that produces the target plunger penetration (6 ± 2 mm or 10 ± 1 mm for EN and ASTM standards respectively) is considered suitable for the normal consistency of mortar. By applying both standards, the normal consistency of the paste is found to be equal to 27%, which corresponds to the water to cement ratio that should be used in the setting time test. This value is within the range of the ordinary Portland cement (25-35%).

The cement paste sample used to carry out the setting time test is then prepared with this value of water to cement ratio. In this test, the plunger in the Vicat apparatus of Figure III.5 is replaced by a needle.

The initial setting time corresponds to the time elapsed between the initial contact of cement and water and the time when the distance between the needle and the base plate of the Vicat apparatus is 6 ± 3 mm (*BS EN 196-3, 2016*) or when the needle penetration reaches 25 mm (*ASTM C191, 2018*). The final setting time is recorded as the time elapsed between the initial contact of cement and water and the time when the penetration does not leave a mark on the specimen surface.

The results are presented in Table III.4. There is a one-hour difference between both standards for the initial setting time, and 35 minutes for the final setting time. These differences could be attributed to the difference in the experimental procedure between both standards.

Despite its high fineness, the cement does not set rapidly since its setting time is regulated by the addition of calcium sulfate to the clinker during cement production. The initial setting time is higher than 75 minutes, conforming to the minimum limit imposed by (*NL 53, 1999*).

Table III.4 Setting times of cement paste

Standard	Initial setting time	Final setting time
BS EN 196-3	2h45min	4h10min
ASTM C191	3h45min	4h45min

- **Mechanical strengths**

To have a better understanding of the mechanical performance of concrete, it is essential to verify the grade of the cement used in concrete mixes. For this purpose, normalized mortar mixes are prepared from the cement of the study to assess their strength.

The normalized mortar mixes are prepared following (*BS EN 196-1, 2005*) by adding 450 ± 2 g of cement, 1350 ± 5 g of normalized sand, and 225 ± 1 g of water. These amounts correspond to the following proportions: one part of cement, 3 parts of the standard sand, and 0.5 part of water, i.e., water to cement ratio of 0.5.

The specimens are prepared by jolting two layers of mortar on 40x40x160 mm prisms molds. They are then covered with a glass plate and stored in a moist room. After 24h, the specimens are de-molded and stored in water at 20 ± 1 °C until the age of testing. The flexural strengths are assessed on 3 prisms at each mortar age: 3, 7, and 28 days.

The results are presented in Table III.5. The compressive strength test is carried out on the halves of the broken prisms of the flexural test according to (*BS EN 196-1, 2005*). As expected, Table III.5 shows that the compressive strength of mortar at 28 days exceeds the minimum required mortar strength (42.5 MPa) and the minimum average compressive strength (55 MPa).

Table III.5 The average values (and the standard deviation values) of the flexural and compressive strengths of the normalized mortars, in MPa

Standard	3 Days	7 Days	28 Days
Flexural strength	6.5 (0.12)	7.1 (0.14)	9.6 (0.17)
Compressive strength	26.6 (0.51)	36.0 (0.22)	57.1 (0.29)

1.1.3 Water

The water added to all concrete mixes is potable water with a pH of 7.7 (at 23 °C). Its characteristics, summarized in Table III.6, confirm that it could be safely used in concrete mixes.

Table III.6 Characteristics of the water used in concrete mixes

Compound	Total dissolved solids	Chloride	Sulfate
Concentration (ppm)	260	20	20
Limits (ASTM C1602, 2006)	(< 50 000)	(< 500)	(< 3 000)

1.1.4 Admixture

To enhance the workability of concrete, the admixture used is a high-range water-reducing superplasticizer (Admix CF 100) provided by Sodamco. It complies with the admixture Type F of (ASTM C494, 2016). For each mix, most of the admixture quantity is introduced into the mixer with the mixing water, while the remaining quantity is added alone at the end of the mixing.

1.2 Mix proportions

During this study, the effect of the total replacement of natural sand by crushed sand is assessed for different concretes to verify that the concrete performance could be maintained during this substitution, whatever the concrete strength.

To be able to study the effects of fine aggregates, the only difference between the compared concrete of each mix is reduced to the fine aggregates type and/or gradation. Several batches of a volume of approximately 0.06 m³ of concrete each are prepared for each type of concrete, to cast all the necessary samples to perform the whole experimental program. The quantity of the needed mixing water is computed taking into consideration the moisture conditions of the aggregates and the water that could be absorbed by these aggregates during mixing. To obtain representative industrial workable concrete, the slump value is fixed to 20 ± 2 cm for all mixes. Thus, for each mix, the dosage of high-range water-reducing admixture is adapted to reach the target slump.

1.2.1 Mixes incorporating normalized crushed sand

The first step of the study consists of assessing the effect on the concrete performance of the different types of fine aggregates which gradations conform to the standard grading requirements. In this part, three different normal strength concrete mixes are designed in addition to one mix of high-strength concrete.

1.2.1.1 Fine aggregates

Three types of fine aggregates are used for each normal strength concrete and only two types of fine aggregates for the high-strength mix.

➤ Normal-strength concrete

Figure III.6 gives the particle size distributions of the three types of fine aggregates used in the normal strength concretes.

The natural sand "NS-Series A" and the "Conventional crushed sand CCS" are mixed in equal mass proportions (50% NS-Series A + 50% CCS) to form the "Control mix combination-A". Thus, this combination is characterized by a fines percentage of 4.8% and a fineness modulus of 2.6. It simulates the typical fine aggregates combination that is currently used in the Lebanese industry to respect the ASTM C33 grading limits. It is incorporated in the "Control mix CM" that serves as the reference concrete of the study.

The particle size distribution of the "Equivalent crushed sand ECS", as seen in Chapter II, is constructed to be strictly similar to the one of the "Control mix combination-A". The "Equivalent mix EM" incorporates this constructed crushed sand as the only fine aggregate without natural sand, to eliminate the effect of the gradation while studying the effect of the total substitution of the conventional combination of sand by the crushed sand.

To study the effect of well-graded crushed sand, the "Modified crushed sand MCS", which construction is detailed in Chapter II, is used as the only fine aggregate in the "Modified mix MM" that does not contain natural sand. It is characterized by a fines percentage of 5% and a fineness modulus of 2.6.

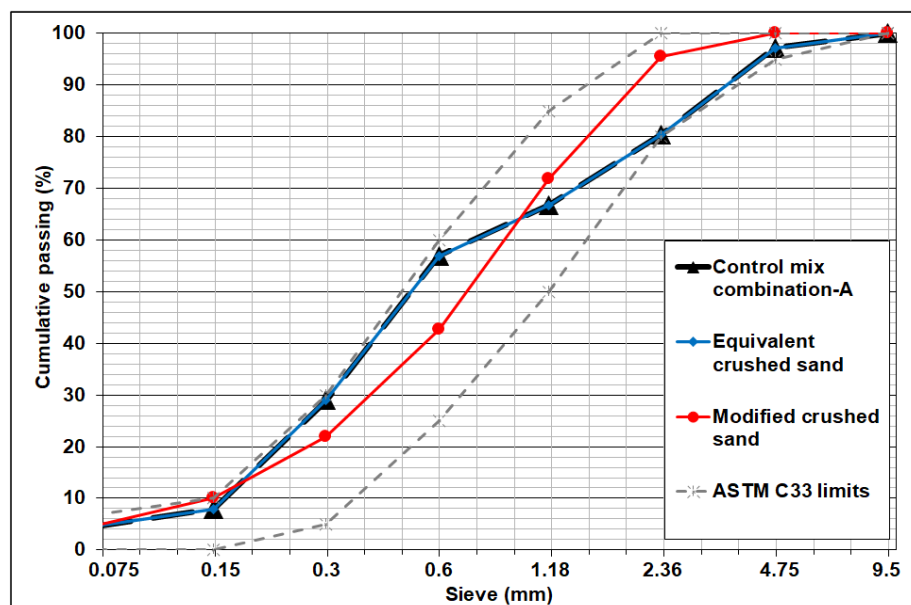


Figure III.6 The particle size distribution of the fine aggregates incorporated in the normal strength concretes compared to the gradation limits of ASTM C33

Table III.7 recapitulates the incorporation of each type of fine aggregates in the different types of concrete.

Table III.7 Nomenclature of the different types of concrete according to the type of the fine aggregates (assessment of the normalized crushed sand effect on normal strength concretes)

Concrete type	Nomination	Fine aggregates type
Control mix	CM	Control mix combination-A: 50% Natural sand-A (NS-Series A) + 50% Conventional crushed sand (CCS) (mass proportions)
Equivalent mix	EM	Equivalent crushed sand (ECS): Only crushed sand, without natural sand Equivalent gradation to the one of the "Control mix combination-A"
Modified mix	MM	Modified crushed sand (MCS): Only crushed sand, without natural sand Well-graded with 5% of fines

➤ High-strength concrete

The gradations of the two types of fine aggregates used in the high-strength concrete mix, the "Control mix combination-B" and the "Modified crushed sand MCS", are represented in Figure III.7.

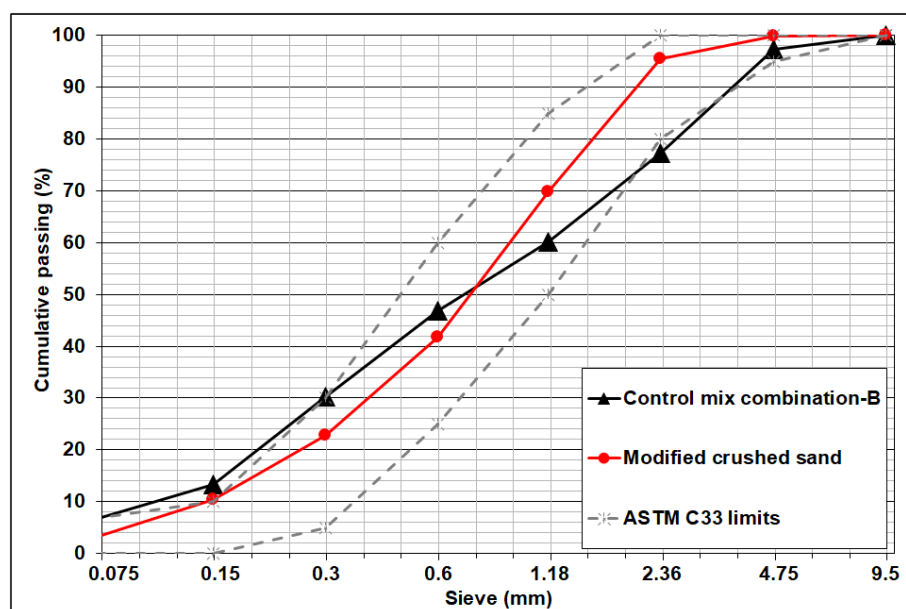


Figure III.7 The particle size distribution of the fine aggregates incorporated in the high-strength concrete compared to the gradation limits of ASTM C33

The "Control mix combination-B", composed of 35% of the natural sand "NS-Series B" and 65% of the "Conventional crushed sand CCS", is incorporated in the "Control mix" (Table III.8). This combination contains 6.9% of fines and presents a fineness modulus of 2.8.

Between the two types of crushed sand concretes, the "Equivalent mix" and the "Modified mix", the latter is chosen to be compared to the control mix of the high-strength concrete. This mix does not contain natural sand and it is constituted of the "Modified crushed sand MCS" as the only fine aggregate (Table III.8). This sand is characterized by a fines percentage of 3% and a fineness modulus of 2.6. The laboratory construction of the "Modified crushed sand MCS" is faster than the one of the "Equivalent crushed sand ECS" and its gradation could be more generalized and applied in the quarries, while the gradation of the "Equivalent crushed sand ECS" depends on the one of the combination of fines aggregates in the conventional concrete mixes.

Table III.8 Nomenclature of the different types of concrete according to the type of the fine aggregates (assessment of the normalized crushed sand effect on the high-strength concrete)

Concrete type	Nomination	Fine aggregates type
Control mix	CM	Control mix combination-B: 35% Natural sand-B (NS-Series B)+ 65% Conventional crushed sand (CCS) (mass proportions)
Modified mix	MM	Modified crushed sand (MCS): Only crushed sand, without natural sand Well-graded with 3% of fines

1.2.1.2 Coarse aggregates

Additionally, to have a well-graded coarse aggregates combination, the mass proportions of MA and CA in each concrete mix are fixed to 43% and 57% respectively, to fit the gradation envelope given in (ASTM C33, 2016) for no. 6.7 aggregate (Figure III.8).

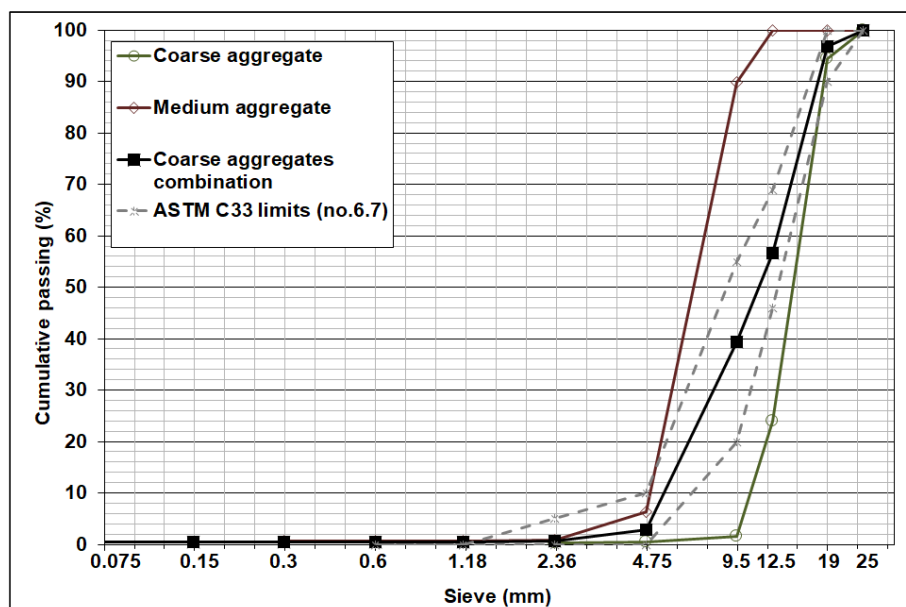
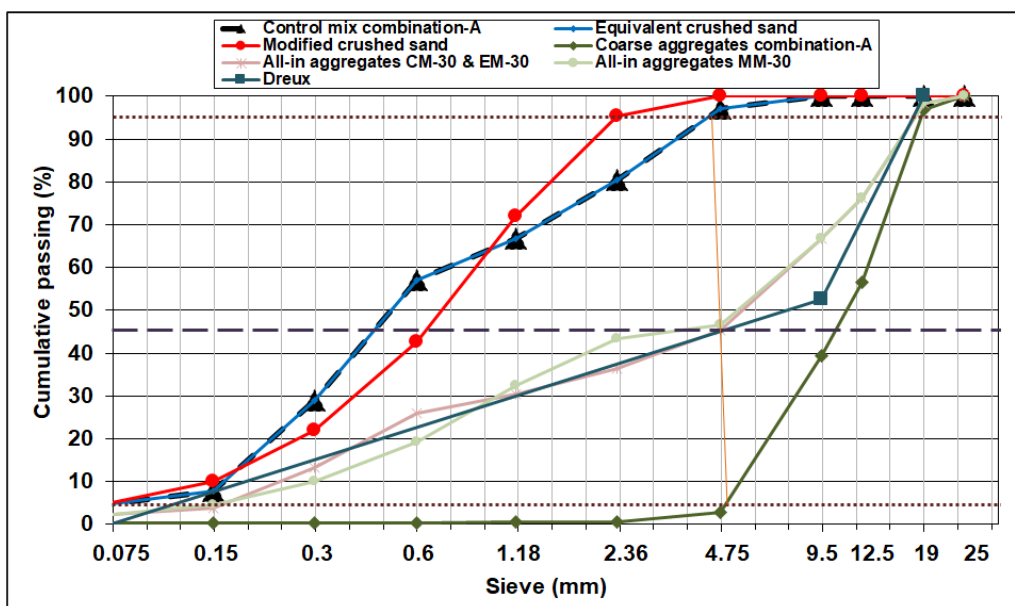


Figure III.8 The particle size distribution of medium and coarse aggregates compared to the gradation limits of no. 6.7 aggregate

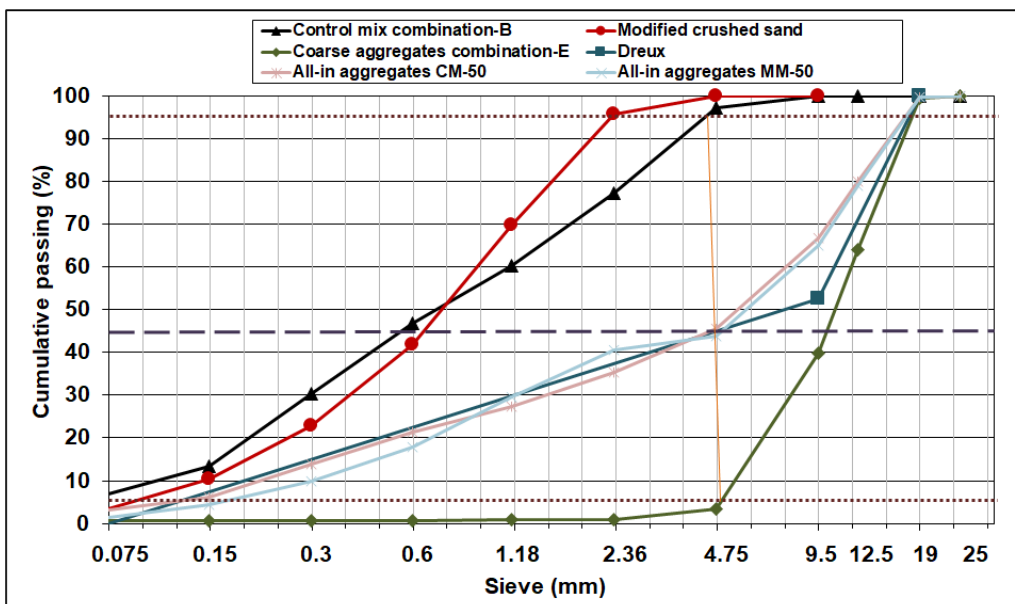
1.2.1.3 All-in aggregates

To avoid segregation and to have well-graded concrete, the all-in aggregates granular distribution is optimized by applying the Dreux method (Dreux and Festa, 1995). The mass proportions are found to be 45% and 55% for the fine and the coarse aggregates combination respectively in all the studied mixes.

Examples of the all-in aggregates of the normal and high-strength concrete mixes are presented in Figure III.9a and Figure III.9b respectively. These figures show that in the range of 1.18-4.75 mm sieves, the graph of the all-in aggregates of MM is higher than the one of CM. The inverse is observed between 0.3 and 0.6 mm sieves. These differences are lower in the high-strength concretes.



(a)



(b)

Figure III.9 Example of the determination of aggregates proportions by Dreux method (assessment of the normalized crushed sand effect) for (a) normal strength concretes and (b) high-strength concrete

1.2.1.4 Concrete mixes

The effects of the different types of fine aggregates on concrete behavior are evaluated for the various concrete mixes. The proportions of the materials are presented in Table III.9. For each mix, the fines aggregates combination of the "Control mix CM" is replaced by an equivalent volume of the "Equivalent crushed sand ECS" and the "Modified crushed sand MCS" in the "Equivalent mix EM" and the "Modified mix MM" respectively.

"Mix 30" is commonly used in the Lebanese concrete industry to reach an average 28-day compressive strength of 30 MPa. This mix is characterized by water to cement ratio of 0.5 and cement content of

350 kg/m³ of concrete. The MA and CA of Series A are used in "Mix 30" and they are fixed to a proportion of 427 kg/m³ and 566 kg/m³ respectively.

To reach a higher strength with the same cement content of 350 kg/m³, the water to cement ratio in "Mix 35-I" is reduced to 0.4 and the aggregates are used in higher amounts. The three types of fine aggregates compared in "Mix 30" are also used for "Mix 35-I". As already mentioned in Chapter II, for different mixes, the coarse and medium aggregates have not been provided on the same day and they have been collected from different pits of the same quarry, thus for this mix, the coarse and medium aggregates of Series B are used instead of those of series A.

Compared to "Mix 30", the water to cement ratio and the cement content in "Mix 35-II" are reduced to 0.4 and 300 kg/m³ respectively, to emphasize more the effects of aggregates and to reach a slightly higher strength while reducing the environmental threats caused by the cement production. The three types of fine aggregates compared in the other two mixes are also used, and the coarse and medium aggregates of series C are incorporated in "Mix 35-II".

"Mix 50" is designed to evaluate the effects of the total substitution of the conventional combination of fine aggregates by well-graded crushed sand when high compressive strength is required in concrete structures. It is characterized by a high cement content of 400 kg/m³ and a low water/cement ratio of 0.3. The two high-strength concretes contain the coarse and medium aggregates of Series E.

Table III.9 Mix design proportions of concretes (assessment of the normalized crushed sand effect) (kg/m³)

Concrete mix	Cement	Effective water	W/C	Admixture*	NS	CCS	ECS	MCS	MA	CA
Mix 30	CM-30			2.47 (0.71%)	406	406	0	0		
	EM-30	350	175	0.5	1.01 (0.29%)	0	0	802	0	427 566
	MM-30			0.00 (0.00%)	0	0	0	802		
Mix 35-I	CM-35-I			8.51 (2.43%)	426	426	0	0		
	EM-35-I	350	140	0.4	4.75 (1.36%)	0	0	840	0	447 593
	MM-35-I			3.86 (1.10%)	0	0	0	840		
Mix 35-II	CM-35-II			10.38 (3.46%)	448	448	0	0		
	EM-35-II	300	120	0.4	6.90 (2.30%)	0	0	884	0	471 624
	MM-35-II			5.99 (2.00%)	0	0	0	884		
Mix 50	CM-50	400	120	0.3	9.61 (2.40%)	300	557	0	0	450 597
	MM-50			10.20 (2.55%)	0	0	0	854		

(*): the value between brackets represents the massic dosage of the admixture as a percentage of the cement mass

1.2.1.5 Additional concrete mix

To be able to conduct additional tests on "Mix 30", specifically the modulus of elasticity and the shrinkage tests, additional quantities of MA and CA aggregates (Series D) have been provided and they are used in mass proportions of 40% and 60% respectively as shown in Table III.10. A batch of 0.03 m³ "Mix 30-a" is prepared for the three types of fine aggregates. The mass proportions vary to 42% and 58% for fine and coarse aggregates combination respectively.

Table III.10 Mix design proportions of "Mix 30-a" (kg/m³)

Concrete mix	Cement	Effective water	W/C	Admixture*	NS	CS	ECS	MCS	MA	CA
Mix 30a	CM-30a			3.74 (1.07%)	378	378	0	0		
	EM-30a	350	175	0.5	2.00 (0.57%)	0	0	747	0	418 627
	MM-30a				1.24 (0.35%)	0	0	0	747	

(*): the value between brackets represents the massic dosage of the admixture as a percentage of the cement mass

1.2.2 Concrete mixes incorporating crushed sand with a high percentage of fines

The objective of the second part of the study is to verify if the "Fine Crushed Sand", characterized by a gradation that does not conform to the ASTM C33 grading requirements in terms of the high percentage of fines, could replace the natural sand without compromising the concrete performance. This replacement could limit the constraints and eliminate the additional cost resulting from the reduction of the high percentage of fines from the fine crushed sand.

In this part, two types of comparisons are developed:

- This first comparison is conducted between the "Control mix" incorporating the "Control mix combination-B" on one hand, and the "Fine mix" containing the "Fine crushed sand FCS" as the only fine aggregate, on the other hand. This comparison aims to ascertain that the "Fine crushed sand" could safely replace the conventional combination of sands in the "Control mix".
- The second comparison consists of assessing the performance of the "Fine mix" on one hand, and the "Modified mix MM" that incorporates the "Modified crushed sand" with a percentage of fines within the standard limits, on the other hand. This comparison is conducted to efficiently investigate the effect of high fines content by comparing two crushed sand concretes differing only by the percentage of fines.

An example of the particle size distribution of each fine aggregate is illustrated in Figure III.10.

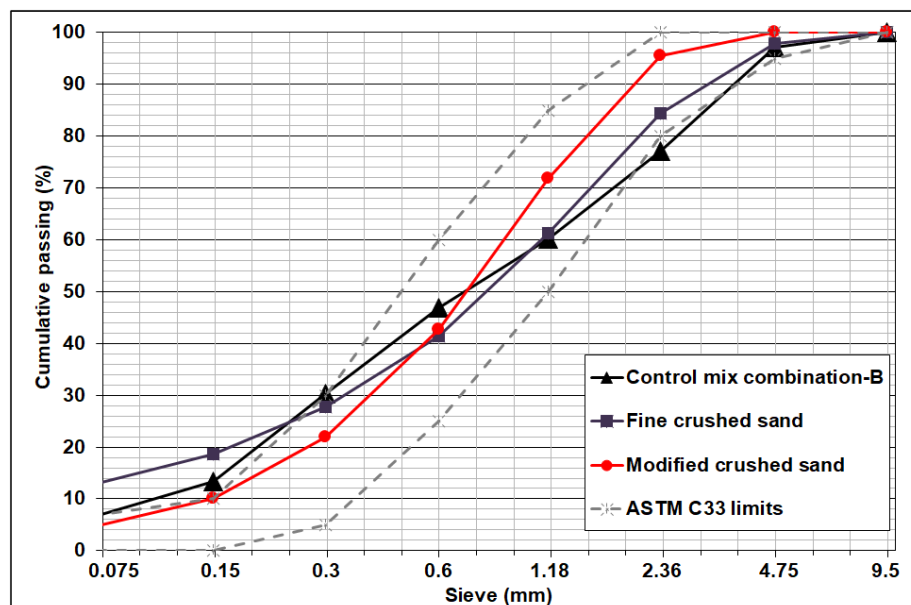


Figure III.10 The particle size distribution of the fine aggregates incorporated in the performance-based approach study compared to the gradation limits of ASTM C33

All the quantity of the "Fine crushed sand FCS" used in this study has been provided from the same crusher but from two different stocks which differ by the fines contents, 18% and 13%, and the fineness moduli, 2.1 and 2.7. Additionally, the "Modified crushed sand" is constructed with two different percentages of fines: 5% and 3% and a fineness modulus of 2.6 (Table III.11).

Table III.11 Nomenclature of the different types of concrete according to the type of the fine aggregates (assessment of the fine crushed sand effect)

Concrete type	Nomination	Fine aggregates type
Control mix	CM	Control mix combination-B: 35% Natural sand-B (NS-Series B) + 65% Conventional crushed sand (CCS) (mass proportions)
Fine mix	FM	Fine crushed sand (FCS): Only crushed sand, without natural sand 18% of fines, exceeding the standard grading requirements (7%)
		Fine crushed sand (FCS): Only crushed sand, without natural sand 13% of fines, exceeding the standard grading requirements (7%)
Modified mix	MM	Modified crushed sand (MCS): Only crushed sand, without natural sand Well-graded with 5% of fines
		Modified crushed sand (MCS): Only crushed sand, without natural sand Well-graded with 3% of fines

The effects of fines are evaluated on a normal strength concrete "Mix 30" and high-strength concrete "Mix 50". The mix design proportions of each mix are presented in Table III.12.

Table III.12 Mix design proportions of concrete mixes incorporating crushed sand with high fines percentage (kg/m^3)

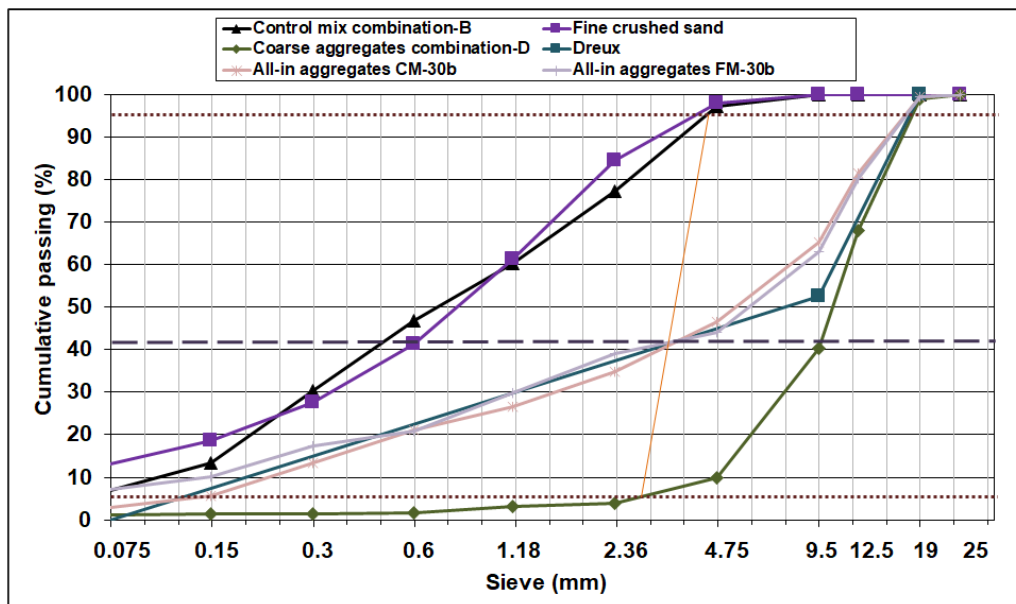
Concrete mix	Cement	Effective Water	W/C	Admixture*	NS	CS	MCS	FCS	MA	CA
Mix 30	CM-30b			4.50 (1.29%)	264	490	0	0	416	625
	FM-30b	350	175	0.5	2.62 (0.75%)	0	0	0	677	442
	MM-30			0.00 (0.00%)	0	0	802	0	427	566
Mix 50	CM-50			9.61 (2.40%)	300	557	0	0		
	FM-50	400	120	0.3	9.81 (2.45%)	0	0	0	854	450
	MM-50			10.20 (2.55%)	0	0	854	0		

(*): the value between brackets represents the massic dosage of the admixture as a percentage of the cement mass

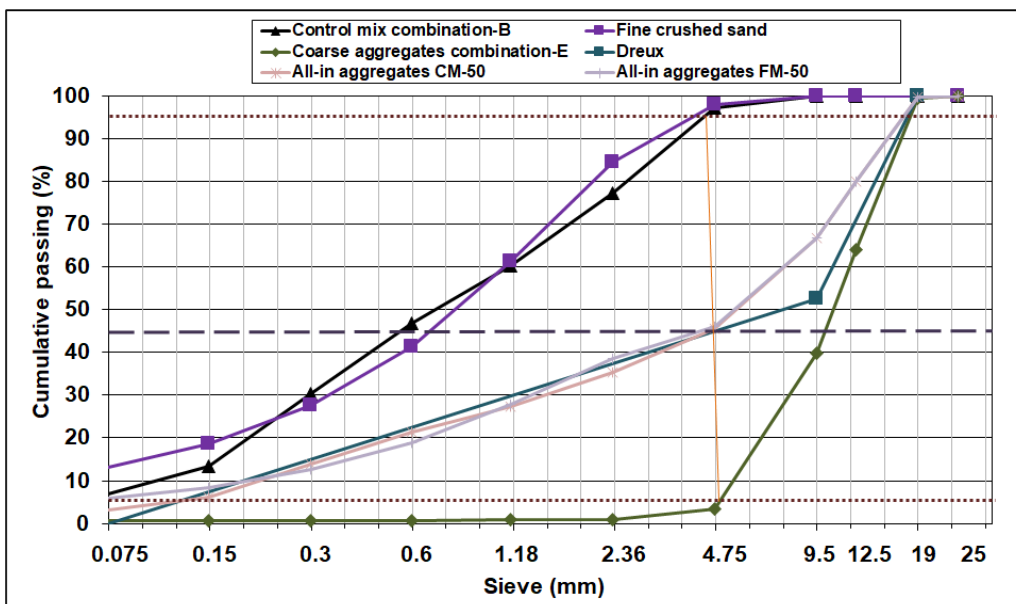
For "Mix 30", the "Fine crushed sand FCS" used is characterized by a content of fines of 18%. The coarse aggregates of Series D are used in mass proportions of 40% and 60% for MA and CA respectively in CM-30b and FM-30b. To obtain a well-graded mix with these aggregates, the "Control mix" is characterized by mass proportions of 42% and 58% for fine and coarse aggregates combination respectively (Figure III.11a). To compensate for the fineness of the "Fine crushed sand FCS", the mass proportion of the fine aggregates in the "Fine mix FM" is reduced to 38% versus 62% for coarse aggregates combination. Due to the closure of the aggregates quarries during the period of this study, the amounts of Series D coarse aggregates have not been enough to cast the "Modified mix MM". Therefore, FM-30b is compared to the "Modified mix MM-30", which is used in the comparison of the

normalized crushed sand concretes (Table III.9) and incorporates the "Modified crushed sand MCS" with 5% of fines.

For "Mix 50", the "Fine crushed sand FCS" presents 13% of fines, while the "Modified crushed sand MCS" incorporates only 3% of fines. The volume of the combination of sands of the "Control mix" is replaced by an equivalent volume of "Fine crushed sand FCS" and "Modified crushed sand MCS" in the "Fine mix FM" and the "Modified mix MM" respectively. The MA and CA of Series E are used for the three types of concrete in mass proportions of 43% and 57% respectively. The total mass proportion of the fine aggregates represents 45% of the total mass of aggregates (Figure III.11b).



(a)



(b)

Figure III.11 Example of the determination of aggregates proportions by Dreux method (assessment of the fine crushed sand effect)

The particle size distribution of the all-in aggregates of the two types of concretes, CM and FM, are close in the case of the normal (Figure III.11a) and the high-strength concrete mixes (Figure III.11b), with smaller differences in the high-strength concretes.

1.2.3 Summary of materials and proportions

Table III.13 summarizes the main characteristics of each concrete mix and the nomenclature used for all the concrete mixes throughout the study.

Table III.13 Concrete mixes nomenclature according to the cement content, the water to cement ratio, and the aggregates series

Mix	Materials	Cement (kg/m ³)			Water/Cement			Aggregates Series				
		300	350	400	0.3	0.4	0.5	A	B	C	D	E
Mix 30	Cement	-	X	-	-	-	-	-	-	-	-	-
	W/C	-	-	-	-	-	X	-	-	-	-	-
	NS	-	-	-	-	-	-	X	-	-	-	-
	CS	-	-	-	-	-	-	X	-	-	-	-
	MA	-	-	-	-	-	-	X	-	-	-	-
	CA	-	-	-	-	-	-	X	-	-	-	-
Mix 30-a	Cement	-	X	-	-	-	-	-	-	-	-	-
	W/C	-	-	-	-	-	X	-	-	-	-	-
	NS	-	-	-	-	-	-	X	-	-	-	-
	CS	-	-	-	-	-	-	X	-	-	-	-
	MA	-	-	-	-	-	-	-	-	-	X	-
	CA	-	-	-	-	-	-	-	-	-	X	-
Mix 30-b	Cement	-	X	-	-	-	-	-	-	-	-	-
	W/C	-	-	-	-	-	X	-	-	-	-	-
	NS	-	-	-	-	-	-	-	X	-	-	-
	CS	-	-	-	-	-	-	X	-	-	-	-
	MA	-	-	-	-	-	-	-	-	-	X	-
	CA	-	-	-	-	-	-	-	-	-	X	-
Mix 35-I	Cement	-	X	-	-	-	-	-	-	-	-	-
	W/C	-	-	-	-	X	-	-	-	-	-	-
	NS	-	-	-	-	-	-	X	-	-	-	-
	CS	-	-	-	-	-	-	X	-	-	-	-
	MA	-	-	-	-	-	-	-	X	-	-	-
	CA	-	-	-	-	-	-	-	X	-	-	-
Mix 35-II	Cement	X	-	-	-	-	-	-	-	-	-	-
	W/C	-	-	-	-	X	-	-	-	-	-	-
	NS	-	-	-	-	-	-	X	-	-	-	-
	CS	-	-	-	-	-	-	X	-	-	-	-
	MA	-	-	-	-	-	-	-	-	X	-	-
	CA	-	-	-	-	-	-	-	-	X	-	-
Mix 50	Cement	-	-	X	-	-	-	-	-	-	-	-
	W/C	-	-	-	X	-	-	-	-	-	-	-
	NS	-	-	-	-	-	-	-	X	-	-	-
	CS	-	-	-	-	-	-	X	-	-	-	-
	MA	-	-	-	-	-	-	-	-	-	-	X
	CA	-	-	-	-	-	-	-	-	-	-	X

(X): chosen criteria

(-): not chosen criteria

1.3 Mixing procedure

A circular pan concrete mixer is used in the mixing process, with a maximum capacity of 60 Liters. The mixing is provided by three blades fixed about the rotating vertical axis of the pan.

To eliminate the effects of different mixing procedures on the comparison between the different types of concrete, the same mixing procedure, based on (*ASTM C192, 2016a*) standard, is applied for all the concrete mixes as follows:

- Dampening the mixture and all the equipment that will be used in the mixing process.
- Introducing the medium and coarse aggregates and mixing them together for 20 seconds.
- Inserting the fine aggregates and mixing for an additional 20 seconds.
- Adding the cement and mixing it with all the other constituents for 30 seconds.
- Bringing in the water with approximately the two-thirds admixture quantity, and mixing continuously for 3 minutes.
- Stopping the mixer to let the mix rest for 2 minutes.
- Turning on the mixer, adding the remaining quantity of the admixture, and mixing all the ingredients for 2 additional minutes.
- Performing the slump test to check if the target slump is reached, and if not, adjusting the admixture content and mixing for an additional 2 minutes.

2. Experimental procedure

The experimental procedure conducted on concrete covers the fresh state properties, mechanical resistances, elastic modulus, deformations, and durability properties. In addition to the macrostructural assessment, a microstructural analysis is carried out at the interface between the cement paste and the sand grains.

2.1 Fresh state properties of concrete

The fresh concrete properties are important criteria to choose the pouring method and to control the transport, the placing time, and the removal of scaffoldings and formworks in construction sites.

To compare the behavior of concrete mixes at the fresh state, several characteristics are measured including the temperature, the density, the air content, the slump, and the setting time for the different concrete types, as shown in Table III.14, except "Mix 30-a". The slump test is the only fresh state test performed on "Mix 30-a" to ensure similar workability for the three types of concrete since this mix is only prepared for shrinkage and modulus of elasticity tests.

Table III.14 The experimental program for measurements of fresh properties

Concrete mix	Fresh temperature	Fresh density	Air content	Slump	Slump retention	Setting time
CM-30	X	X	X	X	X	X
EM-30	X	X	X	X	X	X
MM-30	X	X	X	X	X	X
Mix 30 CM-30a	-	-	-	X	-	-
EM-30a	-	-	-	X	-	-
MM-30a	-	-	-	X	-	-
CM-30b	X	X	X	X	X	X
FM-30b	X	X	X	X	X	X

	Concrete mix	Fresh temperature	Fresh density	Air content	Slump	Slump retention	Setting time
Mix 35-I	CM-35-I	X	X	X	X	X	X
	EM-35-I	X	X	X	X	X	X
	MM-35-I	X	X	X	X	X	X
Mix 35-II	CM-35-II	X	X	X	X	X	X
	EM-35-II	X	X	X	X	X	X
	MM-35-II	X	X	X	X	X	X
Mix 50	CM-50	X	X	X	X	X	-
	MM-50	X	X	X	X	X	-
	FM-50	X	X	X	X	X	-

(X): property measured

(-): property not measured

2.1.1 Fresh concrete temperature

Usually, the objective of this test is to ensure that the temperature of the freshly mixed concrete complies with the specifications of the project. But, in our study, this temperature is mainly recorded to verify that the environmental conditions are conserved for the different types of concrete of each mix since the environmental temperature, the temperature of the concrete constituents, and the fresh concrete temperature could affect the concrete properties. In the experimental program conducted by (Ortiz *et al.*, 2009), the fresh properties of concrete have been affected by the temperature of aggregates, since the absorption rate and the friction of sand increase at high temperature (38 °C) and low temperature (6 °C) respectively, reducing in both cases the workability of mortar.

Directly after mixing, the concrete is placed in a wheelbarrow and the fresh concrete temperature is measured following the (ASTM C1046, 2017). The measuring device is inserted into the container and covered by at least 75 mm of concrete in all directions, as shown in Figure III.12a. The device is kept in this position for 2 to 5 minutes before recording the concrete temperature.

2.1.2 Slump and slump retention

To have an industrial workable concrete, the target slump of all the concrete mixes is 20 ± 2 cm. The slump test is conducted directly after mixing to determine the needed quantity of the admixture for each type of concrete.

Furthermore, to evaluate the loss of workability of the different types of concrete, the concrete is placed in a wheelbarrow, covered and left at rest, due to the difficulty of maintaining a continuous mixing in the conditions of the laboratory. After 30, 60, and 90 minutes, the concrete is only remixed by hand using a scoop, for approximately one minute, and the slump test is conducted. Thus, this test does not translate the real slump loss which could happen in fresh concrete during its transport to the sites.

The slump and the slump retention tests are applied following (ASTM C143, 2015a) standard. The concrete is placed in three layers of equal volume in a mold in the shape of a frustum of a cone, and each layer is rodded 25 times with a tamping rod. Immediately after removing the mold, the slump value is measured by determining the difference between the top of the mold and the displaced original center of the top surface of the specimen (Figure III.12b).

2.1.3 Setting time

The initial setting time is the time when the concrete cement paste starts losing its plasticity. Thus, it represents an important index to control the transport, placing, and compaction of concrete. The final setting time is the time when the paste totally loses its plasticity and it is an indicator that could be used to control the safe removal of formworks.

(ASTM C403, 2008) is used to determine the initial and final setting times of concrete by measuring the time required of the mortar portion of concrete to reach specified values of resistance to needles penetration.

The fresh concrete is sieved over a 4.75 mm sieve (Figure III.12c) and the passing fraction is stored at 20-25 °C. After 3 to 4 hours of the initial contact between cement and water, a vertical force is applied by a needle on the surface of the mortar until a depth of penetration reaches 25 ± 2 mm. The test is repeated every 30 minutes and it is performed at least 6 times until at least one penetration resistance exceeds 27.6 MPa (Figure III.12d). For each penetration test, the resistance of the needle penetration is calculated and the time is recorded.

The penetration resistance is then plotted versus the time elapsed since the initial contact of cement and water. The initial and final setting times are determined as the elapsed time between the initial contact of cement and mixing water and the time when the penetration resistance is equal to 3.5 and 27.6 MPa respectively.



Figure III.12 Illustrations of the tests conducted on the concrete mixes at fresh state: (a) Temperature; (b) Slump and slump retention; (c-d) Setting time; (e) Density; and (f): Air content

2.1.4 Fresh density and air content

The fresh density of concrete is usually used to correct the proportions of the materials in the concrete mix by comparing the experimental mix volume to its theoretical one. It is also necessary to determine the air content of fresh concrete for the different mixes since it could affect the concrete behavior at a hardened state.

To calculate the fresh density, the rodding consolidation method is applied in three consecutive layers of concrete in a 7 Liters measure as per (*ASTM C138, 2017a*) standard. After weighing the empty measure and the measure full of concrete as shown in Figure III.12e, the density (or unit weight) of freshly mixed concrete is calculated as the ratio of the fresh concrete mass to the volume of the measure.

After measuring the fresh concrete mass, the same concrete is used to assess the air content of the freshly mixed concrete by the pressure method in compliance with (*ASTM C231, 2017a*). The test apparatus is shown in Figure III.12f. The method consists of conveying a pressured air to a concrete volume, then the change in the air pressure is detected and converted directly to a percentage of air content in concrete.

2.2 Mechanical behavior of concrete

Mechanical characterization tests are performed on the different types of concrete: compressive strength, modulus of elasticity, and flexural strength. The elastic modulus test is only performed on "Mix 30a" as shown in Table III.15.

Table III.15 The experimental program for mechanical characterization

Concrete mix	Compressive strength	Modulus of elasticity	Flexural strength
CM-30	X	-	X
EM-30	X	-	X
MM-30	X	-	X
Mix 30	CM-30a	X	-
	EM-30a	X	-
	MM-30a	X	-
	CM-30b	X	-
	FM-30b	X	X
Mix 35-I	CM-35-I	X	X
	EM-35-I	X	X
	MM-35-I	X	X
Mix 35-II	CM-35-II	X	X
	EM-35-II	X	X
	MM-35-II	X	X
Mix 50	CM-50	X	X
	MM-50	X	X
	FM-50	X	X

(X): property measured

(-): property not measured

2.2.1 Compressive strength

Compressive strength is the main mechanical criterion to characterize the concrete performance. That is why the concrete is usually defined by the compressive strength grade.

The cylinders are previously prepared following (*ASTM C192, 2016a*) by rodding three layers of concrete in molds of 150 mm in diameter and 300 mm in length. The specimens are kept in a controlled room at 23 ± 2 °C, de-molded after 24 ± 8 h, and cured in water tanks at 23 ± 2 °C until the day of testing: 3,7, 28, 90, and 135 days.

Before conducting the compressive strength tests, the surfaces of the specimens are aligned by sawing, then the diameter and the length of each specimen are measured. The diameter is calculated as the average of two values of diameter measured at a right angle at about mid-height of the cylinder. The length of the specimen corresponds to the lengths' average value of three different lengths measured at locations evenly spaced around the circumference of the cylinder.

The apparent density of each sample is assessed since it is an index of the uniformity in the preparation of the specimens of the same batch. For this purpose, after the water curing and before performing the compressive strength test, the mass of the cylinder is measured by previously removing its surface moisture with a towel. The density of the cylinder is determined as the ratio of its mass to its volume, which is calculated from the average measured diameters and lengths.

Indeed, the previous sawing of the surfaces is not sufficient to ensure their parallelism. Thus, since there is no available parallel grinding machine, neoprene pads are mounted in metallic ring retainers on both ends of each cylinder, as illustrated in Figure III.13, to evenly spread the axial load across the specimen surface. Then, the specimen is adequately placed in the mechanical press, and spacers are added if necessary.

The compressive strength test is carried out according to (*ASTM C39, 2017a*) procedure. It consists of applying a compressive axial load at 0.25 ± 0.05 MPa/s. The maximum load that the specimen could undergo before displaying a well-defined fracture pattern is recorded and the compressive strength of each specimen is calculated as the ratio of this maximum load to the measured sectional area of the cylinder.



Figure III.13 Neoprene pad and compressive strength machine

2.2.2 Modulus of elasticity

The modulus of elasticity is an essential concrete mechanical characteristic required to design concrete structures. Hence, it is necessary to assess the effect of the type of fine aggregate on this hardened concrete property.

This modulus is determined from the axial longitudinal deformation measurement while applying compression stress on concrete samples with the same geometry as the samples used in the compressive strength test, as specified in (*ASTM C469, 2014*). The test is carried out at 28 days.

For this test, the perpendicularity of the surface with the specimen's axis is provided by capping the specimen surface with sulfur mortar, to ensure a uniaxial compressive loading well distributed on cylinder surfaces.

The longitudinal displacement of the sample is determined by the means of a compressometer equipped with a displacement dial gauge. As illustrated in Figure III.14, this measurement device consists of two yokes and a pivot rod A to maintain a constant distance between the two yokes. The lower yoke B is strictly attached to the specimen, while the upper one C is attached at two diametrically opposite points to be free to rotate. Thus, the gauge reading is equal to the sum of the displacement due to the specimen deformation and the one due to the rotation of the yoke about the pivot rod.

After properly adjusting the specimen in the compressometer, the specimen is well-aligned in the loading machine. The test consists of applying three cycles of loading and unloading with maximal stress corresponding to 40% of the concrete compressive strength, previously measured on companion samples. The load is applied continuously and without shock, at a constant rate within the range of 0.25 ± 0.05 MPa/s while recording the displacement by the dial gauge, for each load increment of 50 kN.

The displacement of the specimen is computed as half the dial gauge reading. For each loading value, the average displacement is then calculated from the three loading cycles and the longitudinal strain is determined as the ratio of the measured longitudinal displacement to the initial distance between the two yokes of the compressometer (163 mm). The graph of the stress versus strain could then be plotted and the modulus of elasticity is calculated by:

$$E = \frac{S_2 - S_1}{\epsilon_2 - \epsilon_1} \quad (\text{Eq. III.1})$$

Where:

- S_1 = stress corresponding to a longitudinal strain, ϵ_1 , of 50 millionths (MPa);
- S_2 = stress corresponding to 40% of ultimate load (MPa);
- $\epsilon_1 = 0.000050$;
- ϵ_2 = longitudinal strain produced by stress S_2 .

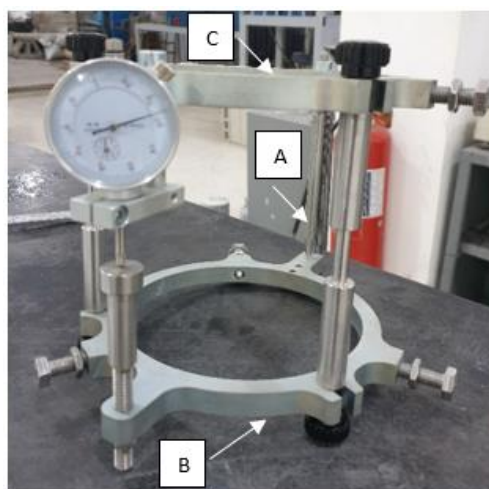


Figure III.14 The compressometer used to measure the longitudinal displacement of a specimen under uniaxial compressive load, allowing the determination of the modulus of elasticity

2.2.3 Flexural strength

The flexural strength test allows assessing the tensile strength of concrete with an easier test than the direct tensile one. This test is conducted following the ASTM standard (*ASTM C78, 2016*) entitled "Standard test method for flexural strength of concrete (using simple beam with third-point loading)" (Figure III.15) which is equivalent to the four points flexural strength test of the European standard (*NF EN 12390-5, 2009*). The test is carried out at 28 days.

For each type of concrete, three prisms are prepared by rodding two layers of fresh concrete in 100x100x500 mm molds, following the (*ASTM C192, 2016a*). The specimens are kept in a controlled room at 23 ± 2 °C, de-molded after 24 ± 8 h, and cured in water tanks at 23 ± 2 °C. The test is made as soon as practicable after removal from water to avoid the reduction of the measured modulus of rupture due to the surface drying.

The depth and width of the specimen are determined by taking the average of three measurements, two at the edges and one at the center of the cross-section, while the specimen is oriented for testing.

During the test, the reactions are parallel to the direction of the applied load, and this load is applied perpendicularly to the face of the specimen, continuously and without shock, at a constant rate of 0.0667 kN/s until fracture. The maximum applied load is recorded. Since the distance between the support and the loading block is third the span of the prism (Figure III.15), the modulus of rupture R , in MPa, is calculated as follows:

$$R = \frac{P L}{b d^2} \quad (\text{Eq. III.2})$$

Where:

- P = maximum applied load (N);
- b = specimen width (mm);
- d = specimen depth (mm).

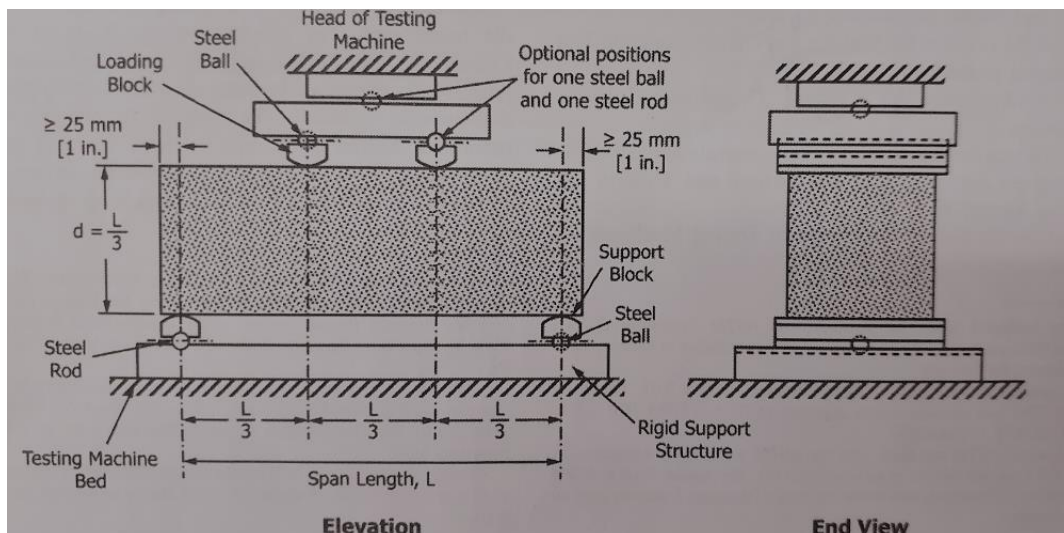


Figure III.15 Schematic of the apparatus of the flexural strength test by third-point loading (*ASTM C78, 2016*)

2.3 Shrinkage of concrete

The concrete shrinkage could cause tensile stresses in concrete if it is restrained, which could lead to cracking. Therefore, it is essential to determine the free deformation variation of concrete caused by any factors other than the externally applied forces and the temperature changes. The shrinkage test consists of measuring the relative length change of concrete specimens at different ages according to (*ASTM C157, 2006*) standard. Due to the important influence of the mixing water on the concrete shrinkage, in this study, the shrinkage test is conducted on the mix which exhibits the highest water to cement ratio, i.e Mix 30a.

For this test, six specimens are prepared from each type of concrete:

- three specimens that can undergo free drying, to assess the total shrinkage;
- three specimens well-wrapped, after de-molding, with a sticking aluminum foil to avoid any humidity exchanges, to assess the autogenous shrinkage.

The concrete should be placed in prisms of minimum dimensions of 75x75x285 mm, whereas, during this study, the dimensions of the available molds for this test were 50x50x200 mm. The geometry indeed influences the kinetic of the drying shrinkage. However, in the case of this study, using samples that differ in dimensions from those of the ASTM standard is not detrimental, since the objective of the test is to compare the shrinkage of concrete to identify the effects of the sand type.

During placing, the concrete is rodded in two equal layers, consolidated by rodding. The prisms are then stored in a controlled room (23 ± 2 °C; $50 \pm 4\%$ Relative Humidity). They are then de-molded after 24 ± 0.5 h of the addition of water to the cement during the mixing operation. The initial mass and the initial comparator reading are taken immediately after demolding and after wrapping the specimens of the autogenous shrinkage with the aluminum foil.

For the rest of the test, the wrapped and unwrapped specimens are placed in a climatic chamber (23 ± 2 °C; $50 \pm 4\%$ Relative Humidity). The mass and the shrinkage measurements (Figure III.16) are recorded at different ages including 3, 7, 14, 21, 28, and 77 days. The test was stopped at 77 days due to unforeseen circumstances. The mass loss is measured throughout the test and the two types of shrinkage strain at any age are determined to the nearest 0.001%, as the ratio of the length change to the initial value of the reference length (200 mm).



Figure III.16 The length change readings to determine the total and autogenous shrinkages

2.4 Durability properties of concrete

Concrete durability is its ability to resist weathering actions and other conditions of service life such as a chemical attack, aggressive ion penetration, freezing and thawing, and abrasion while maintaining its serviceability. For this purpose, many properties could be tested on hardened concrete to simulate its performance under critical conditions. The effects of fine aggregates' characteristics on the durability properties of concrete are not widely developed in the literature (Chapter I), hence the necessity of assessing the durability of concrete when crushed sand totally replaces natural sand.

Among a vast range of durability tests, five tests have been chosen to assess the effects of the fine aggregate on the durability properties. The resistivity and the porosity accessible to water of concrete are good indicators of the pore structure in concrete and its ability to resist the fluid transfer. The resistivity test is rapid, simple, and non-destructive; thus, this property is assessed for all concrete mixes, except "Mix 30a". The porosity test is conducted on "Mix 30", the concrete of the highest water to cement ratio (Table III.16). Furthermore, due to the negative impacts on the long-term structural behavior of reinforced concrete that could be imposed by the high permeability to water and chloride ions, it is primordial to evaluate the resistance to chloride ions penetration, the hardened concrete absorption by immersion, and the depth of the water penetration under pressure in order to compare the durability properties of the different concrete mixes. These tests are the three most demanded durability tests in Lebanon and they are conducted on all concrete mixes, except "Mix 30a" (Table III.16).

All the durability tests have been performed at 90 days, except the three types of concrete of "Mix 50". It was intended to carry out the durability tests of this mix at 90 days, but due to the pandemic imposed circumstances, they were postponed to an age of 135 days. It is worth mentioning that given the applied mix designs and the followed curing conditions, the microstructure of concrete should not present significant differences at both ages since the durability properties usually and principally vary when the concrete age is below three months (AFGC, 2004).

Table III.16 The experimental program for durability properties

Concrete mix	Porosity	Absorption	Depth of water penetration under pressure	Resistance to chloride ions penetration	Resistivity
CM-30	-	X	X	X	X
EM-30	-	X	X	X	X
MM-30	-	X	X	X	X
Mix 30	CM-30a	X	-	-	-
	EM-30a	X	-	-	-
	MM-30a	X	-	-	-
	CM-30b	-	X	X	X
	FM-30b	X	X	X	X
Mix 35-I	CM-35-I	-	X	X	X
	EM-35-I	-	X	X	X
	MM-35-I	-	X	X	X
Mix 35-II	CM-35-II	-	X	X	X
	EM-35-II	-	X	X	X
	MM-35-II	-	X	X	X
Mix 50	CM-50	-	X	X	X
	MM-50	-	X	X	X
	FM-50	-	X	X	X

(X): property measured

(-): property not measured

2.4.1 Porosity accessible to water

Although the concrete porosity test is not commonly required in Lebanon, this test is evaluated in this study since the porosity accessible to water is an essential indicator of the concrete long-term performance because it governs the fluid transfer. The porosity test is performed as per the French recommendations of (*AFPC-AFREM, 1998*).

The porosity test was carried out in LMDC in France. Accordingly, due to the difficulty to transport massive quantities of concrete to France, 4 to 5 small specimens from each type of "Mix 30" concrete (Table III.16) are extracted from the fractured cones of the cylinders which have been submitted to the compressive strength test, after 28 days of water curing. Thus, these fractions are less susceptible to microcracks. Then, the specimens are properly wrapped to avoid undesirable desiccation or humidity absorption. Before conducting the porosity test, the exterior cover of these samples is removed by sawing and the internal part is used for the test.

On the day of testing (90 days), the specimens are placed in a desiccator, and a vacuum is maintained for 4 hours. At the end of this period, water is added in a way to cover the specimens at least 20 mm from all directions, and the vacuum is then maintained for an additional 20 hours.

The second step consists of determining the mass of each specimen when it is totally immersed in water M_w . Afterward, the surface water of the specimen is removed by a cloth and the saturated-surface dried mass is determined M_{SSD} . The specimen is then oven-dried (105 ± 5 °C) to constant mass and the dried mass is determined M_D . The open porosity accessible to water is calculated as follows:

$$\varepsilon = 100 \times \frac{M_{SSD} - M_D}{M_D - M_w} \quad (Eq. III.3)$$

2.4.2 Water absorption by immersion

The absorption ability of concrete is another valuable index for durability. It is assessed through the amount of water that penetrates into concrete samples that have been immersed in water for 30 minutes, in accordance with (*BS 1881-122, 1983*). This test is relatively easy and rapid.

For each mix, the water absorption is measured for three cores that have been water cured until the day of coring, having a diameter and length of 75 mm each. To obtain these cores, the 150x300 mm cylinders are sawed in half, and the upper new surface of the 150x150 mm specimen is perpendicularly drilled.

At the specified age of the test, 90 days for the normal strength concrete and 135 days for "Mix 50", the initial mass of the specimen is determined after drying it in the oven (105 ± 5 °C) for 72 ± 2 hours and cooling it for 24 ± 0.5 hours. Then, the specimen is immersed in water for 30 ± 0.5 minutes, dried with a cloth to remove all free water, and weighed to determine the saturated mass.

The absorption is calculated as the percentage ratio of the difference between the saturated and initial masses to the initial mass of the specimen.

2.4.3 Depth of water penetration under pressure

Knowing that permeable porous concrete will have poor long-term mechanical properties, it is necessary to evaluate the resistance of concrete against the penetration of water under pressure in the durability study.

The depth of water penetration under pressure corresponds to the amount of water migration through concrete when the water is under hydrostatic pressure. In this study, it is determined by the (*BS EN 12390-8, 2009*) standard.

The specimens used are cylinders of 150 mm in diameter and length, obtained after sawing the 150x300 mm cylinders at the middle. The 150x150 mm cylinders have been water-cured until the day of testing: 90 days for the normal strength concretes and 135 days for "Mix 50".

The test consists of applying a water pressure of 500 ± 50 kPa to the specimens' surface for 72 ± 2 hours (Figure III.17a). At the end of this period, the specimen is split in half, perpendicularly to the face on which the water pressure was applied, and the maximum water penetration depth is visually detected by a difference in the color and it is measured by the means of a ruler (Figure III.17b).

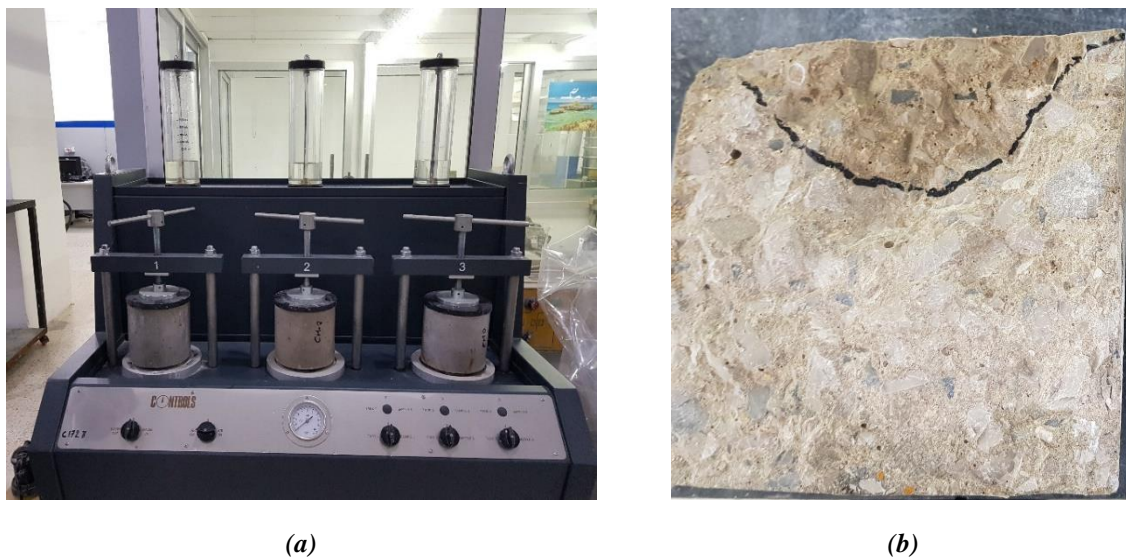


Figure III.17 The test of the depth of water penetration under pressure:
(a) the samples under pressure (b) the sample at the end of the test

2.4.4 Resistance to chloride ion penetration

Due to their highly alkaline nature, the concrete products form a passive and non-corroding protective film around the steel rebars to prevent their corrosions. However, the chloride ions can penetrate the concrete cover, reach this film and cause reinforcement corrosion, expansion, internal stresses, and spalling of concrete due to their aggressive nature. Therefore, it is essential to assess the resistance of concrete to chloride ions penetration.

By studying the electrical conduction of concrete specimens subjected to an electrical voltage for six hours duration, the (*ASTM C1202, 2017*) test provides an indication of the concrete's ability to resist chloride ions penetration. Among the durability tests which assess the resistance of concrete to chloride ion penetration, this test is popular since it is one of the easiest and quickest.

For each mix, three specimens having a diameter and length of 100 and 50 mm respectively are sawed from the inner part of three different 100x200 mm concrete cylinders that have been water cured until the day of sawing.

The steps followed in this test are illustrated in Figure III.18. The specimen's circumference is coated with epoxy, then placed in a vacuum desiccator where a vacuum is applied for 3 hours. After that, de-

aerated water is added and the specimen is left under vacuum for one additional hour. Then, the vacuum pressure is released and the specimen is soaked in water for 18 hours.

At the age of testing, 90 days for the normal strength concretes and 135 days for "Mix 50", the specimen is mounted in the test apparatus formed of two cell compartments filled with a 3% NaCl and 0.3 N NaOH solution. An electrical voltage of 60 V is connected for 6 hours and the current is recorded every 30 minutes. To avoid the boiling of the solutions and the damage of the cells, the temperature is recorded throughout the test to ensure that it does not exceed 90 °C.

The total charge Q passed during the period of this test is estimated using the following formula:

$$Q \text{ (C)} = 900 (I_0 + 2 I_{30} + 2 I_{60} + \dots + 2 I_{300} + 2 I_{330} + I_{360}) \quad (\text{Eq. 3.4})$$

Where:

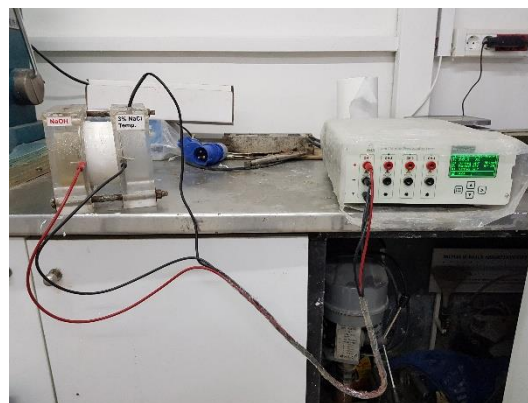
- I_0 = the current immediately after the voltage is applied (A);
- I_t = the current at t minutes after the voltage is applied (A).



(a)



(b)



(c)

Figure III.18 The steps followed in the resistance to chloride ions penetration test:
(a) epoxy coating; (b) vacuum; and (c) charge measurement

2.4.5 Resistivity

The measurement of the concrete resistivity provides useful information about the concrete microstructure and its pores network since the current is essentially carried by the dissolved ions in the liquid pores and it circulates in the intrinsic solution (Polder *et al.*, 2001; AFGC, 2004). By giving an indication of the pores' volume and connectivity and the chemical composition of the intrinsic solution,

the test estimates, in a quick, simple, and non-destructive way, the ability of concrete to resist the water and ions penetration. In this study, the resistivity test is performed based on the (APM 219, 1996) test method.

Before carrying out the compressive strength test of the different types of concrete, at 90 or 135 days, and before adjusting the alignment of their surface, the resistivity test is applied on the cylinders having a diameter and length of 150 and 300 mm respectively. These cylinders have been water-cured until the day of testing.

To conduct a precise comparison between the different types of concrete, the samples should be at the same moisture state. Since the measurements on dried or partially saturated specimens could be unstable (Chen *et al.*, 2014), the specimens should be preferably at the saturated-surface dried state. Thus, immediately after removing the specimens from water, the outer water surface is removed, and the test is performed.

An alternating current of a frequency of 1 kHz is applied between the ends of the concrete specimen that has been previously covered with a damp sponge topped by conductive plates, as shown in Figure III.19. The measuring device (Giatec-RCON) measures the voltage, calculates the impedance value, and directly gives the resistivity of the concrete specimen.



Figure III.19 The apparatus of the resistivity test for concrete specimens

2.5 Microstructural analysis of concrete

The interface between cement paste and sand grains, known as Interfacial Transition Zone (ITZ) is investigated in order to identify a possible difference in the shape and the mineralogy of the hydrates induced by the siliceous rounded sand and the angular limestone sand.

For this purpose, the scanning electron microscope technique SEM, coupled with the Energy Dispersive X-ray spectroscopy EDX, is used. The SEM/EDX combination allows a compositional analysis in addition to the morphological scanning of concrete.

As already detailed for the porosity test, the samples used for the microstructure analysis have been arbitrarily chosen from the fractured cones of concrete cylinders that have been previously water cured for 28 days then submitted to the compressive strength test. Thus, no definitive conclusion could be

drawn on the microcracks observed in the SEM images, because these microcracks could be due to the fracture that occurred during the compressive strength test or due to the preparation of specimens for the SEM observation. Even though the collection of the specimens following this method does not allow the differentiation between the microcracks generated by this preparation and those related to the concrete microstructure, it does not mask the mineralogical and morphological properties of the interface between cement paste and sand grains. Additionally, this method helps to detect the detachment that could occur between the cement paste and the sand grains due to the compressive strength test.

The collected specimens are properly wrapped until the day of the microstructural analysis, to reduce as much as possible the changes in the cement paste microstructure (hydration, carbonation) and the risk of interface cracking that could be induced by the cement paste deformation, due to desiccation or humidity absorption.

This microstructure analysis is led on the four concrete types of "Mix 30", as shown in Table III.17. This mix is characterized by the highest water to cement ratio; thus, it probably presents the weakest interface resistance among all the mixes.

Table III.17 The experimental program for the microstructural analysis

Concrete mix	Microstructural analysis	
Mix 30	CM-30	-
	EM-30	-
	MM-30	-
	CM-30a	X
	EM-30a	X
	MM-30a	X
	CM-30b	-
	FM-30b	X
	CM-35-I	-
Mix 35-I	EM-35-I	-
	MM-35-I	-
	CM-35-II	-
Mix 35-II	EM-35-II	-
	MM-35-II	-
	CM-50	-
Mix 50	MM-50	-
	FM-50	-

(X): property measured

(-): property not measured

2.6 Summary of the concrete experimental program

The tests conducted on the different types of concrete at different ages are summarized in Table III.18. The choice of the standard used for each test depends on the Lebanese market. The ASTM standards are usually required to evaluate the concrete performance, except for some properties where the BS or other standards are applied.

Table III.18 Summary of the conducted tests on concrete

Investigated Property	Standard	Specimens ^a	Curing ^a	Age	
Fresh Properties	Fresh temperature	ASTM C1064-17	-	-	Fresh concrete
	Fresh density	ASTM C138-17a	Measure V: 7 liters	-	Fresh concrete
	Air content	ASTM C231-17a	Measure V: 7 liters	-	Fresh concrete
	Slump	ASTM C143-15a	-	-	Fresh concrete
	Slump retention	ASTM C143-15a	-	-	30, 60, and 90 min
	Setting time	ASTM C403-08	Fraction passing the 4.75 mm sieve	-	3-4 h
Mechanical behavior	Compressive strength	ASTM C39-17a	Cylinders D: 150 mm; L: 300 mm	Water at 23 ± 2 °C	3, 7, 28, and 90 (or 135) days
	Modulus of elasticity	ASTM C469-14	Cylinders D: 150 mm; L: 300 mm	Water at 23 ± 2 °C	28 days
	Flexural strength	ASTM C78-16	Prisms Cross-section: 100x100 mm ² ; L: 500 mm	Water at 23 ± 2 °C	28 days
Deformations^b	Shrinkage	ASTM C157-06	Prisms Cross-section: 50x50 mm ² ; L: 200 mm	- Climatic Chamber (T:23 ± 2 °C RH:50 ± 4%) ^c - No humidity exchange ^d	1 to 77 days
Durability properties	Porosity	AFPC-AFREM-1998	<i>Extracted from 150x300 fractured cylinders</i>	Water at 23 ± 2 °C for 28 days; wrapped for the rest	90 days
	Water absorption by immersion	BS 1881-122:1983	Cylinders D: 75 mm; L: 75 mm <i>Cored from 150x150 cylinders</i>	Water at 23 ± 2 °C	90 or 135 days
	Depth of water penetration under pressure	BS 12390-8: 2009	Cylinders D: 150 mm; L: 150 mm <i>Sawed from 150x300 cylinders</i>	Water at 23 ± 2 °C	90 or 135 days
	Resistance to chloride ions permeability	ASTM C1202-17	Cylinders D: 100 mm; L: 50 mm <i>Sawed from the middle of 100x200 cylinders</i>	Water at 23 ± 2 °C	90 or 135 days
	Resistivity	Based on APM 219, 1996	Cylinders D: 150 mm; L: 300 mm	Water at 23 ± 2 °C	90 or 135 days

(^a): V: Volume; D: Diameter; L: Length; T: Temperature, and RH: Relative humidity;

(^b): For each type of concrete, two types of curing for three different samples each;

(^c): for total shrinkage; and (^d): for autogenous shrinkage.

Conclusions

The objective of the study consists of evaluating the effects of the different types of fine aggregate on concrete performance. To reach this objective, several concrete mixes are designed with differences limited to the fine aggregate type and/or gradation only. The slump value is similar for the different types of concrete and a high-range water-reducing admixture is used to reach the target workable concrete.

Three normal strength concrete mixes are prepared:

- "Mix 30" is characterized by a cement content of 350 kg/m^3 and water to cement ratio of 0.5;
- "Mix 35-I" contains 350 kg/m^3 of cement and water to cement ratio of 0.4;
- "Mix 35-II" presents a cement content of 300 kg/m^3 and a water to cement ratio of 0.4.

To assess the effect of the normalized crushed sand as the only fine aggregate in concrete, for each mix of the normal strength concretes, "Mix 30", "Mix 35-I", and "Mix 35-II", three types of concrete are prepared:

- The "Control Mix" is the conventional concrete made of equal mass proportions of natural sand and conventional crushed sand;
- The "Equivalent Mix" only contains crushed sand with the same particle size distribution as the combination of fine aggregates in the "Control Mix";
- The "Modified Mix" is made of crushed sand with a well-graded size distribution, without natural sand.

For the high-strength concrete "Mix 50", characterized by high cement content (400 kg/m^3) and low water to cement ratio (0.3), two types of concrete are prepared which differ only by the type and gradation of the fine aggregate:

- The "Control Mix" contains a combination of fine aggregates of 35% natural sand and 65% conventional crushed sand;
- The "Modified Mix" does not contain natural sand and it incorporates well-graded crushed sand as the only fine aggregate.

To verify if a performance-based approach could be adopted, "Mix 30" and "Mix 50" are also designed with a "Fine Crushed Sand" which gradation does not comply with the grading requirements imposed by the (*ASTM C33, 2016*) standard. This sand is characterized by a high percentage of fines (13-18%) exceeding the limit imposed by the standard (7%).

To assess the relevance, for the Lebanese construction industry, of the total substitution of natural sand by crushed sand, a wide experimental program is established. It consists of performing several tests characterizing the fresh properties, mechanical behavior, and durability performances (not widely developed in previous studies) of the different types of concrete.

By adopting the described mix designs and by performing the aforementioned experimental program, a comparison in the concrete performance is held in the next two chapters. Accordingly, conclusions could be conducted on the effectiveness of replacing the conventional fine aggregates combination with normalized crushed sand and/or crushed sand with high fines percentage that exceeds the limit imposed by the standard.



Chapter IV

**Experimental Study
on Concrete Mixes
Incorporating
Normalized Crushed
Sand**



IV. Experimental Study on Concrete Mixes Incorporating Normalized Crushed Sand

Introduction

The main objective of this chapter is to check if the concrete performance could be maintained, in terms of fresh properties, mechanical strengths, deformations, and long-term behavior, when the classical combination of natural siliceous rounded sand and conventional crushed limestone sand is totally replaced by crushed limestone sand which gradation conforms to the standard grading requirements.

After applying the experimental procedure for mixing and testing concrete, detailed in the previous chapter, the current chapter presents a comparative analysis between the results of the two types of concrete mixes incorporating normalized crushed sand, "Equivalent mix EM" and "Modified mix MM", and the reference concrete containing a conventional combination of natural sand and crushed sand, "Control mix CM", for four different concrete formulations.

The characterization of concrete behavior is performed at fresh state and hardened state with mechanical and durability properties. Additionally, given its great impact on the concrete performance, the quality of the interfacial transition zone (ITZ) between the cement paste and the sand grains is also investigated by a microstructural analysis.

Since this study aims to resolve the problems of the natural sand in the industrial frame and to present a solution that could be applied in the Lebanese industry, a brief technical, environmental, and economic feasibility study is conducted in the last part of this chapter in order to verify the adequacy of using the normalized crushed sand as the only fine aggregate in concrete.

1. Comparison of concrete performances

In the following section, the results of the fresh properties, compressive strength, flexural strength, and durability properties are presented for 11 different types of concrete. The mix design proportions of the different types were displayed in chapter III.

Three mixes of normal strength concrete, "Mix 30", "Mix 35-I", and "Mix C35-II", are compared for three different fine aggregates each. "Mix 30" is characterized by a water to cement ratio of 0.5 and cement content of 350 kg/m³. For "Mix 35-I", the water to cement ratio is reduced to 0.4 while conserving the same cement content. "Mix C35-II" presents low cement content and water to cement ratio, of 300 kg/m³ and 0.4 respectively. The three concrete types of each mix differ only by the fine aggregates type and/or gradation. The "Control mix CM" contains the reference combination of fine aggregates consisting of equivalent mass proportions of natural sand "NS-Series A" and the "Conventional crushed sand CCS". The "Equivalent mix EM" incorporates the "Equivalent crushed sand ECS" as the only fine aggregate without natural sand. The "Modified mix MM" also does not contain natural sand, the well-graded "Modified crushed sand MCS" is the only fine aggregate in this type of concrete.

In order to reach high compressive strength, "Mix 50" is characterized by a high cement content, 400 kg/m³, and low water to cement ratio, 0.3. As detailed in the mix design in the previous chapter, two

types of concrete are compared for this mix and they differ only by the fine aggregate type and gradation. The "Control mix CM-50" contains a conventional combination of natural sand "NS-Series B" and the "Conventional crushed sand CCS". The "Modified mix MM-50" does not contain natural sand; it incorporates the well-graded "Modified crushed sand MCS" as the only fine aggregate in concrete.

To have an additional quantity of concrete to perform the modulus of elasticity and shrinkage tests, the same cement content and water to cement ratio of "Mix 30" are adopted in the "Mix 30a" but with slightly different proportions of coarse aggregates (originating from different pits of the same quarry). Furthermore, a microstructural analysis is performed at the interfacial transition zone of samples from the three types of concrete of "Mix 30a".

1.1 Fresh properties

To analyze the effect of fine aggregates on concrete properties at fresh state, several fresh properties are assessed and compared for the different types of concrete. As already mentioned in the previous chapter, the aggregates used have been in the air-dry condition.

For each mix, the slump is checked directly after mixing and, if necessary, the admixture content is adjusted to reach a slump of 20 ± 2 cm. After guarantying the reach of the target slump, and within a maximum of 15 minutes after the end of the concrete mixing, the temperature of concrete is recorded.

The fresh concrete temperature and the required admixture content for each mix are presented in Table IV.1.

Table IV.1 Fresh concrete temperature and admixture content of all concrete mixes

Concrete mix	Concrete property	Fresh concrete temperature (°C)	Admixture content/kg of cement (%)
Mix 30 (W/C: 0.5; cement: 350 kg/m ³)	CM-30	21.5	0.71
	EM-30	21.5	0.29
	MM-30	22.0	0.00
Mix 35-I (W/C: 0.4; cement: 350 kg/m ³)	CM-35-I	23.5	2.43
	EM-35-I	22.5	1.36
	MM-35-I	21.5	1.10
Mix 35-II (W/C: 0.4; cement: 300 kg/m ³)	CM-35-II	24.5	3.46
	EM-35-II	24.0	2.30
	MM-35-II	23.0	2.00
Mix 50 (W/C: 0.3; cement: 400 kg/m ³)	CM-50	29.0	2.40
	MM-50	29.5	2.55

After the determination of the fresh concrete temperature, the density and air content are measured, and the samples for the setting times test are collected. The mixes are then covered and left at rest. They are only remixed by hand directly before repeating the slump test after 30, 60, and 90 minutes, to detect the evolution of slump with time. Due to the lack of sufficient aggregates quantities, only one batch of each type of concrete has been prepared for the fresh properties tests. The results of the eleven mixes are displayed in Table IV.2.

Table IV.2 Fresh state properties of all concrete mixes

Concrete Mix	Fresh state properties	CM	EM	MM	
Mix 30 (W/C: 0.5; cement: 350 kg/m ³)	Slump (cm)	<i>Initial</i>	20.5	20.5	20.5
		<i>30 minutes</i>	17.0	17.5	18.5
		<i>60 minutes</i>	12.5	14.0	15.0
		<i>90 minutes</i>	11.5	11.0	14.0
	Setting time	<i>Initial</i>	6h40min	5h00min	5h00min
		<i>Final</i>	9h20min	7h40min	7h30min
	Density (kg/m³)		2390	2363	2341
	Air content (%)		1.3	1.8	1.9
Mix 35-I (W/C: 0.4; cement: 350 kg/m ³)	Slump (cm)	<i>Initial</i>	20.5	21.5	21.5
		<i>30 minutes</i>	17.0	19.5	20.0
		<i>60 minutes</i>	16.0	19.0	20.0
		<i>90 minutes</i>	12.5	18.0	20.0
	Setting time	<i>Initial</i>	8h15min	6h25min	6h05min
		<i>Final</i>	10h45min	8h20min	8h35min
	Density (kg/m³)		2413	2412	2405
	Air content (%)		2.5	2.4	2.9
Mix 35-II (W/C: 0.4; cement: 300 kg/m ³)	Slump (cm)	<i>Initial</i>	20.0	20.0	21.0
		<i>30 minutes</i>	Shear	15.5	11.0
		<i>60 minutes</i>	-	12.0	10.0
		<i>90 minutes</i>	-	10.0	7.5
	Setting time	<i>Initial</i>	12h15min	8h20min	8h00min
		<i>Final</i>	14h45min	10h50min	10h30min
	Density (kg/m³)		2439	2435	2404
	Air content (%)		1.7	2.3	2.7
Mix 50 (W/C: 0.3; cement: 400 kg/m ³)	Slump (cm)	<i>Initial</i>	19.5	-	19.0
		<i>30 minutes</i>	11.0	-	8.0
		<i>60 minutes</i>	7.5	-	7.0
		<i>90 minutes</i>	4.5	-	5.0
	Density (kg/m³)		2449	-	2459
	Air content (%)		2.5	-	2.2

(-): property not measured

1.1.1 Fresh concrete temperature

To be able to conduct a reliable comparison between the fresh properties, the different types of concrete of each mix are cast on the same day and while conserving the same environmental conditions and the same temperature of aggregates.

By comparing the values of the concrete temperature at fresh state (Table IV.1), we can observe a small difference that reaches a maximum of 0.5, 2, 1.5, and 0.5 °C for "Mix 30", "Mix 35-I", "Mix 35-II", and "Mix 50" respectively. These results confirm that, for each mix, the materials temperatures and the environmental conditions could be considered similar during the mixing.

Additionally, the results of the temperatures of all the fresh concretes ensure that these mixes did not reach too high or too low temperatures after mixing, thus the concrete hydration rate will not be affected. "Mix 50" exhibits the highest temperature among the other mixes (29-29.5 °C). This result is related to the higher environmental temperature on the day of mixing CM-50 and MM-50.

1.1.2 Workability

Comparing the admixture content of the normal strength concrete mixes, the highest admixture dosage is required for Mix 35-II. This could be explained by the lowest cement paste volume and water to cement ratio, and also by the highest natural sand content of this mix compared to the two other normal strength concrete mixes. Table IV.1 shows that to reach a slump value of 20 ± 2 cm at fixed water to cement ratio for each one of the three normal strength concretes, "Mix 30", "Mix 35-I", and "Mix C35-II", the content of the water-reducing admixture is the highest in the "Control Mix CM" and it decreases when the natural sand is totally substituted by crushed sand in concrete. In the reference mix CM of "Mix 35-II", this content (3.46%) is the highest and it even exceeds 2.5%, the maximum allowable percentage suggested by the admixture manufacturer. Having the same particle size distribution of fine aggregates, the "Equivalent mix EM" requires lower admixture content than the CM concrete for the three different concrete mixes. Its highest amount is for "Mix 35-II", without exceeding the maximum dosage recommended by the manufacturer. As for "Modified mix MM", it needs the lowest admixture content compared to the other two types of concrete. Moreover, it is remarkable that the MM reaches the target slump without adding admixture in "Mix 30".

In "Mix 50", for the same water to cement ratio, the admixture contents are quite similar in both types of concrete, CM and MM, with a slightly higher value for the modified mix MM. This value reaches the maximum limit (2.5%) recommended by the admixture manufacturer.

➤ Effect of deleterious particles

As seen in chapter II, the natural sand "NS-Series A", used in the three types of normal strength concrete, exhibits a higher percentage of deleterious particles than the crushed sand. This natural sand is characterized by a lower sand equivalent percentage (60 and 73% for NS and CS respectively), higher methylene blue value (1.9 and 0.9 g for NS and CS respectively), and a higher percentage of clay lumps and friable particles (5.3 and 0.7% for NS and CS respectively). Since these particles usually increase the water demand of the concrete mix and reduce its workability, the natural sand in the control mix CM requires a higher content of water-reducing admixture to reach the target slump. Thus, the incorporation of the crushed sand as the only fine aggregate in EM and MM leads to lower admixture demand, thus higher workability compared to CM concrete that contains natural sand.

Previous studies also proved that the deleterious particles increase the water demand of the mixes and negatively affect the fresh performance of concrete. By comparing spherical river sand grains with manufactured sand characterized by angular grains with a rough surface, (*Shen et al., 2016*) have found that the latter exhibited lower clay contents and thus required a lower amount of water-reducing admixture in concrete. Similarly, (*Hasdemir et al., 2016*) found that, in order to obtain the same slump for fixed water to cement ratio, a higher dosage of admixture should be added to concretes incorporating sand samples with higher methylene blue values, to compensate for the dosage of chemical additives absorbed by the clay minerals.

For high-strength concrete, both types of concrete exhibit approximately the same dosage of admixture with slightly higher content in the crushed sand concrete (2.40 and 2.55% for CM-50 and MM-50 respectively), thus approximately the same workability.

The natural sand "NS-Series B" used in the control mix of "Mix 50" is also characterized by a higher content of deleterious particles than the crushed sand. The sand equivalent percentage of the natural sand is lower (58 and 73% for NS and CS respectively), its methylene blue value is higher (1.3 and 0.9 g for NS and CS respectively), and its percentage of clay lumps and friable particles is also higher (5.0 and 0.7% for NS and CS respectively). However, the effect of deleterious particles is less pronounced in the high-strength concrete. This could be attributed to the lowest amount of natural sand in "Mix 50" (300 kg/m^3) compared to the other mixes with a content higher than 400 kg/m^3 .

➤ Effect of shape

The morphological characterizations conducted in chapter II proved that the natural sand grains are sub-rounded while the crushed sand grains are angular with a rough surface. Conventionally, it is believed that the roughness and angularity of crushed sand negatively affect the workability by increasing the water demand of fresh concrete. This effect was confirmed by many studies detailed in Chapter I.

However, the effect of the shape of the fine aggregate is not predominant in the normal strength concretes of this study. Despite the higher angularity and roughness of the crushed sand grains, the concretes incorporating the crushed sand as the only fine aggregate, EM and MM, exhibit better workability than the concrete with the natural rounded sand, CM. This comparison proves that the content of impurities and deleterious particles that could be present in fine aggregates could have a more significant effect on the concrete workability than the shape and surface texture of sand grains.

This observation complies with (*Shen et al., 2016; Shen et al., 2018*) results. They have found that the stone powder, gradation, and clay content of fine aggregate have more influence on concrete workability than the shape and surface roughness of its particles.

For the high-strength concrete "Mix 50", the replacement of the sub-rounded natural sand by normalized crushed sand does not lead to a significant difference in the superplasticizer demand of CM and MM. Thus, the effect of the difference in the shape between the natural sand and the crushed sand tends also to be negligible in the high-strength concrete, knowing that the natural sand content is lower in this mix (300 kg/m^3) compared to that in the normal strength concretes ($400\text{-}450 \text{ kg/m}^3$).

➤ Effect of gradation

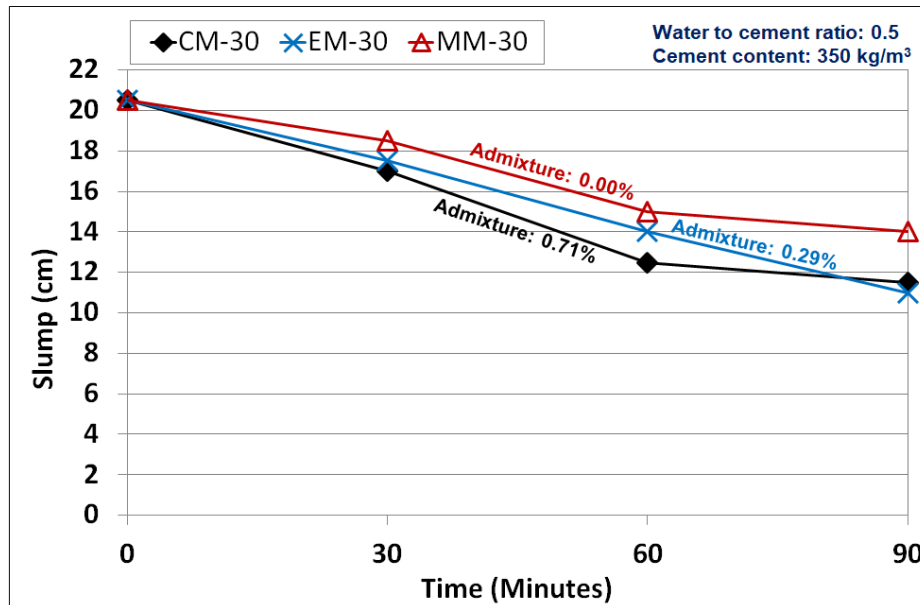
Noting that EM and MM of the normal strength concretes do not contain natural sand, the improvement of the particle size distribution of the crushed sand (Figure III.6 of Chapter III) and the all-in aggregates (Figure III.9a of Chapter III) in MM leads to a decrease in the amount of the admixture content compared to EM. The well-graded modified sand reduces the content of cement needed to fill the voids, leaving a higher quantity of cement grains available to coat the surface of the aggregates and to reduce the friction between aggregates particles, enhancing thereby the workability of concrete (*Santos et al., 2015*).

1.1.3 Loss of workability with time

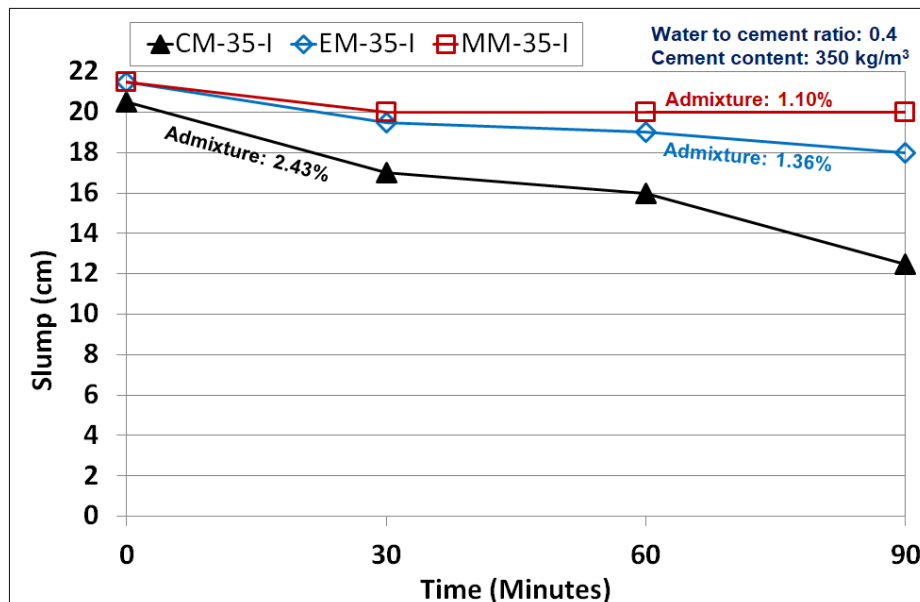
The slump retention test informs on the loss of workability with time. After applying hand mixing, the slump of each concrete mix is measured after 30, 60, and 90 minutes of mixing. For each time, the slump is determined on one sample and the values are presented in Table IV.2.

To have a clearer description of this behavior, these results are expressed in terms of the evolution of slump values with time for each concrete in Figure IV.1.

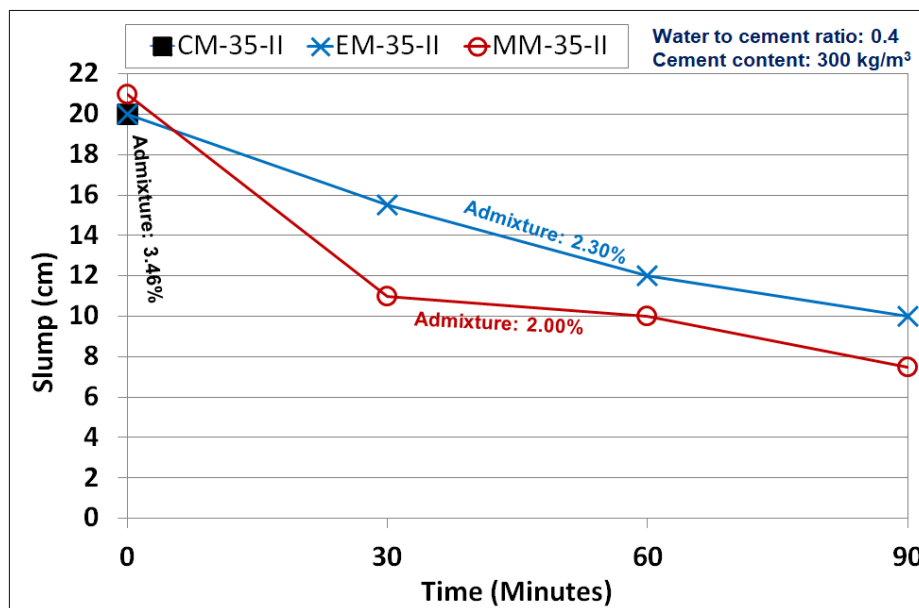
Generally, compared to the three types of concrete of "Mix 35-II", the concretes of "Mix 35-I" maintain more workability after 90 minutes. Having the same water to cement ratio, this difference could be attributed to the lowest cement paste volume and highest admixture content in the concretes of "Mix 35-II". However, the comparison between "Mix 30" and "Mix 35-I" is not concordant with this analysis. Despite the highest water to cement ratio and the lowest admixture content in "Mix 30", the three types of concrete lose their workability faster. The reason behind this discrepancy could be due to the artifact done during the slump retention test of "Mix 30". For the three types of concrete of "Mix 30", the concrete sample was not covered throughout the slump retention test, increasing in this way the workability loss due to desiccation.



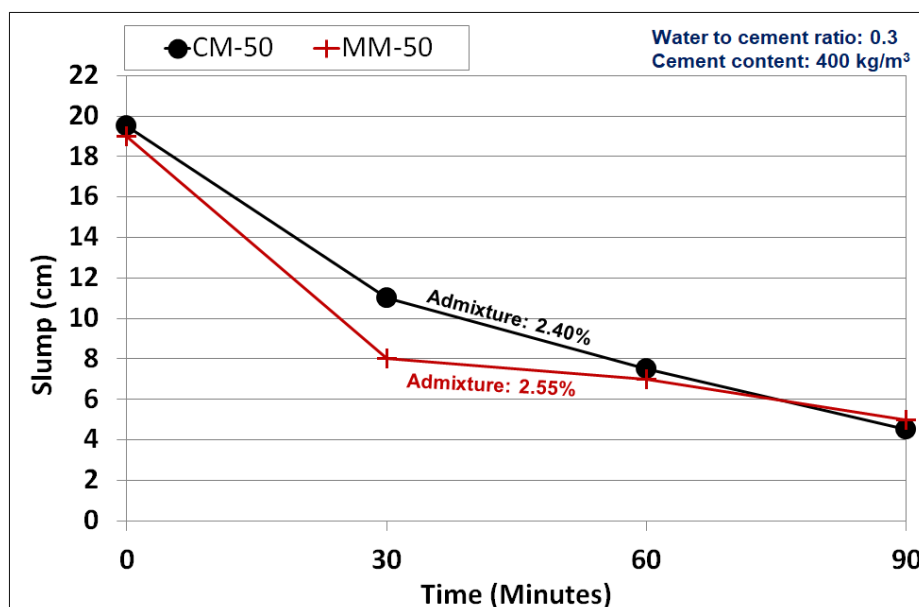
(a)



(b)



(c)



(d)

Figure IV.1 Evolution of slump over time for (a) "Mix 30", (b) "Mix 35-I", (c) "Mix 35-II", and (d) "Mix 50"

The graph of the three types of "Mix 30" (Figure IV.1a) shows that in the 60 minutes, the control mix CM exhibits the highest rate of slump decrease, followed by EM, then MM. Accordingly, the content of the admixture follows the same order in these concretes. After 60 minutes, the decrease of the slump in CM begins to slow down to reach, at 90 minutes, a slump value similar to the value of EM. It should be noted that the difference in the decrease between the three mixes is not significant. The slump values remain close throughout the test with a maximum difference of 3 cm between EM and MM at 90 minutes.

Figure IV.1b reveals that for "Mix 35-I", MM does not lose its initial workability even after 90 minutes. The slump values of EM also remain in the same range of workability with a decrease of 2.5 cm at the

end of the test. However, the reference concrete CM displays a remarkable progressive decrease of workability to reach 12.5 cm after 90 minutes. CM contains a much higher amount of admixture while the other two mixes incorporate close admixture content.

For "Mix 35-II", the reference concrete CM, containing a high amount of admixture which exceeds the maximum limit proposed by the manufacturer, displays a shear behavior after 30 minutes, an indication that this mix could cause difficulties while placing. Regarding the crushed sand concretes of this mix, lower slump values are detected in MM, despite the close amount of admixture in this mix compared to the one of EM concrete (Figure IV.1c). As explained before, this normal strength mix is characterized by the lowest cement paste volume and water to cement ratio which affect the workability.

For high-strength concrete "Mix 50", the slump values and their evolutions are quite similar (Figure IV.1d). With a comparable admixture content, the slump loss follows the same trend with very close values throughout the test. The largest difference is detected after 30 minutes, the MM-50, which contains slightly higher admixture content, presents a slightly lower value (difference of 3 cm). The results of this mix show that both types of concrete are characterized by a high loss of workability after 30 minutes. The slump decreases by 8.5 and 11 cm for CM and MM respectively, probably due to the high dosage of admixture in these two types of concrete.

Hence, the results of all the studied concrete mixes in this study reveal that the water-reducing admixture content in the concrete mixes seems to significantly affect the slump retention results. These results are in accordance with those of (*Makhloufi et al., 2014*).

1.1.4 Setting times

The results of Table IV.2 indicate that the CM presents the longest initial and final setting times for the three normal strength concrete mixes, while EM and MM present very close values whatever the concrete mix. The control mixes need the highest admixture content among the other two types of concrete (Table IV.1). Thus, the difference in setting times between the control concretes and the crushed sand concretes could be explained by the retarder secondary effect of the admixture used in this study. Figure IV.2 clearly shows that the initial and final setting times increase with the admixture content in concrete mixes.

Additionally, the higher quantity of calcite fines in the crushed sand concretes, due to the total replacement of the siliceous sand by pure limestone fine aggregates, could have acted as nucleation sites and accelerated the chemical reaction responsible for the cement hydration. Hence, the initial and final setting times are reduced for EM and MM. In previous studies, the same effect of the limestone fines on the setting times of the cement paste was observed when the limestone powder was used as filler in concrete (*Bentz et al., 2015; Moon et al., 2017*).

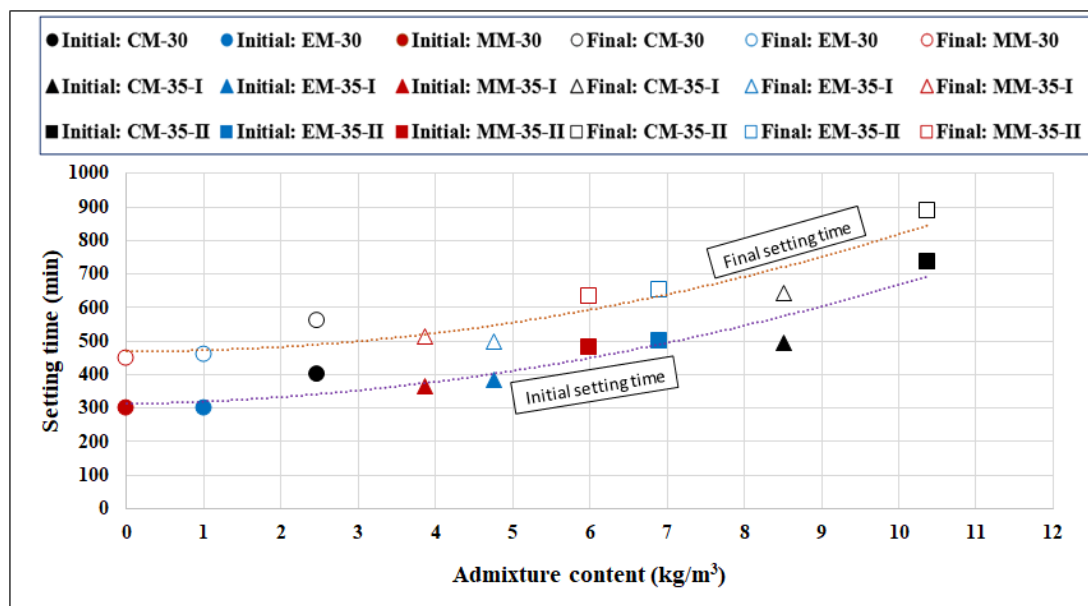


Figure IV.2 Initial and final setting times function of admixture content in the normal strength concrete mixes

1.1.5 Density and air content

During this study, the differences between the experimental and the theoretical values of fresh densities of all concrete mixes are found to be negligible (Annex E).

While comparing the densities of the 11 concretes (Table IV.2), it could be observed that, as expected, the lower water to cement ratio produces concrete with a higher density, thus higher compactness.

By comparing the fresh density and air content of the three types of concrete of each normal strength concrete, Table IV.2 and Figure IV.3 show that the reference concrete CM, which requires the highest amount of admixture, presents the highest density with the lowest air content, except for "Mix 35-I". This mix is characterized by similar density and air content for CM and EM despite the difference in the admixture content between these two types of concrete.

For "Mix 50", since the two types of concrete require approximately the same admixture content to reach a slump of 20 ± 2 cm, the density and air content are almost identical for both types of concrete. The negligibly higher admixture content in MM and better particle size distribution of fine aggregates give a concrete with slightly lower air content and higher density.

The increase of the fresh density and decrease of air content with the increase of admixture proportion may be due to the dispersive effect of the admixture used, which deflocculates the cement particles and limits their agglomeration, reducing in this way the voids in the fresh concrete and enhancing its packing and fresh density. For the different types of concrete of each mix, this effect could be observed in Figure IV.3. (Makhloufi *et al.*, 2014) have detected the same effect of admixture on the concrete density.

Additionally, the aggregates characterization results reported in Chapter II indicated that the specific gravity of natural sand "NS-Series A" (2.62), used in the control mixes of the normal strength concretes, is higher than the specific gravity of the crushed sand (2.55). Knowing that the concrete bulk density is a linear function of the density of aggregates, as seen in the studies of (Qasrawi *et al.*, 2009; Gameiro *et al.*, 2014), then the total replacement of the natural sand by crushed sand with lower specific gravity decreases the fresh density of concrete.

For the high-strength concrete, in addition to the closeness in the air content values, the relative densities of the natural sand "NS-Series B" (2.59) used in CM-50 and the crushed sand CS (2.55) are close, thus they do not provide concretes with different fresh densities in "Mix 50".

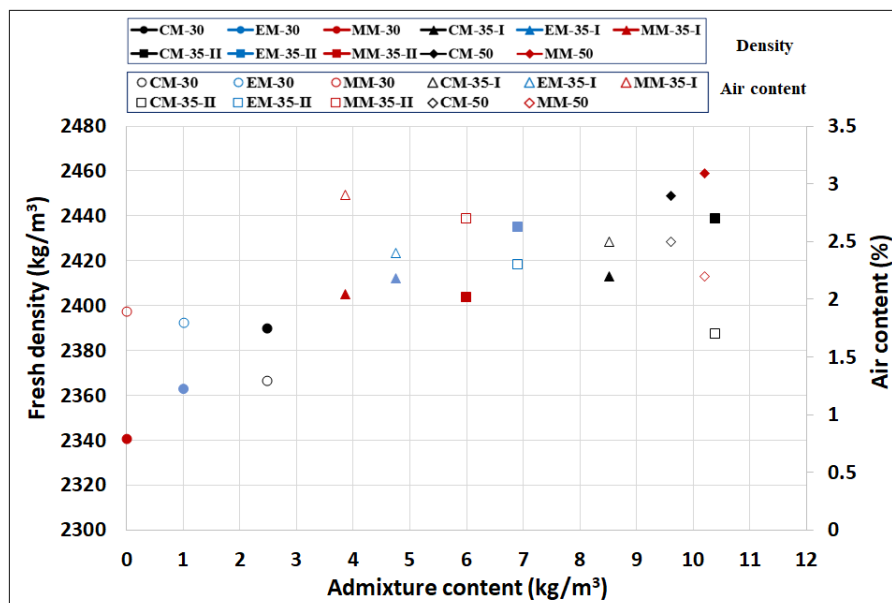


Figure IV.3 Fresh density and air content function of admixture content in all concrete mixes

1.1.6 Summary of fresh properties

The normal strength crushed sand concretes demand lower admixture dosage than the reference concrete incorporating natural sand, probably due to the higher water demand of deleterious particles of the latter. Thus, the lower admixture content in the normalized crushed sand concretes provides a slower loss of workability with time, lower fresh density, and higher air content. In addition to the admixture effect, the crushed sand could play the role of a nucleation site and reduce the setting times of concrete. Consequently, in terms of the admixture content, the normalized crushed sand could give an economic advantage for crushed sand concretes compared to the reference concrete used nowadays in the Lebanese market.

The two types of high-strength concrete are characterized by a close fresh state behavior. The effect of the fine aggregates seems less pronounced since the control mix of the high-strength concrete is characterized by the lowest amount of natural sand compared to the normal strength concrete mixes.

1.2 Mechanical behavior

To assess the effect of the substitution of natural sand by crushed sand on the mechanical behavior of concrete, the compressive strength, modulus of elasticity, and flexural strength of the different types of concrete are compared in this section.

The ability of concrete to undergo load throughout its service life is evaluated by comparing the compressive and flexural strengths of the 11 studied concretes. Additionally, the effect of fine aggregates on the elasticity of concrete is investigated on the three types of "Mix 30a".

Within a maximum duration of 15 minutes after the mixing of concrete, the cylinders and prisms specimens are prepared following the procedures detailed in Chapter III and are kept in water at 23 ± 2 °C until the day of the test.

1.2.1 Compressive strength

Table IV.3 displays the average compressive strength values and the standard deviations of three 150x300 mm concrete cylinders for each type of concrete, water-cured until the day of testing: 3, 7, 28, and 90/135 days. The long-term compressive strength test of the three normal strength concretes is conducted at 90 days, while that of the high-strength concrete, "Mix 50", is carried out at 135 days for the reasons detailed in Chapter III.

Table IV.3 Average values (and standard deviations) of the compressive strength of all concrete mixes at different ages, in MPa

Concrete mix		3 Days	7 Days	28 Days	90/135 Days*
Mix 30 (W/C: 0.5; cement:350 kg/m ³)	CM-30	17.8 (0.63)	24.7 (1.36)	35.1 (0.41)	39.2 (0.26)
	EM-30	17.5 (0.37)	24.6 (0.48)	35.8 (1.29)	39.4 (1.28)
	MM-30	17.5 (1.07)	24.2 (2.13)	33.5 (1.06)	36.0 (1.03)
Mix 35-I (W/C: 0.4; cement:350 kg/m ³)	CM-35-I	32.9 (1.67)	43.6 (0.38)	49.8 (1.90)	61.4 (0.89)
	EM-35-I	29.1 (1.12)	38.4 (1.91)	43.1 (0.63)	57.4 (2.38)
	MM-35-I	29.7 (0.35)	38.4 (0.60)	42.9 (0.76)	53.2 (1.95)
Mix 35-II (W/C: 0.4; cement:300 kg/m ³)	CM-35-II	27.4 (0.03)	39.1 (1.73)	47.8 (0.27)	59.3 (2.63)
	EM-35-II	28.4 (1.59)	39.2 (2.50)	49.5 (1.31)	53.5 (1.58)
	MM-35-II	26.7 (0.27)	39.0 (2.11)	46.1 (0.12)	53.9 (1.02)
Mix 50 (W/C: 0.3; cement:400 kg/m ³)	CM-50	42.1 (0.93)	48.4 (1.76)	66.0 (1.06)	72.5 (3.23)
	MM-50	40.7 (0.04)	46.9 (1.43)	65.4 (1.80)	71.1 (3.03)

(*): the long-term compressive strength test is performed at 90 days for the normal strength concretes, "Mix 30", "Mix 35-I", and "Mix 35-II", and at 135 days for the high-strength concrete "Mix 50"

Generally, for each concrete mix, the 28-day average compressive strengths of concretes with different types of sand, CM, EM, and MM, relatively conform to the expected average compressive strength for each water to cement ratio: 30, 35, and 50 MPa for "Mix 30", "Mix 35-I" and "Mix 35-II", and "Mix 50" respectively. At different ages, the compressive strengths of "Mix 30", "Mix 35-II", and "Mix 50" seem not considerably affected by the total substitution of natural sand by crushed sand in concrete for the same water to cement ratio and cement content. However, in "Mix 35-I" which is characterized by the highest cement content and lowest water to cement ratio between the normal strength concretes, larger differences are detected with higher compressive strength for CM compared to those of crushed sand concretes.

The three concrete types of "Mix 30" display similar compressive strengths at 3 and 7 days. At 28 and 90 days, the compressive strengths remain close in CM and EM, the two types of concrete with the same gradation of fine aggregates. However, the compressive strengths of MM are slightly lower (6 and 9% at 28 and 90 days respectively) compared to the other two mixes.

For "Mix 35-I", at all ages, the control mix CM presents the highest values with a difference varying between 12% (at 3 days) and 13-14% (at 28 and 90 days), compared to the crushed sand concretes. EM and MM are characterized by a comparable behavior, they present similar values at 3, 7, and 28 days,

and a value slightly inferior for the MM (7%) compared to EM at 90 days. "Mix 35-I" is characterized by a high difference in the admixture content between the three types of concrete (2.43, 1.36, and 1.10% for CM, EM, and MM respectively). The difference in the admixture content could explain the highest compressive strengths of CM. By increasing the admixture content, the deflocculation of the cement grains increases, enhancing thereby the hydration reaction and improving the concrete strength, whereas in the crushed sand concretes, the cement grains could be less deflocculated.

The compressive strengths of the three types of concrete of "Mix 35-II" are equivalent whatever the concrete age. The same average values are found at 7 days and little differences of 3% and 7% are observed in the average compressive strength values at 3 and 28 days respectively, with the highest value for EM and lowest value for MM. At 90 days, EM has no longer the highest strength, it presents the same strength as MM, while CM reaches a compressive strength of 59.3 MPa, a 10% higher result compared to the other two types of concrete. This difference could be attributed to the higher dosage of admixture in CM, which is characterized by a secondary retarding effect that could enhance the long-term compressive strength of concrete.

For the three types of normal strength concrete, the lowest compressive strength is obtained by MM, which contains the well-graded modified crushed sand as the only fine aggregate. This sand is the one that fits better the ASTM grading limits compared to the other two types of fine aggregates incorporated in CM and EM. As already observed in the assessment of the concrete properties at fresh state, the better gradation of MM leads to a decrease in the admixture demand. However, this reduced admixture content could lead to the lowest deflocculation of the cement particles which slightly affects their hydration and consequently the concrete compressive strength, compared to the other two types of concrete.

For the high-strength concrete "Mix 50", Table IV.3 reveals similar strengths for both types of concrete, CM and MM, at different concrete ages, with a maximum difference of 3% at 3 and 7 days. As intended, high strength is attained in both types of concrete with 65-66 MPa at 28 days.

The evolutions of compressive strengths over time are investigated through Figure IV.4.

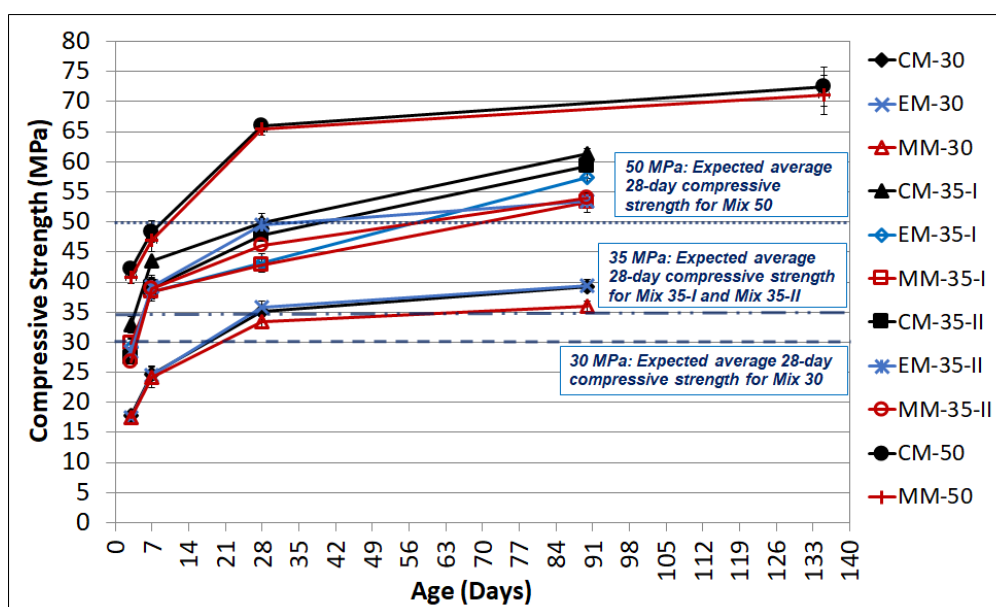
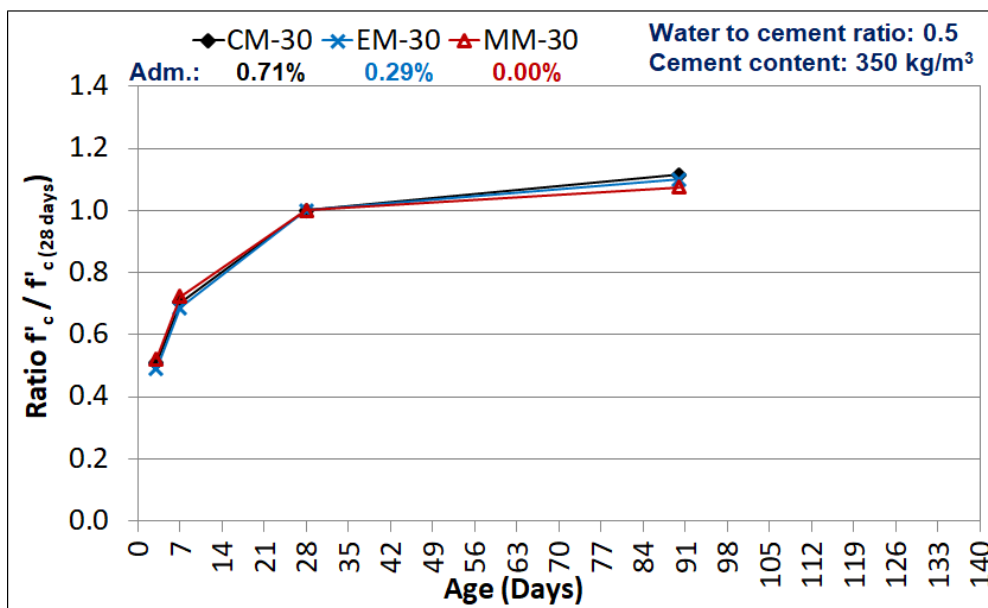


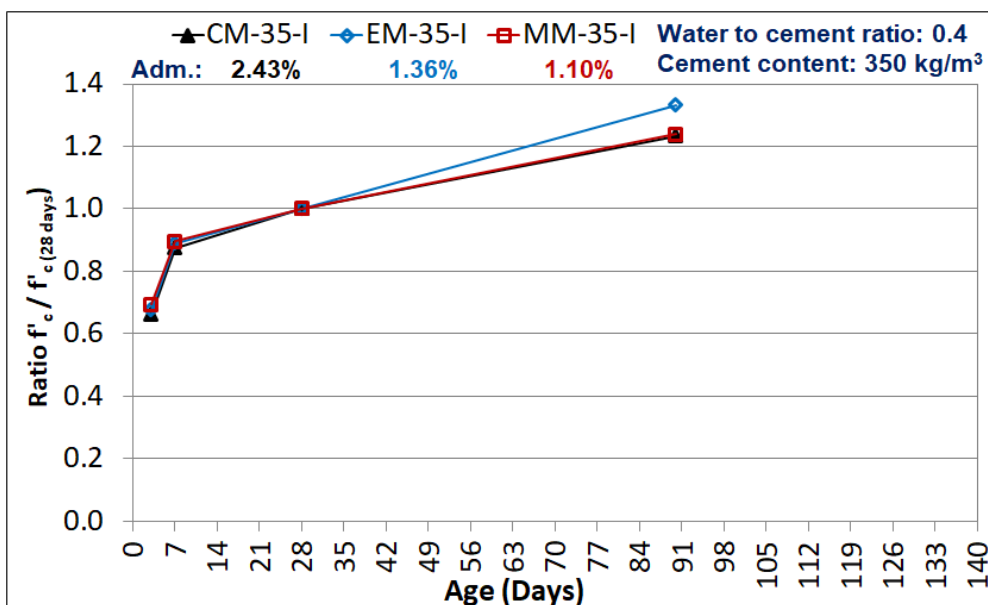
Figure IV.4 Evolution of the compressive strength over time for all the studied concretes

As seen in this figure, by decreasing the water to cement ratio, the magnitude and the kinetics of the compressive strengths increase in "Mix 35-I", "Mix 35-II", and "Mix 50" compared to those of "Mix 30". It should also be noted that, despite the lower cement content in "Mix 35-II" compared to that in "Mix 35-I", for the same water to cement ratio (0.4), the compressive strength is not significantly affected. It is even enhanced in the crushed sand concretes at 7 and 28 days. Despite the cost that could be imposed in the increase of the admixture content in "Mix 35-II", this mix could give economic and environmental advantages since it conforms to the expected average compressive strength (35 MPa) for this water to cement ratio (0.4) with lower cement content.

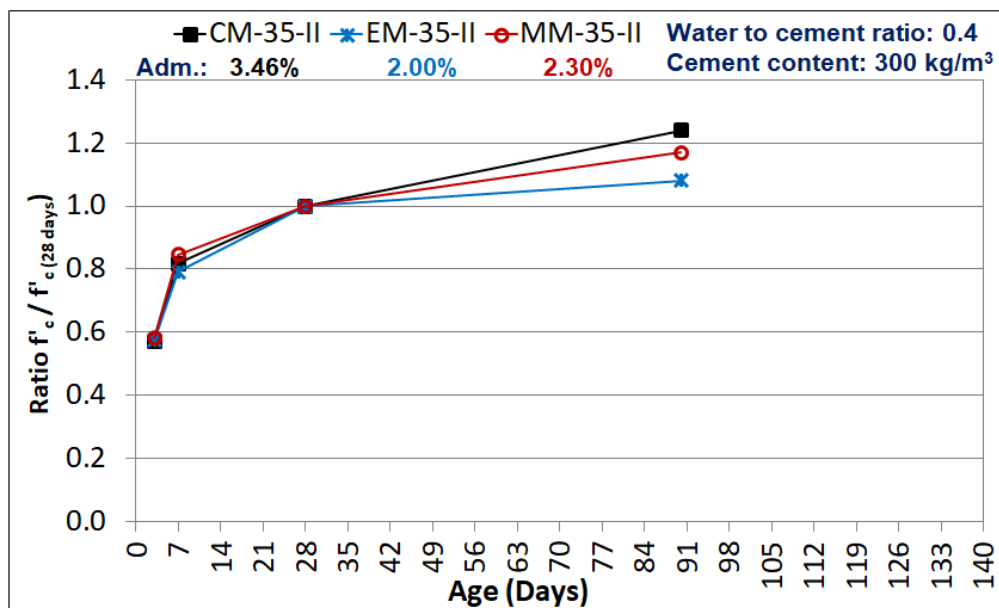
The evolutions of the ratio of the compressive strength at each age to the 28-day compressive strength are presented in Figure IV.5 to focus on the compressive strength kinetics.



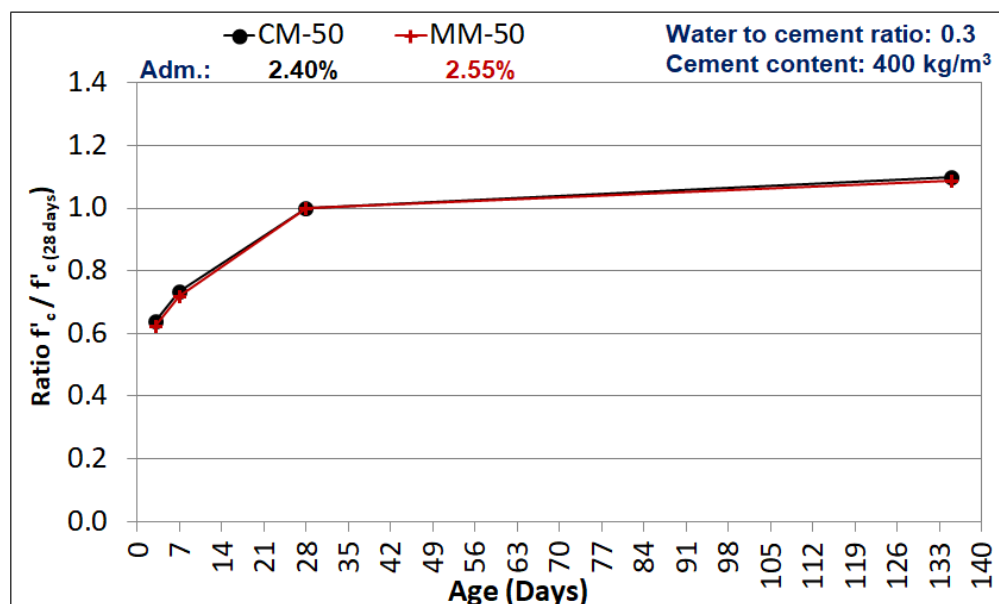
(a)



(b)



(c)



(d)

Figure IV.5 Evolutions of the ratio of the compressive strength at different ages to the 28-day compressive strength for (a) "Mix 30", (b) "Mix 35-I", (c) "Mix 35-II", and (d) "Mix 50"

For the three types of each normal strength concrete mix, Figure IV.5a to Figure IV.5c show that the development of the compressive strength is similar between 3 and 7 days and it slightly diverges between 7 and 28 days. The main differences in terms of kinetics appear over 28 days for some concrete mixes. From 28 to 90 days, approximately the same increase of compressive strength is observed for the three types of "Mix 30" (Figure IV.5a), whereas for the other two mixes, the gain of strength from 28 to 90 days differs according to the type of fine aggregates. For "Mix 35-I", EM exhibits the highest strength gain (33%) while CM and MM strengths evolve similarly (23-24%) (Figure IV.5b). This highest difference for EM-35-I could be related to the highest standard deviation value of the 90-day compressive strength of this mix (2.38) compared to the value of the others (0.89 and 1.95 for CM-35-

I and MM-35-I respectively) (Table IV.3). For "Mix 35-II", at 90 days the CM concrete gains 24% more strength, while the increases for EM and MM are 8% and 17% respectively (Figure IV.5c). Also, CM-35-II is characterized by a 90-day compressive strength with the highest standard deviation (2.63) compared to the others (1.58 and 1.02 for EM-35-II and MM-35-II respectively) (Table IV.3).

Figure IV.5d also demonstrates the similarity in the evolution of the compressive strength over time for the two types of the high-strength concrete "Mix 50", CM-50 and MM-50. Both graphs seem superimposed for all concrete ages.

In previous studies, at fixed water to cement ratio, for different slumps or different admixture content, the crushed sand concrete gives higher compressive strength. The angular and rough surface of the crushed sand particles improves the interfacial transition zone between the sand grains and the cement paste, thus enhancing the concrete performance in terms of compressive strength (*Stefanidou, 2016; An et al., 2017*). However, in the normal strength concretes of our study, the effect of fine aggregate shape and roughness is not significantly pronounced on the compressive strength of concrete. It is probably compensated by the beneficial deflocculation and secondary retarding effect of the higher dosage of admixture in the concrete incorporating natural sand. In this study, concretes globally develop comparable compressive strengths whatever the type of fine aggregates although they differ by their shapes, mineralogy, and gradation. Confirming our results, (*Cordeiro et al., 2016*) also found that the increase of the natural sand substitution by crushed sand does not have a significant or negative effect on the compressive strength of concrete.

1.2.2 Modulus of elasticity

The assessment of the performance of concrete in terms of the 28-day modulus of elasticity is conducted on the three types of "Mix 30a". For each concrete type, three 150x300 mm cylinder specimens are prepared and cured in water until the age of 28 days. The average and the standard deviation values for each concrete type are displayed in Table IV.4.

The experimental results of the 28-day modulus of elasticity of concrete are quite similar for the three types of concrete of "Mix 30a" (33-34 GPa). Hence, knowing that all the other constituents are the same in terms of quality and quantity (coarse aggregate and cement paste), the modulus of elasticity seems not affected by the variation of the type of fine aggregate in concrete. Thus, the possible influences of the proportion, grains shape, type, and modulus of elasticity of sand on the modulus of elasticity of concrete are undetectable.

According to (*ACI 318, 1995*), the 28-day elastic modulus of concrete could be predicted from the 28-day compressive strength and the unit weight of concrete as follows:

$$E_c(\text{MPa}) = W_c^{1.5} \cdot (0.043) \cdot \sqrt{f'_c} \quad (\text{Eq. IV.1})$$

Where W_c : the unit weight of hardened concrete at 28 days (kg/m^3) and f'_c : the mean compressive strength at 28 days (MPa).

On the other hand, the Eurocode 2 (*EN 1992-1-1, 2004*) estimates the 28-day modulus of elasticity from the 28-day compressive strength value by:

$$E_{cm}(\text{MPa}) = 22000 \cdot \left(\frac{f_{cm}}{10}\right)^{0.3} \quad (\text{Eq. IV.2})$$

Where f_{cm} : the mean compressive strength at 28 days (MPa).

By applying these formulas to the studied types of concrete, correct compliance is observed between the experimental values and the calculated ones for both standards (Table IV.4).

Table IV.4 Average experimental values (and standard deviations) of modulus of elasticity "Mix 30a" at 28 days and calculated values according to ACI 318 and Eurocode 2

Mix 30a (W/C: 0.5; cement:350 kg/m ³)	CM-30a	EM-30a	MM-30a
Unit weight of hardened concrete, kg/m ³	2403	2389	2377
Compressive strength, MPa	41.9	43.2	42.4
Average experimental modulus of elasticity (and standard deviations), GPa	34.4 (2.29)	34.0 (1.68)	33.3 (2.18)
Modulus of elasticity ACI 318, GPa	32.8	33.0	32.4
Modulus of elasticity Eurocode 2, GPa	33.8	34.1	33.9

Few studies have been carried out to evaluate the effect of the fine aggregates on the modulus of elasticity of concrete, whereas many studies have investigated the effect of coarse aggregate on this mechanical characteristic. (Makani *et al.*, 2010) conclude that the modulus of elasticity of concrete is dependent on the stiffness and volume fraction of coarse aggregates. By studying the shape effect, (Rocco and Elices, 2009) deduce that the crushed coarse aggregates produce concrete with a higher modulus of elasticity than the concrete made with spherical aggregates. As for fine aggregates and conforming to our results, in the study of (Cordeiro *et al.*, 2016), no significant changes are detected in the modulus of elasticity of concrete when a proportion of crushed granite sand (10%, 30%, and 50% by mass of fine aggregate) replaces the natural siliceous sand in concrete. This similarity could be more pronounced when the stiffness of the different types of sand is similar. Thus, taking into consideration the relatively low volume of fine aggregates in concrete in comparison with that of coarse aggregates, the characteristics of the fine aggregates might not be considered as a significant influential factor on the elastic modulus of concrete.

1.2.3 Flexural strength

The average values and the standard deviations of the 28-day flexural strengths are tabulated in Table IV.5 and presented in Figure IV.6. This test is conducted following (ASTM C78, 2016) on three prisms (100x100x50 mm) from each type of concrete, cured in water at 23 ± 2 °C, until the day of testing.

The three types of concrete of "Mix 30" and "Mix 35-II" generally display close flexural strength values, taking into account the standard deviation. However, contrarily to the compressive strength results in which MM globally presents the lowest values, the flexural strength of MM of both mixes are slightly higher than the values of the other two types of concrete CM and EM (10% higher value compared to CM for "Mix 30" and 11% higher value compared to EM for "Mix 35-II"). Subsequently, the concrete containing natural sand does not develop the highest flexural strength and it is even characterized by the lowest value for "Mix 30". For "Mix 35-I", generally the three types of concrete present good performance with higher strength in the control mix CM compared to the concretes without natural sand, EM and MM. Contrarily to "Mix 30" and "Mix 35-II", in this mix, MM presents the lowest flexural strength value with a difference of 15% with the control mix, while the values of CM and EM are close. The flexural strength values follow then the same trend as the compressive strength values for "Mix 35-I".

Table IV.5 Average values (and standard deviations) of 28-day flexural strength of all the studied concretes

Concrete mix		Flexural strength, in MPa
Mix 30 (W/C: 0.5; cement:350 kg/m ³)	CM-30	5.05 (0.20)
	EM-30	5.44 (0.83)
	MM-30	5.59 (1.08)
Mix 35-I (W/C: 0.4; cement:350 kg/m ³)	CM-35-I	6.76 (0.43)
	EM-35-I	6.11 (0.14)
	MM-35-I	5.76 (0.49)
Mix 35-II (W/C: 0.4; cement:300 kg/m ³)	CM-35-II	5.96 (0.47)
	EM-35-II	5.71 (0.50)
	MM-35-II	6.35 (0.21)
Mix 50 (W/C: 0.3; cement:400 kg/m ³)	CM-50	8.31 (0.73)
	MM-50	7.61 (0.39)

The slight improvement of the flexural strength of MM-30 and MM-35-II could be attributed to the rough surface and the angularity of the crushed sand grains on one hand, and the better distribution of the modified crushed sand grains on the other hand. (Stefanidou, 2016; Li et al., 2011) have found that the effect of the roughness and angularity of crushed sand is significant on the enhancement of the bond between the sand particles and the cement paste. Thus, the crushed sand could improve the performance of mortar and concrete. This positive effect could be more predominant when concrete is submitted to tension as in the case of flexural test, than under uniaxial compressive loading. Nevertheless, this improvement is not observed for "Mix 35-I", where the crushed sand concretes present lower flexural strength than the concrete incorporating natural sand. Similar to the compressive strength results, the highest cement content and lowest water to cement ratio in the three types of concrete of "Mix 35-I", and the relatively lower admixture content in EM and MM, lead to lower hydration and deflocculation of the cement grains in these mixes. Consequently, compared to CM, these mixes present a weaker adherence between the cement paste and the sand grains, thus lower flexural strength.

It is worth mentioning that the three types of concrete of "Mix 35-II" present close flexural strength values to those of "Mix 35-I". This comparison demonstrates that, for the same water to cement ratio, comparable flexural strength could be attained with lower cement content.

As for the 28-day flexural strength results of "Mix 50" (Table IV.5 and Figure IV.6), the value of the reference mix CM-50 is slightly higher (8%) than the value of the crushed sand concrete MM-50. So, in the case of this study, the shape of the well-graded crushed sand does not have a significant effect and does not improve the flexural strength of the high-strength concrete as is the case of the normal strength concretes. This could be related to the lowest amount of natural sand in the high-strength concrete compared to that of the normal strength concrete mixes.

Comparable to our results, when the crushed sand replaced the natural sand, for a constant cement content and water to cement ratio of 0.3, (Donza et al., 1996) have not detected any appreciable difference, neither in compressive strength nor in flexural strength of the high-strength concrete.

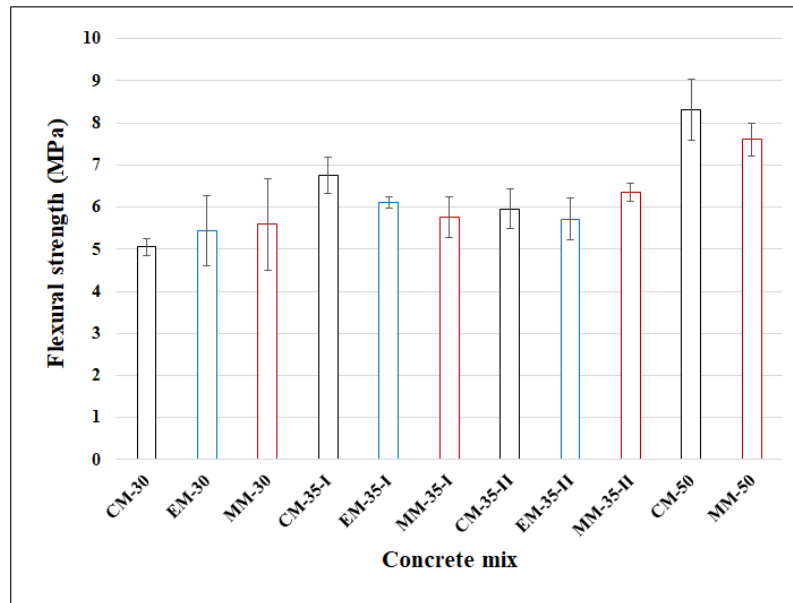


Figure IV.6 Average flexural strength values of all concrete mixes

1.2.4 Summary of the mechanical behavior

The mechanical behavior of the normal strength concrete is maintained when the normalized crushed sand substitutes the conventional combination of fine aggregates in concrete, for the same cement content and water to cement ratio, despite the slight detected differences in compressive and flexural strengths. The crushed sand could enhance the bond between the cement paste and the sand grains and increase the flexural strength of concrete, while the variation of the admixture content, with the different types of fines aggregates, could alter the deflocculation of the cement grains and varies the strength of concrete. On the other hand, the elastic modulus does not seem affected by the change of the sand type.

The effect of the substitution of the conventional combination of natural sand by well-graded crushed sand tends to be negligible on the compressive and flexural strengths of the high-strength concrete.

1.3 Shrinkage

The hydration reaction and the variation of the internal relative humidity that occurs in the cement paste cause a change of volume in an unloaded concrete, normally a shrinkage, at a constant temperature. As detailed in Section 4.2.3 of Chapter I, the sand and coarse aggregates act as rigid inclusions that restrain the shrinkage of the cement matrix, due to their higher stiffness compared to that of the cement paste. Thus, it is essential to verify if the total replacement of natural sand by crushed sand could generate a negative impact on the shrinkage behavior of concrete. By comparing the reference concrete incorporating natural siliceous sand to the two crushed sand concretes, the effects of the shape, the mineralogy, and the rigidity (not measured) of the fine aggregates on the concrete shrinkage could be assessed.

Different types of shrinkage are measured during this study: autogenous shrinkage without moisture exchange, and the total shrinkage for samples in a climatic chamber at 23 ± 2 °C and $50 \pm 4\%$ RH relative humidity. The desiccation shrinkage, which corresponds to the shrinkage part due to the loss of water, is calculated as the difference between the total and autogenous shrinkage. The mass loss is also measured on the total shrinkage samples and is herein correlated to the shrinkage values. Additionally,

the mass loss of the sealed samples is monitored throughout the test to detect any accidental drying that could occur on these samples.

The test of autogenous and total shrinkage is conducted on three samples for each type of "Mix 30a": CM-30a, EM-30a, and MM-30a. The samples of the three types of concrete have been subjected to exactly the same curing conditions, and the measurements have been taken on the same day. The following sections detail the analysis of the evolution of each type of shrinkage from the date of samples demolding at 1 day until the age of 77 days.

1.3.1 Autogenous shrinkage

As seen in Section 4.2.3 of Chapter I, the autogenous shrinkage is induced by Le Chatelier chemical contraction and by capillary tension due to the self-desiccation of these pores when internal water hydrates the cement. The autogenous shrinkage is calculated as the ratio of the length change to the initial length value of the sealed concrete samples (200 mm) while monitoring the constant temperature and avoiding any moisture transfer into or from the concrete.

Figure IV.7 reveals the evolutions of the average values of the autogenous shrinkage function of the concrete age for the three types of concrete, from the demolding day (day 1) until the end of the measurements (day 77).

The three curves are close while there is a slight shift in the development of the average autogenous shrinkage of MM after 49 days. Taking the standard deviation into consideration, this difference could be negligible.

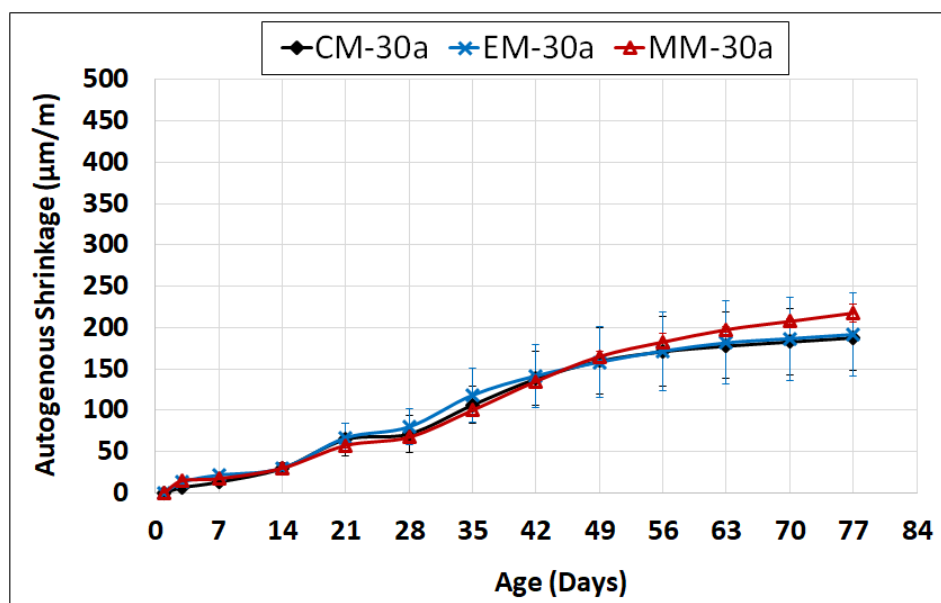


Figure IV.7 Evolution with the concrete age of the autogenous shrinkage for the three types of concrete of "Mix 30a" in sealed conditions without moisture exchange

The three types of concrete present quite similar behavior all over the test, with a maximum difference that does not exceed 12 $\mu\text{m}/\text{m}$ (11%) between CM-30a and EM-30a, and 29 $\mu\text{m}/\text{m}$ (15%) between CM-30a and MM-30a. Since the cement paste that develops shrinkage is the same in terms of volume and composition in the three types of concrete of Mix 30a, the shape, the mineralogy, and the particle size distribution of sand do not seem to affect the autogenous shrinkage of concrete in the case of this study. The sand volume is relatively small, thus changing the fine aggregates between the three types of

concrete does not significantly modify the concrete autogenous shrinkage. Accordingly, since the autogenous shrinkage is related to the size of the capillary pores of the cement paste, the close results of these two types of concrete could reveal a similarity in the size of the capillary pores, as expected since the cement pastes are the same.

Figure IV.8 shows the evolution of the mass loss of the sealed samples. According to these evolutions, an accidental drying shrinkage occurs for the three types of concretes, with a maximum mass loss of 0.5% at the end of the test. Thus, the shrinkage measured on the sealed samples could not be considered as totally autogenous shrinkage. Nevertheless, as the accidental drying is relatively close for all the concretes, the analysis of shrinkage evolution of the sealed samples remains valid.

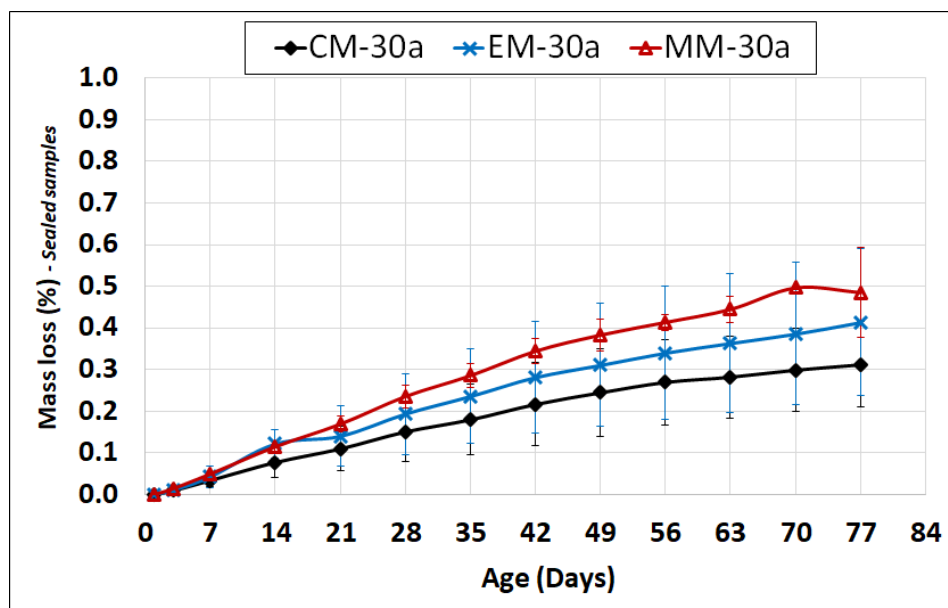


Figure IV.8 Evolution with the concrete age of the accidental mass loss measured on sealed samples of the three types of concrete of "Mix 30a"

1.3.2 Total shrinkage

The total shrinkage corresponds to the strain when the concrete is free to dry. After demolding (day 1), the samples are stored in a climatic chamber, at 23 ± 2 °C and $50 \pm 4\%$ RH.

The average evolution of the total shrinkage strain over time, for the three types of concrete, is presented in Figure IV.9.

The reference concrete CM-30a is characterized by the highest total shrinkage compared to the other two concretes that do not contain the natural siliceous sand. Since the shrinkage of the sealed samples is comparable for the three types of concrete, the highest total shrinkage of the control mix could result from its highest drying shrinkage.

During the first three days, the graphs of CM-30a and EM-30a are superimposed. After the third day, the CM-30a curve begins to shift to reach a maximum difference of $82 \mu\text{m/m}$ (21% higher value compared to the EM-30a value) at 21 days. After this age, the shrinkage of both types of concrete continues to increase but with lower differences that do not exceed 10% after 49 days. This slight reduction in the shrinkage of the crushed sand concrete could be attributed to the ITZ quality that is usually enhanced by the crushed grains of limestone sand. If the grains are still bonded to the cement paste, they could restrain its shrinkage. Moreover, the ability of the sand grains to restrain cement paste

deformation is correlated to their stiffness. However, in the case of this study, the differences are slight, due to the reduced volume of sand in comparison with those of coarser aggregates.

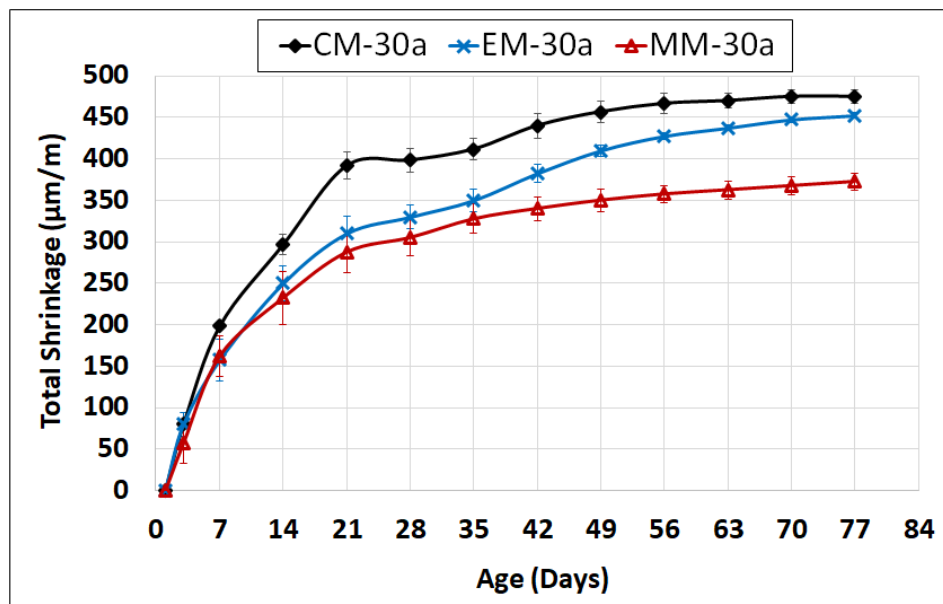


Figure IV.9 Evolution with concrete age of the total shrinkage of the three types of concrete of "Mix 30a", stored in a climatic chamber (23 ± 2 °C and $50 \pm 4\%$ RH)

The reduction of the shrinkage by the total substitution of natural sand has been also confirmed by a study conducted by (Aquino *et al.*, 2010), where the shrinkage of concrete is reduced (15%) when limestone sand totally replaces the mountain siliceous sand in concrete. Similarly, when working with coarse aggregates, (Makani, 2011) has also found that the siliceous aggregates present higher values of total shrinkage than the limestone aggregates. As in our case, these differences are also more significant than those of the autogenous shrinkage. Since the free delayed strains in desiccation conditions are higher, the restraining effect of sand grains, depending on the ITZ bonding and/or the differences in their stiffness, could be more visible.

The MM-30a concrete, with the well-graded crushed limestone sand, exhibits the lowest total shrinkage. The kinetic of the shrinkage evolution is similar to the one of the reference concrete, conserving a nearly constant difference at various concrete ages of around 23%. In addition to the mineralogy and the shape of the crushed sand, the particle size distribution of the well-graded crushed sand could provide a denser ITZ with a better bond with the cement paste. Indeed, the lowest intergranular voids at fresh state, induced by the better gradation, provide higher cement amount available to coat the grains. Thus, the enhancement of the ITZ microstructure probably restrains the cement paste shrinkage in desiccation conditions. However, this enhancement that could be generated in the ITZ is not reflected in the compressive strength of concrete (Table IV.6). It could be compensated by the higher admixture dosage of CM which generally could improve the cement hydration due to a better deflocculation.

Table IV.6 Average values (and standard deviations) of the compressive strength of the three types of concrete of "Mix 30a"

Mix 30a (W/C: 0.5; cement:350 kg/m ³)	CM-30a	EM-30a	MM-30a
Compressive strength, MPa	41.9 (0.82)	43.2 (0.43)	42.4 (0.04)

1.3.3 Drying shrinkage and mass loss

The drying shrinkage corresponds to the part of shrinkage due to the loss of the internal water. Thus, it is mainly governed by the ambient relative humidity. It is related to the water content, its absorption, and its retention into the hardened concrete (Aquino *et al.*, 2010).

The drying shrinkage is usually calculated as the difference between the two independent types of shrinkage, the total shrinkage of the samples subjected to free drying and the autogenous shrinkage of the samples isolated from the ambient moist environment. However, the accidental drying of the sealed samples used for the measurement of the autogenous shrinkage (Figure IV.8) leads to a bias in the calculated values of the drying shrinkage. Therefore, the drying shrinkage could not be presented in this study. However, since the shrinkage and the accidental mass loss measured on sealed samples of the three types of concrete are comparable, the difference in the real autogenous shrinkage is probably negligible.

As already mentioned, the drying shrinkage depends on the hydric gradient between the open pores of concrete and the surrounding environment, hence it is directly related to the concrete porosity structure. Thus, usually, the drying shrinkage is represented as a function of the mass loss of the samples free to dry, to clearly assess the relationship between the drying shrinkage and the reduction of the concrete mass due to the loss of water content of the sample. However, since the values of the drying shrinkage could not be exactly calculated and since the real autogenous shrinkages are estimated to be comparable for the three types of concrete, thus the total shrinkage could be represented as a function of the mass loss, instead of the drying shrinkage, to assess the difference in porosity between the three types of concrete (Figure IV.10).

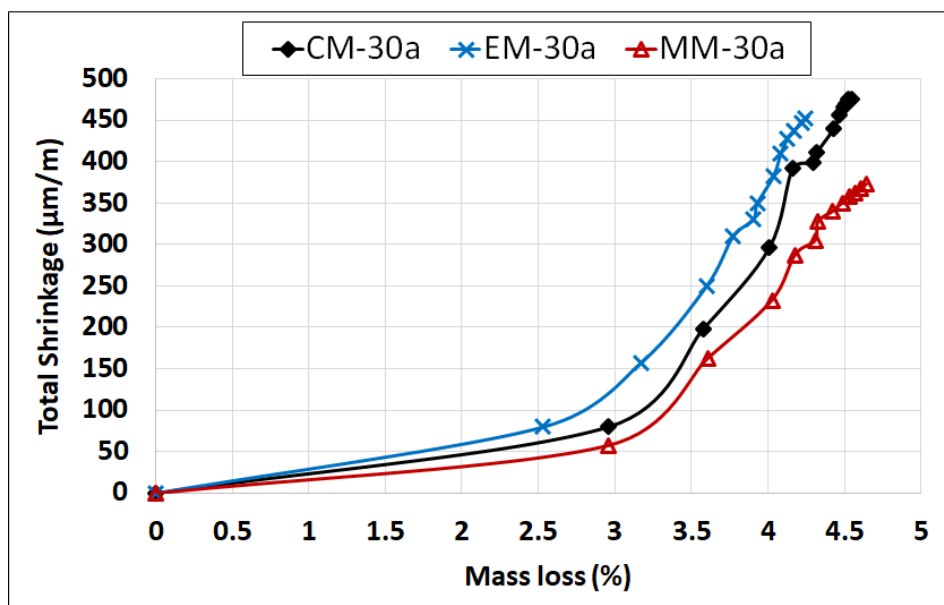


Figure IV.10 Total shrinkage of the three types of concrete of "Mix 30a" as a function of the mass loss of the total shrinkage samples

Usually, this graph could be divided into three phases as detailed in the following.

The first phase of the graph is characterized by a rapid loss of mass with low shrinkage. This observation could be attributed to the evaporation of the free water from open pores or cracks at the surface. These coarse pores are relatively big in size and induce rapid mass loss with lower capillary tensions, thus

lower shrinkage (*Granger, 1995 cited by Makani, 2011*). Figure IV.10 shows that the three types of concrete present superimposed graphs in this first phase, an indication of the presence of pores with similar sizes at the surface of the three types of concrete.

In the second phase, the relation becomes nearly linear because the pores become finer, thus higher drying shrinkage develops in concrete (*Sicard, 1993 cited by Makani, 2011*). In Figure IV.10, the second phase begins with a small difference in the slope between the three types of concrete, and after that, the three curves become parallel revealing a porous structure similar in size. Moreover, this means that the restraining effect of the granular phase on cement paste is rather similar. While all the other parameters of the three types of concrete are identical, the difference due to the variation of sand is low, probably attenuated by the fact that the sand represents only a part of the granular phase.

In the third phase, the loss of mass usually slows down due to the reduction in the moisture gradient with the surrounding. Additionally, a deceleration in the rate of deformations could occur due to the formation of microcracks in concrete around the aggregates, caused by the high capillary tensions. These cracks decelerate the transfer of the capillary tensions into the rest of the sample, reducing thereby its macroscopic shrinkage (*Sellier and Buffo-Lacarrière, 2009 cited by Makani, 2011*). In the case of this study, the third phase is not well demonstrated because of the relatively short period of the test (77 days). The deformation in the three types of concrete continues to evolve following the same trend, indicating a continuous presence of moisture gradient with the surrounding and a probable absence of microcracks at this age.

1.3.4 Summary of the shrinkage

Since the volume of the coarse aggregates is similar for the different types of concrete and the fine aggregates occupy only a part of the granular skeleton, the effect of varying the fine aggregate in each type of concrete tends to be not significantly pronounced.

The three types of normal strength concrete develop approximately the same shrinkage with slightly lower total shrinkage for the normalized crushed sand concretes, maybe due to a restraining effect improved by a better bond with cement paste and/or a higher stiffness of limestone sand compared to siliceous natural sand.

1.4 Durability Properties

The type and quality of sand could be a major factor in determining the long-term performance of concrete (*Huiguang et al., 2011*). As seen in Section 4.2.4 of Chapter I, few studies evaluated the effect of the fine aggregate shape characteristics on the durability properties of concrete. However, by studying the durability properties of the various types of concrete, the effect of fine aggregate has to be estimated. In this study, the assessment of the durability properties is established by comparing the porosity accessible to water, the water absorption percentage, the depth of water penetration under pressure, the resistance to chloride ion penetration, and the resistivity for each type of concrete.

Table IV.7 presents the overall results of the tests conducted according to the standards detailed in the previous chapter, at 90 days for the three types of each normal strength concrete mix and 135 days for "Mix 50".

Table IV.7 Average values (and standard deviations) of the durability properties at 90 days for normal strength concretes and at 135 days for "Mix 50"

Concrete mix		Porosity (%)	Absorption (%)	Water depth (mm)	Passed charge (C)	Resistivity (Ω m)
Mix 30 (W/C: 0.5; cement:350 kg/m ³)	CM-30	16.5 (0.34)	2.6 (0.14)	38 (-)	6729 (170)	41 (1.0)
	EM-30	16.7 (1.09)	3.1 (0.10)	26 (2.1)	7646 (75)	41 (1.4)
	MM-30	16.8 (0.55)	3.1 (0.16)	29 (5.0)	7912 (638)	41 (0.0)
Mix 35-I (W/C: 0.4; cement:350 kg/m ³)	CM-35-I	-	1.7 (0.14)	14 (3.1)	3710 (552)	52 (1.7)
	EM-35-I	-	1.9 (0.08)	17 (0.6)	4636 (220)	50 (1.0)
	MM-35-I	-	1.9 (0.06)	17 (3.2)	4448 (400)	49 (1.2)
Mix 35-II (W/C: 0.4; cement:300 kg/m ³)	CM-35-II	-	1.3 (0.06)	10 (2.0)	3644 (81)	59 (1.5)
	EM-35-II	-	1.6 (0.07)	11 (2.0)	4473 (64)	54 (1.5)
	MM-35-II	-	1.7 (0.07)	10 (2.1)	4048 (17)	55 (0.6)
Mix 50 (W/C: 0.3; cement:400 kg/m ³)	CM-50	-	1.1 (0.05)	11 (2.4)	2387 (169)	87 (2.1)
	MM-50	-	1.2 (0.06)	11 (1.7)	2171 (191)	79 (0.0)

(-): property not measured

1.4.1 Porosity accessible to water

The porosity accessible to water is an important indicator of concrete durability but the assessment of this property is not commonly required in the Lebanese market. In this study, the porosity is determined as per the French recommendations of (AFPC-AFREM, 1998).

At the end of the 28-day compressive strength test, the samples for the porosity test have been collected as detailed in Chapter III and wrapped until the day of the test, 90 days.

The assessment of concrete porosity is done only on the three types of concrete of "Mix 30a", the concrete with the highest water to cement ratio, due to the difficulty to transport massive quantities to LMDC. Table IV.7 indicates that approximately the same porosity is obtained on these concretes (16.5-16.8%). Since these values are around 16%, the three types of concrete could be classified as low durable according to the (AFGC, 2004) guide. Their porosity is in the range of the porosity values (14-16%) for a concrete compressive strength between 25 and 40 MPa (AFGC, 2004).

Despite the difference in the type of fine aggregate in terms of mineralogy, shape, and gradation, and by applying the identical production and curing conditions, the three types of concrete seem to exhibit a similar volume of pores accessible to water. Thus, in the conditions of this study, considering the amount of sand that changes between the three types of concrete, the fine aggregate type could be considered as a non-influent factor on the concrete porosity accessible to water.

1.4.2 Water absorption by immersion

The water absorption by immersion is another important index for durability. The test of water absorption aims to measure the water absorption of concrete after 30 minutes of immersion in water.

At the end of the test, the absorption is calculated as the percentage ratio of the difference between the saturated and initial masses to the initial mass of the specimen, according to (BS 1881-122-Part 122, 1983) standard. The higher this value, the lower the concrete durability. The standard does not specify

a limit value for the water absorption by immersion. Alternatively, according to a study led for durability specifications of the marine structures in the Middle East region, a 30-minute water absorption percentage higher than 2% produces a non-durable concrete in these severe environmental conditions (*Pocock and Corrans, 2007 as cited by Heath, 2016*).

In our study, for each type of concrete, the water absorption after 30 minutes of immersion in water is assessed on three 75x75 mm cylinders cores, cured in water until the date of test: 90 days for all the normal strength concretes and 135 days for "Mix 50".

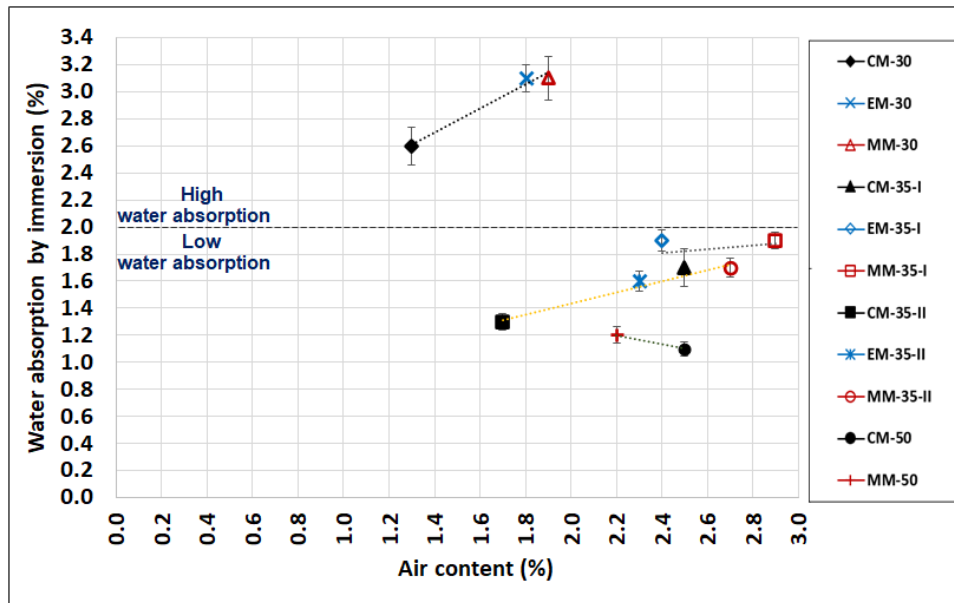
Referring to Table IV.7, the three types of concrete of "Mix 30" could be considered as non-durable concrete, in the previous aforementioned conditions (absorption values: 2.6-3.1% higher than 2%). Since the water absorption values of the three types of concrete of "Mix 35-I", "Mix 35-II", and "Mix 50" do not exceed 2%, they can thus present a durable long-term performance in terms of the water absorption after 30 minutes of immersion. For "Mix 35-I", decreasing the water to cement ratio to 0.4 leads to lower porosity and thus lower water absorption values than the three types of "Mix 30" (absorption values: 1.7-1.9%). On the other hand, for "Mix 35-II", for the same water to cement ratio and lower cement content than "Mix 35-I", the water absorption of concrete decreases to a range between 1.3-1.7%. As expected, the two high-strength concretes of "Mix 50" are characterized by the lowest water absorption by immersion, of around 1%.

Within the same range of durability, Table IV.7 reveals some differences between the three types of concrete of each mix. CM is characterized by the lowest value, while EM and MM present similar water absorption. The highest difference is for EM of "Mix 35-II" (31%) and the lowest for MM of "Mix 50" (9%) while remaining in the same range of durability.

In addition to the effect of the size and volume of the concrete pores, the water absorption by immersion could be related to the air content of the fresh concrete, as shown by the dashed lines of Figure IV.11, for the different types of concrete of each mix.

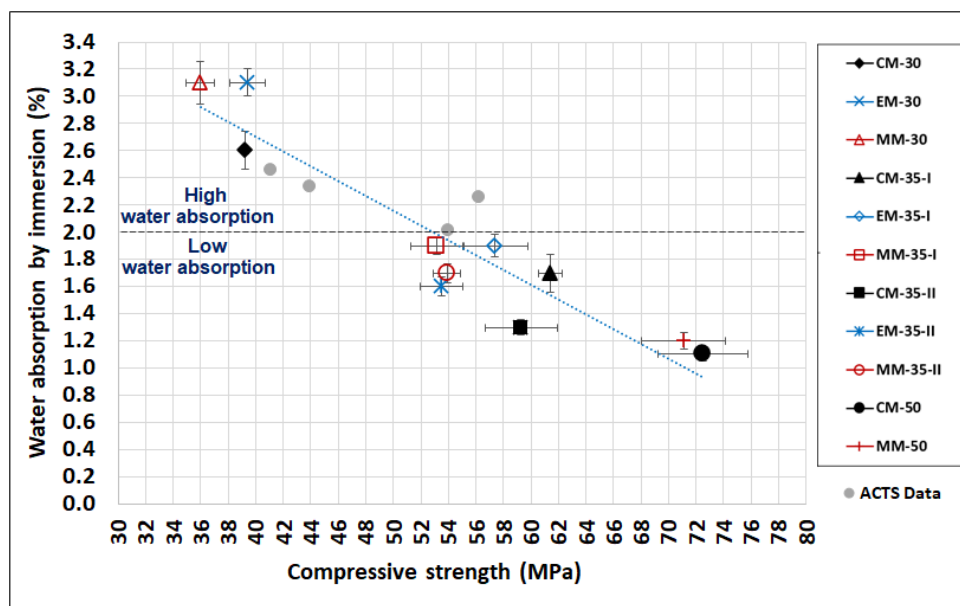
Correspondingly, for "Mix 30" and "Mix 35-II", the lowest 30-minute water absorption is observed for the control mix CM, which presents the lowest air content. For "Mix 35-I" and "Mix 50", the three types of concrete present close air content thus close water absorption. The presence of air bubbles could create open pores in concrete, generating a higher water absorption by immersion (*Gameiro et al., 2014*). However, Figure IV.11 shows that this tendency could not be generally applied at the scale of the different concrete mixes.

Furthermore, Figure IV.12 shows a correlation between water absorption and the compressive strength (same curing for these two tests) at 90 days for the normal strength concretes and 135 days for "Mix 50". Besides, the graph includes some confidential data collected from the Advanced Construction Technology Services ACTS laboratory by internal communication, on samples aged 28 days. The graph shows that the higher the compressive strength of concrete, the lower the water absorption. This figure seems to reveal a linear relationship between these two properties.



* Each dashed line connects the CM, EM, and MM of each normal strength concrete and CM and MM of the high-strength concrete, independently of the other mixes;
 * 2% is the limit given by (Pocock and Corrans, 2007 as cited by Heath, 2016) for the marine structures in the Middle East region.

Figure IV.11 Relation between the average water absorption by immersion and the air content of fresh concrete



* The ACTS values, at 28 days, are confidential data collected by internal communication with the ACTS laboratory, measured following (BS 1881-122-Part 122, 1983);
 * 2% is the limit given by (Pocock and Corrans, 2007 as cited by Heath, 2016) for the marine structures in the Middle East region.

Figure IV.12 Relation between the average water absorption and the average compressive strength at 90 days for normal strength concretes and 135 days for "Mix 50", completed by confidential data from ACTS

1.4.3 Water penetrability under pressure

The importance of this durability value lies in the assessment of the resistance of concrete against the penetration of water under pressure. It gives an accurate indication of the concrete permeability and it is determined by measuring the depth of water penetration under hydrostatic pressure following (*BS EN 12390-8, 2009*) standard. A high depth in this test is associated with low concrete durability.

Similar to the water absorption test, the standard does not specify a limit for the depth of water penetration under pressure. Nevertheless, to be considered as durable concrete, this depth should not exceed 10 mm, according to the study conducted for durability specifications of the marine structures in the Middle East region (*Pocock and Corrans, 2007 as cited by Heath, 2016*).

For this test, the specimens used are 150x150 mm sawed at the middle of 150x300 mm cylinders that have been water cured until the day of the test: 135 days for "Mix 50" and 90 days for all the other mixes. As detailed in Chapter III, at the end of the test, each specimen is split in half and the maximum water penetration depth is measured (Figure IV.13a).

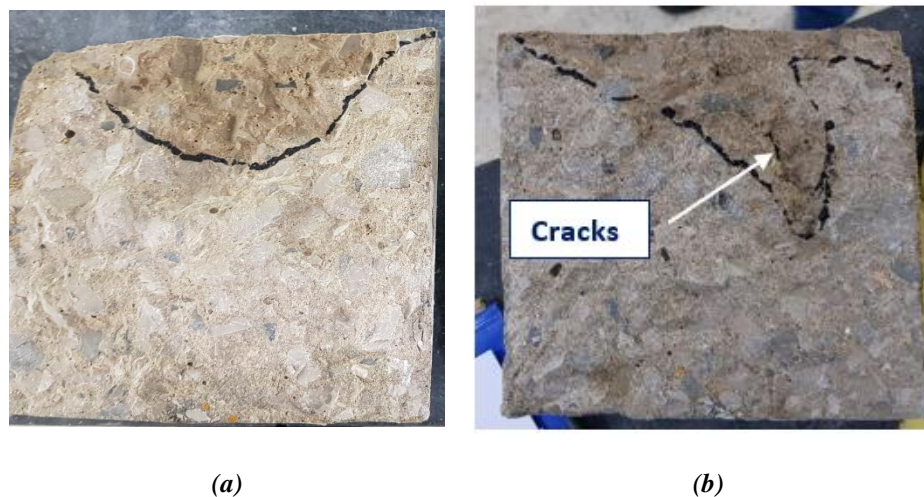


Figure IV.13 An example of the specimens used for the test of water depth under pressure for (a) an uncracked specimen and (b) a cracked specimen

For "Mix 35-II" and "Mix 50", the water penetrability values (10-11 mm) of Table IV.7 are very close to the limit (10 mm) suggested by (*Pocock and Corrans, 2007 as cited by Heath, 2016*), whereas, for the other two mixes, the depth values exceed 10 mm (26-38 mm and 14-17 mm for "Mix 30" and "Mix 35-I" respectively). Accordingly, the three types of concrete of "Mix 30" and "Mix 35-I" are characterized by high permeability to water, while the depths of water penetrability of the different types of concrete of "Mix 35-II" and "Mix 50" are acceptable. Comparing the concrete mixes, the water depth decreases when reducing the water to cement ratio. For the same water to cement ratio of 0.4, its value also reduces with lower cement content.

By comparing the three types of concrete of "Mix 30" (Table IV.7), CM presents the highest depth of water penetrability. The result of CM presented in this table is the result of one specimen and not the average of three because the two other CM samples have been cracked and developed a high permeability. Figure IV.13b illustrates an example of the cracked specimens with a high depth of penetrated water. These undesired cracks could, unfortunately, be the result of an artifact during the sample preparation. However, the three specimens of EM and MM do not display any visible cracks and they present relatively similar penetration depths of 26 and 29 mm respectively. Consequently, the

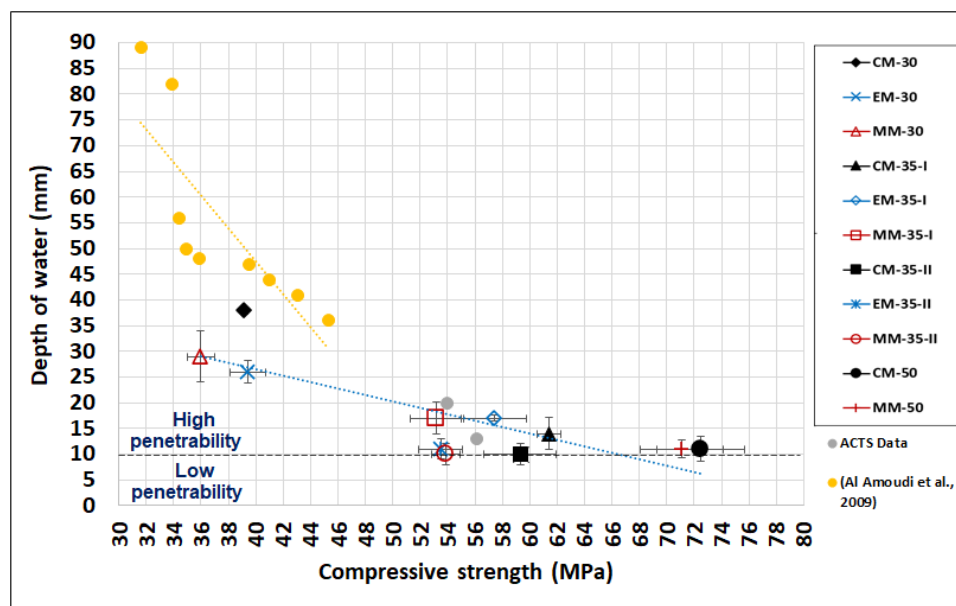
observation of cracks in the CM samples of "Mix 30" limits the possibility of drawing a global conclusion for the three types of concrete of this mix.

For "Mix 35-I", no visible cracks have been detected for the three types of concrete. EM and MM present the same depth of water penetrated under pressure (17 mm), while CM is characterized by the lowest value (14 mm). Then, the reference concrete, incorporating the natural and the conventional crushed sand, presents a slightly better pore structure than the two crushed sand concretes of "Mix 35-I".

The three types of concrete of "Mix 35-II" are characterized by similar low permeability (10-11 mm). These results indicate that the three types of concrete of this mix exhibit the same pore structure.

Similarly, for "Mix 50", the same value of water absorption by immersion (11 mm) is measured on CM and MM.

Figure IV.14 presents the correlation between the depth of water penetration under pressure and the compressive strength of concrete, at 90 days for the normal strength concretes and 135 days for "Mix 50". This figure demonstrates that, similar to the trend observed for the water absorption by immersion, when the compressive strength increases, the depth of water under pressure decreases. The confidential data collected from the ACTS laboratory by internal communication, on samples aged 28 days, show the same trend with values close to the one obtained by our study. However, the same tendency is also observed in the study of (Al-Amoudi et al., 2009) but with significant differences in the values, despite the application of similar test procedures.



* The ACTS values, at 28 days, are confidential data collected by internal communication with the ACTS laboratory, measured following (BS EN 12390-8, 2009);

* (Al-Amoudi et al., 2009) values, at 28 days, are determined by DIN 1048 standard which is similar to the (BS EN 12390-8, 2009) standard;

* 10mm is the limit given by (Pocock and Corrans, 2007 as cited by Heath, 2016) for the marine structures in the Middle East region.

Figure IV.14 Relation between the average water depth and the average compressive strength at 90 days for normal strength concretes and 135 days for "Mix 50", completed by confidential data from ACTS and (Al-Amoudi et al., 2009)

1.4.4 Resistance to chloride ion penetration

As already detailed in Chapter III, it is primordial to assess the resistance of concrete to the chloride ion penetration since, when they penetrate the concrete, these ions reach the protective alkaline film around the reinforcement rebars and reduce the durability of reinforced concrete. The resistance to chloride ions is estimated from the electrical conductance of concrete specimens when they are connected to an electrical cell for 6 hours, following (*ASTM C1202, 2017*) standard.

The higher the value of the charge passed in the resistance to chloride ions penetration RCP test, the higher the ions penetrability, thus the lower the resistance of concrete to the chloride ion penetration and the lower the durability. According to (*ASTM C1202, 2017*) standard, when the passed charge in the RCP test exceeds 4000 C, the concrete exhibits high penetrability to the chloride ions, while concrete with a charge between 2000 and 4000 C is supposed to have moderate penetrability (Table IV.8).

This test is conducted in 100x50 mm saturated concrete specimens, sawed from 100x200 mm cylinders that have been water cured until the age of the test, 90 days for the normal strength concretes and 135 days for "Mix 50".

Table IV.8 Correlation between chloride ions penetrability and the passing charge (ASTM C1202, 2017)

Charge passed (Coulombs)	Chloride ions penetrability	Range of the studied concrete mixes
> 4000	High	CM-30 (6729), EM-30 (7646), MM-30 (7912) EM-35-I (4636), MM-35-I (4448) EM-35-II (4473), MM-35-II (4048)
2000 - 4000	Moderate	CM-35-I (3710) CM-35-II (3644) CM-50 (2387), MM-50 (2171)
1000 - 2000	Low	-
100 - 1000	Very low	-
< 100	Negligible	-

As their charge is higher than 4000 C, the three types of concrete of "Mix 30" are considered as highly penetrable concretes for chloride ions (Table IV.7 and Table IV.8). For "Mix 35-I" and "Mix 35-II", the penetrability of chloride ions in EM and MM (4048-4636 C) are slightly above the threshold of the high limit (4000 C), while CM presents a moderate penetrability but with a value close to 4000 C. For "Mix 50", Table IV.7 and Table IV.8 inform that the penetrability to chloride ion of both types of concrete (2387 and 2171 C for CM-50 and MM-50 respectively) could be considered as moderate since both results deviate around 2000 C, the margin that separates the low and moderate penetrability levels.

These comparisons prove that, for each concrete mix, the different types of concrete are approximately within the same range of durability in terms of the resistance to chloride ions penetrability. Additionally, it could be noticed that the chloride penetrability decreases with the reduction of the water to cement ratio. In a previous study, (*Al-Amoudi et al., 2009*) have compared the passed charge for different cement content and water to cement ratio while using crushed limestone coarse aggregates and dune sand. The results show that, for water to cement ratio of 0.5 and cement content of 350 kg/m³, the 28-day passed charge is 5614 C. For the same cement content, this value decreases to 3639 C when the water to cement ratio is decreased to 0.4. Furthermore, for the same water to cement ratio, by comparing the results of Mix 35-I and Mix 35-II, the values of the chloride ion penetrability are lower when reducing the cement content from 350 to 300 kg/m³.

By carrying a global review on the standard deviations of Table IV.7, they seem high in some types of concrete. Nevertheless, the coefficient of variation for these values is relatively low. These variations are then considered acceptable since they do not exceed the precisions (12%) specified in (*ASTM C1202, 2017*), except for the coefficient of variation of CM-35-I (15%).

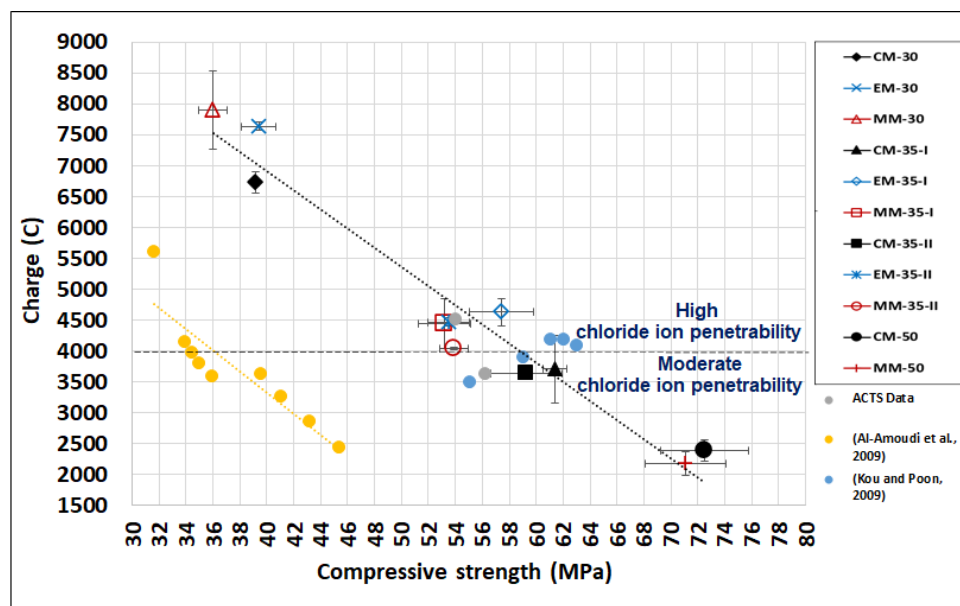
Even though the different types of concrete of each normal strength concrete mix lie approximately within the same range of durability, Table IV.7 and Table IV.8 reveal differences between the control mix and the other two types of concrete. The passing charge in the RCP test for EM and MM is 14-18%, 20-25%, and 11-23% higher than the CM values, for "Mix 30", "Mix 35-I", and "Mix 35-II" respectively. This difference in the amount of the charge conducted throughout the RCP test could be related to lower pore spaces and pore connectivity in the reference concrete compared to EM and MM. The higher dosage of admixture in the reference concrete could be the reason behind the presence of a lower porous microstructure in the control mix. The admixture deflocculates more the cement grains, reducing thus the air content in concrete and increasing the ions dissolved in the solution, before their precipitation as hydrates, which could block the diffusion of chloride ions and increase the resistance of concrete to the penetration of these ions.

Moreover, (*Titi and Tabatabai, 2018*) have shown a strong dependence of the resistance to chloride ion penetration on the coarse aggregates absorption, the lowest the aggregates absorption, the lowest the passed charge. Since the sand absorption and the water content at the surface of the sand grains could influence the type of hydrates and the local porosity at the interfacial transition zone between the sand grains and the cement paste, this observation could be also applied to the absorption of the fine aggregates used in this study. The control mix incorporates natural sand with lower water absorption than the crushed sand (1.1% and 2.6% respectively for natural sand and crushed sand), thus this difference could induce a difference in the pores network, thus lower permeability for the control mix.

For the three studied normal strength concretes, the two crushed sand concretes, EM and MM, that differ only by the crushed sand gradation, present close passed charges values. The resistance to chloride ions penetration seems not affected by the fine aggregate gradation. Likewise, (*Shen et al., 2018*) have examined the effect of the manufactured sand gradation on the concrete permeability and they notice little difference (7%) in the passed charge when the particle size distribution of the manufactured sand is optimized.

The two types of concrete of "Mix 50" develop close values of the passed charge (2387 and 2171 C for CM-50 and MM-50 respectively). Thus, the resistance to chloride ion penetrability seems not modified by the type of fine aggregates in the high-strength concrete, which is characterized by the lowest natural sand content among the other mixes.

Figure IV.15 correlates the average passed charge to the average compressive strength, determined on the same day of the durability tests and for the same curing conditions, 28 days for the data collected from ACTS and the study of (*Al-Amoudi et al., 2009*), 90 days for the normal strength concretes of our study and the data of (*Kou and Poon, 2009*), and 135 days for the high-strength concretes of our study. Globally, a linearly decreasing trend between the passed charge and the compressive strength is observed in the area of the study. The reduction of the charge passed in the RCP test is an indication of enhanced pore structure that increases the compressive strength of concrete. The data collected from the ACTS laboratory and those of (*Kou and Poon, 2009*) follow approximately the same regression line as the results of our study. However, the data of (*Al-Amoudi et al., 2009*) are situated far from the others, although they follow the same trend.



* The ACTS values, at 28 days, are confidential data collected by internal communication with the ACTS laboratory, determined following (ASTM C1202, 2017);

* (Al-Amoudi et al., 2009) and (Kou and Poon, 2009) values are determined following (ASTM C1202, 2017) at 28 and 90 days respectively;

* 4000 C is the limit given by (ASTM C1202, 2017).

Figure IV.15 Relation between the average passed charge and the average compressive strength at 90 days for normal strength concretes and 135 days for "Mix 50", completed by confidential data from ACTS and (Al-Amoudi et al., 2009; Kou and Poon, 2009)

1.4.5 Resistivity

Since the current is carried out by the ions dissolved in concrete pores, the resistivity could be related to the volume and size of pores. The resistivity measurement could indicate the risk of chloride penetration and the risk of corrosion of reinforced concrete with a rapid and non-destructive test. Within a particular structure, the higher the resistivity, the lower the probability that the concrete undergoes high penetration to chloride ions and severe corrosion (ACI, 2001).

As already mentioned in Chapter III, to conduct a precise and reliable comparison between the resistivities of the different concretes, the same geometry (cylinders of 150x300 mm) and preparation of the specimens have been adopted. Also, since the resistivity of concrete depends on the moisture condition of the specimens, all the concrete samples have been in the saturated-surface dried condition during the resistivity measurements.

(Shane et al., 1999 as cited by the manual of the resistivity measuring machine Giatec-RCON) have associated the values of the saturated bulk resistivity at 28 days and those of the charge passed at 56 days, of the same concrete, to characterize its ability to resist the chloride ions penetration. This correlation is presented in Table IV.9.

Table IV.9 Correlation between concrete resistivity and chloride ions penetration (Shane et al., 1999)

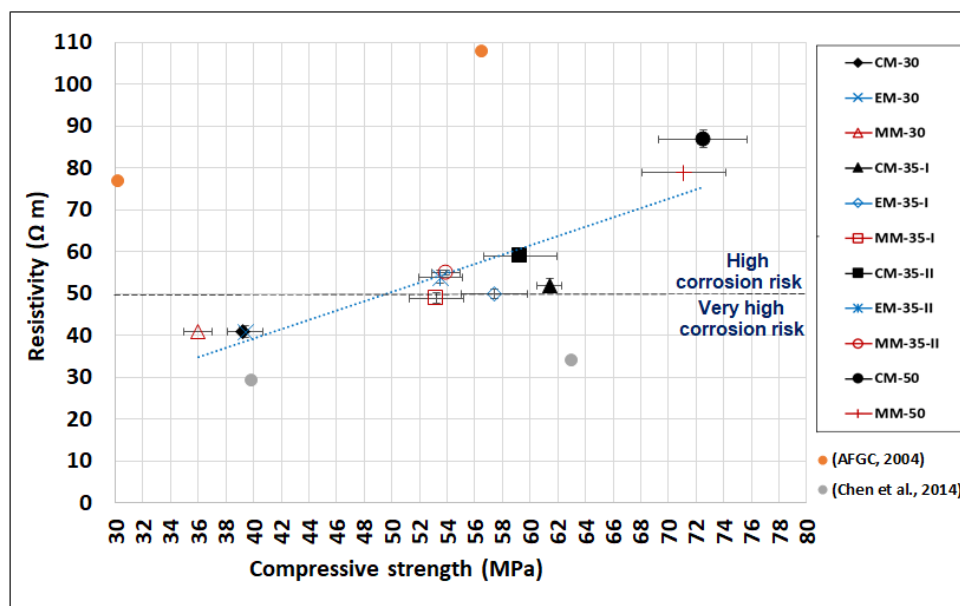
28-day bulk resistivity of saturated concrete (Ω m)	56-day charge passed as per ASTM C1202 (C)	Chloride penetration	Range of the studied concrete mixes at 90/135 days*
> 2000	< 100	Negligible	-
200 - 2000	100 - 1000	Very low	-
100 - 200	1000 - 2000	Low	-
50 - 100	2000 - 4000	Moderate	CM-35-I (52), CM-35-II (59), EM-35-II (54), MM-35-II (55), CM-50 (87), MM-50 (79)
< 50	> 4000	High	CM-30 (41), EM-30 (41), MM-30 (41), EM-35-I (50), MM-35-I (49)

*The tests are conducted at 90 days for "Mix 30", "Mix 35-I", and "Mix 35-II", and at 135 days for "Mix 50"

By applying these notions to the results of our study, but for 90/135-day age specimens, this interrelation is confirmed. Referring to Table IV.7 and Table IV.9, the three types of concrete of "Mix 30" present a resistivity lower than 50 Ω m, hence they are characterized by a high risk of chloride penetration (> 4000 C) (Table IV.9). The results are confirmed by (Polder, 2001) who states that a low resistivity of 50 Ω m is associated with concrete of quite high water to cement ratio. On the other hand, the reduction of the water to cement ratio in "Mix 35-I" and "Mix 35-II" increases the resistivity and slightly reduces the penetration to chloride ions from high to moderate (resistivity values in the range of 50 Ω m and charge in the range of 4000 C). For these mixes, "Mix 35-I" and "Mix 35-II", with the same water to cement ratio, the reduction of cement content leads to a slight increase of the resistivity. As for "Mix 50", the two types of concrete present the highest resistivity with the lowest passed charge. They are considered moderately susceptible to penetration to chloride ions since their resistivity values range between 50 and 100 Ω m (87 and 79 for CM-50 and MM-50 respectively).

From Table IV.7 and Table IV.9, the same value of resistivity (41 Ω m) is measured on the three types of concrete of "Mix 30". For the other two mixes, "Mix 35-I" and "Mix 35-II", the values are also very close whatever the type of concrete of each mix, and the differences could be considered negligible. The resistivity of the reference concrete is slightly higher than the resistivity of the crushed sand concretes. The difference does not exceed 6% and 8% for "Mix 35-I" and "Mix 35-II" respectively. For "Mix 50", the resistivity of CM is also slightly higher (9%) than that of MM.

Furthermore, Figure IV.16 shows that the resistivity and the compressive strength are correlated for all the studied concretes. The resistivity increases with the compressive strength value, measured at the same age, on water cured samples. The high resistivity is an indication of a dense microstructure and low porosity, thus a high compressive strength. These results are in correlation with those of (Chen et al., 2014) and (AFGC, 2004) guide for the surface and bulk resistivity respectively. Figure IV.16 also demonstrates that the results of the current study are lower than those of concrete with comparable compressive strengths (resistivity between 100 and 250 Ω m for a compressive strength between 30 and 60 MPa in (AFGC, 2004) guide).



* (Chen et al., 2014) and (AFGC, 2004) values are determined at 28 and 90 days respectively;
 * 50 Ω m is the limit given by (Shane et al., 1999 as cited by the manual of the resistivity measuring machine Gatec-RCON).

Figure IV.16 Relation between the average resistivity and the average compressive strength at 90 days for normal strength concretes and 135 days for "Mix 50", completed by data from (Chen et al., 2014) and (AFGC, 2004) guide

1.4.6 Overall durability performance

The results of all the durability properties and the long-term compressive strengths are represented, in Figure IV.17, relative to the control mix values, to set an effective and clearer comparison between the crushed sand concretes and the reference concrete of each mix.

For the long-term compressive strength and the resistivity, the normalized values (ratio of EM or MM values to the value of CM) are directly presented in Figure IV.17. A represented value higher than one means that the crushed sand concretes exhibit higher compressive strength or higher resistivity than the reference concrete, thus better durability.

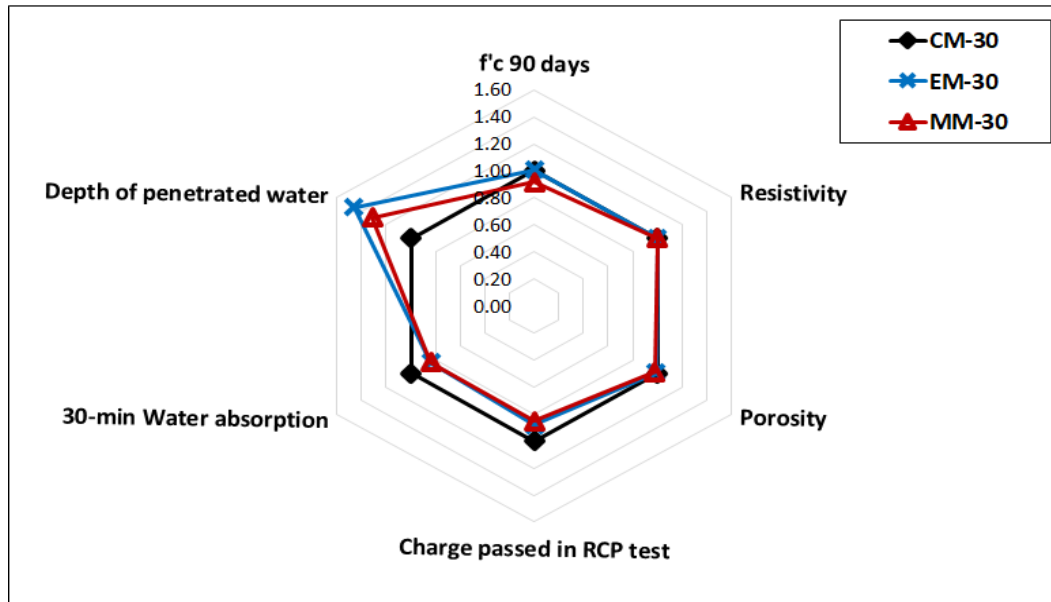
For the porosity accessible to water, the passing charge in the RCP test, the water absorption percentage, and the depth of water penetrability, the reciprocal normalized values are displayed in Figure IV.17 (ratio of the CM value to the value of EM or MM). When the represented values are higher than one, the crushed sand concretes yield lower results, thus they display better durability properties compared to the reference concrete.

The crushed sand concretes of the three normal strength concrete mixes are characterized by lower durability than the reference concrete. Figure IV.17a to Figure IV.17c show that the represented values are slightly lower than 1 for all the durability properties, except for the depth of water under pressure in "Mix 30" (Figure IV.17a). The slightly better durable behavior of the reference concrete could be attributed to the higher dosage of admixture in this type of concrete. The cement grains are more deflocculated; thus, the amount of pores is reduced and the durability is increased.

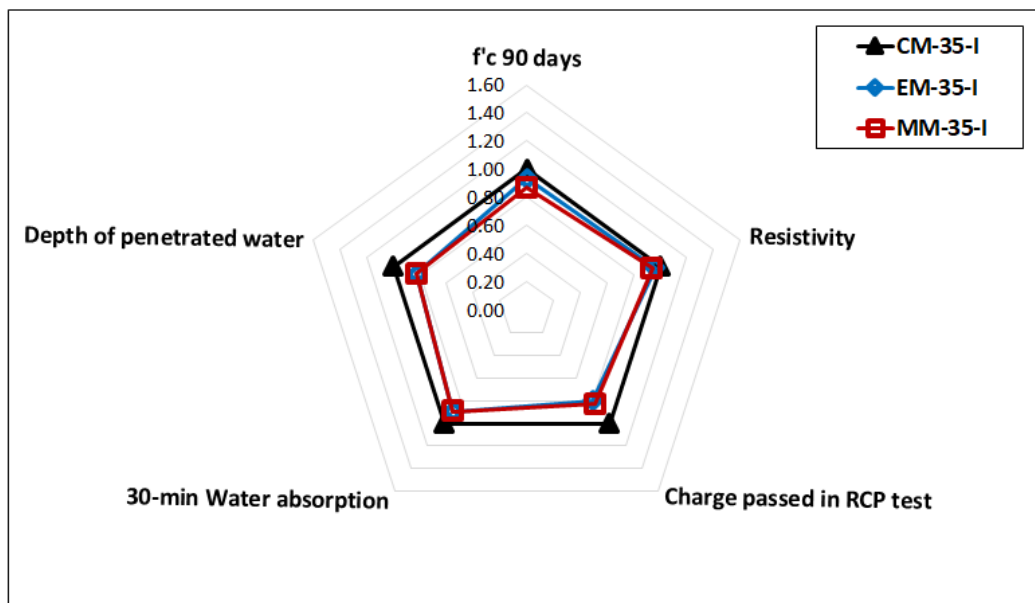
Figure IV.17a to Figure IV.17c demonstrate that the crushed sand concretes express similar behavior reflected by superimposed points in these figures. EM and MM do not contain natural sand but only

crushed limestone sand with different particle size distribution within the standard grading limits. This comparison reveals that the variation of the sand gradation, within the standard grading requirements, does not affect the durability properties of 90 days old concrete.

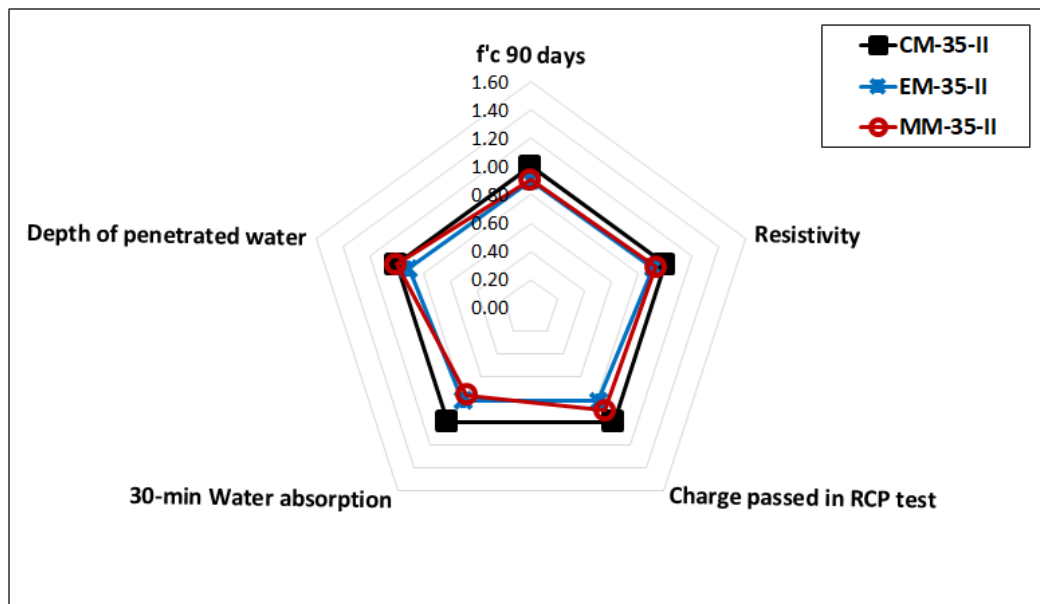
Figure IV.17d clearly shows the similarity in the long-term performance, at 135 days, of the high-strength conventional concrete CM-50 and the high-strength crushed sand concrete MM-50.



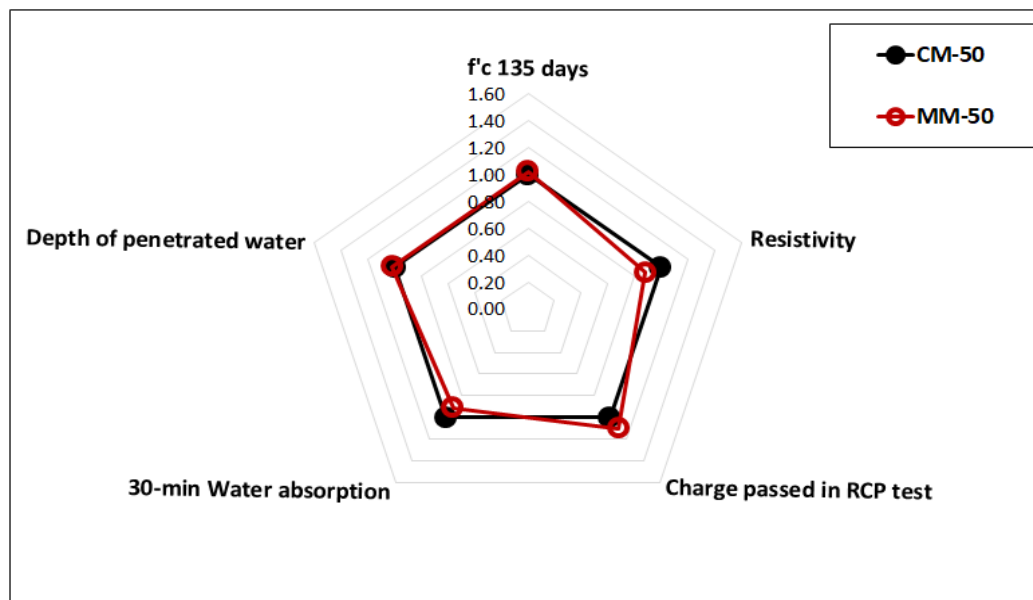
(a)



(b)



(c)



(d)

Figure IV.17 Durability properties for (a) "Mix 30", (b) "Mix 35-I", (c) "Mix 35-II", and (d) "Mix 50"

1.4.7 Summary of the durability properties

Generally, for each normal strength concrete mix, the different types of concrete are in the same range of durability with slightly better performance for the reference concrete. Thus, these mixes seem to exhibit a close permeability and pores structure.

Additionally, the fine aggregate and its intrinsic properties (mineralogy, morphology, and gradation) do not seem to have a significant impact on the durability of the high-strength concrete characterized by a lower natural sand content compared to the normal strength mixes. The differences between the

durability properties of the two types of concretes are slight and lower than those of the normal strength concrete.

Furthermore, for the 11 studied concretes, in a range of 28-day compressive strength between 30 and 60 MPa, a linear correlation exists between the compressive strength and the assessed durability properties. The higher compressive strength leads to concrete with higher durability.

1.5 Microstructural analysis and correlation with the concrete performance

As already introduced in Section 4.2.5 of Chapter I, the interfacial transition zone ITZ is known as the weakest zone in concrete and its quality could affect the mechanical and durability properties of concrete. Since this effect could be more pronounced for coarse aggregates than for fine aggregates, few studies have been interested in the effect of fine aggregates on the ITZ quality. Nevertheless, it is primordial to assess the influence of fine aggregate type on the quality of the cement-sand interface and consequently on the mechanical and durability behavior of the different types of studied concrete.

In this study, the microstructural analysis is carried out on concrete fractions arbitrarily recuperated from fractured cones after the 28-day compressive strength test, for the three types of concrete of "Mix 30a" (Chapter III). Before conducting the compressive strength test, the samples have been water cured. Then, the fractured samples have been wrapped until the day of the microstructural analysis. SEM/EDX analysis is applied to detect any possible difference in shape and mineralogy of the hydrates that could be present in the ITZ of the siliceous natural sand and limestone crushed sand. Since this study mainly concerns the morphology and the mineralogy at the interface, the analysis is not influenced by the microcracks which could be generated during the compressive strength test or due to the preparation of specimens under vacuum, for the SEM observation.

To obtain detailed information on the topography of the ITZ, the secondary electron images SEI are captured. During this comparative investigation, an important number of images are collected and analyzed. For each type of concrete, Figure IV.18 shows one of these representative images at the cement-sand grains interface.

Generally, the comparative observations conducted between the reference concrete incorporating natural sand and the crushed sand concretes indicate that the total substitution of natural siliceous sand by crushed limestone sand could be beneficial for the ITZ quality. By observing the siliceous grains of natural sand in the reference concrete CM of Figure IV.18a, we can notice that the surface of these grains seems smooth, not etched, and barely covered by cement paste. However, in EM and MM, the limestone sand grains are covered by cement paste and there is a clear continuity of the cementitious matrix on the rough surface of these crushed sand grains (Figure IV.18b and Figure IV.18c).

From these images, a smooth layer of portlandite that surrounded the natural siliceous sand grains is also detected. On the other hand, in the crushed sand concretes, the portlandite is oriented by epitaxial growth towards the crushed rough sand grains creating a better interlocking between the cement paste and the sand particles. In addition to the mechanical interlocking, the bond between the cement and aggregates could be the result of the chemical reaction provided by the calcite ions at the interface (*Javelas et al., 1975; Struble and Skalny, 1980*). As seen in Section 4.2.5 of Chapter I, the calcium carbonate from the limestone aggregate's surface could dissolve and then react with the surrounding cement paste and its hydration products to form carbo-aluminates (*Grandet and Ollivier, 1980; Ollivier et al., 1995*). This reaction densifies the cement paste around the aggregates and reduces its local

porosity. It could also enhance the cohesiveness and the bond between the paste and the aggregates due to the increase in the roughness of the aggregate surface after the attack of calcite by the liquid phase. However, there is no such chemical and mineralogical compatibility to enhance the bond between the cement paste and the siliceous aggregate (*Bachiorrini and Murat, 1987; Bederina et al., 2013*).

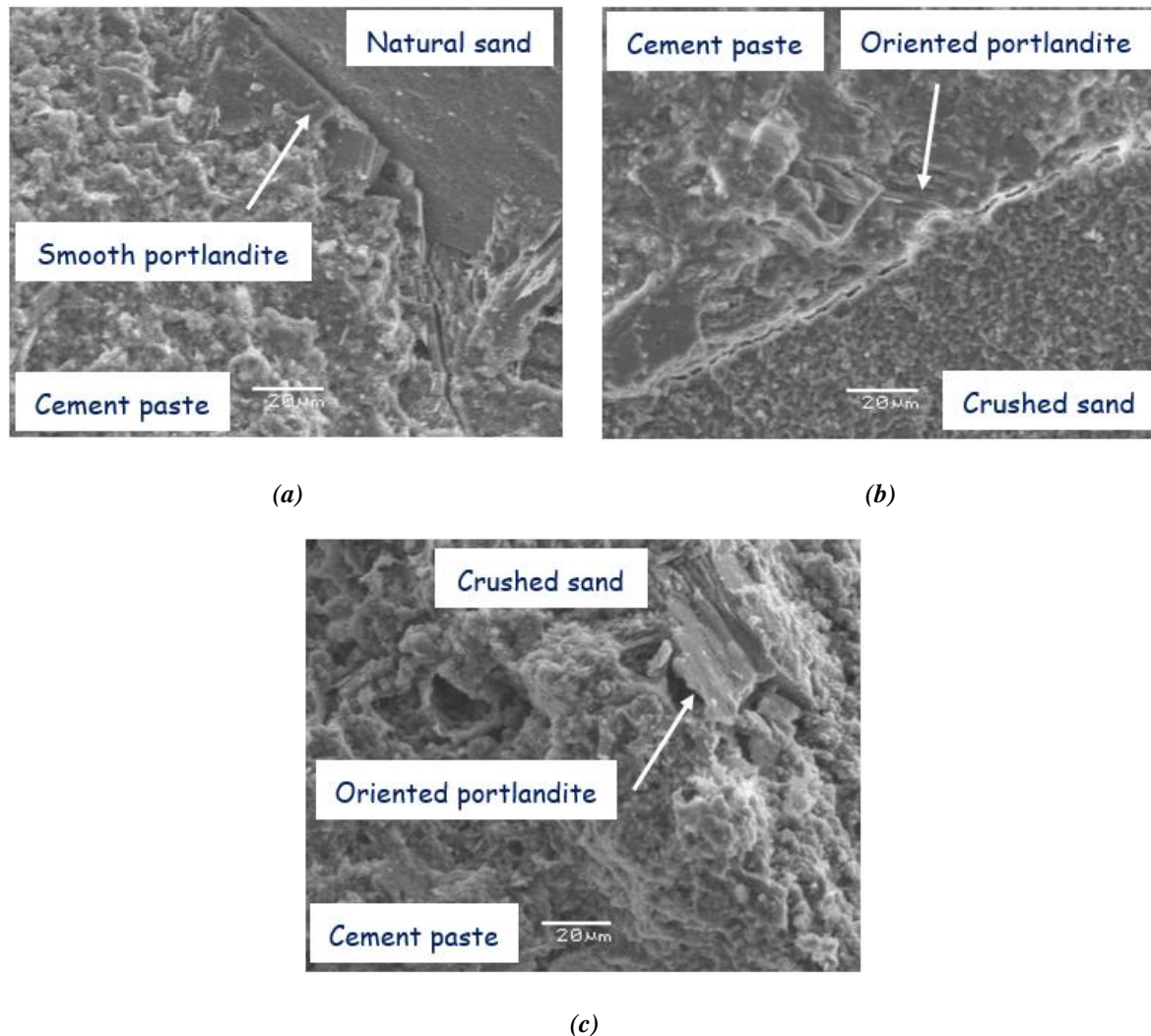
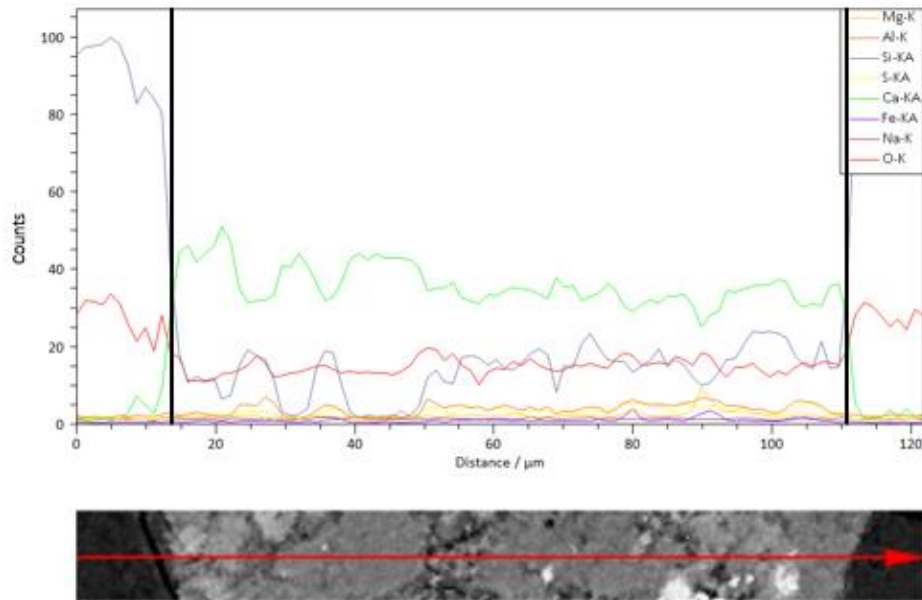


Figure IV.18 SEI images (x800) for (a) CM, (b) EM, and (c) MM of "Mix 30a"

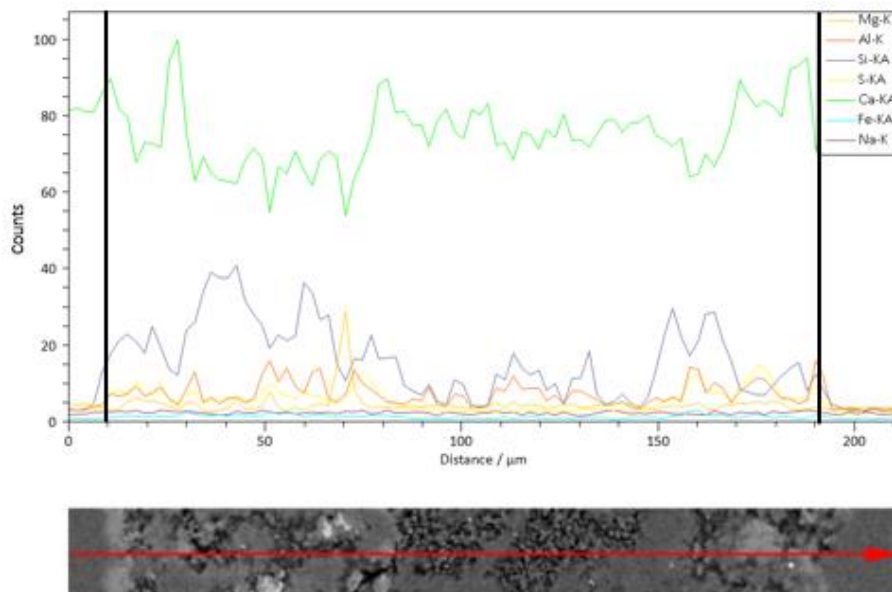
To evaluate the effect of the fine aggregates on the chemical reaction in the ITZ, the EDX technique is employed to obtain the elements map of the concrete samples. To obtain a plane surface, the samples have been polished and the backscattered electron images have been captured. This technique is applied to the three types of concrete.

An example of the elemental distribution of the reference concrete CM and the crushed sand concrete MM is illustrated in Figure IV.19. Since the elemental distribution in the crushed sand concretes, EM and MM, is nearly the same, only the ITZ of the crushed sand grain of MM is chosen to be compared to that of CM (Figure IV.19). This analysis covers the distance between two siliceous natural sand in CM (Figure IV.19a), while Figure IV.19b shows the distribution of the elements between two limestone crushed sand grains in MM. Accordingly, the figures are presented in two different scales. The curves correspond to a space between the measuring points of 1.2 and 2.1 μm for Figure IV.19a and Figure IV.19b respectively (analysis done on 100 points). The elements assessed include magnesium Mg, aluminum Al, silicon Si, sulfur S, calcium Ca, iron Fe, sodium Na, and oxygen O.

The analysis of the graphs of both types of concrete detects a higher calcium silicate ratio at the vicinity of crushed sand grains compared to the siliceous ones. This observation is an indication of the reactivity of the limestone sand with the cement paste and the formation of calcium aluminate hydrates. It could also be related to the higher percentage of limestone fines (5%) in the crushed sand concrete MM, while in the control mix CM the fines content is formed of approximately 1.2% of natural sand fines and 3.6% of crushed limestone sand fines.



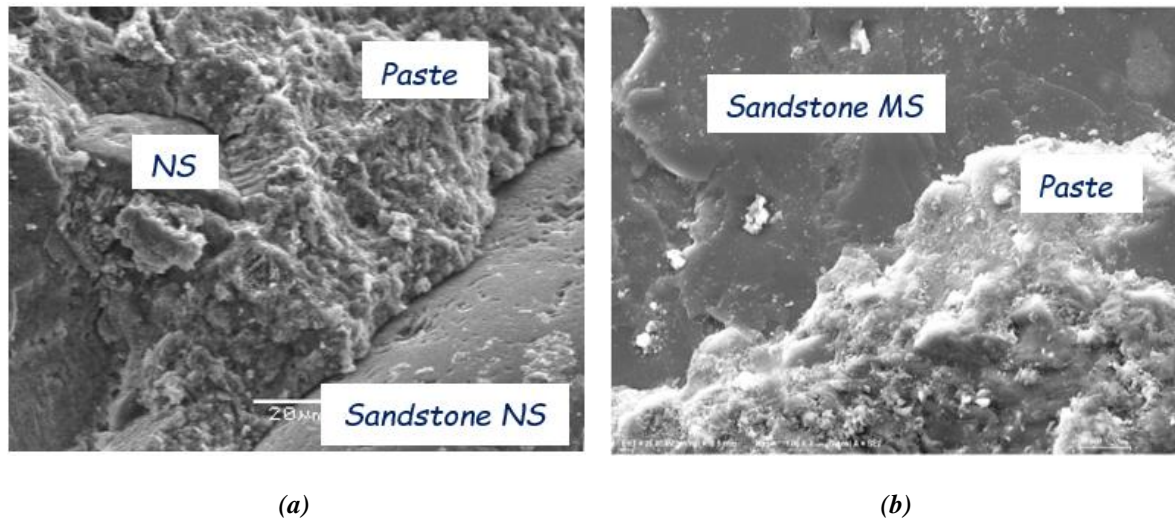
(a)



(b)

Figure IV.19 Graph of the elemental distribution (a) between two natural siliceous sand grains in CM and (b) two crushed limestone sand grains in MM

Similarly, (Shen *et al.*, 2017) have observed an SEM image of the interface between the cement paste and the sandstone grain, comparable to those of our study (Figure IV.20). There seems no adherence to the hydration products on the surface of the sandstone sand grains.



*NS: Natural sandstone; *MS: Manufactured sandstone

Figure IV.20 Interfacial transition zone between the sandstone and cement paste as observed by SEM (a) in our study and (b) by (Shen et al., 2017)

Likewise, the microstructural studies led on coarse aggregates show that the limestone coarse aggregate contributes to a better anchorage between the cement paste and the aggregate compared to the siliceous aggregate with a smooth surface (Ribeiro et al., 2011; Bentz et al., 2015). (Monteiro et al., 1985) also detect an epitaxial growth of some hydration products on the limestone coarse aggregates surface that is not detected in the ITZ of quartzite aggregate.

As already mentioned, the mechanical and durability properties of concrete do not only depend on the nature of the cement paste and the mechanical resistance and porosity of aggregates. They also depend on the reactivity characteristic of the aggregate and the quality of the concrete microstructure (Bachiorrini and Murat, 1987; Bederina et al., 2013). However, the differences in the ITZ status of the three types of concrete compared in our study do not induce strong differences in the mechanical and durability behavior at the macroscale of concrete.

The improvement in the microstructure of the limestone crushed sand concretes does not enhance the concrete compressive strengths, since the three types of concrete present comparable values with a negligible difference. However, it leads to lower shrinkage and higher flexural strength for EM and MM compared to those of the reference concrete that incorporates natural siliceous sand. A similar correlation has been established by (Akçaoğlu et al., 2005) who conclude that the ITZ quality influences the tensile strength while it does not affect the compressive strength of concrete. This result tends to prove that the bond resistance of ITZ could influence the macroscale behavior of concrete if the mesoscopic stress state, due to mechanical test or restrained deformation, leads to tensile stress higher than the bond resistance. Regarding the long-term performance of concrete, the crushed sand concretes and the reference concrete present durability properties within the same range, with slightly better behavior for the latter.

Besides, the effect of differential deformation between the cement paste and the sand, as in the case of the paste shrinkage, is probably masked by the continuous water curing conditioning of the concrete specimens before conducting the compressive strength test. Subsequently, in further microstructural analysis, the effect of the type of fine aggregate on the ITZ state and thus on the mechanical and durability behaviors of concrete should be evaluated in more severe drying conditions.

2. Feasibility study for using the normalized crushed sand as the only fine aggregate

Using a fine aggregate that gives good concrete performance is not the only concern in the construction industry. The technical feasibility of the production process and the environmental and economic impacts are essential elements to choose the sand in concrete.

Accordingly, to be an effective alternative to natural sand, the production of the normalized crushed sand should also be environmentally and economically acceptable. Otherwise, our study will remain a theoretical scientific proposal without useful practicability.

In the present section, a succinct overview is delivered to analyze, on one hand, the technical feasibility of the production of the normalized crushed sand, and on the other hand, its environmental and economic benefits and restrictions. The advantages and disadvantages of the normalized crushed sand from the environmental and economic points of view are detailed in the following sections and summarized in Table IV.10.

In addition to a literature review on these matters, the feasibility study has been prepared after site visits to concrete plants and quarries, to discuss their concerns on these issues since they are directly involved parties. It should be noted that the prices are presented in \$ per bulk volume and this study has been conducted in June-July 2020, thus the below-mentioned prices could have been subjected to some variations after this period.

2.1 Technical overview

During the production of crushed sand, an important interest is given to its quality. The crushed sand should not be elongated and flaky and its percentage of fines should not exceed the standardized limit (7%). Thereby, the generation of well-shaped particles with a high reduction ratio is desired. However, the more the produced well-shaped particles, the more the generated fines (*Bengtsson and Evertsson, 2006*). Thus, the intent to limit the content of fines during the crushing process could reduce the quality of the produced crushed sand by negatively affecting its shape.

Therefore, to avoid the worsening of the shape of sand particles, the quarries usually produce crushed sand with a high percentage of fines, followed by a classification process to reduce the percentage of generated fines.

Technically, to be able to produce, in the future, the normalized crushed sand which conforms to the standard requirements in terms of gradation and fines content, two classification methods could be adopted by the Lebanese quarries. After applying the crushing process steps detailed in Chapter II, the limitation of the high percentage of fines could be applied either by wet processing using different washing techniques or by dry treatment using the air classification method.

The washing technologies improve the quality of crushed sand. They could include, as listed by (*Lagowski and Saramak, 2016*), washing by vibrating screen washers, wet screening, vibratory and rotary drum washers, log washers, turbo washers, and high-pressure washers. Nevertheless, the crushed sand should not be completely washed, because a small quantity of fines is beneficial to the workability of mortars and concretes (*Kabbani, 1967*) and their microstructures. This fact imposes more technical and economic constraints on the quarries since they should control the washing process to eliminate only the exact content of fines, treat the water used for washing, and dry the sand before transporting it

from the quarry. It should be noted also that this method could lead to an agglomeration of the limestone fines.

The air classification method consists of separating the fine particles according to their shape, weight, and density, by the means of the application of counteracting gravitational and/or centrifugal forces versus the drag force of the air (*Aslaksen Aasly et al., 2014 cited by Cepuritis et al., 2017*). For this process, several machines could be used, i.e., bag filters, cyclones, scrubbers, and electrostatic precipitators. Using one of these techniques, the fines could be reduced from 20 to 7% (*Goodquarry, 2011*). Thus, the strategy of coupling the crushing process by air classification techniques is effective in the full-scale production of aggregates and concrete (*Cepuritis et al., 2015*). It could separate the fines into different sections before storing them into silos and then adequately combine them if necessary. Moreover, when separated, the generated fines could be used as limestone filler in mortar and concrete.

2.2 Environmental overview

As seen in Chapter I, the excessive exploitation of natural sand resources affects the ecological equilibrium. In Lebanon, good quality natural sand is usually located under pine trees. Therefore, to be able to create sand quarries, huge pine forests are eliminated. So, one of the main negative environmental impacts of natural sand excavation is the deforestation and desertification of lands. Consequently, in some regions, the panorama is irreversibly damaged (*Weltzien, 2006*). Additionally, most of these land quarries are located close to populated areas.

Conversely, the use of crushed sand as the only fine aggregate in concrete could prevent unnecessary damages to the environment. To produce crushed sand, there is no need to create new quarries. The quarries already exist for coarse aggregates. In this way, the exploitation of resources is optimized. Furthermore, if more legal quarries are necessary, they could be well designed and planned to have a minimum impact on the environment. They could be located in the mountains with no vegetation and far from the populated areas, thus the environmental impacts and the negative effects of the noise and dust on the inhabitants could be minimized. In this way, their location will be more beneficial than that of the actual siliceous sand quarries, even though the transport of the sand will be more expensive. Also, an important caution could be attributed to their location in such a way to avoid the demolition of the underground caves or pollution of the underground water.

On the other hand, if the quarries shifted their crushed sand production to the normalized crushed sand while reducing the content of fines, some environmental disadvantages will be imposed. The wet techniques reduce the release of dust in the air, creating a safer environment, internally within the plant and externally in the neighborhood atmosphere. However, the wetting process should be continued, heavily increasing the water consumption in regions where water resources could not even be available. Additionally, if the fines are removed by washing, they will probably remain stockpiled without significant use or thrown in nature in a way that does not respect the environmental conditions. Hence, by applying the wet processing, we face the problems of lack of space in the quarry area, pushing the owners to widen their working plant, increasing thereby the negative environmental impacts. Moreover, the necessity of de-watering the ponds poses another environmental threat if the water is not adequately discharged. According to the Lebanese journal (*The daily star, 2016*), the increase of the pollution level in the Litani river, due to discharge of the water used to wash the excavated sand from one of the quarries of the Marjayoun area, is an example of the environmentally threatening throwing away activities.

To overcome the settling lagoons' problems and the neighborhood run-off of polluted water, filter press systems could be used, where the washing water is recovered to be reused in the washing plants (*Goodquarry, 2011*). Furthermore, the air classification method could be safely used without negatively affecting the environment.

2.3 Economic overview

For environmental reasons, in 2003, the Lebanese government has decided to stop the work of all sand quarries all over the country (*Yager, 2004*). The scarcity of this sand leads to an increase in its cost. Additionally, to respond to the need of the Lebanese market, the sand has been imported at high prices from different countries, including Egypt and Syria. Consequently, the cost of concrete has raised, risking in this way the construction sector. Nowadays, even the bad quality natural sand is expensive and its cost, as received by the concrete plants, is around 20-25 \$/m³ (32-40 \$/tons). As for better quality, if available, its cost reaches 25-30 \$/m³ (40-48 \$/tons).

In contrast, the crushed limestone sand is very abundant in Lebanon. It is widely available throughout the country and rock quarries are located in almost all the Lebanese districts. That is why the conventional crushed sand is more cost-effective than the natural sand. It is sold to the concrete plants at acceptable prices that vary between 10-13 \$/m³ (17-22 \$/tons).

However, as already mentioned, the production of the normalized crushed sand imposes the use of washing or air classification techniques. These procedures require the implementation of specific machines that require additional charges on the quarries, and consequently on the sand production. Furthermore, by adding these operations, the efficiency of the crushed sand production is affected. For the same period of time, the produced quantity will be decreased, increasing in this way the maintenance cost of the machines with a reduced effective economic profit.

The optimization of the crushed sand gradation and the application of the fines classification techniques raise the crushed sand price by around 15%. Despite this increase, the price of the normalized crushed sand remains below the cost of the natural sand available in the Lebanese market and the imported crushed sand. Additionally, the manufacturing of crushed sand could ensure a continuous supply at a relatively fixed price, whereas the continuous supply of natural sand is not guaranteed.

Additionally, the use of the normalized crushed limestone sand is more economical than the use of the classical combination of natural sand and conventional crushed sand, incorporated nowadays in concrete mixes, since the normalized crushed sand concretes demand lower admixture dosage (Section 1.1.2). Moreover, by eliminating the use of natural sand in concrete mixes, the cost of transport, storage, and testing of this material is subtracted from the cost of concrete materials.

Table IV.10 Environmental and economic advantages and disadvantages of the normalized crushed sand as the only fine aggregate in concrete mixes

	Environmental impacts	Economic impacts
Advantages	<ul style="list-style-type: none"> - Reduction of environmental damages - No need for new quarries - If needed, possibility of creating new quarries with minimum negative impacts - Reduction of the dust released in the environment 	<ul style="list-style-type: none"> - Continuous supply - Acceptable and relatively fixed price - Relatively fixed concrete price - Reduction of the admixture dosage in concrete - Decrease in the cost of transport, storage, and testing of concrete materials
Disadvantages	<ul style="list-style-type: none"> - Settling ponds due to the washing process - Inadequate discharge of polluted water - Excessive exploitation of water resources 	<ul style="list-style-type: none"> - Additional production cost for classification techniques - Decrease in the production rate

Conclusions

Since the currently available natural sand, in Lebanon, is deficient to be directly used in concrete production, in the aspects of its quality and cost, the effect of total replacement of natural siliceous sand by normalized crushed limestone sand in concrete is evaluated in terms of the fresh, hardened and durability properties for three different types of normal strength concrete, and two different types of high-strength concrete, commonly used in the Lebanese market.

For the three different formulations of normal strength concrete, the comparison is held between three types of concrete each, having the same slump and water to cement ratio and mainly differing by the type and gradation of fine aggregates and the admixture content. The gradation of fine aggregates, in any case, conforms to the ASTM C33 grading requirements, and the admixture content is adopted to reach a similar slump of 20 ± 2 cm.

For the three normal strength concretes, the crushed sand concretes require a lower admixture dosage than the conventional concrete, due to the higher content of deleterious particles of the natural siliceous sand used in the reference concrete. Accordingly, the workability of the crushed sand concrete decreases slower with time than the reference concretes. The setting times of the control mixes are higher, probably because of the retarder secondary effect of the admixture. Also, due to their lower content in admixture and the lower specific gravity of crushed sand, the crushed sand concretes generally display slightly lower fresh density and higher air content.

Regardless of the type of fine aggregate, the mechanical properties of the normal strength concretes are globally maintained. The compressive strengths are comparable for the three types of concrete, and the expected average compressive strength for each water to cement ratio is attained for each mix. However, in "Mix 35-I", for water to cement ratio of 0.4 and cement content of 350 kg/m^3 , the reference concrete presents slightly higher strengths (maximum difference of 8 MPa at 90 days) than the crushed sand concretes. This could be attributed to the higher admixture content in this mix, which deflocculates more the cement grains, enhances the hydration, and increases the compressive strength of concrete. The elastic modulus of concrete seems barely affected by the total substitution of natural siliceous sand by the normalized crushed limestone sand. The flexural strength and the shrinkage are improved in the crushed sand concretes.

In terms of durability, the crushed sand concretes and the control mix are within the same range and they present comparable properties, even though the durability properties of the reference concrete are slightly better in the normal strength concrete mixes. Thus, the replacement of the conventional combination of natural and crushed sand by normalized crushed sand does not induce significant differences in the permeability and the pores structure of concrete.

The microstructural analysis demonstrates that the angularity, surface roughness, and mineralogy of the crushed sand provide an interfacial transition zone between sand grains and cement paste of better quality compared to that with the natural sand grains. This microstructural enhancement could explain the slight increase in the flexural strength of the crushed sand concretes and the slight reduction of their shrinkage. However, it does not significantly affect the macrostructural behavior in terms of durability and other mechanical properties.

Additionally, the comparisons conducted between the concretes that only contained normalized crushed sand with a particle size distribution within the limits of the ASTM C33 standard show that they globally present similar behavior. The use of the well-graded crushed sand with a better dispersion of particles within these limits does not significantly improve the overall concrete performances, except for the workability, allowing the reduction in the superplasticizer content but consequently to a lower deflocculation and hydration of cement grains.

Similarly, for high-strength concrete, the comparison between the reference mix and the modified crushed sand concrete reveals that the effect of the fine aggregate type and gradation on the fresh, strength, and durability of the high-strength concrete seems negligible.

Based on the results of this experimental comparison, despite the differences between the natural sand and the crushed sand in terms of the morphology of their grains, their mineralogy, their physical properties, and their particle size distributions, the normalized crushed sand could be considered as an effective alternative to natural siliceous sand in normal and high-strength concretes without compromising the concrete performance. Furthermore, the optimization of the particle size distribution of this normalized crushed sand, to have a better distribution within the ASTM C33 grading limits, is not indispensable to maintain concrete properties. It is sufficient to have a particle size distribution that conforms to the limits imposed by this standard even if it is not well-distributed within these limits.

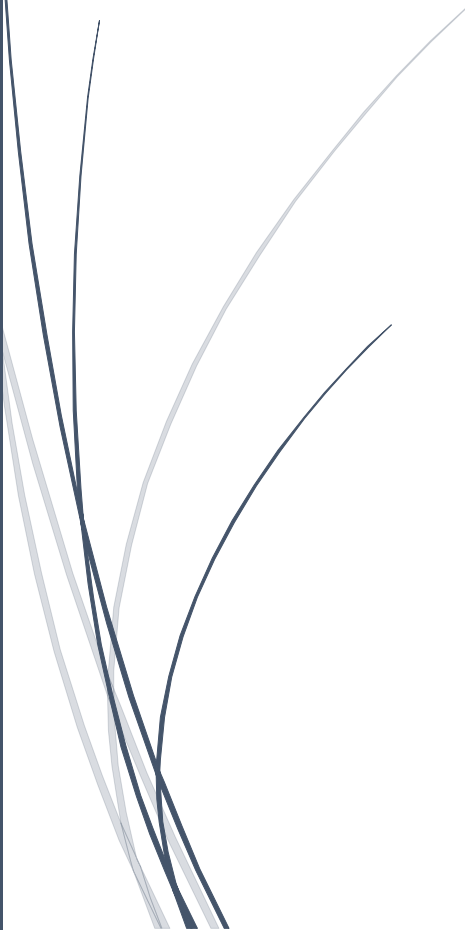
Technical, environmental, and economic feasibility studies of the production of the normalized crushed sand have been conducted, to be able to incorporate it as the only fine aggregate in concrete. These studies show that, even if the fines reduction techniques could induce additional costs on the crushed sand production, this solution is effective to overcome the scarcity and high cost of the natural sand.

Nevertheless, to reduce the few constraints that could be imposed by this solution, it is necessary to assess, in the next chapter, the effect of the fine crushed sand on the concrete performance, without reducing its high percentage of fines.



Chapter V

**Performance-Based
Approach Study on
Concrete Mixes
Incorporating Crushed
Sand with High
Percentage of Fines**



V. Performance-Based Approach Study on Concrete Mixes Incorporating Crushed Sand with High Percentage of Fines

Introduction

The previous chapter covered the comparison between different types of concrete, incorporating crushed sand, with a percentage of fines ($< 75 \mu\text{m}$ sieve) lower than the maximum allowable limit (7%) set by ASTM C33 (ASTM C33, 2016), the current applied regulation in Lebanon. However, the reduction of the crushed sand fines in order to conform to the standard limitations could impose many industrial and economic constraints.

Therefore, this chapter consists of evaluating the performance of concrete incorporating crushed sand with a percentage of fines exceeding 7%, following a performance-based approach. The study investigates if the fresh properties, the mechanical behavior, and the long-term performance of concrete could be maintained when the conventional combination of fine aggregates (natural sand and conventional crushed sand) is replaced by fine crushed limestone sand with a high percentage of fines (13%-18%).

The behaviors of the normal strength concrete "Mix 30b" and the high-strength concrete "Mix 50" are assessed during this study for three different types of sand each. As detailed in Chapter III, "Mix 30b" is characterized by a water to cement ratio of 0.5 and cement content of 350 kg/m^3 , whereas in "Mix 50", the water to cement ratio is reduced to 0.3 and the cement content is increased to 400 kg/m^3 , to reach a high strength.

For each one of these mixes, two types of comparisons are conducted. First, the characterization results of fine crushed sand concrete FM are compared to those of the conventional concrete CM, to be sure that the fine crushed sand could safely replace the conventional combination of fine aggregates. Then, a comparison is carried out between the fine crushed sand concrete FM and the normalized crushed sand concrete MM, having a percentage of fines within the limits, to efficiently evaluate the single effect of the high percentage of fines.

The three types of "Mix 50" have the same types and proportions of coarse aggregates and they are cast on the same day. The conventional combination of fine aggregates in CM is characterized by a content of fines of 7%. The fine crushed sand concrete FM presents crushed sand with a high percentage of fines of 13%, while the normalized crushed sand in the modified mix MM contains only 3% of fines.

However, for the normal strength concrete "Mix 30b", the coarse aggregates quantities have not been enough to cast the three types of concrete, due to the closure of the aggregates quarries in Lebanon during this study. Thus, we could not design a modified concrete MM with coarse aggregates provided from the same stock as those in CM and FM. Therefore, the comparison is conducted with the MM-30 of the previous chapter, taking into consideration the effects that could be imposed by the variation of the physical characteristics of coarse aggregates and their proportions. For "Mix 30b", the fine crushed sand incorporated in FM contains 18% of fines, while the modified crushed sand in MM is characterized by a low percentage of fines of 5%. The conventional combination of fine aggregates used in the control mix of "Mix 30b" is similar to the one of "Mix 50" with a fines content of 7%.

Additionally, a microstructural analysis is carried out at the interfacial transition zone between the cement paste and the sand grains of the normal strength concrete, to detect the possible differences that could be developed by the high percentage of fines at the microscale, and to try to understand the origins of the variations in the concrete behaviors at the macroscale, if any.

Furthermore, the last section of this chapter presents an overview of the technical part of this approach, in addition to an economic and environmental comparison, to introduce the advantages of the valorization of the high percentage of fines, generated during the production of crushed limestone sand.

1. Fresh properties

This section focuses on the effect of the high percentage of fines on the fresh properties of concrete. After applying the mixing procedure detailed in Chapter III and adjusting the admixture content to reach a 20 ± 2 cm slump, the fresh concrete temperature is recorded. Table V.1 presents the fresh concrete temperature and the required admixture content for each type of concrete.

Table V.1 Fresh concrete temperature and admixture content of all concrete mixes

Concrete mix Concrete property	Mix 30 (W/C: 0.5; cement: 350 kg/m ³)			Mix 50 (W/C: 0.3; cement: 400 kg/m ³)		
	CM-30b +7%	FM-30b 18%	MM-30* 5%	CM-50 7%	FM-50 13%	MM-50 3%
Fresh concrete temperature (°C)	27.0	30.5	22.0	29.0	29.0	29.5
Admixture content/kg of cement (%)	1.29	0.75	0.00	2.40	2.45	2.55

(*): The physical characteristics and proportions of coarse aggregates in MM-30 differ from those in CM-30b and FM-30b;

(+): Content of fines.

Several fresh properties tests have been performed on one batch of each type of concrete. They include slump, slump retention, density, and air content. Due to the lack of a sufficient quantity of materials, the setting time has been conducted only on the normal strength concretes "Mix 30". The results of the three types of normal strength concrete "Mix 30" and high-strength concrete "Mix 50" are presented in Table V.2.

Table V.2 Fresh state properties of all concrete mixes

Concrete mix Concrete property	Mix 30 (W/C: 0.5; cement: 350 kg/m ³)			Mix 50 (W/C: 0.3; cement: 400 kg/m ³)			
	CM-30b +7%	FM-30b 18%	MM-30* 5%	CM-50 7%	FM-50 13%	MM-50 3%	
Slump (cm)	Initial	20.5	20.0	20.5	19.5	19.0	19.0
	30 minutes	9.0	13.5	18.5	11.0	10.0	8.0
	60 minutes	7.5	9.5	15.0	7.5	9.5	7.0
	90 minutes	6.5	5.0	14.0	4.5	8.0	5.0
Setting time	Initial	6h00min	4h10min	5h00min	-	-	-
	Final	8h45min	6h10min	7h30min	-	-	-
Density (kg/m ³)	2381	2378	2341	2449	2476	2459	
Air content (%)	1.3	1.7	1.9	2.5	2.0	2.2	

(*): The physical characteristics and proportions of coarse aggregates in MM-30 differ from those in CM-30b and FM-30b;

(+): content of fines;

(-): property not measured.

1.1 Fresh concrete temperature

The fresh concrete temperature depends on the temperature of the concrete constituents and the environmental temperature on the day of casting.

For practical reasons, the three types of normal strength concrete, CM-30b, FM-30b, and MM-30, have been cast at different days with different environmental temperatures, hence the difference in their fresh concrete temperature (Table V.1). FM-30b which presents the highest fresh concrete temperature has been cast on the hottest day.

For "Mix 50", cast on the same day with the same environmental and mixing conditions, the three types of concrete display identical fresh temperatures.

1.2 Workability

Since the slump is fixed for all the studied types of concrete, the effect of fine aggregates on the concrete workability is assessed by the admixture dosage needed to reach the target slump (20 ± 2 cm).

Table V.1 shows that for normal strength concrete "Mix 30", the admixture content is lower in the fine crushed sand concrete FM-30b (0.75%) compared to the reference concrete CM-30b (1.29%), which incorporates natural sand. Thus, to reach similar workability, despite the angularity and rough surface of the crushed sand grains, the total replacement of the natural sub-rounded sand by crushed sand decreases the admixture demand of concrete. This reduction could be attributed to the lower content of deleterious particles in the crushed sand. As already explained in Chapter IV, the effect of the high content of deleterious particles in the fine aggregate supersedes that of the fine aggregate shape. The natural sand "NS-Series B" used in the control mix of the normal strength concrete, CM-30b, is characterized by a higher percentage of deleterious particles than the crushed sand. Compared to the fine crushed sand, the sand equivalent percentage of the natural sand is lower (58 and 62% for NS and fine CS respectively) and its methylene blue value is higher (1.3 and 0.61 g for NS and fine CS respectively). The angularity of the crushed sand grains and its high percentage of fines do not increase the admixture demand. Thus, the shape of the crushed sand grains and its fines percentage seem to be non-dominant factors in altering the workability of the studied concretes. These results are confirmed by those of the previous chapter and the studies of (*Hasdemir et al., 2016; Shen et al., 2016*).

On the other hand, the comparison between the two types of crushed sand concrete, FM-30b and MM-30, depicts a higher admixture content in the concrete with a high percentage of fines (0.75 and 0% for FM-30b and MM-30 respectively). In addition to the effect of the higher temperature in FM-30b on reducing the workability (30.5 and 22 °C for FM-30b and MM-30 respectively), the high content of fines in the fine crushed sand used in FM-30b (18%) could increase the surface area of the fine aggregate and thus the water demand. It requires a higher dosage of admixture to reach the same slump as in MM-30. Similarly, in the study conducted by (*Ding et al. 2016*), the increase of the percentage of fines from 5 to 13%, has to be associated with a higher admixture dosage varying from 0.7% to 1% to maintain the workability of a normal strength concrete (cement content: 320 kg/m³ and water to cement ratio: 0.56).

Given the high cement content and low water to cement ratio in the high-strength concrete "Mix 50", CM-50 and FM-50 require a high amount of admixture of 2.40 and 2.45% respectively (Table V.1). However, this value does not exceed the maximum content recommended by the admixture manufacturer (2.5%). This comparison shows that both types of concrete demand approximately the

same admixture content for the same water to cement ratio. Despite the high content of the deleterious particles in the natural sand and the angularity of the crushed sand particles, both types of concrete are characterized by the same workability, thus the fine aggregates tend to have a negligible effect on the workability of high-strength concrete.

By comparing FM-50 and MM-50, Table V.1 shows that the admixture dosage in MM is close to that of FM (2.45 and 2.55% for FM-50 and MM-50 respectively), and it slightly exceeds the limit of the admixture dosage recommended by the supplier (2.5%). Accordingly, the content of fines in the crushed sand (13%) does not seem to affect the workability of the high-strength concrete. Thus, it is noticeable that the effect of fines on the concrete workability is less pronounced in the high-strength concrete compared to the normal strength concrete probably due to the lower percentage of fines and the higher content of cement in the high-strength concrete (fines content of 13 and 18% and cement content of 400 and 350 kg/m³ for "Mix 50" and "Mix 30" respectively), to the similarity of the fresh concrete temperature of FM-50 and MM-50 (Table V.1), and to the negligible differences in the particle size distribution of the all-in aggregates of the high-strength concretes (Figure III.11b in Chapter III). Similarly, in the study of (*Shen et al., 2018*), when the powder content in the manufactured metasandstone varies from 0 to 12.5%, for the same water reducer dosage, small differences are depicted in the slump (20 ± 2 cm) and the concretes remained in the same range of workability.

1.3 Loss of workability with time

The loss of workability of concrete is monitored for 90 minutes after initial mixing, at an interval of 30 minutes. Throughout this period, the mixes have been covered at rest and only mixed by hand directly before performing the slump test, on one sample for each testing time.

The evolution of slump versus time is presented in the graphs of Figure V.1 for the different types of concrete.

Figure V.1a shows different slumps values for the reference concrete CM and the fine crushed sand concrete FM of "Mix 30" in the first 30 minutes which become close later. CM-30, which demands a higher amount of admixture, is characterized by a higher kinetic of slump reduction than the fine crushed sand concrete FM-30. The slump of CM-30 decreases by 11.5 cm in the first 30 minutes to produce a significant difference with the FM-30 (which decreases by 6.5 cm). In contrast, at 90 minutes, CM-30 exhibits a slightly higher slump (difference of 1.5 cm) than the FM-30.

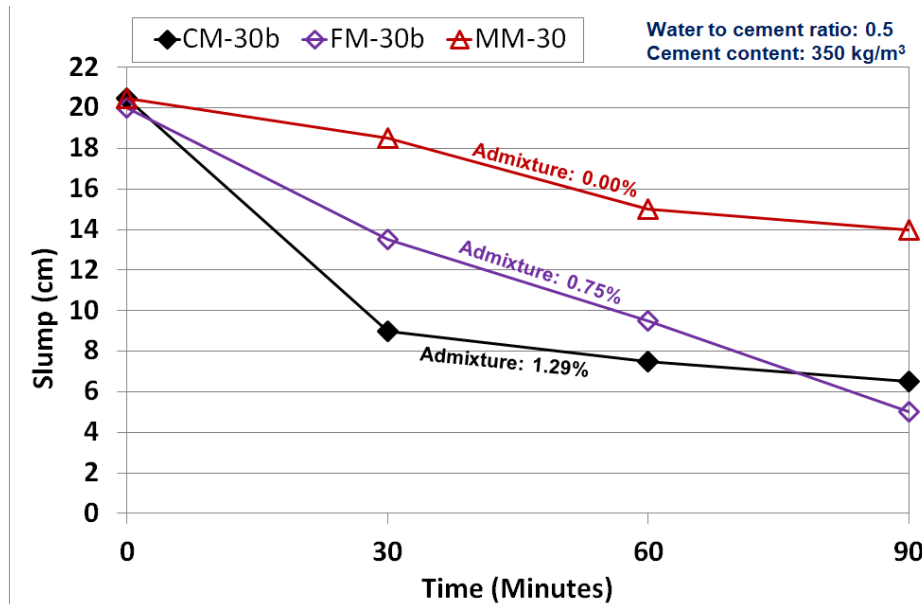
The comparison between FM-30 and MM-30 reveals that the FM-30 is characterized by remarkable higher kinetics of slump loss. This difference could also be the result of the higher dosage of admixture in FM-30, which accelerates the slump loss of concrete, as observed for the normal strength concretes of Chapter IV. The higher fresh temperature of FM-30 (30.5 and 22 °C for FM-30b and MM-30 respectively) could also contribute to its higher kinetics of slump loss.

For high-strength concrete "Mix 50", Figure V.1b depicts a rapid loss of workability for the three studied types of concrete, due to the relatively high admixture content in these concretes and their high temperature.

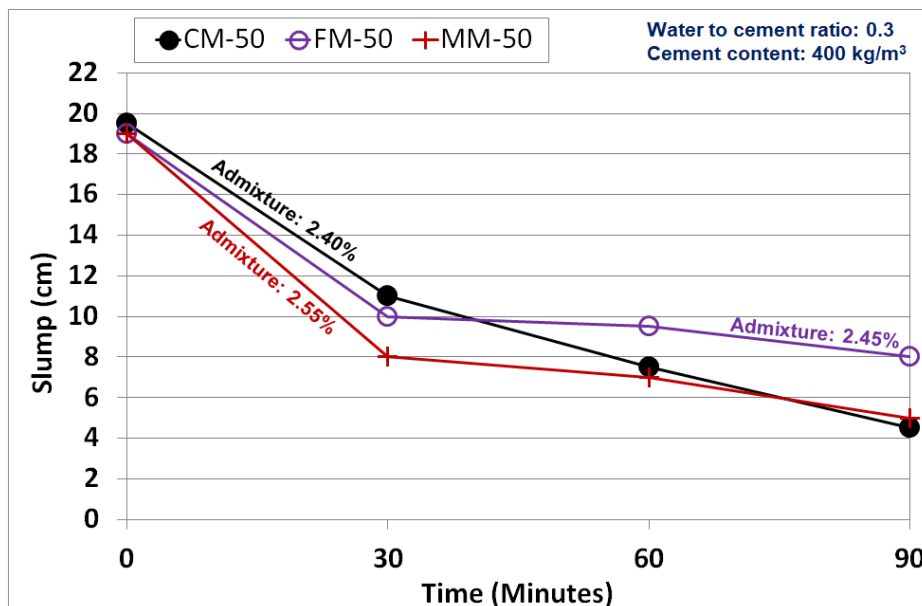
The slump loss of CM-50 and FM-50 is similar during the first 30 minutes. After this period, the deviation begins to increase, to reach a difference of 3.5 cm after 90 minutes, in the favor of FM-50. These similar results in the first 60 minutes could be attributed to the same admixture content between both types of concrete.

Containing a higher admixture content, which slightly exceeds the maximum recommended dosage (2.55%) (Table V.1), MM-50 presents slightly higher kinetics of slump loss compared to the one of FM-50. The maximum difference between the slump values of these two types of concrete is not significant and it reaches 3 cm after 90 minutes.

Generally, the slump evolution over time seems affected by the admixture content, as observed in the results of the previous chapter and the results of (Makhloufi *et al.*, 2014).



(a)



(b)

Figure V.1 Slump evolution over time for (a) "Mix 30" and (b) "Mix 50"

1.4 Setting times

Table V.2 shows that the fine crushed sand concrete FM-30b presents lower initial and final setting times than the reference concrete CM-30b. This difference in the setting times (110 min and 155 min for the initial and final setting times respectively) could result from the difference in the admixture content between both mixes. Since the dosage of admixture is higher in CM-30b, the secondary retarding effect of this admixture could decelerate the setting of this concrete. This result is in correlation with the results of the normalized crushed sand concretes, studied in the previous chapter.

Additionally, the high percentage of fines in the fine crushed sand could have played the role of a limestone filler that acts as a nucleation site and contributes to the chemical hydration of cement during the early ages (*Donza et al., 2002*), reducing thereby the setting times of concrete, as seen in previous studies by (*Bentz et al., 2015; Moon et al., 2017*).

Furthermore, since the rate of setting is affected by the fresh concrete temperature (*Kosmatka and Wilson, 2011*), the higher fresh concrete temperature in FM-30b (30.5 °C) compared to the one of CM-30b (27.0 °C), could be an additional reason in the decrease in the setting times of the fine crushed sand concrete FM-30b.

By comparing the setting times of FM-30b and MM-30, Table V.2 indicates that FM displays lower setting times than MM, a difference of 50 min and 80 min for the initial and final setting times respectively. Despite the lower admixture content in MM-30 (Table V.1) (0.75 and 0% for FM and MM respectively), it displays higher setting times than those of FM-30b. The higher percentage of fines in the crushed sand used in FM could be responsible for increasing the proportion of nucleation sites and reducing the setting time of concrete. In addition to the effect of fines, the higher fresh concrete temperature in FM-30b (30.5 °C) compared to the one of MM-30 (22.0 °C), could also have played a role in reducing the setting times of the fine crushed sand concrete.

1.5 Density and air content

For normal strength concrete "Mix 30", CM-30b presents lower air content than FM-30b (1.3 and 1.7% for CM-30b and FM-30b respectively) (Table V.2). This difference could be resulting from the admixture dosage in the two types of concrete. CM-30b, which requires a higher dosage of admixture (1.29 and 0.75% for CM-30b and FM-30b respectively) (Table V.1), is characterized by lower air content, as observed for Mix-30 and Mix-35-II in the previous chapter (see Chapter IV). The deflocculation effect of the admixture disperses the cement grains and tends to reduce the air content. This difference in the air content between both types of concrete does not induce a significant difference in their fresh density. Since the density of concrete could be directly related to the density of the aggregates (*Qasrawi et al., 2009; Gameiro et al., 2014*), the close values of density in CM-30b and FM-30b could be explained by similar values of specific gravities of the natural sand NS-Series B used in CM-30b and the crushed sand (2.59 and 2.55 for NS-Series B and CS respectively).

The comparison between the two types of crushed sand concretes, FM-30b and MM-30, reveals that the concrete with a higher content of fines, FM-30b, develops lower air content and higher density than the concrete incorporating well-graded crushed sand with a content of fines within the standard limits, MM-30. Similarly, the difference in the admixture content between both types of concrete (0.75 and 0% for FM-30b and MM-30 respectively) (Table V.1), could be at the origin of these results. In addition to the deflocculation effect of the admixture, the high percentage of fines could have played a positive role in increasing the compactness of concrete, decreasing hence the air content and increasing the fresh

density. (*Çelik and Marar, 1996*) have also found a reduction of the air content with the increase in the percentage of fines.

Concerning the high-strength concrete "Mix 50", having approximately the same admixture content, the same deflocculation effect could have occurred in CM-50 and FM-50. However, the high percentage of crushed sand fines of FM increases the compacity of concrete and reduces its air content (2.5 and 2.0% for CM-50 and FM-50 respectively) (Table V.2). Since the natural sand "NS-Series B", used in CM-50, and the crushed sand CS are characterized by a very close specific gravity (2.59 and 2.55 for "NS-Series B" and CS respectively), the slightly higher density in FM-50 (2449 and 2476 kg/m³ for CM-50 and FM-50 respectively) could be attributed to the lower air content in this concrete.

The same conclusions could be applied in the comparison between FM-50 and MM-50. For almost the same admixture content (2.45 and 2.55% for FM-50 and MM-50 respectively) (Table V.2), the crushed sand concrete with the highest content of fines, FM-50, develops the lowest air content and the highest fresh density (2476 and 2459 kg/m³ for FM-50 and MM-50 respectively) (Table V.2).

1.6 Summary of fresh properties

Despite the tendency of the fines to absorb water and admixture, the total replacement of the conventional combination of fine aggregates by crushed limestone sand with a high percentage of fines (18%) does not seem to negatively affect the workability of the normal strength concrete. The admixture dosage of the fine crushed sand concrete could even be reduced.

Similarly, the high-strength concrete tends to be not influenced by the high percentage of fines (13%) in the crushed sand.

2. Mechanical behavior

The following section assesses the effect of fines on the mechanical behavior of concrete. A comparative study is conducted between the reference concrete CM and the fine crushed sand concrete FM on one hand, and the fine crushed sand concrete FM and the concrete incorporating normalized crushed sand MM on the other hand. The three types of concrete are studied in terms of compressive and flexural strengths for normal and high strength concrete mixes, "Mix 30" and "Mix 50".

2.1 Compressive strength

The average values and the standard deviation of the compressive strength measured on three 150x300 mm cylinders of each type of concrete are displayed in Table V.3.

All the samples have been water cured at 23 ± 2 °C. The compressive strength of each type of concrete is studied at 3, 7, and 28 days. The long-term compressive strength is assessed at 90 days for the three types of normal strength concrete "Mix 30", and at 135 days for those of the high-strength concrete "Mix 50", due to the inability to perform the test of the latter at 90 days, as explained in Chapter III.

Overall, this table shows that for all the types of concrete, the 28 day-compressive strength relatively conforms to the expected average compressive strength for each water to cement ratio in concrete mixes (30 and 50 MPa for "Mix 30" and "Mix 50" respectively).

Table V.3 Average values (and standard deviations) of the compressive strength of all concrete mixes at different ages, in MPa

Concrete mix Age of concrete	Mix 30 (W/C: 0.5; cement: 350 kg/m ³)			Mix 50 (W/C: 0.3; cement: 400 kg/m ³)		
	CM-30b +7%	FM-30b 18%	MM-30* 5%	CM-50 7%	FM-50 13%	MM-50 3%
3 days	21.1 (0.34)	20.0 (0.50)	17.5 (1.07)	42.1 (0.93)	43.7 (1.45)	40.7 (0.04)
7 days	29.8 (0.78)	27.3 (0.64)	24.2 (2.13)	48.4 (1.76)	47.6 (2.64)	46.9 (1.43)
28 days	40.7 (1.42)	39.5 (1.28)	33.5 (1.06)	66.0 (1.06)	66.4 (1.05)	65.4 (1.80)
90/135 days [#]	47.4 (0.74)	42.4 (0.84)	36.0 (1.03)	72.5 (3.23)	74.1 (2.34)	71.1 (3.03)

(*): The physical characteristics and proportions of coarse aggregates in MM-30 differ from those in CM-30b and FM-30b;

(+): content of fines;

(#): the long-term compressive strength test is performed at 90 days for "Mix 30" and 135 days for "Mix 50".

For normal strength concrete "Mix 30", small differences are detected between the compressive strength of the reference concrete and the fine crushed sand concrete at 3, 7, and 28 days. The values of CM-30b are 5%, 8%, and 4% higher than those of FM-30b at 3, 7, and 28 days respectively. However, this difference increases to 11% at 90 days.

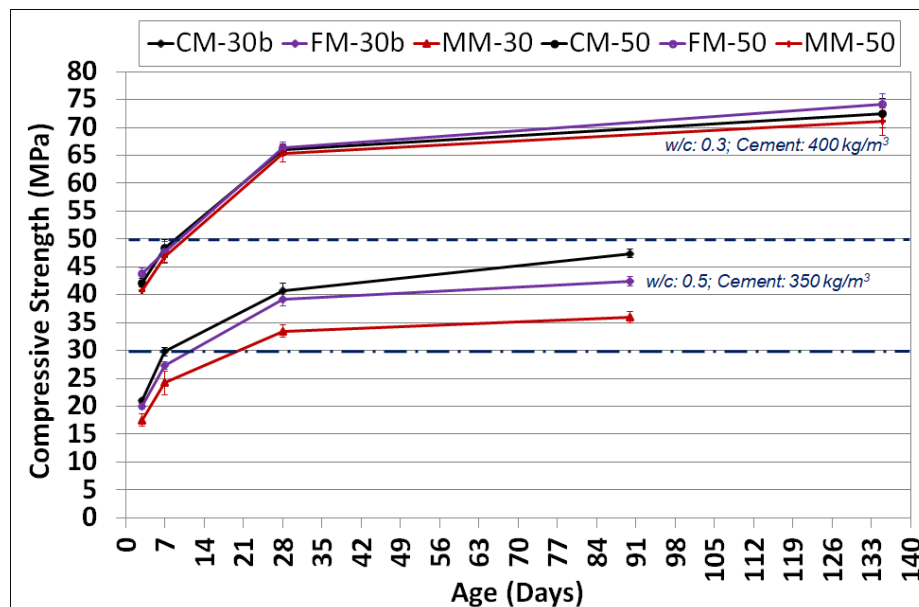
Table V.3 depicts a high difference in the compressive strength values between the two crushed sand concretes, FM-30b and MM-30. FM-30b, the concrete which contains the crushed sand with a high percentage of fines (18%), presents 11-15% higher compressive strength values than the normalized crushed sand concrete with a low content of fines (5%).

Comparing the values of the two types of the high-strength concrete "Mix 50", CM-50 and FM-50 present very close values with a maximum difference of 4% at 3 days (Table V.3). Similarly, the compressive strengths of FM-50 and MM-50 are also close throughout the test.

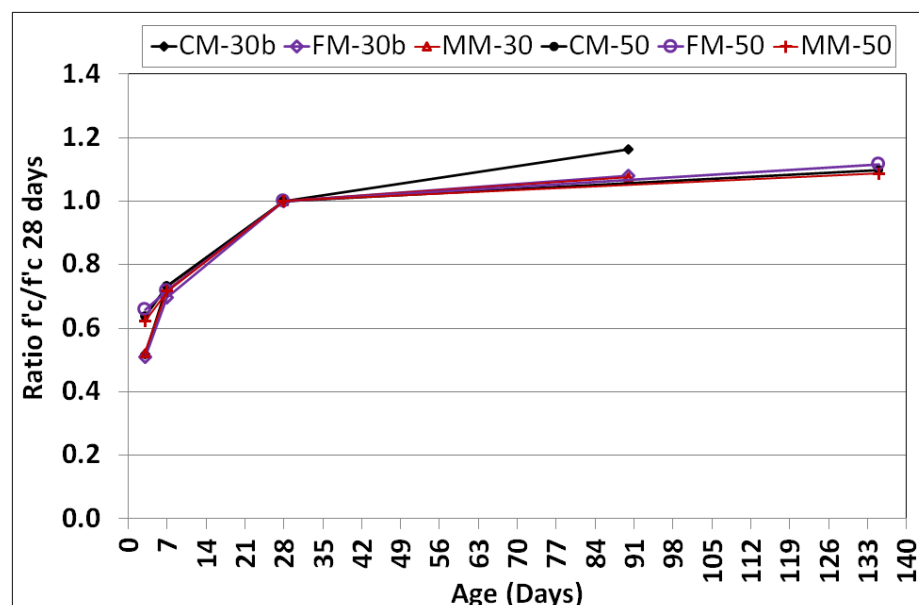
Additionally, to demonstrate the evolution of the compressive strength with age, Figure V.2a illustrates the kinetics of gain of compressive strength function of time. On each day, Figure V.2b also presents the ratio of the compressive strength to the 28-day compressive strength, for the three types of concrete of each mix.

These figures show that for "Mix 30", the compressive strength increases, between 3 and 28 days, at approximately the same rate, for CM-30b and FM-30b. However, from 28 to 90 days, the gain of strength differs since it is higher in CM-30b (16%) compared to that in FM-30b (8%). As for the normalized crushed sand concrete MM-30, the rate of gain of compressive strength is the same as that of the fine crushed sand concrete FM-30b at all ages.

On the other side, these figures reveal almost an identical evolution of the compressive strength between the three types of the high-strength concrete "Mix 50".



(a)



(b)

Figure V.2 Evolution of (a) the compressive strength and (b) the compressive ratio versus time for all the studied concretes

As already mentioned, by comparing CM-30b and FM-30b, slightly lower compressive strengths are displayed by the fine crushed sand concrete at 3, 7, and 28 days. These results are in correlation with the results of the comparison conducted in the previous chapter, between the control mix and the modified mix, for the same water to cement ratio (0.5) and cement content (350 kg/m^3). Hence, the total replacement of natural sand by crushed sand tends to have a negligible effect on the compressive strength at these ages, even though the crushed sand is characterized by a high percentage of fines (18%). Similarly, the increase in the stone powder from 5% to 13% has not affected the 28-day compressive strength of the normal strength crushed sand concrete in the study of (Ding et al., 2016).

However, at a late age (90 days), the difference of 11% between the compressive strength of the crushed sand concrete with a high percentage of fines and that of the reference concrete, is more significant than the difference between those of the normalized crushed sand concretes and the reference concrete of "Mix 30" of the previous chapter (8%). This difference could be interpreted by two different explanations:

First, at the ages below 28 days, the limestone fines generated by the crushed sand could accelerate the hydration reaction (*Li et al., 2009*) and reduce the difference between the compressive strengths of the reference and the fine crushed sand concretes. However, at a late age (90 days), the contribution of the limestone fines in the acceleration of the hydration reaction is reduced, increasing thereby the difference between the compressive strength values of CM-30b and FM-30b. Similarly, in the study conducted by (*Menadi et al., 2009*), for water to cement ratio of 0.65 and cement content of 350 kg/m^3 , the use of crushed limestone with 15% of fines, as the only fine aggregate in concrete, has not affected the concrete compressive strength at 28 days. However, at 90 days, this concrete displays a 15% reduction in compressive strength compared to the concrete incorporating crushed sand without fines.

Second, the dosage of admixture is higher in CM-30b than in FM-30b. Thus, this admixture could have contributed to the enhancement of the compressive strength at a late age, due to its deflocculation effect on the cement grains. This effect is less pronounced in the comparisons between the reference concrete and the normalized crushed sand concretes of "Mix 30" of the previous chapter since the dosage of admixture is relatively low for the different types of concrete of this mix.

For the normal strength concrete "Mix 30", the high difference between the compressive strength values of FM-30b and MM-30 could be mainly related to the difference in the physical characteristics and proportions of coarse aggregates since the compressive strengths of CM-30b and FM-30b are also globally higher than those of CM-30 and EM-30 of Chapter IV, which exhibit for example 28-day compressive strength of 35.1 and 35.8 MPa respectively. Thus, the effect of the high percentage of fines could not be directly concluded from the comparison of the compressive strengths of these two types of concrete since these fines are not the only influential factor on the concrete strengths. Also, the difference could be related to the absence of admixture in MM-30b which limits the good deflocculation of cement and its reactivity.

For the high-strength concrete "Mix 50", a high percentage of fines (13%), which exceeds the limit imposed by the ASTM standard (7%), does not seem to negatively affect the compressive strength. Then, the high percentage of fines in sand tends to be a non-influential factor in the compressive strength of high-strength concrete, at an early and late age. The low water to cement ratio in these mixes, associated with the high cement content, creates a dense microstructure that does not rely on the fines to fill the voids between aggregates and increase the compressive strength. These results are also confirmed by a previous study done by (*Gokce et al., 2016*), where the compressive strength seems independent of the fines content presented in the crushed limestone sand, for low water to cement ratio (0.38) and high cement content (380 kg/m^3).

2.2 Flexural strength

The 28-day flexural strength is obtained on three different 100x100x500 mm prisms, water-cured until the day of testing. The test has been applied using a simple beam with third-point loading, following (*ASTM C78, 2016*).

Table V.4 displays the average value and the standard deviation of the results of each type of concrete.

Generally, these results indicate a close behavior in terms of flexural strength in the three types of the normal strength concrete "Mix 30". On the other hand, the results show a difference between the flexural strengths of the different types of high-strength concrete "Mix 50". Despite this difference, the three types of concrete of "Mix 50" present a relatively high flexural strength.

Table V.4 Average values (and standard deviations) of the 28-day flexural strength of all concrete mixes, in MPa

Concrete mix Flexural strength	Mix 30 (W/C: 0.5; cement: 350 kg/m ³)			Mix 50 (W/C: 0.3; cement: 400 kg/m ³)		
	CM-30b +7%	FM-30b 18%	MM-30* 5%	CM-50 7%	FM-50 13%	MM-50 3%
Experimental	5.3 (0.42)	5.7 (0.60)	5.6 (1.08)	8.3 (0.73)	7.0 (0.08)	7.6 (0.39)

(*): The physical characteristics and proportions of coarse aggregates in MM-30 differ from those in CM-30b and FM-30b;

(+): content of fines;

For "Mix 30", contrarily to the compressive strength results, the little difference between the flexural strength values goes in the favor of the fine crushed sand mix. FM-30b displays an 8% higher value compared to the flexural strength of CM-30b. So, the substitution of the conventional combination of natural and crushed sand by an angular limestone crushed sand with a high percentage of fines could slightly improve the flexural strength of normal strength concrete.

In the previous chapter, the same trend is observed in the comparison between the normalized crushed sand concrete MM and the reference concrete CM of "Mix 30". The flexural strength of the normalized crushed sand concrete exceeds the strength of the reference concrete by 10%. Since a close difference is found for CM-30b and FM-30b (8%) and since FM-30b and MM-30 develop nearly the same flexural strength, the improvement of the flexural strength in FM-30b is probably due to the rough surface and the angularity of the crushed sand grains and not to the high percentage of fines, knowing that the rough surface of the crushed sand grains could enhance the bond at the interface and increase the flexural strength of concrete, as found in the studies of (Stefanidou, 2016; Li et al., 2011).

In the case of "Mix 50", the total replacement of the conventional combination of fine aggregates by fine crushed sand seems not positively affecting the flexural strength of concrete. Despite the similarity in the compressive strength results, FM-50, containing crushed sand with a higher percentage of fines, produces concrete with lower flexural strength (16 and 10% lower values than the ones of CM-50 and MM-50 respectively).

For the high-strength concrete of this study, which is characterized by a dense microstructure, the high content of fines could have exceeded the needed quantity necessary to fill the voids. Thus, the excessive quantity increases the surface area of aggregates. Hence, a higher amount of cement is required to coat the aggregates, leading to a weaker bond between the cement and aggregates and reducing the concrete flexural strength. This observation is in correlation with the results of (Çelik and Marar, 1996; Vijayalakshmi et al., 2013). In their studies, the flexural strength has decreased gradually when the fines content exceeds the optimum percentage needed to fill the voids.

2.3 Summary of the mechanical behavior

In this study, the compressive and flexural strengths of the normal strength concretes are maintained when the conventional combination of natural and crushed sand is replaced by crushed limestone sand with a high percentage of fines (18%).

For the high-strength concrete, a high content of fines of (13%) which exceeds the maximum allowable limit (7%), does not seem to deteriorate the compressive strength of concrete. However, it could decrease the flexural strength, since in a dense microstructure with few voids, the excess quantity of fines, provided from the crushed limestone sand, could not be well coated by the cement paste. Hence it could affect the bond between the cement and the aggregates and reduce the flexural strength of concrete. This assumption could be verified through a microstructural analysis of the high-strength concrete in future studies.

3. Durability Properties

The fines content in crushed sand could affect the long-term performance of concrete. Then, for each mix, a comparative study is carried out between the durability properties of the three types of concrete: the reference concrete CM, the fine crushed sand concrete FM, and the normalized crushed sand concrete MM.

Table V.5 presents the results of the durability tests performed at 90 and 135 days for "Mix 30" and "Mix 50" respectively.

As explained in Chapter III, the durability properties evaluated in this section are the most common tests required in the Lebanese market to characterize the performance of concrete at a late age. For each mix, the tests include water absorption after 30 minutes immersion, depth of water penetration under pressure, resistance to chloride ion penetration, and resistivity. Additionally, the porosity test, not widely recommended in Lebanon, has been conducted on the three types of concrete of "Mix 30" due to its importance as an index of concrete durability.

The global observation of Table V.5 reveals slight differences in some durability properties of the normal strength concrete and similarity in the long-term behavior between the different types of high-strength concrete.

Table V.5 Average values (and standard deviations) of durability properties of all the studied concretes at 90 days for "Mix 30" and at 135 days for "Mix 50"

Concrete mix	Mix 30 (W/C: 0.5; cement: 350 kg/m ³)			Mix 50 (W/C: 0.3; cement: 400 kg/m ³)		
	CM-30b +7%	FM-30b 18%	MM-30* 5%	CM-50 7%	FM-50 13%	MM-50 3%
Concrete property						
Porosity (%)	16.5 (0.34)	16.4 (1.27)	16.8 (0.55)	-	-	-
Water absorption (%)	3.6 (0.12)	3.7 (0.14)	3.1 (0.16)	1.1 (0.05)	1.1 (0.06)	1.2 (0.06)
Water depth (mm)	15 (1.5)	19 (2.1)	29 (5.0)	11 (2.4)	11 (2.0)	11 (1.7)
Passed charge (C)	6801 (117)	8295 (279)	7912 (638)	2387 (169)	2246 (88)	2171 (191)
Resistivity (Ω m)	42 (0.6)	41 (0.6)	41 (0.0)	87 (2.1)	76 (0.6)	79 (0.0)

(*): The physical characteristics and proportions of coarse aggregates in MM-30 differ from those in CM-30b and FM-30b;

(+): content of fines;

(-): property not measured.

3.1 Porosity accessible to water

The porosity accessible to water is an essential indicator of concrete durability. The high porosity induces a high permeability of concrete, thus low durability. The test is conducted as per the French

recommendations of (*AFPC-AFREM, 1998*) on the three types of "Mix 30". As detailed in Chapter III, 4 to 5 samples have been collected from the fractured cones after the compressive strength test applied on 150x300 mm cylinders that have been water-cured for 28 days. The collected specimens are then wrapped until the day of testing (90 days).

The same value of porosity accessible to water is measured on the control mix (16.5%), the fine crushed sand concrete (16.4%), and the normalized crushed sand concrete (16.8%) (Table V.5). Accordingly, for the same water to cement ratio and at a fixed slump, the increase in the percentage of fines from 5 to 18% tends to be a non-influential factor on the porosity accessible to water of concrete.

Similar to these results, for the same cement content (350 kg/m³) and higher water to cement ratio (0.65), the porosity values in the study of (*Menadi et al., 2009*) are approximately in the same range of porosity (15 to 17.5%), for fines content varying between 0 to 15%. Besides, the porosity values are in the same range as those specified in the (*AFGC, 2004*) guide (14-16%), for the same range of compressive strength (25-40 MPa). According to this guide, the three types of concrete of this study could be considered as low durable concretes, since their porosity is around 16%.

3.2 Water absorption by immersion

The water absorption by immersion test consists of measuring the 30-minute water absorption on three samples for each type of hardened concrete, following (*BS 1881-122-Part 122, 1983*). The permeability of concrete increases with water absorption, affecting thereby its durability. As discussed in Chapter IV, the standard does not set a maximum limit value for the water absorption by immersion. However, according to a study done for durability specifications of the marine structures in the Middle East region, a 30-minute water absorption percentage higher than 2% is associated with non-durable concrete (*Pocock and Corrans, 2007 as cited by Heath, 2016*).

For the three types of concrete of "Mix 30" and "Mix 50", Table V.5 presents the results of the water absorption after 30 minutes of immersion of 75x75 mm cylinders, that have been water-cured until the day of the test, i.e., 90 days for "Mix 30" and 135 days for "Mix 50".

By comparing the values of the water absorption to the limit values set by (*Pocock and Corrans, 2007 as cited by Heath, 2016*) for the classification of the concrete durability of the marine structures in the Middle East region, the three types of concrete of "Mix 30" could not be considered as durable concretes since their absorption percentages exceed 2% (3.6, 3.7, and 3.1% for CM-30b, FM-30b, and MM-30 respectively). Within the same range of durability, the reference concrete and the fine crushed sand concrete of "Mix 30" are characterized by nearly the same water absorption by immersion, while the normalized crushed sand concrete presents slightly lower water absorption.

On the other hand, Table V.5 shows that the absorption percentages of the three types of high-strength concrete "Mix 50" are lower than 2% (1.1-1.2%). Thus, they could be regarded as durable in terms of their 30-minute water absorption by immersion. It is also remarkable that the three types of "Mix 50" present the same 30-min water absorption by immersion.

Hence, the total replacement of the conventional combination of fine aggregates by crushed sand with a high percentage of fines does not seem to present significant effects on the 30-minute water absorption of the normal and high-strength concretes.

3.3 Water penetrability under pressure

The water penetrability under pressure is also an index of the concrete permeability. This property is determined following (*BS EN 12390-8, 2009*) standard by measuring the depth of water penetration under hydrostatic pressure. A high depth of water denotes a high permeability of concrete and low durability. A maximum depth is not specified in the standard. Nevertheless, concrete with a depth lower than 10 mm is considered durable according to the study conducted for durability specifications of the marine structures in the Middle East region (*Pocock and Corrans, 2007 as cited by Heath, 2016*).

The test is carried out on three samples of each type of concrete. The samples are 150x150 mm cylinders sawed at the middle of 150x300 mm cylinders that have been water cured until the day of the test: i.e., at 90 days for the three types of concrete of "Mix 30" and 135 days for those of "Mix 50". All the results are given in Table V.5.

High values are detected in the three types of normal strength concrete, (15, 19, and 29 mm for CM-30b, FM-30b, and MM-30 respectively). As per the study of (*Pocock and Corrans, 2007 as cited by Heath, 2016*), these concretes are considered non-durable since the depth of penetrated water exceeds 10 mm. The depth of water penetration under pressure for the normal strength concretes of previous studies are also higher than this limit, since they range between 12 and 27 mm in the study of (*Gokce et al., 2016*), and they even exceed 50 mm in the study of (*Menadi et al., 2009*).

Within this same range of durability, CM-30b presents a slightly lower value (15 mm) than the crushed sand concrete with a high percentage of fines FM-30b (19 mm). Taking the standard deviation into consideration, this difference could be considered non-significant.

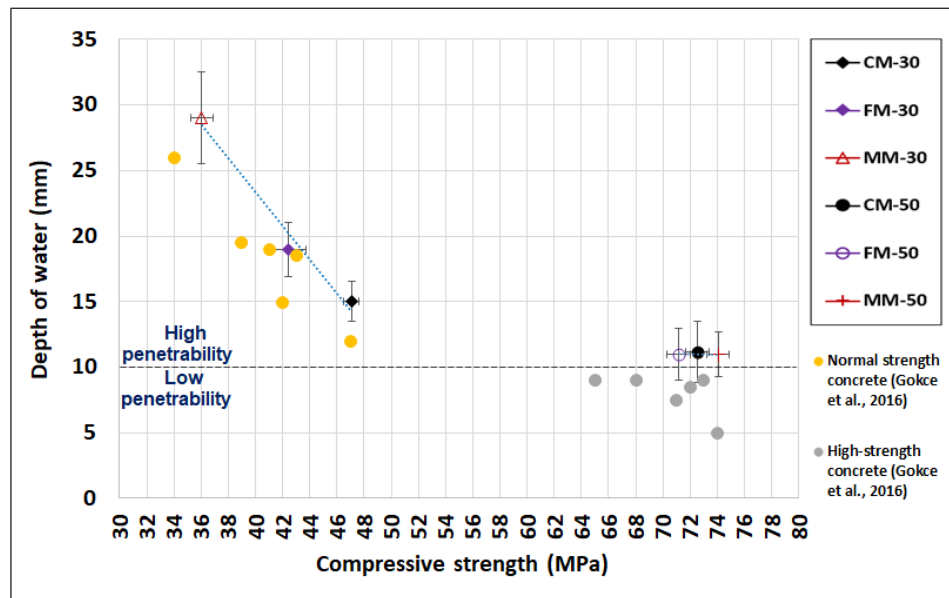
Comparing the depth of water of FM-30b (19 mm) to the one of the normalized crushed sand concrete MM-30 (29 mm), the difference is high with a relatively high standard deviation in MM-30. Many reasons could explain this result. First, since the fines could act as filler that reduces the connectivity of the pores by blocking the water passage, the higher content of fines in FM-30b (18%) could be responsible for the decrease of the depth of water penetration under pressure, compared to MM-30 with a fines content of 5%. Thus, the high content of fines could attenuate the permeability of concrete and increase its durability (*Çelik and Marar, 1996; Menadi et al., 2009; Gokce et al., 2016*). Second, MM-30 does not contain admixture contrarily to FM-30b. Accordingly, the cement particles could be more deflocculated in FM-30b and the pores could be reduced. Third, the difference in the depth of water between FM-30b and MM-30 could be related to that of the concrete formulation between both types of concrete, i.e., the change in the type and proportions of coarse aggregates, since the three types of concrete of "Mix 30" of the previous chapter exhibit a relatively higher depth of water penetration compared to those of "Mix 30b" of this chapter.

For the high-strength concrete, Table V.5 shows that the crushed sand concrete with a high percentage of fines is characterized by the same depth of water as the control concrete and the normalized crushed sand concrete. The water depth (11 mm) is relatively low and it is very close to the 10 mm limit. Hence, the three types of high-strength concrete could be considered durable with low permeability.

This observation is also a confirmation that the three types of high-strength concrete present the same pore structure and the same permeability. The fines content does not seem to be a significant influential factor in the depth of water penetration under pressure for the dense microstructure of the high-strength concrete. The same observation has also been found in the study of (*Gokce et al., 2016*) with values that do not exceed the 10 mm limit, for water to cement ratio of 0.38 and cement content of 380 kg/m³.

Moreover, the depth of water under pressure follows the same trend with respect to the long-term compressive strength (Table V.3 and Table V.5). The higher the water penetration (15, 19, and 29 mm)

the lower the 90-day compressive strength (47.4, 42.4, and 36.0 MPa) for CM-30b, FM-30b, and MM-30 respectively. Likewise, the three types of high-strength concrete, characterized by a similar depth of water penetration under pressure (11 mm), present very close 135-day compressive strengths (72.5, 74.1, and 71.1 MPa for CM-50, FM-50, and MM-50 respectively). Figure V.3 presents this correlation completed by the results of (Gokce et al., 2016).



* (Gokce et al., 2016) values, at 28 days, are determined by (BS EN 12390-8, 2009);

* 10mm is the limit given by (Pocock and Corrans, 2007 as cited by Heath, 2016) for the marine structures in the Middle East region.

Figure V.3 Relation between the average depth of water and the average compressive strength at 90 days for "Mix 30" and 135 days for "Mix 50", completed by data from (Gokce et al., 2016)

3.4 Resistance to chloride ions penetration

The resistance to chloride ion penetration test RCP is determined by (ASTM C1202, 2017) standard. A high charge value characterizes a low resistance to chloride ions penetration, thus revealing low concrete durability. According to this standard, concrete with a passed charge higher than 4000 C is characterized by high penetrability to the chloride ions, while concrete with a charge between 2000 and 4000 C has moderate penetrability.

Three 100x50 mm samples from each type of concrete are used for the RCP test. They have been sawed from 100x200 mm saturated cylinders, that have been water cured until the age of the test, i.e., 90 days for "Mix 30" and 135 days for "Mix 50".

Table V.5 shows that the three types of concrete of "Mix 30" lie in the same range of durability (6801, 8295, and 7912 C for CM-30b, FM-30b, and MM-30 respectively). They are all characterized by a high penetrability since the charge passed in the RCP test exceeds 4000 C (Table V.6). Similarly, due to the high water to cement ratio (0.65) and for a cement content of 350 kg/m³, the concrete mixes in the study of (Menadi et al., 2009) also show a high risk of chloride ion penetrability.

For the high-strength concrete, the charges passed in the RCP test for the three types of concrete are close and slightly higher than 2000 C (2387, 2246, and 2171 C for CM-50, FM-50, and MM-50 respectively). Thus, the chloride ions penetrability of these three types of concrete could be considered as moderate (Table V.5 and Table V.6).

It is worth mentioning that the standard deviations displayed in Table V.5 for the three types of concrete of each mix, "Mix 30" and "Mix 50", are acceptable. The maximum coefficient of variation (9% for MM-50) is lower than 12%, the maximum acceptable variation indicated in (*ASTM C1202, 2017*).

Table V.6 Correlation between chloride ions penetrability and the passing charge (*ASTM C1202, 2017*)

Charge passed (C)	Chloride ions penetrability	Range of the studied concrete mixes
> 4000	High	CM-30b (6801), FM-30b (8295), MM-30 (7912)
2000 - 4000	Moderate	CM-50 (2387), FM-50 (2246), MM-50 (2171)
1000 - 2000	Low	-
100 - 1000	Very low	-
< 100	Negligible	-

For the same range of durability, in the normal strength concrete, FM-30b which incorporates crushed sand with a high percentage of fines presents a 22% higher passing charge than the reference concrete CM-30b. This difference could be due to the higher dosage of admixture in the control mix. The cement particles could be more deflocculated, enhancing thus the cement hydration and increasing the ions dissolved in the pores which could block the diffusion of chloride ions.

Compared to MM-30, FM-30b is characterized by a slightly higher passing charge (5%). This comparison is an indication that the increase of the content of fines in the crushed sand, from 5 to 18%, tends to be a non-influential factor in the resistance of concrete to the penetration of chloride ions. Similarly, in the study of (*Menadi et al., 2009*), the incorporation of 15% limestone fines in the crushed sand does not induce a variation in the 90-day resistance to chloride-ion penetration of concrete, compared to the reference concrete containing crushed sand without fines.

The similarity in the RCP results of the different types of high-strength concrete also proves that the limestone fines have little or no effect on the resistance to chloride ions penetration of high-strength concrete. The high cement content (400 kg/m³) and low water to cement ratio (0.3) in the high-strength concrete create a dense microstructure with few pores. Consequently, the high percentage of fines in the fine crushed sand would not contribute to the densification of the structure and does not modify the pores structure which controls the permeability of concrete. These results are confirmed by previous studies conducted by (*Li et al., 2009; Vijayalakshmi et al., 2013*) which have evaluated the effect of fines percentage up to 15%.

Furthermore, a correlation could be depicted between the 90-day compressive strength and the charge passed in the different types of normal strength concrete (Table V.3 and Table V.5) measured at the same age after a similar water cure. The comparison between CM and FM of "Mix 30" reveals that CM presents the lowest charge, thus the highest compressive strength (6801-8295 C, and 47.4-42.4 MPa for CM-30b and FM-30b respectively). Consequently, the lower the charge passed in the RCP test, the better the pores structure, thus the higher the long-term compressive strength of concrete. Contrarily, compared to MM-30, the slightly higher charge in FM-30b does not develop a lower compressive strength (8295-7912 C, and 42.4-36.0 MPa for FM-30b and MM-30 respectively).

Additionally, the three types of high-strength concrete display close charge (2387, 2246, and 2171 C) and close 135 days compressive strength values (72.5, 74.1, and 71.1 MPa).

3.5 Resistivity

The resistivity of a saturated concrete could be correlated to the volume and sizes of its pores since the current is carried out by the ions dissolved in these pores. The resistivity test estimates the severity of chloride penetration and corrosion of reinforced concrete. Thus, a high resistivity implies high concrete durability and low severity of corrosion (ACI, 2001). For three samples of each type of concrete, the resistivity test is performed on 150x300 mm cylinders, in saturated-surface dried conditions.

In the study of (Shane et al., 1999 as cited by the manual of the resistivity measuring machine Giatec-RCON), the values of the saturated bulk resistivity at 28 days are associated with those of the charge passed at 56 days, of the same concrete. The correlation, presented in Table V.7, is applied to the bulk resistivity and charge passed in the RCP test at 90 days for "Mix 30" and 135 days for "Mix 50" (Table V.5). Since the resistivity of the three types of concrete of "Mix 30" is below 50 Ω m, they are characterized by a high penetrability to chloride ions penetration (> 4000 C). These concretes, which display approximately the same resistivity (41-42 Ω m), exhibit a resistivity lower than those of concrete with close cement content (353 kg/m³) and water to cement ratio (0.49), presented in the (AFGC, 2004) guide (100 Ω m).

For the high-strength concrete, the three types of concrete are in the same range of resistivity (values higher than 50 Ω m and lower than 100 Ω m), showing moderate resistance to chloride ions penetration with a value that ranges between 2000 and 4000 C. However, a slightly higher resistivity (87 Ω m) is measured on the reference concrete with the conventional combination of fine aggregates, CM-50, whereas the two crushed sand concretes develop close resistivity (76 and 79 Ω m for FM-50 and MM-50 respectively).

The comparison between the fine crushed sand concrete FM and the normalized crushed sand concrete MM shows that the percentage of fines does not induce a significant difference in the concrete resistivity, neither for the normal nor for the high-strength concrete.

Table V.7 Correlation between concrete resistivity and chloride ions penetration (Shane et al., 1999 cited by the manual of the resistivity measuring machine Giatec-RCON)

28-day bulk resistivity of saturated concrete (Ω m)	56-day charge passed as per ASTM C1202 (C)	Chloride penetration	Range of the studied concrete mixes at 90/135 days*
> 2000	< 100	Negligible	-
200 - 2000	100 - 1000	Very low	-
100 - 200	1000 - 2000	Low	-
50 - 100	2000 - 4000	Moderate	CM-50 (87), FM-50 (76), MM-50 (79)
< 50	> 4000	High	CM-30b (42), FM-30b (41), MM-30 (41)

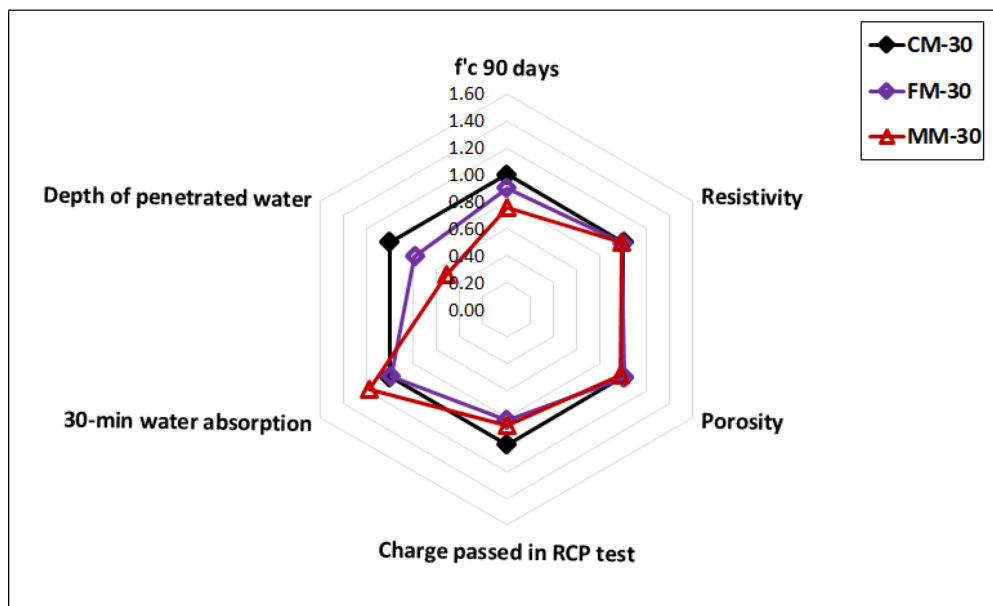
(*): the resistivity test is performed at 90 days for "Mix 30" and 135 days for "Mix 50".

3.6 Overall durability performance

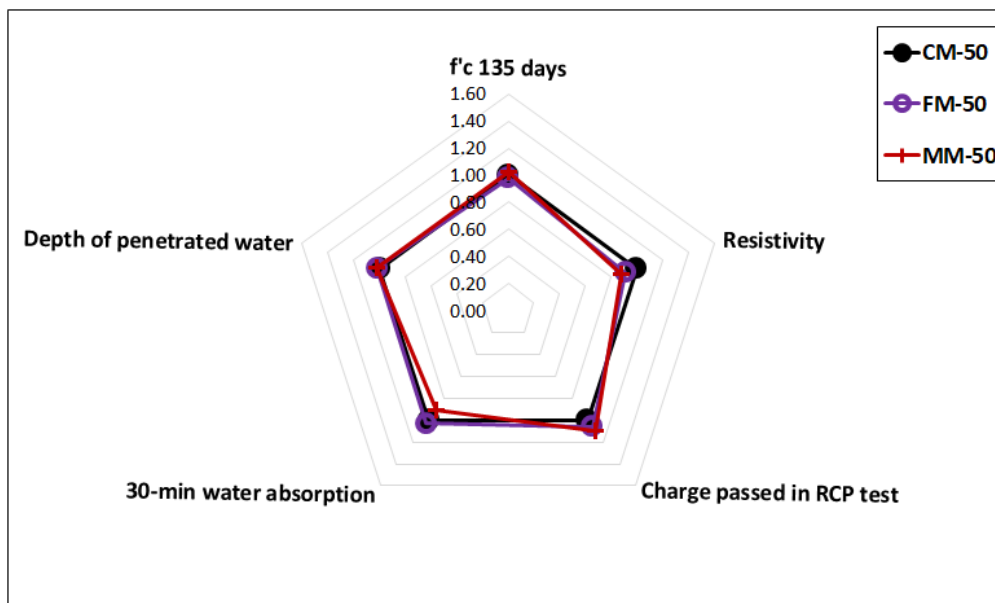
To have a clearer presentation of the durability properties, Figure V.4 depicts the small differences between the three types of concrete of each mix, even though they are in the same range of durability.

This figure presents the normalized values of the long-term compressive strength and concrete resistivity (ratio of the values of the crushed sand concretes, FM and MM, to those of the reference concrete, CM). Consequently, the values higher than one are an indication of higher resistivity and compressive strength for the crushed sand concretes, thus better durability behavior.

For the remaining durability properties, i.e., the porosity, the 30-minute water absorption by immersion, the depth of water penetration under pressure, and the charge passed in the resistance to chloride ions penetration test, this figure features the inversed normalized values (ratio of the result of CM to the result of FM or MM). When the represented value is higher than one, the results of these properties are lower in the crushed sand concretes, indicating higher durability and better long-term performance than the reference concrete.



(a)



(b)

Figure V.4 Durability properties for the different types of concrete of (a) "Mix 30" and (b) "Mix 50"

Figure V.4a proves that, in this study, the resistivity, porosity, and resistance to the chloride ions are not significantly affected by the use of crushed sand with a high percentage of fines. However, the difference in the other properties exceeds 10%. As already detailed in the previous sections, this difference could be related to many factors, i.e., the difference in the coarse aggregates' proportions and characteristics between MM and the two other types of concrete, the deflocculation effect of the admixture, and the filler effect of the particles of fines.

For the high-strength concrete, Figure V.4b reveals approximately a similar long-term behavior for the three types of concrete. This similarity could be an indication of a close microstructure between the different types of high-strength concrete, CM-50, FM-50, and MM-50.

3.7 Summary of durability properties

The results of the durability properties demonstrate that, for each mix, the three types of concrete, CM, FM, and MM, globally lie in the same range of durability.

Regardless of the type of fine aggregates, the normal strength concrete could not be considered durable. Even though the durability of the conventional mix is slightly better, the incorporation of high fines content in crushed sand concrete does not affect its durability compared to the normalized crushed sand concrete.

The three types of high-strength concrete are similar. They are considered durable in terms of all the studied indicators, showing no negative effect of the high percentage of fines in the long-term performance of this concrete.

Globally, the results obtained on crushed sand concrete with high fines content (13-18%) are close to those of the control mix, demonstrating that the increase of the fine content above the limit (7%) seems not significantly affecting the concrete behavior.

4. Microstructural analysis and correlation with the concrete performance

The concrete microstructure could be affected by the amount of limestone fines in the sand. Thus, this section details a microstructural analysis of the fine crushed sand concrete and compares it to that of the conventional and normalized crushed sand concretes.

In this objective, the compositional analysis and the mapping of the elements are assessed by the SEM/EDX method to detect the morphological and mineralogical differences that could be located at the interface between the cement paste and the sand particles in the control mix concrete CM, the fine crushed sand concrete FM, and the normalized crushed sand MM, of "Mix 30". As detailed in Chapter III, the samples studied in this analysis have been arbitrarily extracted from the fractured cones after the 28-day compressive strength test. Before the compressive test, the samples have been water cured. After the compressive strength test, the collected fractured samples have been wrapped until the day of the microstructural analysis. It should be noted that this analysis does not include the analysis of the possible microcracks at the interface, since they could result from the compressive strength test or the preparation of the samples for the microstructure observations.

As already observed in the microstructural analysis of the previous chapter, the smooth rounded siliceous grains in the control mix could limit the adherence of sand grains with the cement paste (Figure V.5a). However, the angularity, rough surface, and mineralogy of the crushed sand grains in the crushed

sand concrete enhance a better adherence and mechanical continuity with the cement paste (Figure V.5b and Figure V.5c). The images at the interface of the cement paste and the grains of the two crushed sand concretes, FM and MM, seem very similar despite the difference in the fines content between these two mixes.

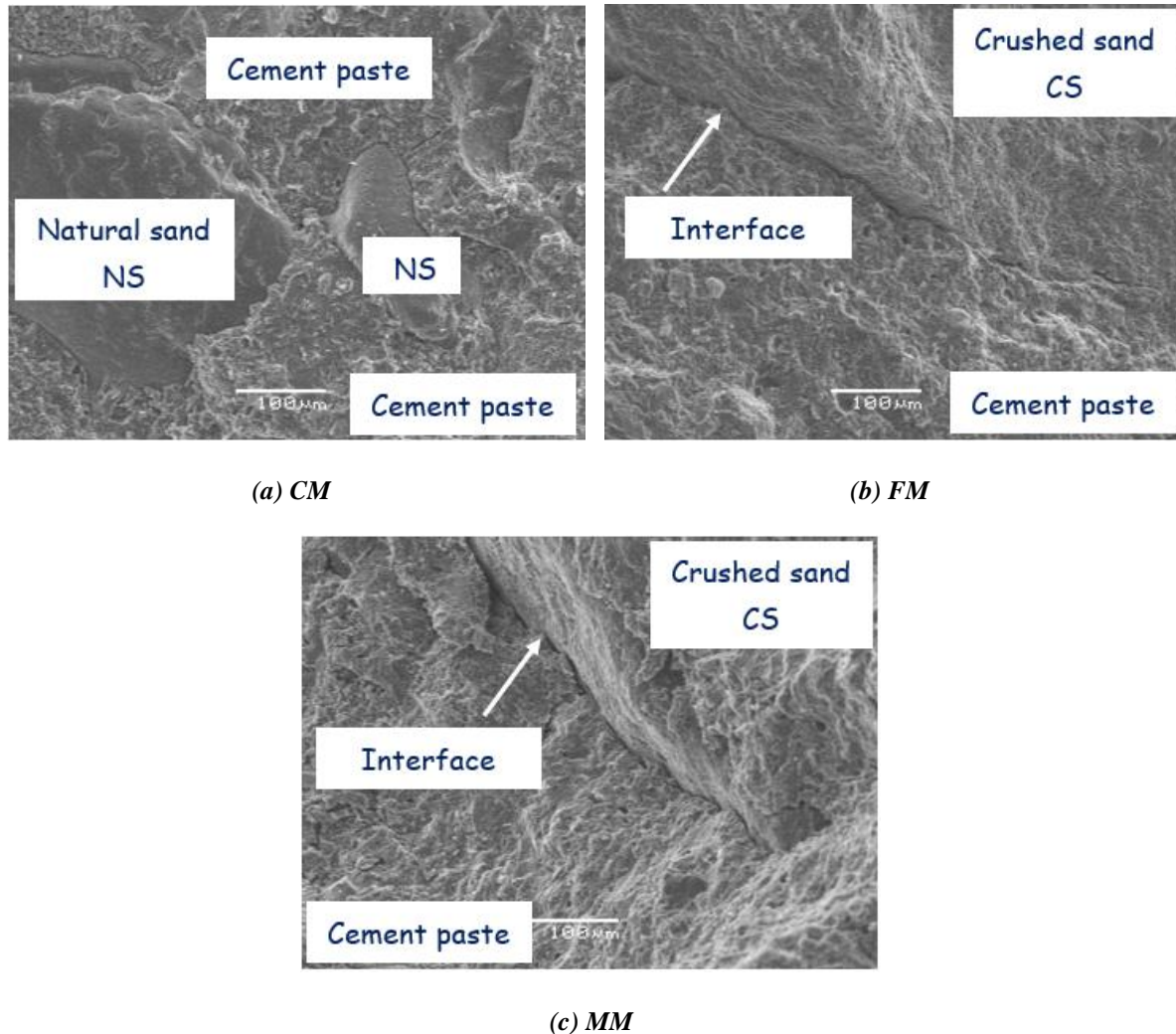


Figure V.5 SEI images (x200) at ITZ of (a) natural sand grains CM-30a, (b) crushed sand grain FM-30b, and (c) crushed sand grain MM-30a

To be able to investigate if the high percentage of limestone fines favors the formation of a denser and more homogeneous microstructure at the ITZ, the elemental mapping analysis is conducted. Two examples of the distribution map of the calcium element are shown in Figure V.6.

This presentation also unfolds a comparable distribution of the Ca element at the interface between the cement paste and the crushed sand grains. Thus, the high percentage of limestone fines does not seem to induce a remarkable difference in the elements distribution in the concrete microstructure.

Similarly, by elemental mapping analysis, (Shen *et al.*, 2018) have found that the high percentage of fines in concrete does not cause elemental enrichment. However, these fines improve the ITZ quality by filling the voids, densifying the interfacial transition zone between the cement paste and aggregates, and leading to a more homogenous paste.

This similarity in the microstructure of the two types of crushed sand concrete also results in equivalent concrete performances at the macroscale since the mechanical and durability properties of concrete incorporating crushed sand with a high percentage of fines are comparable to those of the normalized crushed sand concrete.

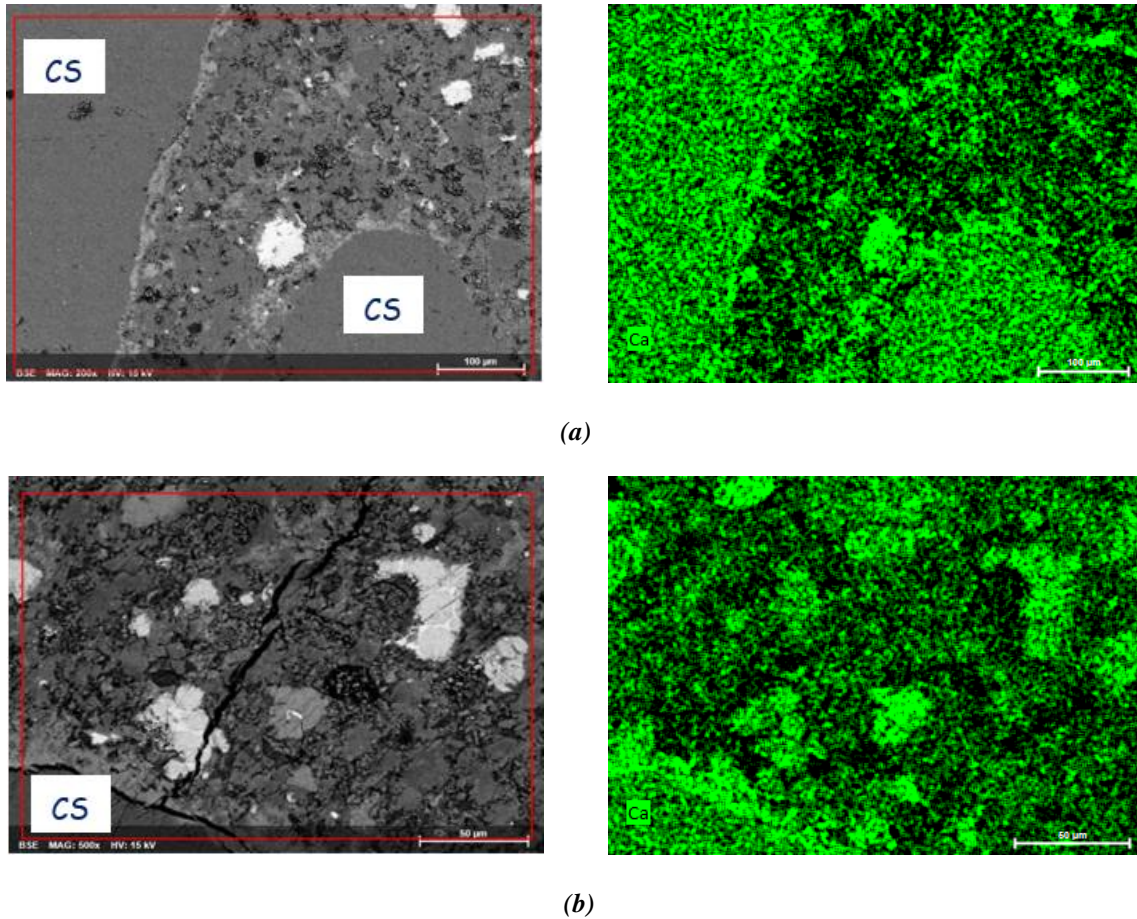


Figure V.6 The distribution map of calcium at the interface between the cement paste and the crushed sand grains of (a) FM-30b (x200) and (b) MM-30a (x500)

5. Feasibility study for using the fine crushed sand as the only fine aggregate

The feasibility study conducted in Chapter IV has revealed that the use of normalized crushed sand offers many environmental and economic benefits. However, the fact of applying a classification technique to reduce the high percentage of fines, generated during the crushing process, could increase the crushed sand production cost and imply some environmental disadvantages.

Therefore, the suitability assessment of using fine crushed sand as the only fine aggregate in concrete is not limited to its effect on the concrete performance, it is coupled with a technical, environmental, and economic overview to evaluate the feasibility of this crushed sand as the only fine aggregate in concrete.

As noted in the previous chapter, the prices mentioned in the section below are presented in \$ per bulk volume and could have been subjected to some changes after the period of this study (June-July 2020).

5.1 Technical overview

As already mentioned, the better the shape of the particles, the higher the production of fines (*Bengtsson and Evertsson, 2006; Guimaraes et al., 2007*). Thus, by valorizing the high percentage of fines formed during the crushed sand production, the well-shaped crushed sand could be produced at high speed and high energy, without worrying about the generation of the high amount of fines as a by-product (*Cepuritis et al., 2015*).

Technically, compared to the production of the conventional crushed sand, the only addition consists of introducing a supplementary sieve, to collect the fine crushed sand with a gradation that lies within the acceptable grading limits, except for the high percentage of fines.

5.2 Environmental overview

Compared to the use of natural sand in conventional concrete mixes, the fine crushed sand presents the same environmental advantages as the normalized crushed sand. The use of the fine crushed sand as the only fine aggregate in concrete is more environmentally beneficial than the use of natural sand. It contributes to the preservation of the pine trees' forests and the reduction of the desertification and deforestation of lands. Thus, the environmental damages are limited and the consumption of natural resources is optimized. Besides, the fines generated from the crushed sand originate from the limestone rocks and do not contain toxic elements or high content of deleterious particles.

Additionally, the production of the fine crushed sand without washing out the high percentage of fines, plays a positive role in the preservation of water resources, avoiding the creation of settling lagoons in the crusher area and eliminating the discharge of polluted water after washing.

5.3 Economic overview

Economically, the use of fine crushed sand as the only fine aggregate in concrete is an advantageous solution. The crushed sand is abundant in limestone quarries all over Lebanon and its supply is guaranteed at a lower cost than that of the natural siliceous sand.

Moreover, as seen in the previous chapter, an additional cost is applied to reduce the percentage of fines to be in accordance with the standard requirements. However, contrary to the normalized crushed sand, the fine crushed sand does not require the implementation of fines classification techniques and/or fines disposal methods that increase the crushed sand cost. Thus, the price of fine crushed sand, 15-17 \$/m³ (25.5-29 \$/tons), is lower than the price of the normalized crushed sand, 18-20 \$/m³ (31-34 \$/tons).

Sometimes, depending on the crushed rock characteristics, the crushing process does not generate a sufficient quantity of fine crushed sand. Thus, an additional crusher could be introduced, increasing thereby the cost of the fine crushed sand compared to that of the conventional crushed sand (10-13 \$/m³ or 17-22 \$/tons). However, despite this increase, the fine crushed sand remains less expensive than the natural sand, which price could reach 30 \$/m³ (48 \$/tons).

Furthermore, as already mentioned in the previous chapter, the highest amount of energy is usually consumed on non-commercial products (*Guimaraes, et al. 2007*). Thus, by avoiding the limitation of fines content after production, the crushed sand production will be more efficient. The huge energy consumed to produce the fines will not be vainly dissipated on a by-product. In contrast, it is used in the generation of a valuable product that is beneficial for concrete and aggregates producers.

Conclusions

To be able to valorize the high percentage of fines (13-18%) generated during the crushed sand production, which exceeds the maximum limit imposed by the ASTM C33 standard (7%), the effect of crushed limestone fines is evaluated by a comparison conducted between the conventional concrete, the fine crushed sand concrete, and the normalized concrete, for normal and high strength concrete mixes.

The non-harmless nature of the crushed limestone fines permits the use of crushed limestone sand with a high percentage of fines in concrete without significantly affecting the fresh, mechanical, and durability properties of the normal strength concrete. To keep the same workability, fine crushed sand concrete requires lower admixture content than control concrete. As assumed for the normal strength concrete results of Chapter IV, the lower induced cement deflocculation slightly decreases the compressive strength at 90 days and the durability of concrete. However, the flexural strength is better for the fine crushed concrete probably due to a better bond between the cement paste and sand grains.

For high-strength concrete, the three types of concrete also have very close behavior, there is no significant effect of the high percentage of fines on the fresh properties, compressive strength, and the long-term performance of the high-strength concrete. However, due to the dense microstructure, the excess content of fines that does not fill the voids could require a higher amount of cement and could adversely affect the bond at the ITZ and the flexural strength of the high-strength concrete.

The approach of optimizing the production of crushed sand, without reducing the high percentage of fines necessary to conform to the limit imposed by the standard, is an effective ecological and economic solution that permits the shift to 100% crushed sand concretes, in order to respond to the need of the Lebanese market, without compromising the concrete properties.



General Conclusions and Future Studies

General Conclusions and Future Studies

Conclusions

The resources of the good quality natural siliceous sand are almost depleted in Lebanon and the mining of the remaining quantity is prohibited for environmental concerns. These problems lead to a rise in the natural sand cost and consequently the concrete cost. In addition to that, the available natural sand is too fine and is always combined with an appropriate amount of crushed limestone sand to conform to the limits imposed by ASTM C33, the standard applied in Lebanon.

Similar to Lebanon, several countries also undergo a lack of natural sand for concrete construction. The good quality natural sand becomes less available and its mining creates negative environmental impacts. Subsequently, in order to limit its exploitation and to reduce the environmental impacts of the disposal of these substitutes, many studies have analyzed the use of crushed rocks, construction and demolition wastes, domestic wastes, and industrial products as a partial or total replacement to natural sand in concrete. In the Lebanese case, the crushed limestone sand tends to be the most effective solution to totally replace the natural sand, in order to limit the economic and environmental problems of the latter. However, this solution is not so far applied since there is no scientific evidence, across the country, to convince the construction sector of its feasibility. Accordingly, this study is the first in Lebanon to assess the effect of the total replacement of natural siliceous sand by crushed limestone sand and to verify if the concrete performance could be maintained by this substitution.

The literature review shows that the concrete performance could be influenced by the fine aggregates' characteristics. The shape of sand grains and their particle size distribution could control the workability of fresh concrete, while the effect of fines and deleterious particles depends on their nature and their percentage in the mix. The mechanical resistance of concrete is influenced on one hand by the bond between the cement paste and the sand grains, determined by the mineralogy and morphology of sand, and on the other hand by the compactness of the mix, regulated by the particle size distribution. Few studies have detailed the effects of fine aggregates properties on the shrinkage and durability of concrete. The effect on shrinkage does not seem significant while the durability could mainly depend on the fines content of sand and its mineralogy. The concrete microstructure at the interfacial transition zone ITZ between the cement paste and the sand grains is not widely investigated in the literature contrarily to ITZ of the coarse aggregates, but it could depend on the mineralogy, morphology, and fines content of sand.

The experimental program conducted on the aggregates highlights the differences in the shape, chemical composition, mineralogy, and physical characteristics between the natural sand and the crushed sand. The natural sand is siliceous and formed of sub-rounded angular grains, characterized by a particle size distribution finer than the limits imposed by the ASTM C33 standard. The crushed sand consists of angular limestone grains with a particle size distribution coarser than these limits. In addition to these differences, the two types of sand differ also by some physical properties: the fineness, specific gravity, percentage of deleterious particles, and soundness are higher in the natural sand, while the absorption and the fines content are lower. Since the fines in the crushed sand are generated from the secondary crushing process, they have a better quality than those of the natural sand. Even though the content of clay lumps and the soundness percentage of the natural sand exceed the maximum limit imposed by the standard, this sand is used currently in concrete provided that it is mixed with the crushed limestone sand.

General Conclusions and Future Studies

To evaluate the effect of the normalized crushed sand, which particle size distribution conforms to the grading limits, three normal strength concrete mixes and one high-strength concrete, commonly used in the Lebanese market, are prepared:

- "Mix 30" incorporates a cement content of 350 kg/m^3 and water to cement ratio of 0.5;
- "Mix 35-I" contains 350 kg/m^3 of cement and a water to cement ratio of 0.4 to reach a higher compressive strength than "Mix 30".
- "Mix 35-II" presents a cement content of 300 kg/m^3 and a water to cement ratio of 0.4 to get a greater highlight on the effects of aggregates and to limit the environmental threats caused by cement production, by reducing the cement content while getting a slightly higher strength.
- "Mix 50" is a high-strength concrete characterized by high cement content of 400 kg/m^3 and low water to cement ratio of 0.3.

To allow a comparison based on the only effect of the fine aggregates, while fixing the effective water to cement ratio, the cement content, and the coarse aggregates proportions, for each concrete mix, the conventional combination of the natural sand and crushed sand in the control mix is replaced, in the crushed sand concretes, by an equivalent volume of normalized crushed sand. For this purpose, two types of normalized crushed sand are constructed in the laboratory to conform to the standard grading limits: the "Equivalent crushed sand" with a particle size distribution similar to that of the fine aggregates' combination in the control mix, to study the effect of the shape and physicochemical characteristics of fine aggregates; the "Modified crushed sand" with a better particle size distribution within the standard limits, to evaluate the effect of gradation. A high-range water-reducing admixture is used to reach a slump value of $20 \pm 2 \text{ cm}$ for all concrete mixes.

The experimental program includes the evaluation of concrete properties at fresh state: initial workability, loss of workability with time, fresh density, air content, and setting time. The mechanical behavior is assessed in terms of compressive strength, elastic modulus, flexural strength, and shrinkage deformations. The determination of the long-term performance of concrete covers its porosity accessible to water, 30-minute water absorption by immersion, depth of water penetration under pressure, resistance to chloride ion penetration, and resistivity.

Taking into consideration the dispersion between the different results, the comparisons drive to the conclusion that the normalized crushed sand could effectively replace the natural siliceous sand in normal and high strength concretes, without compromising the concrete performance, in terms of fresh, mechanical, and durability properties:

- In the normal strength concrete, the effect of the deleterious particles supersedes the effect of the grains shape. These particles increase the water demand for fresh concrete. Thus, the concrete incorporating natural sand with sub-rounded grains and a higher percentage of deleterious particles demands a higher dosage of superplasticizer than the crushed sand concretes, formed of angular crushed limestone sand with lower content of deleterious particles. In the high-strength concrete, the natural sand and crushed sand, differing mainly by their mineralogy and morphology, do not present different behaviors.
- The mechanical behavior of concrete is comparable for the different types of fine aggregates in normal and high-strength concretes. A slight improvement is detected in the flexural and shrinkage of the normal strength crushed sand concretes, probably due to the angularity and mineralogy of the crushed limestone sand grains which improve their bond with cement paste. The expected average compressive strength is attained, with slightly higher values (maximum difference $< 8 \text{ MPa}$ at 90 days in "Mix 35-I") for the reference concrete containing a higher admixture content, due to the deflocculation effect of the admixture which enhances the hydration of the cement grains.

General Conclusions and Future Studies

- For the same range of compressive strength, the different types of concrete lie in the same range of durability, hence the characteristics of the fine aggregates do not induce a difference in the permeability and pores structure of normal and high-strength concrete.
- The microstructural analysis confirms the beneficial effect of the angularity and rough surface of the crushed sand grains since the quality of the interfacial transition zone between the cement paste and these grains is better than that with the natural sand grains.

The two types of normalized crushed sand concretes, that contain normalized crushed sand with a particle size distribution within the limits of the ASTM C33 standard, globally exhibit similar behavior, proving that the crushed sand which presents more optimized particle size distribution within this limit does not significantly improve the concrete performance at hardened state. At the fresh state, the workability is improved due to the lowering of interparticle voids, leaving a higher available amount of cement paste to cover the particles. Thus, this effect allows reducing the admixture dosage.

Technical, environmental, and economic feasibility studies of the production of the normalized crushed sand show that, even if the reduction of the high percentage of fines generated by the crushing process could induce some industrial constraints and additional costs on the crushed sand production, this solution is effective to overcome the scarcity and high cost of the natural sand.

To avoid the few constraints that could be imposed by the production of the normalized crushed sand, it is necessary to evaluate the use of the crushed limestone sand with a percentage of fines that exceeds the limit imposed by the standard (7%). For this purpose, "Mix 30" and "Mix 50" are also designed with a fine crushed limestone sand, which gradation does not comply with the grading requirements in terms of the high percentage of fines (13-18%). The comparisons show that this alternative is an effective economic and ecological solution that permits the valorization of the limestone fines without compromising the concrete performance:

- For the normal strength concretes, the fine crushed sand concrete demands a lower admixture dosage than the control mix. It is characterized by slightly lower durability and 90-day compressive strength, maybe due to the lower deflocculation of cement particles. It also presents a higher flexural strength, probably due to a higher bond between the crushed sand grains and the cement paste.
- For the high-strength concretes, the high percentage of fines does not seem to affect the fresh properties, compressive strength, and durability of concrete. However, the high content of fines that does not fill the voids of this dense microstructure could negatively affect the bond between the cement paste and the crushed sand grains and consequently the flexural strength of concrete.

Generally, for fixed water to cement ratio, cement content, and coarse aggregates proportions, and for different dosages of admixture to reach the same slump value, the total replacement of the natural siliceous sand, by normalized crushed sand or by crushed sand with high fines percentage that exceeds the limit imposed by the ASTM standard, could resolve the industrial problems related to the natural sand in Lebanon.

Accordingly, the following recommendations are offered to the different parties in the construction field:

- The contractors, consultants, and concerned authorities are invited to accept the use of the normalized and fine crushed sand as the only fine aggregate in concrete.
- The concrete plants are encouraged to start producing concrete mixes without natural sand.

- The quarries are solicited to optimize the production of the conventional crushed sand in order to manufacture crushed sand that conforms to the grading specifications imposed by the standard or fine crushed sand with a high percentage of fines that exceeds the standard limit.

Future studies

Based on this study, a range of suggestions for new studies can be proposed.

Due to time frame limitations and some restrictions related to the transport of samples to France, the microstructural analysis and some concrete tests, such as porosity and shrinkage, have not been conducted on all concrete mixes. It is interesting to complete the study by performing these tests on all concrete mixes especially the high-strength concretes since the autogenous shrinkage is usually significant in the dense microstructure and to be able to explain the slight reduction in the flexural strength of the concrete incorporating the fine crushed limestone sand.

Furthermore, the effect of the total replacement of natural sand by normalized crushed sand or fine crushed sand on the creep of normal and high-strength concretes could be analyzed as well. The creep is a necessary mechanical behavior to design concrete constructions, such as bridges and prestressed concrete structures. Since the sustained loading induces microstructural damage around the aggregate, in particular when coupled with desiccation, some differences could then occur depending on the type of sand and its bond with cement paste. Thus, a campaign of creep tests has to be led to analyze the effects of the fine aggregates' type on this mechanical behavior and consequently the effect of the microstructural damage on the durability of concretes with different types of fine aggregates.

When designing concrete mixes, the choice has been done to fix a maximum number of parameters and to adjust the superplasticizer dosage to reach the same slump. However, the slightly better behavior of the reference concrete could be attributed to its higher dosage in superplasticizer. Therefore, a complementary experimental program based on fixing the admixture dosage between the different concrete mixes allows confirming or not this assumption.

During this experimental program, all the concrete properties have been evaluated according to the laboratory curing conditions suggested by the standards, which could differ from the real in-situ conditions. Since continuous curing could mask the differential deformation between the cement paste and the sand grains and since inadequate curing could result in a weak concrete with a porous surface, hence the time and method of curing could affect the concrete microstructure, strength, and durability. To ensure that the concrete properties could be maintained in severe drying conditions, future studies seem necessary to assess the effect of the total replacement of the natural subrounded siliceous sand by angular crushed limestone sand, in different curing conditions. Such drying conditions could also allow a better highlight of the bond strength with cement paste depending on the type of sand grains and thus a better identification of the effects of sand characteristics on the hardened state behavior of concrete.

The effects of sand on the fresh, mechanical, and durability properties of concrete, as well as those of the other concrete constituents, depend on its volume in the concrete mix. The thesis program focuses on concrete performances to provide information for the concrete industry in a short time. However, to increase the effects of sand and reveals more clearly the influence of the various fine aggregates' characteristics on the hardened state behavior, some complementary experimental tests could be carried out on mortars. The results obtained on mortars and concretes could then be analyzed using some homogenization methods in order to propose a relevant model able to assess the concrete behavior from the characteristics of its constituents: such as the water to cement ratio, binder constitution and volume,

General Conclusions and Future Studies

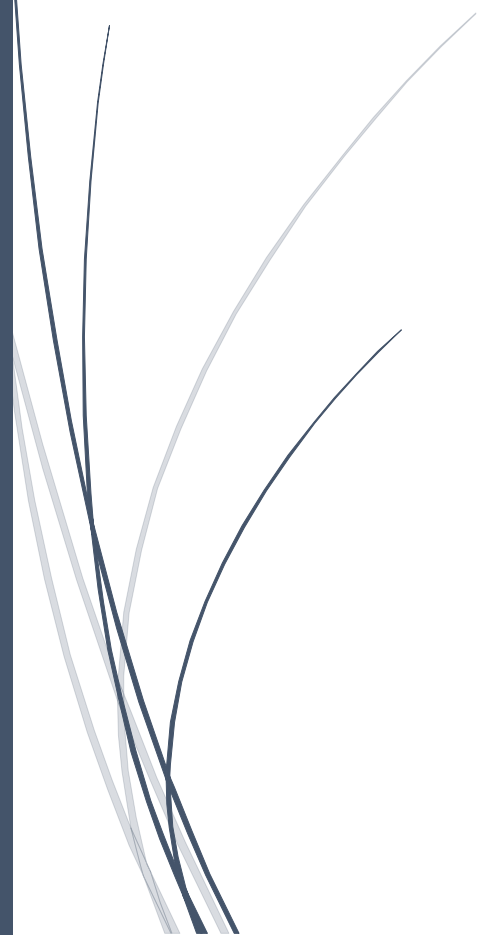
optimization of the granular stacking, and volume fraction, morphology, mineralogy and physical parameters of aggregates. Some experimental investigation could be proposed to try to assess the bond strength at the ITZ.

The effect of the crushed limestone sand could also be assessed on the performance of concretes with pozzolanic additions since this sand creates nucleation sites for hydration products that could enhance the low short-term compressive strength associated with these concretes.

It is interesting also to develop a detailed life-cycle assessment for all the studied concrete mixes to highlight the environmental advantages of the crushed limestone sand as an effective, quick, and feasible solution for the Lebanese construction field. However, in the long term, it is essential to manage the waste disposal in Lebanon and find a more ecological solution, limiting thereby the disappearance of the limestone mountains.



Résumé Substantiel



Résumé Substantiel

Introduction

Le secteur de la construction au Liban souffre de la dégradation de la qualité du sable naturel siliceux, de sa raréfaction suite à des mesures gouvernementales imposant une législation stricte sur son extraction et des effets néfastes sur l'environnement liés à sa surexploitation. Par conséquent, ce sable est fourni du marché noir ou importé à des prix très élevés, affectant ainsi le coût du béton. Etant trop fin pour être utilisé comme seul sable dans le béton, selon la norme ASTM C33 en vigueur au Liban, il est toujours mélangé avec un pourcentage approprié d'un sable calcaire concassé de carrière.

Les problèmes reliés à la surexploitation du sable naturel ne sont pas limités au Liban à cause de l'expansion mondiale des travaux de construction. Sa qualité et quantité se détériorent mondialement et son extraction affecte gravement l'environnement. Par conséquent, beaucoup de gouvernements ont imposé des taxes et des restrictions sur son exploitation, augmentant ainsi son prix. Afin de résoudre ces problèmes, plusieurs pays ont trouvé des alternatives qui consistent à remplacer partiellement ou totalement le sable naturel par d'autres types de sable provenant des carrières, du recyclage des bétons, déchets domestiques et des sous-produits industriels.

Le sable concassé calcaire est l'un de ces alternatives internationales. Il pourrait présenter des avantages sur les résistances du béton et sa durabilité grâce à sa minéralogie, morphologie et son contenu de fines. Actuellement, parmi les autres alternatives, ce sable peut être le plus fiable dans le contexte libanais puisqu'il n'y a pas d'autres solutions provenant du recyclage des déchets à court terme et puisque ce sable se trouve en abondance dans tout le pays. Par contre, malgré l'abondance de ce sable et les avantages économiques et environnementaux qui peuvent résulter de son unique usage dans le béton, cette solution n'est pas jusqu'à présent appliquée au Liban, principalement puisqu'il n'y a pas de référence scientifique à l'échelle du pays pour convaincre les parties concernées dans le marché libanais de la pertinence de cette solution.

Pour cette raison, cette thèse, réalisée en cotutelle académique et faisant l'objet d'une coopération industrielle avec une entreprise Libanaise, vise à introduire le sable concassé calcaire comme une solution de substitution à l'usage du sable naturel siliceux, en répondant aux interrogations suivantes :

- Est-ce que le sable calcaire concassé conforme à la norme peut être utilisé comme seul sable dans le béton, au lieu d'être utilisé comme sable additionnel au sable naturel siliceux ?
- Est-ce que les propriétés du béton à l'état frais, son comportement mécanique, sa durabilité et sa microstructure seront ils affectés par cette substitution pour le même dosage en ciment, rapport E/C et maniabilités ?
- Est-ce que le sable concassé à un pourcentage de fines dépassant la limite de la norme peut aussi être une solution effective ?

Cette étude aide à augmenter la connaissance sur les effets positifs de l'optimisation de la production du sable concassé et de la valorisation de ses fines. Elle incite à l'usage de la bonne qualité du sable concassé comme le seul sable dans le béton, dans le but de limiter la dépendance actuelle du secteur de la construction libanais à l'utilisation du sable naturel siliceux.

En vérifiant la performance des bétons sans sable naturel et en les comparant aux mélanges conventionnels, cette étude permet d'analyser les effets des différentes caractéristiques du sable (morphologie, minéralogie, propriétés physiques, granulométrie et contenu des fines) sur les propriétés

des bétons ordinaires et bétons à hautes-performances, couramment utilisés au Liban, aux états frais et durci. De même, l'étude porte sur les effets des caractéristiques du sable sur les déformations, durabilité et microstructure peu abordés dans la littérature.

Deux approches différentes ont été suivies dans cette étude. Premièrement, pour respecter les exigences de la granulométrie et contenu des fines de la norme ASTM, l'effet du sable concassé calcaire, dont la granulométrie a été construite au laboratoire pour être conforme à la norme, a été étudié. Deuxièmement, pour valoriser les fines provenant du concassage du sable concassé calcaire, une approche performantielle a été menée sur des bétons contenant un sable concassé avec un pourcentage de fines élevé (13-18%) dépassant la limite de la norme ASTM (7%).

Le programme expérimental a été mené dans le laboratoire des matériaux de la société ACTS au Liban, sauf les caractérisations chimiques, minéralogiques et morphologiques des granulats, la porosité accessible à l'eau du béton et son analyse microstructurale qui nécessitaient des équipements spécifiques disponibles au Laboratoire Matériaux et Durabilité de Construction LMDC en France.

La thèse est composée de cinq chapitres.

Le premier chapitre de la thèse comporte une étude bibliographique sur les problématiques du sable naturel sur les plans national et international. Il introduit aussi les alternatives évaluées dans plusieurs pays. De même, cette partie détaille les effets des différentes caractéristiques du sable sur les propriétés du béton à différentes échelles macro et micro structurales et à plusieurs échéances.

Afin de vérifier si les granulats utilisés dans cette étude respectent les spécifications de la norme ASTM C33 utilisée au Liban, et de pouvoir expliquer les différences entre les bétons qui pourraient provenir des écarts entre le sable naturel et les différents sables concassés étudiés, le deuxième chapitre présente les caractéristiques morphologiques, chimiques, minéralogiques et physiques des granulats grossiers et des sables.

Le troisième chapitre détaille les différentes formulations du béton pour évaluer les effets de différents sables sur le comportement de bétons ordinaire et à haute performance. Pour chaque classe, les écarts entre les différents types de béton sont limités au type de sable et au dosage du superplastifiant pour atteindre une même maniabilité.

Le chapitre IV est consacré à l'étude de différents bétons dont les sables sont conformes à la norme ASTM C33, pour trois formulations de béton ordinaire et une formulation de béton à haute-performance. Puisque le sable concassé actuel présente une granulométrie non conforme à la norme ASTM C33, la granulométrie de ce sable durant cette étude est modifiée au laboratoire de façon à respecter cette norme. Ce sable normalisé est introduit dans le béton dans deux différentes granulométries et ces deux types de bétons sont ainsi comparés avec le béton de référence comportant le mélange conventionnel sable naturel - sable concassé actuel.

Le chapitre V étudie la possibilité d'utiliser des sables dont les teneurs en éléments fins seraient non conformes à la norme ASTM C33, pour une formulation de béton ordinaire et une autre de béton à haute-performance. En effet, puisque le sable concassé actuel ne peut pas seul remplacer le sable naturel à cause de ses grains qui sont relativement gros, certaines carrières essaient de produire un nouveau sable concassé plus fin. Ce sable est caractérisé par un pourcentage de fines élevé (13-18 %) qui dépasse la limite imposée par la norme ASTM C33 (7 %). Pour éviter les contraintes industrielles, environnementales et économiques qui peuvent résulter de la réduction de pourcentage des fines, ce chapitre étudie la possibilité de valoriser ces fines en utilisant ce sable fin comme alternative au sable

naturel siliceux en comparant les performances de bétons contenant comme seul sable le sable concassé avec un pourcentage de fines élevé, avec celle de bétons de référence comportant le mélange conventionnel sable naturel - sable concassé actuel et de bétons contenant le sable conforme à la norme.

En outre, la viabilité de la substitution totale du sable naturel par du sable concassé est évaluée sur les plans technique, environnemental et économique afin de présenter une solution pratique et effective pour l'industrie. Cette évaluation est menée dans le quatrième chapitre pour le sable normalisé et dans le cinquième pour le sable fin.

Etude bibliographique

Plusieurs pays souffrent de la rareté des différents types du sable naturel, leurs effets négatifs sur le béton et les effets néfastes de leur surexploitation sur l'environnement. L'excavation du sable des fleuves réduit ainsi le niveau de l'eau, perturbe la faune et flore du voisinage et cause une érosion du lit du fleuve. En plus, ce sable peut contenir un pourcentage élevé d'impuretés et particules délétères qui peuvent affecter la performance du béton. Le sable de mer doit être lavé avant d'être utilisé dans le béton et peut contenir un pourcentage élevé d'ions qui peuvent causer la corrosion des aciers d'armatures. L'excavation de ce sable perturbe aussi l'écosystème de la plage et menace les infrastructures qui se situent sur la côte. Enfin, l'exploitation du sable provenant des carrières présente des impacts négatifs sur l'environnement et la qualité de ce sable décroît à un taux alarmant. Le sable des déserts quant à lui n'est pas largement utilisé dans le béton malgré sa grande disponibilité dans plusieurs pays. Il est en effet caractérisé par une granulométrie mal distribuée et une grande finesse, menant ainsi à de faibles maniabilité et résistance dans le béton.

Pour limiter ces inconvénients, des solutions consistant à remplacer, totalement ou partiellement, le sable naturel par plusieurs matériaux alternatifs, dans les bétons et mortiers, ont déjà été envisagées. Ainsi, l'exploitation des ressources du sable naturel sera atténuée et l'utilisation de ces matériaux alternatifs dans les bétons pourra réduire les effets négatifs de leur traitement. L'utilisation des sables calcaire, marbre et granite dans le béton aide à valoriser les fines générées lors du concassage des roches. Le béton, briques, verre et plastiques sont des déchets de constructions et démolitions et des déchets domestiques, qui peuvent être recyclés pour remplacer le sable naturel dans le béton. Ce sable peut aussi être remplacé par les sous-produits industriels, tel que les cendres, les laitiers, le sable de fonderie...

Toutefois, parmi ces alternatifs, le sable calcaire concassé semble être la solution la plus effective pour remplacer totalement le sable naturel dans le béton au niveau du marché libanais. Ce sable peut contenir un pourcentage élevé de fines dû au processus de concassage et diffère du sable naturel puisqu'il est formé de grains de calcite anguleux alors que le sable naturel est caractérisé par des grains de silice semi-arrondis.

L'étude bibliographique couvre l'effet des caractéristiques du sable sur les différentes propriétés du béton. Les principales analyses peuvent être résumées comme suit.

➤ Effets sur les propriétés du béton à l'état frais

La minéralogie du sable ne semble pas être un facteur influençant sur les propriétés du béton à l'état frais. Par contre, la morphologie des grains de sable peut contrôler la maniabilité du béton. La surface rugueuse de ces grains et leur forme anguleuse favorisent un frottement intergranulaire qui réduit la maniabilité du béton. La granulométrie bien distribuée produit un béton bien compact alors qu'une granulométrie mal distribuée augmente la demande en ciment pour remplir les vides intergranulaires dans le mélange du béton. Un pourcentage de fines adéquat contribue à la lubrification des particules

plus grossières en remplissant les vides intergranulaires et laissant un excès de ciment. En revanche, quand ce pourcentage dépasse sa valeur optimale dans le mélange de béton, l'excès de fines peut augmenter la demande en eau et affecter la maniabilité du béton. De même, les particules délétères présentent un effet négatif sur les propriétés du béton à l'état frais puisqu'elles augmentent la demande en eau du mélange.

➤ Effets sur le comportement mécanique du béton

La compatibilité chimique des grains de sable avec les produits de la réaction d'hydratation crée une forte liaison avec la pâte de ciment. La forme des grains présente aussi une influence importante sur le comportement mécanique du béton. Le sable caractérisé par une surface rugueuse et des formes de grains anguleuses permet d'améliorer l'adhérence avec la pâte de ciment et de conférer de meilleures performances mécaniques au béton que celles conférées par le sable à grains plus sphériques et surface lisse. En plus, la résistance mécanique du béton peut être améliorée par un sable de bonne distribution granulométrique puisqu'il rend le mélange plus compact et réduit les vides intergranulaires. Cependant, un pourcentage de fines très élevé peut augmenter la quantité des grains non couverts par du ciment, affectant ainsi défavorablement la performance mécanique du béton. Les impuretés et les particules délétères peuvent atténuer l'adhérence des grains de sable avec la pâte de ciment et réduire la résistance du béton.

Le retrait du béton semble moins affecté par les caractéristiques de sable que par celles des gravillons. Les quelques études qui portent sur l'effet du sable sur le retrait relient cet effet à la porosité du sable.

➤ Effets sur la durabilité du béton

L'effet des caractéristiques du sable sur la durabilité du béton n'est pas largement évalué dans les études bibliographiques. L'effet du pourcentage de fines sur la durabilité est le plus abordé. Le contenu des fines peut dépasser les limites imposées par les normes à condition qu'il reste bénéfique ou sans effet sur la durabilité du béton. Le pourcentage élevé des fines peut soit remplir les vides dans le béton et améliorer sa durabilité, soit avoir l'effet opposé en couvrant les particules plus grossières et limitant la liaison entre ces grains et la pâte du ciment. La minéralogie des grains de sable peut aussi avoir un impact sur la durabilité du béton. Certains types de sables, comme les sables calcaires, réagissent avec les produits de la réaction d'hydratation du ciment et réduisent la porosité du béton, alors que d'autres, comme certains sables siliceux ou gypseux, peuvent avoir un effet négatif en induisant des expansions et microfissures.

➤ Effets sur la microstructure du béton

Pour expliquer l'origine des différences dans les propriétés des bétons formés de plusieurs types de sable, l'étude bibliographique porte aussi sur la microstructure du béton. Les quelques études qui évaluent l'effet du sable sur la microstructure à l'interface entre la pâte du ciment et les grains de sable trouvent que la réactivité chimique de certains types de sable, comme le sable calcaire, peut rendre la microstructure du béton plus dense et réduire la porosité suite à la production des produits d'hydratation secondaires. En outre, comme déjà mentionné, la liaison à l'interface peut dépendre de la morphologie des grains de sable, et le pourcentage des fines peut être bénéfique pour la densification de la microstructure du béton.

Suite à cette étude bibliographique, plusieurs points peuvent être pris en considération dans cette thèse sur l'évaluation de la substitution totale du sable naturel siliceux par du sable calcaire concassé.

Premièrement, il est primordial de déterminer les caractéristiques des deux types de sable avant de les utiliser dans les formulations de béton et de conduire le programme expérimental sur les bétons de classes de résistance différentes. Cette caractérisation permet de révéler leurs effets sur les propriétés des différents bétons, en particulier celles non largement développées dans la bibliographie, telles que le retrait et la durabilité.

Dans certaines études, les effets des différentes caractéristiques du sable ne peuvent pas être clairement conclus, suite à l'existence de plusieurs variables dans les différents mélanges comparés qui ne peuvent pas être découplés afin de juger l'effet de chaque paramètre séparé. Il est donc nécessaire de limiter les variables dans le mélange et de fixer, en particulier, le dosage en ciment, le rapport eau efficace sur ciment et la maniabilité. Pour compenser la perte de la maniabilité suite à l'utilisation de certains types de sable, un superplastifiant devra être incorporé dans les formulations des bétons, sans augmenter le contenu en eau.

Enfin, puisque les études bibliographiques montrent que les propriétés des bétons ne sont pas significativement affectées par le pourcentage des fines qui dépasse les limites imposées par les différentes normes, il est important de déterminer l'effet, sur les bétons du marché libanais, du sable calcaire concassé ayant un pourcentage de fines supérieur aux limites réglementaires.

Ainsi, le programme expérimental sur les granulats et les bétons vise à vérifier si le remplacement total du sable naturel siliceux par différentes granulométries de sable calcaire concassé peut résoudre le problème industriel et de déterminer les effets des caractéristiques de ces sables sur la performance du béton.

Caractérisation des granulats

Au Liban, les gravillons, globalement retenus sur le tamis de diamètre 4.75 mm, sont fournis pour les formulations de béton en deux tailles différentes : petite (D_{max} 10-12 mm) et grosse (D_{max} 20 mm). Ces gravillons proviennent des carrières du concassage des montagnes libanaises calcaires. Les sables, globalement passant le tamis de diamètre 4.75 mm, sont divisés en deux types : le sable concassé d'origine calcaire et le sable naturel siliceux fourni par simple excavation de la mer, fleuve, ou principalement des carrières terrestres.

Pour ce travail, le sable naturel est fourni par une carrière localisée à Mayrouba, Mont-Liban, alors que le sable concassé et les deux tailles des gravillons sont fournis par une carrière à Bikfaya, Mont-Liban.

Afin de s'assurer que les différentes propriétés des granulats sont conformes aux spécifications de l'ASTM, un programme de caractérisation expérimentale est mené sur des échantillons représentatifs de chaque type de granulats. Les analyses morphologiques sont menées en utilisant le microscope optique et le microscope électronique à balayage. Pour déterminer la composition chimique, la spectrométrie à couplage inductif et l'analyse thermogravimétrique sont utilisées. La minéralogie des granulats est évaluée par la technique de diffraction par rayonnements X. Les propriétés physiques mesurées (granulométrie, pourcentage des particules délétères, densité relative, absorption, résistance à l'abrasion et à l'impact, résistance à l'altération) sont déterminées suivant la norme ASTM, alors que la valeur du bleu de méthylène est évaluée selon la norme européenne.

Le programme expérimental mené sur les sables montre que le sable naturel NS est principalement formé de grains de silice semi-arrondis avec un pourcentage de silice SiO_2 de 87.25%, tandis que le sable concassé CS est de nature calcaire composé en 97.23% de grains de calcite CaCO_3 anguleux. Le sable naturel se distingue par une distribution granulométrique très fine qui le situe globalement au-dessus de la limite maximale imposée par la norme ASTM C33. Le sable concassé classique présente une fraction granulométrique plus grossière qui le situe globalement au-dessous de la limite inférieure. Par conséquent, pour respecter le fuseau de cette norme, les deux types de sable sont toujours mélangés en proportions adéquates dans toutes les formulations de béton vendues sur le marché libanais (généralement 50-50). Outre leurs différences minéralogique et granulométrique, les deux types de sable diffèrent aussi par leurs propriétés physiques. Le sable concassé présente des valeurs d'absorption et un pourcentage de fines (2.6 et 7.2% respectivement) supérieurs à ceux du sable naturel (1.1 et 2.3-6.3% respectivement), alors que celui-ci présente une finesse (module de finesse de 1.6-1.8 et 3.4 pour NS et CS respectivement), densité relative (2.59-2.62 et 2.55 pour NS et CS respectivement), particules délétères (contenu en argile de 5-5.3 et 0.7%, valeur de méthylène de 1.3-1.8 et 0.9 g et équivalent de sable de 58-60 et 73% pour NS et CS respectivement) et une perte par altérabilité (11 et 5% pour NS et CS respectivement) plus élevés. Cette comparaison montre que même si le sable concassé est caractérisé par un pourcentage de fines plus élevé, ces fines sont de bonne qualité puisqu'elles résultent de la fragmentation des roches mères calcaires durant leur concassage secondaire. Les pourcentages élevés d'argile et de la perte par altérabilité du sable naturel siliceux dépassent le pourcentage limite imposé par la norme en vigueur au Liban. Malgré la qualité réduite de ce sable naturel, il est actuellement utilisé dans les formulations des bétons avec le sable concassé puisque jusqu'à présent il n'y a pas d'alternatives validées scientifiquement.

Les gravillons concassés calcaire utilisés (D_{\max} 10-12 mm et D_{\max} 20 mm) proviennent de la même carrière que celle du sable concassé. Ils sont généralement de bonne qualité : leurs résistances à l'altérabilité, à l'impact et à l'abrasion sont élevées avec une absorption et un pourcentage de particules délétères réduits.

En outre, une étude supplémentaire a été menée pour caractériser les gravillons et le sable concassé provenant de plusieurs ressources de sept différentes régions libanaises. Cette étude a montré que les propriétés des granulats concassés sont comparables, à l'exception des densités et absorptions. Ainsi, compte tenu de ces similitudes, nous pouvons estimer que les résultats finaux de la thèse obtenus sur des granulats issus d'une seule carrière pourront être généralisés aux autres carrières à condition que les densités et absorptions soient déterminées pour chaque ressource avant de formuler le béton.

Production du sable calcaire concassé

Le sable concassé conventionnel, "Conventional crushed sand" dans le mémoire, est considéré comme un sable relativement grossier, donc la granulométrie doit être optimisée pour pouvoir l'utiliser comme seul sable dans le béton. Pour cette raison, certaines carrières commencent à produire un sable concassé, "Fine crushed sand" dans le mémoire, avec une granulométrie plus fine et un pourcentage de fines (particules passant le tamis de 75 μm) plus élevé.

➤ **Sable concassé conventionnel**

Le sable concassé conventionnel est utilisé comme sable supplémentaire dans toutes les formulations de béton du marché libanais afin de compenser la finesse du sable naturel et sa non-conformité aux normes.

La première étape de production de ce sable consiste à utiliser un broyeur rotatif pour réduire la taille des roches mères, exploitées des montagnes libanaises. Les parties les plus fines (poussière et particules du sol) sont séparées des roches concassées et convoyées vers un tas séparé qui peut être utilisé comme matériau de remblai dans la construction des routes. Les matériaux concassés sont criblés à 100 mm et transportés vers un nouveau broyeur (broyeur à marteaux) alors que les refus à 100 mm sont réintroduits dans le premier broyeur.

Les matériaux concassés provenant du premier broyage passent dans le broyeur à marteaux pour subir un second concassage. En aval de ce broyeur, une bande transporteuse convoie les produits du concassage sur trois cribles différents, 20, 10 et 5 mm, pour collecter respectivement les gros gravillons 10/20 mm et les petits gravillons 5/10 mm. Pour produire le sable concassé conventionnel, une partie du petit gravillon est concassé de nouveau dans un broyeur à marteaux et puis tamisé sur le crible de diamètre 5 mm. Pour chacun des cribles cités, les particules surdimensionnées repassent dans le broyeur pour être concassées.

Pour cette étude, le sable concassé conventionnel est fourni à partir d'un seul stock d'une même carrière. Afin d'obtenir une granulométrie qui se situe à l'intérieur du fuseau de la norme ASTM C33, ce sable concassé est mélangé, à masse équivalente ou avec une proportion de 65% avec le sable naturel dans les bétons de référence.

➤ **Sable concassé fin**

Pour être utilisé seul dans les mélanges de béton, certaines carrières essaient depuis peu de produire un sable concassé fin dont la granulométrie respecte la norme ASTM C33, à l'exception du pourcentage de fines qui varie entre 13 et 18% et dépasse la limite normative imposée (7%).

La première étape de production de ce sable est similaire à la production du sable concassé conventionnel. Cependant, pour produire un sable plus fin, une grille supplémentaire est ajoutée. Une partie des matériaux passant la grille de 4.75 mm est convoyée vers un crible de 2.36 mm. Les particules passant ce dernier crible forment le sable concassé fin, alors que les particules retenues (entre 3 et 5 mm) sont ajoutées au sable concassé conventionnel.

Il faut noter que, parfois, selon les caractéristiques de la roche concassée, le concassage du petit gravillon ne produit pas un volume suffisant de matériaux passant le crible de 2.36 mm. Par conséquent, avant de transporter le sable concassé au crible de 2.36 mm, une étape de concassage supplémentaire doit être ajoutée pour augmenter la production du sable concassé fin.

Dans la dernière partie de cette étude, ce sable est utilisé dans les formulations de béton pour évaluer, en appliquant une approche performantielle, si les performances du béton peuvent être maintenues suite à l'utilisation d'un sable concassé qui ne respecterait pas les limites imposées par la norme en termes de pourcentage des fines. Il est issu de deux stocks différents provenant de la même carrière fournissant le sable concassé conventionnel, avec deux pourcentages de fines distincts : 13 et 18 %.

Construction du sable calcaire concassé

Comme l'étude consiste à remplacer le sable naturel par le sable concassé et puisque les sables avec différentes caractéristiques peuvent se comporter différemment dans le béton, deux types de sables calcaires concassés ont été « construits » durant cette thèse, afin d'évaluer l'effet du type du sable et de sa granulométrie sur la performance du béton.

➤ **Sable concassé équivalent**

Les effets reliés à la morphologie et aux propriétés physicochimiques du sable sont déterminés à l'aide du sable concassé équivalent, "Equivalent crushed sand" dans le mémoire. Ce sable correspond au sable calcaire concassé dont la granulométrie a été reconstruite au laboratoire pour être strictement identique à celle de la combinaison de sable du béton de référence utilisé dans les formulations conventionnelles des bétons, afin de pouvoir étudier les seuls effets de la nature et de la morphologie des grains de sable à même granulométrie et même pourcentage en fines.

Pour construire ce sable au laboratoire, une large quantité du sable concassé conventionnel est séchée et divisée par tamisage en plusieurs fractions retenues sur les tamis de diamètres 4.75, 2.36, 1.18, 0.60, 0.30, 0.15 et 0.075 mm qui sont ensuite remélangées selon les proportions adéquates. Le résultat de cette construction est un sable concassé dont la granulométrie respecte la norme ASTM et est identique à celle du mélange du sable dans le béton de référence.

➤ **Sable concassé modifié**

L'effet de la granulométrie est conclu en utilisant le sable calcaire concassé modifié, noté "Modified crushed sand" dans le mémoire. Ce sable est caractérisé par une granulométrie qui se situe dans une zone plus médiane du fuseau de la norme ASTM C33. Pour construire ce sable, une proportion appropriée du sable concassé fin est lavée par de l'eau pour réduire son pourcentage de fines à 3-5 %.

Formulation des bétons

Après la détermination des caractéristiques des granulats, en particulier la granulométrie, la densité et l'absorption, et après la préparation des différents types de sable concassé, les différents bétons sont formulés.

Le programme expérimental sur les sables a détecté plusieurs différences entre les deux types de sable, tel que la forme de leurs grains, leurs compositions chimiques, minéralogie, absorption, finesse, granulométrie, quantité et qualité des fines. Sachant que les différences entre ces deux sables peuvent directement influencer la performance du béton frais et durci, les mélanges du béton dans cette étude sont formulés pour comparer, pour chaque classe, plusieurs types de bétons différant seulement par le type de sable et/ou sa granulométrie. Afin d'obtenir un béton de bonne maniabilité, l'affaissement visé est de 20 ± 2 cm pour tous les types de béton. Ainsi, pour chaque mélange, le dosage du superplastifiant-réducteur d'eau haut de gamme a été adapté pour atteindre cette valeur. Le ciment utilisé dans tous les mélanges est un ciment calcaire commercial fourni de Holcim dans des sacs de 50 kg chacun.

L'étude expérimentale sur le béton comporte la détermination de ses propriétés à l'état frais, son comportement mécanique et sa durabilité. Les propriétés à l'état frais analysées inclues la température, la densité, l'air occlus, le temps de prise et l'affaissement (initial et après 30, 60 et 90 minutes). Les résistances à la compression sont déterminées aux échéances de 3, 7, 28 et 90/135 jours. Le module d'élasticité et la résistance à la flexion sont mesurés à l'échéance de 28 jours. Les déformations des bétons sont suivies jusqu'à 77 jours. Les essais de durabilité sont menés à 90 jours pour les bétons ordinaires et à 135 jours pour les bétons à haute-performances. Il était prévu de mener les essais de durabilité de tous les bétons à 90 jours mais dû à des circonstances non prévues ils ont été reportés à l'échéance de 135 jours. Ces essais comprennent la porosité accessible à l'eau, absorption de l'eau par immersion, profondeur de la pénétration de l'eau sous pression, résistance à la pénétration des ions chlorures et résistivité. Les essais menés sont les plus recommandés au Liban, normalement établis

suivant la norme américaine ASTM à l'exception de certains essais qui ont été conduits selon les normes européennes. Cette étude expérimentale est divisée en deux parties principales.

La première partie évalue l'effet de la substitution du mélange du sable naturel et du sable concassé conventionnel par un sable concassé normalisé dont la granulométrie est conforme à la norme. Pour ce but, 9 formulations de bétons, couramment utilisés au Liban, sont comparées pour 3 différentes résistances de béton ordinaire, "Mix 30", "Mix 35-I", and "Mix 35-II", et 2 autres formulations pour un béton de haute-performance "Mix 50".

Pour les 3 bétons ordinaires :

- "Mix 30" dans le mémoire, est caractérisé par un rapport eau efficace sur ciment de 0.5 et un contenu de ciment de 350 kg/m^3 , pour atteindre une résistance moyenne de 30 MPa à l'échéance de 28 jours.
- "Mix 35-I" dans le mémoire, comporte un rapport eau efficace sur ciment (0.4) plus réduit et des proportions des granulats plus élevées pour le même contenu du ciment (350 kg/m^3) que celui de "Mix 30" afin d'atteindre une résistance plus élevée.
- "Mix 35-II" dans le mémoire, contient le même rapport eau efficace sur ciment que celui dans "Mix 35-I" pour un contenu du ciment plus atténué (300 kg/m^3), pour mettre en relief les effets des granulats et pour atteindre une résistance un peu plus élevée avec un contenu de ciment plus réduit, réduisant ainsi les menaces environnementales reliées à la production du ciment.

Pour chacun de ces 3 mélanges de béton ordinaire, 3 types de bétons sont comparés avec des proportions fixes d'eau efficace, ciment, et gravillons :

- Le béton de référence, noté "Control Mix" dans le mémoire, qui correspond au mélange conventionnel utilisé au Liban, composé de la combinaison de sable du béton de référence avec des proportions massiques égales de sable naturel et de sable concassé conventionnel.
- Le béton équivalent, noté "Equivalent Mix" dans le mémoire, qui ne contient pas de sable naturel et renferme le sable concassé "Equivalent crushed sand" comme seul sable.
- Le béton modifié, noté "Modified Mix" dans le mémoire, qui ne comporte pas de sable naturel et contient le sable concassé "Modified crushed sand" comme unique sable.

Ainsi, le mélange de sable conventionnel du "Control Mix" est remplacé par un volume équivalent de "Equivalent crushed sand" et "Modified crushed sand" pour le "Equivalent Mix" et "Modified Mix" respectivement.

Le béton "Mix 50" est caractérisé par un contenu en ciment élevé (400 kg/m^3) et un rapport eau efficace sur ciment réduit (0.3). Pour ce béton de haute-performance, deux types de bétons sont comparés :

- Le béton de référence ("Control Mix") qui contient un mélange massique de 35% de sable naturel et 65% de sable concassé conventionnel.
- Le béton modifié ("Modified Mix") qui ne comporte pas de sable naturel et utilise le sable concassé "Modified crushed sand" comme unique sable.

Dans la seconde partie, une approche performantielle est suivie pour examiner l'effet d'un sable concassé avec un pourcentage de fines élevé (13-18 %) que la limite ASTM (7%) sur la performance de "Mix 30" et "Mix 50". Pour chacun de ces mélanges, trois types de béton sont comparés :

- Le béton de référence ("Control Mix") qui contient un mélange massique de 35% de sable naturel et 65% de sable concassé conventionnel.
- Le béton avec mélange fin, noté "Fine Mix" dans le mémoire, qui ne contient pas de sable naturel et est formé du sable concassé fin "Fine crushed sand" comme seul sable.

- Le béton modifié ("Modified Mix") qui ne comporte pas de sable naturel et utilise le sable concassé "Modified crushed sand" comme unique sable.

Etude expérimentale sur les bétons comportant le sable calcaire concassé conforme à la norme

Pour évaluer la pertinence de la substitution totale du sable naturel par du sable concassé conforme à la norme utilisée dans le marché libanais, un large programme expérimental a été établi. Le programme consiste à effectuer plusieurs essais caractérisant les propriétés des différents bétons à l'état frais, leurs comportements mécaniques et leurs durabilités.

➤ **Bétons ordinaires**

Pour chacun des trois mélanges du béton ordinaire, "Mix 30", "Mix 35-I", and "Mix 35-II", détaillés dans le paragraphe précédent, la comparaison est menée entre trois types de béton, avec même affaissement et rapport eau efficace sur ciment et différant principalement par le type et la granulométrie du sable et le dosage en superplastifiant. La granulométrie des sables reconstitués, dans tous ces mélanges, respecte les spécifications granulométriques de la norme ASTM C33. Le dosage du superplastifiant est ajusté pour atteindre un affaissement au cône d'Abrams de 20 ± 2 cm.

• **Propriétés à l'état frais**

Pour ces trois mélanges, les résultats montrent que les bétons contenant le sable calcaire concassé comme seul sable, demandent un dosage en superplastifiant plus faible que celui des bétons contenant le sable naturel. Cette observation peut être due à la quantité plus élevée des particules délétères dans le sable naturel siliceux incorporé dans le béton de référence. De même, la maniabilité des bétons contenant le sable calcaire normalisé décroît plus lentement alors que leurs temps de prise sont plus courts que ceux des bétons de référence. Ces résultats peuvent être associés à la quantité plus élevée du superplastifiant dans les bétons de référence qui peut avoir un effet retardateur. En réduisant l'agglomération des grains de ciment, ce superplastifiant peut aussi être responsable de la densité à l'état frais plus élevée et d'une teneur en air occlus plus faible dans le béton de référence, en addition à la densité plus élevée des grains de sable siliceux qui augmentent la densité du béton de référence.

• **Comportement mécanique**

Le comportement mécanique du béton ordinaire est maintenu quel que soit le type de sable. Les résistances à la compression pour les trois types de béton sont comparables et la résistance à compression moyenne, correspondante à chaque rapport eau sur ciment et contenu du ciment, est atteinte pour chaque mélange entre 7 et 28 jours. Par contre, pour le mélange "Mix 35-I", pour un rapport eau sur ciment de 0.4 et un contenu en ciment de 350 kg/m^3 , le béton de référence présente des résistances légèrement supérieures (différence maximale de 8 MPa à l'échéance de 90 jours) à celles des bétons contenant le sable calcaire concassé comme le seul sable. Cette différence peut être attribuée à la quantité plus élevée du superplastifiant qui déflocule davantage les grains de ciment, améliore leur hydratation et augmente la résistance à la compression à long terme. Le module d'élasticité du béton ne semble pas affecté par la substitution totale du sable naturel siliceux par le sable calcaire concassé. Enfin, la résistance à la flexion et le retrait semblent améliorés dans les bétons contenant le sable calcaire concassé comme seul sable.

- **Durabilité**

En termes de durabilité, les bétons de référence et les bétons incorporant le sable calcaire concassé sont dans la même gamme et présentent des propriétés comparables avec un comportement légèrement plus durable pour le béton de référence. Cette légère différence peut être attribuée au dosage plus élevé du superplastifiant dans le béton de référence qui mène à une meilleure défloculation des grains de ciment et améliore leurs hydratations, réduisant ainsi les pores et augmentant la durabilité.

Compte tenu des essais de durabilité pratiqués, la porosité accessible à l'eau, absorption de l'eau par immersion, profondeur de la pénétration de l'eau sous pression, résistance à la pénétration des ions chlorures et résistivité, on peut en conclure que le remplacement total du mélange conventionnel du sable naturel et sable concassé par le seul sable calcaire concassé conforme à la norme ne produit pas de modifications significatives dans le réseau des pores dans le béton.

Une relation linéaire existe entre la résistance à la compression et les essais de durabilité à la même échéance de 90 jours. La résistance à la compression la plus élevée mène à une durabilité plus importante.

- **Microstructure**

L'analyse microstructurale montre que l'angularité, la rugosité de la surface et la minéralogie du sable calcaire concassé mènent à une interface entre les grains de sable et la pâte du ciment de meilleure qualité que celle avec le sable naturel siliceux. Cette amélioration peut expliquer la légère augmentation de la résistance à la flexion des bétons incorporant le sable calcaire concassé conforme à la norme comme seul sable, ainsi que la réduction de son retrait. Cependant, cette amélioration n'a pas une action significative sur la performance du béton à l'échelle macrostructurale en termes de durabilité et des autres propriétés mécaniques.

- **Comparaison entre les bétons contenant le sable calcaire concassé conforme à la norme**

Les comparaisons conduites entre les deux types de béton qui ne contiennent que le sable calcaire concassé dont la granulométrie est conforme aux limites imposées par la norme ASTM C33, montrent qu'ils présentent globalement le même comportement. L'utilisation du sable calcaire concassé avec une granulométrie mieux distribuée entre ces limites ne modifie pas significativement la performance du béton, à l'exception de la maniabilité qui s'améliore et conduit à une réduction du dosage en superplastifiant.

➤ **Bétons à hautes-performances**

Pour les bétons à haute-performances, les comparaisons entre le béton de référence et le béton contenant le sable calcaire concassé modifié montrent que les effets du type et de la granulométrie du sable sur les propriétés du béton à l'état frais, comportement mécanique et durabilité ne sont pas significatifs.

➤ **Synthèse de la performance des bétons**

Suite aux résultats du programme expérimental, et malgré les différences entre le sable naturel et le sable concassé en termes de la morphologie de leurs grains, leurs minéralogies, leurs propriétés physiques et leurs granulométries, le sable calcaire concassé conforme à la norme peut effectivement

remplacer le mélange classique du sable naturel siliceux – sable concassé conventionnel dans le béton ordinaire et le béton à haute-performance, sans affecter les performances du béton. De plus, l'optimisation de la granulométrie du sable calcaire concassé dont la granulométrie se situe déjà dans les limites de la norme, n'est pas indispensable pour maintenir les propriétés du béton.

➤ **Etude de faisabilité technique, environnementale et économique**

L'utilisation d'un sable qui favorise une bonne performance au béton n'est pas le seul souci dans le secteur de la construction. La faisabilité technique de la procédure de production de ce sable ainsi que les impacts économiques et environnementaux de son utilisation sont des éléments importants pour choisir le bon sable pour le béton. Pour cette raison, cette thèse s'est intéressée aussi à la praticabilité technique et aux avantages ou inconvénients économiques et environnementaux.

La production d'un sable concassé conforme à la norme doit générer un sable de bonne qualité avec un pourcentage de fines qui ne dépasse pas la limite imposée par la norme (7%). Pour réduire le pourcentage de fines résultant de la production du sable concassé, deux méthodes de réduction peuvent être utilisées : par eau ou par air. Le lavage par eau doit être contrôlé pour éliminer exactement le contenu de fines nécessaire, l'eau utilisée pour le lavage doit être ensuite traitée et le sable doit être séché avant son transport de la carrière. La réduction par air peut séparer les fines et les recombinaison en quantité adéquate si nécessaire avec moins de contrainte.

Economiquement, la rareté du sable naturel siliceux et son importation augmentent son coût. En revanche, puisque le sable calcaire concassé est plus abondant au Liban, son prix est plus acceptable. Même si l'utilisation des techniques de réduction des fines par eau ou par air nécessite l'implantation de machines supplémentaires qui augmenteront le coût de ce sable et réduiront le rendement de la production, le sable calcaire concassé conforme à la norme restera moins coûteux que le sable naturel siliceux et son approvisionnement pourra être garanti. Il convient également de mentionner que l'incorporation du sable concassé réduit le dosage de superplastifiant dans le béton ce qui présente un avantage économique pour ce type de sable.

Du point de vue environnemental, l'utilisation du sable concassé comme seul sable aide à réduire les effets néfastes de l'exploitation du sable naturel et de la destruction des forêts de pins. En plus, pour produire ce sable, il n'est pas nécessaire d'ouvrir de nouvelles carrières puisque les carrières existent déjà pour la production des gravillons. Si jamais de nouvelles carrières sont requises, elles pourront être localisées dans des montagnes sans végétation et loin des zones peuplées. De cette façon, leur location sera plus bénéfique que celle des carrières de sable naturel actuelles, même si le transport de ce sable sera un peu plus coûteux. D'autre part, des inconvénients environnementaux peuvent résulter de la réduction de pourcentage des fines dans les carrières. Ainsi, l'utilisation des techniques de réduction des fines par l'eau réduit la poussière dans l'atmosphère mais augmente la consommation de l'eau (qui peut être recyclée). Les fines éliminées sont alors placées dans des bassins de décantation ou déchargées dans la nature d'une façon néfaste. Il conviendra de privilégier la réduction des fines sous air (cyclone) afin de limiter les effets sur l'environnement.

Même si les techniques de réduction de fines peuvent générer des prix supplémentaires sur la production du sable concassé, l'utilisation du sable calcaire concassé conforme à la norme reste une solution pertinente pour résoudre les problèmes liés à la rareté et au prix du sable naturel siliceux.

Néanmoins, pour réduire les contraintes qui peuvent être imposées par la solution de la production d'un sable concassé conforme à la norme avec réduction du pourcentage élevé des fines, il est nécessaire

d'évaluer l'effet du sable concassé présentant une teneur en fines supérieures à la norme sur les performances du béton, sans avoir à réduire ces fines.

Etude expérimentale sur les bétons comportant le sable calcaire concassé avec un pourcentage de fines élevé

Pour étudier l'effet d'un pourcentage de fines élevé (13-18%) généré durant la production du sable concassé et qui dépasse la limite imposée par la norme ASTM C33 (7%), un béton contenant du sable concassé avec un pourcentage de fines élevé est comparé au béton de référence et à un béton avec du sable concassé conforme à la norme. Ces comparaisons sont faites pour une formulation d'un béton ordinaire et une formulation d'un béton à haute-performance.

➤ **Bétons ordinaires**

Pour la formulation étudiée et dans les conditions expérimentales fixées (même dosage en ciment, même rapport E/C, maniabilité constante maintenue par ajustement de la teneur en superplastifiant), la présence de fines calcaires supplémentaires dans le sable calcaire concassé n'affecte pas significativement les propriétés à l'état frais, mécaniques et de durabilité du béton ordinaire.

Pour maintenir la même maniabilité, le sable concassé avec une teneur en fines supérieure à la norme demande un dosage en superplastifiant plus faible que celui du béton de référence. Comme dans le cas des bétons ordinaires contenant le sable concassé conforme à la norme, la résistance à la compression à 90 jours du béton avec sable concassé à teneur en fines non conforme est légèrement plus faible que celle du béton de référence avec sable naturel. Au contraire, la résistance à la flexion est plus élevée pour le béton incorporant le sable calcaire concassé avec une teneur en fines élevée, probablement grâce à une meilleure liaison entre les grains de sable et la pâte du ciment.

➤ **Bétons à hautes-performances**

Les trois types de bétons à haute-performance présentent globalement un comportement très proche. L'effet du pourcentage de fines élevé sur les propriétés du béton à haute-performance, aux états frais et durci, est négligeable. La seule différence est détectée dans la résistance à la flexion. L'excès des fines dans le sable concassé, qui ne remplissent pas les pores intergranulaires dans cette dense microstructure, peut affecter la liaison à l'interface et réduire la résistance à la flexion du béton.

➤ **Etude de faisabilité technique, environnementale et économique**

L'étude de faisabilité sur le sable calcaire concassé conforme à la norme a montré que ce sable offrait plusieurs avantages économiques et environnementaux, cependant réduits par la nécessité d'éliminer une partie des fines. Techniquement, la production d'un sable concassé avec un pourcentage de fines plus élevé que la norme exige seulement l'utilisation d'un crible supplémentaire à 3 mm. Par contre, cette utilisation élimine les inconvénients liés au lavage du sable. Du point de vue économique, le prix du sable concassé à teneur en fines supérieure à la norme est plus réduit que celui du sable concassé conforme à la norme. De même, la production du sable concassé sera plus effective puisque l'énergie consommée pour la production du sable concassé n'est pas dissipée sur des fines non valorisées. Par conséquent, l'optimisation de la production d'un sable concassé sans réduction de la teneur en fines (13-18%) est une solution effective, écologique et économique qui peut résoudre les problèmes liés au sable naturel dans le marché libanais.

Conclusions

Les ressources de sable naturel siliceux sont presque épuisées au Liban et le gouvernement impose des restrictions sur son exploitation. Ces problèmes mènent à une augmentation du prix du sable naturel et par conséquent celui du béton et à une baisse de sa qualité. En outre, ce sable est très fin et doit être combiné avec un sable concassé plus grossier pour respecter les limites granulométriques imposées par la norme ASTM C33.

Dans le contexte libanais, le sable calcaire concassé semble être la solution la plus pertinente pour remplacer totalement le sable naturel siliceux. En conséquence, cette étude, réalisée en cotutelle scientifique et avec un support industriel libanais, a évalué l'effet du remplacement total du sable naturel siliceux par du sable calcaire concassé et vérifié si les performances du béton pouvaient être maintenues suite à cette substitution.

Le programme expérimental mené sur les granulats a souligné les différences dans la forme, composition chimique, minéralogie, et caractéristiques physiques entre le sable naturel et le sable concassé. Le sable naturel est un sable siliceux formé de grains semi-arrondis avec une granulométrie plus fine que les limites imposées par la norme ASTM C33. Le sable concassé est caractérisé par des grains de calcite anguleux et possède une granulométrie plus grosse que ces limites ASTM. En plus, les deux types de sable diffèrent par quelques traits physiques : la finesse, la densité, le pourcentage en particules délétères, et l'altérabilité sont plus élevés dans le sable naturel, alors que l'absorption et le contenu des fines sont plus réduits. Puisque les fines dans le sable calcaire concassé sont générées lors de la procédure du concassage secondaire de roches calcaire, elles sont de meilleure qualité que celles du sable naturel siliceux.

Pour établir une comparaison basée sur le seul effet des caractéristiques du sable, plusieurs types de béton de différentes résistances en compression ont été formulés en limitant les différences seulement au type du sable et/ou sa granulométrie. Le rapport eau efficace sur ciment, le dosage en ciment et les proportions des gravillons sont fixés. L'affaissement est similaire pour les différents types de béton et un superplastifiant est utilisé pour atteindre l'affaissement visé de 20 ± 2 cm.

Les résultats ont montré que le remplacement total du sable naturel siliceux par du sable calcaire concassé, dont la granulométrie respecte le fuseau défini par la norme ASTM C33, peut être considéré comme une solution pertinente par rapport à la problématique de l'exploitation du sable naturel au Liban. Pour les bétons ordinaires, l'effet des particules délétères présentes dans le sable naturel est plus prononcé que celui des formes des grains du sable. Ces particules augmentent la demande en eau du béton frais. Par conséquent, le béton incorporant le sable naturel avec des grains semi-arrondis et un pourcentage élevé de particules délétères demande un dosage plus élevé en superplastifiant que le béton contenant le sable calcaire concassé conforme à la norme composé de grains angulaires avec un pourcentage de particules délétères réduit. Pour les différentes formulations de béton, les résultats ont montré qu'il est possible d'obtenir les résistances moyennes visées et que les performances de béton sont peu affectées par le type de sable, avec des valeurs un peu plus élevées à long terme pour le béton de référence qui contient un dosage plus élevé de superplastifiant qui déflocule les particules du ciment et améliore son hydratation. Une amélioration négligeable avec le sable concassé conforme à la norme est détectée pour la résistance en flexion et le retrait des bétons grâce à l'angularité et la minéralogie des grains du sable calcaire concassé. L'observation de ces bétons au MEB montre une meilleure qualité de l'interface pâte-granat grâce à l'angularité et la rugosité des grains de ce sable. Pour un même rapport eau efficace sur ciment, les différents types de béton, se situent dans la même gamme de durabilité, ce qui montre que les caractéristiques du sable ne mènent pas à des différences dans le réseau

poral du béton. Pour les bétons avec sable concassé, une meilleure distribution de la granulométrie au sein du fuseau normatif n'améliore pas significativement la performance du béton à l'exception de sa maniabilité. Pour le béton à haute-performance, l'utilisation du sable calcaire concassé dont la granulométrie respecte la norme ne modifie pas les performances du béton.

Cependant, pour produire le sable concassé conforme à la norme, il faut réduire la teneur en fines générées durant le concassage ce qui introduit des contraintes industrielles et économiques supplémentaires. Nous avons donc étudié la possibilité d'utiliser un sable calcaire concassé avec un pourcentage de fines plus élevé (13-18%) que ne le permet la norme (7%). Les résultats des comparaisons montrent que cette alternative est une solution effective, économique et écologique qui permet de valoriser les fines du sable concassé sans affecter la performance du béton.

Par conséquent, et dans les conditions de l'étude (même rapport eau efficace sur ciment et même maniabilité maintenue par un superplastifiant), les problèmes industriels liés à l'utilisation du sable naturel siliceux au Liban peuvent être résolus en remplaçant totalement ce sable par du sable calcaire concassé soit avec une granulométrie respectant la norme, soit avec un pourcentage de fines (moins de 20%) qui dépasse la limite imposée par la norme (7%).

Suites aux résultats de cette étude, les recommandations suivantes sont offertes aux différentes parties du secteur de construction :

- Les entrepreneurs, les consultants et les autorités concernées sont invités à accepter l'utilisation du sable concassé calcaire, soit avec une granulométrie respectant la norme, soit avec un pourcentage de fines dépassant la norme, comme seul sable dans le béton.
- Les usines de bétonnage sont encouragées à commencer la production des bétons sans sable naturel.
- Les carrières sont incitées à optimiser la production du sable concassé conventionnel pour produire un sable concassé qui respecte les spécifications de la norme ou un sable fin avec un pourcentage de fines qui dépasse la norme.

Perspectives

Suite à des limitations temporelles, l'analyse microstructurale et certains essais, comme la porosité accessible à l'eau et le retrait, n'ont pas été réalisés sur tous les bétons. Il serait intéressant de compléter l'étude par ces essais sur tous les bétons, en particulier sur les bétons à hautes-performances puisque le retrait endogène peut être significatif dans une microstructure compacte et pour pouvoir expliquer les petites réductions détectées dans la résistance à la flexion avec le sable calcaire à teneur en fines élevée.

En outre, l'effet de la substitution totale du sable naturel par du sable concassé sur le fluage des bétons ordinaires et à hautes-performances peut aussi être analysé. Le fluage est nécessaire pour la conception des constructions en béton, comme les ponts et les bétons précontraints. Puisque le chargement continu induit des endommagements microstructuraux autour des granulats, surtout quand il est combiné à la dessiccation, des différences peuvent se produire dépendant du type de sable et sa liaison à la pâte du ciment. Donc, une campagne d'essais sur le fluage doit être menée pour analyser l'effet du sable sur ce comportement mécanique.

Le choix des formulations des bétons consistait de fixer au minimum le nombre des paramètres et d'ajuster le dosage en superplastifiant pour atteindre le même affaissement. Pourtant, le comportement légèrement meilleur des bétons de référence peut être attribué à leurs dosages supérieurs en

superplastifiant. D'où la nécessité de mener un programme expérimental complémentaire basé sur la fixation du dosage de l'adjuvant entre les différents types de béton pour valider ou non cette hypothèse.

Durant cette étude, les propriétés de béton ont été évaluées selon les conditions de cure proposées par les normes, qui peuvent différer de celles des sites de construction. Étant donné que la durée et la méthode de cure peuvent modifier la microstructure, les résistances et la durabilité du béton, suite au changement de la porosité de sa surface et aux variations des déformations différentielles entre la pâte du ciment et les grains de sable, de futures études devraient évaluer les effets de la substitution totale du sable naturel siliceux par du sable calcaire concassé pour différentes conditions de cure.

Les effets du sable sur les propriétés du béton à l'état frais et durci, ainsi que ceux des autres constituants, dépendent de son volume dans le béton. Le programme expérimental de cette étude s'appuie sur les performances des bétons pour fournir des informations rapides à l'industrie du béton. Pourtant, pour augmenter les effets du sable et montrer plus clairement l'influence de ses caractéristiques, des essais complémentaires peuvent être menés sur le mortier. Les résultats obtenus sur les bétons et les mortiers peuvent alors être analysés pour proposer des modèles pertinents capables de déterminer le comportement du béton à l'aide des caractéristiques de ses constituants : comme le rapport eau sur ciment, la composition et le volume du liant, ainsi que le volume, morphologie, minéralogie et propriétés physiques des granulats. Des analyses expérimentales peuvent être proposées pour évaluer la liaison à l'interface.

Il est aussi important d'évaluer l'effet du sable concassé calcaire sur les propriétés de béton à additions pouzzolaniques, puisque ce sable crée des sites de germination pour les produits de l'hydratation qui peuvent améliorer les résistances à court terme associées à ces types de bétons.

Finalement, c'est intéressant de mener une analyse de cycle de vie détaillée pour toutes les formulations de bétons étudiées, pour accentuer les avantages environnementaux du sable concassé calcaire comme une solution effective, rapide et pratique pour le secteur de la construction libanaise. Pourtant, à long terme, il est indispensable de mener une gestion effective des déchets permettant de trouver une solution plus écologique provenant de ces déchets, afin de limiter l'exploitation des montagnes calcaires libanaises.

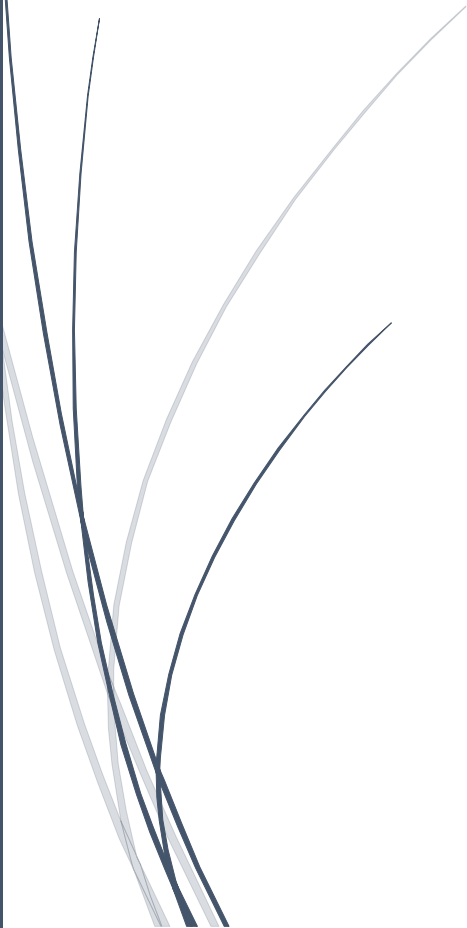


Annexes



Annex A

**Physical
Characterization Tests
for Aggregates**



A. Physical Characterization Tests for Aggregates

Introduction

This annex summarizes the procedures of the tests conducted on the aggregates and the required characteristic of each aggregate type to be used in concrete. All the aggregates characteristics are assessed according to the ASTM standards, except for the Methylene blue value that is determined following the European standard. Furthermore, a comparison is held between ASTM and European standards to depict the differences between these two standards.

1. Standard terminology relating to concrete and concrete aggregates (*ASTM C125, 2016*)

1.1 Aggregates terminology

In this standard, the **aggregate** is defined as a granular material used with a cementing medium to form hydraulic-cement concrete or mortar. It is usually nominated according to its origin and its nominal size as follows:

- **Coarse aggregate:** Aggregate predominantly retained on the 4.75-mm (No. 4) sieve, or that portion of an aggregate retained on the 4.75-mm (No. 4) sieve.
- **Fine aggregate:** Aggregate passing the 9.5-mm (3/8-in.) sieve, almost entirely passing the 4.75-mm (No. 4) sieve, and predominantly retained on the 75- μ m (No. 200) sieve; or that portion of an aggregate passing the 4.75-mm (No. 4) sieve and retained on the 75- μ m (No. 200) sieve.
- **Nominal maximum size (of aggregate):** In specifications for, or description of aggregate, the smallest sieve opening through which the entire amount of the aggregate is permitted to pass.
- **Maximum size (of aggregate):** In specifications for, or description of aggregate, the smallest sieve opening through which the entire amount of aggregate is required to pass.
- **Gravel:** Coarse aggregate resulting from natural disintegration and abrasion of rock or processing of weakly bound conglomerate.
- **Crushed Gravel:** Product resulting from the use of mechanical devices to break gravel particles into smaller fragments.
- **Sand:** Fine aggregate resulting from natural disintegration and abrasion of rock or processing of completely friable sandstone.
- **Manufactured Sand:** Fine aggregate produced by crushing rock, gravel, iron blast-furnace slag, or hydraulic-cement concrete.

1.2 Comparison with European standard

In European standards, the aggregate size is designated in terms of lower (d) and upper (D) sieve sizes. This designation accepts the presence of some particles which will be retained on the upper sieve (oversize) and some which will pass the lower sieve (undersize).

EN 12620:2008 defines **aggregate** as a granular material used in construction that may be natural, manufactured, or recycled.

- **Natural aggregate:** Aggregate from mineral sources that has been subjected to nothing more than mechanical processing.

- **Manufactured aggregate:** Aggregate of mineral origin resulting from an industrial process involving thermal or other modification.
- **Recycled aggregate:** Aggregate resulting from the processing of inorganic material previously used in construction.

This standard also defines the different types of aggregates according to their size:

- **Fine aggregate:** designation given to the smaller aggregate sizes with D less than or equal to 4 mm; it can be produced from natural disintegration of rock or gravel and/or by the crushing of rock or gravel or processing of manufactured aggregate.
- **Coarse aggregate:** designation given to the larger aggregate sizes with D greater than or equal to 4 mm and d greater than or equal to 2 mm.
- **All-in aggregate:** an aggregate consisting of a mixture of coarse and fine aggregates. It can be produced without separating into coarse and fine fractions or it may be produced by combining coarse and fine aggregate.
- **Filler aggregate:** an aggregate, most of which passes a 0.063 mm sieve, which can be added to construction materials to provide certain properties.
- **Fines:** the particle size fraction of an aggregate that passes the 0.063 mm sieve.

2. Standard practice for reducing samples of aggregate to testing size (*ASTM C702, 2011*)

2.1 Procedure

To obtain test portions representative of the field sample, this test aims to minimize the variations in materials characteristics by presenting three methods to reduce the size of large samples.

Method A - Mechanical Splitter (For coarse aggregates and dry fine aggregates):

- Uniformly distribute the original sample in the hopper or pan from edge to edge;
- Introduce the sample at a rate to allow it to flow freely through the chutes and into the receptacle below;
- Take one receptacle and reintroduce the portion of the sample into the splitter as many times as necessary to reduce the sample to the required size specified for each test.

Method B - Quartering (For coarse aggregates and moist fine aggregates):

- Place the original sample on a hard, clean, level surface;
- Mix the material thoroughly by turning the entire sample over 3 times;
- Shovel the entire sample into a conical pile;
- Flatten it to a uniform thickness and diameter by pressing down the apex with a shovel (diameter approximately 4 times the thickness);
- Divide it into four equal quarters and remove two diagonally opposite quarters, including all fine materials by brushing all spaces clean;
- Successively mix and quarter the remaining material until the sample is reduced to the desired size.

Method C - Miniature stockpile sampling (Only for moist fine aggregates):

- Place the original sample on a hard, clean, level surface;
- Mix the material thoroughly by turning the entire sample over 3 times;
- Shovel the entire sample into a conical pile;

- Flatten it to a uniform thickness and diameter by pressing down the apex with a shovel (diameter approximately 4 times the thickness);
- Obtain a sample for each test by selecting at least 5 increments of material at random locations from the miniature stockpile.

2.2 Comparison with European standard

The reduction of the field sample is determined in European standard by **NF EN 932-2-1999, Tests for general properties of aggregates, Part 2: Methods for reducing laboratory samples**. In addition to the mechanical splitter (riffle box) and quartering, the test proposes additional sample reduction techniques using a rotary sample divider and fractional shoveling.

3. Standard test method for sieve analysis of fine and coarse aggregates (*ASTM C136, 2014*)

3.1 Procedure

The test consists of determining the gradation of fine and coarse aggregates by separating a specified mass of the sample through a series of sieves placed in decreasing order from top to bottom according to their openings.

The field sample is reduced to the specified test size according to ASTM C702. For fine aggregates, the sample size shall be a minimum of 300 g after drying. For coarse aggregates, the sample size depends on the nominal maximum size of aggregates (Table A.1).

Table A.1 Sample mass according to the nominal maximum size of aggregates

Nominal maximum size (mm)	Minimum test sample (kg)
9.5	1
12.5	2
19	5
25	10
37.5	15
50	20
63	35
75	60
90	100
100	150
125	300

After drying the sample to constant mass at 110 ± 5 °C, the sample is placed on the top sieve of the sieves' series selected and placed in decreasing opening size from top to bottom. The sieves are agitated by hand or by a mechanical shaker for a sufficient period respecting the following conditions:

- The quantity on a given sieve shall be limited so that all particles have the opportunity to reach sieve openings many times during sieving:
 - For sieves < 4.75mm, quantity should be < 7 kg/m² of surface area
 - For sieves > 4.75mm, quantity should be < 2.5 x sieve opening (mm) x effective sieving area (m²)
- Overload can cause permanent deformation of the sieve; it should be prevented by inserting an additional intermediate sieve, splitting the sample into several portions, or using sieves with a larger frame size to provide greater sieving area

- For each sieve, the sieving should be continued in such a manner that not more than 1% by mass of the material retained will pass that sieve during 1 minute of continuous hand sieving by holding the covered sieve in a slightly inclined position in one hand and striking it sharply of about 150 times/minute (6 revolutions of 25 strokes each)
- If a mechanical shaker is used, it is better to reduce the time of sieving to 10 minutes maximum to avoid sample degradation.

The mass retained on each sieve is determined to the nearest 0.1% of the total original dry sample mass. Then, the cumulative passing percentage of each sieve is calculated to the nearest whole number. Additionally, the fineness modulus is calculated as the sum of the cumulative mass percentage retained on 0.15, 0.30, 0.60, 1.18, 2.36, 4.75, 9.50, 19, 37.5, 75 mm, and larger, divided by 100.

The total mass after sieving should check closely with the original mass of the sample. If the amounts differ by more than 0.3% the results are not accepted.

3.2 Specifications for aggregates used in concrete (*ASTM C33, 2016*)

3.2.1 Fine aggregates

To be used in concrete fine aggregates should have a fineness modulus between 2.3-3.1 and should be graded as displayed in (Table A.2).

Table A.2 Limits of the cumulative passing percentage of fine aggregates

Sieve Diameter (mm)	Minimum Percentage Passing ¹ (%)	Maximum Percentage Passing ¹ (%)
9.50 (3/8 in)	100	100
4.75 (No. 4)	95	100
2.36 (No. 8)	80	100
1.18 (No. 16)	50	85
0.60 (No. 30)	25	60
0.30 (No. 50)	5	30
0.15 (No. 100)	0	10
0.075 (No. 200) ²	0	3 ^{3,4}

Notes:

- ¹ Fine aggregates shall have not more than 45% passing any sieve and retained on the next.
- ² The percentage of particles finer than No. 200 sieve is found by the test complied with ASTM C117: Materials finer than 75 μ m by washing.
- ³ For natural fine aggregates, this value shall be 5% if the concrete is not subjected to abrasion.
- ⁴ For manufactured or recycled aggregate, if the particles finer than 75 μ m (No.200) sieve are essentially composed of dust of fracture derived from the parent rock in the crushing operation and do not contain an applicable level of clay minerals or shale, then this value should be 5% if the concrete is subjected to abrasion, and 7% if the concrete is not subjected to abrasion.

3.2.2 Coarse Aggregates

The grading required for coarse aggregates depends mainly on their nominal size. ASTM C33 details the nomination of each aggregate (grading number) and the grading limits.

3.3 Comparison with European standard

The sieve analysis in European standard is done according to **NF EN 933-1-2012 (Tests for geometrical properties of aggregates Part 1: Determination of particle size distribution - Sieving method)**.

In this standard, the minimum test portion differs from the one of the ASTM standard and the field sample shall be reduced as specified in EN 932-2. The dry sieving is preceded by washing over a 0.063 mm sieve.

The test is adequate if the sum of the masses retained on each sieve and the pan differs by less than 1% from the original mass before the beginning of dry sieving.

4. Standard test method for materials finer than 75µm (No.200) sieve in mineral aggregates by washing (ASTM C117, 2013)

4.1 Procedure

The dry sieve analysis test does not give an accurate percentage of materials finer than 75 µm; ASTM C117 is used for this purpose. It consists of washing the sample over a 75 µm sieve and calculating the percentage of clay and/or other aggregates particles removed after being dispersed by water.

The field sample should be reduced to the specified test size according to ASTM C702. The sample size for this test depends on the nominal maximum size of the aggregate and should be as presented in Table A.3.

Table A.3 Sample mass according to the nominal maximum size of aggregates

Nominal maximum size (mm)	Minimum mass (g)
$d \leq 4.75$	300
$4.75 < d \leq 9.5$	1000
$9.5 < d \leq 19$	2500
$d > 19$	5000

The test procedure consists of washing aggregates unless some clay and bituminous coatings have adhered to the larger particles of aggregates. In this case, the washing process is done first using a wetting agent then followed by using plain water.

After drying the sample to constant mass at $110 \pm 5^\circ\text{C}$, its mass B (g) is determined to the nearest 0.1%. Then the specimen is placed in a container, covered with a sufficient quantity of plain water, and agitated in a way to separate fine particles from coarser particles and to bring the fine materials into suspension. The water is poured into the 0.075 mm sieve and the process is repeated several times until having clear surface water. The material retained on the 0.075 mm sieve is flushed and added to the

washed sample. The new mass C (g) is determined after drying the washed sample to a constant mass at $110 \pm 5^\circ\text{C}$.

The percentage of materials finer than $75 \mu\text{m}$, A (%), is calculated to the nearest 0.1% as follows:

$$A = \frac{B-C}{B} \times 100 \quad (\text{Eq. A.1})$$

4.2 Specifications for aggregates used in concrete (ASTM C33, 2016)

To be used in concrete, natural fine aggregates should have a percentage of materials finer than $75 \mu\text{m} < 3\%$ if the concrete is subjected to abrasion and $< 5\%$ if the concrete is not subjected to abrasion.

For manufactured or recycled aggregate, if the particles finer than $75 \mu\text{m}$ (No.200) sieve are essentially composed of dust of fracture derived from the parent rock in the crushing operation and do not contain an applicable level of clay minerals or shale, then the percentage of materials finer than $75 \mu\text{m}$ should be 5% if the concrete is subjected to abrasion, and 7% if the concrete is not subjected to abrasion.

For coarse aggregates, the percentage of materials finer than $75 \mu\text{m}$ is limited to 1%.

4.3 Comparison with European standard

As already mentioned, the content of fines in the fine aggregates is determined in the European standard according to **NF EN 933-1-2012 (Tests for geometrical properties of aggregates, Part 1: Determination of particle size distribution - Sieving method)**.

The dry mass is recorded before and after the washing process over 0.063 mm sieve to know the percentage of materials finer than 0.063 mm .

5. Standard test method for clay lumps and friable particles in aggregates (ASTM C142, 2017)

5.1 Procedure

This test aims to determine an approximate percentage of clay lumps and friable particles in coarse and fine aggregates.

The method is applied in the portion of aggregates remaining from the "Materials finer than $75 \mu\text{m}$ test". For fine aggregates, the portion coarser than 1.18 mm is used with a minimum mass of 25g. For coarse aggregates, the sample should be divided into several portions having minimum masses as shown in Table A.4.

Table A.4 Sample mass according to the nominal maximum size of aggregates

Size of particles (mm)	Minimum mass (g)
4.75 to 9.5	1000
9.5 to 19	2000
19 to 37.5	3000
Over 37.5	5000

The exact mass of the sample is measured B (g), spread in a thin layer on the bottom of a container, and soaked with distilled water for 24 ± 4 h. At the end of the soaking period, each particle of the sample should be rolled and squeezed into smaller sizes between the thumb and the forefinger (the use of fingernails or the pressure of aggregates against a hard surface or on each other should be avoided). After all discernible particles have been broken, the detritus should be separated from the remainder of the sample by wet sieving through the appropriate sieve as follows (Table A.5):

Table A.5 Sieve choice according to the nominal maximum size of aggregates

Size of particles (mm)	Size of sieve for removing residue (mm)
Fine aggregates (retained on 1.18 mm sieve)	0.85
4.75 - 9.5	2.36
9.5 - 19	4.75
19 - 37.5	4.75
Over 37.5	4.75

The retained particles should be collected, dried to constant mass at 110 ± 5 °C, and weighted C (g).

For fine aggregate and each fraction of coarse aggregates, the percentage of clay lumps and friable particles is calculated as follows:

$$A = \frac{B-C}{B} \times 100 \quad (\text{Eq. A.2})$$

For coarse aggregates, the percentage of clay lumps and friable particles is the average of the percentage in each sieve fraction. If any size of the aggregate presented in **Table A.5** contains less than 5% of aggregates, the percentage of clay lumps and friable particles of this size should be considered equal to the next larger or next smaller size, in order to calculate the average.

5.2 Specifications for aggregates used in concrete (ASTM C33, 2016)

ASTM C33 limits the percentage of clay lumps and friable particles in fine aggregates used in concrete to 3%. For coarse aggregates, the percentage may vary from 2 to 10% depending on the weathering regions.

6. Standard test method for lightweight particles in aggregates (ASTM C123, 2014)

6.1 Procedure

The objective of this test is to determine the percentage of lightweight particles in aggregates.

The heavy liquid used in this test to separate coal or lignite is a solution of zinc chloride and has a specific gravity of 2. For chert and shale, heavier liquids are used, a solution of zinc bromide, having a specific gravity of 2.4. Other solutions or mixtures can also be used.

The field sample should be reduced, according to ASTM C702, to an adequate test size depending on the nominal maximum size of the aggregates (Table A.6).

Table A.6 Sample mass according to the nominal maximum size of aggregates

Nominal Maximum Size (mm)	Minimum Sample size (g)
≤ 4.75	200
9.5	1500
12.5 to 19	3000
25 to 37.5	5000
≥ 50	10000

The test sample should be dried to constant mass at 110 ± 5 °C and sieved over 300 µm and 4.75 mm sieve for fine and coarse aggregates respectively. The mass retained is measured W_2 (g), brought to the saturated-surface dry condition, then introduced into the heavy liquid in a suitable container (V liquid ≥ 3 x absolute volume of aggregates).

For fine aggregates, the liquid and the floating particles are poured into a second container by passing through a skimmer then returned to the first container. The decanting process is repeated after further agitation by stirring until the specimen is free of floating particles. The sank fine aggregates particles should not be decanted onto the skimmer.

For coarse aggregates, the floating particles are removed by the skimmer after repeated agitation.

The decanted particles are washed, dried at 110 ± 5 °C, and weighed W_1 (g).

The percentage of lightweight particles is described as follows:

$$L = \frac{W_1}{W_2} \times 100 \quad (\text{Eq. A.3})$$

6.2 Specifications for aggregates used in concrete (ASTM C33, 2016)

ASTM C33 limits the percentage of coal and lignite in fine aggregates to 0.5% if the appearance of concrete is important and to 1% for all other concretes. For coarse aggregates, the limit varies from 0.5 to 1% depending on weathering regions.

6.3 Comparison with European standards

The determination of lightweight particles content in European standard according to **NF EN 1744-1-2009 (Tests for chemical properties of aggregates - Part 1: Chemical analysis-14.2: Determination of lightweight contaminators)** follows the same procedure as the ASTM one. The only difference between both standards is the test portion.

7. Standard test method for sand equivalent value of soils and fine aggregate (ASTM D2419, 2014)

7.1 Procedure

The test aims to determine the proportions of clay-size particles in fine aggregates, and the particle sizes are defined as follows:

- Clay size: particles finer than 0.002 mm (0.005 mm in some cases).
- Fine aggregate: particles passing the 9.5 mm sieve, almost entirely passing 4.75 mm sieve, and predominantly retained on 0.075 mm sieve.
- Sand: particles passing 4.75 mm and retained on 0.075 mm sieve.

The test should be performed at a location free from vibration and the plastic cylinders should not be exposed to direct sunlight. The working solution which is more than 2 weeks old shall be discarded and its temperature should be maintained at 22 ± 3 °C.

The field sample should be reduced, according to ASTM C702, to 1.5 kg after discarding the materials coarser than 4.75 mm. The sampling method consists of filling four measure tins of the tested material and tapping their bottom edge on a hard surface at least four times. The mass of each tin is measured, then the material is returned back to the sample, split, or quartered until obtaining the total weight of the four tins. Two additional splitting or quartering are applied to finally obtain the weight of one tin that consists of the final test specimen.

To perform the test, the working calcium chloride solution should be placed on a shelf 90 ± 5 cm above the working surface. 4" of the solution is added in the cylinder, and using a funnel the sample in the tin is poured. The bottom of the cylinder is tapped by the heel of the hand several times and then it is allowed to stand for 10 ± 1 minutes. The cylinder is then closed and well shook and inverted to loosen the material from its bottom. This step is followed by a shaking procedure by the mean of a mechanical shaker, manual shaker, or hand shaker (by holding it in a horizontal position and shake it for 90 cycles in 30 seconds). Afterward, the solution is added to fill 15" of the cylinder and while adding it, the irrigation pipe should be gently stabbed and twisted to force the fine materials in the bottom of the cylinder to suspend over the coarser particles. The cylinder is then allowed to stand for $20 \text{ min} \pm 15 \text{ s}$. At the end of the standing period, the level of the top of the suspension is recorded as a "clay reading". Using the weighted foot, the "sand reading" is recorded after substituting from the level indicated by the extreme top edge of the indicator 25.4 cm (distance between the extreme top and bottom edge of the indicator).

The sand equivalent value SE (%) is then calculated as follows:

$$SE = \frac{\text{Sand Reading}}{\text{Clay Reading}} \times 100 \quad (\text{Eq. A.4})$$

7.2 Comparison with European standards

The Sand Equivalent Value is determined in European standard by **EN 933-8-2012 (Tests for geometrical properties of aggregates-Part 8: Assessment of fines-Sand equivalent test)**. This standard differs from the ASTM by the preparation of the sample and it is conducted on the fraction of sand smaller than 2 mm, not 4.75 mm.

8. Assessment of fines – Methylene blue test (BS EN 933-9, 1999)

8.1 Procedure

This method is used for the determination of the methylene blue value of the 0/2mm fraction in fine aggregates. After drying, the sample should contain at least 200 g of 0/2 mm particle size and its mass is recorded M_1 (g)

The Methylene Blue solution (dye solution) is composed of 10 ± 0.1 g/L of methylene blue. Its maximum period of use is 28 days and should be stored away from light.

The preparation of the suspension solution consists of adding to the test sample 500 ± 5 mL of distilled water and agitating it well with 5 mL of the dye solution. The agitation rate is fixed at 600 ± 60 r/min for the first 5 minutes and subsequently, it becomes 400 ± 40 r/min for the remainder of the test.

The stain test is done after each injection of 5 mL of dye solution; it consists of taking a drop of suspension (such that the diameter is between 8 and 12 mm) and depositing it on the filter paper. The stain formed is composed of a generally solid blue color surrounded by a colorless wet zone. The test is positive if, in the wet zone, a halo consisting of a persistent light blue ring of about 1 mm is formed around the central deposit, and remains for 5 minutes.

If the test is negative, a further 5 mL of methylene blue solution is added and the stain test is repeated. If the test is positive, the total added volume V_1 to produce a halo that persists for 5 minutes is recorded. If insufficient fines are present to obtain a halo, 30 ± 0.1 g of dried Kaolinite is added, and the volume of dye solution absorbed by 30g of Kaolinite is recorded $V' = 30$ MBK.

The methylene blue value MB (g/kg) is expressed as follows:

$$MB = \frac{V_1}{M_1} \times 10 \quad (\text{Eq. A.5})$$

With the addition of Kaolinite, the expression of the methylene blue value becomes:

$$MB = \frac{V_1 - V'}{M_1} \times 10 \quad (\text{Eq. A.6})$$

8.2 Specifications for aggregates used in concrete (ASTM C33, 2016)

According to ASTM C33, the manufactured sand with a percentage less than 4% of material finer than $2 \mu\text{m}$ and $MB < 5$ mg/g is suitable for concrete. The fine aggregates with higher values may also be suitable, provided that the fresh and hardened properties of concrete are acceptable.

9. Standard Test Method for Organic Impurities in Fine Aggregates for Concrete (ASTM C40, 2016)

9.1 Procedure

This test gives a qualitative value of organic impurities in fine aggregates. The field sample should be reduced to 450 g according to ASTM C702.

The reagent sodium hydroxide solution (3%) is prepared by dissolving 3 parts by mass of reagent grade sodium hydroxide (NaOH) in 97 parts of water.

The preparation of the standard color solution consists of dissolving reagent grade potassium dichromate ($\text{K}_2\text{Cr}_2\text{O}_7$) in concentrated sulfuric acid (sp gr. 1.84) at the rate of 0.25 g/100 mL of acid. It must be freshly made (not more than 2 hours).

The sodium hydroxide solution is added to a glass bottle leveled by 130 mL with the sample solution, to form a volume of 200 mL after shaking. The bottle is closed, shook vigorously, then allowed to stand for 24 hours.

The quality of the sample solution is determined by comparing its color to a standard color solution or glass standard plates colors:

- Standard color solution: The color of a bottle filled with 75 ml of the standard color solution is compared to the color of the supernatant liquid above the sample solution. If the sample color is lighter or similar to the standard color solution then the sample can be considered free of organic impurities.
- Glass color standard procedure: The comparison of the solution is done with 5 glass standard colors as mentioned in Table A.7.

Table A.7 Color standards plates

Gardner Color Standard No.	Organic Plate No.
5	1
8	2
11	3 (Standard)
14	4
16	5

9.2 Specifications for aggregates used in concrete

When the sample produces a color darker than the standard color or plate no.3, the fine aggregate shall be considered to possibly contain injurious organic impurities. It's advisable to perform further tests before approving the aggregate for use in concrete.

9.3 Comparison with European standards

The determination of organic impurities in European standard is done according to **NF EN 1744-1-2009 (Tests for chemical properties of aggregates, Part 1: Chemical analysis- Determination of organic components affecting the setting and the hardening of cement-15.1: Determination of potential presence of humus)**.

This standard follows the same procedure as the ASTM standard with variation in the heights of the solution (80 mm) and the test portion (120 mm) into the glass. It could also be applied to the fraction of coarse aggregates that passes the 4 mm sieve.

10. Standard test method for relative density (specific gravity) and absorption of fine (*ASTM C128, 2015*) and coarse aggregate (*ASTM C127, 2015*)

10.1 Procedure

These tests aim to determine the relative density (specific gravity) and the absorption of fine and coarse aggregates. By definition, the Relative Density (Specific gravity) is the ratio of the mass of an aggregate to the mass of a volume of water equal to the volume of the aggregate particles (also referred to as the absolute volume of the aggregate particles); it is also defined by the ratio of the density of the aggregate particles to the density of water. It differs from "Bulk Density or Unit Weight" which includes

the volume of voids between the aggregates particles and it is used to calculate the volume occupied by the aggregate in a concrete mixture. Three types of Relative Density can be calculated in this test:

- Saturated Surface Dry (SSD) density: It is used when the absorption of aggregates is satisfied and they are in their SSD condition;
- Oven Dry (OD) density: It is used when the aggregates are dry or assumed to be dry;
- Apparent relative density (specific gravity): It pertains to the solid material making up the constituent particles excluding the pore space, within the particle, that can be filled with water.

10.1.1 Fine aggregate

The field sample should be reduced to 1 kg according to ASTM C702 and it should be dry to constant mass at 110 ± 5 °C. The sample is covered with water either by immersion or by the addition of at least 6% moisture to the fine aggregates and left for 24 ± 4 hours. At the end of the immersion period, the sample is stirred and air-dried homogeneously. Afterward, the surface moisture should be tested using a specified mold. The mold is placed on a smooth nonabsorbent surface, the sample is overflowed in the mold and is lightly tamped with 25 light drops of the tamper (each drop should be started 5 mm above the top surface and the tamper is freely fell under gravitational attraction). The loose sand is removed from the base and the mold is lifted vertically. If there is a slight slumping, then the saturated surface dry condition is reached. If fine aggregate remains molded shape, then moisture is still present and the sample should be dried and tested repeatedly for moisture. If the sample slumped from the first trial, this means that it has been dried past the saturated-surface dried condition; so, a few mL of water should be mixed with the sample and permitted to stand for 30 minutes before resuming the drying process.

When the saturated-surface-dry condition is reached, the test is continued according to one of the following methods:

- **Gravimetric Procedure (Pycnometer):**

A mass S consisting of 500 ± 10 g of saturated-surface dry fine aggregates is introduced into the pycnometer which is partially filled with water. Additional water to approximately 90% of the pycnometer's capacity is added and the pycnometer is agitated to eliminate all visible air bubbles. The agitation could be done manually (roll, invert, or agitate for 15 to 20 minutes) or mechanically. After eliminating all air bubbles, the water level in the pycnometer is brought to its calibrated capacity (after adjusting if necessary, the temperature to 23 ± 2 °C) and the total mass (pycnometer, specimen, and water) is determined C (g). Then, the sample is removed from the water, dried to constant mass at 110 ± 5 °C and its mass is determined A (g). Additionally, the mass of the pycnometer filled to its calibrated capacity with water at 23 ± 2 °C is determined B (g).

The three different specific gravities are calculated as follows:

- The oven-dried relative density (specific gravity) S_d :

$$S_d = \frac{A}{B+S-C} \quad (\text{Eq. A.7})$$

- The saturated-surface dry relative density (specific gravity) S_s :

$$S_s = \frac{S}{B+S-C} \quad (\text{Eq. A.8})$$

- The apparent relative density (specific gravity) S_a :

$$S_a = \frac{A}{B+A-C} \quad (\text{Eq. A.9})$$

- **Volumetric Procedure (Le Chatelier Flask):**

At 23 ± 2 °C, the flask is initially filled with water to a point between 0 and 1 mL, and its initial reading R_1 is recorded. A mass S_1 of 55 ± 5 g of fine aggregate in the saturated-surface dry condition is added. The flask is closed, rolled in an inclined position, or gently whirled in a horizontal circle to dislodge all entrapped air (the process is continued until no further bubbles rise to the surface) and a final reading R_2 is recorded within 1 °C of the original temperature. For determination of absorption, a separate mass S of 500 ± 10 g portion of saturated-surface dry fine aggregate is used and its dried mass A (g) is determined.

The three different specific gravities are calculated as follows:

- The oven-dried relative density (specific gravity) S_d :

$$S_d = \frac{S_1 \left(\frac{A}{S}\right)}{0.9975 (R_2 - R_1)} \quad (\text{Eq. A.10})$$

- The saturated-surface dry relative density (specific gravity) S_s :

$$S_s = \frac{S_1}{0.9975 (R_2 - R_1)} \quad (\text{Eq. A.11})$$

- The apparent relative density (specific gravity) S_a :

$$S_a = \frac{S_1 \left(\frac{A}{S}\right)}{[0.9975 (R_2 - R_1)] - \left[\frac{S_1}{S}(S - A)\right]} \quad (\text{Eq. A.12})$$

In both methods, the absorption (%) is expressed by:

$$\text{Absorption} = \frac{S-A}{A} \times 100 \quad (\text{Eq. A.13})$$

10.1.2 Coarse aggregate

The field sample should be reduced to the test sample size according to ASTM C702. The materials passing 4.75 mm sieve should be rejected and the minimum sample size should conform with Table A.8.

Table A.8 Sample mass according to the nominal maximum size of aggregates

Nominal maximum size (mm)	Minimum mass of test (kg)
12.5 or less	2
19	3
25	4
37.5	5
50	8
63	12
75	18
90	25
100	40
125	75

After rejecting all materials passing 4.75 mm sieve (or 2.36 mm sieve if the coarse aggregate contains a substantial quantity of material finer than 4.75 mm), the sample is washed to remove the dust or other coatings from the surface. If the sample contains more than 15% retained on 37.5 mm, it should be divided into several fractions. The sample is dried to constant mass at 110 ± 5 °C and immersed in water for 24 ± 4 h. At the end of the immersion period, the sample is removed from the water and rolled in a large absorbent cloth until all visible films of water are removed and its saturated-surface dry mass B (g) is determined. After determining the mass in air, immediately the sample is placed in a specific container and its apparent mass C (g) is determined in the water at 23 ± 2 °C (all entrapped air should be removed before determining this mass, by shaking the container while immersed). Afterward, the sample is dried to constant mass at 110 ± 5 °C and then its dried mass is determined A (g).

The following formulas are applied for the calculations of relative densities and absorption:

- The oven-dried relative density (specific gravity) S_d :

$$S_d = \frac{A}{B-C} \quad (\text{Eq. A.14})$$

- The saturated-surface dry relative density (specific gravity) S_s :

$$S_s = \frac{B}{B-C} \quad (\text{Eq. A.15})$$

- The apparent relative density (specific gravity) S_a :

$$S_a = \frac{A}{A-C} \quad (\text{Eq. A.16})$$

- The absorption (%):

$$\text{Absorption} = \frac{B-A}{A} \times 100 \quad (\text{Eq. A.17})$$

If the sample is tested in separate size fractions, and knowing the relative density G_i and the absorption A_i of each fraction, the following formulas are applied to calculate the relative density G and the absorption of the total sample.

$$G = \frac{1}{\frac{P_1}{100 \times G_1} + \frac{P_2}{100 \times G_2} + \dots + \frac{P_n}{100 \times G_n}} \times 100 \quad (\text{Eq. A.18})$$

$$\text{Absorption} = \frac{1}{\frac{P_1 A_1}{100} + \frac{P_2 A_2}{100} + \dots + \frac{P_n A_n}{100}} \times 100 \quad (\text{Eq. A.19})$$

$$\text{Where, } P_i = \frac{m_i}{\Sigma m_i} \times 100 \quad (\text{Eq. A.20})$$

Other interpolations could also be done in this test, for both types of aggregates:

$$S_s = 1 + \frac{\text{Absorption}}{100} \times S_d \quad (\text{Eq. A.21})$$

$$S_a = \frac{1}{\frac{1}{S_d} - \frac{\text{Absorption}}{100}} = \frac{S_d}{1 - \frac{\text{Absorption} \times S_d}{100}} \quad (\text{Eq. A.22})$$

$$S_a = \frac{1}{1 + \frac{\text{Absorption}}{100} \frac{\text{Absorption}}{S_s}} = \frac{S_s}{1 - \frac{\text{Absorption}}{100} x (S_s - 1)} \quad (\text{Eq. A.23})$$

$$\text{Absorption} = \left(\frac{S_s}{S_d} - 1 \right) x 100 \quad (\text{Eq. A.24})$$

$$\text{Absorption} = \frac{S_a - S_s}{S_a (S_s - 1)} x 100 \quad (\text{Eq. A.25})$$

10.2 Comparison with European standards

The determination of density in European standard is done following **NF EN 1097-6 (Tests for mechanical and physical properties of aggregates, Part 6: Determination of particle density and water absorption)**.

This test requires the use of the pycnometer method not only for fine aggregates as in ASTM standard but also for aggregates passing 37.5 mm and retained on 0.063 mm. But the pycnometer usage defers in both standards by the soaking procedure and by the moist condition of aggregates at the beginning of the test (dry in ASTM and moist in European Standard).

11. Standard test method for soundness of aggregates by use of sodium sulfate or magnesium sulfate (*ASTM C88, 2013*)

11.1 Procedure

This test helps to simulate the expansion of water on freezing, by an internal expansion force derived from successive hydration and dehydration of salts in the pores of a specimen subjected to cycles of immersion in a sodium sulfate or magnesium sulfate solution.

The field sample should be reduced to test size according to ASTM C702.

The fine aggregate should pass through a 9.5 mm sieve then washed on a 300 μm sieve, and dried to constant weight at 110 ± 5 °C. The sample is separated into different sizes by sieving and it is selected of sufficient size to yield more than 100 g of each of the following sizes in amounts of 5% or more (Table A.9):

Table A.9 Fine aggregates separation by sieving

Passing sieve (mm)	Retained on sieve (mm)
0.6	0.3
1.18	0.6
2.36	1.18
4.75	2.36
9.5	4.75

For coarse aggregates, the particles finer than 4.75 mm sieve are removed. The sample should be washed and dried to constant weight A (g) at 110 ± 5 °C. It is then separated into different sizes by sieving and it shall yield the amounts in Table A.10 of indicated sizes that are available in amounts of 5% or more. In the case of sizes greater than 19 mm, the number of particles is recorded in the test samples.

Table A.10 Coarse aggregates separation by sieving

Passing sieve (mm)	Retained on sieve (mm)	Mass (g)
9.5	4.75	300±5
19	9.5	1000±10
	Consisting of:	
12.5	9.5	330±5
19	12.5	670±10
37.5	19	1500±50
	Consisting of:	
25	19	500±30
37.5	25	1000±50
63	37.5	5000±300
	Consisting of:	
50	37.5	2000±200
63	50	3000±300
	Larger sizes consisting of:	
75	63	7000±1000
90	75	7000±1000
100	90	7000±1000

The samples are immersed in the solution for not less than 16 h and not more than 18 h in such a manner that the solution covers them to a depth of at least 0.5 in. During immersion, the temperature is maintained at 21 ± 1 °C and the containers are covered to reduce evaporation and to prevent accidental addition of extraneous substances. At the end of the soaking period, the aggregates are removed and permitted to drain for 15 ± 5 min before being oven-dried at 110 ± 5 °C to constant mass (check the weight loss of test sample at intervals of 2 to 4 h, the constant weight will be considered to have been achieved when weight loss is less than 0.1% of sample weight in 4 h drying). After cooling, the samples are introduced again into the solution. The process of alternate immersion and drying is repeated for 5 cycles. After the completion of the final cycle and after the sample has cooled, the samples are washed by circulated water at 43 ± 6 °C with barium chloride (BaCl_2) to be free from the sodium or magnesium sulfate.

For test samples coarser than 19 mm, the particles are separated into groups and the number of particles is recorded, showing each type of distress that occurred after immersion (splitting, crumbling, cracking, and flaking).

After the removal of the solution, each sample is dried to constant weight at 110 ± 5 °C and sieved over specified sieves. The retained mass is measured B (g). For fine aggregates, each fraction is sieved over the same sieve on which it was retained before, in the same manner as for sample preparation. For coarse aggregate, for each fraction, the sieve is chosen according to Table A.11.

The loss by soundness for each fraction is expressed by:

$$L = \frac{A-B}{A} \times 100 \quad (\text{Eq. A.26})$$

In order to calculate the weighted average, the fractions that contain less than 5% of the sample are considered to have the same loss as the average of the next smaller and the next larger sizes. If one of these is absent, the loss is considered equal to the loss of the next larger or the next smaller size.

Table A.11 Loss determination according to sieve diameter

Passing sieve (mm)	Retained on sieve (mm)	Sieve used to determine loss (mm)
100	90	75
90	75	63
75	63	50
63	37.5	31.5
37.5	19	16
19	9.5	8
9.5	4.75	4

11.2 Specifications for concrete aggregates (*ASTM C33, 2016*)

ASTM C33 sets limits for the loss percentage due to five cycles of immersion in both types of solution. For fine aggregates, the loss by sodium and magnesium sulfate solution is limited to 10% and 15% respectively. For coarse aggregates, the maximum allowable loss by sodium sulfate is 12%, while it is 18% for the magnesium sulfate.

11.3 Comparison with European standards

The determination of soundness resistance of aggregates in the European standard is studied using only a magnesium sulfate solution in accordance with **NF EN 1367-2-2010 (Tests for thermal and weathering properties of aggregates, Part 2: Magnesium sulfate test)**.

Usually, this test is done on 500 g of the portion retained on 10 mm sieve and passing 14 mm sieve, but it could also be done outside this size range by respecting some specifications. The European standard differs also from the ASTM standard by the period of drainage after each cycle; it shall be 2 ± 0.25 h and not 15 ± 5 min.

12. Standard test method for resistance to degradation of small-size coarse aggregate by abrasion and impact in the Los Angeles machine (*ASTM C131, 2014*)

12.1 Procedure

This test covers the study of resistance to degradation in the Los Angeles machine of coarse aggregates with a maximum size of 37.5 mm. The field sample should be reduced, according to ASTM C702, to adequate sizes.

The sample should be washed, oven-dried to a constant mass at 110 ± 5 °C, separated into individual size fractions, and recombined to one of the following gradings, before recording the final mass A (g):

- Grading A (Total weight: 5000 ± 10 g)
 - Passing 37.5mm, retained on 25mm: 1250 ± 25 g
 - Passing 25mm, retained on 19mm: 1250 ± 25 g
 - Passing 19mm, retained on 12.5mm: 1250 ± 10 g
 - Passing 12.5mm, retained on 9.5mm: 1250 ± 10 g
- Grading B (Total weight: 5000 ± 10 g)
 - Passing 19mm, retained on 12.5mm: 2500 ± 10 g
 - Passing 12.5mm, retained on 9.5mm: 2500 ± 10 g

- Grading C (Total weight: 5000 ± 10 g) Passing 9.5mm, retained on 6.3mm: 2500 ± 10 g
Passing 6.3mm, retained on 4.75mm: 2500 ± 10 g
- Grading D (Total weight: 5000 ± 10 g) Passing 4.75mm, retained on 2.36mm: 5000 ± 10 g

The sample is introduced in the Los Angeles machine with a specific number of spheres. The number of spheres used depends on the sample grading: 12, 11, 8, and 6 for Grade A, B, C, and D respectively. The machine is then rotated at a rate of 30 to 33 rpm for 500 revolutions. At the end of the revolutions, the discharged material is sieved on a 1.7 mm sieve, washed, dried to constant mass at 110 ± 5 °C, and weighed B (g).

The loss by abrasion of the sample L (%) is calculated as follows:

$$L = \frac{A-B}{A} \times 100 \quad (\text{Eq. A.27})$$

12.2 Specifications for aggregates used in concrete (ASTM C33, 2016)

ASTM C33 limits the loss percentage by abrasion of coarse aggregates to 50%.

12.3 Comparison with European standards

The determination of resistance by abrasion and impact in European standard is done per **NF EN 1097-2-2010 (Tests for mechanical and physical properties of aggregates, Part 2: Methods for the determination of resistance to fragmentation)**.

ASTM and European standards follow the same test procedure and sample preparations, but they use different sieve diameters, grading, and number of balls. Additionally, after discharging the machine, the material should be washed and sieved on a 1.6 mm sieve in the European standard.

13. Standard test method for total evaporable moisture content of aggregates by drying (ASTM C566, 2013)

13.1 Procedure

This test aims to determine the percentage of moisture in a sample of aggregates by drying. The field sample should be reduced, according to ASTM C702, to test sizes shown in Table A.12.

Table A.12. Sample mass according to the nominal maximum size of aggregates

Nominal Maximum Size (mm)	Sample Mass (kg)
4.75	0.5
9.5	1.5
12.5	2
19	3
25	4
37.5	6
50	8
63	10
75	13
90	16
100	25
150	50

The method consists of determining the original mass of the sample W (g), drying it to a constant mass (<0.1% additional mass loss), then measuring the dried mass after it has cooled D (g).

The drying process could be conducted by one of the following sources of heat: ventilated oven (110 ± 5 °C), electric or gas hot plate, electric heat lamps, and ventilated microwave oven.

The total evaporable moisture content p (%) is calculated by:

$$p = \frac{W-D}{D} \times 100 \quad (\text{Eq. A.28})$$

The surface moisture content (%) is estimated as the difference between the total evaporable moisture and the absorption determined by ASTM C127 or ASTM C128.

13.2 Comparison with European standards

The total Evaporable moisture is determined in European standard by **NF EN 1097-5-2008 (Tests for mechanical and physical properties of aggregates, Part 5: Determination of the water content by drying in a ventilated oven)**.

This test differs mainly from ASTM by the size of the test sample. The field sample shall be reduced as specified in EN 932-2 and the test portion depends on the upper size of aggregates forming the sample:

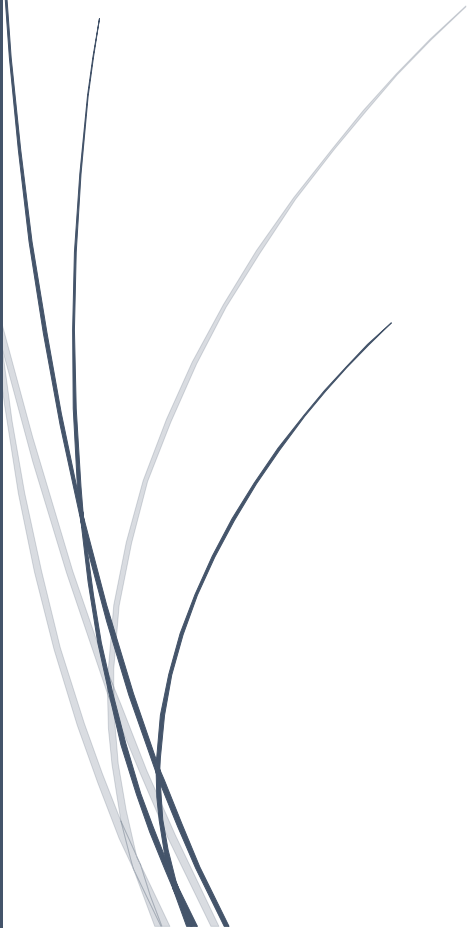
- if $D \geq 1.0$ mm, the minimum mass (in kilograms) shall be $0.2 D$;
- if $D < 1.0$ mm, the minimum mass shall be 0.2 kg.

This standard describes only one heating procedure to determine the moisture content, the ventilated oven procedure at 110 ± 5 °C.



Annex B

**Crushed Aggregates
Properties
from Different
Lebanese Resources**



B. Crushed Aggregates Properties from Different Lebanese Resources

Introduction

During our study, the "Conventional crushed sand" used in all concrete mixes was provided from the same quarry located in Bikfaya, Mount-Lebanon region. Recalling that the main objective of the thesis is to totally replace the natural sand with crushed sand in concrete, it is essential to ascertain that the crushed sand properties do not significantly differ from one quarry to another, to be able to generalize the conclusions of the thesis, regardless of the source of the crushed sand.

Additionally, it is important to investigate the characteristics of different sources of medium and coarse aggregates, to be sure that they could be used in concrete and do not majorly differ from those of the ones studied in the thesis.

For this purpose, in addition to the characterization of aggregates from the Mount-Lebanon region, a parallel study was conducted on seven resources of crushed aggregates from three different Lebanese regions: Beqaa governate, South governate, and North governate.

This supplementary study consists of comparing the physical properties of these aggregates, determined by the same tests' standards applied on the aggregates used in the concrete mixes of the thesis.

1. Quarries locations



Figure B.1 The location of the aggregates resources

Seven aggregates resources from three different Lebanese regions were investigated during this study. Figure B.1 illustrates the location of these quarries. From the Beqaa regions, aggregates were provided from three different quarries: Zahle, Majd Al Anjar, and Ras Baalbek. Quarries from Tyre and Ansar served as aggregates resources from the South region, while Dahr Nassar and El Biri were the chosen locations from the North region.

Similar to the aggregates used in the thesis (from Bikfaya quarries), all the studied crushed aggregates are of limestone nature.

The provided aggregates are crushed sand CS, medium aggregate MA, and coarse aggregate CA. During this study, the government imposed restrictions on the work of the quarries, therefore some types of these aggregates were not provided from all the regions.

2. Aggregates properties

2.1 Clay lumps and friable particles

The clay lumps and friable particles test was applied on crushed aggregates samples following (*ASTM C142, 2017*). The results are presented in Table B.1.

The three types of aggregates are characterized by a low percentage of clay lumps and friable particles (between 0.02 and 0.16%). This percentage does not exceed the maximum allowable limit (3%) specified by (*ASTM C33, 2016*).

Table B.1 Clay lumps and friable particles of crushed aggregates (%)

Aggregates Type*	Mount-Lebanon	Beqaa			South Lebanon		North Lebanon	
	Bekfaya	Zahle	Majd El Anjar	Ras Baalbek	Tyre	Ansar	Dahr Nassar	El Biri
CS	0.7	0.04	0.02	0.10	0.03	0.09	-	-
MA	0.2	0.08	0.12	-	0.09	0.07	-	-
CA	0.2	0.08	0.14	0.15	0.12	0.16	0.08	0.15

(*): CS crushed sand; MA: medium aggregate, and CA: coarse aggregate;

(-): aggregates not provided.

2.2 Sand equivalent

(*ASTM D2419, 2014*) is used to determine the sand equivalent percentage for crushed sand.

The sand equivalent values vary between 61% and 78% in all regions (Table B.2). There is no specific limit for the sand equivalent percentage in fine aggregates in (*ASTM C33, 2016*). However, a sand equivalent value higher than 70% is usually accepted in concrete mixes. The results show that some crushed sand resources could exhibit low sand equivalent.

Table B.2 Sand equivalent of crushed aggregates (%)

Aggregates Type*	Mount-Lebanon	Beqaa			South Lebanon		North Lebanon	
	Bekfaya	Zahle	Majd El Anjar	Ras Baalbek	Tyre	Ansar	Dahr Nassar	El Biri
CS	73	78	66	74	77	61	-	-

(*): CS crushed sand;

(-): aggregates not provided.

2.3 Methylene blue value

The Methylene Blue value for all the crushed sand samples is investigated following the (*BS EN 933-9, 1999*) standard.

The results presented in Table B.3 show that all the crushed sand samples presented a low methylene blue value (between 0.5 and 3.3 g). These quantities do not exceed the maximum allowable limit (5 g) imposed by (*ASTM C33, 2016*). These results mean that the clay contents are low in the crushed sand of all resources.

Table B.3 Methylene Blue value of crushed aggregates (g)

Aggregates Type*	Mount-Lebanon	Beqaa			South Lebanon		North Lebanon	
	Bekfaya	Zahle	Majd El Anjar	Ras Baalbek	Tyre	Ansar	Dahr Nassar	El Biri
CS	0.9	0.5	1.7	1.4	1.3	3.3	-	-

(*): CS crushed sand;

(-): aggregates not provided.

2.4 Organic impurities

(*ASTM C40, 2016*) is used to qualitatively detect the presence of organic impurities in different crushed sand resources. An example of the test results is shown in Figure B.2.

All the tested samples showed a lighter solution compared to the color of the standard solution. This is an indication of the absence of organic impurities.



Figure B.2. Comparison of the crushed sand solution (at the left) to the standard color solution (at the right) to detect organic impurities in crushed sand

2.5 Relative densities

The oven-dry, saturated-surface dry, and apparent relative densities are measured following (*ASTM C128, 2015*) for crushed sand and (*ASTM C127, 2015*) for medium and coarse aggregates.

Table B.4 shows a variation in the values between the different resources. However, they all present values that are common for these types of aggregates since they range between 2.4 and 2.9 (*Kosmatka and Wilson, 2011*).

Table B.4 Relative densities of crushed aggregates

Relative Density	Aggregates Type*	Mount-Lebanon	Zahle	Beqaa		South Lebanon		North Lebanon	
		Bekfaya ⁺		Majd El Anjar	Ras Baalbek	Tyre	Ansar	Dahr Nassar	El Biri
Oven dry	CS	2.55	2.52	2.49	2.62	2.44	2.43	-	-
	MA	2.66	2.65	2.66	-	2.53	2.55	-	-
	CA	2.67	2.67	2.61	2.75	2.56	2.53	2.61	2.62
Saturated Surface dry	CS	2.62	2.59	2.57	2.70	2.56	2.53	-	-
	MA	2.67	2.67	2.68	-	2.60	2.61	-	-
	CA	2.68	2.68	2.65	2.76	2.62	2.59	2.64	2.65
Apparent	CS	2.74	2.70	2.70	2.86	2.72	2.69	-	-
	MA	2.71	2.70	2.71	-	2.72	2.73	-	-
	CA	2.70	2.71	2.69	2.80	2.73	2.69	2.69	2.71

(*): CS crushed sand; MA: medium aggregate, and CA: coarse aggregate;

(+): This column presents the average values for the aggregates densities presented in Chapter II;

(-): aggregates not provided.

2.6 Absorption

(*ASTM C128, 2015*) and (*ASTM C127, 2015*) are also used to determine the absorption of crushed sand, and medium and coarse aggregates respectively.

Table B.5 shows that the absorption of aggregates varies considerably from one quarry to another (2.6 to 5.2%, 0.6 to 2.8%, and 0.5 to 2.5% for crushed sand, medium, and coarse aggregate respectively), even between some aggregates from different quarries of the same region (for example, 4.1 to 5.2% for crushed sand in the South Lebanon region). This variation is reasonable since the absorption property could also vary with the different zones and depths of the same quarry, the higher the depth, the softer the aggregate and the higher could be its absorption (*Ioannou et al., 2014*)

Table B.5 Absorption of crushed aggregates (%)

Aggregates Type*	Mount-Lebanon	Zahle	Beqaa		South Lebanon		North Lebanon	
	Bekfaya ⁺		Majd El Anjar	Ras Baalbek	Tyre	Ansar	Dahr Nassar	El Biri
CS	2.6	2.6	3.2	3.2	5.2	4.1	-	-
MA	0.7	0.6	0.7	-	2.8	2.6	-	-
CA	0.6	0.5	1.1	0.7	2.5	2.3	1.1	1.2

(*): CS crushed sand; MA: medium aggregate, and CA: coarse aggregate;

(+): This column presents the average values for the aggregates absorptions presented in Chapter II;

(-): aggregates not provided.

2.7 Soundness loss by sodium sulfate solution

The soundness loss by a sodium sulfate solution is determined as per (*ASTM C88, 2013*).

The three types of tested aggregates, from all the studied resources, present low values (between 0.4 and 9) (Table B.6) compared to the limits imposed by (*ASTM C33, 2016*) standard (10% and 12% for fine and coarse aggregates respectively).

Table B.6 Soundness loss by sodium sulfate solution for the crushed aggregates (%)

Aggregates Type*	Mount-Lebanon	Beqaa			South Lebanon		North Lebanon	
	Bekfaya	Zahle	Majd El Anjar	Ras Baalbek	Tyre	Ansar	Dahr Nassar	El Biri
CS	5	3	4	1	3	4	-	-
MA	9	3	9	-	1	0.4	-	-
CA	8	2	3	2	1	0.5	1	1

(*): CS crushed sand; MA: medium aggregate, and CA: coarse aggregate;

(-): aggregates not provided.

2.8 Abrasion loss by Los Angeles machine

(*ASTM C131, 2014*) standard is used to determine the abrasion loss of medium and coarse aggregates by the Los Angeles machine, and the results are presented in Table B.7. For both types of aggregates and all the studied regions, the abrasion loss percentage is less than 50% (between 19 and 26), hence the aggregates are characterized by good resistance to abrasion according to (*ASTM C33, 2016*) standard.

Table B.7 Abrasion loss (%) by Los Angeles machine for the crushed aggregates

Aggregates Type*	Mount-Lebanon	Beqaa			South Lebanon		North Lebanon	
	Bekfaya	Zahle	Majd El Anjar	Ras Baalbek	Tyre	Ansar	Dahr Nassar	El Biri
MA	24	24	23	-	22	23	-	-
CA	24	22	24	19	20	21	26	25

(*): CS crushed sand; MA: medium aggregate, and CA: coarse aggregate;

(-): aggregates not provided.

Conclusion

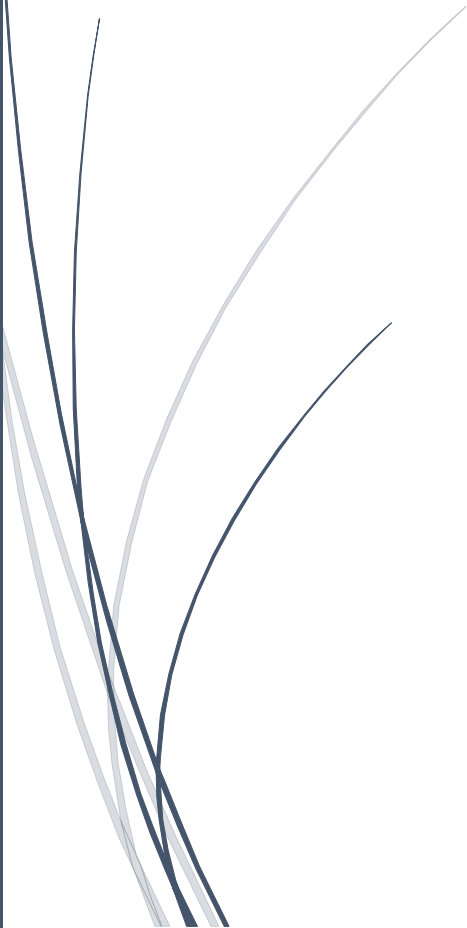
This study demonstrates that all the studied regions are characterized by aggregates of acceptable and comparable properties for the use in concrete in terms of the deleterious particles content and the resistance to soundness and abrasion. However, the relative densities and the absorption percentages differ from one quarry to another, that is why it is primordial to determine the density and the absorption of each aggregate before estimating the aggregates' proportions in concrete mixes.

Generally, this study proves that regardless of the quarries' location, the "Conventional crushed sand" in Lebanon exhibits physical properties (deleterious particles content and resistance to soundness) that respect the ASTM C33 standard requirements for aggregates in concrete.



Annex C

Physical Characterization Tests for Cement



C. Physical Characterization Tests for Cement

Introduction

Hydraulic cement is defined as the cement that sets and hardens by chemical reaction with water and is capable of doing so underwater.

Both standards, ASTM and European, could be required in the specifications of the construction projects in the Lebanese market. Hence, the cement characteristics were determined according to these two standards and the tests are elaborated in this annex.

1. Specification for standard sand

To be used in mortar, the required characteristics of the sand are presented in (ASTM C778, 2017) for the American standard and (EN 196-1, 2005) for the European standard.

1.1 Standard specification for standard sand (ASTM C778, 2017)

The ASTM standard specifies the characteristics listed in Table C.1 for the natural sand.

Table C.1 The characteristics of the standard sand

Characteristics	20-30 Sand	Graded Sand
1.180	100	100
0.850	85-100	-
Grading % passing sieve (mm)	0.600	0-5
	0.425	-
	0.300	-
	0.150	-
		96-100
	60-75	16-30
	0-4	
Max difference in air content of mortars made with washed and unwashed sand (% air)	2.0	1.5
Source of sand	Ottawa, IL or LeSuer, MN	Ottawa, IL

1.2 Method of testing cement – Part 1: Determination of strength (EN 196-1, 2005)

CEN Reference sand is natural siliceous sand consisting of rounded particles and has a silica content of at least 98%. To be used in mortar, its moisture content should not exceed 0.2% after drying at 105-110 °C. Its particle size distribution, determined for a total mass not less than 1345 g, should be as shown in Table C.2.

Table C.2 The particle size distribution of the standard sand

Square mesh size (mm)	2.00	1.60	1.00	0.50	0.16	0.08
Cumulative sieve residue (%)	0	7 ± 5	33 ± 5	67 ± 5	87 ± 5	99 ± 1

2. Procedure for mixing hydraulic cement paste and mortar

(*ASTM C305, 2014*) presents the mixing procedures for cement paste and mortar in the American standards. For the European standard, the mixing procedure for cement paste is presented in (*EN 196-3, 2016*), while the one for mortar is presented in (*EN 196-1, 2005*).

2.1.1 Standard practice for mechanical mixing for hydraulic cement pastes and mortars of plastic consistency (*ASTM C305, 2014*)

2.1.1.1 Procedure for mixing cement paste

The paddle and the bowl should be dried and placed in the mixing position in the mixer. The cement is added to the total quantity of the mixing water previously placed in the bowl. After allowing 30 s for the absorption of the water, the mixer should start at a low speed of 140 ± 5 r/min for 30 s. The mixer is then stopped for 15 s during which all the adhering paste on the sides of the bowl should be scrapped down into the batch. The mixer is then restarted at a medium speed of 285 ± 10 r/min for 60 s.

2.1.1.2 Procedure for mixing mortar

The paddle and the bowl should be dried and placed in the mixing position in the mixer. The cement is added to the total quantity of the mixing water previously placed in the bowl. After allowing 30 s for the absorption of the water, the mixer should start at a low speed of 140 ± 5 r/min for 30 s. While mixing at low speed, the entire quantity of sand is added slowly for 30 s. The mixer is then stopped, the speed changed to a medium speed of 285 ± 10 r/min and restarted again for 30 s. At the end of this period, the mixer is stopped and the mortar is allowed to stand for 90 s. During the first 15 s of this interval, the mortar that may have been collected on the side of the bowl should be quickly scraped down into the batch, then for the remainder of this interval, the mixer enclosure should be closed or the bowl covered with the lid. The mixer is turned on for an additional 60 s at a medium speed of 285 ± 10 r/min. In any case, requiring a remixing interval, any mortar side of the bowl shall be quickly scraped down the batch with the scraper before remixing.

2.1.2 Method of testing cement – Part 3: Determination of setting times and soundness (*EN 196-3, 2016*)

The total mixing time for cement paste shall be 3 minutes. Within 10 s, the water and the cement are introduced into the bowl without loss. The mixer is started, immediately at low speed, and the time is recorded as "zero time". After 90 s, the mixer is stopped for 30 s during which all the paste adhering to the wall and the bottom part of the bowl is removed using a suitable rubber or plastics scraper and placed in the middle of the bowl. The mixer is restarted and run at low speed for a further 90 s.

2.1.3 Method of testing cement – Part 1: Determination of strength (*EN 196-1, 2005*)

For this standard, the water and the cement should be introduced into the bowl without loss. The mixer is then started immediately at low speed (Rotation: 140 ± 5 r/min; Planetary movement: 62 ± 5 r/min) and the time is recorded as "zero time". After 30 s of mixing, the sand is added steadily for 30 s. The mixer is then switched to the high speed (Rotation: 285 ± 10 r/min; Planetary movement: 125 ± 10

r/min) and the mixing is continued for an additional 30 s. The mixer is stopped for 90 s, during the first 30 s all the paste adhering to the wall and the bottom part of the bowl should be removed using a suitable rubber or plastic scraper and placed in the middle of the bowl. The mixer is then restarted and run at high speed for a further 90 s.

3. Determination of normal consistency of hydraulic cement paste

This test aims to determine the amount of water required to prepare hydraulic cement pastes with normal consistency. The cement paste is prepared according to (*ASTM C305, 2014*) and (*EN 196-3, 2016*).

3.1 Standard test method for amount of water required for normal consistency of hydraulic cement paste (*ASTM C187, 2011*)

The cement paste is prepared by mixing 650 g of cement with a measured quantity of water following the procedure prescribed in the procedure for mixing pastes of practice C305. The cement paste shall be quickly shaped in the form of a ball and tossed six times through a free path of about 150 mm from one hand to another.

With a minimum amount of additional manipulation and by introducing the ball into the larger end of the conical ring held in one hand, the Vicat ring is filled with the cement paste.

The excess of the sample is then removed by a single movement and the ring is placed on its larger end on the base plate. If necessary, the excess paste is sliced off by a single oblique stroke of a trowel. The paste should not be compressed during the cutting and smoothing.

The ring should be resting on the plate of the Vicat apparatus, which shall be free of vibration during the test. The plunger is attached to the end of the rod and the set-screw is tightened. After setting the movable indicator to the upper zero mark of the scale, or taking an initial reading, the rod is immediately released with a time not exceeding 30 s after completion of mixing.

If the indicator shows 10 ± 1 mm then the paste is of normal consistency. If not, the test should be repeated with different percentages of water until normal consistency is obtained.

The amount of water required for normal consistency is equal to the percentage of the ratio of the mass of water used to the mass of dry cement.

3.2 Method of testing cement – Part 3: Determination of setting times and soundness (*EN 196-3, 2016*)

500 g of cement is mixed with a measured quantity of water following the mixing procedure of cement paste of this standard detailed in the previous section. The plunger of the Vicat apparatus is lowered to rest on the base plate and the pointer is adjusted to read zero at this position. The mold of the cement paste is then transferred into the apparatus and centered under the rod. The plunger should then rest on the surface of the paste for 1-2 seconds, and the moving parts are quickly removed to allow the plunger to penetrate vertically into the center of the paste (within $4 \text{ min} \pm 10 \text{ s}$ after zero time). The scale is read at least 5 s after the end of the penetration or 30 s after the release of the plunger, whichever is earlier. If the scale reading (the distance between the bottom face of the plunger and the base plate)

shows 6 ± 2 mm, the water content of the paste expressed as a percentage by mass of the cement is considered as the water for standard consistency. If not, the test is repeated with different water to cement ratios.

4. Determination of the time of setting of hydraulic cement paste

This test method aims to determine the amount of initial and final setting times of hydraulic cement paste. The cement paste should be prepared according to (*ASTM C305, 2014*) and (*EN 196-3, 2016*) with a water to cement ratio equal to the normal consistency of cement.

4.1 Standard test method for time of setting of hydraulic cement paste by Vicat needle (*ASTM C191, 2018a*)

The initial setting time is defined in this standard as the time elapsed between the initial contact of cement and water and the time when the penetration is 25 mm. The final setting time is the time elapsed between the initial contact of cement and water and the time when the needle does not make a complete circular impression on the paste surface.

The cement is prepared following practice (*ASTM C187, 2011*), and the temperature of the air in the vicinity of the mixing slab, the dry cement, molds, base plates, and mixing water shall be maintained at 23 ± 3 °C and the relative humidity of the mixing room shall be not less than 50%. The test specimen is left in the moist room for 30 minutes after molding.

The needle of the rod is lowered to rest on the surface of the cement paste, the setscrew is tightened and the indicator is set at zero. The rod is then released quickly by releasing the screw, and the needle is allowed to settle for 30 seconds. In this way, the needle penetration is determined every 15 minutes until penetration of 25 mm or less is obtained. Each penetration should be made at least 5 mm away from any previous penetration and at least 10 mm away from the inner side of the ring.

The Vicat time of setting is calculated as an interpolation between the time of the last penetration greater than 25 mm and the time of the first penetration less than 25 mm.

The first penetration measurement that does not mark the specimen surface with a complete circular impression is the penetration that determines the final setting time. Verification shall be made by two additional penetrations measured on different areas of the specimen surface within 90 seconds.

4.2 Method of testing cement – Part 3: Determination of setting times and soundness (*EN 196-3, 2016*)

The initial setting time is defined in this standard as the time elapsed between the zero time and the time at which the distance between the needle and the base plate is 6 ± 3 mm. The final setting time is the time elapsed between the zero time and the time of penetration that does not mark the specimen surface.

The mold and the base plate should be placed in a container at 20 ± 1 °C and positioned under the needle of 1.13 ± 0.05 mm diameter, where the surface of the plate should be submerged at least 5 mm. The needle is lowered to rest on the paste surface for 1 to 2 seconds, and the moving parts are quickly removed to allow the needle to penetrate vertically into the center of the paste. The scale should be read at least 5 s after the end of the penetration or 30 s after the release of the needle, whichever is earlier.

The scale reading (the distance between the bottom face of the plunger and the base plate) is then recorded and the penetration is repeated at spaced positions (8 mm from the rim of the mold or 5 mm from each other and at least 10 mm from the last penetration position). The needle should be cleaned immediately after each penetration. The initial setting time is reported as the elapsed time between the zero time and the time at which the distance between the needle and the base plate is 6 ± 3 mm.

To determine the final setting time, a ring attachment of a diameter of 5 mm is fixed to the needle to facilitate the observation of small penetration. The final setting time is recorded as the elapsed time between the zero time and the time of penetration that does not mark the specimen surface.

5. Determination of strength of cement mortar

This test method aims to determine the strength of cement mortar in terms of the compressive strength in the ASTM standard, and the flexural and compressive strengths in the European standard. The mortar specimen should be prepared according to (*ASTM C305, 2014*) and (*EN 196-3, 2016*).

5.1 Standard test method for compressive strength or hydraulic cement mortars using 50 mm cube specimens (*ASTM C109, 2016a*)

Two or three 50 mm cube specimens shall be made from a batch of mortar for each period of the test or test age, cast in a controlled room, at a temperature of 23 ± 2 °C and humidity not less than 50%.

The proportions of materials for the standard mortar shall be one part of Portland cement by weight to 2.75 parts of graded standard sand with a water-cement ratio of 0.485.

Table C.3 presents the quantities of materials to be mechanically mixed at one time in the batch of mortar, under the procedure given in Practice C305.

Table C.3 Materials proportions for mortar batches

Number of specimens	6	9	12
Cement, g	500	740	1060
Sand, g	1375	2035	2915
Water, mL	242	359	514

After completion of the mixing of the mortar batch, the molding should be started within a maximum of 2 minutes and 30 s. The first layer is placed of about 25 mm in each cube compartments and tamped 32 times in about 10 s in 4 rounds by applying sufficient pressure to ensure uniform filling. Each round should be at right angles to the other and consist of eight adjoining strokes over the surface of the specimen. The consolidation of one cube should be completed before going to the next. The same tamping process is repeated for the second layer of mortar in all the cubes compartments. The excess mortar is removed with a trowel and the surface is smoothed.

The molded specimens are stored in a moist room for 20 to 72 hours, then de-molded after a minimum of 24 hours and immersed in saturated lime water.

At the age of testing, the specimens are removed from the water, wiped to remove the surface water, and cleared from any loose sand grains or incrustations from the faces that will be in contact with the

bearing blocks of the testing machine. Then, the straightness of these faces is checked before placing the specimen in the testing machine.

The load is applied to the faces of the specimen that were in contact with the true plane surfaces of the mold at a rate within the range of 900 to 1800 N/s, and the maximum load P indicated by the machine is recorded.

The compressive strength is then calculated as follows:

$$f_m = \frac{P}{A} \quad (\text{Eq. C.1})$$

Where:

f_m : Compressive strength (MPa), P : Total maximum load (N), and A : Area of the specimen (mm²).

5.2 Method of testing cement – Part 1: Determination of strength (EN 196-1, 2005)

The room where the preparation of the specimens takes place shall be maintained at a temperature of 20 ± 2 °C and relative humidity greater or equal to 50%. To mix the mortar, the proportions by mass shall be one part of the cement, three parts of CEN standard sand, and one-half part of water (water/cement ratio 0.50). Each batch for the three test specimens shall consist of 450 ± 2 g of cement, 1350 ± 5 g of sand, and 225 ± 1 g of water.

5.2.1 Flexural strength

The mold used for this test is formed of three compartments to prepare three prisms of 40x40 mm in cross-section and 160 mm in length each. Immediately after the preparation of the mortar, the first of two layers of mortar is introduced into the mold, spread uniformly using the large spreader, and compacted with 60 jolts of the jolting table. The second layer of mortar is then introduced while ensuring that there is a surplus of mortar, leveled with the small spreader, and compacted with a further 60 jolts. After gently lifting the mold from the jolting table, the excess mortar is immediately stroked off and the mortar left on the perimeter of the mold is wiped off.

The mold is covered with a plate of glass, steel, or other impermeable material that does not react with cement, of approximate size 210x185x6 mm. For 24 h tests, the de-molding is carried out not more than 20 min before the specimens are tested. For tests at ages greater than 24 h, the demolding is carried out between 20 and 24h after molding. Without delay, the de-molded specimens are submerged conveniently, either horizontally or vertically, in the water at 20 ± 1 °C.

The specimens are removed from water not more than 15 min before the test is carried out at any particular age and covered with a damp cloth until tested. Any deposit on the test faces should be removed and the strength tests are carried out at 24 h \pm 15 min; 48 h \pm 30 min; 72 h \pm 45 min; 7 d \pm 2 h; \geq 28 d \pm 8 h.

The apparatus for the determination of flexural strength shall be capable of applying three-points loading up to 10 kN at a rate of loading of 50 ± 10 N/s until fracture. The apparatus shall be provided with a flexure device incorporating two steel supporting rollers of 10 ± 0.5 mm diameter, spaced 100 ± 0.5 mm apart, and a third steel loading roller of the same diameter placed centrally between the other

two. The length of these rollers shall be between 45 and 50 mm. The three vertical planes through the axes of the three rollers shall be parallel and remain parallel, equidistant and normal to the direction of the specimen under test.

The flexural strength R_t is calculated as the average of three individual tests as follows:

$$R_t = \frac{1.5 \times F_t \times l}{b^3} \quad (\text{Eq. C.2})$$

Where:

R_t : Flexural strength (MPa), F_t : Load applied to the middle of the prism at fracture (N), l : the distance between the supports (mm), and b : the side of the square section of the prism (mm).

5.2.2 Compressive strength

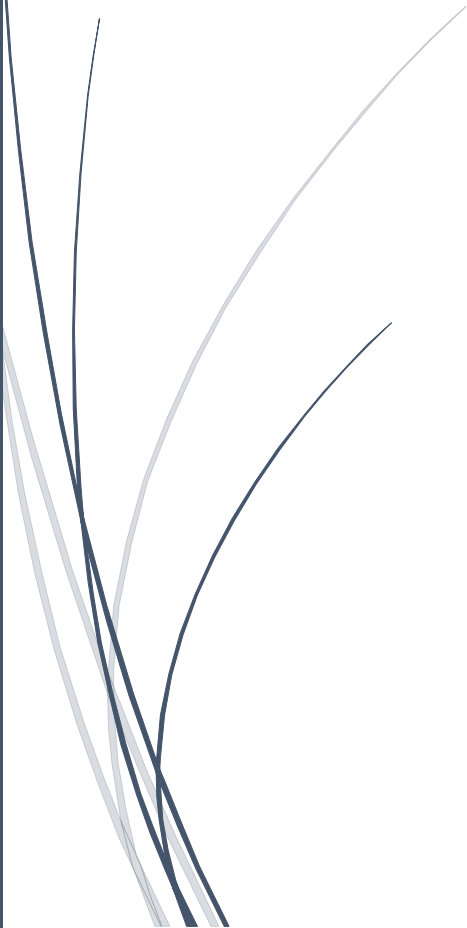
The compressive strength is carried out on halves of the prism broken at the flexural strength test. The rate of the load increase is 2400 ± 200 N/s. The maximum load at fracture F_C is recorded in N and the compressive strength is calculated in MPa as:

$$R_C = \frac{F_C}{1600} \quad (\text{Eq. C.3})$$



Annex D

Concrete Tests



D. Concrete Tests

Introduction

This annex consists of detailing the procedure of the tests conducted on concrete in this study. The differences between the ASTM and the European standards are also presented in this annex.

1. Standard terminology relating to concrete and concrete aggregates (*ASTM C125, 2016*)

In this standard, **Concrete** is defined as a composite material that consists essentially of a binding medium within which are embedded particles or fragments of aggregate; in hydraulic-cement concrete, the binder is formed from a mixture of hydraulic cement and water.

When the concrete possesses enough of its original workability so that it could be placed and consolidated by the intended methods, it is a **Fresh Concrete**.

Hardened Concrete is concrete that has developed sufficient strength to serve some defined purpose or resist a stipulated loading without failure.

2. Standard test method for temperature of freshly mixed hydraulic-cement concrete (*ASTM C1064, 2017*)

2.1 Procedure

This test aims to measure the temperature of freshly mixed concrete at the time of testing.

This temperature could be measured in either the transporting equipment, the forms after discharge, or in a sample container after discharging the concrete.

The measuring device should be placed in the container so that the device sensing portion is covered by at least 75 mm of concrete in all directions and at least three times the nominal maximum size of the coarse aggregate. Then, gentle pressure should be applied around the measuring device to close the void left by the placement of the device and to prevent ambient air temperature from affecting the reading.

After 2 to 5 minutes maximum, the temperature could be recorded to the nearest 0.5 °C without removing the device from the container while reading the temperature.

2.2 Comparison with European standard

The European Standard does not present a specific method to determine the temperature of freshly mixed concrete.

3. Standard test method for slump of hydraulic-cement concrete (*ASTM C143, 2015a*)

3.1 Procedure

This test aims to measure the slump of freshly mixed concrete, having coarse aggregates size up to 37.5 mm, by using a mold in the shape of a frustum of a cone. Samples with slump lower than 15 mm may not be adequately plastic and samples with slump higher than 230 mm may not be adequately cohesive for this test to have significance.

Before conducting the test, the mold should be dampened and placed on a rigid, flat, level, moist, nonabsorbent, and free of vibration surface.

While holding the mold firmly in place, the concrete should be placed, by moving the scoop around the perimeter of the mold to ensure even distribution and to avoid segregation, in three layers of equal volume (one-third of mold volume corresponds to 70 mm depth; two-thirds of the volume corresponds to 160 mm depth). Each layer of concrete should be rodded uniformly over the cross-section of the mold with 25 strokes of the tamping rod. The bottom layer should be rodded throughout its depth. While rodding the two other layers the rod should penetrate through the layer being rodded and into the layer below approximately 25 mm. While filling the third layer, an excess of concrete should be kept above the top of the mold. Then, the concrete surface should be struck off by rolling the tamping roll over it.

While keeping the mold firm in place, the concrete should be removed from the area surrounding the mold. Afterward, the mold should be removed immediately (5 ± 2 seconds) by raising it vertically to a distance of 300 mm.

Immediately, the slump should be measured and recorded (to the nearest 5 mm) by determining the difference between the top of the mold and the displaced original center of the top surface of the specimen. If the test falls away or shears off from one side, the test should be disregarded and repeated.

3.2 Comparison with European standard

The European standard, **NF EN 12350-2-2012 (Testing fresh concrete-Part 2: Slump test)**, specifies the suitability of the test only for concretes with a maximum size of aggregates lower than 40 mm and slump values between 10 mm and 210 mm. The same procedures are followed to determine the slump as the ones in the ASTM standard.

4. Standard test method for density (unit weight), yield, and air content (gravimetric) of concrete (*ASTM C138, 2017a*)

4.1 Procedure

This test consists of measuring the density of freshly mixed concrete and it presents methods to calculate the yield (the volume of concrete produced from a mixture of known quantities of the component materials), the cement content, and the air content of concrete (by the gravimetric method).

The measure could be filled using one of the following consolidation methods, depending on the slump value. The rodding method is applied for concretes with a slump greater than 75 mm and the vibration

method is applied for concretes with a slump lower than 25 mm. For concretes with a slump between 25 and 75 mm, one of the two methods could be applied.

- The rodding method consists of placing the concrete in three layers of equal volume. Each layer is rodded uniformly over the cross-section of the measure with 25 strokes of the tamping rod when nominal 14-L or smaller measures are used, 50 strokes when nominal 28 L measures are used, and one stroke per 20 cm² of surface for larger measures. The bottom layer is rodded through its depth. For the other two layers, the rod is allowed to penetrate into the layer below to approximately 25 mm. After rodding each layer, the sides of the measure are tapped 10 to 15 times with an appropriate mallet using such force to close any voids left by the tamping rod and to release any large bubbles of air that may have been trapped.
- The vibration method consists of placing the concrete in two equal layers. The internal vibrator of 50 Hz is inserted in three different points of each layer and is penetrated to 25 mm in the underlying layer. The vibrator is not allowed to touch the bottom or the sides of the measure. The duration of vibration for each layer depends upon the concrete workability and the vibrator's effectiveness. Care should be taken to avoid forming air pockets when removing it.

The interior of the measure should be dampened and any standing water should be removed from the bottom. The empty mass M_m of the measure is determined. After placing the measure on a flat, level, firm surface, the concrete is placed while the scoop is moved around the perimeter of the measure opening to ensure an even distribution of the concrete with minimal segregation, according to the chosen consolidation method. An excess of concrete protruding approximately 3 mm above the top of the mold is optimum. Then, the surface is strike-off by a sawing motion to cover 2/3 of the measure surface, then the whole surface is strike-off. Final strokes should be performed with the edge of the plate in order to have a smooth surface. After cleaning all the excess concrete from the exterior of the measure, the final mass M_C is determined.

Many concrete characteristics could be measured from this test:

- Density (unit weight):

$$D = \frac{M_C - M_M}{V_M} \quad (\text{Eq. D.1})$$

- Theoretical density (unit weight):

$$T = \frac{M}{V} \quad (\text{Eq. D.2})$$

- Absolute volume of each ingredient:

$$V_i = \frac{M_i}{1000 \times D_i} \quad (\text{Eq. D.3})$$

- Yield:

$$Y = \frac{M}{D} \quad (\text{Eq. D.4})$$

- Relative yield:

$$R_Y = \frac{Y}{Y_D} \quad (\text{Eq. D.5})$$

- Cement content:

$$C = \frac{C_b}{Y} \quad (\text{Eq. D.6})$$

- Air content:

$$A = 100 \times \frac{T-D}{T} \quad \text{or} \quad A = 100 \times \frac{Y-V}{Y} \quad (\text{Eq. D.7})$$

Where:

M_c : Mass of the measure filled with concrete (kg); M_m : Mass of the empty measure (kg);

V_m : Volume of the measure (m^3); M_i : Mass of each ingredient (kg);

D_i : specific gravity of each ingredient; M : total mass of all materials batched (kg);

V : total absolute volume of the component ingredients in the batch (m^3);

Y_d : volume of concrete which the batch was designed to produce (m^3);

C_b : Cement mass in the batch (kg).

4.2 Comparison with European standard

In **NF EN 12350-6-2012 (Testing fresh concrete-Part 6: Density)** the vibration could also be applied externally by the means of a vibration table (minimum 40 Hz), while the internal vibrator should have a minimum frequency of 120 Hz.

This standard follows the same rodding procedure as that in ASTM C138 and the calculations are limited only to the density.

5. Standard test method for air content of freshly mixed concrete by the pressure method (*ASTM C231, 2017a*)

5.1 Procedure

This test determines the air content of freshly mixed concrete exclusive of any air that may exist inside voids within aggregates particles; it applies to concrete made with relatively dense aggregates. The determination of air content by the pressure method consists of the determination of the air content from the observation of the change in concrete volume with a change in pressure.

If concrete contains aggregate particles coarser than 50 mm sieve, wet sieving should be done over 37.5 mm to yield sufficient material to fill the measure. The mortar adhering on the surface of the coarse aggregate should not be wiped during sieving.

The measure could be filled using one of the following consolidation methods, depending on the slump value. The rodding method is applied for concretes with a slump greater than 75 mm and the vibration method is applied for concretes with a slump lower than 25 mm. For concretes with a slump between 25 and 75 mm, one of the two methods could be applied.

- The rodding method consists of placing the concrete in three layers of equal volume. Each layer is rodded uniformly over the cross-section of the measure with 25 strokes of the tamping rod when nominal 14-L or smaller measures are used, 50 strokes when nominal 28 L measures are used, and one stroke per 20 cm² of surface for larger measures. The bottom layer is rodded through its depth. For the other two layers, the rod is allowed to penetrate into the layer below to approximately 25 mm. After rodding each layer, the sides of the measure are tapped 10 to 15 times with an appropriate mallet using such force to close any voids left by the tamping rod and to release any large bubbles of air that may have been trapped.
- The vibration method consists of placing the concrete in two equal layers. The internal vibrator of 50 Hz is inserted in three different points of each layer and is penetrated to 25 mm in the underlying layer. The vibrator is not allowed to touch the bottom or the sides of the measure. The duration of vibration for each layer depends upon the concrete workability and the vibrator's effectiveness and care should be taken to avoid forming air pockets when removing it.

The interior of the measure should be dampened and any standing water should be removed from the bottom. After placing the measure on a flat, level, firm surface, the concrete is placed while moving the scoop around the perimeter of the measure opening to ensure an even distribution of the concrete with minimal segregation, according to the chosen consolidation method. An excess of concrete protruding approximately 3 mm above the top of the mold is optimum. Then, the surface is strike-off by a sawing motion to cover 2/3 of the measure surface, then the whole surface is strike-off. Final strokes should be performed with the edge of the plate in order to have a smooth surface.

Type A or type B meters can be used to determine the air content. Type B is generally used and the procedure of its use is detailed in the following. After cleaning the flanges or rims of the measuring bowl and the cover assembly, the apparatus is assembled. The main air valve between the air chamber and the measuring bowl is closed and both petcocks are opened. Water is added through one petcock until water emerges from the opposite petcock. Then, the main air bleeder valve on the air chamber is closed and the air is pumped into the chamber until the gauge hand is on the initial pressure line. The compressed air is allowed to cool for few seconds. The gauge hand is stabilized at initial pressure by pumping or bleeding-off air as necessary, and the gauge is tapped lightly by hand. The petcocks are closed, and the main air valve is opened. The sides of the bowl should be tapped with the mallet and the pressure gauge should be tapped by hand to be stabilized. The air content is recorded and the main air valve is released.

The air content is measured as follows:

- Air content of the tested sample (%)

$$A_s = A_1 - G \quad (\text{Eq. D.8})$$

- Air content of the full mixture (%)

$$A_t = \frac{100 A_s V_c}{100 V_t - A_s V_a} \quad (\text{Eq. D.9})$$

- Air content of the mortar fraction (%)

$$A_m = \frac{100 A_s V_c}{100 V_m + A_s (V_c - V_m)} \quad (\text{Eq. D.10})$$

Where:

A_1 : Apparent air content tested (%);

G : aggregate correction factor determined by a detailed procedure in this standard;

V_c : absolute air-free volume of ingredients passing 37.5 mm from original batch weights (m^3);

V_t : absolute air-free volume of all ingredients of the mixture (m^3);

V_a : absolute volume of aggregates coarser than 37.5 mm from original batch weights (m^3);

V_m : absolute volume of ingredients of the mortar fraction of the mixture (cement + water + fine aggregates + coarse aggregates (4.75 to 37.5 mm)).

5.2 Comparison with European standard

NF EN 12350-7-2012 (Testing fresh concrete- Part 7: Air content - Pressure methods) is the European standard used to determine the air content under pressure and it follows the same procedures detailed in ASTM C231, but in this standard, the maximum nominal size of aggregates could reach 63 mm.

As for the compaction methods, the vibration could be applied externally by the means of a vibration table (minimum 40 Hz), the internal vibrator should have a minimum frequency of 120 Hz, and the rodding procedure is similar to the one in the ASTM standard.

6. Standard test method for time of setting of concrete mixtures by penetration resistance (*ASTM C403, 2008*)

6.1 Procedure

The time of setting of concrete is defined by the time required for the mortar portion of concrete to reach specified values of resistance to needles penetration. This test shall be performed on a mortar portion sieved from the concrete mixture and not on a prepared mortar intended to simulate the mortar fraction of the concrete.

Three specimens for each sample should be prepared with compliance with the following conditions:

- Record the time at which initial contact was made between cement and mixing water.
- After determining and recording the slump (ASTM C143) and air content (ASTM C231) of the fresh concrete, select a representative portion of sufficient volume of concrete to provide enough mortar to fill the test container to a depth of at least 140 mm.
- In accordance with (ASTM C172), obtain a mortar sample by wet-sieving the selected portion of concrete through a 4.75 mm sieve and onto a non-absorptive surface.
- Remix the mortar, measure, and record its temperature then place it in a single layer in the container.
- Consolidate the sample to eliminate air pockets and level the top surface (the mortar surface shall be at least 10 mm below the top edge of the container).
- Store the specimens at 20-25 °C.

Each test is performed for at least 6 penetrations, and it should be continued until at least one penetration resistance reading equals or exceeds 27.6 MPa. In subsequent penetration tests, the areas where the mortar has been disturbed by previous tests should be avoided.

For concrete mixtures at lab temperature (20 to 25 °C), the initial test should be performed 3 to 4 h after initial contact between cement and water, and subsequent tests should be made at 0.5 to 1 h intervals.

For concrete mixtures containing accelerators or at a higher temperature, the initial test should be performed 1 to 2 h after initial contact between cement and water, and subsequent tests should be made at 0.5 h intervals. For concrete mixtures containing retarders or at a lower temperature, the initial test should be performed 4 to 6 h after initial contact between cement and water and time intervals for subsequent tests depend on the rate of setting.

The ambient air temperature is measured and recorded at the start and the finish of the test. A block is placed under one side of the container to form an angle of approximately 10° to facilitate the process of removing the bleed water from the surface by a pipet. A needle of appropriate size (depending upon the degree of setting) is inserted in contact with the mortar surface. A vertical force is applied until the needle penetrates the mortar to a depth of 25 ± 2 mm (the time required for penetration shall be 10 ± 2 s). The force required for the penetration of 25 mm and the time of application (measured as elapsed time after initial contact of cement and water) are recorded.

For each penetration test, the penetration resistance is calculated as the ratio between the recorded force and the bearing area of the needle. The test results are plotted (penetration resistance as ordinates and elapsed time as abscissa) and the initial and the final setting times are determined from the plots as the time when the penetration resistance reaches 3.5 MPa and 27.6 MPa respectively.

7. Standard test method for making and curing concrete test specimens in the laboratory (ASTM C192, 2016a)

7.1 Procedure

This test covers the requirements for mixing concrete, preparing, and curing specimens under laboratory conditions.

Before mixing, the materials should be at room temperature in the range of 20-30 °C, unless the concrete temperature is stipulated. Cement should be stored in a dry place, mixed, and passed through 850 µm sieve to remove all lumps. To avoid segregation, coarse aggregates should be separated into individual size fractions then combined in proper gradation to produce the desired grading. The same method could be applied for fine aggregates or they could be maintained in damp condition until use.

The weight of aggregates to be used in mixes could be determined by one of the following procedures:

- If aggregates absorption is low (less than 1%), the mass of aggregates in the room-dry condition is determined with allowance made for the amount of water that will be absorbed from the unset concrete (useful when aggregates are separated into individual size fractions).
- The individual size fractions are weighed, recombined, and immersed in water at least 24 h before use. The excess of water is decanted, and the combined weight of aggregates and the mixing water is determined. The allowance shall be made for the amount of water absorbed.

- The aggregates are brought to a saturated condition (surface moisture in sufficiently small amounts) at least 24 h prior to use. The quantity of surface water must be counted as part of the required mixing water. This method is particularly useful for fine aggregates. If used with coarse aggregates, each size fraction should be separated.
- The aggregates are brought to a saturated surface dry condition SSD until used. This method is used primarily for batches $\leq 0.007 \text{ m}^3$

Insoluble powdered admixtures containing no hygroscopic salts and are to be added in small quantities should be mixed with cement. Insoluble admixtures with amounts $> 10\%$ by mass of cement, should be added in the same manner as cement. Insoluble powdered admixtures but containing hygroscopic salts should be mixed with sand. Water-soluble and liquid admixtures should be added with mixing water and should be included in the calculation of water content. Admixtures, incompatible in concentrated form, such as solutions of CaCl_2 and certain air-entraining and set-retarding admixtures should not be intermixed prior to use.

Mixing concrete could be done by one of the following procedures with batch size calculated as to leave 10% excess after molding specimens:

- **Hand mixing:**

The hand-mixing procedure is not applicable to air-entrained concrete or concrete with no slump, it is also limited to batches volume $\leq 0.007 \text{ m}^3$:

- The cement is mixed with the powdered insoluble admixtures and fine aggregates, without adding water until they are blended.
- The coarse aggregates are added and mixed without adding water until they are uniformly distributed throughout the batch.
- The water is added and mixed with all ingredients until the concrete is homogenous.

- **Machine mixing:**

- The coarse aggregates are added with some of the mixing water and the solution of admixtures.
- The mixer is started then the fine aggregates are added with the cement and water while the mixer is running (components may be added to stopped mixer after permitting it to turn few revolutions).
- All the ingredients are mixed for 3 minutes, followed by 3 minutes rest, then 2 minutes of final mixing.

The cylinders could be filled using one of the following consolidation methods, depending on the slump value. The rodding or vibration methods are applied for concretes with a slump greater or equal to 25 mm, while the vibration method is applied for concretes with a slump lower than 25 mm. Internal vibration should not be used for cylinders with a diameter less than 100 mm and for beams or prisms with a breadth or depth less than 100 mm.

- The rodding method consists of placing the concrete in the required number of layers (depending on the cylinder dimension). Each layer is rodded uniformly over the cross-section of the measure with the specified number of strokes of the tamping rod. The bottom layer is rodded through its depth. For the other layers, the rod is allowed to penetrate into the layer below to approximately 25 mm. After rodding each layer, the sides of the mold are tapped 10 to 15 times with an appropriate mallet using such force to close any voids left by the tamping

rod and to release any large bubbles of air that may have been trapped. The concrete surface is spaded with a trowel or other suitable tool.

- The vibration method consists of placing the concrete in the required number of approximately equal layers. For cylinders, the internal vibrator is slowly inserted with the required number of insertions, uniformly within each layer (the vibrator is not allowed to touch the bottom or the sides of the cylinder). For beams, the internal vibrator is inserted at intervals not exceeding 150 mm along the centerline of the long dimension of the specimen (alternating insertions are used along two lines for specimens wider than 150 mm). The vibrator is penetrated to 25 mm in the underlying layer. The sides of the mold are tapped 10 to 15 times with an appropriate mallet using such force to close any voids left by the tamping rod and to release any large bubbles of air that may have been trapped. The duration of vibration for each layer depends upon the concrete workability and the vibrator's effectiveness and care should be taken to avoid forming air pockets when removing it. The concrete is struck off the surface.

To prevent the loss of moisture from the specimens, they are covered immediately after casting. The molds should be removed 24 ± 8 h after casting (molds shall not be removed before 20 ± 4 h for prolonged setting time) and storage shall be free of vibration during the first 48 h.

Curing temperature shall be 23 ± 2 °C in water storage tanks or moist rooms. For flexural strength, and for a minimum period of 20 h before testing, specimens should be cured in water saturated with calcium hydroxide solution $\text{Ca}(\text{OH})_2$. Drying the surfaces prior to testing shall be prevented).

7.2 Comparison with European standard

In addition to cylinder specimens, **NF EN 12390-1-2012 (Testing hardened concrete-Part 1: Shape, dimensions and other requirements for specimens and molds)** specifies the dimensions and tolerances for cubes and prisms specimens.

NF EN 12390-2-2012 (Testing hardened concrete-Part 2: Making and curing specimens for strength tests) specifies that the specimens can be kept in the molds for a minimum of 16 hours and a maximum of 3 days protected against shock, vibration, and dehydration at a temperature of 20 ± 5 °C (or 25 ± 5 °C in hot climates).

Curing the test specimens should be in water at a temperature of 20 ± 2 °C, or in a chamber at 20 ± 2 °C and relative humidity ≥ 95 %, till immediately before testing.

As for the compaction methods, the vibration could be applied externally by the means of a vibration table (minimum 40 Hz), the internal vibrator should have a minimum frequency of 120 Hz, and the rodding procedure is similar to the one in ASTM C192.

8. Standard test method for compressive strength of cylindrical concrete specimen (*ASTM C39, 2017a*)

8.1 Procedure

This test aims to measure the compressive strength of cylinders or cores by applying a compressive axial load, and it is limited to concrete having a density higher than 800 kg/m³.

If the test is performed to determine the compressive strength on laboratory tests, the specimens should be prepared according to ASTM C192 standard. At the end of the specified curing period, the specimens shall be tested in moist condition as soon as practical.

If the ends of the specimen are not plane within 0.05 mm and differ from orthogonality to the axis by more than 0.5°, the specimen should be discarded.

Two values of diameter are measured at a right angle at about mid-height of the specimen and the average of the two values is recorded to the nearest 0.25 mm. Specimens should be discarded if any individual diameter of a cylinder differs from any other diameter of the same cylinder by more than 2%.

The average length of the specimen is determined to the nearest 1 mm at 3 locations evenly spaced around the circumference. When the density calculation is not required and the ratio of length into diameter is smaller than 1.8 or larger than 2.2, the length of the specimen is measured to the nearest 0.05 D.

The mass of the specimen is determined before capping, after removing its surface moisture with a towel.

The volume can be calculated after weighing the specimen in air, and its submerged mass is determined in water at 23 ± 2 °C.

The bearing faces of the bearing blocks of the compressive strength machine, the spacers, and the specimen are cleaned from dust. The specimen is placed on the lower bearing block of the machine by aligning its axis with the center of thrust of the upper bearing block. The load indicator is set to zero, and the load is applied continuously and without shock at a rate of 0.25 ± 0.05 MPa/s until the load indicator shows that the load is decreasing steadily, and the specimen displays a well-defined fracture pattern.

The maximum applied load, the type of the fracture pattern, and any defects on the specimen are recorded. The compressive strength is calculated, in MPa, by:

$$f_{cm} = \frac{4000 P_{max}}{\pi D^2} \quad (Eq. D.11)$$

Where:

P: the maximum applied load (kN);

D: the average measured diameter (mm).

If $L/D \leq 1.75$, the calculated compressive strength should be multiplied by a correction factor following Table D.1 (interpolation is used for intermediate values).

Table D.1 Correction factor function of L/D

L/D	1.75	1.5	1.25	1
Correction factor	0.98	0.96	0.93	0.87

In order to calculate the density, the specimen volume is determined by the measurements of the average length and average diameter or by applying the following equation:

$$V = \frac{W - W_s}{\gamma_w} \quad (Eq. D.12)$$

Where:

W: The mass of the specimen in air (kg);

W_s: The apparent mass of the submerged specimen (kg);

γ_w: The water density at 23 °C = 997.5 kg/m³.

When required, the density of the specimen is determined, in kg/m³, by:

$$\text{Density} = \frac{W}{V} \quad (\text{Eq. D.13})$$

Where:

W: The mass of the specimen (kg);

V: The volume of the specimen (m³).

8.2 Comparison with European standard

The compressive strength for concrete specimens is determined by the European standard **NF EN 12390-3-2012 (Testing hardened concrete-Part 3: Compressive strength of test specimens)** and it differs from ASTM C39 only by the rate of load applied; it should be 0.6 ± 0.2 MPa/s. This standard specifies that the initial load applied should not exceed approximately 30% of the failure load.

9. Standard test method for static modulus of elasticity and Poisson's ratio of concrete in compression (ASTM C469, 2014)

9.1 Procedure

This test aims to determine the modulus of elasticity (stress to strain value) and Poisson's ratio (lateral to longitudinal strain) of hardened concrete by applying compression stress (0-40% of the ultimate concrete strength).

The test specimens can be molded cylinders prepared according to ASTM C192 or drilled cores with a length to diameter ratio greater than 1.5.

A bonded or unbonded sensing device is used to measure to the nearest 5 millionths the average deformation of two diametrically opposite gauge lines, each parallel to the axis, and each centered about mid-height of the specimen.

Gauge points embedded in or cemented to the specimen could be used. The effective length of each gauge line shall be not less than three times the maximum size of the aggregate in the concrete nor more than two-thirds the height of the specimen; the preferred length of the gauge line is one-half the height of the specimen.

The compressometer of Figure D.1 could also be used. This measurement device consists of two yokes and a pivot rod A to maintain a constant distance between the two yokes. The lower yoke B is strictly attached to the specimen, while the upper one C is attached at two diametrically opposite points to be free to rotate. Thus, the gauge reading is equal to the sum of the displacement due to the specimen deformation and the one due to the rotation of the yoke about the pivot rod.

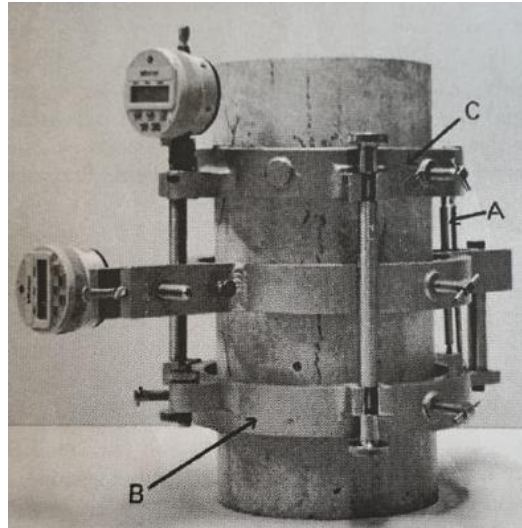


Figure D.1 Suitable compressometer

If the distances of the pivot rod and the gauge from the vertical plane passing through the support points of the rotating yoke are equal, the deformation of the specimen is equal to one-half the gauge reading. If these distances are not equal, the deformation d (μm) is calculated as follows:

$$d = \frac{g e_r}{e_r + e_g} \quad (\text{Eq. D.14})$$

Where:

g : the gauge reading (μm);

e_r : the perpendicular distance, measured to the nearest 0.2 mm from the pivot rod to the vertical plane passing through the two support points of the rotating yoke;

e_g : the perpendicular distance, measured to the nearest 0.2 mm from the gauge to the vertical plane passing through the two support points of the rotating Yoke.

If Poisson's ratio is desired, an extensometer is used. If the distances of the hinge and the gauge from the vertical plane passing through the support points of the middle are equal, the transverse deformation of the specimen diameter r_s is equal to one-half the gauge reading. If these distances are not equal, the transverse deformation d' (μm) of the specimen diameter is calculated in accordance with:

$$d' = \frac{g' e'_h}{e'_h + e'_g} \quad (\text{Eq. D.15})$$

Where:

g' : the gauge reading (μm);

e'_h : the perpendicular distance, measured to the nearest 0.2 mm from the pivot rod to the vertical plane passing through the two support points of the rotating yoke;

e'_g : the perpendicular distance, measured to the nearest 0.2 mm from the gauge to the vertical plane passing through the two support points of the rotating yoke.

Before applying the following procedure to determine the modulus of elasticity and the Poisson's ratio, compressive strength shall be determined for at least two companion specimens. The specimens should be tested within 1 hour after removal from curing, with a constant surrounding temperature not varying by more than 2 °C.

The specimen is aligned in the machine and it is loaded a minimum of three times (do not record any data during 1st loading), the load is applied continuously and without shock (at a rate of 1 mm/minute or 250 ± 50 kPa/s), until the applied load is 40% of the average ultimate load of companion specimens (this is the maximum load for the modulus of elasticity test).

Without interruption of loading, the applied load is recorded when the longitudinal strain (the measured longitudinal deformation of the specimen divided by the effective gauge length) is 50 microstrain. Additionally, the longitudinal strain is recorded when the applied load is equal to 40% of the ultimate load of the specimens. The transverse strain (ratio of the measured gauge in specimen diameter to the original diameter) is also recorded at the same points.

To plot the stress-strain curve take readings at two or more intermediate points or use an instrument that makes a continuous record.

The modulus of elasticity E is calculated to the nearest 200 MPa by:

$$E = \frac{S_2 - S_1}{\epsilon_2 - 0.000050} \quad (\text{Eq. D.16})$$

Where:

S_2 : the stress corresponding to 40% of the ultimate load (MPa);

S_1 : the stress corresponding to a longitudinal strain, ϵ_2 , of 50 millionths (MPa);

ϵ_2 : the longitudinal strain produced by stress S_2 .

The Poisson's ratio μ is calculated by:

$$E = \frac{\epsilon_{t2} - \epsilon_{t1}}{\epsilon_2 - 0.000050} \quad (\text{Eq. D.17})$$

Where:

ϵ_{t2} : the transverse strain at mid-height of the specimen produced by stress S_2 ;

ϵ_{t1} : the transverse strain at mid-height of the specimen produced by stress S_1 .

9.2 Comparison with European standard

In the European standard, the modulus of elasticity is determined by **BS EN 12390-13:2013 (Testing hardened concrete - Part 13: Determination of secant modulus of elasticity in compression)**. In this test, the gauges used should have the same requirements as in ASTM C469.

In Method A (Figure D.2a), the wiring stability and the specimen positioning are checked by three preloading cycles. The initial secant modulus is determined by:

$$E_{C,0} = \frac{\Delta\sigma}{\Delta\epsilon_0} = \frac{\sigma_a^m - \sigma_b^m}{\epsilon_{a,1} - \epsilon_{b,0}} \quad (\text{Eq. D.18})$$

And the stabilized secant modulus is calculated as:

$$E_{C,S} = \frac{\Delta\sigma}{\Delta\varepsilon_S} = \frac{\sigma_a^m - \sigma_b^m}{\varepsilon_{a,3} - \varepsilon_{b,2}} \quad (\text{Eq. D.19})$$

In Method B (Figure D.2b), three loading cycles are carried out. The wiring stability and the specimen positioning are checked at the end of the second and third cycles. The stabilized secant modulus is determined from the third cycle by:

$$E_{C,S} = \frac{\Delta\sigma}{\Delta\varepsilon_S} = \frac{\sigma_a^m - \sigma_p^m}{\varepsilon_{a,3} - \varepsilon_{p,2}} \quad (\text{Eq. D.20})$$

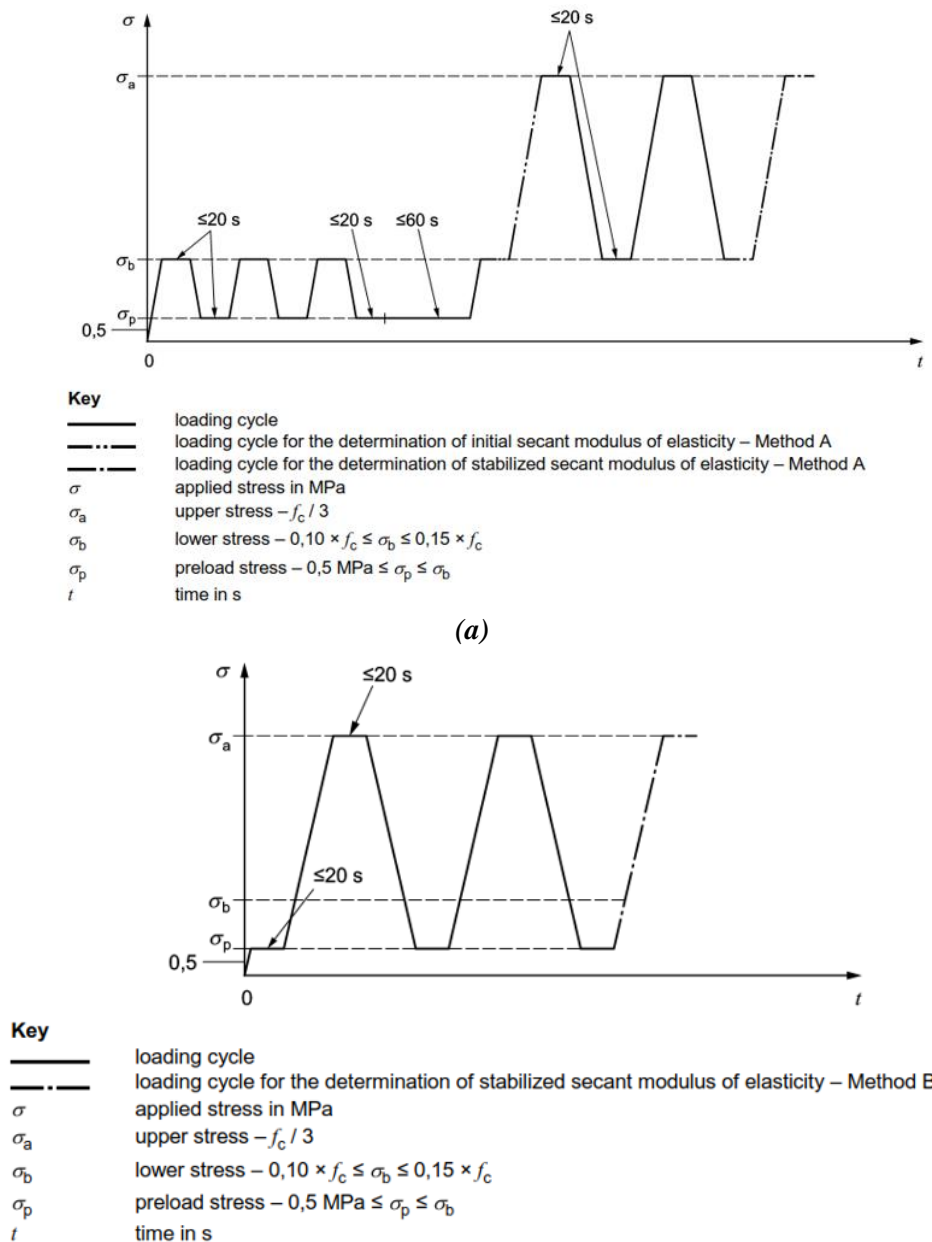


Figure D.2 Determination of the modulus of elasticity by (a) Method A, and (b) Method B (BS EN 12390-13, 2013)

10. Standard test method for flexural strength of concrete (using simple beam with third-point loading) (*ASTM C78, 2016*)

10.1 Procedure

This test aims to determine the flexural strength of hardened concrete using a simple beam with third-point loading.

The specimens should be prepared according to ASTM C192 and tests shall be made as soon as practical after removal from moist storage (surface drying leads to a reduction of the measured modulus of rupture).

The specimen's depth shall be equal to the third of the span and the sides shall be at 90° with top and bottom. All specimen surfaces shall be smooth and free of scars, indentations, holes, or inscribed identification marks.

During the test, the load should be applied perpendicularly to the face of the specimen without eccentricity and reactions shall always be parallel to the direction of the applied load. The ratio of the horizontal distance between the point of application of the load and the point of application of the reaction to the depth of the beam shall be 1 ± 0.03 .

The test specimen is turned on its side with respect to its position as molded and centered on the support blocks. The specimen is loaded continuously and without shock at a constant rate until the breaking point. The rate (N/min) is computed as follows:

$$r = \frac{S b d^2}{L} \quad (\text{Eq. D.21})$$

Where:

S: the rate of increase in the maximum stress on the tension face (0.9-1.2 MPa/min);

b: the average width of the specimen as oriented for testing (mm);

d: the average depth of the specimen as oriented for testing (mm);

L: the span length (mm).

The calculation of modulus of rupture R (MPa) depends on the fracture location.

- If the fracture initiates in the tension surface within the middle third of the span length:

$$R = \frac{P L}{b d^2} \quad (\text{Eq. D.22})$$

- If the fracture initiates in the tension surface outside of the middle third of the span length by not more than 5% of the span length:

$$R = \frac{3 P a}{b d^2} \quad (\text{Eq. D.23})$$

- If the fracture initiates in the tension surface outside of the middle third of the span length by more than 5% of the span length, discard the results of the test.

Where a is the average distance between the line of fracture and the nearest support measured on the tension surface of the beam (mm).

10.2 Comparison with European standard

In European standard, **NF EN 12390-5-2009 (Testing hardened concrete-Part 5: Flexural strength of test specimens)** the rate of increase in the maximum stress on the tension face varies from 0.04 to 0.06 MPa/s and there is no 5% tolerance for a fracture to be outside the loading rollers.

This standard specifies that the initial load applied should not exceed approximately 20% of the failure load.

11. Standard test method for length change of hardened hydraulic-cement mortar (*ASTM C157, 2006*)

11.1 Procedure

This test aims to determine the length change, an increase or decrease in the length, of a laboratory test specimen caused by any factor other than externally applied forces and temperature changes.

The air in the room shall be maintained at a temperature of 23 ± 2 °C and relative humidity of $50 \pm 4\%$.

The concrete test specimens are in the form of prisms of 100x100 mm cross-section and $L=285$ mm (if all aggregates pass 50 mm sieve), or prisms of 75x75 mm cross-section and $L=285$ mm (if all aggregates pass 25 mm sieve).

Three test specimens shall be prepared for each test and cured in a moist cabinet. The concrete is placed in the molds in two equal layers and consolidated by rodding.

After completion of molding, the device should be loosening by holding the gage studs in position at both ends of the mold to prevent any restraint of studs before the specimens are de-molded.

The specimens are removed from the molds at an age of 23.5 ± 0.5 h after the addition of water to the cement during the mixing operation (not more than 24 h).

After removing the specimens from the mold at the age of 24 ± 0.5 h, they should be placed in lime-saturated water (23 ± 0.5 °C) for a minimum of 15 minutes for a 25x25 mm square cross-section and a minimum of 30 minutes for 75 or 100x100 mm square cross-sections.

At an age of 24 ± 0.5 h after the addition of water to the cement during the mixing operation, the specimens should be removed from water storage one at a time, wiped with a damp cloth, and immediately the initial comparator reading should be taken.

The specimens can be stored in lime-saturated water and the comparator readings of each specimen are taken when it has reached an age of 8, 16, 32, and 64 weeks.

When the specimens are cured in air storage, they should have a clearance \geq of 25mm on all sides. The readings should be taken at relative humidity 50 ± 4 % at a temperature of 23 ± 2 °C after curing of 4, 7, 14, and 28 days and 8, 16, 32, and 64 weeks.

The length change at any age is calculated, to the nearest 0.001%, by:

$$\Delta L_x = \frac{CRD - \text{initial CRD}}{\text{gage length}} \quad (\text{Eq. D.24})$$

Where:

CRD: the difference between comparator reading of the specimen and the reference bar at any age;

Gage length: 250 mm.

11.2 Comparison with European standard

BS EN 12390-16:2019 (Testing hardened concrete-Part 16: Determination of the shrinkage of concrete) is used to determine the shrinkage of concrete. The samples should be cured in a room or cabinet at 20 ± 2 °C and relative humidity between 50 and 70%.

In this test, the total shrinkage strain is calculated, at time t, by:

$$E_{CS}(t, t_0) = \frac{l(t_0) - l_{cs}(t)}{L_0} \quad (\text{Eq. D.25})$$

Where:

L_0 : the gauge length (mm);

$l(t_0)$: the initial length at time t_0 (mm);

$l_{cs}(t)$: the length at time t (mm);

$E_{cs}(t, t_0)$: the total shrinkage strain of the specimen at time t.

12. Standard test method for electrical indication of concrete's ability to resist chloride ion penetration (ASTM C1202, 2017)

12.1 Procedure

By studying the electrical conduction of concrete specimens, this test indicates the concrete's ability to resist chloride ion penetration. It is not valid for specimens containing reinforcing steel positioned longitudinally, thus providing a continuous electrical path between the two ends of the specimen. Also, this test will be skewed if the sample is exposed to chlorides and other anion aggressive chemicals.

This test applies to specimens with a diameter of 95 to 100 mm. If $D > 95$ mm, adjustments shall be made. If $D < 95$ mm, care must be taken to ensure that the solutions can contact the entire area.

At least two cylinders or cores of 100 mm diameter are prepared, moist cured for 28 days (if only Portland cement is used), or extended moist cured for 56 days (if supplementary cementitious materials are used), or accelerated moist cured for 7 days and immersed in lime saturated water for 21 days if specified.

By using a water-cooled diamond saw or silicon carbide saw, a 50 ± 3 mm slice should be cut from the top of the core or specimen.

At the end of the curing period, the specimen is allowed to surface dry in air for at least 1h. The side surfaces are then coated by brushing a rapid setting coating. After allowing the coating to cure, the

specimen is placed in a vacuum desiccator (pressure shall decrease to less than 50 mmHg within a few minutes) and the vacuum is maintained for 3 h. The specimen is covered with de-aerated boiled water (after cooling it to ambient temperature) and the vacuum pump is allowed to run for one additional hour. The pump is then turned off and the specimen is soaked in the beaker under the same prepared water for 18 ± 2 hours.

The specimen is removed from water to a sealed can that will maintain it in 95% or higher relative humidity until the beginning of testing. On the day of testing, the specimen is sealed with the test cells. The first side of the cell containing the top surface is filled with 3% NaCl (connected to the negative terminal of the power supply), while the other side of the cell with 0.3N NaOH solution (connected to the positive terminal of the power supply). The cells should be retained fill during the test. The lead wires are attached, the electrical connections made, and the power supply (set to 60 ± 0.1 V) turned on.

The room temperature should be at 20-25 °C throughout the test. The current is recorded initially and at least every 30 minutes. After 6 h, the specimen is removed, the cells are rinsed in tap water, and the residual sealant is stripped out and discarded.

$I(t)$ is plotted and a smooth curve is drawn. Then the area underneath the curve is integrated if automatic data processing equipment is not used.

The total charge passed is a measure of the electrical conductance of the concrete and could be estimated by:

$$Q(C) = 900 (I_0 + 2 I_{30} + 2 I_{60} + \dots + 2 I_{300} + 2 I_{330} + I_{360}) \quad (\text{Eq. D.26})$$

Where:

I_0 = the current immediately after the voltage is applied (A);

I_t = the current at t minutes after the voltage is applied (A).

If the specimen is different than 95 mm diameter then the charge passed through a 95 mm diameter is calculated by:

$$Q_s = \frac{Q_x}{\frac{95}{x^2}} \quad (\text{Eq. D.27})$$

Where x is the diameter (mm).

Based on the value of the passed charge, Table D.2 gives an indication of the chloride ion penetrability.

Table D.2 The chloride ion penetrability function of the charge passed

Charge passed (Coulombs)	Chloride ion penetrability
>4000	High
2000-4000	Moderate
1000-2000	Low
100-1000	Very low
<100	Negligible

12.2 Comparison with European standard

The European Standard NF EN 13396-2004 (Products and systems for the protection and repair of concrete structures-Test methods-Measurement of chloride ion ingress) specifies a method for determining the resistance to chloride ion penetration of hardened concrete by calculating

the chloride ion content of the powder of the specimen at different increments after immersion in NaCl solution.

13. Method for determination of water absorption (*BS 1881-122, 1983*)

This test aims to determine the water absorption in hardened concrete specimens.

The samples shall consist of three individual cores of 75 mm long and 75 ± 3 mm diameter.

They should be drilled, as far as possible, perpendicular to the surface. The cores should be marked and their orientation recorded.

The specimens should be placed in the oven for 72 ± 2 hours (105 ± 5 °C). At the end of this period, the specimens are cooled for 24 ± 0.5 hours in the desiccator. Then, the weight A of the specimen is measured. Afterward, the specimens are immersed in water with their longitudinal axis horizontal (25 ± 5 mm of water should cover the specimens) for 30 ± 0.5 minutes. The specimens are then removed from the water, shook to remove the bulk of water, and dried with a cloth to remove all free water. The weight B is then measured as the final mass.

The absorption is then calculated as the ratio of the increase in mass resulting from the immersion to the dry mass:

$$\mathbf{Absorption} = \frac{B-A}{A} \quad (\text{Eq. D.28})$$

A correction factor shall be applied if the core length is different than 75 mm.

14. Testing hardened concrete: depth of penetration of water under pressure (*BS EN 12390-8, 2009*)

This test presents a method to determine the penetration of water under pressure in hardened concrete (at least 28 days old) that has been water cured. During the test, the water pressure can be applied to the surface of the test specimen either from the bottom or the top.

The specimen shall be cubic, cylindrical, or prismatic of the length of edge or diameter not less than 150 mm and no other dimension less than 100 mm. Immediately after the specimen is de-molded, the surface to be exposed to water pressure is roughened with a wire brush.

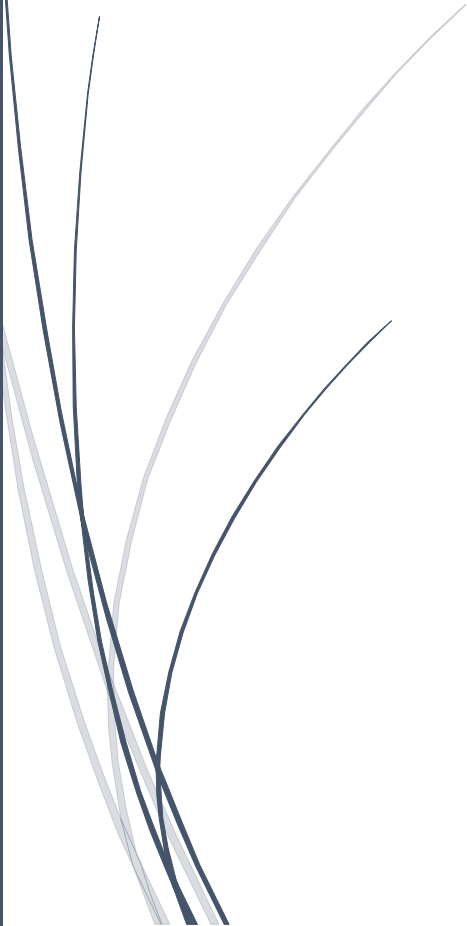
The specimen should be placed in the apparatus and water pressure of 500 ± 50 kPa should be applied for 72 ± 2 hours. After the pressure has been applied for the specified time, the excess of water is removed and the specimen is split in half perpendicularly to the face on which the water pressure was applied (during splitting the face exposed to water pressure should be kept on the bottom).

As soon as the split face has dried to such an extent that the water penetration front can be clearly seen, the waterfront is marked on the specimen and the maximum depth of penetration under the test area is measured. If leakage is observed during the test period, the validity of the result should be considered and the fact recorded.



Annex E

**Comparison Between
Calculated and
Experimental Fresh
Concrete Densities**



E. Comparison Between Calculated and Experimental Fresh Concrete Densities

Introduction

This annex presents a comparison between the calculated and experimental air content and density of fresh concrete.

Calculations

For each concrete mix, the calculated mass of each material, in one cubic meter of concrete, is determined in Table E.1 to Table E.5, taking into consideration the measured air content presented in Table E.6. For each concrete mix, Table E.6 compares the calculated fresh density to the measured one.

Table E.1 Calculated masses of Mix 30 materials

Mix 30	Materials	SSD mass (kg)	SSD specific gravity	Calculated volume (m ³)	Calculated mass (kg)
CM-30	Cement	350	3090	0.11	353.2
	Water	175	1000	0.18	176.6
	Admixture	2.47	1200	0.002	2.5
	Natural sand	411	2640	0.16	414.6
	Crushed sand	417	2620	0.16	420.8
	Medium aggregate (10 mm)	430	2670	0.16	433.7
	Coarse aggregate (20 mm)	569	2680	0.21	574.3
EM-30	Cement	350	3090	0.11	352.2
	Water	175	1000	0.18	176.1
	Admixture	1.01	1200	0.001	1.0
	Natural sand	0	2640	0.00	0.0
	Crushed sand	823	2620	0.31	828.1
	Medium aggregate (10 mm)	430	2670	0.16	432.3
	Coarse aggregate (20 mm)	569	2680	0.21	572.5
MM-30	Cement	350	3090	0.11	351.8
	Water	175	1000	0.18	175.9
	Admixture	0	1200	0.000	0.0
	Natural sand	0	2640	0.00	0.0
	Crushed sand	823	2620	0.31	827.2
	Medium aggregate (10 mm)	430	2670	0.16	431.9
	Coarse aggregate (20 mm)	569	2680	0.21	572.0

Table E.2 Calculated masses of Mix 30b materials

Mix 30b	Materials	SSD mass (kg)	SSD specific gravity	Calculated volume (m ³)	Calculated mass (kg)
CM-30b	Cement	350	3090	0.11	353.6
	Water	175	1000	0.18	176.8
	Admixture	4.5	1200	0.004	4.5
	Natural sand	267	2640	0.10	269.7
	Crushed sand	503	2620	0.19	508.1
	Medium aggregate (10 mm)	420	2660	0.16	424.3
	Coarse aggregate (20 mm)	628	2680	0.23	634.4
FM-30b	Cement	350	3090	0.11	353.6
	Water	175	1000	0.18	176.8
	Admixture	2.62	1200	0.002	2.6
	Natural sand	0	2640	0.00	0.0
	Crushed sand	699	2620	0.27	706.2
	Medium aggregate (10 mm)	445	2660	0.17	449.6
	Coarse aggregate (20 mm)	667	2680	0.25	673.9

Table E.3 Calculated masses of Mix 35-I materials

Mix 35-I	Materials	SSD mass (kg)	SSD specific gravity	Calculated volume (m ³)	Calculated mass (kg)
CM-35-I	Cement	350	3090	0.11	347.5
	Water	140	1000	0.14	139.0
	Admixture	8.51	1200	0.007	8.4
	Natural sand	430	2640	0.16	427.3
	Crushed sand	437	2620	0.17	433.6
	Medium aggregate (10 mm)	451	2670	0.17	447.4
	Coarse aggregate (20 mm)	597	2680	0.22	593.0
EM-35-I	Cement	350	3090	0.11	349.3
	Water	140	1000	0.14	139.7
	Admixture	4.75	1200	0.004	4.7
	Natural sand	0	2640	0.00	0.0
	Crushed sand	862	2620	0.33	860.2
	Medium aggregate (10 mm)	451	2670	0.17	449.6
	Coarse aggregate (20 mm)	597	2680	0.22	596.0
MM-35-I	Cement	350	3090	0.11	347.9
	Water	140	1000	0.14	139.1
	Admixture	3.86	1200	0.003	3.8
	Natural sand	0	2640	0.00	0.0
	Crushed sand	862	2620	0.33	856.7
	Medium aggregate (10 mm)	451	2670	0.17	447.8
	Coarse aggregate (20 mm)	597	2680	0.22	593.6

Table E.4 Calculated masses of Mix 35-II materials

Mix 35-II	Materials	SSD mass (kg)	SSD specific gravity	Calculated volume (m ³)	Calculated mass (kg)
CM-35-II	Cement	300	3090	0.10	299.4
	Water	120	1000	0.12	119.8
	Admixture	10.38	1200	0.009	10.4
	Natural sand	453	2640	0.17	452.0
	Crushed sand	460	2620	0.18	458.7
	Medium aggregate (10 mm)	474	2670	0.18	473.2
	Coarse aggregate (20 mm)	629	2680	0.23	627.9
EM-35-II	Cement	300	3090	0.10	298.8
	Water	120	1000	0.12	119.5
	Admixture	6.9	1200	0.006	6.9
	Natural sand	0	2640	0.00	0.0
	Crushed sand	907	2620	0.35	903.3
	Medium aggregate (10 mm)	474	2670	0.18	472.2
	Coarse aggregate (20 mm)	629	2680	0.23	626.6
MM-35-II	Cement	300	3090	0.10	297.6
	Water	120	1000	0.12	119.0
	Admixture	5.99	1200	0.005	5.9
	Natural sand	0	2640	0.00	0.0
	Crushed sand	907	2620	0.35	899.6
	Medium aggregate (10 mm)	474	2670	0.18	470.3
	Coarse aggregate (20 mm)	629	2680	0.23	624.0

Table E.5 Calculated masses of Mix 50 materials

Mix 50	Materials	SSD mass (kg)	SSD specific gravity	Calculated volume (m ³)	Calculated mass (kg)
CM-50	Cement	400	3090	0.13	396.7
	Water	120	1000	0.12	119.0
	Admixture	9.6	1200	0.008	9.5
	Natural sand	303	2610	0.12	300.5
	Crushed sand	572	2620	0.22	567.3
	Medium aggregate (10 mm)	453	2680	0.17	449.3
	Coarse aggregate (20 mm)	600	2700	0.22	595.1
MM-50	Cement	400	3090	0.13	397.6
	Water	120	1000	0.12	119.3
	Admixture	10.2	1200	0.009	10.1
	Natural sand	0	2610	0.00	0.0
	Crushed sand	820	2620	0.31	815.0
	Medium aggregate (10 mm)	478	2680	0.18	475.1
	Coarse aggregate (20 mm)	633	2700	0.23	629.1
FM-50	Cement	400	3090	0.13	399.6
	Water	120	1000	0.12	119.9
	Admixture	9.81	1200	0.008	9.8
	Natural sand	0	2610	0.00	0.0
	Crushed sand	876	2620	0.33	875.1
	Medium aggregate (10 mm)	451	2680	0.17	450.5
	Coarse aggregate (20 mm)	597	2700	0.22	596.4

Table E.6 Differences between the calculated and measured densities of all concrete mixes

Concrete mix		Calculated air content	Measured air content	Calculated mass (kg)	Calculated density (kg/m ³)	Measured density (kg/m ³)	Difference in densities (kg/m ³)
Mix 30	CM-30	0.022	0.013	2376	2376	2390	14
	EM-30	0.024	0.018	2362	2362	2363	1
	MM-30	0.024	0.019	2359	2359	2341	18
Mix 30b	CM-30b	0.023	0.013	2372	2372	2381	9
	FM-30b	0.027	0.017	2363	2363	2378	15
Mix 35-I	CM-35-I	0.018	0.025	2396	2396	2413	17
	EM-35-I	0.022	0.024	2400	2400	2412	12
	MM-35-I	0.023	0.029	2389	2389	2405	16
Mix 35-II	CM-35-II	0.015	0.017	2441	2441	2439	2
	EM-35-II	0.019	0.023	2427	2427	2435	8
	MM-35-II	0.019	0.027	2416	2416	2404	12
Mix 50	CM-50	0.017	0.025	2438	2438	2449	11
	MM-50	0.016	0.025	2446	2446	2459	13
	FM-50	0.019	0.020	2451	2451	2476	25

Conclusion

The comparisons between the calculated and experimental fresh densities show small differences, for all the studied concrete mixes.



References



References

- Abbas, I.I., Chaaban, J.K., Al-Rabaa, A.R., and Shaar, A.A. (2017), "Solid Waste Management in Lebanon: Challenges and Recommendations," *Journal of Environment and Waste Management*, 4(2), October, pp. 053-063.
- Achour, T., Lecomte, A., Ben Ouezdou, M., Mensi, R., and Joudi, I. (2008), "Contribution of the Fillers Limestones to the Paste-Aggregate Bond: Tunisian Examples," *Materials and Structures*, 41, pp. 1427-1439. doi:10.1617/s11527-007-9287-0.
- ACI 318 (1995), "Building Code Requirements for Reinforced Concrete", American Concrete Institute, Farmington Hills, Michigan.
- ACI Committee 222R-01 (2001), "Protection of Metals in Concrete Against Corrosion", American Concrete Institute, Farmington Hills, Michigan.
- AFGC (2004), "Conception des Bétons Pour Une Durée de Vie Donnée des Ouvrages - Indicateurs de Durabilité", Association Française de Génie Civil.
- AFPC-AFREM (1997), "Méthodes Recommandées pour La Mesure des Drandeurs Associées à La Durabilité," Toulouse.
- Aggarwal, Y., and Siddique, R. (2014), "Microstructure and Properties of Concrete Using Bottom Ash and Waste Foundry Sand as Partial Replacement of Fine Aggregates," *Construction and Building Materials*, 54, pp. 210-223. <https://doi.org/10.1016/j.conbuildmat.2013.12.051>.
- Agrawal, U.S., Wanjari, S.P., and Naresh, D.N. (2017), "Characteristic Study of Geopolymer Fly Ash Sand as a Replacement to Natural River Sand," *Construction and Building Materials*, 150, pp. 681-688. <https://doi.org/10.1016/j.conbuildmat.2017.06.029>.
- Akçaoğlu, T., Tokyay, M., and Çelik, T. (2005), "Assessing the ITZ Microcracking Via Scanning Electron Microscope and Its Effect on the Failure Behavior of Concrete," *Cement and Concrete Research*, 35(2), pp. 358-363. <https://doi.org/10.1016/j.cemconres.2004.05.042>.
- Akrout, K., Mounanga, P., Ltifi, M., and Ben Jamaa, N. (2010), "Rheological, Mechanical and Structural Performances of Crushed Limestone Sand Concrete," *International Journal of Concrete Structures and Materials*, 4(2), pp. 97-104. <https://doi.org/10.4334/IJCSM.2010.4.2.97>.
- Al-Amoudi, O.S.B., Al-Kutti, W.A., Ahmad, S., and Maslehuddin, M. (2009), "Correlation Between Compressive Strength and Certain Durability Indices of Plain and Blended Cement Concretes", *Cement and Concrete Composites*, 31(9), pp. 672-676. <https://doi.org/10.1016/j.cemconcomp.2009.05.005>.
- Al-Jabri, K.S., Al-Saidy, A.H., and Taha, R. (2011), "Effect of Copper Slag as a Fine Aggregate on the Properties of Cement Mortars and Concrete," *Construction and Building Materials*, 25 (2), pp. 933-938. <https://doi.org/10.1016/j.conbuildmat.2010.06.090>.
- Alves, A.V., Vieira, T.F., De Brito, J., and Correia, J.R. (2014), "Mechanical Properties of Structural Concrete with Fine Recycled Ceramic Aggregates," *Construction and Building Materials*, 64, pp. 103-113. <https://doi.org/10.1016/j.conbuildmat.2014.04.037>.

References

- An, J., Kim, S.S., Nam, B.H., and Durham, S.A. (2017), "Effect of Aggregate Mineralogy and Concrete Microstructure on Thermal Expansion and Strength Properties of Concrete," *Applied Sciences*, 7(12), 1307. <https://doi.org/10.3390/app7121307>.
- APM 219 (1996), "Test Method: Concrete Testing, Hardened Concrete: Electrical Resistivity", 1st Edition, May 1996.
- Aquino, C., Masumi, I., Hiroaki, M., Maki, M., and Takahisa, O. (2010), "The Effects of Limestone Aggregate on Concrete Properties," *Construction and Building Materials*, 24(12), pp. 2363-2368. <https://doi.org/10.1016/j.conbuildmat.2010.05.008>.
- Aslaksen Aasly, K., Danielsen, S., Wigum, B., Norman, S.H., Cepuritis, R., Onnela, T. (2014), "Review Report on Dry and Wet Classification of Filler Materials for Concrete, State-of-the-Art", COIN Project Report, 52- 2014, SINTEF, Oslo.
- ASTM C33 (2016), "Standard Specification for Concrete Aggregates," ASTM International, West Conshohocken, PA.
- ASTM C39 (2017a), "Standard Test Method for Compressive Strength of Cylindrical Concrete Specimen," ASTM International, West Conshohocken, PA.
- ASTM C40 (2016), "Standard Test Method for Organic Impurities in Fine Aggregates for Concrete," ASTM International, West Conshohocken, PA.
- ASTM C78 (2016), "Standard Test Method for Flexural Strength of Concrete (Using Simple Beam with Third-Point Loading)," ASTM International, West Conshohocken, PA.
- ASTM C88 (2013), "Standard Test Method for Soundness of Aggregates by Use of Sodium Sulfate or Magnesium Sulfate," ASTM International, West Conshohocken, PA.
- ASTM C109 (2016a), "Standard Test Method for Compressive Strength of Hydraulic Cement Mortars Using 50 mm Cube Specimens," ASTM International, West Conshohocken, PA.
- ASTM C114 (2004), "Standard Test Method for Chemical Analysis of Hydraulic Cement," ASTM International, West Conshohocken, PA.
- ASTM C117 (2013), "Standard Test Method for Materials Finer than 75 μ m (No.200) Sieve in Mineral Aggregates by Washing," ASTM International, West Conshohocken, PA.
- ASTM C123 (2014), "Standard Test Method for Lightweight Particles in Aggregates," ASTM International, West Conshohocken, PA.
- ASTM C125 (2016), "Standard Terminology Relating to Concrete and Concrete Aggregates," ASTM International, West Conshohocken, PA.
- ASTM C127 (2015), "Standard Test Method for Relative Density (Specific Gravity) and Absorption of Coarse Aggregates," ASTM International, West Conshohocken, PA.
- ASTM C128 (2015), "Standard Test Method for Relative Density (Specific Gravity) and Absorption of Fine Aggregates," ASTM International, West Conshohocken, PA.

References

ASTM C131 (2014), "Standard Test Method for Resistance to Degradation of Small-Size Coarse Aggregate by Abrasion and Impact in the Los Angeles Machine," ASTM International, West Conshohocken, PA.

ASTM C136 (2014), "Standard Test Method for Sieve Analysis of Fine and Coarse Aggregates," ASTM International, West Conshohocken, PA.

ASTM C138 (2017a), "Standard Test Method for Density (Unit Weight), Yield, and Air Content (Gravimetric) of Concrete," ASTM International, West Conshohocken, PA.

ASTM C142 (2017), "Standard Test Method for Clay Lumps and Friable Particles in Aggregates," ASTM International, West Conshohocken, PA.

ASTM C143 (2015a), "Standard Test Method for Slump of Hydraulic-Cement Concrete," ASTM International, West Conshohocken, PA.

ASTM C157 (2006), "Standard Test Method for Length Change of Hardened Hydraulic-Cement Mortar and Concrete," ASTM International, West Conshohocken, PA.

ASTM C187 (2011), "Standard Test Method for Amount of Water Required for Normal Consistency of Hydraulic Cement Paste," ASTM International, West Conshohocken, PA.

ASTM C188 (2017), "Standard Test Method for Density of Hydraulic Cement," ASTM International, West Conshohocken, PA.

ASTM C191 (2018a), "Standard Test Method for Time of Setting of Hydraulic Cement by Vicat Needle," ASTM International, West Conshohocken, PA.

ASTM C192 (2016a), "Standard Test Method for Making and Curing Concrete Test Specimens in the Laboratory," ASTM International, West Conshohocken, PA.

ASTM C204 (2017), "Standard Test Methods for Fineness of Hydraulic Cement by Air-Permeability Apparatus," ASTM International, West Conshohocken, PA.

ASTM C231 (2017a), "Standard Test Method for Air Content of Freshly Mixed Concrete by the Pressure Method," ASTM International, West Conshohocken, PA.

ASTM C305 (2014), "Standard Practice for Mechanical Mixing for Hydraulic Cement Pastes and Mortars of Plastic Consistency," ASTM International, West Conshohocken, PA.

ASTM C403 (2008), "Standard Test Method for Time of Setting of Concrete Mixtures by Penetration Resistance," ASTM International, West Conshohocken, PA.

ASTM C469 (2014), "Standard Test Method for Static Modulus of Elasticity and Poisson's Ratio of Concrete in Compression," ASTM International, West Conshohocken, PA.

ASTM C494 (2016), "Standard Specification for Chemical Admixtures for Concrete," ASTM International, West Conshohocken, PA.

ASTM C566 (2013), "Standard Test Method for Total Evaporable Moisture Content of Aggregates by Drying," ASTM International, West Conshohocken, PA.

References

- ASTM C595 (2017), "Standard Specification for Blended Hydraulic Cements," ASTM International, West Conshohocken, PA.
- ASTM C702 (2011), "Standard Practice for Reducing Samples of Aggregate to Testing Size," ASTM International, West Conshohocken, PA.
- ASTM C778 (2017), "Standard Specification for Standard Sand," ASTM International, West Conshohocken, PA.
- ASTM C1064 (2017), "Standard Test Method for Temperature of Freshly Mixed Hydraulic-Cement Concrete," ASTM International, West Conshohocken, PA.
- ASTM C1202 (2017), "Standard Test Method for Electrical Indication of Concrete's Ability to Resist Chloride Ion Penetration," ASTM International, West Conshohocken, PA.
- ASTM C1260 (2001), "Standard Test Method for Potential Alkali Reactivity of Aggregates (Mortar Bar Method)," ASTM International, West Conshohocken, PA.
- ASTM C1602 (2006), "Standard Specification for Mixing Water Used in the Production of Hydraulic Cement Concrete," ASTM International, West Conshohocken, PA.
- ASTM D2419 (2014), "Standard Test Method for Sand Equivalent Value of Soils and Fine Aggregate," ASTM International, West Conshohocken, PA.
- ASTM D4791 (2019), "Standard Test Method for Flat Particles, Elongated Particles, or Flat and Elongated Particles in coarse Aggregates," ASTM International, West Conshohocken, PA.
- Atkinson, A., and Nickerson, A.K. (1984), "The Diffusion of Ions Through Water-Saturated Cement," *Journal of Materials Science*, 19, pp. 3068-3078.
- Bachiorrini, A., and Murat, M. (1987), "Evolution Microstructurale des Composites du Système Ciment Alumineux-Granulat Calcaire. I. Mode de Propagation de la Fissure," *Cement and Concrete Research*, (17), pp. 242-248.
- Bachiorrini, A., and Murat, M. (1987), "Evolution Microstructurale des Composites du Système Ciment Alumineux-Granulat Calcaire. II. Influence sur la Porosité et les Résistances Mécaniques," *Cement and Concrete Research*, (17), pp. 397-403.
- Bai, Y., Darcy, F., and Basheer, P.A.M. (2005), "Strength and Drying Shrinkage Properties of Concrete Containing Furnace Bottom Ash as Fine Aggregate," *Construction and Building Materials*, 19 (9), pp. 691-697. <https://doi.org/10.1016/j.conbuildmat.2005.02.021>.
- Bederina, M., Makhloufi, Z., Bounoua, A., Bouziani, T., and Quéneudec, M. (2013), "Effect of Partial and Total Replacement of Siliceous River Sand with Limestone Crushed Sand on the Durability of Mortars Exposed to Chemical Solutions", *Construction and Building Materials*, 47, pp. 146-158. <https://doi.org/10.1016/j.conbuildmat.2013.05.037>.
- Belaribi, N., Pons, G., and Perrin, B. (1997), "Delayed Behavior of Concrete: Influence of Additions and Aggregate Characteristics in Relation to Moisture Variations," *Cement and Concrete Research*, 27 (9), pp. 1429-1438.

References

- Bellanger, M., Homand, F., and Remy, J.M. (1993), "Water Behaviour in Limestones as a Function of Pores Structure: Application to Frost Resistance of Some Lorraine Limestones," *Engineering Geology*, 36 (1–2), pp. 99-108. [https://doi.org/10.1016/0013-7952\(93\)90022-5](https://doi.org/10.1016/0013-7952(93)90022-5).
- Bengtsson, M., and Evertsson, C.M. (2006), "Measuring Characteristics of Aggregate Material from Vertical Shaft Impact Crushers," *Minerals Engineering*, 19 (15), pp. 1479-1486. <https://doi.org/10.1016/j.mineng.2006.08.003>.
- Bentz, D.P., Ardani, A., Barrett, T., Jones, S.Z., Lootens, D., Peltz, M.A., Sato, T., Stutzman, P.E., Tanesi, J., and Weiss, W.J. (2015), "Multi-Scale Investigation of the Performance of Limestone in Concrete," *Construction and Building Materials*, 75, pp. 1-10. <https://doi.org/10.1016/j.conbuildmat.2014.10.042>.
- Benyamina, S., Menadi, B., Bernard, S.K., and Kenai, S. (2019), "Performance of Self-Compacting Concrete with Manufactured Crushed Sand," *Advances in Concrete Construction*, 7(2), pp. 87-96. <https://doi.org/10.12989/acc.2019.7.2.087>.
- Binici, H., and Aksogan, O. (2018), "Durability of Concrete Made with Natural Granular Granite, Silica Sand and Powders of Waste Marble and Basalt as Fine Aggregate," *Journal of Building Engineering*, 19, pp. 109-121. <https://doi.org/10.1016/j.jobbe.2018.04.022>.
- BLOMINVEST Bank (2016), "The Lebanese Cement Industry Facing Low Domestic Demand and Fierce Competition Abroad," Research Department, Beirut, Lebanon.
- Bonavetti, V.L., and Irassar, E.F. (1994), "The Effect of Stone Dust Content in Sand," *Cement and Concrete Research*, 24(3), pp. 580-590.
- Breton, D., Carles-Gibergues, A., Ballivy, G., and Grandet, J. (1993), "Contribution to the Formation Mechanism of the Transition Zone Between Rock-Cement Paste," *Cement and Concrete Research*, 23, pp. 335-346.
- BS 882 (1992), "Specification for Aggregates from Natural Sources for Concrete," British Standards Institution, London, UK.
- BS 1881-122 (1983), "Method for Determination of Water Absorption," British Standards Institution, London, UK.
- BS EN 196-1 (2005), "Method of Testing Cement - Part 1: Determination of Strength, European Standards," European Standards, British Standards Institution, London, UK.
- BS EN 196-3 (2016), "Method of Testing Cement - Part 3: Determination of Setting Times and Soundness," European Standards, British Standards Institution, London, UK.
- BS EN 197-1 (2011), "Cement: Composition, Specifications and Conformity Criteria for Common Cements," European Standards, British Standards Institution, London, UK.
- BS EN 933-9 (1999), "Assessment of Fines – Methylene Blue Test," European Standards, British Standards Institution, London, UK.
- BS EN 1097-6 (2013), "Tests for Mechanical and Physical Properties of Aggregates - Part 6: Determination of Particle Density and Water Absorption," European Standards, British Standards Institution, London, UK.

References

- BS EN 12390-8 (2009), "Testing Hardened Concrete: Depth of Penetration of Water Under Pressure," European Standards, British Standards Institution, London, UK.
- BS EN 12390-13 (2013) "Testing Hardened Concrete - Part 13: Determination of Secant Modulus of Elasticity in Compression," European Standards, British Standards Institution, London, UK.
- BS EN 12390-16 (2019) "Testing Hardened Concrete - Part 16: Determination of the Shrinkage of Concrete," European Standards, British Standards Institution, London, UK.
- BS EN 12620 (2002), "Aggregates for Concrete," European Standards, British Standards Institution, London, UK.
- Çelik, T., and Marar, K. (1996), "Effects of Crushed Stone Dust on Some Properties of Concrete", *Cement and Concrete Research*, 26 (7), pp. 1121-1130. [https://doi.org/10.1016/0008-8846\(96\)00078-6](https://doi.org/10.1016/0008-8846(96)00078-6).
- Cepuritis, R., Garboczi, E.J., and Jacobsen, S. (2017), "Three Dimensional Shape Analysis of Concrete Aggregate Fines Produced by VSI Crushing", *Powder Technology*, 308, pp. 410-421. <https://doi.org/10.1016/j.powtec.2016.12.020>.
- Cepuritis, R., Jacobsen, S., and Onnela, T. (2015) "Sand Production with VSI Crushing and Air Classification: Optimising Fines Grading for Concrete Production with Micro-Proportioning," *Minerals Engineering*, 78, pp. 1-14. <https://doi.org/10.1016/j.mineng.2015.03.025>.
- Chang, Z.T., Song, X.J., Munn, R., and Marosszeky, M. (2005), "Using Limestone Aggregates and Different Cements for Enhancing Resistance of Concrete to Sulphuric Acid Attack," *Cement and Concrete Research*, 35 (8), pp. 1486-1494. <https://doi.org/10.1016/j.cemconres.2005.03.006>.
- Chen, C.T., Chang, J.J., and Yeih, W.C. (2014), "The Effects of Specimen Parameters on the Resistivity of Concrete," *Construction and Building Materials*, 71, pp. 35-43. <https://doi.org/10.1016/j.conbuildmat.2014.08.009>.
- Chen, X., Huang, W., and Zhou, J. (2012), "Effect of Moisture Content on Compressive and Split Tensile Strength of Concrete," *Indian Journal of Engineering and Materials Sciences*, 19 (6), pp. 427-435.
- Chia, K.S., and Zhang, M.H. (2002), "Water Permeability and Chloride Penetrability of High-Strength Lightweight Aggregate Concrete," *Cement and Concrete Research*, 32 (4), pp. 639-645. [https://doi.org/10.1016/S0008-8846\(01\)00738-4](https://doi.org/10.1016/S0008-8846(01)00738-4).
- Choi, Y.W., Moon, D.J., Kim, Y.J., and Lachemi, M. (2009), "Characteristics of Mortar and Concrete Containing Fine Aggregate Manufactured from Recycled Waste Polyethylene Terephthalate Bottles," *Construction and Building Materials*, 23(8), pp. 2829-2835. <https://doi.org/10.1016/j.conbuildmat.2009.02.036>.
- Cohen, M.D, Olek J., and Dolch, W.L. (1990), "Mechanism of Plastic Shrinkage Cracking in Portland Cement and Portland Cement-Silica Fume Paste and Mortar," *Cement and Concrete Research*, 20, pp. 103-119.

References

- Coppio, G.J.L., De Lima, M.G., Lencioni, J.W., Cividanes, L.S., Dyer, P.P.O.L., and Silva, S.A. (2019), "Surface Electrical Resistivity and Compressive Strength of Concrete with the Use of Waste Foundry Sand as Aggregate," *Construction and Building Materials*, 212, pp. 514-521. <https://doi.org/10.1016/j.conbuildmat.2019.03.297>.
- Cordeiro, G.C., De Alvarenga, L.M.S.C., and Rocha, C.A.A. (2016), "Rheological and Mechanical Properties of Concrete Containing Crushed Granite Fine Aggregate", *Construction and Building Materials*, 111, pp. 766-773. <https://doi.org/10.1016/j.conbuildmat.2016.02.178>.
- Cortas, R., Rozière, E., Staquet, S., Hamami, A., Loukili, A., and Delplancke-Ogletree, M.P. (2014), "Effect of the Water Saturation of Aggregates on the Shrinkage Induced Cracking Risk of Concrete at Early Age," *Cement and Concrete Composites*, 50, pp. 1-9. <https://doi.org/10.1016/j.cemconcomp.2014.02.006>.
- Cortes, D.D., Kim, H.K., Palomino, A.M., and Santamarina, J.C. (2008), "Rheological and Mechanical Properties of Mortars Prepared with Natural and Manufactured Sands," *Cement and Concrete Research*, 38 (10), pp. 1142-1147. <https://doi.org/10.1016/j.cemconres.2008.03.020>.
- Debieb, F., and Kenai, S. (2008), "The Use of Coarse and Fine Crushed Bricks as Aggregate in Concrete," *Construction and Building Materials*, 22(5), pp. 886-893. <https://doi.org/10.1016/j.conbuildmat.2006.12.013>.
- De Castro, S., and De Brito, J. (2013), "Evaluation of the Durability of Concrete Made with Crushed Glass Aggregates," *Journal of Cleaner Production*, 41, pp. 7-14.
- De Larrard, F., and Belloc, A. (1997), "The Influence of Aggregate on the Compressive Strength of Normal and High-Strength Concrete," *ACI Materials Journal*, 94(5), pp. 417-426.
- Ding, X., Li, C., Xu, Y., Li, F., and Zhao, S. (2016), "Experimental Study on Long-Term Compressive Strength of Concrete with Manufactured Sand," *Construction and Building Materials*, 108, pp. 67-73. <https://doi.org/10.1016/j.conbuildmat.2016.01.028>.
- Dolage, D.A.R., Dias, M.G.S., and Ariyawansa, C.T. (2013), "Offshore Sand as a Fine Aggregate for Concrete Production," *British Journal of Applied Science & Technology*, 3(4), pp. 813-825. <https://doi.org/10.9734/bjast/2014/3290>.
- Donza, H., and Cabrera, O. (1996), "The Influence of Kinds of Fine Aggregate on Mechanical Properties of High Strength Concrete", *Proceedings of 4th International Symposium of High-Strength/High-Performance Concrete*, Paris, France, vol. 2, pp. 153-160.
- Donza, H., Cabrera, O., and Irassar, E.F. (2002), "High Strength Concrete with Different Fine Aggregate," *Cement and Concrete Research*, 32, pp. 1755-1761.
- Dos Anjos, M.A.G., Sales, A.T.C., and Andrade, N. (2017), "Blasted Copper Slag as Fine Aggregate in Portland Cement Concrete," *Journal of Environmental Management*, 196, pp. 607-613. <https://doi.org/10.1016/j.jenvman.2017.03.032>.
- Dreux, G., and Festa, J. (1995), "Nouveau guide du béton," Edition Eyrolles.
- Eguchi, K., and Teranishi, K. (2005), "Prediction Equation of Drying Shrinkage of Concrete Based on Composite Model," *Cement and Concrete Research*, 35(3), pp. 483-493.

References

- El-Fadel, M., Sadek, S., and Chahine, W. (2001), "Environmental Management of Quarries as Waste Disposal Facilities," *Environmental Management*, 27 (4), pp. 515-531. <https://doi.org/10.1007/s002670010167>.
- El-Fadel, M., Zeinati, M., El-Jisr, K., and Jamali, D. (2001), "Industrial-Waste Management in Developing Countries: The Case of Lebanon," *Journal of Environmental Management*, 61 (4), pp. 281-300. <https://doi.org/10.1006/jema.2000.0413>.
- Elsharief, A., Cohen, M.D., and Olek, J. (2003), "Influence of Aggregate Size, Water Cement Ratio and Age on the Microstructure of the Interfacial Transition Zone," *Cement and Concrete Research*, 33, pp. 1837-1849. [https://doi.org/10.1016/S0008-8846\(03\)00205-9](https://doi.org/10.1016/S0008-8846(03)00205-9).
- EN 933-8 (2012), "Tests for Geometrical Properties of aggregates - Part 8: Assessment of Fines -Sand Equivalent Test," European Standards.
- EN 933-9 (2010), "Assessment of Fines – Methylene Blue Test," European Standards.
- EN 1992-1-1 (2004), "Eurocode 2: Design of Concrete Structures - Part 1-1: General Rules and Rules for Buildings", European Standards.
- EN 12620 (2008), "Aggregates for Concrete," European Standards.
- Environmental Justice Organization (2014), "Building an Economy on Quicksand," Environmental Justice Organization, Liabilities and Trade, August 5th. <http://www.ejolt.org/2014/08/building-an-economy-on-quicksand>.
- Farran, J. (1956), "Contribution Minéralogique à l'Etude de l'Adhérence entre les Constituants Hydratés des Ciments et les Matériaux Enrobés," *Revue des Matériaux de Construction*.
- Gameiro, F., De Brito, J., and Correia da Silva, D. (2014), "Durability Performance of Structural Concrete Containing Fine Aggregates from Waste Generated by Marble Quarrying Industry," *Engineering Structures*, 59, pp. 654-662. <https://doi.org/10.1016/j.engstruct.2013.11.026>.
- Giatac RCON, "Concrete Electrical Resistivity Meter," Giatac Scientific Inc., Ottawa, Canada.
- GIZ (2014), "Country Report on the Solid Waste Management in Lebanon", The Regional Solid Waste Exchange of Information and Expertise Network in Mashreq and Maghreb Countries.
- Gokce, A., Beyaz, C., and Ozkan, H. (2016), "Influence of Fines Content on Durability of Slag Cement Concrete Produced with Limestone Sand," *Construction and Building Materials*, 111, pp. 419-428. <https://doi.org/10.1016/j.conbuildmat.2016.02.139>.
- Gonçalves, J.P., Tavares, L.M., Toledo Filho, R.D., Fairbairn, E.M.R., and Cunha, E.R. (2007), "Comparison of Natural and Manufactured Fine Aggregates in Cement Mortars," *Cement and Concrete Research*, 37(6), pp. 924-932. <https://doi.org/10.1016/j.cemconres.2007.03.009>.
- González-Gómez, W.S., Quintana, P., May-Pat, A., Avilés, F., May-Crespo, J. and Alvarado-Gil, J.J. (2015), "Thermal Effects on the Physical Properties of Limestones from the Yucatan Peninsula," *International Journal of Rock Mechanics and Mining Sciences*, 75, pp. 182-189. <https://doi.org/10.1016/j.ijrmms.2014.12.010>.

References

- Goodquarry Article (2011), "Goodquarry," Output of the MIST Quarry Fines Minimisation' and Waterless Fines Removal' projects. <https://www.goodquarry.com>
- Grandet, J., and Ollivier, J.P. (1980), "Etude de la Formation du Monocarboaluminate de Calcium Hydraté au Contact d'un Granulat Calcaire dans une Pâte de Ciment Portland," *Cement and Concrete Research*, 10, pp. 759-770.
- Granger, L. (1995), "Comportement Différé du Béton dans les Enceintes de Centrales Nucléaires: Analyse et Modélisation," Ph.D. Thesis, Ecole Nationale des Ponts et Chaussées, Paris, France.
- Guimaraes, M.S., Valdes, J.R., Palomino, A.M, and Santamarina, J.C. (2007), "Aggregate Production: Fines Generation during Rock Crushing," *International Journal of Mineral Processing*, 81 (4), pp. 237-247. <https://doi.org/10.1016/j.minpro.2006.08.004>.
- Gupta, T., Chaudhary, S., and Sharma, R.K. (2014), "Assessment of Mechanical and Durability Properties of Concrete Containing Waste Rubber Tire as Fine Aggregate," *Construction and Building Materials*, 73, pp. 562-574. <https://doi.org/10.1016/j.conbuildmat.2014.09.102>.
- Hama, S.M., and Hilal, N.N. (2017), "Fresh Properties of Self-Compacting Concrete with Plastic Waste as Partial Replacement of Sand," *International Journal of Sustainable Built Environment*, 6 (2), pp. 299-308. <https://doi.org/10.1016/j.ijbsbe.2017.01.001>.
- Hamad, B.S, Yassine, M.Y., and Khawlie, M.R. (1996), "Survey Study on Geology and Location of Major Sand Resources in Lebanon, Eastern Mediterranean," *Bulletin of the International Association of Engineering Geology*, No. 53, Paris, April.
- Hasdemir, S., Tuğrul, A., and Yilmaz, M. (2016), "The Effect of Natural Sand Composition on Concrete Strength," *Construction and Building Materials*, 112, pp. 940-948. <https://doi.org/10.1016/j.conbuildmat.2016.02.188>.
- He, H., Courard, L., Pirard, E., and Michel, F. (2016), "Shape Analysis of Fine Aggregates Used for Concrete," *Image Analysis and Stereology*, 35(3), pp. 159-166. <https://doi.org/10.5566/ias.1400>.
- Heath, K. (2016), "Chapter 9: Marinas in the Arabian Gulf Region," *Marine Concrete Structures- Design Durability and Performance*, Clough Murray and Roberts, Cape Town, South Africa. <https://doi.org/10.1016/B978-0-08-100081-6.00009-X>.
- Huiguang, Y., Yan, L., Henglin, L., and Quan, G. (2011), "Durability of Sea-Sand Containing Concrete: Effects of Chloride Ion Penetration", *Mining Science and Technology*, 21(1), pp. 123-127. <https://doi.org/10.1016/j.mstc.2010.07.003>.
- Idir, R., Cyr, M., and Tagnit-Hamou, A. (2010), "Use of Fine Glass as ASR Inhibitor in Glass Aggregate Mortars," *Construction and Building Materials*, 24 (7), pp. 1309-1312. <https://doi.org/10.1016/j.conbuildmat.2009.12.030>.
- Ioannou, I., Petrou, M.F., Fournari, R., Andreou, A., Hadjigeorgiou, C., Tsikouras, B., and Hatzipanagiotou, K. (2014), "Crushed Limestone As An Aggregate in Concrete," *The Geological Society*, 331, pp. 127-135. <https://doi.org/10.1144/SP331.11>.
- Ismail, Z.Z., and AL-Hashmi, E.A. (2009), "Recycling of Waste Glass as a Partial Replacement for Fine Aggregate in Concrete," *Waste Management*, 29 (2), pp. 655-659. <https://doi.org/10.1016/j.wasman.2008.08.012>.

References

- Javelas, R., Maso, J.C., Ollivier, J.P., and Thenoz, B. (1975), "Observation Directe au Microscope Electronique par Transmission de la Liaison Pâte de Ciment - Granulats dans des Mortiers de Calcite et de Quartz", *Cement and Concrete Research*, 5, pp. 285-294.
- Jiao, D., Shi, C., Yuan, Q., An, X., Liu, Y., and Li, H., (2017), "Effect of Constituents on Rheological Properties of Fresh Concrete-A Review," *Cement and Concrete Composites*, 83, pp. 146-159. <https://doi.org/10.1016/j.cemconcomp.2017.07.016>.
- Kabbani, M. (1967), "Various Types of Sand in Lebanon and their Effect on the Strength of Concrete and Mortar", Master Thesis of Engineering, American University of Beirut, Lebanon.
- Khatib, J.M., and Mangat, P.S. (1995), "Absorption Characteristics of Concrete as a Function of Location Relative to Casting Position," *Cement and Concrete Research*, 25 (5), pp. 999-1010.
- Khawlie, M.R., and Hinai, K. (1980), "Geology and Production of Construction Material Resources of Lebanon: A Preliminary Study," *Engineering Geology*, 15, pp. 223-232.
- Khouadjia, M.L.K., Mezghiche, B., and Drissi, M. (2015), "Experimental Evaluation of Workability and Compressive Strength of Concrete with Several Local Sand and Mineral Additions," *Construction and Building Materials*, 98, pp. 194-203. <https://doi.org/10.1016/j.conbuildmat.2015.08.081>.
- Kim, I.S., Choi, S.Y., and Yang, E.I. (2018), "Evaluation of Durability of Concrete Substituted Heavyweight Waste Glass as Fine Aggregate," *Construction and Building Materials*, 184, pp. 269-277. <https://doi.org/10.1016/j.conbuildmat.2018.06.221>.
- Kosmatka, S.H., and Wilson, M.L. (2011), "Design and Control of Concrete Mixtures," EB001, 15th edition, Portland Cement Association, Skokie, Illinois, USA, 460 pages.
- Kou, S.C., and Poon, C.S. (2009), "Properties of Concrete Prepared with Crushed Fine Stone, Furnace Bottom Ash and Fine Recycled Aggregate as Fine Aggregates," *Construction and Building Materials*, 23 (8), pp. 2877-2886.
- Kronlof, A. (1994), "Effect of Very Fine Aggregate on Concrete Strength," *Materials and Structures*, 27, pp. 15-25.
- Kurda, R., De Brito, J., and Silvestre, J.D. (2019), "Water Absorption and Electrical Resistivity of Concrete with Recycled Concrete Aggregates and Fly Ash," *Cement and Concrete Composites*, 95, 169-182. <https://doi.org/10.1016/j.cemconcomp.2018.10.004>.
- Labidi, I., Boughanmi, S., and Khelidj, A. (2019), "Effect of Low Calcite Addition on Sulfate Resisting (SR) Portland Cements: Hydration Kinetics at Early Age and Durability Performance After 2 Years," *Chemistry Africa*, 2, pp. 401-414. <https://doi.org/10.1007/s42250-019-00047-0>.
- Lagerblad, B., Gram, H.E., and Westerholm, M. (2014), "Evaluation of the Quality of Fine Materials and Filler from Crushed Rocks in Concrete Production," *Construction and Building Materials*, 67, pp. 121-126. <https://doi.org/10.1016/j.conbuildmat.2013.10.029>.
- Lagowski, J., and Saramak, D. (2016), "Improving Gravel and Crushed Aggregates Washing Technology Efficiency through Application of High Pressure Washer", *E3S Web of Conferences*, MEC2016, 8, 01041. <https://doi.org/10.1051/e3sconf/20160801041>.

References

- LBCI News (2019), "Unlicensed Quarries and Crushers to Be Forced to Close Soon," News Bulletins Reports, April 28. <https://www.lbcgroup.tv/news/d/news-bulletin-reports/441260/unlicensed-quarries-and-crushers-to-be-forced-to-c/en>.
- Le Chatelier, H. (1900), "Sur les Changements Volumiques Qui Accompagnent le Durcissement des Bétons," Bulletin de la Société de l'Encouragement pour l'Industrie Nationale, 5ème Série, Tome 5.
- Lee, E., Park, S., and Kim, Y. (2016), "Drying Shrinkage Cracking of Concrete Using Dune Sand and Crushed Sand," *Construction and Building Materials*, 126, pp. 517-526. <https://doi.org/10.1016/j.conbuildmat.2016.08.141>.
- Lerch, W. (1957), Title No. 53-44, *Journal of ACI*, 28 (8), pp. 797-802.
- Li, B., Ke, G., and Zhou, M. (2011), "Influence of Manufactured Sand Characteristics on Strength and Abrasion Resistance of Pavement Cement Concrete," *Construction and Building Materials*, 25 (10), pp. 3849-3853. <https://doi.org/10.1016/j.conbuildmat.2011.04.004>.
- Li, B., Wang, J., and Zhou, M. (2009), "Effect of Limestone Fines Content in Manufactured Sand on Durability of Low- and High- Strength Concrete," *Construction and Building Materials*, 23 (8), pp. 2846-2850. <https://doi.org/10.1016/j.conbuildmat.2009.02.033>.
- Li, L.G., and Kwan, A.K.H. (2014), "Packing Density of Concrete Mix under Dry and Wet Conditions," *Powder Technology*, 253, pp. 514-521. <https://doi.org/10.1016/j.powtec.2013.12.020>.
- Limeira, J., Etxeberria, M., Agulló, L., and Molina, D. (2011), "Mechanical and Durability Properties of Concrete Made with Dredged Marine Sand," *Construction and Building Materials*, 25(11), pp. 4165-4174. <https://doi.org/10.1016/j.conbuildmat.2011.04.053>.
- Liu, W., Huang, R., Fu, J., Tang, W., Dong, Z., and Cui, H. (2018), "Discussion and Experiments on the Limits of Chloride, Sulphate and Shell Content in Marine Fine Aggregates for Concrete," *Construction and Building Materials*, 159, pp. 725-733. <https://doi.org/10.1016/j.conbuildmat.2017.10.078>.
- Liu, X., Li, T., Tian, W., Wang, Y., and Chen, Y. (2020), "Study on the Durability of Concrete with FNS Fine Aggregate," *Journal of Hazardous Materials*, 381, 120936. <https://doi.org/10.1016/j.jhazmat.2019.120936>.
- L'Orient Le Jour (2016), "Les Travaux se Poursuivent et le Sable Disparu est Irremplaçable," *L'Orient Le Jour Magazine*, 10 Octobre.
- Makani, A. (2011), "Influence de la Nature Minéralogique des Granulats sur le Comportement Mécanique Différé des Bétons", Ph.D. Thesis, University of Toulouse, France.
- Makani, A., Vidal, T., Pons, G., and Escadeillas, G. (2010), "Time-Dependent Behaviour of High Performance Concrete: Influence of Coarse Aggregate Characteristics," 14th International Conference on Experimental Mechanics, *EPJ Web of Conferences*, 6, 03002. <https://doi.org/10.1051/epjconf/20100603002>.
- Makhloufi, Z., Bouziani, T., Bédérina, M., and Hadjoudja, M. (2014), "Mix Proportioning and Performance of a Crushed Limestone Sand - Concrete," *J. Build. Mater. Struct*, 1, pp. 10-22.

References

- Mazzucco, G., Majorana, C., Salomini, V., and Xotta, G. (2013), "Aggregate Behaviour in Concrete Materials Under High Temperature Conditions," *MATEC Web of Conferences*, 05008(6), pp. 3-4. <https://doi.org/10.1051/mateconf/20130605008>.
- Menadi, B., Kenai, S., Khatib, J., and Aït-Mokhtar, A. (2009), "Strength and Durability of Concrete Incorporating Crushed Limestone Sand," *Construction and Building Materials*, 23(2), pp. 625-633. <https://doi.org/10.1016/j.conbuildmat.2008.02.005>.
- Metha, P.K., and Monteiro, P.J.M. (2006), "Concrete: Microstructure, Properties and Materials," McGraw-Hill Publishers, New York, 514.
- Miličević, I., Štirmer, N., and Pečur, I.B. (2016), "Residual Mechanical Properties of Concrete Made with Crushed Clay Bricks and Roof Tiles Aggregate after Exposure to High Temperatures," *Materials*, 9 (4). <https://doi.org/10.3390/ma9040295>.
- Mindess, S., Young, J.F., and Darwin, D. (1981), "Concrete," Prentice Hall, Englewood Cliffs, NJ, USA.
- Ministry of Environment (2006), "Quarries in Lebanon," ABQUAR Project, Ministry of Environment. <http://www.moe.gov.lb/abquar/en/1b-en.htm>.
- Ministry of Environment (2018), "Solid Wastes Sustainable Policy," Conference Beirut, February 16th, www.moe.gov.lb.
- Monteiro, P.J.M., Maso, J.C., and Ollivier, J.P. (1985), "The Aggregate-Mortar Interface", *Cement and Concrete Research*, 15(6), pp. 953-958. [https://doi.org/10.1016/0008-8846\(85\)90084-5](https://doi.org/10.1016/0008-8846(85)90084-5).
- Moon, G.D., Oh, S., Jung, S.H., and Choi, Y.C. (2017), "Effects of the Fineness of Limestone Powder and Cement on the Hydration and Strength Development of PLC Concrete," *Construction and Building Materials*, 135, pp. 129-136. <https://doi.org/10.1016/j.conbuildmat.2016.12.189>.
- Mundra, S., Sindhi, P.R., Chandwani, V., Nagar, R., and Agrawal, V. (2016), "Crushed Rock Sand - An Economical and Ecological Alternative to Natural Sand to Optimize Concrete Mix," *Perspectives in Science*, 8, pp. 345-347. <https://doi.org/10.1016/j.pisc.2016.04.070>.
- Neithalath, N., and Jain, J. (2010), "Relating Rapid Chloride Transport Parameters of Concretes to Microstructural Features Extracted from Electrical Impedance," *Cement and Concrete Research*, 40 (7), pp. 1041-1051. <https://doi.org/10.1016/j.cemconres.2010.02.016>.
- Neville, A.M., and Brooks, J.J. (1990), "Concrete Technology," Longman Scientific and Technical, United Kingdom.
- New Yorker Magazine (2017), "The World is Running Out of Sand," *New Yorker Magazine*, Annals of Geology, May 29th. <https://www.newyorker.com/magazine/2017/05/29/the-world-is-running-out-of-sand>.
- NF EN 196-2 (2013), "Méthodes d'Essais des Ciments - Partie 2: Analyse Chimique des Ciments," Normes Européennes, AFNOR.
- NF EN 196-6 (2018), "Méthodes d'Essais des Ciments - Détermination de la Finesse," Normes Européennes, AFNOR.

References

- NF EN 933-1 (2012), "Tests for Geometrical Properties of Aggregates Part 1 - Determination of Particle Size Distribution - Sieving Method," Normes Européennes, AFNOR.
- NF EN 932-2 (1999), "Tests for General Properties of Aggregates - Part 2: Methods for Reducing Laboratory Samples," Normes Européennes, AFNOR.
- NF EN 1097-2 (2010), "Tests for Mechanical and Physical Properties of Aggregates - Part 2: Methods for the Determination of Resistance to Fragmentation," Normes Européennes, AFNOR.
- NF EN 1097-5 (2008), "Tests for mechanical and physical properties of aggregates, Part 5: Determination of the water content by drying in a ventilated oven," Normes Européennes, AFNOR.
- NF EN 1367-2 (2010), "Tests for Thermal and Weathering Properties of Aggregates - Part 2: Magnesium Sulfate Test," Normes Européennes, AFNOR.
- NF EN 1744-1 (2009), "Tests for Chemical Properties of Aggregates - Part 1: Chemical Analysis-14.2: Determination of Lightweight Contaminators," Normes Européennes, AFNOR.
- NF EN 1744-1 (2009), "Tests for Chemical Properties of Aggregates, Part 1: Chemical Analysis-Determination of Organic Components Affecting the Setting and the Hardening of Cement-15.1: Determination of Potential Presence of Humus," Normes Européennes, AFNOR.
- NF EN 12350-2 (2012), "Testing Fresh Concrete - Part 2: Slump Test," Normes Européennes, AFNOR.
- NF EN 12350-6 (2012), "Testing Hardened Concrete - Part 6: Density," Normes Européennes, AFNOR.
- NF EN 12350-7 (2012), "Testing Hardened Concrete - Part 7: Air Content - Pressure Methods," Normes Européennes, AFNOR.
- NF EN 12390-1 (2012), "Testing Hardened Concrete - Part 1: Shape, Dimensions and Other Requirements for Specimens and molds," Normes Européennes, AFNOR.
- NF EN 12390-2 (2012), "Testing Hardened Concrete - Part 2: Making and Curing Specimens for Strength Tests," Normes Européennes, AFNOR.
- NF EN 12390-3 (2012), "Testing Hardened Concrete - Part 3: Compressive Strength of Test Specimens," Normes Européennes, AFNOR.
- NF EN 12390-5 (2009), "Testing Hardened Concrete - Flexural Strength of Test Specimens", Normes Européennes, AFNOR.
- NF EN 13396 (2004), "Products and Systems for the Protection and Repair of Concrete Structures-Test Methods-Measurement of Chloride Ion Ingress," Normes Européennes, AFNOR.
- NF P 18-452 (2017), "Bétons - Mesure du Temps d'Écoulement des Bétons et des Mortiers au Maniabilimètre," AFNOR.
- NL 53 (1999), "Hydraulic Binders: Cement - Portland Type P, Portland With Additives Type PA, Composite Type C," Normes Libanaises, Liban.
- Noufal E.R., and Manju, U. (2016), "I-Sand: An Environment Friendly Alternative to River Sand in Reinforced Cement Concrete Constructions," *Construction and Building Materials*, 125, pp. 1152-1157. <https://doi.org/10.1016/j.conbuildmat.2016.08.130>.

References

- Ollivier, J.P., Maso, J.C., and Bourdette, B. (1995), "Interfacial Transition Zone in Concrete", *Advanced Cement Based Materials*, 2(1), pp. 30-38. [https://doi.org/10.1016/1065-7355\(95\)90037-3](https://doi.org/10.1016/1065-7355(95)90037-3).
- Ortiz, J., Aguado, A., Agulló, L., García, T., and Zermeño, M. (2009), "Influence of Environmental Temperature and Moisture Content of Aggregates on the Workability of Cement Mortar," *Construction and Building Materials*, 23, pp. 1808-1814. <https://doi.org/10.1016/j.conbuildmat.2008.09.016>.
- Panda, C.R., Mishra, K.K., Panda, K.C., Nayak, B.D., and Nayak, B.B. (2013), "Environmental and Technical Assessment of Ferrochrome Slag as Concrete Aggregate Material," *Construction and Building Materials*, 49, pp. 262-271. <https://doi.org/10.1016/j.conbuildmat.2013.08.002>.
- Patra, R.K., and Mukharjee, B.B. (2017), "Properties of Concrete Incorporating Granulated Blast Furnace Slag as Fine Aggregate," *Advances in Concrete Construction*, 5 (5), pp. 437-450. <https://doi.org/10.12989/acc.2017.5.5.437>.
- Pocock, D., and Corrans, J. (2007), "Concrete Durability Testing in Middle East Construction," *Concrete Engineering International*, 11, pp. 52-54.
- Polder, R.B. (2001), "Test Methods for on Site Measurement of Resistivity of Concrete- a RILEM TC-154 Technical Recommendation," *Construction and Building Materials*, 15, pp. 125-131. <https://doi.org/10.1007/bf02480599>.
- Pons, G. (1998), "Caractérisation du Comportement Différé des Bétons : De La Réalité du Matériau à La Note de Calcul," *Bulletin des Laboratoires des Ponts et Chaussées, Spécial XX*, pp. 61-71.
- Pons, G., and Torrenti, J.M. (2008), "Chapitre 5 : Le Retrait et le Fluage," *La Durabilité des Bétons*, Presses de l'Ecole Nationale des Ponts et Chaussées.
- Powers, T.C., and Brownyard, T.L. (1946), "Studies of the Physical Properties of Hardened Portland Cement Paste," *Journal Proceedings of the American Concrete Institute*, 43 (9) pp. 469-504.
- Qasrawi, H., Shalabi, F., and Asi, I. (2009), "Use of Low CaO Unprocessed Steel Slag in Concrete as Fine Aggregate," *Construction and Building Materials*, 23(2), pp. 1118-1125. <https://doi.org/10.1016/j.conbuildmat.2008.06.003>.
- Rafieizonooz, M., Salim, M.R., Mirza, J., Hussin, M.W., Salmiati, Khan, R., and Khankhaje, E. (2017), "Toxicity Characteristics and Durability of Concrete Containing Coal Ash as Substitute for Cement and River Sand," *Construction and Building Materials*, 143, pp. 234-246. <https://doi.org/10.1016/j.conbuildmat.2017.03.151>.
- Rajabipour, F., Maraghechi, H., and Fischer, G. (2010), "Investigating the Alkali-Silica Reaction of Recycled Glass Aggregates in Concrete Materials," *Journal of Materials in Civil Engineering*, 22 (12), pp.1201-1208. [https://doi.org/10.1061/\(asce\)mt.1943-5533.0000126](https://doi.org/10.1061/(asce)mt.1943-5533.0000126).
- Rajan, B., and Singh, D. (2017), "Understanding Influence of Crushers on Shape Characteristics of Fine Aggregates Based on Digital Image and Conventional Techniques," *Construction and Building Materials*, 150, pp. 833-843.
- RECYBETON Recommendations (2018), "Comment Recycler le Béton dans le Béton," Recommendations du projet national RECYBETON, Novembre 2018.

References

- Rezvani, M., and Proske, T. (2017), "Influence of Chemical-Mineralogical Properties of Limestone on the Shrinkage Behaviour of Cement Paste and Concrete Made of Limestone-Rich Cements," *Construction and Building Materials*, 157, pp. 818-828. <https://doi.org/10.1016/j.conbuildmat.2017.09.101>.
- Ribeiro, S., Ribeiro, D. de C., Souza Dias, M.B. de S., Garcia, G.C.R., and Dos Santos, É.M.B. (2011), "Study of the Fracture Behavior of Mortar and Concretes with Crushed Rock or Pebble Aggregates," *Materials Research*, 14(1), pp. 46-52. <https://doi.org/10.1590/S1516-14392011005000004>.
- Rocco, C.G., and Elices, M. (2009), "Effect of Aggregate Shape on the Mechanical Properties of a Simple Concrete," *Engineering Fracture Mechanics*, 76 (2), pp. 286-298. <https://doi.org/10.1016/j.engfracmech.2008.10.010>.
- Sabih, G., Tarefder, R.A., and Jamil, S.M. (2016), "Optimization of Gradation and Fineness Modulus of Naturally Fine Sands for Improved Performance as Fine Aggregate in Concrete," *Procedia Engineering*, 145, pp. 66-73. <https://doi.org/10.1016/j.proeng.2016.04.016>.
- Sadeghi, S.H.R., and Harchegani, M.K. (2012), "Effects of Sand Mining on Suspended Sediment Particle Size Distribution in Kojour Forest River, Iran," *Journal of Agricultural Science and Technology*, 14, pp. 1637-1646.
- Safiddine, S., Debieb, F., Kadri, E.H., Menadi, B., and Soualhi, H. (2017), "Effect of Crushed Sand and Limestone Crushed Sand Dust on the Rheology of Cement Mortar," *Applied Rheology*, 27, 14490, <https://doi.org/10.3933/APPLRHEOL-27-14490>.
- Saikia, N., and De Brito, J. (2014), "Mechanical Properties and Abrasion Behaviour of Concrete Containing Shredded PET Bottle Waste as a Partial Substitution of Natural Aggregate," *Construction and Building Materials*, 52, pp. 236-244. <https://doi.org/10.1016/j.conbuildmat.2013.11.049>.
- Santos, A.C.P., Ortiz-Lozano, J.A., Villegas, N., and Aguado, A. (2015), "Experimental Study about the Effects of Granular Skeleton Distribution on the Mechanical Properties of Self-Compacting Concrete (SCC)," *Construction and Building Materials*, 78, pp. 40-49. <https://doi.org/10.1016/j.conbuildmat.2015.01.006>.
- Saxena, S., and Pofale, A.D. (2017), "Effective Utilization of Fly Ash and Waste Gravel in Green Concrete by Replacing Natural Sand and Crushed Coarse Aggregate," *Materials Today: Proceedings*, 4 (9), pp. 9777-9783. <https://doi.org/10.1016/j.matpr.2017.06.266>.
- Scrivener, K.L., Crumbie, A.K., and Laugesen, P. (2004), "The Interfacial Transition Zone (ITZ) Between Cement Paste and Aggregate in Concrete," *Interface Science*, 12, pp. 411-421.
- Sellier, A., and Buffo-Lacarrière, L. (2009), "Vers une Modélisation Simple et Unifiée du Fluage Propre, du Retrait et du Fluage en Dessiccation du Béton," *Revue Européenne de Génie Civil*, 13(10), pp. 1161-1182.
- Senhadji, Y., Escadeillas, G., Benosman, A.S., Mouli, M., Khelafi, H., and Ould Kaci, S. (2015), "Effect of Incorporating PVC Waste as Aggregate on the Physical, Mechanical, and Chloride Ion Penetration Behavior of Concrete," *Journal of Adhesion Science and Technology*, 29 (7), pp. 625-640. <https://doi.org/10.1080/01694243.2014.1000773>.

References

- Shane, J.D., Aldea, C.M., Bouxsein, N.F., Mason, T.O., Jennings, H.M., and Shaw, S.P. (1999), "Microstructural and Pore Solution Changes Induced by Rapid Chloride Permeability Test Measured by Impedance Spectroscopy," *Concrete Science and Engineering*, 1, pp. 110-119.
- Shen, W., Liu, Y., Cao, L., Huo, X., Yang, Z., Zhou, C., He, P., and Lu, Z. (2017), "Mixing Design and Microstructure of Ultra High Strength Concrete with Manufactured Sand," *Construction and Building Materials*, 143, pp. 312-321. <https://doi.org/10.1016/j.conbuildmat.2017.03.092>.
- Shen, W., Liu, Y., Wang, Z., Cao, L., Wu, D., Wang, Y., and Ji, X. (2018), "Influence of Manufactured Sand's Characteristics on its Concrete Performance," *Construction and Building Materials*, 172, pp. 574-583. <https://doi.org/10.1016/j.conbuildmat.2018.03.139>.
- Shen, W., Yang, Z., Cao, L., Cao, L., Liu, Y., Yang, H., Lu, Z., and Bai, J. (2016), "Characterization of Manufactured Sand: Particle Shape, Surface Texture and Behavior in Concrete," *Construction and Building Materials*, 114, pp. 595-601. <https://doi.org/10.1016/j.conbuildmat.2016.03.201>.
- Sicard, V. (1993), "Origine et Propriétés du Retrait et du Fluage de Bétons à Hautes Performances à Partir de 28 Heures de Durcissement", Ph.D. Thesis, INSA, Toulouse, France.
- Silva, J., De Brito, J., and Veiga, R. (2009), "Incorporation of Fine Ceramics in Mortars," *Construction and Building Materials*, 23 (1), pp. 556-564. <https://doi.org/10.1016/j.conbuildmat.2007.10.014>.
- Singh, G., and Siddique, R. (2016), "Strength Properties and Micro-Structural Analysis of Self-Compacting Concrete Made with Iron Slag as Partial Replacement of Fine Aggregates," *Construction and Building Materials*, 127, pp. 144-152. <https://doi.org/10.1016/j.conbuildmat.2016.09.154>.
- Singh, M., and Siddique, R. (2014), "Strength Properties and Micro-Structural Properties of Concrete Containing Coal Bottom Ash as Partial Replacement of Fine Aggregate," *Construction and Building Materials*, 50, pp. 246-256.
- Srour, I.M., Chehab, G.R., and Gharib, N. (2012), "Recycling Construction Materials in a Developing Country: Four Case Studies," *Int. J. Engineering Management and Economics*, 3(1/2), pp. 135-151.
- Stefanidou, M. (2016), "Crushed and River-Origin Sands Used as Aggregates in Repair Mortars," *Geosciences*, 6(2), 23. <https://doi.org/10.3390/geosciences6020023>.
- Struble, L., Skanly, J., and Mindess, S. (1980), "A Review of the Cement - Aggregate Bond," *Cement and Concrete Research*, 10, pp. 277-286.
- Tasong, W.A., Cripps, J.C., and Lynsdale, C.J. (1998), "Aggregate-Cement Chemical Interactions," *Cement and Concrete Research*, 28(7), pp. 1037-1048.
- Tasong, W.A., Lynsdale, C.J., and Cripps, J.C. (1998), "Aggregate-Cement Paste Interface. II: Influence of Aggregate Physical Properties," *Cement and Concrete Research*, 28(10), pp. 1453-1465.
- Tasong, W.A., Lynsdale, C.J., and Cripps, J.C. (1999), "Aggregate-Cement Paste Interface. Part I. Influence of Aggregate Geochemistry," *Cement and Concrete Research*, 29(7), pp. 1019-1025.
- Tazawa, E.I., and Miyazawa, S. (1995), "Experimental Study on Mechanism of Autogenous Shrinkage of Concrete," *Cement and Concrete Research*, 25 (8), pp. 1633-1638.

References

- Tazawa, E.I., and Miyazawa, S. (1995), "Influence of Cement and Admixture on Autogenous Shrinkage of Cement Paste," *Cement and Concrete Research*, 25 (2), pp. 281-287.
- Tazawa, E.I., Miyazawa, S., and Kasai, T. (1995), "Chemical shrinkage and Autogenous Shrinkage of Hydrating Cement Paste," *Cement and Concrete Research*, 25 (2), pp. 288-292.
- The Daily Star (2013), "Tyre Mayor, Residents Fight Sand Mining Project," *The Daily Star - Lebanon News*, Mohammed Zaatari, November 18th.
- The Daily Star (2016), "Machnouk Plan to Clean Litani Faces Hurdle," *The Daily Star*, 12-07-2016. <https://www.moe.gov.lb>.
- Thomas, M.D.A., and Wilson, M.L. (2002), "Admixtures Use in Concrete," CD039, PCA, Skokie, IL.
- Tillin, H.M., Houghton, A.J., Saunders, J.E., Drabble, R., and Hull, S.C. (2011), "Direct and Indirect Impacts of Aggregate Dredging," Marine Aggregate Levy Sustainability Fund (MALSF), *Science Monograph Series*, 1, pp. 1-46.
- Titi, H., and Tabatabai, H. (2018), "Effect of Coarse Aggregate Type on Chloride Ion Penetration in Concrete," *Construction and Building Materials*, 162, pp. 871-880. <https://doi.org/10.1016/j.conbuildmat.2018.01.090>.
- Topçu, I.B., and Bilir, T. (2010), "Experimental Investigation of Drying Shrinkage Cracking of Composite Mortars Incorporating Crushed Tile Fine Aggregate," *Materials and Design*, 31 (9), pp. 4088-4097. <https://doi.org/10.1016/j.matdes.2010.04.047>.
- UNEP (2014), "Sand, Rarer Than One Thinks," United Nations Environment Program, Global Environmental Alert Service (GEAS).
- Vijayalakshmi, M., Sekar, A.S.S., and Ganesh Prabhu, G. (2013), "Strength and Durability Properties of Concrete Made with Granite Industry Waste," *Construction and Building Materials*, 46, pp. 1-7. <https://doi.org/10.1016/j.conbuildmat.2013.04.018>.
- Walley, C.D. (1997), "The Geology of Lebanon," *Al Mashriq*, in collaboration with the American University of Beirut, <http://almashriq.hiof.no/ddc/projects/geology/geology-of-lebanon>.
- Wang, J., Yang, Z., Niu, K., Ke, G., and Zhou, M. (2009), "Influence of MB-Value of Manufactured Sand on the Shrinkage and Cracking of High Strength Concrete," *Journal of Wuhan University of Technology-Mater.*, April, pp. 321-325. <https://doi.org/10.1007/s11595-009-2321-z>.
- Weltzien, J. (2006), "Quarries and Worries or Cut and Fill, The Case of Lebanon", *Presse de l'Université de Montréal, Workshop Tunisie*, pp. 116-119. <https://books.openedition.org/pum/14028>.
- Westerholm, M., Lagerblad, B., Silfwerbrand, J., and Forsberg, E. (2008), "Influence of Fine Aggregate Characteristics on the Rheological Properties of Mortars," *Cement and Concrete Composites*, 30 (4), pp. 274-282. <https://doi.org/10.1016/j.cemconcomp.2007.08.008>.
- Wimpenny, D.E., Slater Ravinda, D., Dhir, K., Roderick Jones, M., and Li, Z. (2015), "Thaumasite in Concrete Structure: Some UK Case Studies," *Challenge of Concrete Construction: Volume 3, Repair, Rejuvenation and Enhancement of Concrete*. <https://doi.org/10.1680/rraeoc.31753.0014>.

References

- Xiao, J., Qiang, C., Nanni, A., and Zhang, K. (2017), "Use of Sea-Sand and Seawater in Concrete Construction: Current Status and Future Opportunities," *Construction and Building Materials*, 155, pp. 1101-1111. <https://doi.org/10.1016/j.conbuildmat.2017.08.130>.
- Yager, T.R. (2004), "The Mineral Industry of Lebanon," *U.S. Geological Survey Minerals Yearbook*, 2004-2005, pp. 51.1-51.2.
- Yajurved, R.M., Swetha, D.V., and Yajdani, S.K. (2015), "Studies on Properties of Concrete with Manufactured Sand as Replacement to Natural Sand," *International Journal of Civil Engineering and Technology (IJCIET)*, 6(8), pp. 29-42.
- Yamei, H., and Lihua, W. (2017), "Effect of Particle Shape of Limestone Manufactured Sand and Natural Sand on Concrete," *Procedia Engineering*, 210, pp. 87-92. <https://doi.org/10.1016/j.proeng.2017.11.052>.
- Yang, C.C., Cho, S.W., and Wang, L.C. (2006), "The Relationship between Pore Structure and Chloride Diffusivity from Ponding Test in Cement-Based Materials," *Materials Chemistry and Physics*, 100 (2-3), pp. 203-210. <https://doi.org/10.1016/j.matchemphys.2005.12.032>.
- Yüksel, I., Bilir, T., and Özkan, Ö. (2007), "Durability of Concrete Incorporating Non-Ground Blast Furnace Slag and Bottom Ash as Fine Aggregate," *Building and Environment*, 42, pp. 2651-2659. <https://doi.org/10.1016/j.buildenv.2006.07.003>.
- Zeghichi, L., Benghazi, Z., and Baali, L. (2012), "Comparative Study of Self-Compacting Concrete with Manufactured and Dune Sand," *Journal of Civil Engineering and Architecture*, 6 (10), pp. 1429-1434.
- Zhang, Y., Sun, Q., and Geng, J. (2017), "Microstructural Characterization of Limestone Exposed to Heat with XRD, SEM and TG-DSC," *Materials Characterization*, 134, pp. 285-295. <https://doi.org/10.1016/j.matchar.2017.11.007>.
- Zhao, H., Xiao, Q., Huang, D., and Zhang, S. (2014), "Influence of Pore Structure on Compressive Strength of Cement Mortar," *The Scientific World Journal*, pp. 1-12. <https://doi.org/10.1155/2014/247058>.